

Peptides and Polypeptides Derived from *4S/R-(hyp/amp)*-Proline: Synthesis and Characterisation of β -Structure

A thesis

Submitted in partial fulfillment of the requirements

of the degree of

Doctor of Philosophy

By

Nitin D. Bansode

ID: 20093028



INDIAN INSTITUTE OF SCIENCE EDUCATION AND RESEARCH, PUNE

2015

This Thesis is dedicated to...

My late younger brother Sachin

And

My Family



भारतीय विज्ञान शिक्षा एवं अनुसंधान संस्थान, पुणे

INDIAN INSTITUTE OF SCIENCE EDUCATION AND RESEARCH (IISER), PUNE

(An Autonomous Institution, Ministry of Human Resource Development, Govt. of India)

900 NCL Innovation Park, Dr. Homi Bhabha Road, Pune 411008

Prof. Krishna N. Ganesh

Professor and Coordinator, Chemistry

Director, IISER Pune

J. C. Bose Fellow (DST), NCL Pune

CERTIFICATE

I certify that the work incorporated in the thesis entitled “**Peptides and Polypeptides Derived From 4S/R-(hyp/amp)-Proline: Synthesis and Characterisation of β -structure**” submitted by **Mr. Nitin D. Bansode** was carried out by the candidate, under my supervision. The work presented here or any part of it has not been included in any other thesis submitted previously for the award of any degree or diploma from any other university or institution.

Date: 28th Dec.2015

Prof. Krishna N. Ganesh

(Research Supervisor)

DECLARATION

I declare that, this written submission represents my ideas in my own words and where others' ideas have been included, I have adequately cited and referenced the original sources. I also declare that I have adhered to all principles of academic honesty and integrity and have not misrepresented or fabricated or falsified any idea / data / fact/ source in my submission. I understand that violation of the above will be cause for disciplinary action by the Institute and can also evoke penal action from the sources which have thus not been properly cited or from whom proper permission has not been taken when needed.

Date: 28th Dec. 2015, Pune

Mr. Nitin D. Bansode

ID: 20093028

Acknowledgements

It gives me an immense pleasure to express my deep sense of gratitude towards my research supervisor Prof. Krishna N. Ganesh for his support and guidance. He has been the constant source of inspiration throughout my doctoral research. He has always taken efforts to instill independent thinking, writing skills, presentation skills and many more things to develop a researcher in me. He has been the 'real mentor' in my life; he has guided not only in scientific problems but also in personal difficulties.

I sincerely thank Director, IISER Pune for providing fantastic facilities to carry out doctoral research. Also, I am thankful to each and every chemistry faculty in IISER-Pune for their help.

I am very grateful to my research advisory committee members Dr. S. G. Srivatsan and Dr. H. V. Thulasiram for their fruitful suggestions, comments and encouragement through various RAC meetings. I would like to specially thank Dr. H. N. Gopi who always gave me solution whenever I had problem regarding research. I sincerely thank Dr. Ramkrishna G. Bhatt for his encouragement and support by one or the other way. I would like to acknowledge UGC India for providing research fellowship during the last five years.

I admire the co-operation of my seniors, colleague and juniors for cheerful atmosphere in the lab. I thank my seniors Dr. Mahesh, Dr. Roopa, Dr. Shridhar, Dr. Ashwani, Dr. Gitali, Dr. Amit, Dr. Manaswini, Dr. Tanpreet and Mrs. Pradnya for their help in initial years of research in NCL. I thank Dr. Deepak, my colleague with whom I started my research career and shared every moment of frustration as well as joy. I thank my juniors cum colleagues, Vijay, Satish, Dr. Dhruvajyoti Datta (Dhrup), Madhan, Prabhakar, Shahaji, Pramod (Topi), Pramod (Bhingardave) and Manoj for always keeping healthy atmosphere around. My all labmates actually gave the relaxation needed in tough times of research.

Acknowledgements

I must acknowledge the help from Pooja Lunawat for NMR analysis, Yatish for FESEM instrument, Swati Dixit for MALDI TOF/TOF mass analysis. My Special thank to Mr. Nitin Dalvi and Mr. Mahesh Jadhav for assisting my research with purchase orders and other help. I am thankful to Mayuresh for the administrative help.

Life becomes boring if I would not have met wonderful friends) Dr Prakash and Dr. Sachin (Mali). As we have been together for long time and shared every moment and experience of life. Their kind and helping attitude always supported me in my difficult time. I present my deepest thank for you both guys for bearing me for such a long time.

I had a wonderful company with my friends Shekhar, Dr. Amar, Dr. Maroti, Dr. Sandip, Anupam, Arun, Ashok, Pramod (Sabala), Dnyaneshwar (gangan), Sharad, Susheel, Ganesh, Gopal, Rajkumar, Rahi, Anindita, Santosh, Trimbek, Tushar, Balu Navle, Bapu, Satish, Sanjog, Kundan and all friend from chemistry department who helped me to release the sort of tension in difficult times of research in one way or other. I cannot forget the time spent in Sutarwadi. I enjoyed unforgettable 5 years of my life with Sandeep (sandya) and Ganesh (Ganpat).

I shall always remain indebted to my parents, brother and my entire family, for their unconditional love, blessings, sacrifices, patience and support. My brother Laxman (Bhau) always insisted me to do better, I present my thanks for believing in me. The values and virtues they have instilled in me have made me achieve whatever I have achieved so far. I would like to thank a very very special person my lovely wife, Shobha for her continuous support, faith and patience during the last days of my PhD. Her love and helpful spirit have made this dissertation possible. Finally, I would like to thank my two sweet nieces Janvi and Vaishnavi. They always made me forget all the tension & frustration. I hope with my hard work and dedication, I would be able to translate their dreams into reality.

Nitin

Contents

Abbreviations	vii-x
Abstract	xi-xxi

Chapter 1

Introduction and importance of polyproline conformations

1	Introduction	2
1.1	Conformational Analysis of Polypeptides	2
1.1.1	Ramachandran plot	3
1.2	Protein Secondary Structures: the α Helix and the β Sheet	5
1.2.1	The α helix	5
1.2.2	The β -sheet	6
1.3	Other Secondary Structures: 3_{10} helix, β -hairpin and turns	7
1.4	Polyproline conformation	9
1.4.1	Peptidyl prolyl <i>cis-trans</i> isomerisation	9
1.5	Polyproline conformations	10
1.5.1	Stability of polyproline conformation	12
1.5.2A	Crystal Structure of an Oligoproline PPII-Helix	12
1.5.3	A survey of left-handed polyproline II helices	13
1.5.4	Conformational preference and <i>cis-trans</i> isomerisation of 4(<i>R/S</i>)-substituted proline	14
1.6	Factors Affecting Polyproline Conformation	15
1.7	Biological Significance of Polyproline Conformation	25
1.8	Methodology	35
1.9	Characterization of Polyproline Structures	40
1.10	Scope of present work	44
1.11	References	47

Chapter 2

Synthesis and study of foldamer properties of unnatural (N-amino ethyl)glycyl and pyrrolidine peptides of different length

2	Introduction	60
2.1	Present work: Rationale	63
2.5	Results	64
2.5.1	Synthesis of fully protected monomers	64
2.5.2	Solid phase synthesis of homo oligopeptides 1-4	70
2.6	CD Spectroscopic Studies	73
2.6.1	Circular Dicroism (CD) studies at pH-7.2	75
2.6.2	Circular Dicroism (CD) studies in trifluoroethanol (TFE)	76
2.7	FT-IR studies	80
2.7.1	FT-IR studies in TFE	82
2.8	Discussion	86
2.9	Conclusion	88
2.10	Experimental	90
2.11	References	109
2.12	Appendix	112

Chapter 3

Poly-4*S*(hyp/amp)proline peptides: Characterization of β -structure

3	Introduction	139
3.1	Present work: Rationale	140
3.2	Results	141
3.2.1	Synthesis of protected (2 <i>S</i> ,4 <i>R</i>)- and (2 <i>S</i> ,4 <i>S</i>)-hydroxyproline monomers for polypeptide synthesis	141
3.2.2	Synthesis of homo oligopeptides 5-8 by using solid phase protocol	144
3.2.3	CD Spectroscopic Studies	146

3.2.4	Identification of PPII by UV-CD spectroscopy in water	147
3.2.6	Effect of urea on peptides 5-7	149
3.2.7	Effect of salt (NaCl) on peptides 5-7	152
3.2.8	Effect of NaClO ₄ on peptides 7	155
3.2.9	Effect of trifluoroethanol on peptides 5-7	157
3.3	Identification of β -structure by Raman Spectroscopy	160
3.4	Water-induced switching of β -structure to PPII conformation in the 4S- <i>hyp</i> ₉	162
3.5	Effect of O-acylation on β -structure	162
3.6	β -Structure requires <i>cis</i> -disposition of 4-OH and C2-CO groups	163
3.6.1	Conformational study of 4R-D-peptide 9 (4R-D- <i>hyp</i> ₉) in water	164
3.6.2	Conformational study of (4R-D- <i>hyp</i> ₉) peptide 9 in TFE	165
3.6.3	Effect of N-terminal Phenylalanine	166
3.7	Discussion	167
3.9	Conclusion	174
3.10	Experimental	176
3.12	References	184
3.13	Appendix	190

Chapter 4

Orientation of β -Structure: parallel or antiparallel?

Section 1: Distinguishing the β -structure arrangements by FRET

4.0	Introduction	206
4.2	Rationale of the work	209
4.3	Results and discussion	211
4.3.1	Peptide synthesis and labeling	211
4.3.1a	Fluorescent peptides	211

4.3.1b	Peptides conjugated with fatty acids	212
4.3.3	CD Spectroscopic Studies	216
4.4	Fluorescence spectroscopic studies	218
4.4.1.	Fluorescence emission of peptide 10 and 11 in sodium phosphate buffer (pH 7.2)	218
4.4.2	Fluorescence emission of peptides 10 and 11 in TFE	219
4.5	The FRET experiments	220

Section 2. Morphology and polymorphism of self-assembling polyproline peptides conjugated with fatty acid chains

4.7	Rationale of work	226
4.8	Results and discussion	227
4.8.1	Circular dichroism studies of 4 <i>R</i> -peptides 13-15 in buffer	227
4.8.2	Circular dichroism studies of 4 <i>R</i> -peptides 13-15 in TFE	228
4.8.3	Circular dichroism studies of 4 <i>S</i> -peptides 7, 16-18 in water	229
4.8.4	Circular dichroism studies of 4 <i>S</i> -peptide 7, 16-18 in TFE	230
4.9	Field Emission Scanning Electron Microscopy (FESEM)	231
4.9.1	4 <i>R</i> -peptides 6, 13-15 in water	231
4.9.2	4 <i>S</i> -peptides 7, 16-18 in water	232
4.9.3	FESEM of 4 <i>R</i> -peptides 6, 13-15 in TFE	233
4.9.4	FESEM of 4 <i>S</i> -peptides 7, 16-18 in TFE	234
4.10	FT-IR Studies	236
4.12	Discussion	238
4.13	Conclusion	241
4.14	Experimental	243
4.15	References	249
4.16	Appendix	254

Abbreviations & Symbols

Ac	Acetyl
Ac ₂ O	Acetic anhydride
Aib	α-Aminoisobutyric acid
Ala	Alanine
Amp	(2 <i>S</i> ,4 <i>R</i>)-Aminoproline
amp	(2 <i>S</i> ,4 <i>S</i>)-aminoproline
Arg	Arginine
Asn	Asparagine
Azp	(2 <i>S</i> ,4 <i>R</i>)-Azidoproline
azp	(2 <i>S</i> ,4 <i>S</i>)-azidoproline
(Boc) ₂ O	Boc anhydride
°C	Degree Celsius
Cbz	Benzyloxycarbonyl
CBMIT	1,1'-Carbonylbis(3-Methylimidazolium), Triflate
CD	Circular Dichroism
CDI	1,1'-Carbonyldiimidazole
CMPs	Collagen mimetic peptides
CMBI	2-chloro-1,3-dimethyl-1 <i>H</i> -benzimidazolium hexafluorophosphate
COSY	Correlation Spectroscopy
CRPs	Collagen Related Peptides
Cys	Cystine
D-	Dextro-
DCC	<i>N,N'</i> -Dicyclohexylcarbodiimide
DCM	Dichloromethane
DSC	Differential scanning calorimetry
Δ <i>G</i>	Change in Gibb's free energy
Δ <i>H</i>	Change in enthalpy
Δ <i>T</i> _m	Difference in melting temperature
DIAD	Diisopropyl azodicarboxylate
DIPEA	<i>N,N</i> -Diisopropylethylamine
DMF	<i>N,N</i> -Dimethylformamide
DMS	Dimethyl sulfide
DNA	Deoxyribonucleic acid
<i>E</i>	<i>entgegen</i>
ECM	Extracellular matrix
EDC	1-ethyl-3-(3-dimethylaminopropyl) carbodiimide
EG	Ethylene glycol
eq.	equivalents
ESI-MS	Electro Spray Ionization Mass Spectrometry
Et	Ethyl

Flp	(2 <i>S</i> ,4 <i>R</i>)-Fluoroproline
flp	(2 <i>S</i> ,4 <i>S</i>)-fluoroproline
Fmoc	9-Fluorenylmethoxycarbonyl
g	Gram
Glu	Glutamine
Gly	Glycine
h	Hours
HATU	O-(7-azabenzotriazol-1-yl)-1,1,3,3-tetramethyluronium hexafluorophosphate
HBTU	(2-(1 <i>H</i> -Benzotriazole-1-yl)-1,1,3,3-tetramethyl-uronium- hexafluorophosphate)
HOAt	1-Hydroxy-7-azabenzotriazole
HOBt	N- Hydroxybenzotriazole
HPLC	High Performance Liquid Chromatography
Hyp	(2 <i>S</i> ,4 <i>R</i>)-Hydroxyproline (<i>trans</i> -4-hydroxy-L-proline)
hyp	(2 <i>S</i> ,4 <i>S</i>)-hydroxyproline (<i>cis</i> -4-hydroxy-L-proline)
Hz	Hertz
<i>in situ</i>	In the reaction mixture
<i>in vivo</i>	Within the living organism
<i>in vitro</i>	outside the living organism
IR	Infra Red
K	Kelvin/Kilo/Binding Constant
kJ	kilojoules
$K_{trans/cis}$	Ratio of <i>trans/cis</i>
L-	Levo-
LCMS	Liquid Chromatography-Mass Spectrometry
Leu	Leucine
Lys	Lysine
M	Molar
MACIT	Membrane associated with interrupted triple-helices
MALDI-TOF	Matrix Assisted Laser Desorption Ionization-Time of Flight
MBHA	p-methoxybenzhydramine
MECN	Acetonitrile
MeOH	Methanol
Mep	(2 <i>S</i> ,4 <i>R</i>)-Methylproline
mep	(2 <i>S</i> ,4 <i>S</i>)-methylproline
Mg	milligram
mL	millilitre
MHz	megahertz
min	minutes
μ	Micron
μl	Microliter
μM	Micromolar
mL	Microliter

mmol	millimolar
MS	Mass spectrometry
MsCl	methanesulfonylchloride
Nd:YAG	Neodymium-doped yttrium aluminium garnet; Nd:Y ₃ Al ₅ O ₁₂
ν	nu (frequency)
NaN ₃	Sodium azide
Nm	Nanometer
NMP	N-Methyl-2-pyrrolidone
NMR	Nuclear Magnetic Resonance
NOE	Nuclear Magnetic Overhauser Effect
Pd-C	Palladium on carbon
Phe	Phenylalanine
Pro	L-Proline
PNA	Peptide Nucleic Acid
ppm	parts per million
PPII	Polyproline II
PPI	Polyproline I
psi	pound per square inch
PyBOP	Benzotriazol-1-yloxytri(pyrrolidino)-phosphonium-hexafluorophosphate
<i>R</i>	Rectus
ROA	Raman optical activity
$R_{p/n}$	Ratio of positive to negative band intensities
RP	Reverse phase
RNA	Ribonucleic acid
<i>S</i>	Sinister
SDS-PAGE	Sodium dodecyl sulfate polyacrylamide gel electrophoresis
Ser	Serine
SPPS	Solid Phase Peptide Synthesis
τ	Tau
TBTU	O-(benzotriazol-1-yl)-1,13,3-tetramethyluronium hexafluorophosphate
<i>t</i> -Boc	<i>tert</i> -butyloxycarbonyl
TFA	Trifluoroacetic acid
TFMSA	Trifluoromethane sulfonic acid
TFE	2,2,2-Trifluoroethanol
THF	Tetrahydrofuran
TIS	Triisopropylsilane
TMS	Tetramethylsilane
T_m	Melting temperature
Trp	Tryptophan
TSTU	2-succinimido-1,1,3,3-tetramethyluronium tetrafluoroborate
Tyr	Tyrosine

Abbreviations & Symbols

Val	Valine
VCD	Vibrational Circular Dichroism
v/v	volume to volume ratio
Z	zusammen

Abstract

The thesis entitled “**Peptides and Polypeptides Derived from 4*S/R*-(*hyp/amp*)-Proline: Synthesis and Characterisation of β -structure**” is comprised of studies towards the design and synthesis of peptides based on 4-substituted prolines in hybrid amides and polyproline and study of their conformational behavior under variable physical environments which may have importance in understanding their biological functions. The work describes different conformational behavior of 4-amino/hydroxy hybrid amides and polyproline peptides under different solute and solvent conditions and characterisation of β -structure. The investigation of β -structure in 4*S*-*hyp*₉ may gives new directions of future research work in protein engineering. The thesis is presented as four chapters

Chapter 1: Introduction and importance of polyproline conformations

Chapter 2: Synthesis and study of foldamer properties of unnatural (N-amino ethyl)glycyl and pyrrolidine peptides of different length

Chapter 3: Poly-4*S*(*hyp/amp*)proline peptides: Characterization of β -structure

Chapter 4: Orientation of β -Structure: parallel or antiparallel?

Chapter 1: Introduction and importance of polyproline conformations

This chapter gives an overview on the background literature for undertaking the research work, emphasizing recent advancements in the field of polyproline peptides and their applications.

The polyproline type conformations PPI and PPII have been recognized for their presence in both folded and unfolded protein structures. PPI helix as all backbone tertiary amide bonds are in the *cis* ($\omega_0=0^\circ$) disposition, while in PPII, these bonds are all *trans* ($\omega_0=180^\circ$). The right handed PPI helix is thus compact while the PPII helix is a fully extended left-handed structure.

$n \rightarrow \pi^*$ interaction is the main structural feature responsible for the stabilization of polyproline structures. Polyproline conformations are affected by different factors

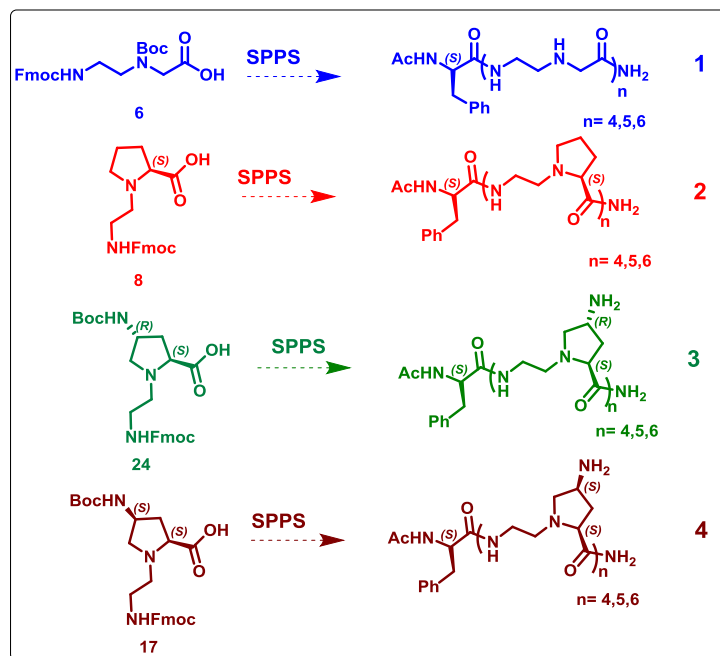
including *endo/exo* pucker for prolyl ring, *cis-trans* isomerism, stereoelectronic (*gauche* interactions). Recent literature and advancements in the area of polyproline emphasize on the utility of proline, and synthesis of series of peptides functionalized with substitution to examine the effects of proline substitution on PPI and PPII conformations with combination of stereoelectronic and steric effects on proline conformation and thus consequently on peptide main-chain conformation and to develop new biologically important tools.

Chapter 2: Synthesis and study of foldamer properties of unnatural (N-amino ethyl)glycyl and pyrrolidine peptides of different length

This chapter is directed towards the comparative study of hybrid amides (aminoethyl-glycyl, aminoethyl-prolyl, *ae-4(R/S)*-aminoprolyl-polyamides) to understand the effect of chain length, proline conformation and stereochemistry of proline C4 substituent on the secondary structures adopted by (*ae-pro*) polyamides in water and Fluoro-alcohols and investigation of conformation adopted by these polyamides by different spectroscopy.

Fully protected monomers (Scheme1) aminoethyl glycine (*aeg*) (**6**), aminoethyl prolyl (*ae-Pro*) (**8**), aminoethyl 4*S*-hydroxyprolyl (*ae-4S-Hyp*) (**17**), and aminoethyl 4*R*-hydroxyprolyl (*ae-4R-hyp*) (**24**) were synthesized and these were incorporated into the homo oligopeptides **1** (*aeg*)_n, **2** (*ae-pro*)_n, **3** (*ae-4R-Hyp*)_n, and **4** (*ae-4S-hyp*)_n, of various length from tetramer to hexamer by solid phase synthesis on Rink amide resin, using Fmoc chemistry with *t*-Boc protection for the 4-amino function on proline (Scheme 1).

Scheme 1.



The conformational studies of oligopeptides were carried out by CD and FT-IR spectral analysis in water (sodium phosphate buffer pH 7.2) and trifluoroethanol (TFE). The peptides **1** and **2** had no ordered secondary structure in both water and TFE due to non-chiral amino acid glycine and unsubstituted proline. In peptide **3**, with 4*R*-NH₂ substitution on proline, no CD or FT-IR signal indicated secondary structure, reflecting the steric inability of 4*R*-NH₂ group to engage in any H-bonding. However, the peptide **4**, with 4*S*-amino substituent on proline can take part in intermolecular hydrogen bonding between two strands (Figure1).

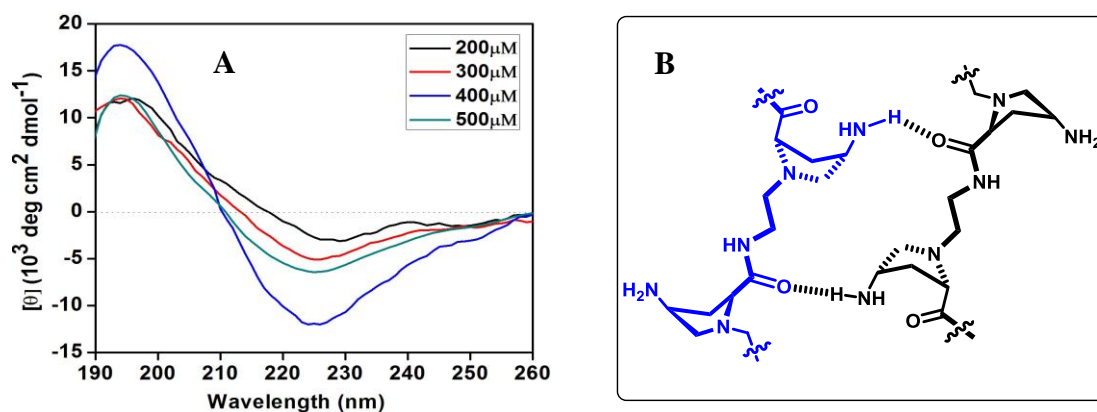


Figure 1. (A) CD profile of peptides *aeg-4S-amp*₆ at concentration 200 to 500 μM in TFE; (B) Possible intermolecular H-bonding

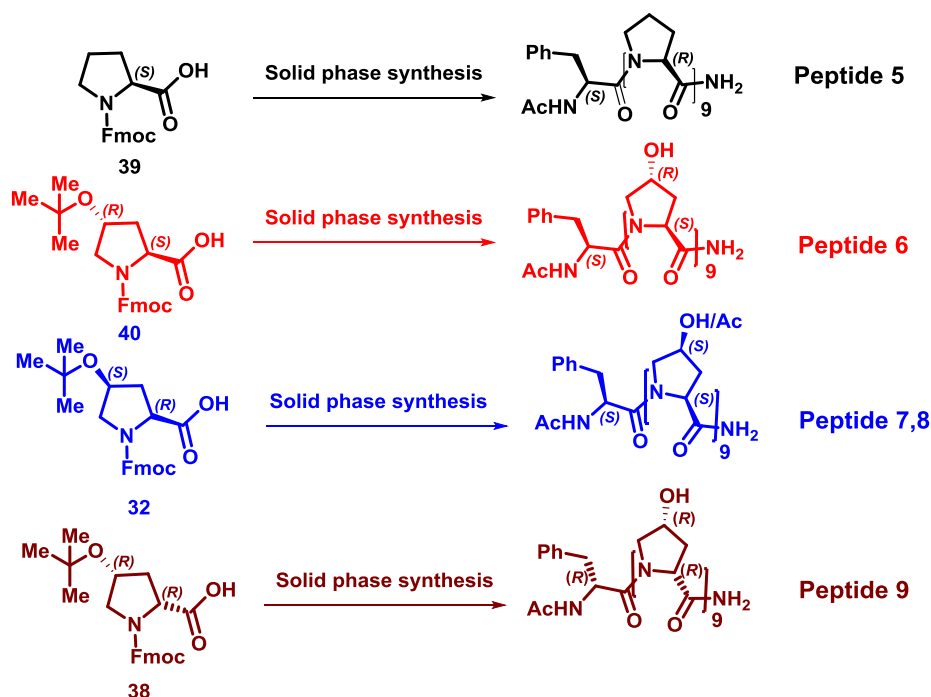
Chapter 3: Poly-4*S*(*hyp/amp*)proline peptides: Characterization of β -structure

Structural and conformational analyses of biopolymers reveal the fact that most of the biological events result from their stable compact conformation, stabilized by a collection of non-covalent interactions. Polyproline *helices*, along with α -helices and β -sheets, are the three most important types of protein secondary structure that exist in nature.

Compared to the other common secondary structure elements found in protein, absence of local hydrogen bonds involving main chain atoms is one of the distinctive structural properties of PPII helices. This structural feature leaves several unsatisfied hydrogen bond acceptors free to establish *intra* or *inter*-molecular interactions. A recent computational study¹ as well as Chapter 2 has suggested that in 4*S*-aminoproline, intramolecular hydrogen bond that is feasible between 4*S*-NH₂ and the carbonyl carbon of same proline moiety², leads to increase in the *trans/cis* ratio of peptide bond. In view of these findings, it was proposed to study the effect of 4*R/S*-amino/hydroxyl group, which unlike fluorine³ or azide⁴ can participate in intramolecular and intermolecular hydrogen bonding. 4-Hydroxy group should act like the 4-amino group in terms of its ability to form hydrogen bonding and influence the PPI and PPII conformation of proline polypeptides.

The 4*S*-L-hydroxyproline (**32**) and 4*R*-D-hydroxyproline (**38**) monomers were synthesized (Scheme 2). These were incorporated into the homo oligopeptides **7** (4*S*-L-hyp₉) and **9** (4*R*-hyp₉) by solid phase synthesis on Rink amide resin, using Fmoc chemistry with *t*-butyl protection for the 4-hydroxy function on proline (Scheme 2). The readily available N-Fmoc proline (**39**) and 4*R*-hydroxyproline (**40**) was used for the synthesis of control proline oligomer **5** (Pro₉) and **6** (4*R*-Hyp₉). The peptide **8** (4*S*-Achyp₉) was obtained by treatment of peptide **7** (4*S*-hyp₉) with acetic anhydride.

Scheme 2.



The conformational studies of oligopeptides were carried out by CD spectral analysis as a function of different solvents trifluoroethanol (TFE) aliphatic alcohol and solutes (urea, sodium chloride and sodium perchlorate). It is commonly known that urea denatures proteins by promoting disorder in peptide backbone. The first step of unfolding is opening up of the hydrophobic core, which then gets solvated by water and later by urea. It is well known that urea promotes PPII helicity while salt (NaCl) disrupts the PPII helix.⁵ The effects of these solutes on the conformation of peptides (**5-7**) were examined by CD spectroscopy. It was found that the PPII helicity of peptides **5**

(*Pro*₉) and **6** (*4R-Hyp*₉) increases smoothly with increase in concentration of urea, while it enhanced rapidly in case of peptide **7** (*4S-hyp*₉). The addition of salt slightly decreases the PPII helicity for peptides **5** (*Pro*₉) and **6** (*4R-Hyp*₉), while drastic decrease was seen in case of peptide **7** (*4S-hyp*₉).

The hydrophobic solvent like trifluoroethanol (TFE) affects the conformational properties of peptide and hence the effect of TFE on peptides (**5-9**) was investigated by CD spectroscopic study. Peptides **5** (*Pro*₉) and **6** (*4R-Hyp*₉) retained PPII conformation in trifluoroethanol. In this solvent, very interestingly β -structure formed in case of peptide **7** (*4S-hyp*₉) which transformed (Figure 2B) to PPII by addition of tiny amount of water. It is seen that the peptide **8** *4S*-(OAc)-*Pro*₉ failed to form β -structure in TFE unlike the hydroxyl peptide **7** *4S*-(OH)-*Pro*₉ and remains in PPII conformation even in TFE like peptide **6** *4R*-(OH)-*Pro*₉.

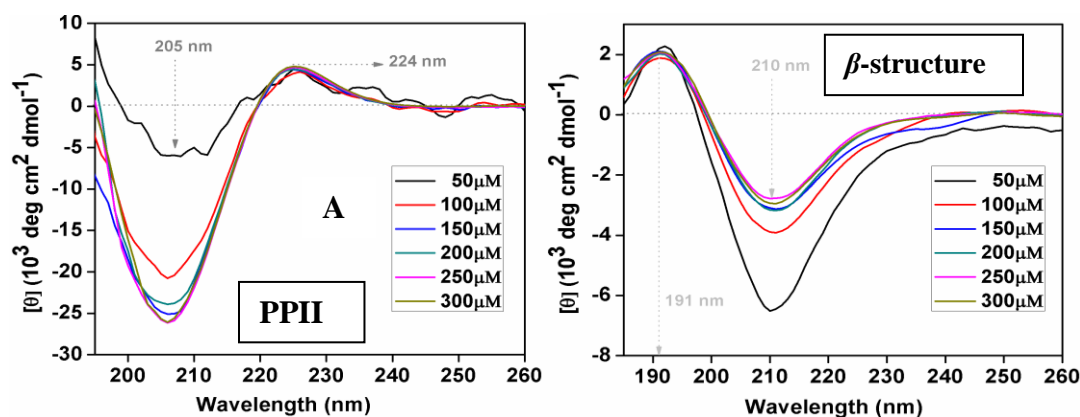


Figure 2. CD profiles of peptides **7** (*4S-hyp*₉) (A) in sodium-phosphate buffer (pH 7.2). (B) in TFE; All measurements done at concentration 50 to 300 μM .

The *cis* position of 4-OH (L) and 2-carboxyl can also be realized with *4R*-OH (D) but with D-proline and the peptide **9** (*4R-hyp*₉) is derived from *4R*-OH-D-proline (Figure 4). The D-prolyl peptide exhibited PPII form of opposite handedness compared to the natural right-handed PPII form in water (mirror image CD) (Figure 3A) and mirror β -structure in TFE (Figure 3B). Although the reversal of sign of CD bands is seen, the CD profile amplitudes are not exactly inverted (Figure 3B).

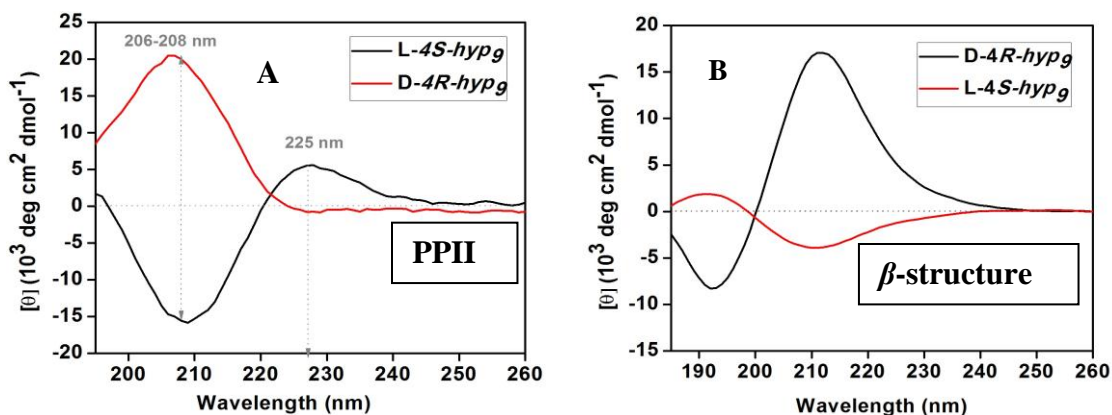


Figure 3. CD profiles of peptide **7** (*4S-L-hyp*₉, red) and **9** (*4R-D-hyp*₉, black) (A) Sodium-phosphate buffer (pH 7.2). (B) in TFE at concentration 100 μ M.

The presence of β -structure in TFE for peptide **7** (*4S-hyp*₉) was supported by Raman spectroscopy. The present results will add a new design principle to a growing repertoire of strategies for engineering peptide secondary structural motifs for new biomaterials. The structural conversion illustrates a fine balance between stereoelectronic and H-bonding effects in novel tuning of the secondary structure of *4R/S*-hydroxyproline polypeptides is discussed in this chapter.

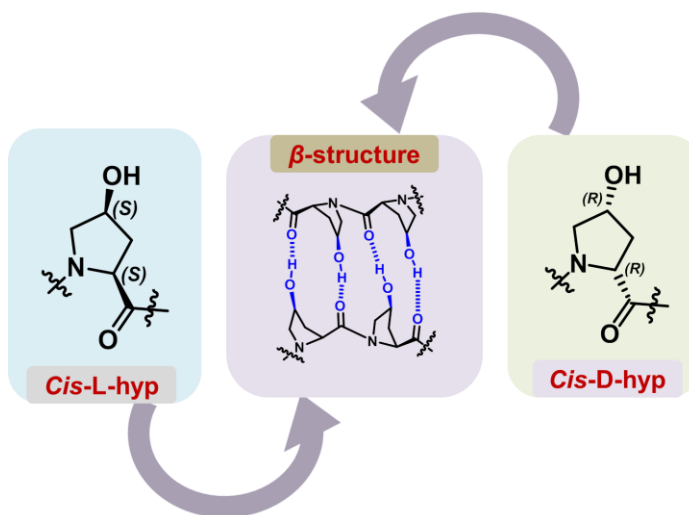


Figure 4. β -structure formed in case of peptide **7** (*4S-L-hyp*₉) and **9** (*4R-hyp*₉).

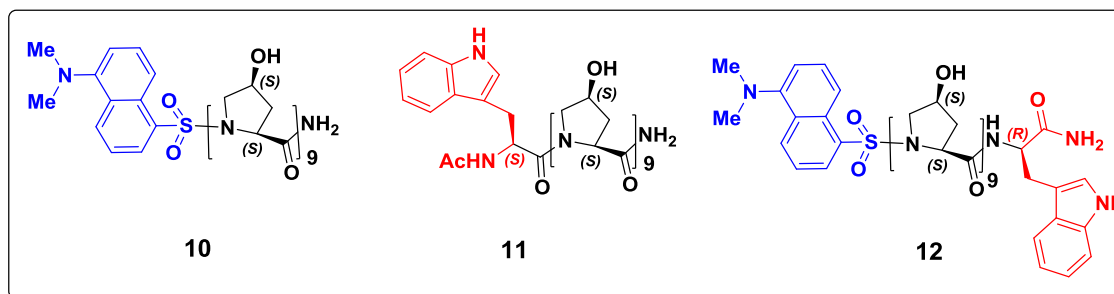
Chapter 4: Orientation of β -Structure: parallel or antiparallel?

This chapter is directed towards distinguishing the parallel/antiparallel orientation of possible β -structure in *4S*-hydroxy-L-proline and *4R*-hydroxy-D-proline

peptides in TFE by using polyhydroxyproline peptides modified with FRET probes, hydrophobic interaction of fatty acid chain which are attached at the N-terminal and FT-IR studies.

Section 1: Distinguishing the β -structure arrangements by FRET

For FRET studies, peptides **10-12** were synthesized to contain a tryptophan or dansyl at N-terminus in two different peptides and both in same peptides with tryptophan at C-terminus and dansyl at N-terminus. Tryptophan as donor and dansyl as acceptor are well known to serve as a FRET pairs to monitor biomolecular geometries.



CD spectroscopic studies suggest that the ability of the fluorescent peptides labeled at N-terminus **10** (4*S*-hyp₉-Ds), **11** (4*S*-hyp₉-Trp) and dual labeled **12** (Trp-4*S*-hyp₉-Ds) to form PPII in water and β -structure in TFE is not altered by FRET probe labeling at various concentrations.

In FRET experiments, concentration of either donor or acceptor peptide was kept constant and the second component peptide was added in 0.5 or 1.0 equivalent. Emission signal from acceptor (Dansyl) was recorded at the excitation frequency (287 nm) of donor (Tryptophan).

Increasing amounts of acceptor peptide **10** (4*S*-hyp₉-Ds) were added to the constant amount of donor peptide **11**(4*S*-hyp₉-Trp) and vice versa in separate experiments. Upon excitation of tryptophan at 287 nm, emission was observed only at tryptophan emission 351 nm. The non-observance of FRET signal after addition of peptide **10** (4*S*-hyp₉-Ds) and **11** (4*S*-hyp₉-Trp) can be attributed to an antiparallel orientation of two strands with the FRET components at opposite termini. After

addition of acceptor peptide **10** (*4S-hyp₉-Ds*) to **12** (*Trp-4S-hyp₉-Ds*), it is found that emission signal intensity at 549 nm corresponding to dansyl fluorescence increased upon excitation at Trp 287 nm. Importantly, the emission corresponding to donor tryptophan decreases which is due to transfer of fluorescence energy from tryptophan to excite dansyl followed by emission from dansyl at 541 nm (Figure 5). All these results can be explained only when peptide associates in an antiparallel orientation which was also well supported by FT-IR studies.

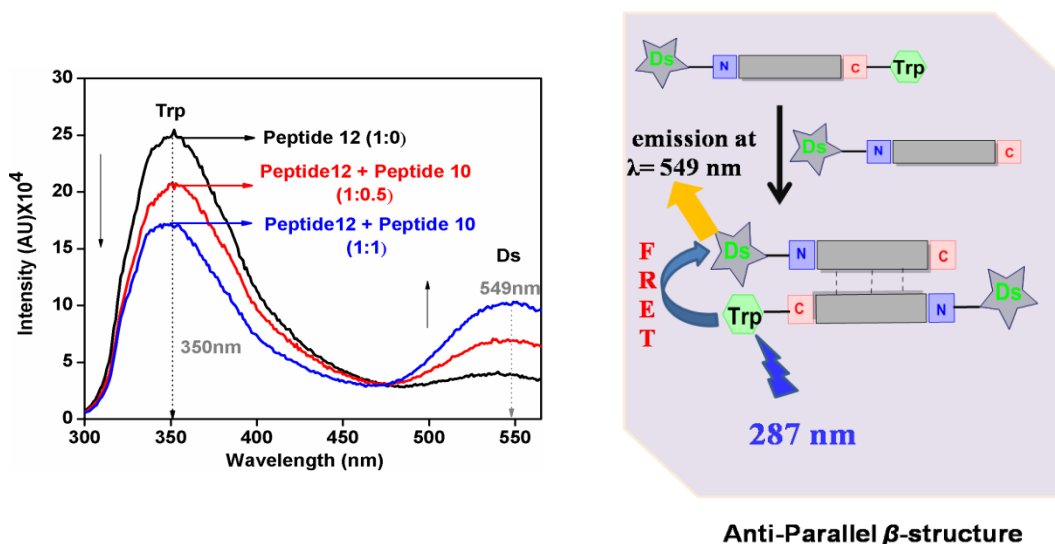
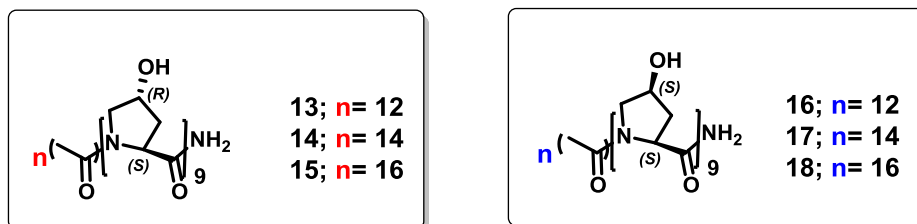


Figure 5. (A) Emission spectra of the modified peptide **12** (*Trp-4S-hyp₉-Ds*) before and after addition of **10** (*4S-hyp₉-Ds*); For FRET, donor excited at λ_{287} nm (donor emission monitored at $\lambda_{351\text{nm}}$ emission and acceptor emission $\lambda_{549\text{nm}}$), (B) Plausible orientation of peptides in β -structure.

Section 2. Morphology and polymorphism of self-assembling polyproline peptides conjugated with fatty acid chains

The peptides (**13-18**) were synthesized to monitor the relative orientation dependent morphology.



The antiparallel disposition of β -structure of 4*S*-peptides seen in TFE is further substantiated from morphological structures of nano-structure formed visualized through FESEM images of their fatty acid conjugates. The hydrophobic interactions among the chains are superimposed on the interchain hydrogen bonding in β -structure.

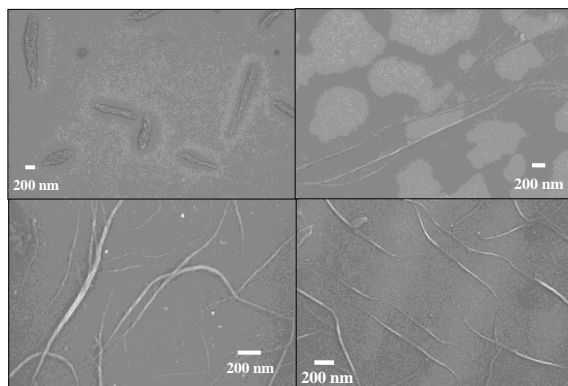


Figure 6. FESEM images for peptides (A) **7** (4*S*-hyp₉), (B) **16** (4*S*-hyp₉-C₁₂), (C) **17** (4*S*-hyp₉-C₁₄) and (D) **18** (4*S*-hyp₉-C₁₆) in TFE at 50 μ M.

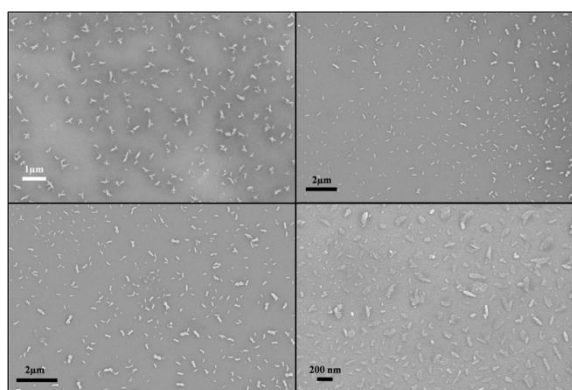


Figure 7. FESEM images for 4*R*-peptides (A) **6** 4*R*-Hyp₉, (B) **13** (4*R*-Hyp₉-C₁₂), (C) **14** 4*R*-Hyp₉-C₁₄ and (D) 4*R*-Hyp₉-C₁₆ in water at 300 μ M.

Only the 4*S*-peptides-lipid conjugates that show β -structure exhibit nanofiber structures (Figure 6) while those from 4*R*-peptides remains as rods (Figure 7). These nanostructures arise from an antiparallel arrangement in which fatty acid chains from opposite strands can hydrophobically interact leading to continuous extension of structures to form nanofibers. A parallel arrangement of strands will remain as non-extendible rods.

The 4*S*-NH₂/OH substitution on proline with *S*-stereochemistry leads to formation of β -structure in TFE, assembled by interchain hydrogen bonding. The extent of β -structure increases with chain lengths and critical at lengths of pentamer and hexamer. The *cis* position of 4-NH₂/OH and 2-carboxyl is important since β -structure observed in peptide derived from 4*S*-OH-L-proline, was also found in peptide composed of 4*R*-OH-D-proline.

β -Structure formed by 4*S*-peptides is a result of association of two polyproline strands through *interchain* H-bond and addition of fatty acid tail at the end of these peptides formed elongated fibers. The FRET experiment and formation of fiber exhibit the antiparallel orientation of two strands in β -structure.

References

1. (a) Flores-Ortega, A.; Casanovas, J.; Nussinov, R.; Alemán, C., Conformational Preferences of β - and γ -Aminated Proline Analogues. *J. Phys. Chem. B* **2008**, *112*, 14045-14055; (b) Flores-Ortega, A.; Casanovas, J.; Assfeld, X.; Alemán, C., Protonation of the Side Group in β - and γ -Aminated Proline Analogues: Effects on the Conformational Preferences. *J. Org. Chem.* **2009**, *74*, 3101-3108.
2. Sonar, M. V.; Ganesh, K. N., Water-Induced Switching of β -Structure to Polyproline II Conformation in the 4*S*-Aminoproline Polypeptide via H-Bond Rearrangement. *Org. Lett.* **2010**, *12*, 5390-5393.
3. Horng, J.-C.; Raines, R. T., Stereoelectronic effects on polyproline conformation. *Protein Sci. : Publ. Protein Soc.* **2006**, *15*, 74-83.
4. Kuemin, M.; Sonntag, L.-S.; Wennemers, H., Azidoproline containing helices: Stabilization of the polyproline II structure by a functionalizable group. *J. Am. Chem. Soc.* **2007**, *129*, 466-467.
5. Whittington, S. J.; Chellgren, B. W.; Hermann, V. M.; Creamer, T. P., Urea Promotes Polyproline II Helix Formation: Implications for Protein Denatured States. *Biochemistry* **2005**, *44*, 6269-6275.

Chapter-1

Introduction

1. Introduction

Nature is an excellent source of inspiration in the design of stimulus responsive materials. Proteins and peptides that encompass in nature forming variety of functional structures should be good as building blocks for design of materials. They have the ability to self-assemble into complex architectures, respond to environmental stimuli such as pH, temperature, solvent, presence of small molecules or enzymes, and oxidising/reducing environment. Unlike proteins that are highly fragile molecules, peptides are small, rigid units that have protein-mimicking properties. They are ideally suited due to the range of distinct physical properties thrust on them from the naturally occurring amino acids.¹

The basic properties of peptides are ultimately defined by their primary amino acid sequence. The different amino acid residues provide diversity via non-covalent interactions such as hydrophobic interactions, aromatic stacking, hydrogen bonding, disulfide bridges and electrostatic interactions. The individual interactions are weak, but as an ensemble they give rise to stable secondary structure and tertiary structure essential for function.²

1.1. Conformational analysis of polypeptides

Proteins are linear chains of amino acids that fold into precise three-dimensional shapes which are crucial to perform a wide range of the functions in cell, the sequence of their amino acid residues directing the folding to a particular native state conformation.³ Polypeptide conformations can be described in terms of three main chain torsion angles; (a) the torsion angle about C_{α} -N σ -bond (R- C_{α} -N-H) ϕ (*phi*), (b) the angle about the σ -bond between carbonyl group and C_{α} (R- C_{α} -C-O) ψ (*psi*), and (c) the angle about the amide bond (O-C-N-H) ω (Figure 1). The σ -bonds (except in the imino acid proline) are relatively flexible and the preferred values for ϕ and ψ angles depend primarily on the nature of the α -substituent. Allowed values for ϕ and ψ are graphically revealed in a Ramachandran when ϕ is plotted *versus* ψ .⁴ The torsional angles of each residue in a peptide define the geometry of its attachment to its two adjacent residues by positioning its planar peptide bond relative to the two adjacent planar peptide bonds. Thus torsion angles are among the most important local structural parameters that control protein folding.

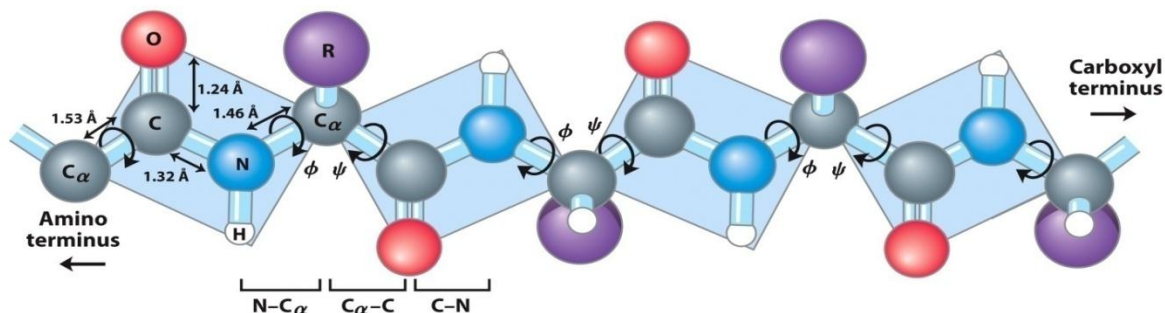


Figure 1. Illustration of peptide plane and the torsion angles.⁵

1.1.1 Ramachandran plot

The sterically allowed values of ϕ and ψ can be determined by calculating the distances between the atoms of a tripeptide at all values of ϕ and ψ for the central peptide unit. Sterically forbidden conformations, such as the one shown in Figure 2A, are those in which any nonbonding interatomic distance is less than its corresponding Van der Waals distance. Such calculations lead to Ramachandran plot⁴ (Figure 2B), which defines the energetically allowed secondary structures for all sets of combinations of ϕ and ψ angles.

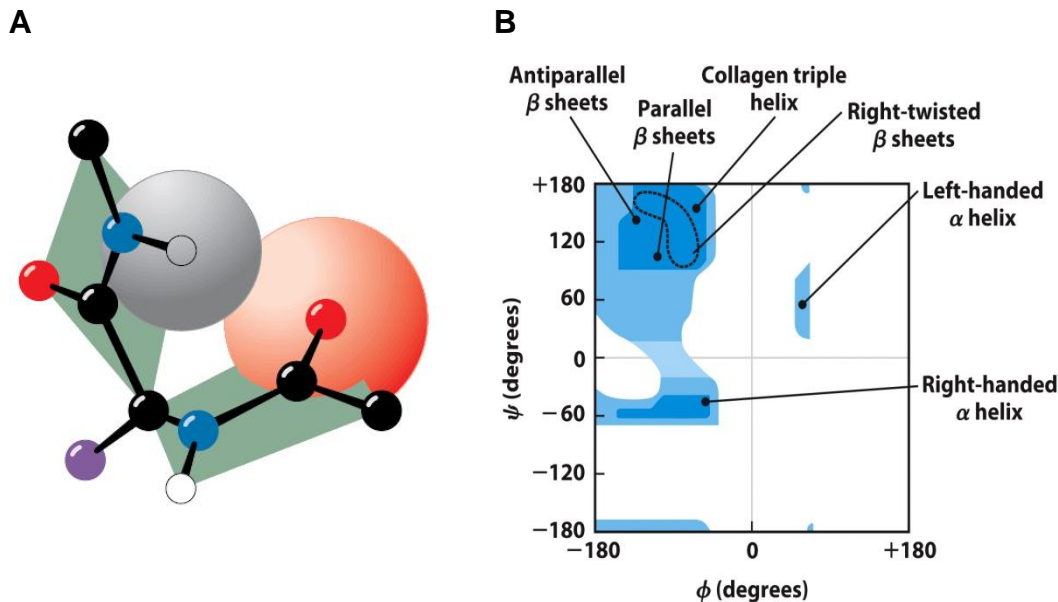


Figure 2. (A) Steric interference between adjacent residues, the collision between carbonyl oxygen and the following amide hydrogen prevents the conformation $\phi = -60^\circ$, $\psi = -30^\circ$, (B) Ramachandran plot for variety of peptide structures.⁶

Ramachandran observed that ϕ and ψ values of accurately determined structures fall within the allowed regions that ϕ - ψ plot. The contours indicate the extent of allowed (light blue) and most favored (dark blue) combinations of (ϕ , ψ). The black circles show the locations of the ideal phi, psi values for the most common regular secondary structural features, β -strands (in antiparallel and parallel sheets) and α -helices. Outside the contours, the corresponding conformations are disfavored or disallowed. There are, however, some notable exceptions:

- ❖ Glycine is less sterically hindered, allows high flexibility in the polypeptide chain as well as torsion angles and is often found in loop regions, where the polypeptide chain takes a sharp turn. This is also the reason for the high conservation of glycine residues in protein families, since the presence of turns at certain positions is a characteristic of a particular fold of protein structure.
- ❖ Proline is often found at the end of helices and functions as a helix disruptor. In contrast to glycine, proline fixes the torsion angles at values, which are very close to those of an extended conformation of the polypeptide (like in a β -sheet).

The three-dimensional geometry of a protein molecule thus optimized due to structural and conformational constraints is vital to its function. Four levels of structure are used to describe a protein. The short regions of proteins called as peptides and basic structures are determined by the primary amino acid sequence. The diversity provided by residues is based on the possible non-covalent interactions such as hydrophobic interactions, aromatic stacking, hydrogen bonding, disulfide bridges and electrostatic interactions. The most common secondary structures are α -helix and β -sheets, although other structures such as the 3_{10} helix, polyproline helix and the π -helix also exist. The nature of secondary structure formed indicated by the primary structure and different amino acids have different secondary structure propensities.²

1.2 Protein secondary structures: the α helix and the β -sheet

Secondary structures arise from intra chain interactions in a stretch of peptide and are mainly composed of α -helices, β -sheets, turns and rest associated with random coils. The various secondary structures are characterised by their specific geometric and derived biophysical properties .⁷

1.2.1 The α helix

α -Helix (Figure 3) is a common secondary structural element of protein and consists of right hand coiled or spiral conformation. An ideal α -helix has a pitch 0.54 nm, rise of 0.15 nm, and the number of amino acid residues for one complete turn is 3.6 (Figure 3). However, α -helices are slightly distorted in proteins with 3.5 to 3.7 amino acid residues per turn.

In an α -helix, carbonyl oxygen of i^{th} residue of polypeptide backbone is hydrogen-bonded to amide NH of the $i+4^{\text{th}}$ residue toward the C-terminus. Each hydrogen bond closes a loop containing 13 atoms (the carbonyl oxygen, 11 backbone atoms, and the amide hydrogen) and α -helix is also termed as 3.6_{13} helix. The hydrogen bonds stabilizing the helix are nearly parallel to the long axis of the helix.

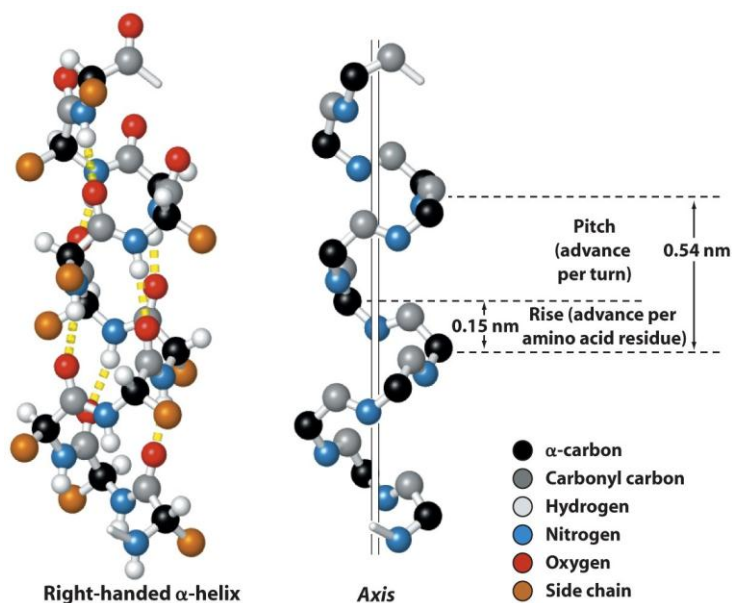
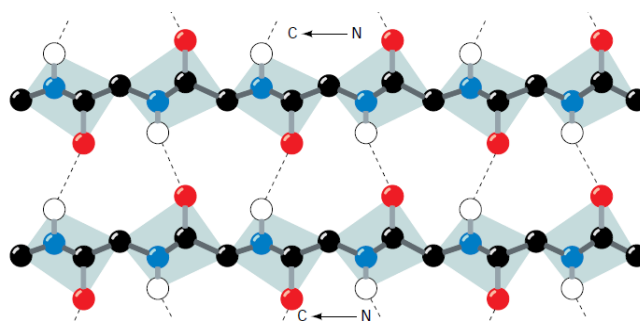


Figure 3. The α helix, dashed lines indicate hydrogen bonds between polypeptide strands.

1.2.2 The β -sheet

A β -sheet (Figure 4) is made up of individual strands of peptide chains held together by hydrogen bonding between the neighbouring chains (interstrand) rather than in the same chain as in an α -helix (intrastrand). The side chains project above or below the sheet, and well placed to interact with side chains of adjacent sheet. β -sheets are stabilized by (i) hydrogen bonds, (ii) their side chains interactions, (iii) favorable (ϕ , ψ) angles (in the β -region of the Ramachandran map), and (iv) van der Waals attractions.

A Parallel



B Antiparallel

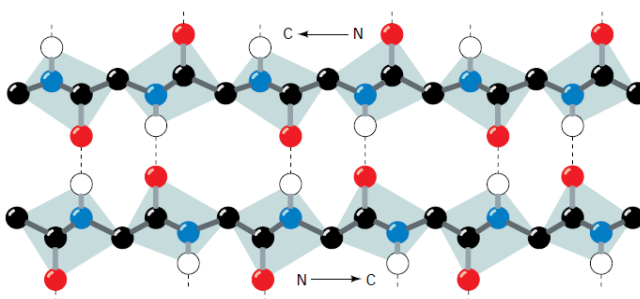


Figure 4. The β -sheets with dashed lines indicating hydrogen bonds between polypeptide strands, (A) an antiparallel β -sheet, (B) a parallel β -sheet.⁶

Depending upon relative orientations of adjacent chains, which can run in either same or opposite directions, β -sheets are categorised as two types

- The antiparallel β -sheet, in which the neighboring hydrogen-bonded polypeptide chains run in opposite directions (Figure 4A). (N→C; C→N)

- The parallel β -sheet, in which both the hydrogen-bonded chains extend in the same direction (Figure 4B). (N \rightarrow C; N \rightarrow C).

Successive side chains of polypeptides in a β -sheet extend in opposite sides of the sheet with a two-residue repeat distance of 7.0 Å.

1.3 Other Secondary Structures: 3_{10} helix, β -hairpin and turns

1.3.1 The 3_{10} -helix

The 3_{10} helix (Figure 5A) is a structural form present in globular proteins and differs from α -helix in hydrogen bonding pattern. The $-\text{C}=\text{O}\cdots\text{H}-\text{N}$ hydrogen bond occurs between residues i and $i+3$ with 10 atoms in rings of 3_{10} -helix (Figure 5B), while in α -helix hydrogen bonds occur between residues i and $i + 4$.

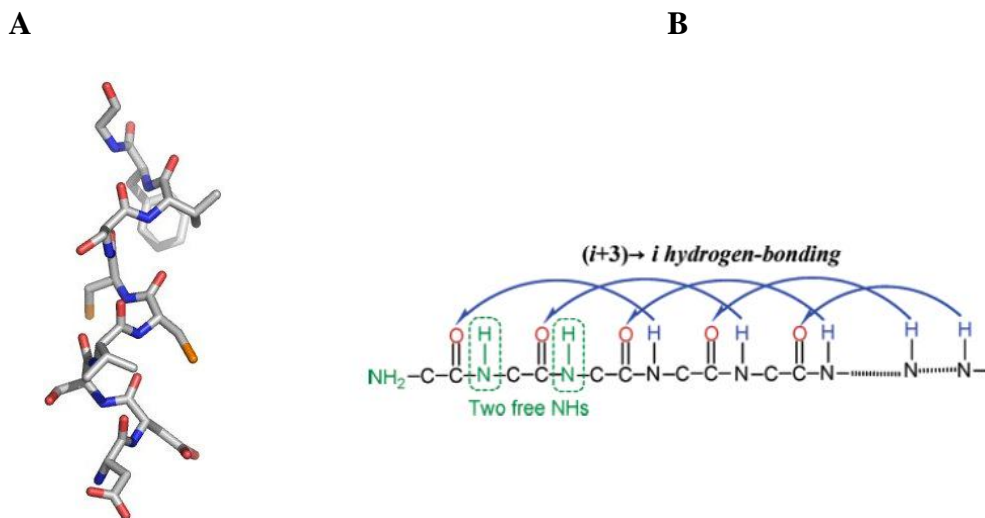


Figure 5. (A) A representative model of 3_{10} helix, (B) Intramolecular hydrogen-bonding pattern of a 3_{10} -helix.

The amino acids in a 3_{10} helix are arranged in a right-handed form with each amino acid taking a 120° turn on the helix axis corresponding to three residues per turn, and a translation of 2.0 Å along the helical axis. 3_{10} -helical conformation has been implicated as an intermediate in unfolding of α -helices to form extended conformation.

1.3.2 The β -hairpin

β -Hairpins (Figure 6) are widespread in globular protein structures and arise from a β -turn connecting two strands of an antiparallel β -sheet.⁹ Characteristic average values for the ϕ and ψ angles of β -strand residues in antiparallel β -sheets are -139° and $+135^\circ$, respectively. β -hairpins can occur in isolation or as part of a series of hydrogen bonded strands that collectively comprise a β -sheet/ β -barrel. β -Hairpin motifs adopt specific conformations, depending upon the number of residues in the turn and the number of interstrand hydrogen bonds between the residues flanking the turn.

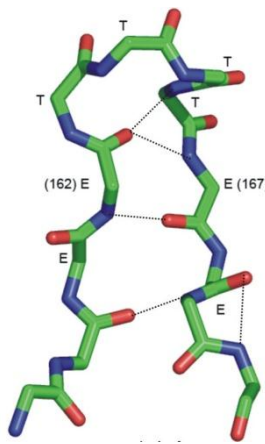


Figure 6. A representative model of β -hairpin.⁶

1.3.3 Turns

Depending upon the number of intervening atoms in a turn before the first H-bond is formed, the types of turns are identified. β -Turns have been identified based on criterion that the distance between $C^\alpha(i)$ and $C^\alpha(i+3)$ is less than 7 \AA and the chain is not in a helical conformation.¹⁰ In contrast to helices, the backbone dihedral angles are not constant for all the residues in the turn. Although the close proximity of the two terminal C^α atoms correlate with the formation of one or two hydrogen bonds between the corresponding residues, such hydrogen bonds are not strictly required in the definition of the turn.

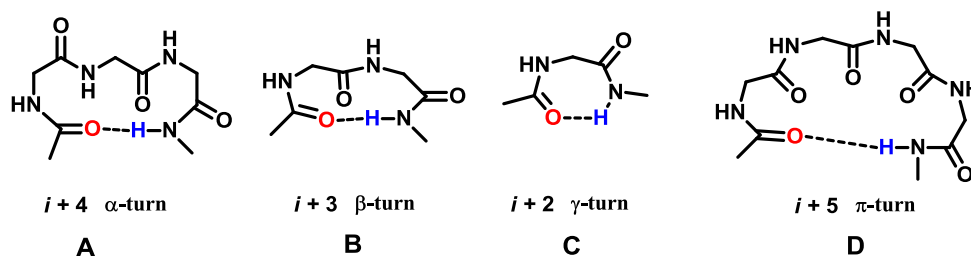


Figure 7. Representation of (A) α -turn, (B) β -turn, (C) γ -turn and (D) π turn.

In an α -turn, the end residues are separated by four peptide bonds ($i \rightarrow i \pm 4$) (Figure 7A); in a β -turn (the most common form), by three bonds ($i \rightarrow i \pm 3$) (Figure 7B), in a γ -turn, by two bonds ($i \rightarrow i \pm 2$) (Figure 7C), in a δ -turn, by one bond ($i \rightarrow i \pm 1$) (Figure 7D) and in a π -turn, by five bonds ($i \rightarrow i \pm 5$) (Figure 7E).

1.4. Polyproline conformation

Apart from the above regular secondary structures and turns, another important characterized secondary structure is the Polyproline II (PPII) helix which is present in both folded and unfolded proteins. Proline is the only naturally occurring imino acid in proteins and plays unique structural and role in guiding protein folding, fiber formation and protein-protein interactions.¹¹

1.4.1 Peptidyl prolyl *cis-trans* isomerisation

Cis-trans isomerization of the peptide bond plays an important role in many protein-folding pathways.¹² Proline being imino acid forms tertiary amide bonds in proteins and can exist in distinct *cis* and *trans* peptide bond conformations. It is estimated that 5-7% of the proteins possess peptidyl-prolyl bonds and switch to a *cis* conformation during normal physiological processes, leading to their proper folding, assembly or transport. The *cis-trans* isomerization is a relatively slow process and serves as a rate-limiting step of protein folding. However, this process is significantly accelerated by peptidyl-prolyl *cis-trans* isomerases (PPIases) that catalyze protein folding by *cis-trans* conversion of peptide bonds preceding the amino acid proline.¹³

1.5 Polyproline conformations

Polyproline helix in proteins comprises of repeating proline residues displaying a specific type of protein secondary structure. The poly-L-proline II (PPII) helix is an important structural class not only of fibrillar proteins like collagen, but also of the folded and unfolded proteins. Apart from the structure, PPII conformation plays an important role in a wide variety of biologically important protein-protein and protein-nucleic acid interactions and a major role in signal transduction and protein complex assembly. This structure is often found in numerous binding sites, specifically those of widely spread SH3 domains. PPII helices are also present in functional proteins involved in transcription, cell motility, self-assembly, elasticity, and bacterial and viral pathogenesis.

Two types of poly-(L-Pro)_n helices are known, termed as polyproline I (PPI) and polyproline II (PPII). The most interesting aspect of PPI and PPII conformation is that, being tertiary amides, thus lack N-H bond to form any interchain or intrachain H-bonds to stabilize helical structures. PPI helix has all backbone tertiary amide bonds in the *cis* ($\omega_0 = 0^\circ$) disposition, while in PPII, these bonds are all *trans* ($\omega_0 = 180^\circ$). The right handed PPI helix is thus compact with all amide bonds in the *cis* conformation, while the PPII helix is a fully extended left-handed structure with all amide bonds in the *trans* conformation.

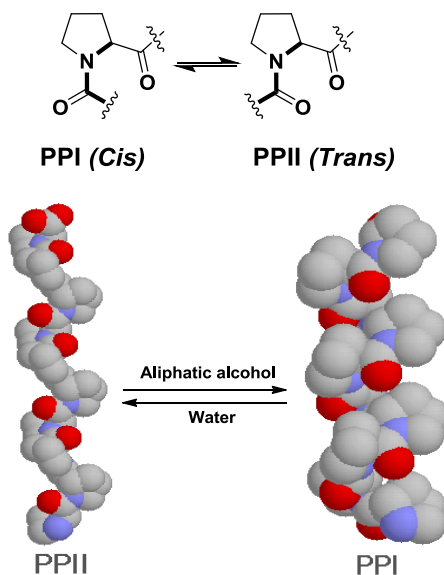


Figure 8. Solvent induced switching between PPII \leftrightarrow PPI conformations.

Polyprolines adopt PPII conformation in water and PPI conformation in hydrophobic solvents (Figure 8). Table 1 summarizes the structural parameters of PPI and PPII forms and Figure 9 gives the conformational models of the two structure.

Table 1. Shows a comparison between PPII and PPI conformations in peptides

Parameter	PPII conformation	PPI conformation
Direction of helix	Left handed	Right handed
Amide bond conformation	<i>Trans</i>	<i>Cis</i>
Nature of helix	Fully extended	More compact
Dihedral angles	$\omega=180^\circ$, $\phi = -75^\circ$, $\psi = +145^\circ$	$\omega=0^\circ$, $\phi = -75^\circ$, $\psi = +160^\circ$
Helical pitch	9.4 Å per turn, 3.3 proline residues per turn	5.6 Å per turn, 3.3 proline residues per turn
Orientation of amide bond in peptide backbone	Nearly perpendicular to the helix axis	Nearly parallel to the helix axis
Preferred solvent	Water	Aliphatic alcohols

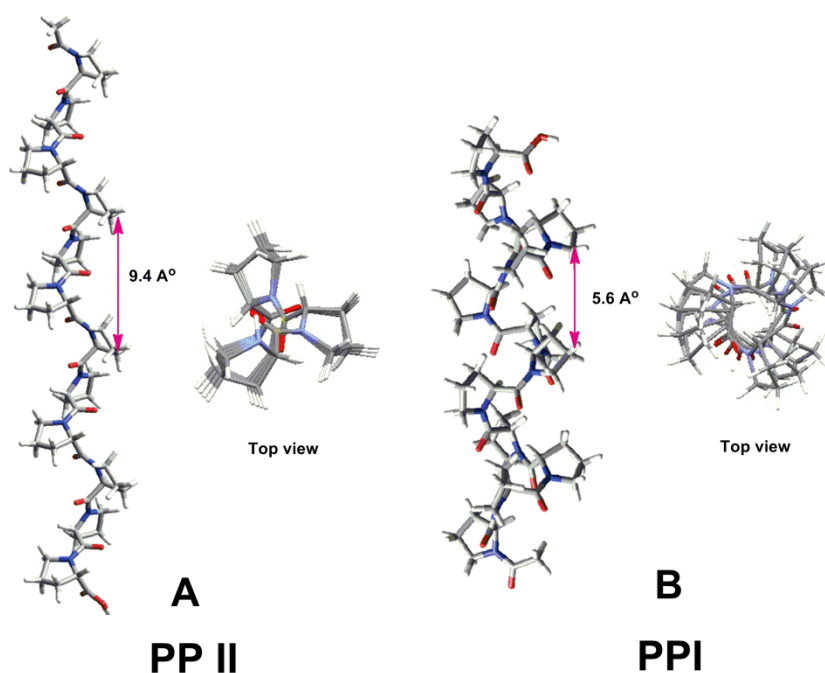


Figure 9. (A) Model structure of polyproline II (PPII) conformation along with top view. (B) Model structure of polyproline I (PPI) conformation along with top view.

1.5.1 Stability of polyproline conformation

Absence of local hydrogen bonds involving main chain atoms is one of the distinctive structural properties of PPII helices, compared to the other common secondary structure elements found in protein. This structural feature leaves several unsatisfied hydrogen bond acceptors free to establish *intra* or *inter*-molecular interactions. Due to the absence of specific hydrogen bonding patterns, formation of long PPII *helices* is rather unusual in globular proteins. It has been proposed that the backbone conformations of unfolded proteins often include short stretches of PPII structural motifs interspersed with turns and bends.¹⁴

In addition to the entropic effects favoring the formation of PPII structures by imino acids, the $n \rightarrow \pi^*$ electronic interaction between lone pair (n) on one carbonyl (O_i) and the empty, electrophilic π^* orbital on the subsequent carbonyl (C_{i+1}) atom provides stabilization to the left-handed PPII.¹⁵ Different studies also suggested the importance of coordinating water molecules for the stability of the PPII helix.¹⁶ In the absence of coordinating water molecules, a PPII helix with all *cis*-amide bonds predicted to be most stable.¹⁷

1.5.2 A Crystal Structure of an Oligoproline PPII-Helix

Recently, Wennemers et al.¹⁸ reported crystal structure of hexaproline crystallized by vapor diffusion using acetonitrile as solvent and tetrahydropyran as cosolvent (Figure 10). Analysis of the dihedral angles showed correlation between ϕ and ψ angles and the ring pucker. If ϕ and ψ are close to -65° and $+140^\circ$, more pronounced the C^γ -*exo* ring pucker was observed. Conversely, ϕ and ψ angles around -73° and $+155^\circ$, respectively, are realized in the C^γ -*endo* puckers.

Crystal structure suggested the importance of coordinating water molecules for the stability of the PPII helix, but hydration is not a prerequisite for PPII helicity. Crystallographic data showed that the amide bonds within the oligoproline helix interact with each other and the degree of interaction is largest in the C^γ -*exo* ring puckered residues indicating $n \rightarrow \pi^*$ interactions are favored by C^γ -*exo* and disfavored by C^γ -*endo* puckering.

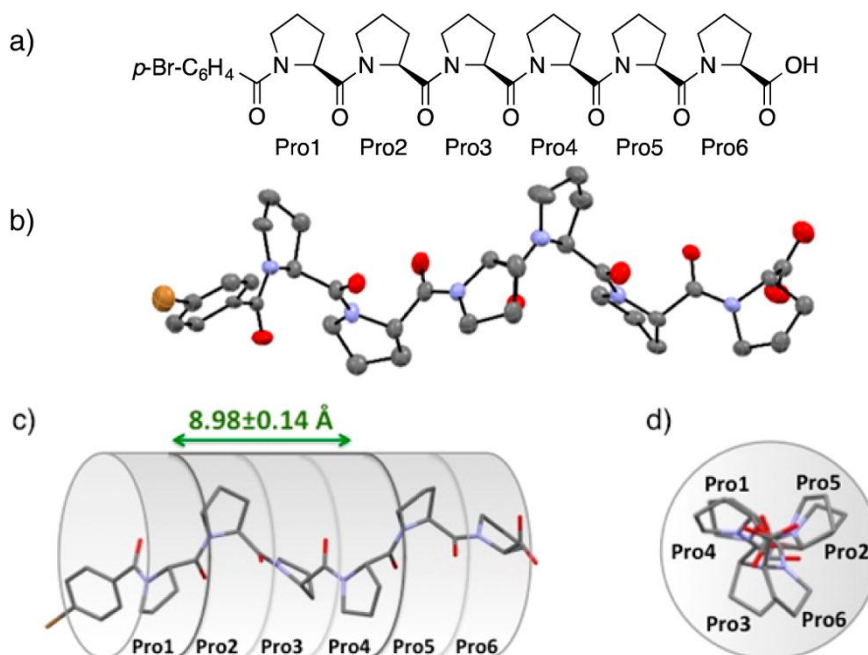


Figure 10. (a) Hexaproline $p\text{-Br-C}_6\text{H}_4\text{-Pro}_6\text{-OH}$ (b) Crystal structure of hexaproline (c) segmental side view (d) View along the axis¹⁸

1.5.3 A survey of left-handed polyproline II helices

Adzhubei and Sternberg¹⁹ in their first systematic search, found 96 PPII helices in a protein databank of 80 proteins. They are composed of not only proline successions but also without proline, e.g. short stretches of polyglutamines adopt PPII conformation. Stapley and Creamer²⁰ presented a survey of 274 non-homologous polypeptide chains from proteins of known structure for regions that form PPII structures. Although such regions are rare, majority of proteins contain at least one PPII helix. Most PPII helices are shorter than five residues, the longest one containing 12 amino acids. Proline predominates in PPII helices, but glutamine and positively charged residues are also favoured. The basis of glutamine prevalence is its ability to form an i to $i+1$ side-chain to main-chain hydrogen bond with the backbone carbonyl oxygen of the preceding residue; this helps to fix the ψ angle of the glutamine and the ϕ and ψ of the preceding residue in PPII conformations and explains why glutamine is favoured at the first position in a PPII helix.

1.5.4 Conformational preference and *cis-trans* isomerization of 4(*R/S*)-substituted proline peptides

Song and Kang²¹ reported the conformational preference and prolyl *cis-trans* isomerization of 4(*R/S*)-substituted proline dipeptides, *N*-acetyl-*N'*-methylamides of 4(*R/S*)-hydroxy-L-proline and 4(*R/S*)-fluoro-L-proline (Ac-Hyp-NHMe and Ac-Flp-NHMe, respectively), using quantum calculations. It was found that the 4*R*-substitution by electron-withdrawing groups did not result in significant changes in backbone torsion angles as well as endocyclic torsion angles of the prolyl ring. However, small changes in backbone torsion angles ϕ and ψ and the decrease in bond lengths $r(C^\beta-C^\gamma)$ or $r(C^\beta-C^\gamma)$ appear to enhance the relative stability of the *trans* *exo*-puckered conformation. The population of *trans* *exo*-puckered conformation increased in the order Ac-Pro-NHMe < Ac-Hyp-NHMe < Ac-Flp-NHMe in chloroform and water.²² This increase in population for *trans* *exo*-puckered (Figure 11) conformation in solution is attributed to favoured steric and stereoelectronic factors in polyproline-II like conformation with *exo* puckering.

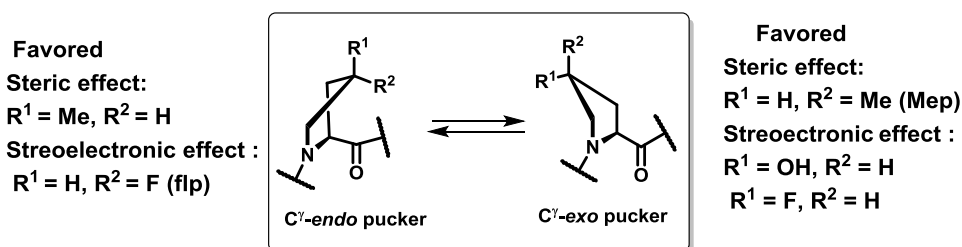


Figure 11. Ring conformations of 4-substituted proline residues.²²

For 4*S*-substitution by electron-withdrawing groups, opposite effect is obtained. The population of *cis* *endo*-puckered conformations increased in the order Ac-Pro-NHMe < Ac-Hyp-NHMe < Ac-Flp-NHMe in aliphatic alcohols. This increase in population for *cis* *endo*-puckered conformations in solution is attributed to an increase in population for the polyproline-I like conformations with *endo* puckering.

1.5.5 Conformational preferences of β - and γ -aminated proline analogues

Aleman and co-worker²³ investigated theoretically, the effect of incorporation of an amino group at the $C^\beta(3)$ - or $C^\gamma(4)$ -positions of the pyrrolidine ring. This affects the

intrinsic conformational properties of the proline. Specifically, a conformational study of the *N*-acetyl-*N'*-methanamide derivatives of four isomers of aminoproline, which differ not only in the β - or γ -position of the substituent but also in its *cis* or *trans* relative disposition, has been studied. A seven membered intramolecular hydrogen bond is possible between 4*S* amino group and carbonyl oxygen. The formation of this intra-residue hydrogen bond (Figure 12) explains the higher stability of the *Ac*- γ -*cis*Amp-NHMe and *Ac*- β -*cis*-Amp-NHMe dipeptides, compared to that of the corresponding analogues with *trans* amino group.

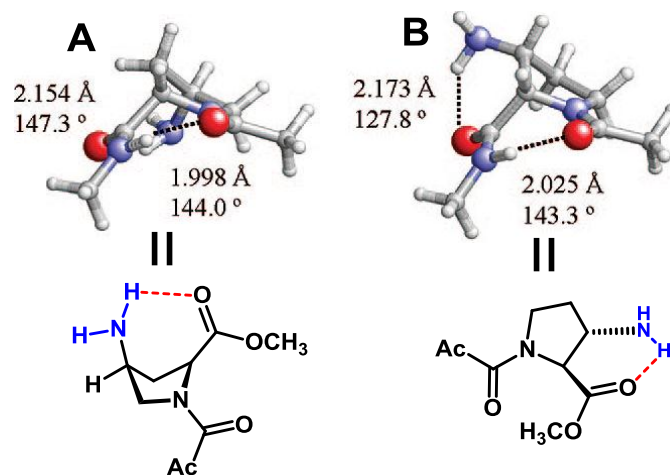


Figure 12. Representation of minimum energy conformations characterized in the gas phase for the Amp-containing dipeptides studied (A) *Ac*- γ -*cis*Amp-NHMe (B) *Ac*- β -*cis*Amp-NHMe.

The conformational properties may be altered by protonation of amino group to a charged ammonium group. This equilibrium in aqueous solution can be used to control the conformation of the 4*R/S*-aminoproline derivatives by altering pH. The conformational preferences of the protonated 4*R/S*-aminoproline derivatives indicated that protonation reduces the backbone conformational flexibility and destabilizes.²⁴

1.6 Factors Affecting Polyproline Conformation

1.6.1 *Cis/trans* peptide bond

Proline has two key conformational equilibria: *endo* versus *exo* ring pucker,²⁵ and *trans* versus *cis* amide bond²⁶ (Figure 13). The analysis of protein structures have indicated

that there is a correlation between proline puckering and the *cis/trans* peptide bond conformation.²⁷

Trans versus *cis* amide bond conformation defines the ω torsion angle (Figure 13A) and proline ring pucker correlates with protein ϕ and ψ main-chain conformation (Figure 13B). *Exo* ring pucker favors more compact conformations (PPII) and an *endo* ring pucker more extended conformations. The *exo* ring pucker stabilizes the *trans* amide bond, whereas an *endo* ring pucker is strongly favored in a *cis* amide bond. Thus, control of proline ring pucker permits control of all protein backbone torsion angles.²⁶

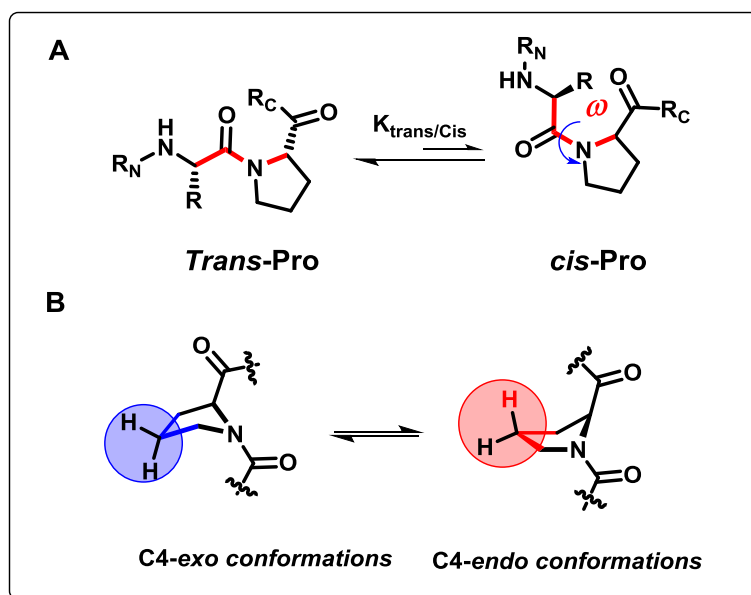


Figure 13. A) *Cis-trans* isomerism of prolyl amide bond B) *Exo* and *endo* ring pucker of proline.²⁸

1.6.2 $n \rightarrow \pi^*$ interaction

Stereoelectronic effect (Figure 14) is the relationship between structure, conformation and reactivity resulting from the alignment of filled or unfilled electronic orbitals. Raines and co-workers^{29,15g} suggested that the backbone $n \rightarrow \pi^*$ interaction could play a key factor in stabilizing the PPII helices by enhancing stereoelectronic effects that favour the *trans* prolyl peptide bond and increase the folding stability of the triple-helical collagen structure comprised of PPII helices.

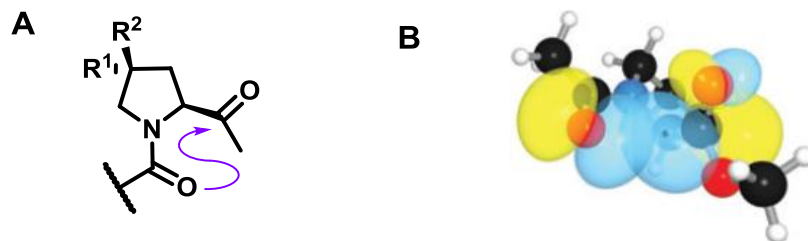


Figure 14. A) An $n \rightarrow \pi^*$ interaction stabilizes the *trans* isomer of the peptide bond but is substantial only when Pro derivatives are in the C^γ -*exo* ring pucker (e.g., $R^1 = \text{OH}$ or F , $R^2 = \text{H}$), B) Depiction of overlap between n and π^* natural bond orbitals in a Pro residue with C^γ -*exo* pucker.

In studies using short polyproline peptides, it has been shown that the stereoelectronic effects have a significant impact on polyproline conformation.²⁹ The substitution of proline by 4*R*-hydroxyproline (Hyp) or 4*R*-Fluoroproline (Flp) was found to enhance the backbone $n \rightarrow \pi^*$ interaction and stabilize PPII conformation by inhibiting the conversion of PPII to PPI. On the other hand, the 4*S*-fluoroproline (flp) substitution favoured conversion of PPII to PPI and destabilized PPII conformation due to steric effects. An electron-withdrawing substituent in the 4*R* position constrains the ϕ and ψ dihedral angles to be close to that in a PPII helix and favors its requisite *trans* peptide bond by enhancing the $n \rightarrow \pi^*$ interaction between O_{i-1} and C_i .^{29b} An electron-withdrawing substituent in the 4*S* position obviates the $n \rightarrow \pi^*$ interaction and thereby alters the relative free energy in favour of the PPI helix.

Recently, Horng and co-workers³⁰ used host-guest peptides to demonstrate that an electron-withdrawing substituent in the 4*R* or 4*S* position has a substantial impact on the kinetics of PPII \rightarrow PPI conversion. The kinetic consequences from stereoelectronic effects lead to difference in the stability of PPII helices. Accordingly, stereoelectronic effects provide a rational means to modulate polyproline conformation.

1.6.3 Gauche effect

Complex balance of noncovalent interactions (e.g., ionic interactions, H-bonding), steric hindrance, and stereoelectronic effects determine the conformations of flexible molecules. In the absence these effects, comparatively weak stereoelectronic effects, like “gauche effect”, can have a large influence on the conformation of molecules. This effect

describes the hyperconjugative electron donation of the bonding orbital (σ) into the antibonding orbital (σ^*), consequently placing the best σ -donor bond *anti* to the best σ -acceptor bond³¹ (Figure 16C, 16D), with preference of *gauche* conformer over the corresponding *anti* conformer.

In proline, it has been demonstrated that electron-withdrawing groups in the 4-position inductively withdraw electron density from the peptide bond and reduce the bond order of the C-N linkage, which facilitates the interconversion of the *cis* and *trans* species to favor the form with lower energy. In the case of 4*R*-substitution, *trans*-disposition of electron withdrawing group (EWG) with respect to α -carbonyl, leads to a strong preference for a *C γ -exo* puckering of the pyrrolidine ring (Figure 15A) due to *gauche* effect (Figure 16D).

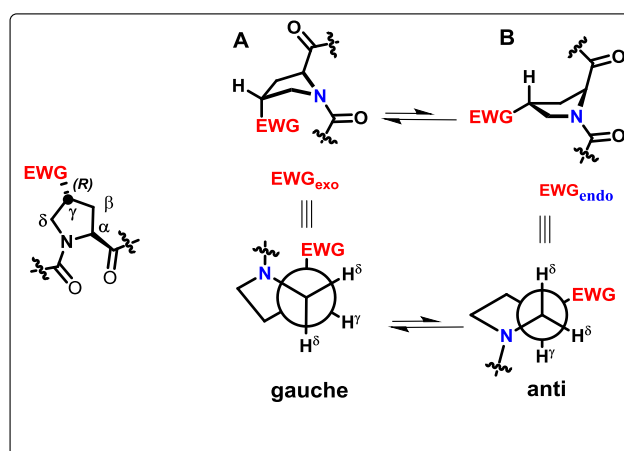


Figure 15. A) Stereoelectronic effect in 4*R*-substituted proline favors of $C\gamma$ - $C\delta$ -bond *gauche* between the amine and electron withdrawing (EWG), B) unfavored *anti* conformation.²⁸

Gauche conformation with 4*S*-substitution leads to a strong preference for *C γ -endo* ring puckering of the pyrrolidine ring due to relative hyperconjugative interactions (Figure 16A and Figure 16E).^{31f}

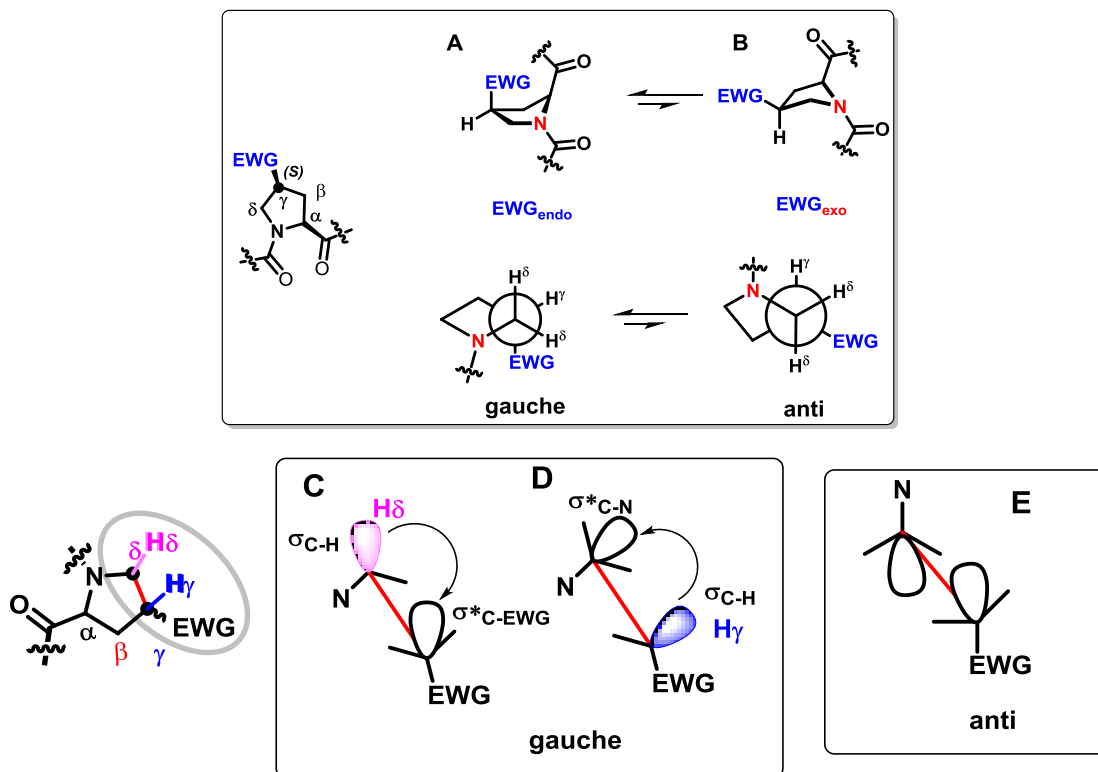


Figure 16. (A) Stereoelectronic effect in 4S-substituted proline favors C γ -C δ -bond gauche between the amine and electron withdrawing (EWG) (B) anti conformation, (C) two hyperconjugative interactions stabilize the gauche conformation by orbital overlap between bonding (C-H δ) and antibonding orbitals (EWG) and (D) orbital overlap bonding (C-H γ) and antibonding (N1). (E) When N and EWG are anti neither stabilizing interaction is possible.²⁸

The *exo* or *endo* preference thus depends on both the stereochemistry of the substitution and the electron-withdrawing nature of the substituent. For sterically demanding and non-electron-withdrawing substituents, the reverse preferences will be observed due to a steric preference for *anti* over gauche conformation (Figure 16E).

1.6.4 Azidoproline as conformational directing element and functionalizable site

Wennemers and co-workers³² demonstrated that 4(*R/S*)-azidoproline can be used both as conformation directing element of the PPII structure and as a functionalizable site for the development of proline-based molecular scaffolds. The conformational analyses in Ac[(4*R*)-Azp]₉OH and Ac[(4*S*)-azp]₉OH demonstrate that the PPII helix is stabilized by (4*R*)-Azp and destabilized by (4*S*)-azp, whereas the PPI helix has opposite behavior and is

stabilized by (4*S*)-azp and destabilized by (4*R*)-Azp. The stabilizing effect of (4*R*)-Azp is due to an enhancement of the $n \rightarrow \pi^*$ interactions which have been proposed to stabilize the PPII conformation.

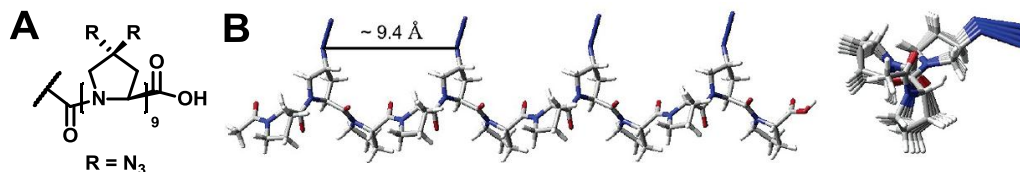


Figure 17. (A) 4(*R/S*)-azidoproline oligomer, (B) Model of an oligoproline PPII-helix with Azp residues in every third position.

The 4*R/S*-azido groups provide site for further functionalization which can be done by “click chemistry” leading to Azp containing polyprolines as attractive molecular scaffolds.

1.6.5 Effect of *O*-Galactosylation of 4*R*-Hydroxyproline on PPII conformation

The hydroxyproline-rich glycoproteins (HRGPs) are the major structural proteins of the extracellular matrix of algae and land plants. They are characterized by a rigid PPII conformation and extensive *O*-glycosylation of 4*R*-hydroxy-L-proline (Hyp) residues, which is a unique post-translational modification of proteins. Schweizer and co-workers³³ investigated the effects of naturally occurring β -*O*-galactosylation of Hyp in a series of well-defined model peptides Ac-(Pro)₉-NH₂, Ac-(Hyp)₉-NH₂ and Ac-[Hyp(β -D-galactose)]₉-NH₂ (Figure 18A). They demonstrated that contiguous *O*-glycosylation of Hyp residues causes a dramatic increase in the thermal stability of the PPII helix according to analysis of thermal melting curves. Molecular modeling indicates that the increase in conformational stability may be due to a regular network of inter-glycan and glycan-peptide hydrogen bonds (Figure 18B), in which the carbohydrate residues form a hydrophilic “overcoat” of the PPII helix.

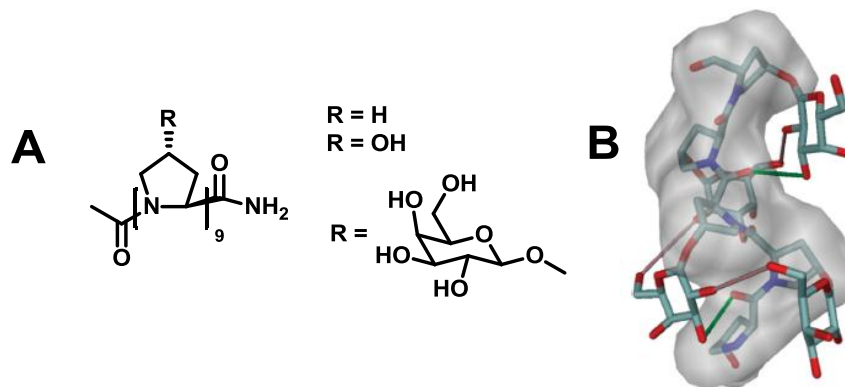


Figure 18. (A) Model polyproline peptides. (B) Molecular modeling of truncated of *O*-Galactosylation peptides shows the surface area of the PPII backbone (shaded) with the D-galactose residues lying in the grooves of the PPII helix. Also shown are inter-glycan H-bonds ($C6(OH)_i \cdots (OH)C2_{i+1}$) (pink) and glycan-peptide carbonyl backbone H-bonds ($C3-(OH)_i \cdots OC_{i-2}$) (green).³³

1.6.6 Effects of terminal functional groups on the stability of the PPII structure

The conformational stability of the PPII helix with respect to the functional groups at the C- and N-terminus has been examined both experimentally and theoretically.³⁴ The oligoprolines (a) AcN-[Pro]₁₂-CONH₂ (b) H-[Pro]₁₂-CONH₂ (c) AcN-[Pro]₁₂-CO₂H and (d) H-[Pro]₁₂-CO₂H with charged and capped termini served as model compounds shown (Figure 19).

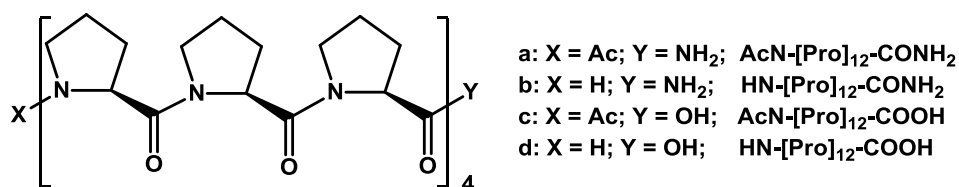


Figure 19. Oligoprolines a-d with different functional groups at the C- and N-terminal.

The conversion of PPII to the PPI was studied by the CD spectroscopy which show that a positively charged N-terminus and a negatively charged C-terminus destabilize the PPII helix and favour the PPI helix, while the capped termini favour the PPII over the PPI helix. These findings are supported by the energy differences computed by *ab initio* methods between the PPII and PPI helices of oligoprolines (Figure 19, a-d).

1.6.7 Control of polyproline helix (PPII) structure via aromatic electronic effects

Aromatic amino acids play distinct structural and functional roles, because of the combination of hydrophobicity and unique interactions through negatively charged aromatic faces and the positively charged aromatic edges (Figure 20).³⁵ Aromatic residues exhibit special interactions with proline residues, which promote *cis* amide bonds through local aromatic-proline interactions. In aromatic-proline sequences, the populations of *cis* amide bonds are dominant due to C–H/ π interaction (Figure 20). These interactions occur between the partial positively charged hydrogen (i.e., H α or H δ , adjacent to the electron-withdrawing amide carbonyl or amide nitrogen) of a polarized proline C–H bond and negatively charged face of the aromatic ring to stabilize the *cis* amide bond, in a manner comparable to a classical cation- π interaction.³⁶

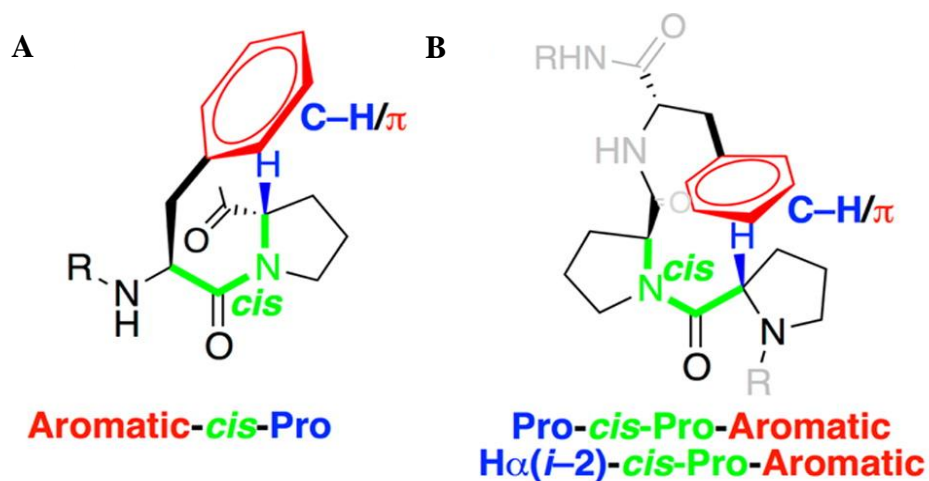


Figure 20. Aromatic-proline interactions that favor *cis* amide bonds in proline-rich sequences. (A) Aromatic-*cis*-proline interaction. (B) H α -*cis*-proline–aromatic interaction. H α (*i*-2)-*cis*-proline-aromatic interactions.

Zondlo *et al.*³⁷ demonstrated the ability of aromatic electronic effects to tune *cis-trans* isomerism in polyproline helix conformation. Electron-rich aromatic residues strongly disfavor polyproline helix and exhibit large population of *cis* amide bonds, while electron-poor aromatic residues exhibit less population of *cis* amide bonds and favor polyproline helix. Electron-poor aromatic amino acids provide special capabilities to integrate aromatic residues into polyproline helices and to serve as the basis of aromatic electronic switches to change structure.

1.6.8 Effect of urea on polyproline II conformation

It is commonly assumed that urea denatures proteins by promoting backbone disorder, resulting in a random-coil behavior. Creamer *et.al*³⁸. demonstrated that even denatured states possess significant amounts of locally ordered backbone structure and that urea promotes polyproline II helix formation in oligomers of proline, alanine, valine and some proteins.³⁹

The mechanism by which urea promotes polyproline II helical structure is not clear. Nozaki and Tanford⁴⁰ and Robinson and Jencks⁴¹ (Figure 21) proposed that urea interacts favourably with the polypeptide backbone influencing the conformation to favour the PPII helical form. This effect is modulated by the nature of the side chains, leading to the observed sequence dependence. Tiffany and Krimm⁴² suggested that urea and guanidine hydrochloride interact with proteins through hydrogen bonding to the backbone carbonyl group.

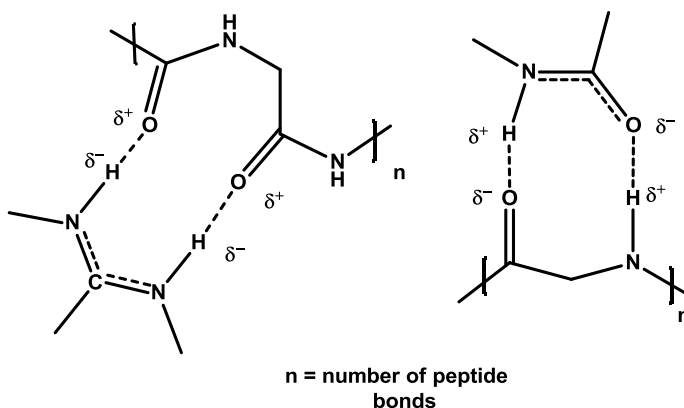


Figure 21. Mechanism of rigidification by urea

1.6.9 Effect of salt on polyproline structure

Mattice and Mandelkern⁴³ found that the PPII helical content of proline oligomers or peptides decreased with increasing salt concentration. PPII helical structures are disrupted by addition of sodium chloride in case of proline and polylysine oligomers.⁴⁴ It has also been demonstrated that neutralization of side chain charges in polylysine at higher pH induces α -helix formation, suggesting the important role of electrostatic interaction in stabilizing the PPII helices.⁴⁵ This may occur by increase in the rotational freedom about

the -C=O and C^α in poly-L-proline,⁴⁶ and about the $\text{C=O}\cdots\text{NH}$ bond,^{47,46b} and the barrier to *cis-trans* isomerization in polyproline due in part to electrostatic interactions.⁴⁸ This reduces the energy difference between the *cis* and *trans* isomers of planar peptide bond.⁴⁹ It has been suggested that there may be direct binding of the salt to the peptide group.⁵⁰ The decrease in PPII structure was recently proposed as a result of chaotropic action of concentrated salt. The existence of metal ion effect on amide groups in the presence of water was proposed by Jencks and co-workers⁴¹ (Figure 22).

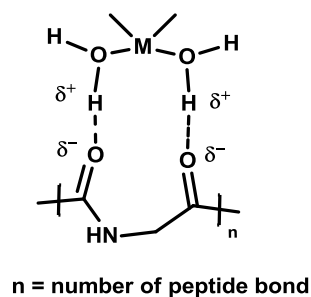


Figure 22. Mechanism of salt binding to peptide backbone.

1.6.10 Effect of aliphatic alcohols on polyproline conformation

Solvents play an important role in isomerization of tertiary amides inducing a conformational change through the *cis-trans* isomerism about X-Pro peptide bonds, where X is any amino acid residue. All amide bonds in proteins and peptides prefer to exist predominantly in the *trans* conformation in water, while about 25% of X-Pro groups adopt *cis* conformation in water⁵¹ but intramolecularly hydrogen-bonded *trans* conformer becomes less populated as solvent polarity increases.⁵² It is well-known that polyprolines adopt PPII conformation in water and PPI conformation in hydrophobic solvents (Figure 23). PPII conformation is stabilized by solvation of the backbone,^{44,53} although the way water influences the tendency of peptides to adopt a PPII conformation is still not well understood.

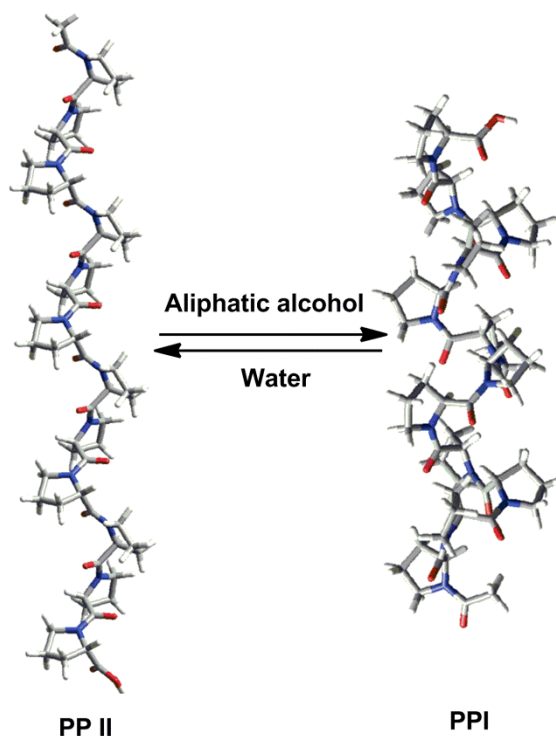


Figure 23. Solvent induced switching between PPII \leftrightarrow PPI conformations.

1.7 Biological Significance of Polyproline Conformation

Short peptides do not fold because they are unable to develop long range cooperative interactions required to form α helix or β -sheets. Recently, a number of spectroscopic studies⁵⁴ on the conformation of the smallest protein subunits revealed that these small peptides adopt PPII structure in water. Some of representative list of major functions carried by the PPII structure^{16b} are given in Table 2.

Table 2. PPII helix major function^{16b}

Function associated with PPII	PPII structure	Protein and description
Structural function PPII maintains three-dimensional structure in natively unfolded proteins and peptides.	PPII helix, PPII conformation of individual residues	Natively unfolded proteins. PPII is one of the predominant conformational states. Provides local order, flexibility, facilitates chain hydration.

Chapter 1

PPII maintains three-dimensional structure in folded proteins.	PPII helix, PPII conformation of individual residues	Folded (globular) proteins. PPII is one of the major regular structures. Provides extended flexible structural blocks, conserved, mostly exposed. Forms interdomain linker regions, N- and C-terminal regions, interactions sites. Forms linkers between other secondary-structure segments based on single-residue structure switches, changing the chain chirality.
PPII in interdomain linkers, structural domains	PPII helix (Pro ⁺) 2FB4:110-QPKANPT-116 1FC1:338-KAKGQPREPQ-347 2FL5:109-PKAAPS-114 3FZU: 108L-RTVAAPS-114L 3FZU: 118H-SASTKGP-124H	IgG1 FAB, light chain (human) IgG1 FC fragment, heavy chain (human). IgG-GAR (yellow antibody), light chain. IgG1 FAB, light chain, heavy chain. PPII helix forms whole or part of interdomain linker
PPII in interdomain linkers, functional domains	PPII helix (Pro ⁻ , conserved) 1RWY: 74-ARDLSA-79	α -Parvalbumin (rat).PPII forms linker between the CD and EF Ca ²⁺ binding functional domains, contains Arg ⁷⁵ forming a single invariant salt bridge with Glu ⁸¹ . β -parvalbumin (avian thymic hormone, ATH) (chicken).PPII forms linker between functional domains
PPII forms structural motifs	PPII helix	LRR proteins. Proteins with short LLRs have PPII helices as structural elements on their convex side, PPII also forms cysteinecapping motif.
PPII is involved in protein self-assembly, elasticity	PPII helix, PPII conformation	Amelogenin. Tooth enamel protein, PRP, IDP. Lampirin. Extracellular matrix protein. Elastin, titin, abductin. Elastomeric proteins. PPII participates in and ensures protein self-assembly; PPII is a key structure in the elasticity mechanism of elastomeric proteins

PPII participates in maintaining three-dimensional structure in the proteins associated with conformational diseases	PPII helix	Prion PrPC proteins, α -synuclein, tau protein, Alzheimer extracellular amyloid β peptide fragment 1–28. Proteins involved in conformational disorders. High content of the PPII is identified, PPII possibly participates in pathogenic conformational changes.
Protein–protein interactions PRDs binding to peptide ligands that adopt PPII helical structure.	PPII helix peptide ligands (Pro+)	Src tyrosine kinases and other SH3-containing proteins. SH3 domain binding PPII helical protein ligands. WW domain. WW domain binding PPII helical protein ligands. GYF domain. GYF domain binding PPII helical protein ligands. EVH1 domain. EVH1 domain binding PPII helical protein ligands. UEV domain. UEV domain binding PPII helical protein ligands. Binding to PPII helical ligands is essential for PRD domain function.

1.7.1 Oligoproline as cell penetrating agents

It has been reported that proline-rich peptides⁵⁵ and proline dendrimer⁵⁶ can be internalized by eukaryotic cells. The most important advantage of proline-rich peptides in biological systems is their solubility in water. In this context, Royo and co-workers⁵⁷ synthesized the *cis*- γ -amino-L-proline oligomers functionalized at the proline α -amine with groups that mimic the side chains of natural amino acids, including alanine, leucine, and phenylalanine. These γ -peptides enter into different cell lines (COS-1 and HeLa) *via* an endocytic mechanism.⁵⁸ In addition to their capacity for cellular uptake, these unnatural short length oligomers offer advantages over the well-known cell penetrating TAT peptide, being less toxic and protease resistance.

Chimielewski and co-workers⁵⁹ have synthesized cell penetrating agents that introduce cationic and hydrophobic moieties along the backbone of a polyproline helix in an amphiphilic manner. This was done by O-alkylation of hydroxyproline monomer to yield a scaffold that displays both hydrophobic and cationic moieties. Introduction of an isobutyl group onto hydroxyproline led to a proline-based mimic of leucine, whereas functionalization with amino or guanidinium groups led to proline-based mimics of lysine

or arginine respectively (Figure 24). Dramatic increases in uptake with MCF-7 cells when upto six guanidinium groups were positioned on the polyproline helix, whereas only modest increases in cellular uptake were observed with the amine-containing polyproline compounds as compared to their flexible counterparts. Amphiphilicity played a key role in the enhanced cell translocation, as scrambled versions of the designed agents, with hydrophobic and cationic groups on all faces of the helix, were only as effective as their flexible peptide counterparts. Interestingly, the most potent peptide, P11LRR, demonstrated efficiency of cellular uptake by an order of magnitude as compared to that of the well-studied Tat peptide, with lower cytotoxicity. The longer CPP sequence, P14LRR, displayed a 7 to 12-fold higher uptake in MCF-7 cells as compared to its shorter counterpart, P11LRR.⁶⁰

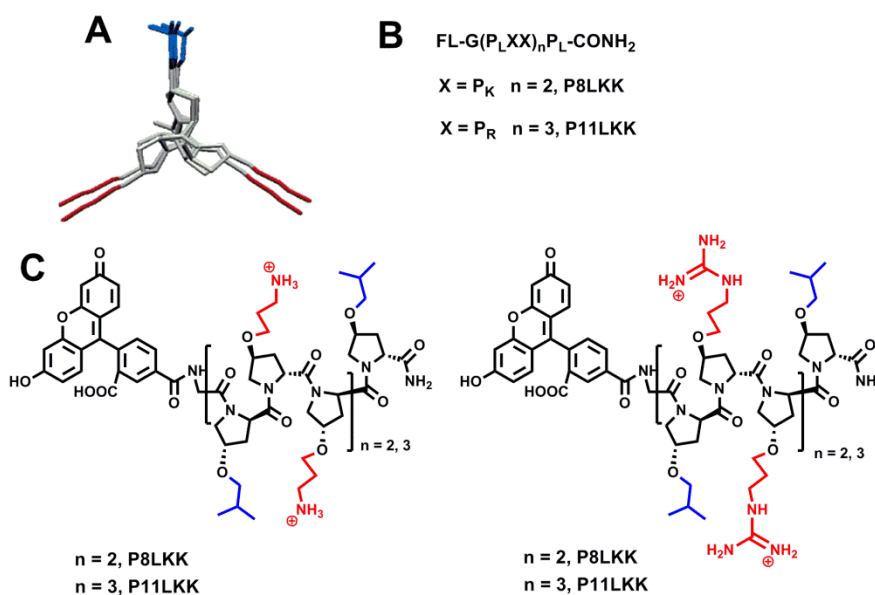


Figure 24. (A) Top view of an amphiphilic polyproline helix containing modified side chains (red, cationic; blue, hydrophobic), (B) Sequences, and (C) Structures of modified polyproline oligomers containing amino (PK) or guanidinium (PR) functionality.⁵⁹

1.7.2 Drug delivery properties of proline-rich peptides

A common challenge in drug development is the *in vivo* and cellular distribution in the treatment of disease. Cell penetrating peptides (CPPs) are promising candidates for the delivery of drugs to both bacterial and eukaryotic cells.⁶¹ Although CPPs are potential drug

delivery candidates, they can display cytotoxicity depending on cargo used and cargo linkage position.⁶² However, proline rich peptides are, translocated across cellular membranes without inducing lysis or causing damage and display much less toxicity to mammalian cells. Thus, these peptides may have significant potential as CPPs or transport systems to deliver drugs to the target cells but may also be used to enhance antimicrobial activity (Table 3).⁶³

Table 3. Proline-rich AMPs able to penetrate cell membranes and cross blood brain barrier as novel potential carriers for drug delivery^{63b}

Cell penetrating peptides (CPP) Pyrrhocoricin	Delivery of peptidic/epitope based cargo Bactenecin 7 Carrier for protein cargo and phosphorescent oxygen sensor. PR39 Delivery of siRNA into 4T1 cells
Blood brain barrier (BBB) crossing Oncocin Apidacacin (Api137) Drosocin Drosocin (Pro5Hyp)	Mostly destined for endothelial cells Mainly trapped in the brain parenchyma

1.7.3 Polyproline conformation in elastic function

PPII conformation is widely present in titin, abductin, and elastin, which are elastomeric proteins and therefore it could play a pivotal role in the genesis of elasticity. The giant elastic protein titin, whose complete domain organization has been revealed,⁶⁴ gives rise to an elastic sarcomere matrix in striated muscle. Precisely, the I-band region of the sarcomere is involved in the elastic response upon stretch and is composed of two main domains. The first domain is made of tandem repeats of about 100 residue immunoglobulin and the second domain is a motif consisting of tandem repeat of four amino acid residues, PEVK. The extension of the PEVK segment is important for the elastic response of striated muscle to passive stretch and behaves mechanically as an entropic spring.⁶⁵ Structural studies of PEVK motif indicated the likely presence of PPII structure with flexible joints. In aqueous solution PEVK contains multiple PPII helices in equilibrium which are flexible and make significant entropic contribution to elasticity. Table 4 represents list of proteins comprising significant stretches of PPII conformation and technique used for conformation studies.

Table 4. Proteins comprising significant stretches of PPII conformation⁶⁶

Protein	Technique
Human tropoelastin	CD
Exon 30 of human tropoelastin	CD
Abductin	CD
Titin	CD
Collagen	CD, X-ray
C hordein	CD
Antigenic peptide of foot and mouth disease virus (FMDV)	CD, X-ray
Wheat glutenin	CD
Bowman-Birk inhibitor	ROA
Amyloidogenic prefibrillar intermediate of human lysozyme	ROA
Protein kinase inhibitor	X-ray
p85 subunit of P13-kinase	CD
Profilin and class II major histocompatibility complexes	X-ray
Mucin	CD
γ -zein protein of maize	CD
Casein milk proteins	ROA
α -synuclein proteins	ROA
Tau proteins	ROA
Syp (Tyr phosphatase)	X-ray
Ligand-acceptor complex of SH3 of Src	X-ray
Ligand-acceptor complex of SH3-5(Tyr kinase)	X-ray
Antigens(mixture)-MHC class II	X-ray

Another elastomeric protein abductin, is a major constituent of the abductor muscle in the bivalve shellfish “*Pecten jacobaeus*.” The ligament lets the mollusc swim by opposing the opening movement of the bivalve of the shellfish. The sequence of abductin⁶⁷ shows the motif FGGMGGNAG contained protein in tandem repeat. This decapeptide studied by CD at different temperatures suggests the presence of a mixture of PPII conformation and random coil in equilibrium which may be important in relation to the mechanism of elasticity of the protein.

Polyproline conformation is also present in elastin, the protein responsible for the elasticity of many vertebrate tissues, including skin, lungs, ligaments, and large arteries.⁶⁸ The elasticity of this protein is entropy driven, in restoring the force responsible for the elastic behavior originating from an increase of disorder accompanying the transition of the stretched to the relaxed state. The octapeptide ALGGGALG of elastin containing GG

adopts mainly the PPII conformation which seems to be important for the elastic behavior of the protein

1.7.4 Intramolecular electron transfer in a helical oligoproline assembly

Molecular assemblies based on oligoproline spacers have a special appeal because of easy synthesis of oligomeric structures and the well-defined, stable secondary structures that dominate when the oligoproline chain contains at least five consecutive proline residues.⁶⁹ Even with large ligand substituents, the oligoproline has ability to fold into a proline helix in solution.⁷⁰

Papanikolas *et al.*⁷¹ synthesized phosphonate oligoproline assemblies containing different Ru^{III} polypyridyl chromophores coupled by click reaction. In water or methanol this assembly adopts PPII helical structure, which brings the chromophore in close contact. Oligoproline scaffolds maintain their secondary structure in solution and on surfaces as well as provide the necessary arrangement of chromophores for directional energy transfer followed by electron injection into TiO₂ (Figure 25).⁷¹⁻⁷²

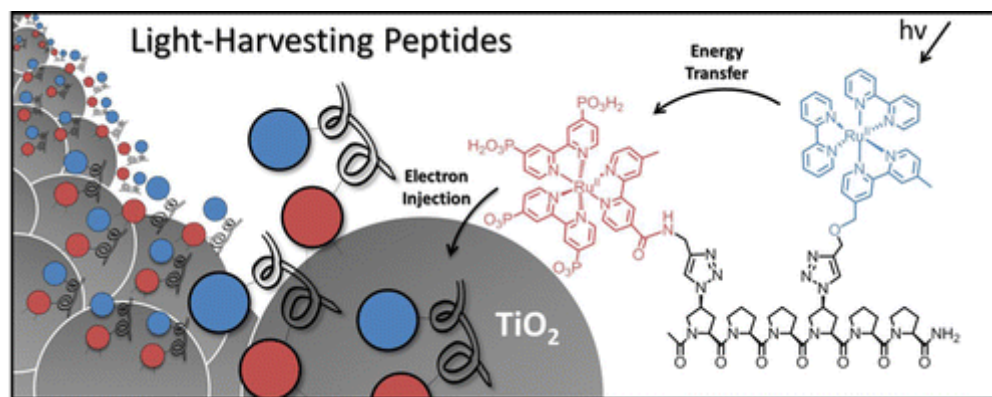


Figure 25. Schematic representation of photophysical events on nanocrystalline TiO₂.⁷¹

Excitation of the assembly results in a rapid, efficient, intra-assembly energy transfer to the inner Ru^{II}. Thus oligoproline holds great promise for the preparation of interfacial assemblies for energy conversion based on a family of assemblies having controlled compositions and distances between key functional groups.

1.7.5 Self-assembly of polyproline rod and a cell-penetrating peptide tat coil

As the cyclic structure of proline induces conformational constraints in the pyrrolidine ring, the proline-rich sequences tend to form stiff helical rod structures, called a polyproline type II (PPII) helix, in aqueous solution. Three nonpolar methylene groups are aligned at the outer part of the rod after PPII helix formation. Based on these facts Myongsoo Lee *et al.*⁷³ hypothesized that the stiff rod character and the nonpolar nature of the outer surface of the PPII helix might impart microphase separation characteristics to the rod-coil of a PPII rod and a hydrophilic Tat-CPP coil, leading to the anisotropic orientational ordering of the rod and self assembly (Figure 26).

Stiff rod character of the polyproline helix enables microphase separation of the slightly hydrophobic rod and the hydrophilic peptide coil, leading to the formation of self-assembled nanocapsules, which are stable enough to cross the cytoplasmic membrane barrier of the cell.

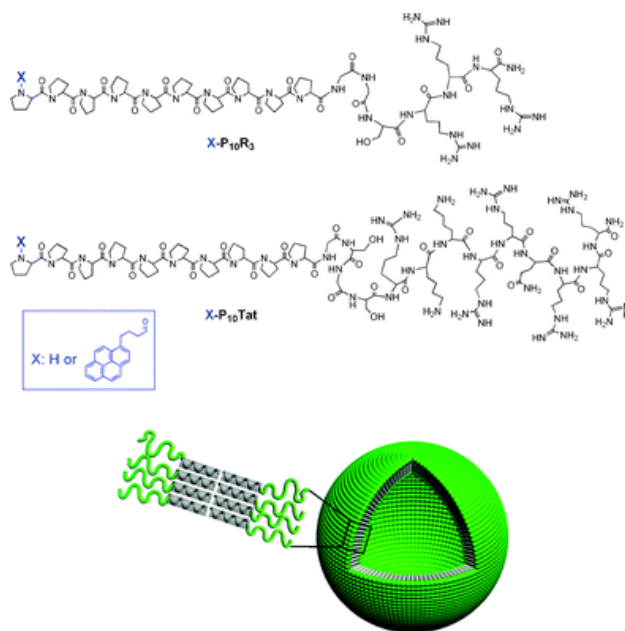


Figure 26. Structures of peptide rod-coil building blocks and their self-assembly into nanocapsule structures.^{73a}

Wennemers *et al.*⁷⁴ demonstrated the value of functionalizable peptidic scaffolds that have no tendency to self-aggregate but govern the spatial orientation between π -systems for directed self-assembly (Figure 27). The length of the conjugate and the

absolute configuration of stereocenters at the outside of the helix, allowed for tuning the supramolecular aggregation.

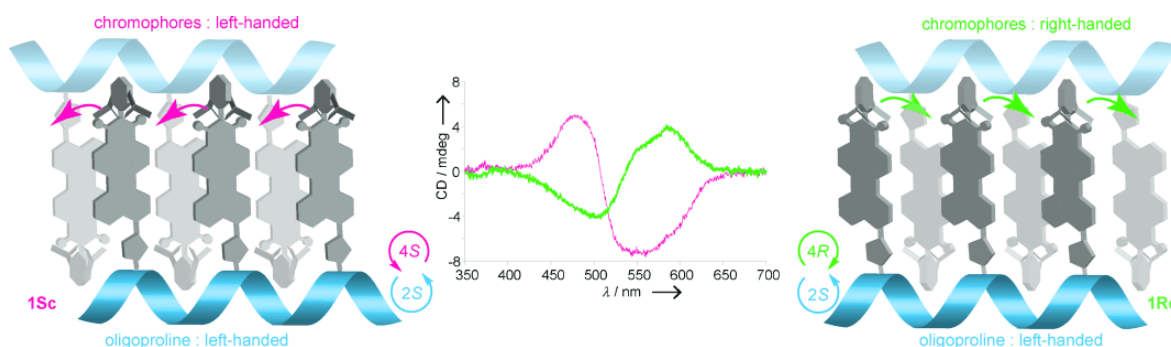


Figure 27. CD spectra of diastereoisomers in THF/H₂O (30:70, 50 μ M, 294 K; middle), Representation of the counter-clockwise and clockwise orientation of chromophores.⁷⁴

With increasing length of the oligoproline- π -system conjugates, higher ordered nanostructures form that range from flexible worm-like threads via fibrils to nanosheets and nanoribbons (Figure 28)

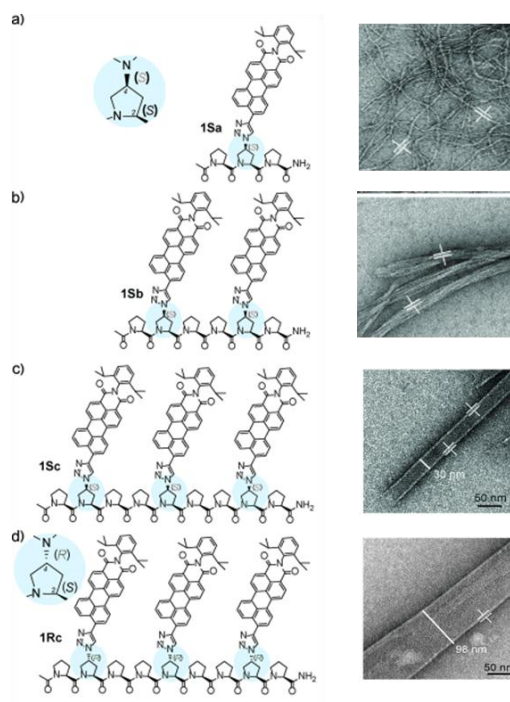


Figure 28. (a) to (d) Structures of oligoproline-PMI conjugates and corresponding supramolecular organization.⁷⁴

1.7.6 Polyproline as a “spectroscopic ruler” for single-molecule fluorescence

In protein folding very large number of microscopic pathways connect the countless unfolded conformations to the unique conformation of the native structure. The investigations of the structural and dynamic properties of short polypeptides (≥ 20 residues) are of most importance for the understanding of the folding mechanism and function of proteins. Popular experimental techniques for the study of short polypeptides are NMR and CD spectroscopy. Fluorescence Resonance Energy Transfer (FRET) has been less routinely useful as it generally occurs over distances larger (20-50 Å) than those characteristic for short polypeptides (5-20 Å), with challenges to derive complex structural and dynamic information in such short peptides that are generally random-coiled and consequently flexible.⁷⁵

Polyproline presents an exception in this respect, because of its ability to form secondary structures at short lengths and the cyclic proline residue providing relatively rigid and elongated backbones.⁷⁶ Polyproline peptides were first used in the context of FRET in the work of Stryer and Haugland,⁷⁷ who experimentally observed the distance dependence of the transfer efficiency assuming polyproline to be a rigid rod. Eaton *et al.*⁷⁸ measured FRET efficiency distributions for donor and acceptor dyes attached to the ends of freely diffusing polyproline molecules of various lengths. By using polyproline peptides Nau *et al.*⁷⁶ obtained donor-acceptor distances from MD simulations (Figure 29). Thus polyproline peptides have become an important standard for calibrating, testing measurements and refining new experimental methods. It has been used as a spectroscopic reference for single-molecule fluorescence experiments.

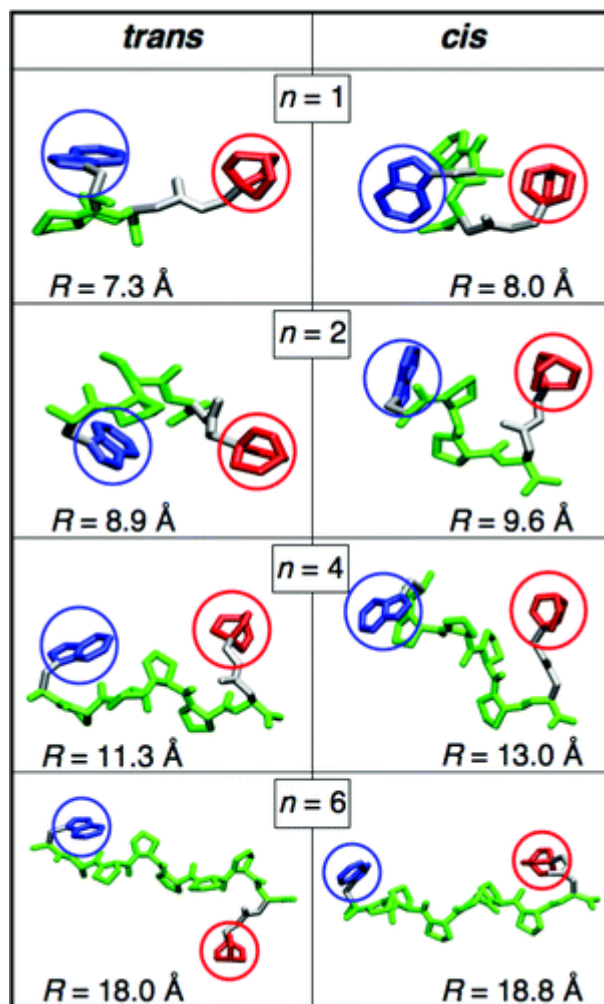
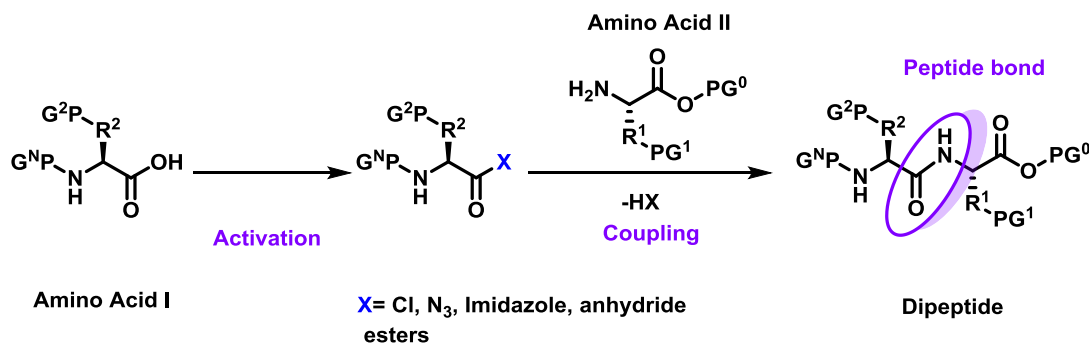


Figure 29. The average donor-acceptor distance in *cis* and *trans* form of polyproline.⁷⁶

1.8 Methodology

1.8.1 Peptide Bond Formation: Methods and Strategies

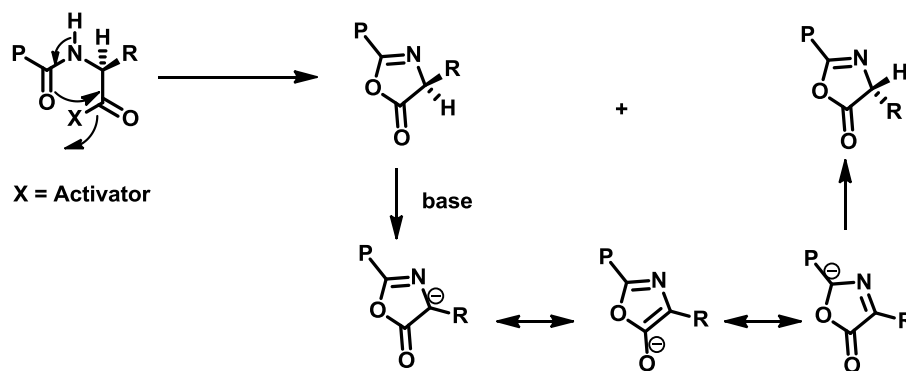
The key step in the peptide synthesis is the formation of the amide bond between two amino acid segments. Carboxy acid function is activated as acyl halides, acyl azides, acylimidazoles, anhydrides, esters etc. There are different ways of coupling reactive carboxy derivatives with an amine:

Scheme 1. Simplified general mechanism of peptide bond formation.

- ❖ An intermediate acylating agent (R-CO-) formed is isolated and then subjected to aminolysis.
- ❖ A reactive acylating agent is formed from the acid in a separate step, followed by immediate treatment with the amine.
- ❖ The acylating agent is generated *in situ* from the acid in the presence of the amine, by the addition of an activating or coupling agent.

The activation of the carboxyl group of the first amino acid is followed by a nucleophilic attack of the amino group of the second amino acid to form the peptide bond. In order to prevent undesirable peptide bond formation, the amino group of the first amino acid and functional side chain groups need to be blocked. Repeated de-blocking, activation and coupling leads to the desired final peptide sequence (Scheme 1).

However, due to the presence of various functional groups in natural and unnatural amino acids and particularly the requirement for full retention of chiral integrity, the coupling of amino acids and peptides under mild conditions can be challenging. A plethora of coupling reagents has been developed superseding each other in efficiency and suitability for specific applications. Racemisation can occur at the C-terminal amino acid residue in the course of a coupling reaction due to the ionization of the α -hydrogen and the formation of an oxazolone intermediate (Scheme 2).

Scheme 2. Racemization mechanism in the course of peptide bond formation

In recent years, peptide coupling reactions have significantly advanced with the development of new peptide coupling agents. DCC as a peptide-coupling reagent is replaced by onium-type coupling reagents to smoothly incorporate sterically hindered amino acids including N-methylated and α,α -dialkylated amino acids into the corresponding peptides. Racemisation suppressants are also used as additives to the peptide coupling reagents which also act as a rate enhancer.⁷⁹ Table 3 evaluates the advantages, disadvantages, and effectiveness of various peptide coupling reagents, based on phosphonium, uronium, immonium, carbodiimide, imidazolium, organophosphorous, acid halogenating reagents.

1.8.1a Racemisation suppressants

Geiger⁸⁰ first reported the use of HOBt as a racemisation suppressant in peptide coupling reactions with carbodiimide coupling reagents. Several additives such as HOBt, HOAt, HODhbt, N-hydroxytetrazole, HOCT, and PTF have been developed which not only suppress racemisation, but also enhance the reactivity.

HOAt has been reported to be more efficient than HOBt because of an anchimeric assistance caused by the pyridine co-workers ring.⁸¹ Later, N-hydroxytriazoles and N-hydroxytetrazole were examined for their coupling efficiency.⁸² Ramage et al.⁸³ reported the coupling reaction of dipeptide with DIC and the newly designed HOCT for a racemisation study. The racemisation with EDC/HOCT activation was negligible for all amino acids except histidine.

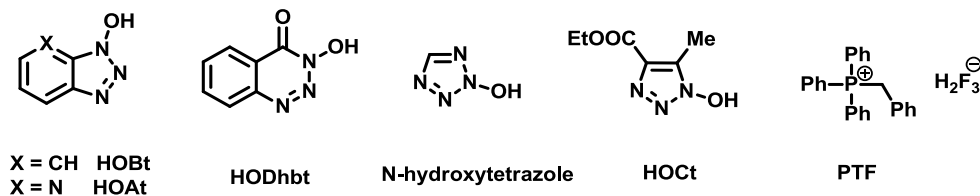


Figure 30. Some examples of racemisation suppressant in peptide coupling reactions.

1.8.1b Solution phase peptides synthesis

This technique has been used for the synthesis of small peptides composed of only a few amino acid residues. Its main advantage is that the intermediate products can be isolated and purified after each step of synthesis, deprotected and recombined to obtain larger peptides of the desired sequence. This technique is highly flexible with respect to the chemistry of coupling and the combination of the peptidic blocks. New strategies for synthesis in solution have been developed, going from the design of functional groups for the side chains and condensation of fragments for the synthesis of large molecules⁸⁴ to the use of new coupling reagents.⁸⁵

1.8.1c Solid phase peptide synthesis (SPPS)

In solid phase synthesis chemical transformations are carried out on solid support by sequential addition of α -amino and side-chain protected amino acid residues to an insoluble polymeric support. Acid labile Boc group or base labile Fmoc group is used for N- α -protection. After removal of the protecting group, the next protected amino acid is added by using either a coupling reagent or pre-activated protected amino acid derivative. The resulting peptide is attached to the resin *via* a linker or directly through its C-terminus and may be cleaved to yield a peptide acid or amide, depending on the linker. Side-chain protecting groups are often chosen so as to cleave them simultaneously with detachment of the peptide from the resin. Cleavage of the Boc protecting group is achieved by trifluoroacetic acid (TFA) and the Fmoc protecting group by piperidine or diethyl amine. Final cleavage of the peptidyl resin and the side-chain deprotection requires strong acid, such as hydrogen fluoride (HF) or trifluoromethanesulphonic acid (TFMSA) in case of Boc

chemistry and 20% TFA in DCM in case of Fmoc chemistry. Table 5 shows the merits and demerits for solid phase peptide synthesis *versus* solution phase peptide synthesis.

Table 5: Solid phase *versus* solution phase peptide synthesis

Solid phase peptide synthesis	Solution phase peptide synthesis
Good for short chain as well as long chain peptides	Good for only short chain peptides
Limitation for large-scale synthesis of peptides	The large-scale synthesis of peptides can be carried out
Isolation and purification is not possible	Need to isolate and purify intermediates
Problems of handling large amounts of expensive resins or large excesses of reagents	Easy to handle the reagents
Generally racemisation not observed	In some cases racemisation observed
This technique is highly flexible with respect to the chemistry of coupling and the combination of the peptidic blocks	This technique has limited flexibility with respect to the chemistry of coupling and the combination of the peptidic blocks

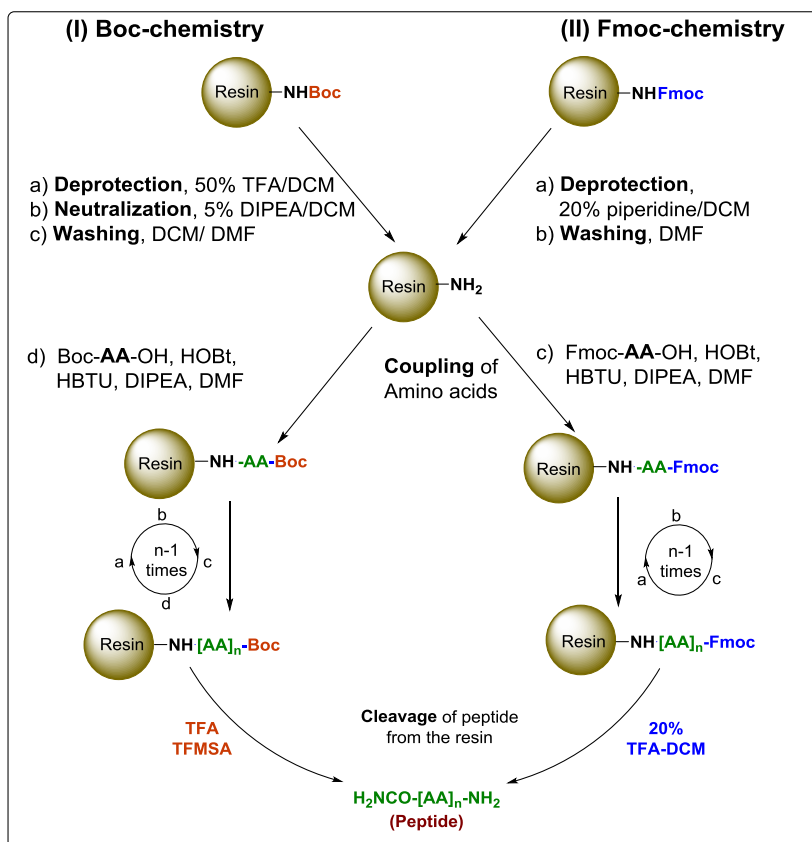
1.8.1d Comparison of *Fmoc* and *Boc* chemistry

There are two major protocols for the routine synthesis of peptides by solid phase method using Fmoc strategy (base-labile α -amino protecting group) or Boc strategy (acid-labile protecting group). First protocol uses fluorenylmethyloxycarbonyl (Fmoc) group as N^α -protection which is extremely stable to acidic conditions but can be cleaved efficiently with a secondary base such as piperidine. The alternative protocol is to use the *t*-butoxycarbonyl (*t*-Boc) group as N^α -protection and reactive side chains are protected with groups that are stable to *t*-Boc deprotection conditions and can be removed under strongly acidic conditions.

For Fmoc deprotection, the growing peptide is subjected to mild base treatment using piperidine/diethylamine during Fmoc deprotection and 20% TFA in DCM is required only for the final cleavage and deprotection of peptidyl resin. By contrast, the cleavage and deprotection in Boc strategy requires the use of dangerous HF or TFA/TFMSA. The removal of a Boc group with TFA yields a positively-charged α -amino group, whereas the removal of an Fmoc group yields a neutral α -amino group. Scheme 3 shows the general

protocol for solid phase peptide synthesis of Fmoc strategy (base-labile alpha-amino protecting group) and Boc strategy (acid-labile protecting group).

Scheme 3. General protocol for SPPS *via* (A) Boc chemistry (B) Fmoc chemistry.



1.9 Characterization of Polyproline Structures

1.9.1 Circular dichroism

Circular dichroism is a spectroscopic method, which depends on the fact that certain molecules interact differently with right and left circularly polarized light. Circularly polarized light is chiral and hence to discriminate between the two chiral forms of light, a molecule must be chiral, which includes the vast majority of biological molecules. CD is useful in determining the PPII helical content of proteins and conformational analysis of nucleic acids and their interaction with other ligands. CD spectra are particularly valuable in characterization of the self assembly of strands to

duplex/triplex/tetraplex for higher order structure and distinguish conformation of hybrid structures such as DNA-peptide complexes. CD spectra can be readily used to estimate the fraction of a molecule that is in the alpha-helix, the beta-sheet, the beta-turn structure, the PPII or PPI conformations and random coil (Figure 31).⁸⁶

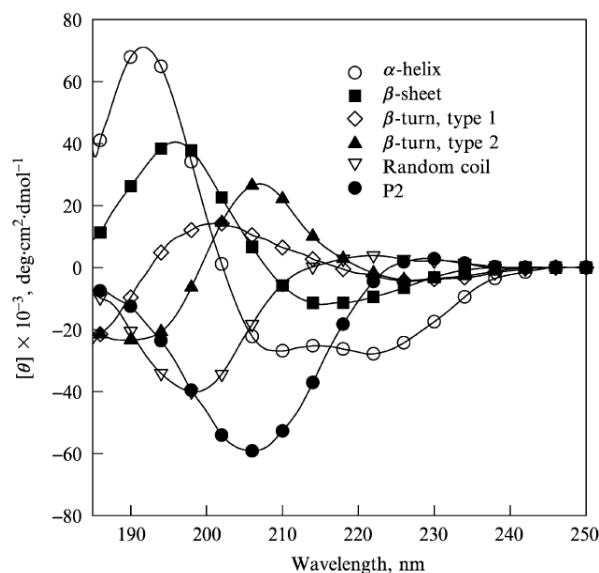


Figure 31. Representative circular dichroism curves corresponding to common secondary structural protein elements.⁸⁶

In general, this phenomenon is seen in absorption bands of any optically active molecule. As a consequence, structure of biological molecules imparts a distinct CD profile specific to its composite secondary structures. The alpha helix of proteins and the double helix of nucleic acids have CD spectral signatures characteristic of their structures. Thus CD can be used to probe structural changes arising from varying solvent conditions, temperature, pH, ionic strength and interaction with ligands. Circular dichroism is a useful technique to study the kinetics of protein folding and protein–ligand interactions. It is an indirect method useful for measurement of thermodynamics and binding. The far-UV CD spectrum of proteins can reveal important characteristics of their secondary structure.

1.9.1a Identification of polyproline II by UV-CD spectroscopy

Polyproline peptides show two different conformations i.e. PPI and PPII in different solvent and can be characterized by UV-CD. Polyproline I helix is found in

solvents of low polarity, e.g. higher alcohols (1-propanol). The type II helix is the conformation occurring in water. A weak, positive band near 225 nm and a strong, negative band at about 205 nm characterize a CD spectrum of PPII. In contrast, PPI exhibits an unusually strong, positive band in the 215-nm region accompanied by two much weaker, negative bands around 195 and 235 nm, respectively⁸⁷ (Figure32).

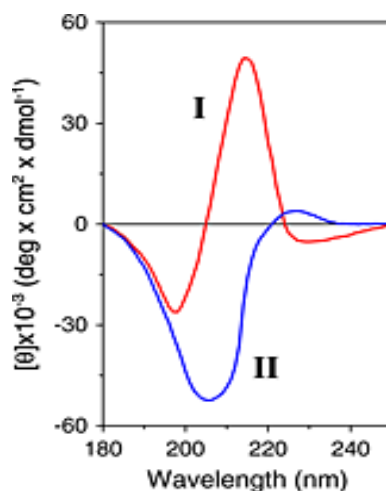


Figure 32. Far-UV CD spectra of I) polyproline I (red) and II) polyproline II (blue) in 1-propanol and in water solution, respectively.

Although the spectra for poly-Lys and poly-Glu are qualitatively similar to polyproline II CD, the negative bands for these peptides had smaller magnitudes. These change can be observed due to charged end effects which alter peptide conformation.⁸⁸ Helbecque *et al.*⁸⁸ also found little effect of varying the pH on the CD of these peptides. The thermal denaturation study of polyproline peptides can be monitored by observing the changes in ellipticity at 222-225 nm with temperature. The thermal denaturation curves uniformly show a decrease in molar ellipticity with increase in temperature for the peptides.

1.9.1b Polyproline II conformation by VCD

VCD (Vibrational Circular Dichroism) is the measurement of the differential absorbance of left and right-circularly polarized IR by fundamental vibrational modes of a molecule. VCD provides a simpler method of interpreting the conformation of polypeptides than IR or Raman alone. Both the spectra of random coil and PPII

conformation exhibit a negative VCD couplet (+, – with decreasing frequency), the difference between them being the shift of the carbonyl stretch of the amide group of PPII, which is 23 cm^{-1} lower than that of random coil conformation. On the other hand, the PPI conformation gives rise absorption that is nearly indistinguishable from that of the PPII in the solid state.^{89,90}

1.9.2 Polyproline II conformation by ROA

Raman optical activity (ROA) measures vibrational optical activity by means of a small difference in the intensity of Raman scattering from chiral molecules in right and left circularly polarized incident laser light.⁹¹ Vibrational circular dichroism (VCD) and ROA spectra reflect the conformation of the main peptide chain. However, the peptide side chains (often hydrophobic hydrocarbon structures) provide strong Raman and ROA signals within almost the entire frequency region due to the polarizability changes during their vibrational motion.⁹² Ring conformations in the poly-L-proline chain are clearly reflected by the ROA spectra and the presence of two conformers (*endo*, *exo*) can be manifested.⁹⁰

The polyproline band positions and intensities are remarkably similar for the TFE as well as water in ROA, except for the amide I peak. This mode (C=O stretching, 1648 cm^{-1} in TFE, 1633 cm^{-1} in H_2O) is most influenced by formation of hydrogen bonds and solvent polarity. The ROA sign patterns within $900\text{--}1010\text{ cm}^{-1}$ and $1164\text{--}1207\text{ cm}^{-1}$ seem to be characteristic in the PPII conformation and correspond well to spectra of other proline-containing peptides.⁹³

1.9.3 Polyproline II conformation by ^{15}N NMR spectroscopy

Unlike α -helices and β -sheets, there is no characteristic main chain hydrogen bonding patterns in PPI and PPII helices making it very difficult to detect their structures directly by NMR spectroscopy. So, PPII helices are often assigned as disordered structures or random coils in aqueous solution due to lack of direct structural information but Lam and Hsu⁹⁴ showed polyproline II possess several NMR characteristics ($\delta^{15}\text{N}$, $^3J_{\text{HN}\alpha}$, and $^1J_{\text{C}\alpha\text{H}\alpha}$) that are differentiable from random coils.

Lam and Hsu⁹⁴ measured the amide ¹⁵N chemical shifts and incorporating temperature and sequence effect corrections, which can be used together with ³J_{HNα} and ¹J_{CαHα} to differentiate helices from random coils with high confidence. With temperature and sequence corrections on the predicted random coil ¹⁵N chemical shifts, a significant ¹⁵N chemical shift deviation was observed for the model peptide. The ¹⁵N chemical shift differences also correlate well with the molar ellipticities (at 220 nm) of the CD spectra at different temperatures, indicating that the ¹⁵N chemical shift is a sensitive probe for helices. The average ³J_{HNα} and ¹J_{CαHα} values of the model peptide are determined to be 6.5 and 142.6 Hz, respectively, which are consistent with the values calculated from the geometry of helices. Based on these observations, a strategy was developed for probing left-handed PPII helical structures from other secondary structures

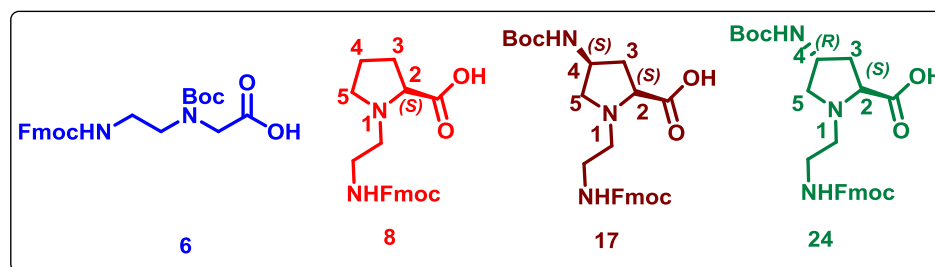
1.10 Scope of present work

The important hallmark of native, functional proteins is the adoption of a stable, highly conformation restricted structure. Structural and conformational analyses of biopolymers reveal the fact that most of the biological events result from their stable compact conformation, stabilized by a collection of non-covalent interactions. Strategies to enable conformational restriction and stabilization of peptides and proteins may be used to interrogate protein structure-function relationships. Short peptides provide model of polypeptide conformational properties to study the protein structure-function relation. The polyproline type conformations PPI and PPII have been recognized for their presence in both folded and unfolded protein structures. Hence, polyproline is an ideal candidate to address these problems because of easy functionalization by chemical synthesis.

Chapter 2: Synthesis and study of foldamer properties of unnatural (*N*-aminoethyl)glycyl and pyrrolidine peptides

This chapter is directed towards the comparative study of hybrid amides (aminoethyl-glycyl, aminoethyl-prolyl, *ae*-4(*R/S*)-aminoprolyl-polyamides) to understand the effect of chain length, proline conformation and stereochemistry of proline C4 substituent on the secondary structures adopted by (*ae-pro*) polyamides in water and

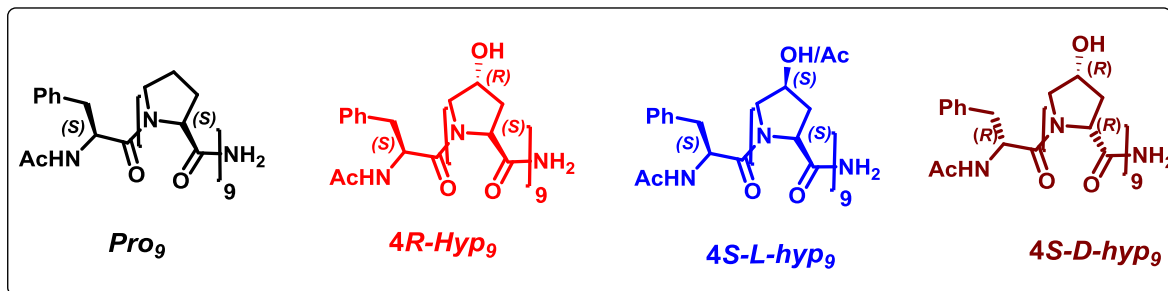
Fluoro-alcohols and investigation of conformation adopted by these polyamides by different spectroscopy.



Chapter 3: Poly-4*S*(hyp)/4*R*(Hyp)proline peptides, characterization of β - structure

The most common stable secondary structures of peptides are α -helix and antiparallel β -pleated sheet and these secondary structures are formed by intermolecular or intramolecular H-bonding. Absence of local hydrogen bonds involving main chain atoms is one of the distinctive structural properties of PPII helices, compared to the other common secondary structure elements found in protein. This structural feature leaves several unsatisfied hydrogen bond acceptors free to establish *intra* or *inter*-molecular interactions. A recent computational study has suggested that in 4*S*-aminoproline, intramolecular hydrogen bond that is feasible between 4*S*-NH₂ and the carbonyl carbon of same proline moiety, leads to increase in the *trans/cis* ratio of peptide bond.

This chapter deals with the study of molecular conformations adopted by 4-hydroxyproline polypeptides. Such study would lead to an understanding of the importance of 4(*R/S*)-OH group in dictating the PPII conformation and influence the ring puckering. 4-Hydroxy group should act like the 4-amino group in terms of its ability to form hydrogen bonding and influence the PPI and PPII conformation of proline polypeptides. The target polypeptides for this work are



Chapter 4: Orientation of β -Structure: parallel or antiparallel

This chapter is directed towards distinguishing the parallel/antiparallel orientation of possible β -structure in 4S-hydroxy-L-proline and 4R-hydroxy-D-proline peptides in TFE by using polypeptides modified with FRET probes and hydrophobic interaction of fatty acid chain, which are attached at the N-terminus.

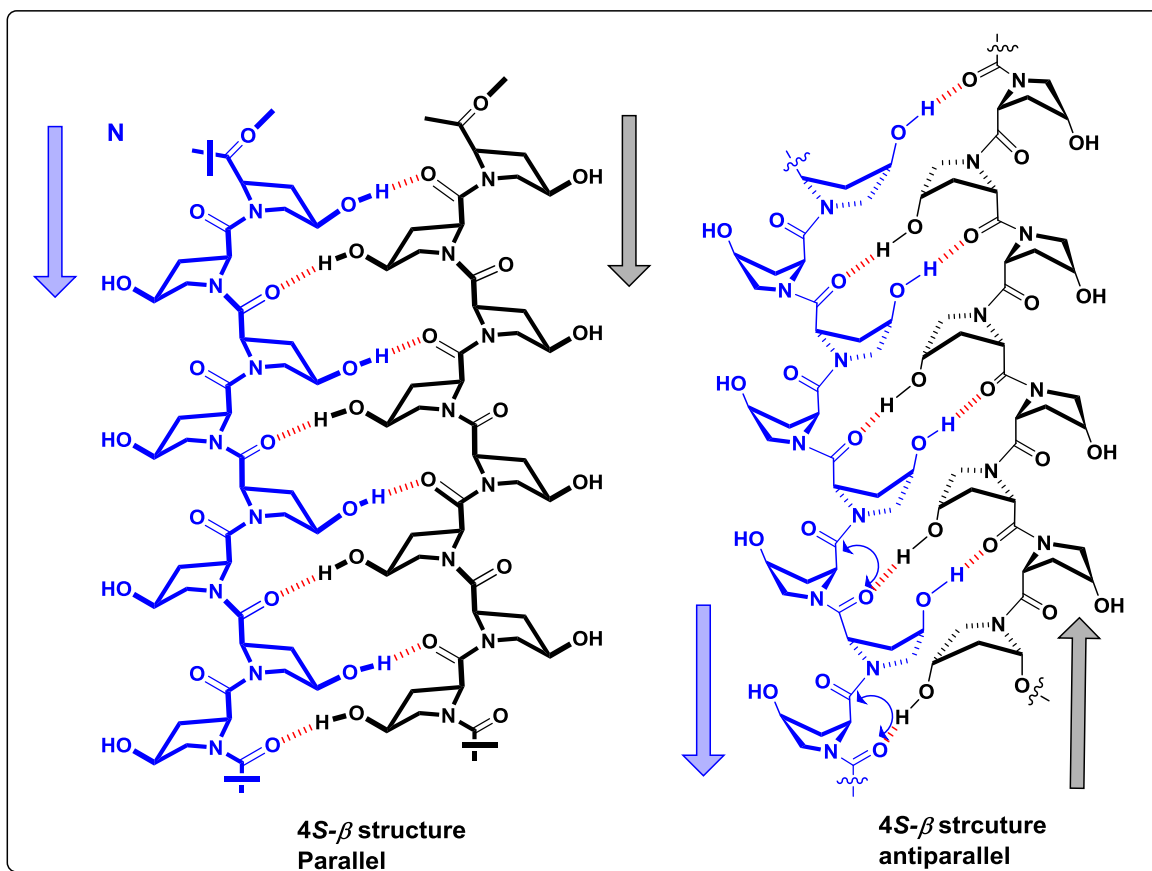


Figure 33. Predicted β -structure (Intermolecular H-bonding).

1.11. References

1. Mart, R. J.; Osborne, R. D.; Stevens, M. M.; Ulijn, R. V., Peptide-based stimuli-responsive biomaterials. *Soft Matt.* **2006**, *2*, 822-835.
2. Lowik, D. W. P. M.; Leunissen, E. H. P.; van den Heuvel, M.; Hansen, M. B.; van Hest, J. C. M., Stimulus responsive peptide based materials. *Chem. Soc. rev.* **2010**, *39*, 3394-3412.
3. Anfinsen, C. B., Principles that Govern the Folding of Protein Chains. *Science* **1973**, *181* (4096), 223-230.
4. Creighton, T. E., *Proteins: Structures and Molecular Properties*. W. H. Freeman: 1993.
5. Nelson, D. L.; Cox, M. M., *Lehninger Principles of Biochemistry*. W.H. Freeman: 2013.
6. Voet, D.; Pratt, C. W.; Voet, J. G., *Principles of Biochemistry*. Wiley: 2012.
7. Mansiaux, Y.; Joseph, A. P.; Gelly, J. C.; de Brevern, A. G., Assignment of PolyProline II Conformation and Analysis of Sequence-Structure Relationship. *PLoS ONE* **2011**, *6*, e18401.
8. Zhang, L.; Hermans, J., 3_{10} Helix Versus α -Helix: A Molecular Dynamics Study of Conformational Preferences of Aib and Alanine. *J. Am. Chem. Soc.* **1994**, *116*, 11915-11921.
9. Sibanda, B. L.; Blundell, T. L.; Thornton, J. M., Conformation of β -hairpins in protein structures: A systematic classification with applications to modelling by homology, electron density fitting and protein engineering. *J. Mol. Biol.* **1989**, *206*, 759-777.
10. (a) Wilmot, C. M.; Thornton, J. M., Analysis and prediction of the different types of β -turn in proteins. *J.Mol. Biol.* **1988**, *203*, 221-232; (b) Richardson, J. S., The Anatomy and Taxonomy of Protein Structure. In *Adv. protein chem.* C.B. Anfinsen, J. T. E.; Frederic, M. R., Eds. Academic Press: 1981; *34*, 167-339. (c) Rose, G. D.; Gierasch, L. M.; Smith, J. A., Turns in Peptides and Proteins. In *Adv. protein chem.*, C.B. Anfinsen, J. T. E.; Frederic, M. R., Eds. Academic Press: 1985; *37*, pp 1-109.
11. Deber, C. M.; Brodsky, B.; Rath, A., Proline Residues in Proteins. In *eLS*, John Wiley & Sons, Ltd: 2001.

12. Brandts, J. F.; Brennan, M.; Lung-Nan, L., Unfolding and refolding occur much faster for a proline-free proteins than for most proline-containing proteins. *Proc. Natl. Acad. Sci. U. S. A.* **1977**, *74*, 4178-4181.
13. Isakov, N., A new twist to adaptor proteins contributes to regulation of lymphocyte cell signaling. *Trends Immunol.* **2008**, *29*, 388-396.
14. Shi, Z.; Woody, R. W.; Kallenbach, N. R., Is polyproline II a major backbone conformation in unfolded proteins? *Adv.protein chem.* **2002**, *62*, 163-240.
15. (a) Bretscher, L. E.; Jenkins, C. L.; Taylor, K. M.; DeRider, M. L.; Raines, R. T., *J. Am. Chem. Soc.* **2001**, *123*, 777-778; (b) DeRider, M. L., *J. Am. Chem. Soc.* **2002**, *124*, 2497-2505; (c) Hinderaker, M. P.; Raines, R. T., *Protein Sci.* **2003**, *12*, 1188-1194; (d) Hodges, J. A.; Raines, R. T., *Org. Lett.* **2006**, *8*, 4695-4697; (e) Horng, J. C.; Raines, R. T., *Protein Sci.* **2006**, *15*, 74-83; (f) Zondlo, N. J., Non-covalent interactions: Fold globally, bond locally. *Nat. chem.l biol.* **2010**, *6*, 567-568; (g) Bartlett, G. J.; Choudhary, A.; Raines, R. T.; Woolfson, D. N., $n \rightarrow \pi^*$ interactions in proteins. *Nat. chem.biol.* **2010**, *6*, 615-620.
16. (a) Zafra-Ruano, A.; Luque, I., Interfacial water molecules in SH3 interactions: Getting the full picture on polyproline recognition by protein-protein interaction domains. *FEBS Lett.* **2012**, *586*, 2619-2630; (b) Adzhubei, A. A.; Sternberg, M. J. E.; Makarov, A. A., Polyproline-II Helix in Proteins: Structure and Function. *J. Mol. Biol.* **2013**, *425*, 2100-2132; (c) Fleming, P. J.; Fitzkee, N. C.; Mezei, M.; Srinivasan, R.; Rose, G. D., A novel method reveals that solvent water favors polyproline II over beta-strand conformation in peptides and unfolded proteins: conditional hydrophobic accessible surface area (CHASA). *Protein Sci.* **2005**, *14*, 111-8; (d) Creamer, T. P.; Campbell, M. N., Determinants of the polyproline II helix from modeling studies. *Adv. protein chem.* **2002**, *62*, 263-82; (e) Mezei, M.; Fleming, P. J.; Srinivasan, R.; Rose, G. D., Polyproline II helix is the preferred conformation for unfolded polyalanine in water. *Proteins: Struct., Function, and Bioinformatics* **2004**, *55*, 502-507.
17. Kuemin, M.; Schweizer, S.; Ochsenfeld, C.; Wennemers, H., Effects of terminal functional groups on the stability of the polyproline II structure: a combined experimental and theoretical study. *J. Am. Chem. Soc.* **2009**, *131*, 15474-82.

18. Wilhelm, P.; Lewandowski, B.; Trapp, N.; Wennemers, H., A Crystal Structure of an Oligoproline PPII-Helix, at Last. *J. Am. Chem. Soc.* **2014**, *136*, 15829-15832.
19. Adzhubei, A. A.; Sternberg, M. J., Left-handed polyproline II helices commonly occur in globular proteins. *J. Mol. Biol.* **1993**, *229*, 472-93.
20. Stapley, B. J.; Creamer, T. P., A survey of left-handed polyproline II helices. *Protein Sci.* **1999**, *8*, 587-95.
21. Song, I. K.; Kang, Y. K., Conformational Preference and Cis–Trans Isomerization of 4(R)-Substituted Proline Residues. *J. of Phys. Chem. B* **2006**, *110*, 1915-1927.
22. Shoulders, M. D.; Guzei, I. A.; Raines, R. T., 4-Chloroprolines: Synthesis, conformational analysis, and effect on the collagen triple helix. *Biopolymers* **2008**, *89*, 443-454.
23. Flores-Ortega, A.; Casanovas, J.; Nussinov, R.; Alemán, C., Conformational Preferences of β - and γ -Aminated Proline Analogues. *J. Phys. Chem. B* **2008**, *112* , 14045-14055.
24. Flores-Ortega, A.; Casanovas, J.; Assfeld, X.; Alemán, C., Protonation of the Side Group in β - and γ -Aminated Proline Analogues: Effects on the Conformational Preferences. *J. Org. Chem.* **2009**, *74*, 3101-3108.
25. Kang, Y. K.; Young Choi, H., Cis–trans isomerization and puckering of proline residue. *Biophys. Chem.* **2004**, *111*, 135-142.
26. Milner-White, E. J.; Bell, L. H.; Maccallum, P. H., Pyrrolidine ring puckering in cis and trans-proline residues in proteins and polypeptides: Different puckers are favoured in certain situations. *J. Mol. Biol.* **1992**, *228*, 725-734.
27. Milner-White, E. J.; Bell, L. H.; Maccallum, P. H., Pyrrolidine ring puckering in cis and trans-proline residues in proteins and polypeptides. Different puckers are favoured in certain situations. *J. Mol. Biol.* **1992**, *228*, 725-34.
28. Pandey, A. K.; Naduthambi, D.; Thomas, K. M.; Zondlo, N. J., Proline Editing: A General and Practical Approach to the Synthesis of Functionally and Structurally Diverse Peptides. Analysis of Steric versus Stereoelectronic Effects of 4-Substituted Prolines on Conformation within Peptides. *J. Am. Chem. Soc.* **2013**, *135*, 4333-4363.

29. (a) Hodges, J. A.; Raines, R. T., Energetics of an $n \rightarrow \pi^*$ interaction that impacts protein structure. *Org. Lett.* **2006**, *8*, 4695-4697; (b) Horng, J. C.; Raines, R. T., Stereoelectronic effects on polyproline conformation. *Protein Sci.* **2006**, *15*, 74-83.
30. Chiang, Y.-C.; Lin, Y.-J.; Horng, J.-C., Stereoelectronic effects on the transition barrier of polyproline conformational interconversion. *Protein Sci.* **2009**, *18*, 1967-1977.
31. (a) Oh, K.-I.; Kim, W.; Joo, C.; Yoo, D.-G.; Han, H.; Hwang, G.-S.; Cho, M., Azido Gauche Effect on the Backbone Conformation of β -Azidoalanine Peptides. *J. Phys. Chem. B* **2010**, *114*, 13021-13029; (b) Sonntag, L.-S.; Schweizer, S.; Ochsenfeld, C.; Wennemers, H., The "Azido Gauche Effect" Implications for the Conformation of Azidoprolines. *J. Am. Chem. Soc.* **2006**, *128*, 14697-14703; (c) DeRider, M. L.; Wilkens, S. J.; Waddell, M. J.; Bretscher, L. E.; Weinhold, F.; Raines, R. T.; Markley, J. L., Collagen Stability: Insights from NMR Spectroscopic and Hybrid Density Functional Computational Investigations of the Effect of Electronegative Substituents on Prolyl Ring Conformations. *J. Am. Chem. Soc.* **2002**, *124*, 2497-2505; (d) Kotch, F. W.; Guzei, I. A.; Raines, R. T., Stabilization of the Collagen Triple Helix by O-Methylation of Hydroxyproline Residues. *J. Am. Chem. Soc.* **2008**, *130*, 2952-2953; (e) Choudhary, A.; Gandla, D.; Krow, G. R.; Raines, R. T., Nature of Amide Carbonyl-Carbonyl Interactions in Proteins. *J. Am. Chem. Soc.* **2009**, *131*, 7244-7246; (f) Taylor, C. M.; Hardré, R.; Edwards, P. J. B., The Impact of Pyrrolidine Hydroxylation on the Conformation of Proline-Containing Peptides. *J. Org. Chem.* **2005**, *70*, 1306-1315.
32. Kümin, M.; Sonntag, L.-S.; Wennemers, H., Azidoproline Containing Helices: Stabilization of the Polyproline II Structure by a Functionalizable Group. *J. Am. Chem. Soc.* **2007**, *129*, 466-467.
33. Owens, N. W.; Stetefeld, J.; Lattová, E.; Schweizer, F., Contiguous O-Galactosylation of 4(R)-Hydroxy-L-proline Residues Forms Very Stable Polyproline II Helices. *J. Am. Chem. Soc.* **2010**, *132*, 5036-5042.
34. Kuemin, M.; Schweizer, S.; Ochsenfeld, C.; Wennemers, H., Effects of Terminal Functional Groups on the Stability of the Polyproline II Structure: A Combined Experimental and Theoretical Study. *J. Am. Chem. Soc.* **2009**, *131*, 15474-15482.

35. (a) Meyer, E. A.; Castellano, R. K.; Diederich, F., Interactions with aromatic rings in chemical and biological recognition. *Angew. Chem. Int. ed.* **2003**, *42*, 1210-50; (b) Salonen, L. M.; Ellermann, M.; Diederich, F., Aromatic rings in chemical and biological recognition: energetics and structures. *Angew. Chem. Int. ed.* **2011**, *50*, 4808-42; (c) Hunter, C. A.; Lawson, K. R.; Perkins, J.; Urch, C. J., Aromatic interactions. *J. Chem. Soc., Perkin Trans. 2* **2001**, (5), 651-669; (d) Ma, J. C.; Dougherty, D. A., The Cation- π Interaction. *Chem. Rev.* **1997**, *97*, 1303-1324; (e) Koide, S.; Sidhu, S. S., The Importance of Being Tyrosine: Lessons in Molecular Recognition from Minimalist Synthetic Binding Proteins. *ACS Chem. Biol.* **2009**, *4*, 325-334.
36. (a) Pal, D.; Chakrabarti, P., Cis peptide bonds in proteins: residues involved, their conformations, interactions and locations. *J. Mol. Biol.* **1999**, *294*, 271-88; (b) Thomas, K. M.; Naduthambi, D.; Zondlo, N. J., Electronic Control of Amide cis-trans Isomerism via the Aromatic-Prolyl Interaction. *J. Am. Chem. Soc.* **2006**, *128*, 2216-2217; (c) Zondlo, N. J., Aromatic-Proline Interactions: Electronically Tunable CH/ π Interactions. *Acc. Chem. Res.* **2013**, *46*, 1039-1049.
37. Pandey, A. K.; Thomas, K. M.; Forbes, C. R.; Zondlo, N. J., Tunable Control of Polyproline Helix (PPII) Structure via Aromatic Electronic Effects: An Electronic Switch of Polyproline Helix. *Biochemistry* **2014**, *53*, 5307-5314.
38. Aurora, R.; Creamer, T. P.; Srinivasan, R.; Rose, G. D., Local interactions in protein folding: lessons from the alpha-helix. *J. Biol. Chem.* **1997**, *272*, 1413-6.
39. Whittington, S. J.; Chellgren, B. W.; Hermann, V. M.; Creamer, T. P., Urea promotes polyproline II helix formation: implications for protein denatured states. *Biochemistry* **2005**, *44*, 6269-75.
40. Nozaki, Y.; Tanford, C., THE SOLUBILITY OF AMINO ACIDS AND RELATED COMPOUNDS IN AQUEOUS UREA SOLUTIONS. *J. Biol. Chem.* **1963**, *238*, 4074-81.
41. Robinson, D. R.; Jencks, W. P., THE EFFECT OF COMPOUNDS OF THE UREA-GUANIDINIUM CLASS ON THE ACTIVITY COEFFICIENT OF ACETYLTETRAGLYCINE ETHYL ESTER AND RELATED COMPOUNDS. *J. Am. Chem. Soc.* **1965**, *87*, 2462-70.

42. Tiffany, M. L.; Krimm, S., Extended conformations of polypeptides and proteins in urea and guanidine hydrochloride. *Biopolymers* **1973**, *12*, 575-587.
43. Mattice, W. L.; Mandelkern, L., Conformational properties of poly-L-proline in concentrated salt solutions. *Biochemistry* **1970**, *9*, 1049-58.
44. Rucker, A. L.; Creamer, T. P., Polyproline II helical structure in protein unfolded states: Lysine peptides revisited. *Protein Science : A Publication of the Protein Society* **2002**, *11*, 980-985.
45. Arunkumar, A. I.; Kumar, T. K.; Yu, C., Non-specific helix-induction in charged homopolypeptides by alcohols. *Biochim. biophys. Acta* **1997**, *1338*, 69-76.
46. (a) Steinberg, I. Z.; Harrington, W. F.; Berger, A.; Sela, M.; Katchalski, E., The Configurational Changes of Poly-L-proline in Solution. *J. Am. Chem. Soc.* **1960**, *82*, 5263-5279; (b) Kurtz, J.; Harrington, W. F., Interaction of poly-L-proline with lithium bromide. *J. Mol. Biol.* **1966**, *17* 440-55; (c) Schleich, T.; Von Hippel, P. H., Specific ion effects on the solution conformation of poly-L-proline. *Biopolymers* **1969**, *7*, 861-877.
47. Mandelkern, L.; Halpin, J. C.; Diorio, A. F.; Posner, A. S., Dimensional Changes in Fibrous Macromolecules: The System α -Keratin-Lithium Bromide. *J. Am. Chem. Soc.* **1962**, *84*, 1383-1391.
48. Holzwarth, G.; Backman, K., Electrostatic effects on polyproline I-II transitions. *Biochemistry* **1969**, *8*, 883-7.
49. Harrington, W. F.; Sela, M., Studies on the structure of poly-l-proline in solution. *Biochim. biophys. Aacta* **1958**, *27*, 24-41.
50. Mandelkern, L.; Stewart, W. E., THE EFFECT OF NEUTRAL SALTS ON THE MELTING TEMPERATURE AND REGENERATION KINETICS OF THE ORDERED COLLAGEN STRUCTURE. *Biochemistry* **1964**, *3*, 1135-7.
51. Zimmerman, S. S.; Scheraga, H. A., Stability of cis, trans, and nonplanar peptide groups. *Macromolecules* **1976**, *9*, 408-16.
52. Madison, V.; Kopple, K. D., Solvent-dependent conformational distributions of some dipeptides. *J. Am. Chem. Soc.* **1980**, *102*, 4855-4863.
- 53.(a) Kelly, M. A.; Chellgren, B. W.; Rucker, A. L.; Troutman, J. M.; Fried, M. G.; Miller, A. F.; Creamer, T. P., Host-guest study of left-handed polyproline II helix

- formation. *Biochemistry* **2001**, *40* (48), 14376-83; (b) Eker, F.; Griebenow, K.; Schweitzer-Stenner, R., Stable conformations of tripeptides in aqueous solution studied by UV circular dichroism spectroscopy. *J. Am. Chem. Soc.* **2003**, *125*, 8178-85; (c) Chen, K.; Liu, Z.; Kallenbach, N. R., The polyproline II conformation in short alanine peptides is noncooperative. *Proc. Natl. Acad. Sci. U S A* **2004**, *101*, 15352-7.
54. (a) Poon, C.-D.; Samulski, E. T.; Weise, C. F.; Weisshaar, J. C., Do Bridging Water Molecules Dictate the Structure of a Model Dipeptide in Aqueous Solution? *J. Am. Chem. Soc.* **2000**, *122*, 5642-5643; (b) Woutersen, S.; Hamm, P., Structure Determination of Trialanine in Water Using Polarization Sensitive Two-Dimensional Vibrational Spectroscopy. *J. Phys. Chem. B* **2000**, *104*, 11316-11320; (c) Woutersen, S.; Hamm, P., Isotope-edited two-dimensional vibrational spectroscopy of trialanine in aqueous solution. *J. Chem. Phys.* **2001**, *114*, 2727-2737; (d) Schweitzer-Stenner, R.; Eker, F.; Huang, Q.; Griebenow, K., Dihedral Angles of Trialanine in D₂O Determined by Combining FTIR and Polarized Visible Raman Spectroscopy. *J. Am. Chem. Soc.* **2001**, *123*, 9628-9633.
55. (a) Li, W.; Tailhades, J.; O'Brien-Simpson, N.; Separovic, F.; Otvos, L., Jr.; Hossain, M. A.; Wade, J., Proline-rich antimicrobial peptides: potential therapeutics against antibiotic-resistant bacteria. *Amino Acids* **2014**, *46*, 2287-2294; (b) Sadler, K.; Eom, K. D.; Yang, J. L.; Dimitrova, Y.; Tam, J. P., Translocating proline-rich peptides from the antimicrobial peptide bactenecin 7. *Biochemistry* **2002**, *41*, 14150-7; (c) Hittinger, E.; Kokil, A.; Weder, C., Synthesis and Characterization of Cross-Linked Conjugated Polymer Milli-, Micro-, and Nanoparticles. *Angew. Chem. Int. Ed.* **2004**, *43*, 1808-1811; (d) Fernandez-Carneado, J.; Kogan, M. J.; Pujals, S.; Giralt, E., Amphipathic peptides and drug delivery. *Biopolymers* **2004**, *76*, 196-203.
56. Crespo, L.; Sanclimens, G.; Montaner, B.; Pérez-Tomás, R.; Royo, M.; Pons, M.; Albericio, F.; Giralt, E., Peptide Dendrimers Based on Polyproline Helices. *J. Am. Chem. Soc.* **2002**, *124*, 8876-8883.
57. Farrera-Sinfreu, J.; Giralt, E.; Castel, S.; Albericio, F.; Royo, M., Cell-Penetrating γ -Amino-L-Proline-Derived Peptides. *J. Am. Chem. Soc.* **2005**, *127*, 9459-9468.
58. Farrera-Sinfreu, J.; Giralt, E.; Castel, S.; Albericio, F.; Royo, M., Cell-penetrating γ -amino-L-proline-derived peptides. *J. Am. Chem. Soc.* **2005**, *127*, 9459-68.

59. Fillon, Y. A.; Anderson, J. P.; Chmielewski, J., Cell Penetrating Agents Based on a Polyproline Helix Scaffold. *J. Am. Chem. Soc.* **2005**, *127*, 11798-11803.
60. Geisler, I.; Chmielewski, J., Probing length effects and mechanism of cell penetrating agents mounted on a polyproline helix scaffold. *Bioorg. Med. Chem. Lett.* **2007**, *17*, 2765-2768.
61. Stewart, K. M.; Horton, K. L.; Kelley, S. O., Cell-penetrating peptides as delivery vehicles for biology and medicine. *Org. Biomol. Chem.* **2008**, *6*, 2242-2255.
62. El-Andaloussi, S.; Jarver, P.; Johansson, H. J.; Langel, U., Cargo-dependent cytotoxicity and delivery efficacy of cell-penetrating peptides: a comparative study. *Biochem. J.* **2007**, *407*, 285-92.
63. (a) Otvos, L., Jr., The short proline-rich antibacterial peptide family. *Cell. mol. life sci. : CMLS* **2002**, *59*, 1138-50; (b) Li, W.; Tailhades, J.; O'Brien-Simpson, N. M.; Separovic, F.; Otvos, L., Jr.; Hossain, M. A.; Wade, J. D., Proline-rich antimicrobial peptides: potential therapeutics against antibiotic-resistant bacteria. *Amino Acids* **2014**, *46*, 2287-94.
64. Labeit, S.; Kolmerer, B., Titins: giant proteins in charge of muscle ultrastructure and elasticity. *Science* **1995**, *270*, 293-6.
65. Gutierrez-Cruz, G.; Van Heerden, A. H.; Wang, K., Modular motif, structural folds and affinity profiles of the PEVK segment of human fetal skeletal muscle titin. *J. biol. chem.* **2001**, *276*, 7442-9.
66. Bochicchio, B.; Tamburro, A. M., Polyproline II structure in proteins: identification by chiroptical spectroscopies, stability, and functions. *Chirality* **2002**, *14*, 782-92.
67. Cao, Q.; Wang, Y.; Bayley, H., Sequence of abductin, the molluscan 'rubber' protein. *Curr. biol. : CB* **1997**, *7*, R677-8.
68. Royce, P. M.; Steinmann, B. U., *Connective tissue and its heritable disorders: molecular, genetic, and medical aspects*. Wiley-Liss: 1993.
69. (a) Deber, C. M.; Bovey, F. A.; Carver, J. P.; Blout, E. R., Nuclear magnetic resonance evidence for cis-peptide bonds in proline oligomers. *J. Am. Chem. Soc.* **1970**, *92*, 6191-8; (b) Okabayashi, H.; Isemura, T.; Sakakibara, S., Steric structure of L-proline oligopeptides. II. Far-ultraviolet absorption spectra and optical rotations of L-proline oligopeptides. *Biopolymers* **1968**, *6*, 323-30.

70. (a) McCafferty, D. G.; Friesen, D. A.; Danielson, E.; Wall, C. G.; Saderholm, M. J.; Erickson, B. W.; Meyer, T. J., Photochemical energy conversion in a helical oligoproline assembly. *Proc. Natl. Acad. Sci.* **1996**, *93*, 8200-8204; (b) McCafferty, D. G.; Slate, C. A.; Nakhle, B. M.; Graham Jr, H. D.; Austell, T. L.; Vachet, R. W.; Mullis, B. H.; Erickson, B. W., Engineering of a 129-residue tripod protein by chemoselective ligation of proline-II helices. *Tetrahedron* **1995**, *51*, 9859-9872.
71. Ma, D.; Bettis, S. E.; Hanson, K.; Minakova, M.; Alibabaei, L.; Fondrie, W.; Ryan, D. M.; Papoian, G. A.; Meyer, T. J.; Waters, M. L.; Papanikolas, J. M., Interfacial Energy Conversion in RuII Polypyridyl-Derivatized Oligoproline Assemblies on TiO₂. *J. Am. Chem. Soc.* **2013**, *135*, 5250-5253.
72. Leem, G.; Morseth, Z. A.; Puodziukynaite, E.; Jiang, J.; Fang, Z.; Gilligan, A. T.; Reynolds, J. R.; Papanikolas, J. M.; Schanze, K. S., Light Harvesting and Charge Separation in a π -Conjugated Antenna Polymer Bound to TiO₂. *J. Phys. Chem. C* **2014**, *118*, 28535-28541.
73. (a) Yoon, Y.-R.; Lim, Y.-b.; Lee, E.; Lee, M., Self-assembly of a peptide rod-coil: a polyproline rod and a cell-penetrating peptide Tat coil. *Chem. Commun.* **2008**, *16*, 1892-1894; (b) Lim, Y.-b.; Moon, K.-S.; Lee, M., Recent advances in functional supramolecular nanostructures assembled from bioactive building blocks. *Chem. Soc. rev.* **2009**, *38*, 925-934.
74. Lewandowska, U.; Zajaczkowski, W.; Chen, L.; Bouillière, F.; Wang, D.; Koynov, K.; Pisula, W.; Müllen, K.; Wennemers, H., Hierarchical Supramolecular Assembly of Sterically Demanding π -Systems by Conjugation with Oligoprolines. *Angew. Chem. Int. Ed.* **2014**, n/a-n/a.
75. (a) Haas, E.; Wilchek, M.; Katchalski-Katzir, E.; Steinberg, I. Z., Distribution of end-to-end distances of oligopeptides in solution as estimated by energy transfer. *Proc. Natl. Acad. Sci. U. S. A.* **1975**, *72*, 1807-11; (b) Haas, E.; Katchalski-Katzir, E.; Steinberg, I. Z., Brownian motion of the ends of oligopeptide chains in solution as estimated by energy transfer between the chain ends. *Biopolymers* **1978**, *17*, 11-31.
76. Sahoo, H.; Roccatano, D.; Hennig, A.; Nau, W. M., A 10-Å Spectroscopic Ruler Applied to Short Polyprolines. *J. Am. Chem. Soc.* **2007**, *129*, 9762-9772.

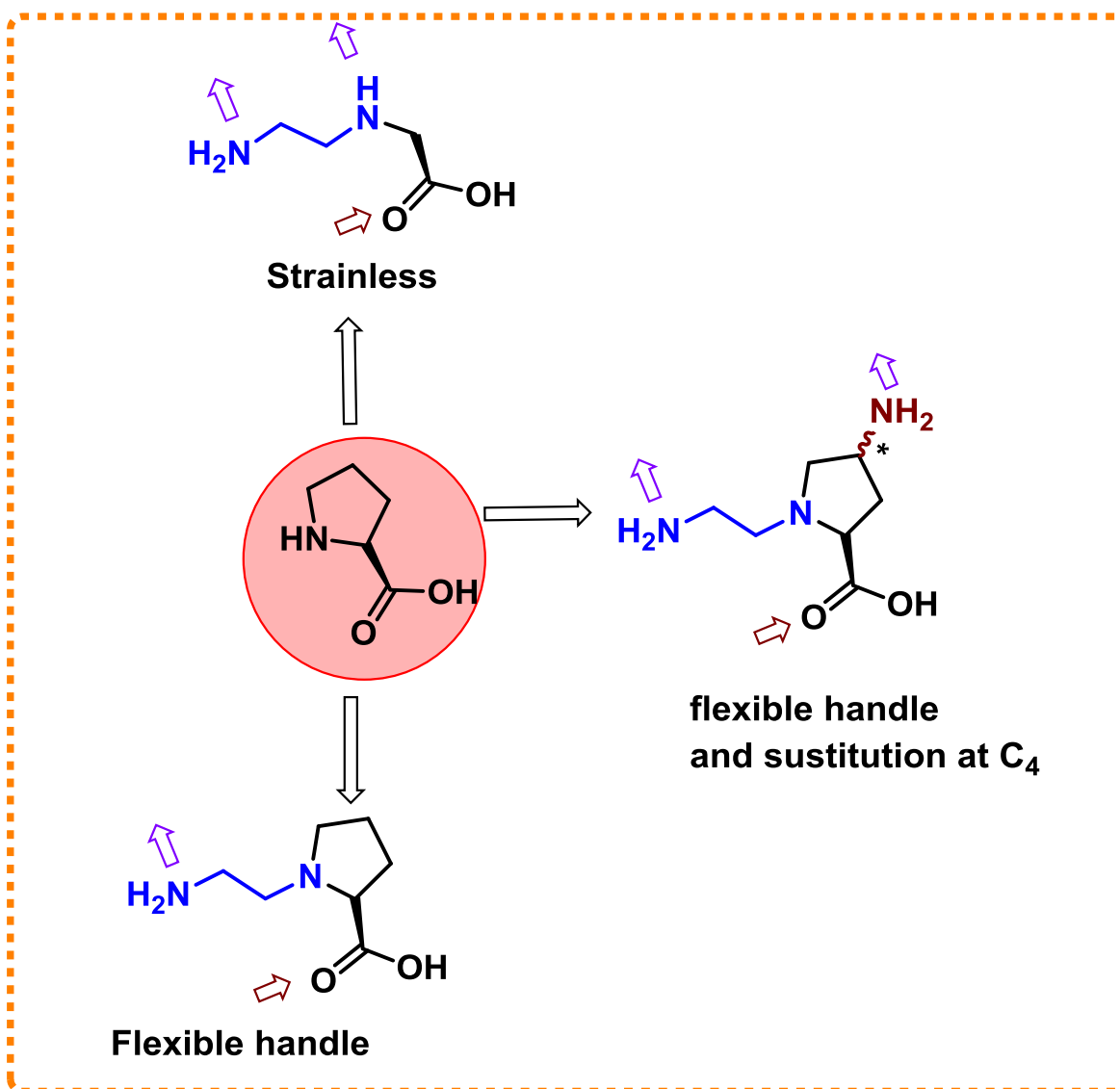
77. Stryer, L.; Haugland, R. P., Energy transfer: a spectroscopic ruler. *Proc. Natl. Acad. Sci. USA* **1967**, *58*, 719-726.
78. Schuler, B.; Lipman, E. A.; Steinbach, P. J.; Kumke, M.; Eaton, W. A., Polyproline and the “spectroscopic ruler” revisited with single-molecule fluorescence. *Proc. Natl. Acad. Sci. USA* **2005**, *102*, 2754-2759.
79. Barrett, G. C.; Elmore, D. T., *Amino Acids And Pept.* Cambridge University Press: New York, 1998.
80. (a) König, W.; Geiger, R., Eine neue Methode zur Synthese von Peptiden: Aktivierung der Carboxylgruppe mit Dicyclohexylcarbodiimid unter Zusatz von 1-Hydroxybenzotriazolen. *Chem. Bericht.* **1970**, *103*, 788-798; (b) Robertson, N.; Jiang, L.; Ramage, R., Racemisation studies of a novel coupling reagent for solid phase peptide synthesis. *Tetrahedron* **1999**, *55*, 2713-2720.
81. (a) Nishiyama, Y.; Ishizuka, S.; Kurita, K., O-(7-Azabenzotriazol-1-yl)-1,1,3,3-tetramethyluronium hexafluorophosphate-1-hydroxy-7-azabenzotriazole-copper(II) chloride: a promising epimerization-free segment coupling system for peptide synthesis. *Tetrahedron Lett.* **2001**, *42*, 8789-8791; (b) Nishiyama, Y.; Tanaka, M.; Saito, S.; Ishizuka, S.; Mori, T.; Kurita, K., A Racemization-Free Coupling Method for Peptides Having N-Methylamino Acids at the Carboxy-Termini. *CHEM. PHARM. BULL.* **1999**, *47*, 576-578.
82. Carpino, L. A.; Ionescu, D.; El-Faham, A.; Beyermann, M.; Henklein, P.; Hanay, C.; Wenschuh, H.; Bienert, M., Complex Polyfluoride Additives in Fmoc-Amino Acid Fluoride Coupling Processes. Enhanced Reactivity and Avoidance of Stereomutation†. *Org.Lett.* **2003**, *5*, 975-977.
83. Jiang, L.; Davison, A.; Tennant, G.; Ramage, R., Synthesis and application of a novel coupling reagent, ethyl 1-hydroxy-1H -1,2,3-triazole-4-carboxylate. *Tetrahedron* **1998**, *54*, 14233-14254.
84. Nishiuchi, Y.; Inui, T.; Nishio, H.; Bódi, J.; Kimura, T.; Tsuji, F. I.; Sakakibara, S., Chemical synthesis of the precursor molecule of the Aequorea green fluorescent protein, subsequent folding, and development of fluorescence. *Proc. Natl. Acad. Sci. USA* **1998**, *95*, 13549-13554.

85. Hiebl, J.; Baumgartner, H.; Bernwieser, I.; Blanka, M.; Bodenteich, M.; Leitner, K.; Rio, A.; Rovenszky, F.; Alberts, D. P.; Bhatnagar, P. K.; Banyard, A. F.; Baresch, K.; Esch, P. M.; Kollmann, H.; Mayrhofer, G.; Weihtrager, H.; Welz, W.; Winkler, K.; Chen, T.; Patel, R.; Lantos, I.; Stevenson, D.; Tubman, K. D.; Undheim, K., Large-scale synthesis of hematoregulatory nonapeptide SK&F 107647 by fragment coupling. *J. Pept. Res.* **1999**, *54*, 54-65.
86. (a) Whitmore, L.; Wallace, B. A., Protein secondary structure analyses from circular dichroism spectroscopy: Methods and reference databases. *Biopolymers* **2008**, *89*, 392-400; (b) Greenfield, N. J., Using circular dichroism spectra to estimate protein secondary structure. *Nat. Protocols* **2007**, *1*, 2876-2890; (c) Fasman, G. D., *Circular Dichroism and the Conformational Analysis of Biomolecules*. Springer US: 1996.
87. (a) Zotti, M. D.; Formaggio, F.; Crisma, M.; Peggion, C.; Moretto, A.; Toniolo, C., Handedness preference and switching of peptide helices. Part I: Helices based on protein amino acids. *J. Pept. Sci.* **2014**, *20*, 307-322; (b) Bovey, F. A.; Hood, F. P., Circular dichroism spectrum of poly-L-proline. *Biopolymers* **1967**, *5*, 325-326; (c) tiffany, M. L.; Krimm, S., Circular dichroism of poly-L-proline in an unordered conformation. *Biopolymers* **1968**, *6*, 1767-1770.
88. Helbecque, N.; Loucheux-Lefebvre, M. H., Critical chain length for polyproline-II structure formation in H-Gly-(Pro)_n-OH. *Int. J. Pept. Protein Res.* **1982**, *19*, 94-101.
89. Dukor, R. K.; Keiderling, T. A.; Gut, V., Vibrational circular dichroism spectra of unblocked proline oligomers. *Int. J. Pept. Protein Res.* **1991**, *38*, 198-203.
90. Dukor, R. K.; Keiderling, T. A., Mutarotation studies of poly-L-proline using FTIR, electronic and vibrational circular dichroism. *Biospectroscopy* **1996**, *2*, 83-100.
91. Barron, L. D.; Hecht, L.; Blanch, E. W.; Bell, A. F., Solution structure and dynamics of biomolecules from Raman optical activity. *Prog. Biophys. Mol. Biol.* **2000**, *73*, 1-49.
92. Nafie, L. A., INFRARED AND RAMAN VIBRATIONAL OPTICAL ACTIVITY: Theoretical and Experimental Aspects. *Ann. Rev. Phys. Chem.* **1997**, *48*, 357-386.
93. Kapitán, J.; Baumruk, V.; Bouř, P., Demonstration of the Ring Conformation in Polyproline by the Raman Optical Activity. *J. Am. Chem. Soc.* **2006**, *128*, 2438-2443.

94. Lam, S. L.; Hsu, V. L., NMR identification of left-handed polyproline type II helices.
Biopolymers **2003**, *69*, 270-281.

Chapter-2

Synthesis and Study of Foldamer Properties of Unnatural (*N*-aminoethyl) Glycyl and Pyrrolidine Peptides of Different Length



2. Introduction

Most of the biological events predominantly result from their compact conformation, stabilized by a collection of non-covalent interactions.¹ The three-dimensional conformations of biopolymers is embedded in the ‘information-rich surfaces’, which include molecular recognition, primarily responsible for various biological processes.² A number of synthetic designs have emerged to study the structural diversity and functional characteristics of polypeptides and many of the structural analogues mimic the molecular functions of natural peptides.

Proteins are polypeptides composed of amino acid residues linked together by amide bond in definite sequences. The two key secondary structural elements are α -helices and β -sheets found in folded proteins, which arise from intrachain and interchain H-bonds respectively. α -Helices (Figure 1A) are formed by hydrogen bonding in peptide backbone via carbonyl carbons and amide protons. The intrastrand hydrogen bonds possible between backbone NH and C=O in residues of i and $i + 4$ can result in a stable secondary structure. Such disposition of H-bonding produces a *helical* coiling of the peptide backbone such that the side chains on backbone lie on the exterior of the helix and perpendicular to its axis.

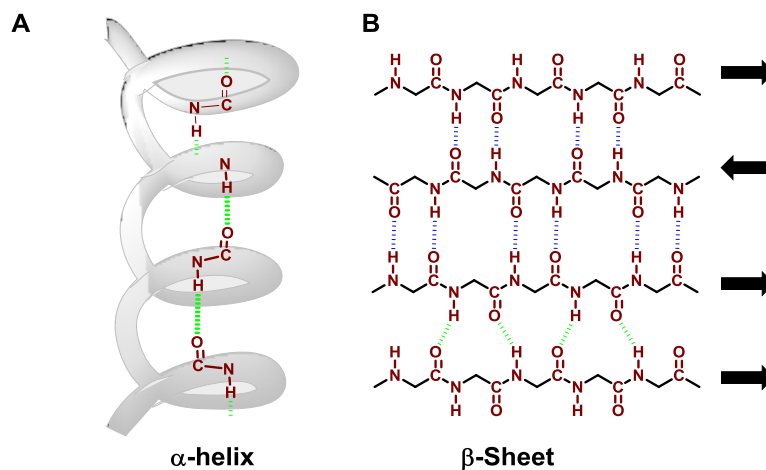


Figure 1. Hydrogen bonding pattern in (A) α -helix, (B) β -sheets.

β -Sheets (Figure 1B) are derived from similar hydrogen bonds but from interchains rather than the intrachain as in the case of α -helix. The two chains of β -sheets can have similar (parallel) or opposite (anti-parallel) orientation.

The 3_{10} -helix (Figure 2) is the fourth most common form of secondary structure in proteins after α -helices, β -sheets, and reverse turns. The 3_{10} -helix is characterized by having at least two consecutive hydrogen bonds between the main-chain carbonyl oxygen of residue i , and the main-chain amide hydrogen of residue $i+3$.

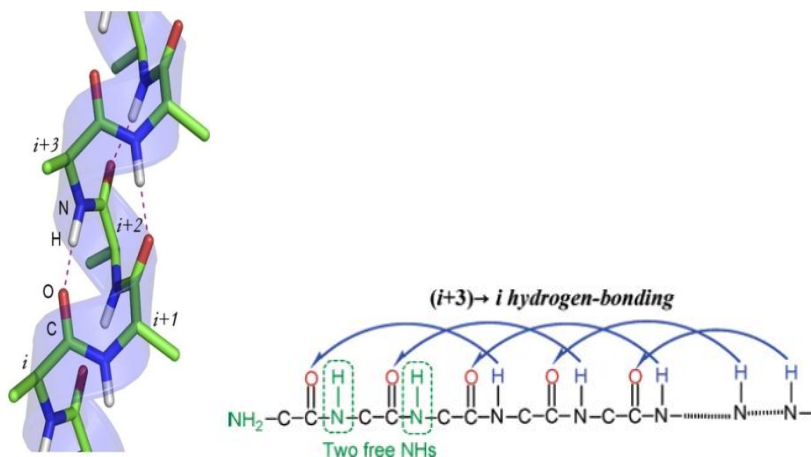


Figure 2. (A) A representative model of 3_{10} helix, (B) Intramolecular hydrogen-bonding pattern of a 3_{10} -helix.

The π -helix (Figure 3) is more packed than the α -helix with i to $i+5$ hydrogen bonding between carbonyl oxygen and nitrogen backbone atoms. A single turn of π -helix contains 16 atoms and hence defined as a 4.4_{16} -helix.³

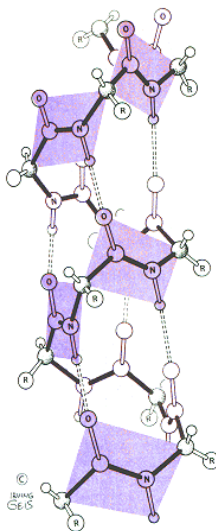


Figure 3. π -helices with the $(i+5, i)$ π -type hydrogen bonds (Black dashed lines).

The two key secondary structural elements found in folded proteins are α -helices and β -sheets, which arise respectively from intrachain and interchain H-bond. Apart from these secondary structures, an important well-characterized secondary structure is the Polyproline II (PPII) helix. The PPII helices correspond to unique local folds and found to occur in numerous globular proteins. As compared to α -helices, and β -sheets, the study of PPII *helices* although important, has attracted less attention, mainly due to four factors:

- ❖ Polyprolines have only H-bond acceptor groups (C=O) and do not have H-bond donor amide protons (Figure 4), necessary for hydrogen bonding and stabilization of secondary structure.
- ❖ Polyproline conformations (PPII and PPI) are stable only due to steric factors.
- ❖ PPII helical conformation, identified as unstable low prolyl intermediate conformation in protein folding/unfolding transitions.
- ❖ Only a few markers are available for unambiguous PPII assignment and the methods using different parameters leads to in variability in assignments.

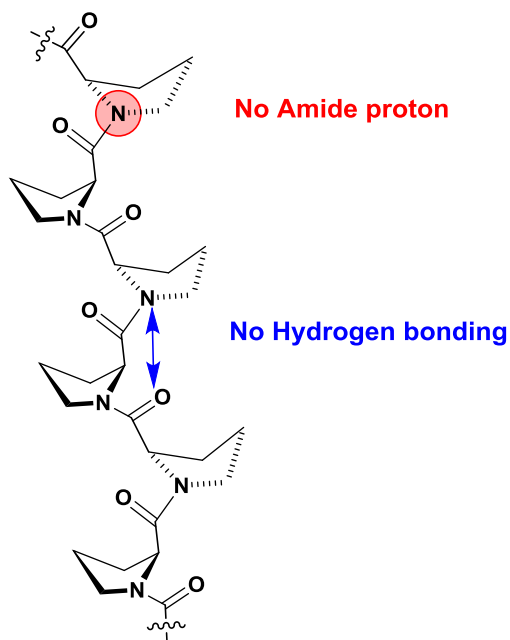


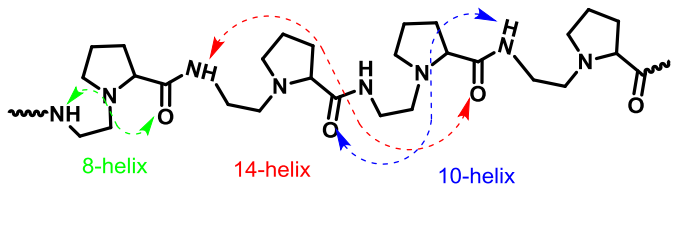
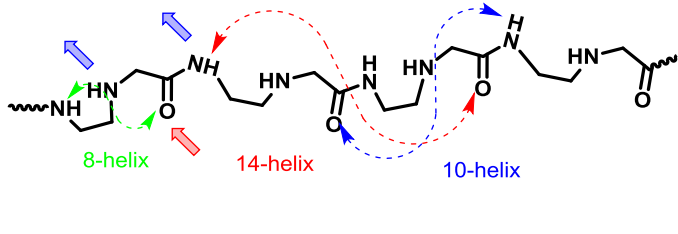
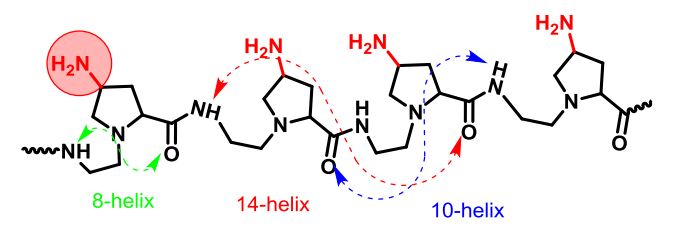
Figure 4. Polyproline.

2.1 Present work: Rationale

α -Helix and β -pleated sheet are formed by intermolecular or intramolecular H-bonding. The peptide backbone contains equal number of H-bond donor and H-acceptor groups. The work presented in this chapter is directed towards introducing H-bonding NH_2 groups as substituents on proline ring to examine their effects on interaction of secondary structure.

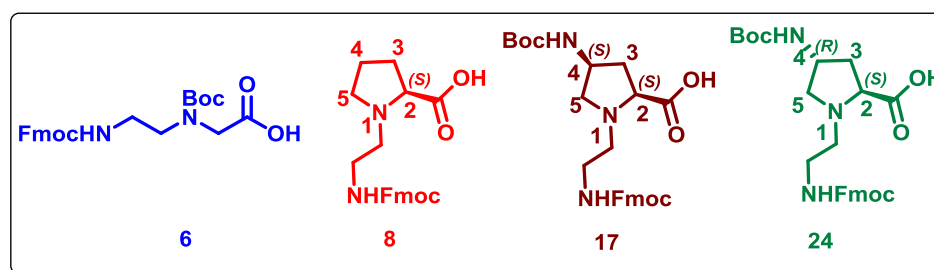
- ❖ Additional flexibility of the alkyl linkage within the backbone peptide provides the torsional freedom in the chain necessary to adopt a variety of conformations
- ❖ An unequal H-bond donor and acceptor group (2:1) in backbone allows investigation of the plethora of possible secondary structures.
- ❖ The effect of stereochemistry of H-bonding substituent at C4 proline ring is important in dictating the secondary structures adopted by the peptides.

Table 1. Modification in polyproline backbone and proposed secondary structures.

H-bond donor	Proposed structures
In backbone	
I) In backbone II) Unequal H-bond donor	
I) In backbone II) Side chain III) Stereochemistry	

The specific objectives of this chapter are

- Synthesis of monomers, N^1 -(Fmoc-aminoethyl)glycine (**6**), N^1 -(Fmoc-aminoethyl) proline (**8**), $(2S,4S)$ - N^1 -(Fmoc-aminoethyl)-4NH-(*t*-Boc)-aminoproline (**17**) and $(2S,4R)$ - N^1 -(Fmoc-aminoethyl)-4NH-(*t*-Boc)-aminoproline (**24**).



- Solid phase synthesis of homo oligomers of different lengths derived from these monomers.
- Cleavage of synthesized peptides from the solid support, purification and characterization.
- Investigation of conformation of these peptides by using CD and FT-IR spectroscopy.
- Effect of different solvents on conformation of the peptides.

2.5 Results

2.5.1 Synthesis of fully protected monomers

The synthesis of N^1 -(Fmoc-aminoethyl)glycine (**6**), N^1 -(Fmoc-aminoethyl)-proline (**8**), $(2S,4S)$ - N^1 -(Fmoc-aminoethyl)-4NH-(*t*-Boc)-aminoproline, (**17**) and $(2S,4R)$ - N^1 -(Fmoc-aminoethyl)-4NH-(*t*-Boc)-aminoproline (**24**) monomers having a combination of N^1 -Fmoc and N^4 -Boc protecting groups were chosen. The peptide synthesis can be achieved by choosing combination chemistry suitable for alternative N-Boc and N-Fmoc protecting groups (Figure 5).

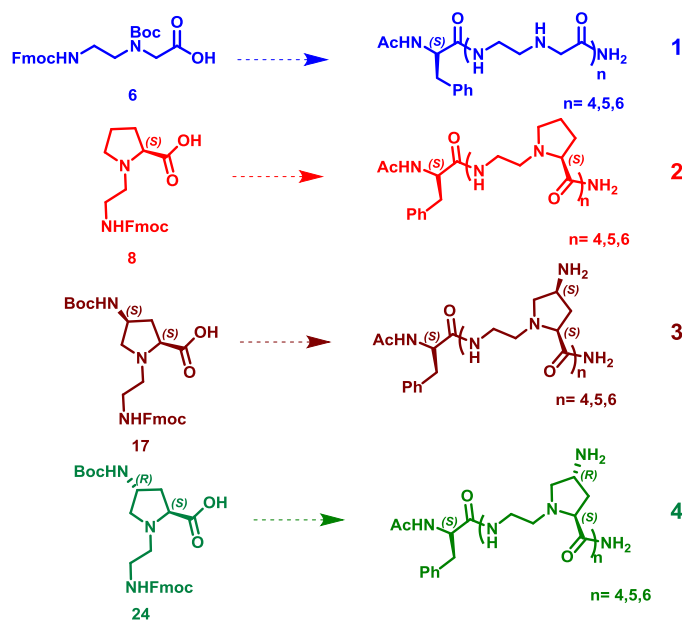


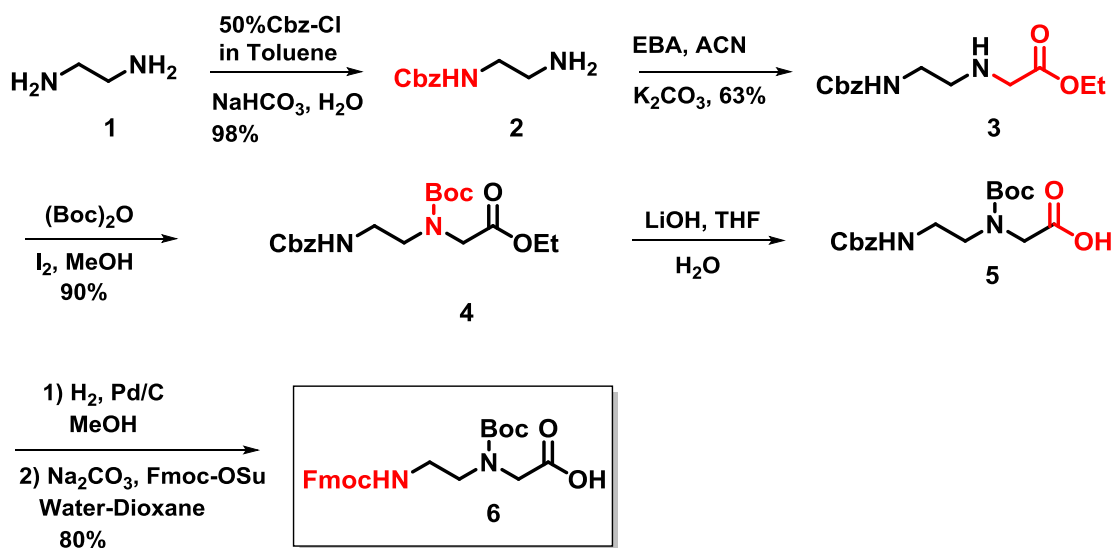
Figure 5. Structures of monomers and opposed oligomers.

2.5.1a Synthesis of N¹-(Fmoc-aminoethyl)glycine (6)

The synthesis of orthogonally protected N¹-(Fmoc-aminoethyl)glycine (**6**) monomer was achieved in five steps from the commercially available ethylenediamine **1** (Scheme 1). Selective monoprotection of ethylenediamine was achieved by its reaction with 1 equivalent benzylchloroformate in water/dioxane, in the presence of Na₂CO₃, to yield benzyl (2-aminoethyl) carbamate **2**. This was then alkylated with ethyl bromoacetate in acetonitrile and triethyl amine to obtain the N-alkylated compound **3**. The appearance of peaks at δ 7.3-7.4 ppm and 1.27 ppm in ¹H NMR shows the presence of Cbz (aromatic) and ester (methyl) respectively in the desired product **3**. The compound **3** upon treatment with (Boc)₂O in presence of molecular iodine as a catalyst yielded N-Boc protected compound **4**, with signals at δ = 1.4 ppm in the ¹H NMR spectrum corresponding to the Boc-group.⁴ The ethyl ester in compound **4** was hydrolysed to acid by using LiOH in THF-water. The N¹-Cbz group was deprotected to amine by hydrogenation using 10%-Pd/C in methanol. The disappearance of aromatic signals of Cbz group in ¹H NMR and the appearance of ninhydrin positive spot on TLC indicated complete deprotection of Cbz group to the amine. The N¹-amine was *in situ* protected as Fmoc, by reaction with Fmoc-Cl to yield the fully protected N¹-(Fmoc-aminoethyl)glycine (**6**). The appearance of ¹H signals

in the aromatic region typical of Fmoc group (δ 7.28-7.37 and 7.53-7.74) confirmed the structure of the monomer **6**.

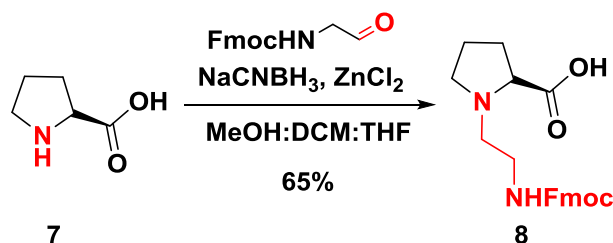
Scheme 1. Synthesis of N¹-(Fmoc-aminoethyl) glycine



2.5.1b Synthesis of N¹-(Fmoc-aminoethyl)-aminoproline (**8**)

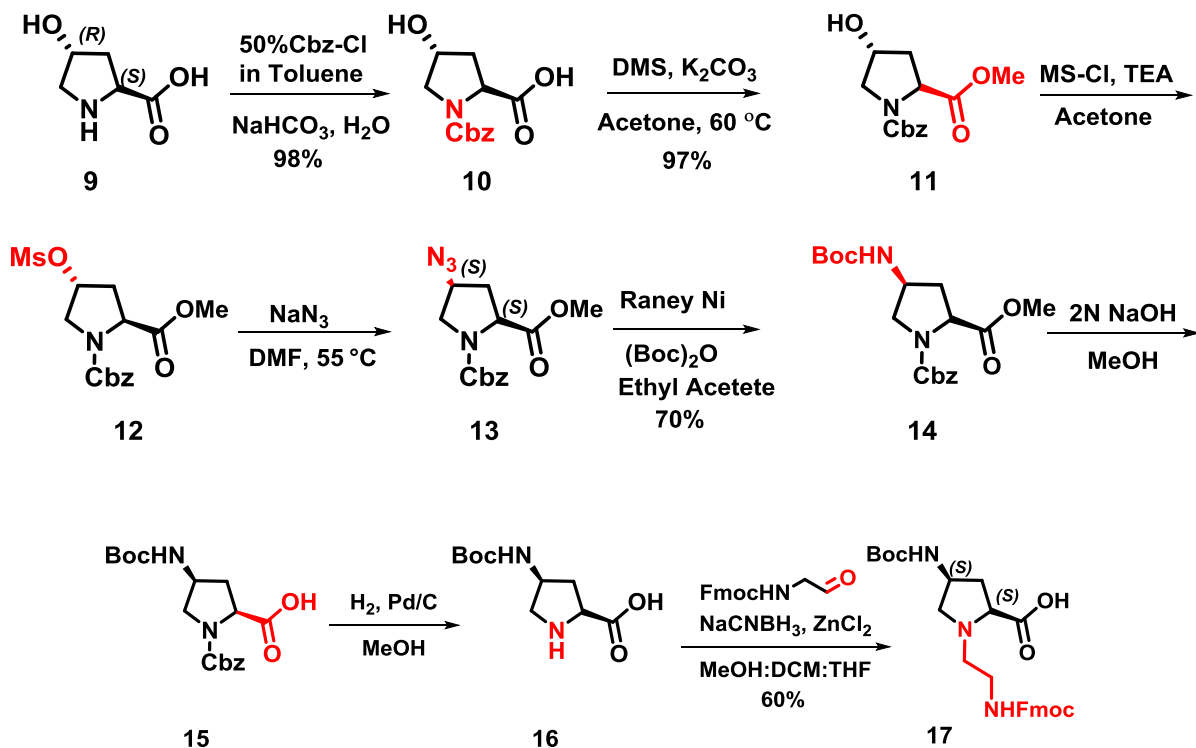
The synthesis of N¹-(Fmoc-aminoethyl)-aminoproline (**8**) was achieved by using reductive amination of the commercially available proline with Fmoc-glycinal in presence of ZnCl₂ as a catalyst to yield **8** with signals at $\delta = 1.4$ ppm in the ¹H NMR spectrum corresponding to the Fmoc-group (δ 7.28-7.37 and 7.53-7.74) (Scheme 2).⁵

Scheme 2. Synthesis of N¹-(Fmoc-aminoethyl)-proline



2.5.1c (2*S*,4*S*)-N¹-(Fmoc-aminoethyl)-4NH-(*t*-Boc)-aminoproline (17)

The synthesis of orthogonally protected (2*S*,4*S*)-N¹-(Fmoc-aminoethyl)-4NH-(*t*-Boc)-aminoproline (**17**) was achieved in eight steps from the naturally occurring *trans*-4*R*-hydroxyproline **9** (Scheme 3). The reaction of *trans*-4*R*-hydroxyproline with benzyloxycarbonylchloroformate in water/dioxane, in the presence of Na₂CO₃, yielded N-benzyloxycarbonyl-4*R*-hydroxyproline **10**. The appearance of aromatic ($\delta = 7.2$ -7.3 and benzylic $\delta = 5.1$) signals in ¹H NMR spectrum of compound **10** confirmed its structure.

Scheme 3. Synthesis of (2*S*,4*S*)-N¹-(Fmoc-aminoethyl)-4NH-(*t*-Boc)-aminoproline

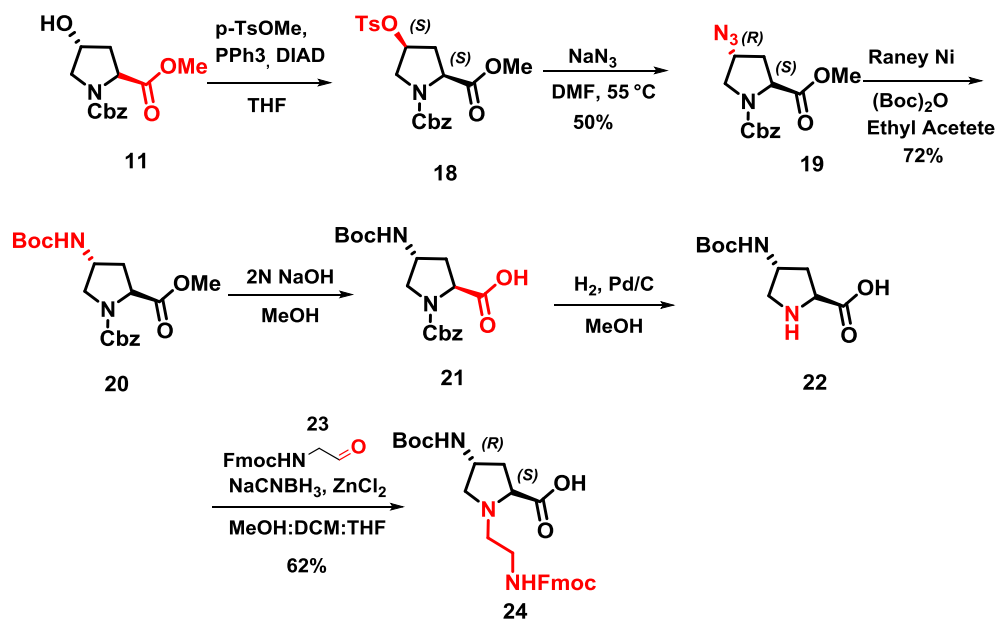
Compound **10** upon treatment with dimethylsulphate (DMS) in acetone/K₂CO₃ yielded the corresponding methyl ester **11**, which showed two signals in ¹H NMR at $\delta = 3.75$ (minor) and 3.54 (major) in corresponding to the methyl (-CH₃) group of the ester arising from two rotamers. The 4*R*-OH group in **11** was converted to the mesyl derivative **12** treatment with methanesulfonylchloride. The mesylate **12** was transformed to the 4*S*-azide **13** by reaction with with NaN₃ in DMF. The reaction was accompanied by inversion of stereochemistry at C-4. A peak at 2108 cm⁻¹ seen in the IR spectrum confirmed the

conversion of mesyl to azide which was selectively reduced to the corresponding amine using Raney-Ni as a catalyst without affecting the N1-Cbz group. The 4*S*-aminogroup was protected *in situ* using Boc anhydride to yield the N⁴-*t*-Boc derivative **14**, confirmed by ¹H signals at δ 1.44 for *t*-Boc and at δ 5.2 for NH protons. The methyl ester **14** was hydrolysed to acid by treating with aq. NaOH (2N) in MeOH:water. The N1-benzyloxycarbonyl group on compound **15** was deprotected by hydrogenation with 10% Pd-C as a catalyst to yield the free amine **16**. The N¹ amine was reacted with Fmoc-glycinal in presence of ZnCl₂/NaCNBH₃ to obtain N1-alkylated compound **17**. The appearance of ¹H signals in the aromatic region indicative of Fmoc group (δ 7.25-7.38 and 7.52-7.73) confirmed the structure of monomer **17**.

2.5.1d Synthesis of (2*S*,4*R*)-N1-(Fmoc-aminoethyl)-4*R*-(*t*-Boc)-N⁴ aminoproline (**24**)

A similar strategy was used for the synthesis of (2*S*,4*R*)-N1-(Fmoc-aminoethyl)-4*R*-(*t*-Boc)-N⁴-aminoproline (**24**) starting from N1-benzyl-2-methyl(2*R*,4*R*)-4-hydroxypyrrolidine-1,2-dicarboxylate **11**. The 4*R*-OH group of compound **11** was converted into 4*S*-O-tosylate **18** by using Mitsunobu reaction with DIAD/PPh₃ and methyl-*p*-toluenesulfonate, the reaction accompanied by an inversion of configuration at C-4.

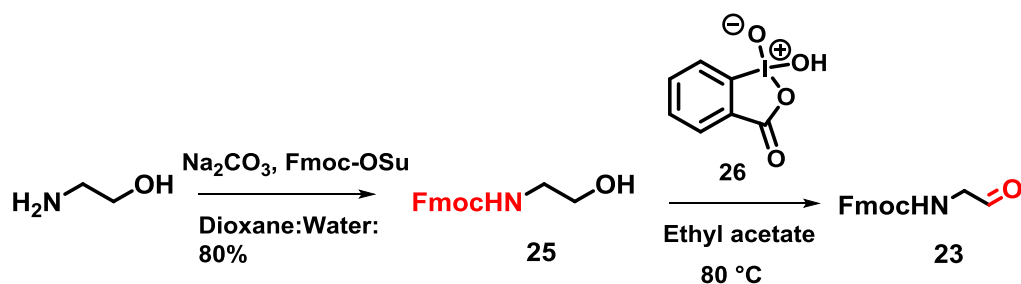
Scheme 4. Synthesis of (2*S*,4*R*)-N1-(Fmoc-aminoethyl)-4NH-(*t*-Boc)-aminoproline



The reaction of 4*S*-O-tosylate **18** with NaN₃ in DMF resulted in a second inversion of stereochemistry at C-4 to yield (2*S*, 4*R*)-N1-(Cbz)-azido-L-proline methyl ester **19**. The appearance of ¹H NMR signals at δ 7.23-7.29 for aromatic protons, at δ 4.93-5.19 for benzylic protons and at δ 4.35-4.43 for C^γ proton and a peak at 2108 cm⁻¹ in IR spectrum of azide confirmed its structure. Compound **19** was selectively reduced using Raney-Ni to the corresponding amine (without affecting the N1-Cbz group) which was *in situ* protected by reaction with Boc anhydride to yield N⁴-*t*-Boc compound **20**, whose structure was confirmed by the appearance of ¹H signals for *t*-Boc at δ 1.40 and at δ 4.70 for NH proton. The methyl ester in compound **20** was hydrolysed to acid by aq. NaOH (2N). N1-Cbz group in **21** was deprotected by hydrogenation using 10% Pd/C to give the imine **22**. The disappearance of aromatic signals of Cbz group in ¹H NMR and the appearance of ninhydrin positive spot on TLC indicated complete deprotection of Cbz group to amine. The N1-amine **22** was reacted with Fmoc-glycinal **23** in presence of ZnCl₂/NaCNBH₃ to obtain the N1-alkylated compound **24**. Conformation of structure was shown by the appearance of ¹H signals in the aromatic region for Fmoc group at δ 7.25-7.38 and 7.52-7.73.

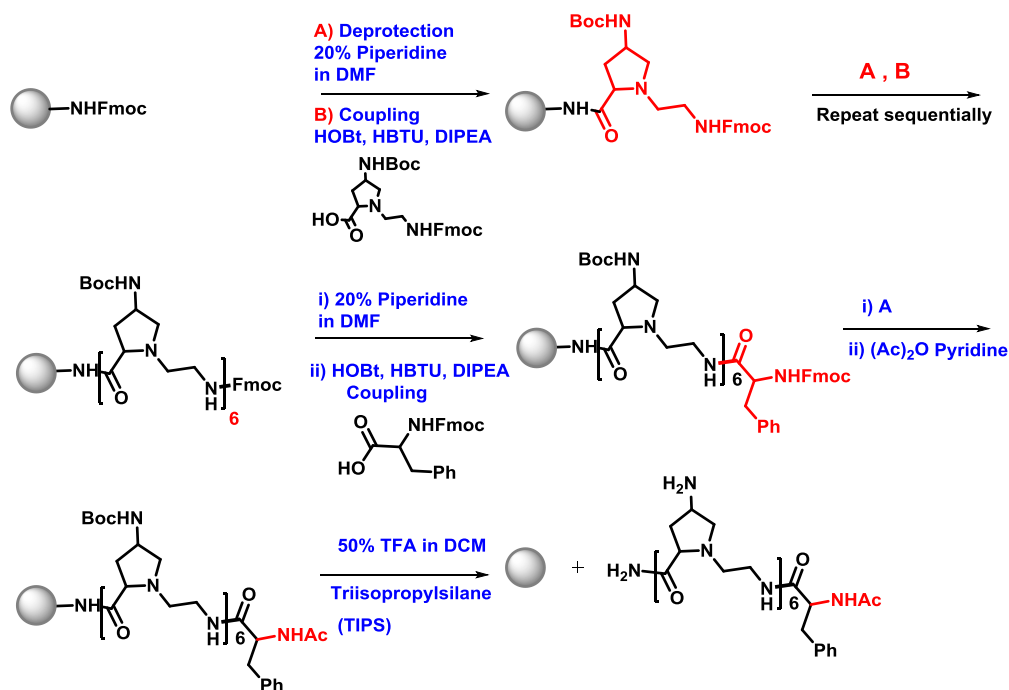
The synthesis of N¹-Fmoc-aminoaldehyde was done from the commercially available ethanolamine which was first protected by Fmoc-Osu (Scheme 5) to The *N*-Fmoc-ethanolamine (**25**). This was then oxidized using 1-hydroxy-1, 2-benziodoxol-3(1*H*)-one 1-oxide (2-Iodoxybenzoicacid, IBX) (**26**) to the corresponding *N*-Fmoc-aminocetaldehyde (**23**) in 90-95 % yield.

Scheme 5. Synthesis of *N*-Fmoc-aminoacetaldehyde



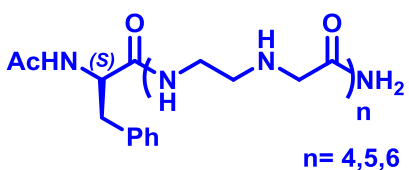
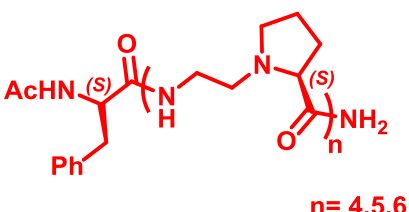
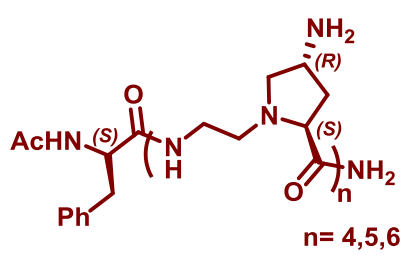
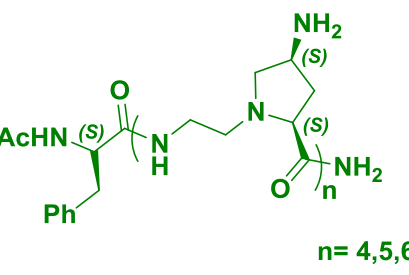
2.5.2 Solid phase synthesis of homo oligopeptides 1-4

The synthesis of homo oligopeptides of different lengths (**n=4, 5, 6**) were done using solid phase peptide synthesis protocols on the commercially available rink amide resin using standard Fmoc chemistry (Scheme 6). The synthesis was done from the C-terminus to the N-terminus using protected monomers (**6, 8, 17, 23**). The Kieselghur supported N,N-dimethylacrylamide resin (with Rink-amide linker) having Fmoc group was deprotected with 20% piperidine in DMF and the monomers as free acids were coupled sequentially using the *in situ* activation of amino acid (3 eq.) in presence of HBTU as a coupling reagent and HOBt and DIPEA as catalyst and racemisation-suppressant. The coupling reaction was repeated by using N-Methyl-2-pyrrolidone (NMP) as solvent. The deprotection reactions were done by using 20% piperidine in DMF and monitored using qualitative Chloranil test⁶ for iminoacids. The terminal amino group of the final peptide was capped with Ac₂O and the peptide was cleaved from the resin using 20% TFA in DCM. As the removal of *t*-Boc requires stronger acidic conditions, the deprotection of N⁴-*t*-Boc group on *Amp* residues of the synthesized peptide was carried out with 90% TFA in DCM. Since *t*-Butyl cation formed during the deprotection of *t*-Boc from the final peptide can lead to N-alkylation of the amines, 0.1% triisopropylsilane (TIPS) was used as a scavenger to prevent such side reactions during peptide-cleavage and *t*-Boc deprotection. The N-terminal acetylated and C-terminal amidated peptides were purified on semi-preparative RP-18 HPLC column using water-acetonitrile gradient containing 0.1% TFA.

Scheme 6. Solid phase synthesis of **1-4**

Thus, the homooligopeptides **1-4** (Table 2) of different lengths (tetramer, pentamer and hexamer) were synthesized from appropriate N-Fmoc-protected monomers N¹-(Fmoc-aminoethyl)glycine (**6**) N¹-(Fmoc-aminoethyl)-proline (**8**), (2*S*,4*S*)-N¹-(Fmoc-aminoethyl)-4NH-(*t*-Boc)-aminoproline (**17**), and (2*S*,4*R*)-N¹-(Fmoc-aminoethyl)-4NH-(*t*-Boc)-aminoproline (**24**) proline monomers. The amino acid phenylalanine (Phe) was included at the N-terminus for all peptides. Since it has aromatic side chain, the concentration of peptide stock-solutions can be determined directly by using UV-absorbance. All peptides contained phenylalanine at N-terminus and hence any effect on polyproline helix stability from this residue is same for all peptides.

Table 2. Synthesis of homooligopeptides **1-4** and Calculated and observed masses for peptides.

Sr No.	Peptides	Mol. Formula	Mass (cal)	Mass (obs)
1	 $n = 4, 5, 6$	n=4 $C_{27}H_{46}N_{10}O_6$	607.72	607.25 [M+1] ⁺
		n=5 $C_{31}H_{54}N_{12}O_7$	707.85	707.36 [M+1] ⁺
		n=6 $C_{35}H_{62}N_{14}O_8$	807.97	807.65 [M+1] ⁺
2	 $n = 4, 5, 6$	n=4 $C_{39}H_{62}N_{10}O_6$	789.96	789.70 [M+Na] ⁺
		n=5 $C_{46}H_{74}N_{12}O_7$	930.15	929.67 [M+Na] ⁺
		n=6 $C_{53}H_{86}N_{14}O_8$	1047.36	1047.51 [M]
3	 $n = 4, 5, 6$	n=4 $C_{39}H_{66}N_{14}O_6$	828.04	827.42 [M+1] ⁺
		n=5 $C_{46}H_{79}N_{17}O_7$	1005.24	1004.77 [M+Na] ⁺
		n=6 $C_{53}H_{92}N_{20}O_8$	1160.43	1159.41 [M+Na] ⁺
4	 $n = 4, 5, 6$	n=4 $C_{39}H_{66}N_{14}O_6$	850.02	850.13 [M+Na] ⁺
		n=5 $C_{46}H_{79}N_{17}O_7$	1005.24	1004.67 [M+Na] ⁺
		n=6 $C_{53}H_{92}N_{20}O_8$	1160.43	1160.20 [M+Na] ⁺

All peptide oligomers were purified by HPLC and characterized by MALDI-TOF. The purity of the peptides as determined using analytical RP-18 HPLC was found to be

greater than 98%. The structural integrity of the peptides was further confirmed by MALDI-TOF mass spectrometry data which agreed closely with the calculated values (Table 2)

2.5.2a Determination of the peptide concentration in stock solution

Determination of the exact concentration of the peptide solutions usually poses a problem. Even after several hours of drying under vacuum, peptides retain significant amounts of water, the amount of which varies with drying conditions and times.⁷ Basic amino acids retain counter ions such as acetyl and trifluoroacetyl, arising from additives used during cleavage and purification procedures. Methods such as quantitative amino acid analysis have been employed to determine the exact concentration of the peptide solutions. However these methods are tedious and the concentration of peptide stock solution may change with time. To discriminate these problems in the present study, the amino acid phenylalanine (Phe) was included at the N-terminus for all peptides. Since it has aromatic side chain, the concentration of peptide stock-solutions can be determined directly by using UV-absorbance ($\epsilon_{259} = 2 \times 10^2 \text{ m}^{-1}\text{cm}^{-1}$). All peptides contained phenylalanine at N-terminus and hence any effect on polyproline helix stability from this residue is same for all peptides.

2.6 CD Spectroscopic Studies

There are several methods for determination of polyproline conformation known in literature which include NMR, UV, resonance Raman spectroscopy and chiroptical spectroscopies. Circular Dicroism (CD) is a quantitative method to determine the secondary structure of protein and synthetic polypeptides that adopt different conformations under different conditions (Figure 6). The spectra of these molecules in the far ultraviolet (UV) regions are dominated by the $n \rightarrow \pi^*$ and $\pi \rightarrow \pi^*$ transitions of amide groups. The different secondary structures in peptides give rise to characteristic CD patterns. The three major electronic transitions in amides are (i) $n \rightarrow \pi^*$ transition at 220-225 nm polarized along the carbonyl bond, (ii) $\pi \rightarrow \pi^*$ transition at 185- 200 nm polarized in the direction of the C-N bond, and (iii) $\pi \rightarrow \pi^*$ transition at 140 nm polarized

approximately perpendicular to the C-N bond direction. The interaction between these transitions gives rise to CD spectra of peptides.

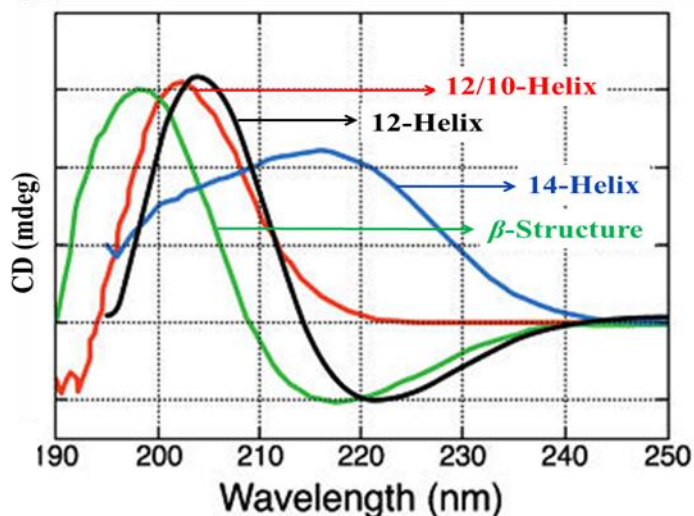


Figure 6. Circular dichroism spectra of secondary structure of different peptides.

The far UV CD spectra of an amide shows bands associated with $\pi \rightarrow \pi^*$ and $n \rightarrow \pi^*$ electronic transitions. The *helices* found in both α - and β -peptides, show the $\pi \rightarrow \pi^*$ band near 205 to 212 nm and $n \rightarrow \pi^*$ transition near 215-225 nm.^{8,9} The CD spectrum of the 12-helix (Figure 6, black) contains the $\pi \rightarrow \pi^*$ transition band at 205 nm and $n \rightarrow \pi^*$ transition near 220 nm.^{10,11} On the other hand, in the 14-helix (Figure 6, blue) $\pi \rightarrow \pi^*$ as well as $n \rightarrow \pi^*$ transitions give only one broad band near 215 nm in solution.^{11,12} The 10/12-helix (Figure 5, red) formed by mixed peptides shows only one broad band with a maximum below 210 nm.¹³

The possible secondary structure of homooligomers **1-4** with respect to oligomer length, at different concentrations, and different solvents were studied with CD spectroscopy. The peptides **3** and **4** both have amino groups and their protonation status may influence their secondary structures. Hence CD spectral studies were done at pH 7.2.

2.6.1 Circular Dichroism (CD) studies at pH-7.2

The conformations of peptides **1** (*aeg*₄, *aeg*₅, *aeg*₆), **2** (*ae-pro*₄, *ae-pro*₅, *ae-pro*₆), **3** (*ae-4R-Amp*₄, *ae-4R-Amp*₅, *ae-4R-Amp*₆) and **4** (*ae-4S-amp*₄, *ae-4S-amp*₅, *ae-4S-amp*₆), were investigated using the CD spectral data recorded sodium phosphate buffer (pH 7.2) shown in Figure 7.

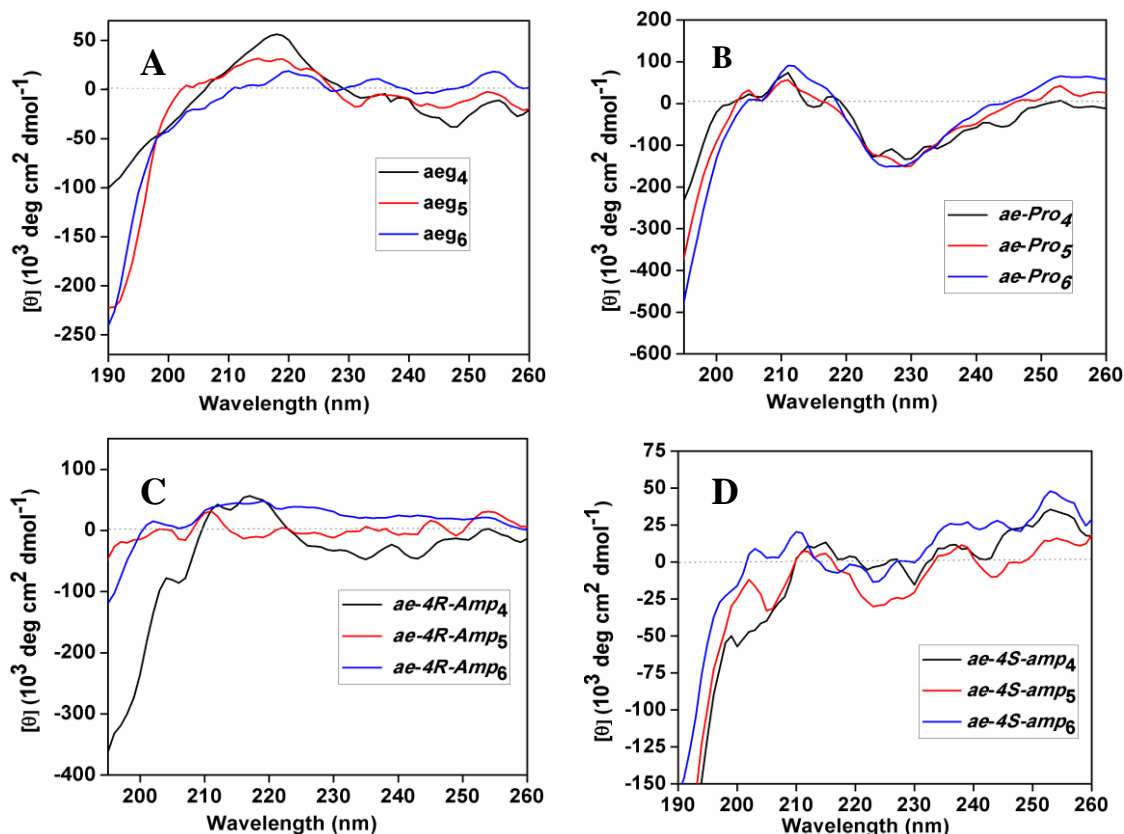


Figure 7. CD spectra of polyamides **1-4** at 25°C in 10 mM phosphate buffer (pH 7.2); (A) **1** (*aeg*₄, *aeg*₅, *aeg*₆), (B) **2**, (*ae-Pro*₄, *ae-Pro*₅, *ae-Pro*₆), (C) **3**, (*ae-4R-Amp*₄, *ae-4R-Amp*₅, *ae-4R-Amp*₆) and (D) **4**, (*ae-4S-amp*₄, *ae-4S-amp*₅, *ae-4S-amp*₆); all measurements are done at peptide concentration of 200μM.

The conformational average resulting from the presence of many local structures can lead to negative or positive ellipticity in 190-260 nm region. No significant CD signals were seen in this region representing any local conformation. The peptides **1-4** therefore have a low structural organization possibly due to i) high content of non-chiral aminoethyl (*ae*) and glycine functionality and ii) multiple interchanging conformations due to flexibility of peptide backbones by lack of any H-bonding in buffer.

2.6.2 Circular Dichroism (CD) studies in trifluoroethanol (TFE)

It is well known that TFE promotes helical structure in peptides.¹⁴ This effect is attributed to enhancement of internal H-bonds in TFE promoting ordered structure. An alternative interpretation involves TFE disrupting the water mediated H-bonding that stabilize unfolded conformations. The CD spectra of peptide **1-4** recorded were in trifluoroethanol (TFE).

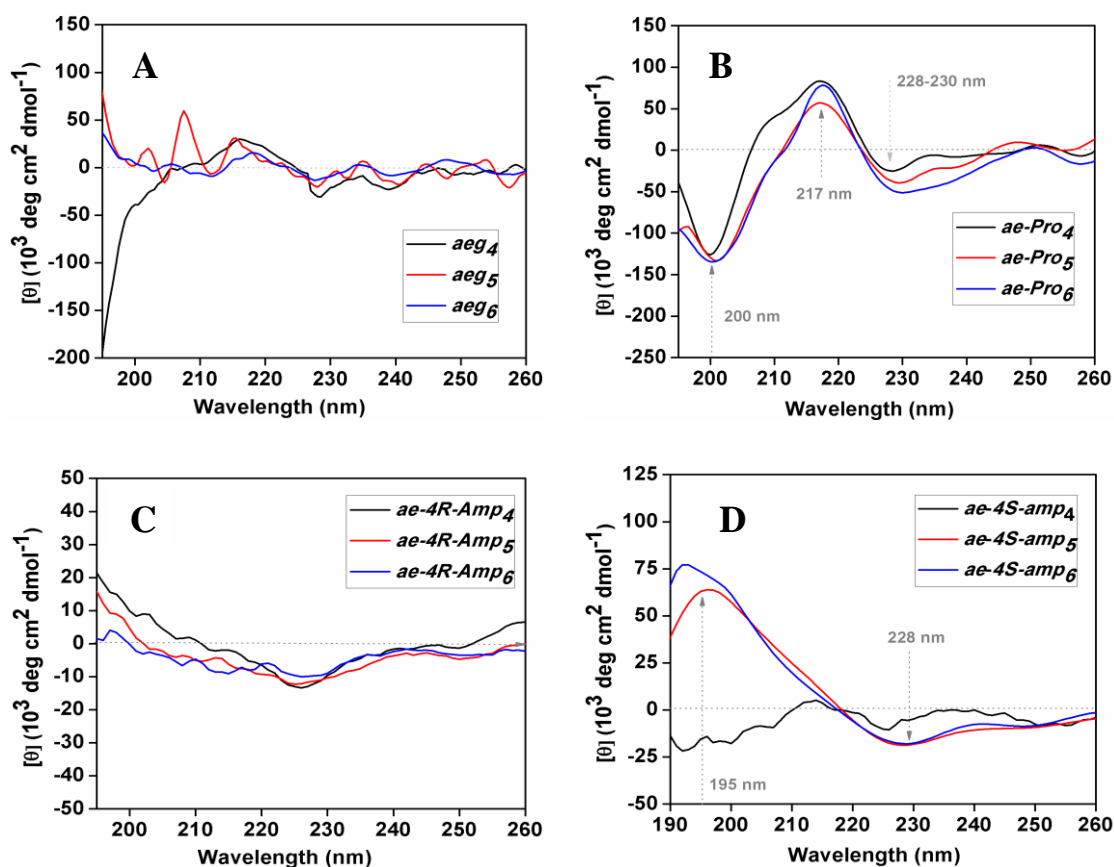


Figure 8. CD spectra of polyamides **1-4** at 25°C in TFE; (A) **1** (*aeg*₄, *aeg*₅, *aeg*₆), (B) **2**, (*ae-Pro*₄, *ae-Pro*₅, *ae-Pro*₆), (C) **3**, (*ae-4R-Amp*₄, *ae-4R-Amp*₅, *ae-4R-Amp*₆) and (D) **4**, (*ae-4S-amp*₄, *ae-4S-amp*₅, *ae-4S-amp*₆); All measurements done at peptide concentrations of 200 μM.

To determine the effect of chain length on the formation of secondary structures, homooligopeptides from tetramer to hexamer were used for measuring CD in TFE. The *ae*-peptides **1** and **3** did not exhibit characteristics of any known secondary structural features of CD signals for tetramer (Figure 8A, 8C) pentamer or hexamer. In comparison, the *ae*-

*Pro*₉ peptide **2** exhibited CD signature with negative peaks at 200, 228-230 nm, and positive peak at 217 nm (Figure 8B) which corresponds to typical PPI conformation and increase with the peptide chain.

On the other hand, *ae-amp* peptide **4** did not exhibit any characteristic and defined spectral features in CD signals for tetramer but exhibited a CD signature with strong and well-defined negative peaks at 228 nm and a strong positive peak at 195 nm (Figure 8D). The intensity of positive band at 195 nm increased slightly with the hexamer. The CD pattern of *ae-amp* peptide **4** closely resembles that of β -structure (Figure 6, green) as seen with 4*S*-aminoproline peptides, which also have been observed to form β -structure.^{15,16}

2.6.3 Concentration dependent CD spectroscopy for peptides

In collagen peptides, the amide NH of glycine is involved in interchain hydrogen bonding, leading to formation of triple helix structure. In contrast, polyproline peptides (without the intervening glycine) lack amide NH and hence are unable to form a triplex *via* interchain H-bonds and consequently end up as a single helix of PPI or PPII type. The formation of triple-helical structure through interchain association is a concentration dependent phenomenon and single stranded chains shift to the triple-helical assemblies with increase in concentration in solution.¹⁷ The magnitude of the ratio of positive to negative band intensity in the CD spectra of collagen peptides ($R_{p/n}$) has been proposed to quantitate the extent of triple-helical strength. The extent of triple-helical structure reaches maximum when the concentration is more than its critical triple-helical concentration. In peptides **3** and **4**, the presence of amino group may influence the formation of other secondary structures, in competition with extended PPII structure.

2.6.3a. Effect of concentration and length of peptide **3** (*ae-4R-Amp*₄, *ae-4R-Amp*₅, *ae-4R-Amp*₆) on the secondary structure

To examine the effect of length on intermolecular interactions as contributors to secondary structure formation and conformational stability of peptide **3**, CD spectroscopic analysis of the peptides was performed in TFE with increasing peptide concentration and data shown in Figure 9.

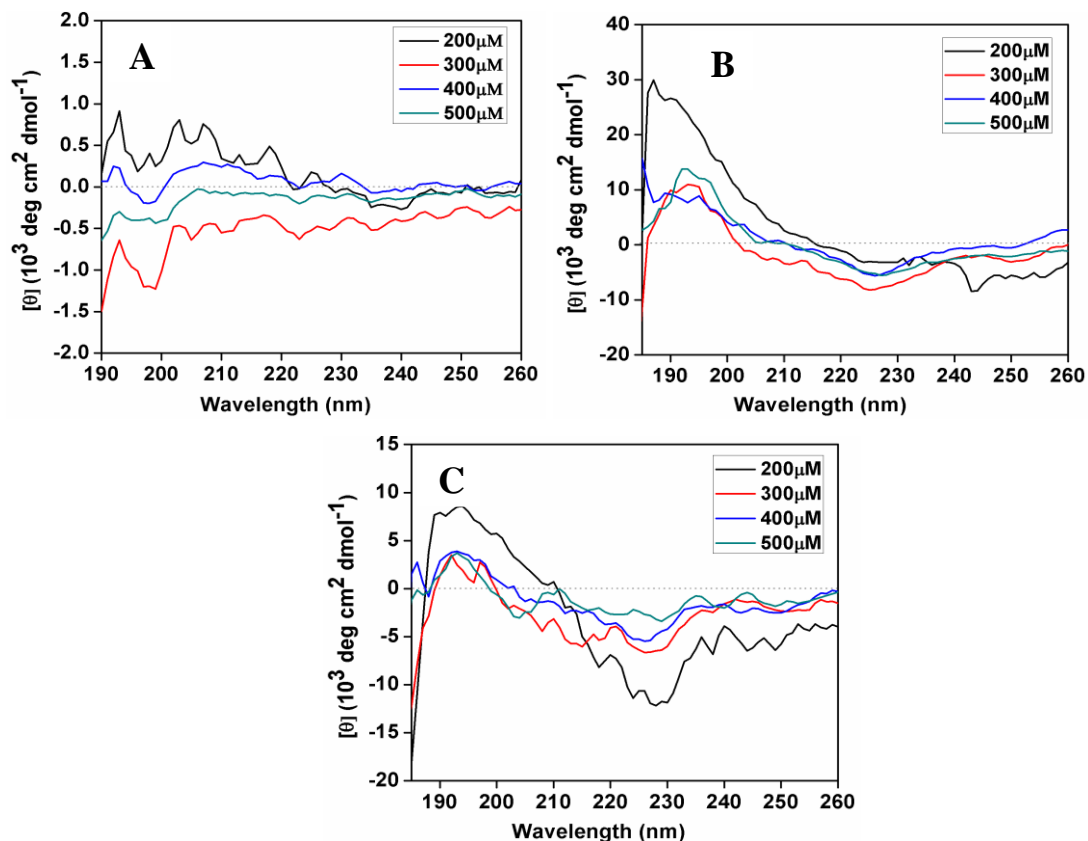


Figure 9. CD profile of peptides (A) *aeg-4R-Amp*₄, (B) *aeg-4R-Amp*₅, (C) *aeg-4R-Amp*₆; All measurements done at concentration 200 to 500 μ M in TFE.

It is seen that only subtle changes occurred in the CD spectra as a function of increasing concentrations or length of peptide **3**. This indicates retention of single stranded structure (no association at higher concentration). The negative band at 225 nm increased slightly.

2.6.3b Effect of concentration and length of peptide peptide 4 (*ae-4S-amp*₄, *ae-4S-amp*₅, *ae-4S-amp*₆) in TFE

Since β -structure arises from the inter-strand interactions, it should be favored at a higher peptide concentration. The CD spectra of peptide **4** were recorded at four different concentrations in TFE and results are shown in Figure 10. The peptide **4** did not exhibit any characteristic and defined spectral features of CD signals for tetramer but it exhibited CD signature with strong and well-defined negative peak at 228 and strong positive signal 195 nm (Figure 10B, 10C).

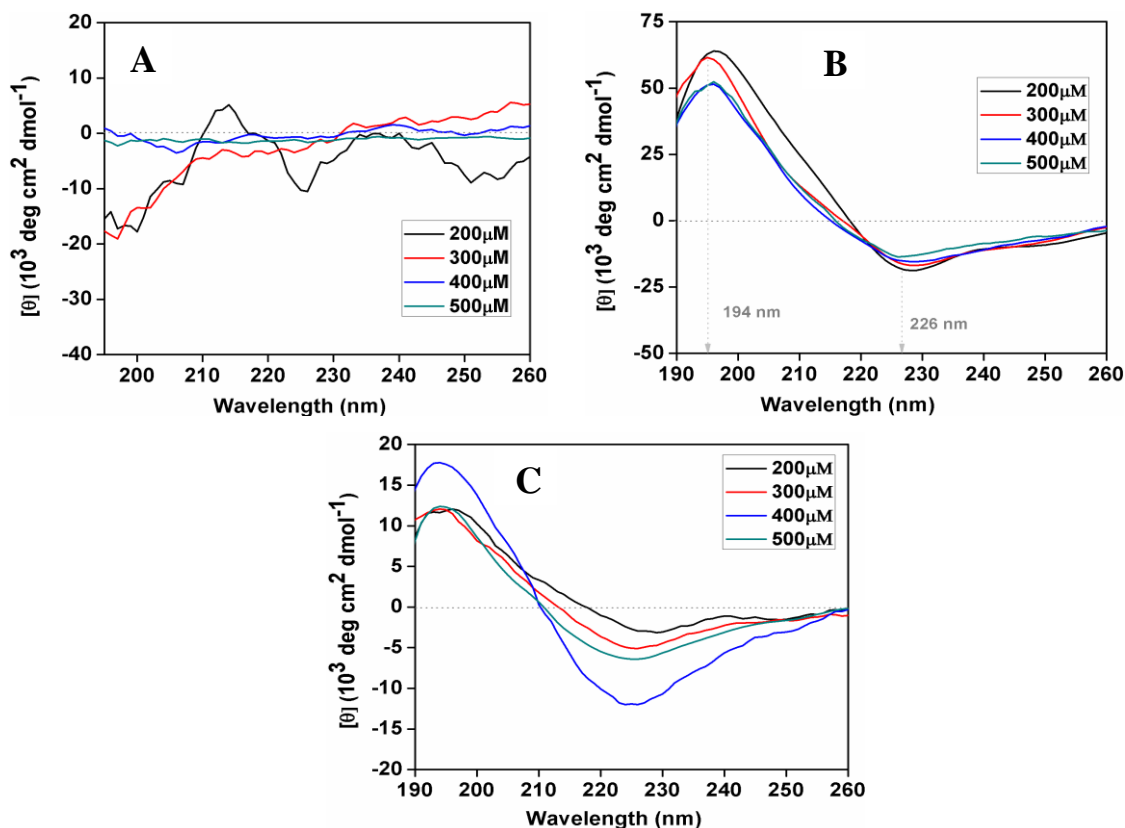


Figure 10 CD profile of peptides (A) *aeg-4S-amp*₄, (B) *aeg-4S-amp*₅ and (C) *aeg-4S-amp*₆; All measurements done at concentration 200 to 500 μ M in TFE.

A bisignate shape in the circular dichroism spectra indicate the existence of favored cooperative binding in the concentration range 200 μ M-500 μ M. The intensities of both positive and negative peaks increase with increase in oligomer length from five to six. These oligomer length-dependent CD signals observed around 224 and 194 nm strongly suggest the adoption of one (or more) regular backbone conformation(s) for oligoproline as short as five residues. The CD profiles of these peptides show no significant changes at higher concentrations, which suggests that β -structure is promoted at significantly higher concentration. The intensity increases with the concentration indicating that β -structure is promoted at higher concentrations. The overall difference in results among the different length of *ae-4S-amp* oligomers implies that the main determinant of the observed differences is the stereochemistry of substituent at C4 position in proline.

2.7 FT-IR studies

FT-IR spectroscopy provides information about the secondary structure content of proteins, like X-ray crystallography and NMR spectroscopy. The FT-IR spectroscopy of protein amide transitions offers a powerful tool for the study of protein conformation and conformational change. The amide vibrations of the protein reflect the couplings between the individual amide vibrations of the peptide units along the polypeptide backbone. The strength of the couplings and the energies of the local peptide vibrations are in turn dictated by the protein conformation and hydrogen bonding to the peptide units. These couplings give rise to delocalized (or excitonic) vibrational states that involve many amide vibrations, leading to infrared transition frequencies that are characteristic of different secondary structures. Amide I and Amide II bands are the characteristic bands found in the infrared spectra of proteins and polypeptides.

Amide I ($\sim 1650 \text{ cm}^{-1}$): The absorption associated with the amide I ($\sim 1650 \text{ cm}^{-1}$) band arises from the stretching vibrations of the C=O bond of the amide (Figure 11) with minor contributions from the out-of-phase CN stretching vibration, the CCN deformation and the NH in-plane bend. The latter is responsible for the sensitivity of the amide I band. The amide I vibration is hardly affected by the nature of the side-chain. However, it depends on the secondary structure of the backbone and therefore the amide vibration is most commonly used for secondary-structure analysis.

Amide II ($\sim 1550 \text{ cm}^{-1}$): Absorption associated with the amide II band originates from the bending vibrations of the N-H bond and the CN stretching vibration (Figure 11) with smaller contributions from the CO in-plane bend and the CC and NC stretching vibrations (Figure 10). Because both the C=O and the N-H bonds are involved in the hydrogen bonding amongst the different elements of secondary structure, the locations of both the Amide I and Amide II bands are sensitive to the secondary structure content of a protein.¹⁸

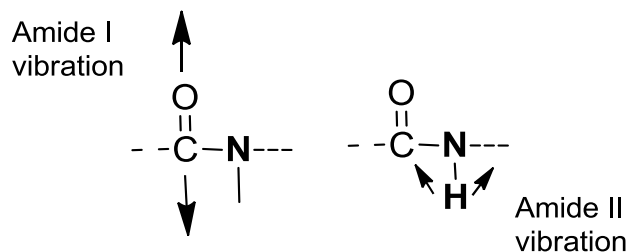


Figure 11. The Amide I band is due to carbonyl stretching vibrations while the Amide II is due primarily to NH bending vibrations.

The other vibrational mode of interest is amide II. Even though the intensity of the amide II region is relatively strong, it is not very sensitive to the secondary structural changes of proteins. Furthermore, the amide II bands strongly overlap with bands originating from amino acid side chain vibrations.¹⁹ Thus, the correlation between secondary structure and frequency is less straightforward for amide II than for the amide I vibration.²⁰ The amide I absorbance maximum of different secondary structures are summarized in Table 3.

Table 3. Assignment of amide I band positions to secondary structure based on experimental data.²⁰

Secondary structure	Band position in H ₂ O/cm ⁻¹		Band position in D ₂ O/cm ⁻¹	
	Average	Extremes	Average	Extremes
α -helices	1654	1648-1657	1654	1642-1660
β -sheet	1633	1623-1641	1633	1615-1638
β -sheet	1684	1674-1695	1684	1672-1694
Turns	1672	1662-1686	1672	1653-1691
Disordered	1654	1642-1657	1654	1639-1654

Thus, the different absorption values of amide bond in FTIR spectroscopy are useful to distinguish amide bonds involved in hydrogen bonding and this is consequently useful in differentiation of secondary structures.

2.7.1 FT-IR studies in TFE

Characteristic amide I mode, represents the CO stretching vibrations in the region between 1600-1700 cm^{-1} . Due to the strong absorption of water between 1640-1650 cm^{-1} , the structure determination by amide I mode are done in D_2O solutions. However, uncertainty in the NH/ND exchange process may result in some degree of ambiguity.²¹ To avoid the strong absorption of water between 1640 and 1650 cm^{-1} , the FT-IR spectra were recorded in anhydrous trifluoroethanol at room temperature.

2.7.1a. FT-IR studies of peptide 1 (*aeg*₄, *aeg*₅ and *aeg*₆) in TFE

In order to explore the secondary structure, the FT IR spectra of peptide 1 with different oligomer lengths were recorded in TFE at room temperature (Figure 12) in transmittance mode.

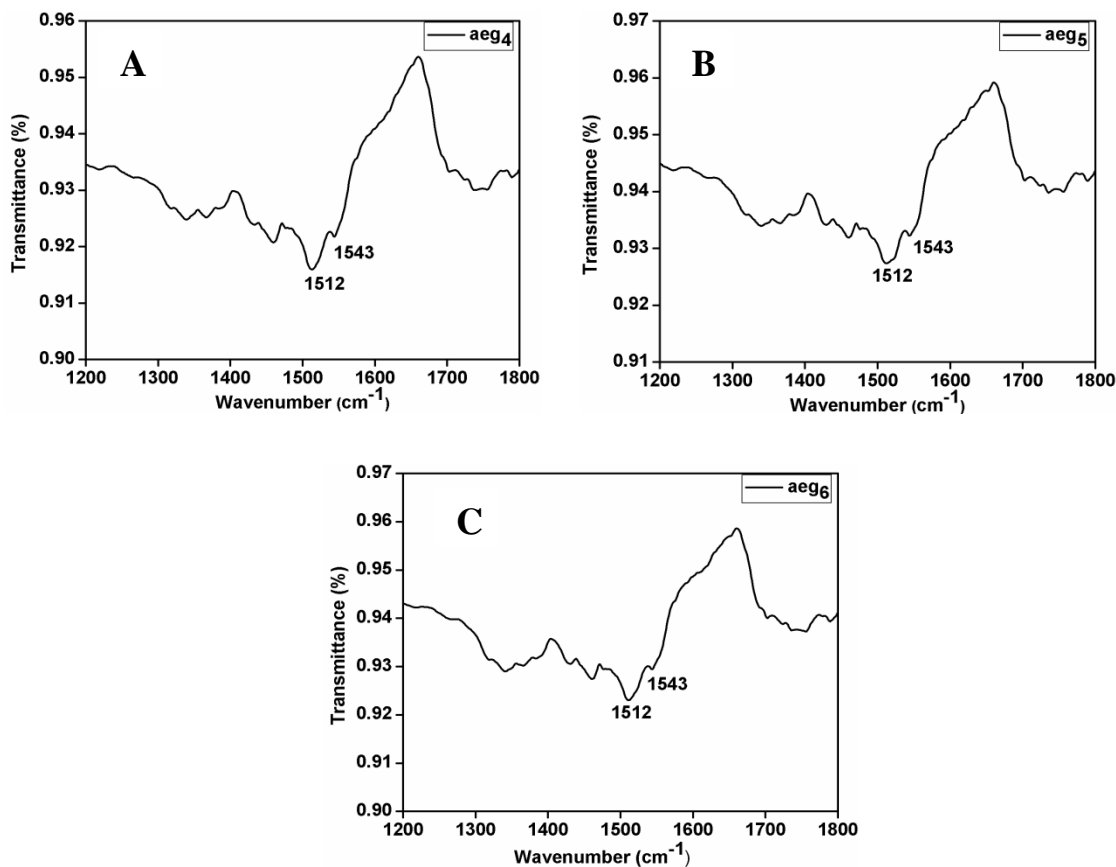


Figure 12. FT-IR spectra of peptides (A) *aeg*₄, (B) for *aeg*₅ and (C) for *aeg*₆ at concentration 100 μM in TFE.

The spectra show bands near 1512 cm^{-1} and 1542 cm^{-1} corresponding to N-H bending vibration/C-N stretching vibration for amide II mode²² originating from the C-N-H bonds peptide **1**. The amide I band frequencies are closely correlated to the molecular geometry and hydrogen bonding pattern but for all three peptide (*aeg*₄, *aeg*₅ and *aeg*₆), no peaks in the region $1600\text{-}1700\text{ cm}^{-1}$ for amide I band²³ were seen.

2.7.1b. FT-IR studies of peptide **2** (*ae-pro*₄, *ae-pro*₅ and *ae-pro*₆) in TFE

In the FT-IR spectra of peptide **2** (*ae-pro*₄, *ae-pro*₅ and *ae-pro*₆) show bands at 1510 cm^{-1} corresponding to amide II and no changes in bands were observed with increase in the length of peptides (Figure 13).

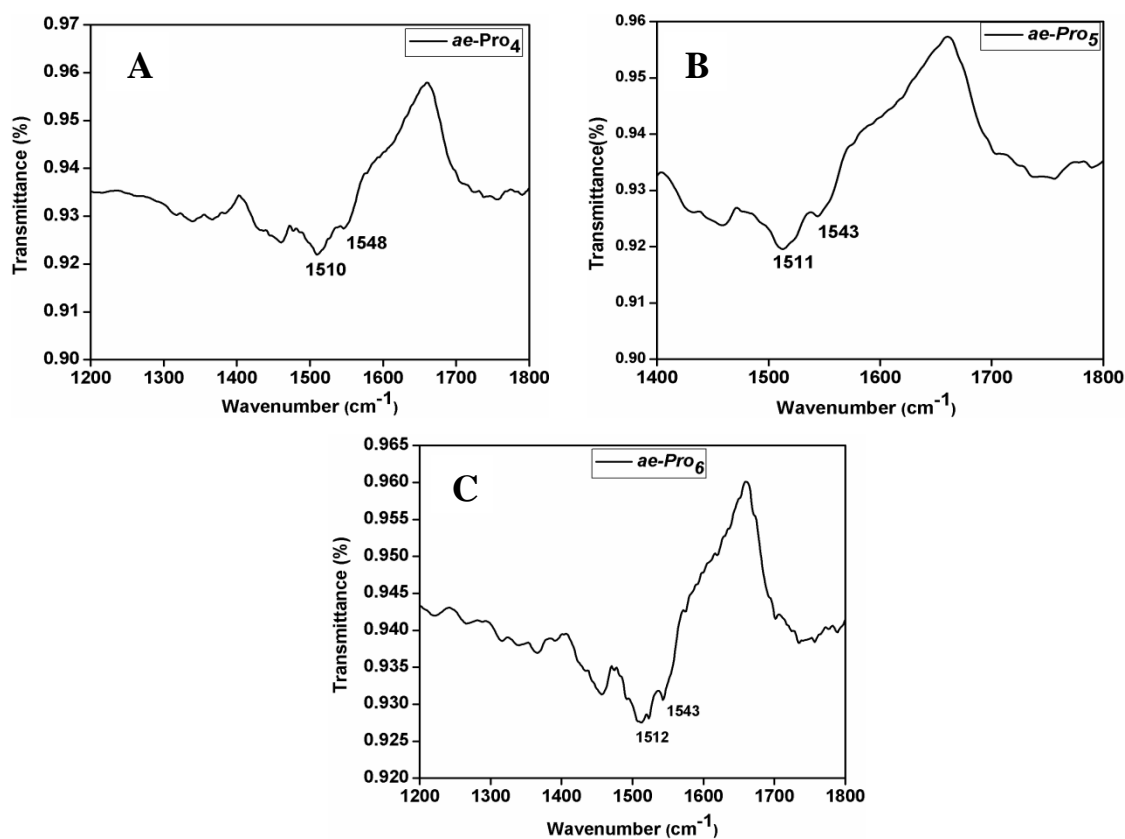


Figure 13. FT-IR spectra of peptides (A) *ae-pro*₄, (B) *ae-pro*₅, (C) *ae-pro*₆ at concentration $100\text{ }\mu\text{M}$ in TFE.

2.7.1c FT-IR studies 3 (*ae-4R-Amp*₄, *ae-4R-Amp*₅, *ae-4R-Amp*₆) in TFE

In order to see the effect of substitution and *R/S* stereochemistry of NH₂ at C₄ of proline, the FT-IR spectra in TFE were recorded. Similar results (Figure 14) were observed for peptide **3** where FT-IR peaks at 1509-1512cm⁻¹ were seen for amide II band with absence of amide I signals.

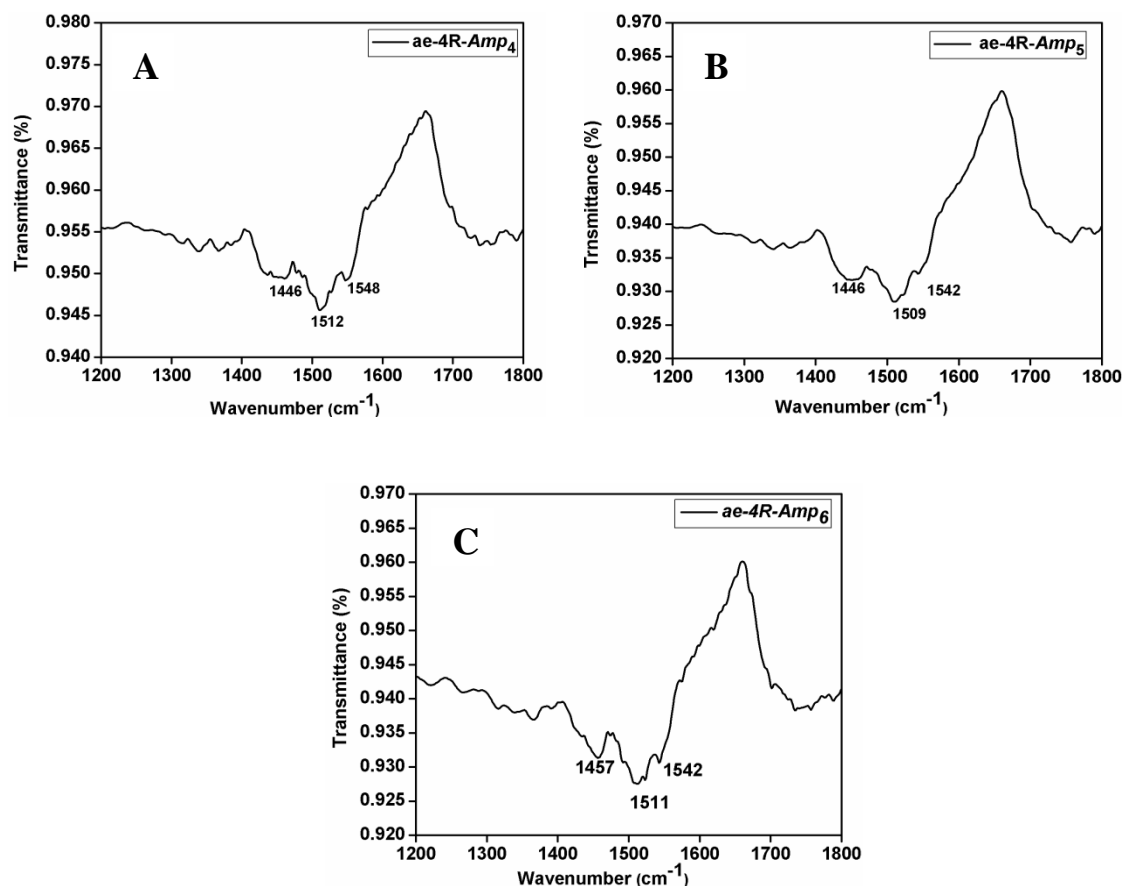


Figure 14. FT-IR spectra of peptides (A) *ae-4R-Amp*₄, (B) *ae-4R-Amp*₅, and (C) for *ae-4R-Amp*₆ at concentration 100 μ M in TFE.

2.7.1d. FT-IR studies 4 (*ae-4S-amp*₄, *ae-4S-amp*₅, *ae-4S-amp*₆) in TFE

In contrast to a single peak observed in the amide II region for peptides **1-3**, the FT IR spectra of *4S*-peptides **4** (*ae-4S-amp*₄, *ae-4S-amp*₅, *ae-4S-amp*₆) in TFE (Figure 13) show bands around near 1512 cm⁻¹ and 1690 cm⁻¹ (Figure 15). These bands correspond to amide II and amide I respectively, suggesting that *4S*-peptides **4** (*ae-4S-amp*₄, *ae-4S-amp*₅,

ae-4S-amp₆) form β -structure in TFE. This is a consequence of stronger inter-molecular hydrogen bonding in TFE arising from a β -structure.

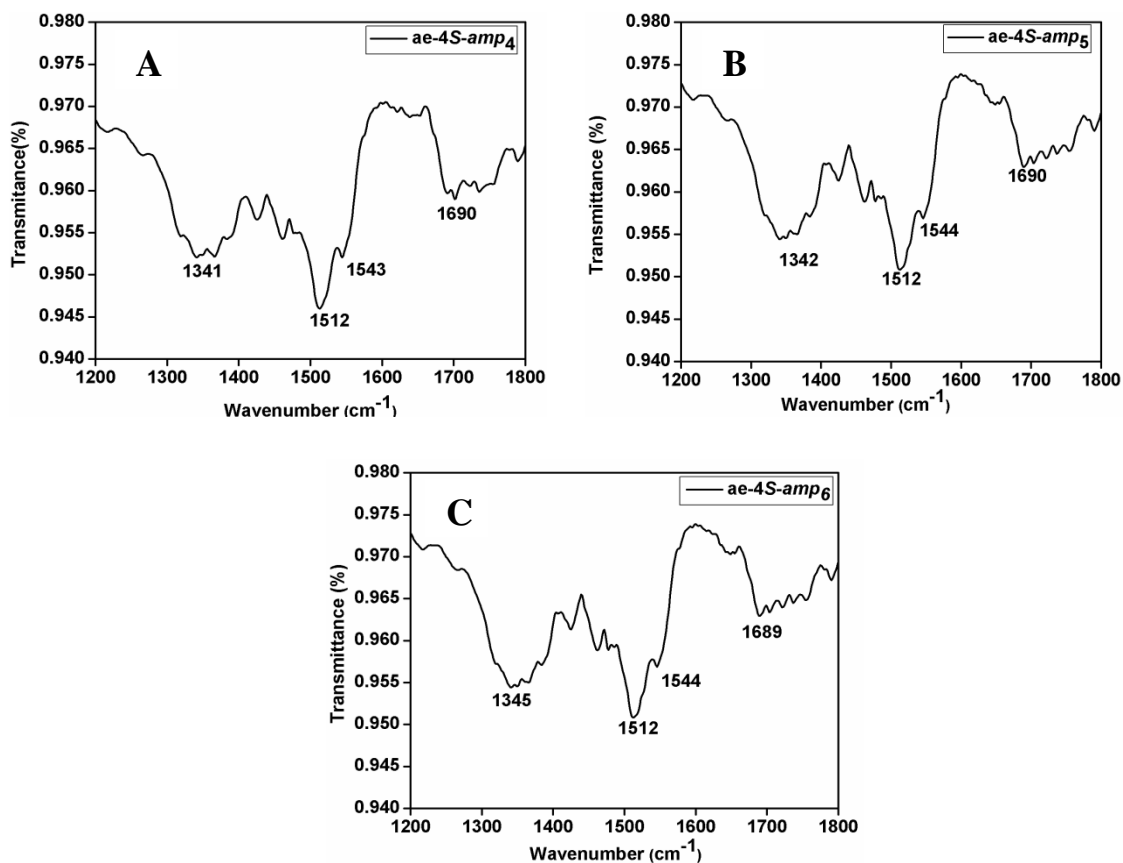


Figure 15. FT-IR spectra of peptides (A) *ae-4S-amp₄*, (B) *ae-4S-amp₅* and (C) for *ae-4S-amp₆* at concentration 100 μ M in TFE.

FT-IR absorption of peptides **1-3** show absorption only in the amide II region around 1542-1548 cm⁻¹ but not in amide I region, indicating the absence of β -structures in TFE (Figure 12, 13, 14). In contrast, FT-IR absorption of *4S*-peptides **4** at 1689-1690 cm⁻¹ could be correlated with the presence of β -structure in TFE (Figure 15) supported by amide II band in the region at 1542-1544 cm⁻¹.

2.8 Discussion

The most common secondary structures found in proteins are α -helix, 3_{10} -helix, and β -sheet, which are defined by characteristic patterns of hydrogen bonding arising from amide hydrogen bond donors (NH) and acceptors (CO).

To establish critical chain length and structural features needed to form the characteristic helix, peptide having spacer chain of two carbon atoms (ethylene diamine) intervening the glycyl prolyl units were designed and synthesized. The CD spectra of such peptides **1** (*aeg*₄, *aeg*₅, *aeg*₆), **2** (*ae-pro*₄, *ae-pro*₅, *ae-pro*₆) **3** (*ae-4R-Amp*₄, *ae-4R-Amp*₅, *ae-4R-Amp*₆) and **4** (*ae-4S-amp*₄, *ae-4S-amp*₅, *ae-4S-amp*₆) were obtained in both aqueous and alcohol solvents (Figure 7, 8). The peptides **1** (*aeg*₄, *aeg*₅, *aeg*₆), **2** (*ae-pro*₄, *ae-pro*₅, *ae-pro*₆) **3** (*ae-4R-Amp*₄, *ae-4R-Amp*₅, *ae-4R-Amp*₆) and **4** (*ae-4S-amp*₄, *ae-4S-amp*₅, *ae-4S-amp*₆) show very low negative and positive bands in in buffer. (Figure 7). Thus, they have a low structural content arising from non-chiral glycine and rigid proline.

Solvent plays a key role in modulating the H-bonding effects. The CD spectra of peptides **1** (*aeg*₄, *aeg*₅, *aeg*₆), **2** (*ae-pro*₄, *ae-pro*₅, *ae-pro*₆) **3** (*ae-4R-Amp*₄, *ae-4R-Amp*₅, *ae-4R-Amp*₆) and **4** (*ae-4S-amp*₄, *ae-4S-amp*₅, *ae-4S-amp*₆) recorded in a non-aqueous fluorinated solvent trifluoroethanol indicated that peptides **1** (*aeg*₄, *aeg*₅, *aeg*₆), **2** (*ae-pro*₄, *ae-pro*₅, *ae-pro*₆) and **3** (*ae-4R-Amp*₄, *ae-4R-Amp*₅, *ae-4R-Amp*₆) do not form any recognizable secondary structure in TFE. Interestingly, the CD profile of peptide **4** (*ae-4S-amp*₄, *ae-4S-amp*₅, *ae-4S-amp*₆) in TFE exhibited a pattern, characteristic of a β -structure, only for pentamer and hexamer but not for tetramer (Figure 8). These observations of peptide CD as a function of chain length suggest that secondary structure is a co-operative process with requirement of a critical length of at least five residues. Formation of a β -structure in any polyproline peptides under any conditions is unprecedented in the literature as they lack H-bond donor sites.

The FT-IR spectroscopy supplements CD-spectroscopy in determination of the conformational studies of peptides and proteins.²⁴ To gain further insight into formation of secondary structure sensitivity, the FTIR spectra of the amide I and amide II bands of the different peptides were studied in TFE. The FTIR spectrum of peptide **1-4** (Table 4), consists of a dominant peak at 1509-1512 cm⁻¹ corresponding to amide II, but amide I

(1640–1700 cm^{-1}) band which is located at 1689-1690 cm^{-1} (Table 4, entry 10 -12) as observed for peptide **4**.

The amide vibrations, intrinsic to the protein backbone are dependent on secondary structure. Based on empirical frequency-secondary structure correlations, formation of β -structure indicated by a strong absorption band at 1680-1690 cm^{-1} .²⁴⁻²⁵ These observations strongly support the CD results which had initially showed the formation of β -structure by peptide **4**.

Table 4: FT-IR spectroscopic data of peptide **1-4**

Sr no.	Peptides	Amide II (1515-1480 cm^{-1})	Amide I (1690-1600 cm^{-1})
1	<i>Pro</i> ₄	1510, 1548	
2	<i>Pro</i> ₅	1511, 1543	-
3	<i>Pro</i> ₆	1512, 1543	-
4	(<i>aegly</i>) ₄	1512, 1543	-
5	(<i>aegly</i>) ₅	1512, 1543	-
6	(<i>aegly</i>) ₆	1512, 1543	-
7	(<i>ae-4R-Amp</i>) ₄	1512, 1548	-
8	(<i>ae-4R-Amp</i>) ₅	1509, 1542	-
9	(<i>ae-4R-Amp</i>) ₆	1511, 1542	-
10	(<i>ae-4S-amp</i>) ₄	1512, 1543	1690
11	(<i>ae-4S-amp</i>) ₅	1512, 1544	1690
12	(<i>ae-4S-amp</i>) ₄	1512, 1542	1689

These results can be rationalised as in peptide **4** (*ae-4S-amp*)_n, where the β -structure arises due to association of strands with the NH_2 group from one strand forming an *intermolecular* H-bond with the amide carbonyl of proline from another strand (Figure 16). Such an association is not possible in *4R*-amino proline. *Intermolecular* H-bonding in *4S*-peptide **4** (*ae-4S-amp*) with pentamers and hexamer was observed but tetramer did not show *intermolecular* H-bonding, due to the fact that small peptides are often highly flexible and are solvated to a greater extent.

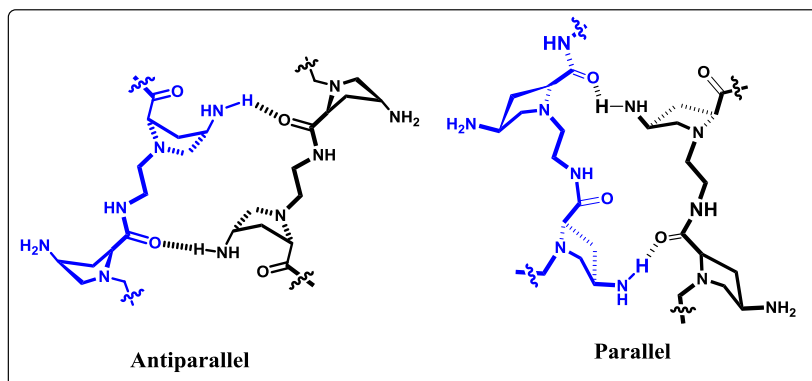


Figure 16. Proposed β -structure for *ae-4S-amp*.

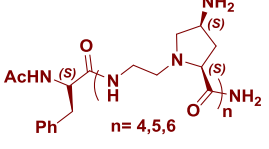
2.9 Conclusion

The comparative study of 15 different hybrid amides (aminoethyl-glycyl, aminoethyl-prolyl, *ae-4(R/S)*-aminopropyl-polyamides) has led to an understanding of the effect of chain length, proline conformation and stereochemistry of proline C4 substituent on the secondary structures adopted by (*ae-pro*) polyamides (Table 5).

The 4*S*-NH₂ substitution on proline with *S*-stereochemistry leads to formation of β -structure in TFE, assembled by interchain hydrogen bonding. The extent of β -structure increases with chain lengths and is critical at lengths of pentamer and hexamer and further depends on four factors: i) solvent (TFE), ii) stereochemistry of substituent at 4-position in proline (*Cis* with respect to acid group) iii) nature of substituent (must have H-bond donor) and iv) length of peptide (length should be more than tetramer) (Table 5).

Table 5. Effect of different parameters on peptide **1-4**

Sr. No.	Peptide	Stereochemistry at C4	Observed Structure in TFE
1		-	No 2° Structure
2		-	Weak PPI in TFE

3	 <p>Chemical structure of peptide 3, shown in green. It features a central proline ring with an R-amino group (NH_2) and a side chain containing a phenyl group (Ph) and an acetyl group (AcHN). The side chain is labeled with $n = 4, 5, 6$. The structure is labeled with (S) and (R) configurations.</p>	R	No 2° Structure
4	 <p>Chemical structure of peptide 4, shown in red. It features a central proline ring with an S-amino group (NH_2) and a side chain containing a phenyl group (Ph) and an acetyl group (AcHN). The side chain is labeled with $n = 4, 5, 6$. The structure is labeled with (S) configurations.</p>	S	$(n=5,6)$ β -sheet like structure

In comparison, the peptides **1** and **2** had no ordered secondary structure in both water and TFE due to non-chiral amino acid glycine and unsubstituted proline. In peptide **3**, with $4R$ - NH_2 substitution on proline, no CD or FT-IR signal indicated secondary structure, reflecting the steric inability of $4R$ - NH_2 group to engage in any H-bonding. However, the chains with $4S$ -amino substituent on proline can take part in intermolecular hydrogen bonding between two strands. These observations may provide a basis for the design of polyamides foldamers that form β -structure in TFE for potential applications in material and biological sciences.

2.10 Experimental

This section describes the detailed synthetic procedures and spectra characterization of the rationally designed monomers.

2.10.1 General

Materials and reagents were of the highest commercially available grade and used without further purification. Reactions were monitored by thin layer chromatography (TLC) were carried out on precoated silica gel 60 F254 plates (E. Merck). TLCs were visualized under UV light, iodine and/or ninhydrin spray followed by heating upto 110 °C with heat gun. Silica gel 60-120 and 100-200 mesh (Merck) was used for routine column chromatography. Elution was done with ethyl acetate/petroleum ether or dichloromethane/methanol mixture depending upon the compound polarity. Flash chromatography was done using 230-400 mesh silica. All solvents were distilled under an inert atmosphere with appropriate desiccant. Reactions in aqueous medium and workup processes were done using double distilled water. Unless otherwise noted, all reactions were carried out at room temperature. IR spectra were recorded on Bruker's Infrared Fourier Transform Spectrophotometer using chloroform and TFE, neat sample. The optical rotation values were measured on Rudolph Research Analytical Autopol V polarimeter. ¹H and ¹³C NMR spectra were recorded on Bruker AV 500 and JEOL AV 400, AV 200 spectrometers. Chemical shifts are reported in ppm using TMS and CDCl₃ as a reference. Spectra were analyzed using ACD spectviewer software from ACD labs. NMR spectra of compounds show two sets of peaks arising from *cis-trans* isomerization of N-CO bond. Analytical HPLC was performed using a Luna 5u C18 (2) (250 mm x 4.6 mm) column from Phenomenex. Preparative HPLC was carried out on a Luna 5u C18 (2) (250 mm x 10 mm) column from Phenomenex. Mass spectra were obtained by ESI-MS technique on Waters-Acquity. Jasco J-815 (Japan) instrument was used for CD measurements. All graphs presented for CD spectra's are drawn by Origin 8 software.

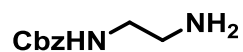
Reagents for the buffer preparation such as NaCl, NaH₂PO₄, Na₂HPO₄, were obtained from Sigma and were of Molecular biology reagent grade. Double distilled water

was demineralized using Millipore MilliQ deionizer and used for the preparation of buffers. pH was adjusted using NaOH and HCl.

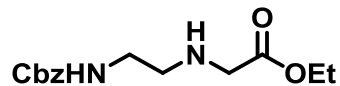
Resins for solid phase peptide synthesis and Fmoc-protected amino acids were bought from Novabiochem and were used without further purification. The term “concentrated under reduced pressure” refers to the removal of solvents and other volatile materials using a rotary evaporator at water aspirator pressure (<20 Torr) while maintaining the water-bath temperature below 40 °C. Residual solvent was removed from samples at high vacuum (<0.1 Torr). The term “high vacuum” refers to vacuum achieved by a mechanical oil pump.

2.10.2 Synthesis of compounds 2-25

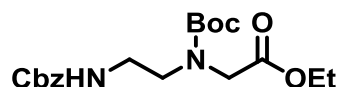
N¹-Benzyl (2-aminoethyl) carbamate (2)



To a solution of ethylenediamine **1** (9.0 g, 150 mmol) in DCM, aqueous NaHCO₃ (25.3 g, 300 mmol) was added and cooled in an ice bath to which a solution of Cbz-Cl (12.8 g, 40 mmol) in toluene (50%) was added. The reaction mixture was stirred for 12 h at room temperature and solvent toluene was removed under vacuum. The aqueous solution was cooled to 0 °C and washed with diethyl ether 3-4 times to remove the unreacted Cbz-Cl and then filtered to remove N,N'-Cbz-bisprotected compound. The aqueous layer extracted with EtOAc (3x100 ml) and the combined organic layer was washed with water followed by saturated brine solution and the organic layer was dried over anhydrous Na₂SO₄ and concentrated under reduced pressure to yield white sticky solid of compound **2**. This compound was used for the next reaction without purification.

Ethyl 2-((N¹-2-(benzyloxy)carbonyl) ethylamino acetate (3)

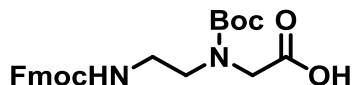
Compound **2** (7.0 g, 36 mmol) was treated with ethylbromoacetate (3.8 mL, 36 mmol) in acetonitrile (80 mL) in the presence of triethyl amine (7.5 g, 54 mmol) and the mixture was stirred at ambient temperature for 5 h. The solvent acetonitrile was removed under vacuum and extracted with ethyl acetate (3x100 ml). The combined organic layers was dried over anhydrous Na₂SO₄ and concentrated under reduced pressure to yield sticky oil compound **3**. (6.3 g, 63% yield); ¹H NMR (CDCl₃, 200 MHz) δ: 7.38-7.30 (m, 5H), 5.66 (br, 1H), 5.10 (s, 2H), 4.18 (q, J=22 Hz, 2H), 3.39 (s, 2H), 3.29 (q, J=16 Hz, 2H), 2.76 (t, J=12 Hz, 2H), 1.27 (t, J=14 Hz, 3H); ¹³C NMR (50 MHz, CDCl₃) δ: 172.3, 156.6, 136.6, 128.4, 128.0, 66.6, 60.9, 50.2, 48.6, 40.5, 14.1; MS (MALDI-TOF) m/z calcd for C₁₄H₂₀N₂O₄ [M+Na]⁺ 303.13, found 303.11.

Ethyl 2-((N¹-2-(((benzyloxy)carbonyl ethyl (N-Boc)amino)acetate (4)

To a magnetically stirred mixture of amine **3** (5.0 g 17.9 mmol) and (Boc)₂O (13 mL, 53.7 mol) a catalytic amount of iodine was added under solvent-free conditions at room temperature. After stirring the reaction mixture for the specified time diethyl ether (50 mL) was added. The reaction mixture was washed with Na₂S₂O₃ and saturated NaHCO₃ and dried over Na₂SO₄, the solvent was evaporated under reduced pressure, and the residue was purified by silica gel column chromatography to afford the corresponding pure product **4**. (6.1 g, 90% yield); ¹H NMR (CDCl₃, 200 MHz) δ: 7.35 (s, 5H), 5.75 (br, 1H), 5.12-5.11 (m, 2H), 4.19 (q, J=6 Hz, 2H), 3.92-3.79 (m, 2H), 3.42-3.31 (m, 4H), 1.45-1.42 (s, 9H), 1.27 (t, J=14 Hz, 3H); ¹³C NMR (50 MHz, CDCl₃) δ: 170.9, 170.6, 156.6, 156.4, 155.5, 136.7, 136.5, 128.4, 128.06, 127.9, 80.6, 66.5, 66.4, 61.3, 50.4, 49.7, 48.8, 48.5, 39.8, 39.6, 28.2, 28.1, 14.2, 14.1; MS (MALDI-TOF) m/z calcd for C₁₉H₂₈N₂O₆ [M+Na]⁺ 403.18, found 403.07.

2-(2-(N¹benzyloxy)carbonyl ethyl (N-Boc)amino acetic acid (5)

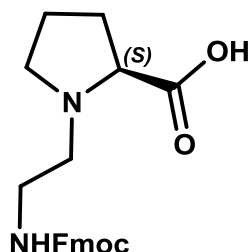
Ethyl ester **4** was (5.0 g, 13.2 mmol) hydrolysed using aqueous LiOH (2N, 15 mL) in methanol (15 mL) and the resulting acid was neutralized with activated Dowex H⁺ till the pH of the solution becomes slightly acidic. The resin was removed by filtration and the filtrate was concentrated to obtain the **5**. This compound was used for the next reaction without purification. MS (MALDI-TOF) *m/z* calcd for C₁₇H₂₄N₂O₆ [M+Na]⁺ 375.19, found 375.19.

N¹-(2-(((9H-fluoren-9-yl)methoxy)carbonyl)amino)ethyl)-N-(tert butoxycarbonyl)glycine (6)

Compound **5** (5.0 g, 14.2 mmol) was dissolved in dry methanol (15 mL) to which 10% Pd/C (0.2 g) was added. The mixture was subjected to hydrogenation under H₂ gas (60-psi pressure) for 6 h. Water (200 mL) was added to the reaction mixture which was filtered through Whatman filter paper and the filtrate was concentrated under reduced pressure. It was dissolved in of dioxane:water (15 ml, 1:1) and the pH was adjusted to ~10 by the slow addition of solid Na₂CO₃ (17.4 mmol). Fmoc-Cl (3.5 g, 14.2 mmol) added slowly to the reaction mixture for 45 min. and was stirred overnight at RT. After completion of the reaction, the reaction mixture was acidified with aq. HCl (20 mL, 1N) in cold condition. The product was extracted with ethyl acetate (3 x 50 mL) and the combined organic layers was washed with brine (30 mL) and dried over anhydrous Na₂SO₄. The solvent was concentrated under reduced pressure to give **6**. (5 g, 80% yield); ¹H NMR (CDCl₃, 400 MHz) δ: 7.75-7.77 (2H, t, J = 8.28), 7.58-7.60 (2H, dd, J = 7.53), 7.29-7.41 (4H, m), 5.66 (br, 1H), 4.51-4.55 (m, 1H), 4.18-4.40 (m, 2H), 3.71-3.97 (m, 2H), 3.10-3.21 (m, 4H), 1.40-1.44 (s, 9H); ¹³C NMR (100 MHz, CDCl₃) δ: 172.6, 143.9, 141.3, 127.7,

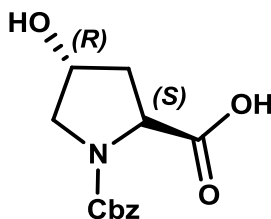
127.1, 124.8, 120.0, 81.2, 49.8, 49.1, 42.2, 31.0, 28.20; MS (MALDI-TOF) m/z calcd for $C_{24}H_{28}N_2O_6$ $[M+1]^+$ 440.19 found 440.98.

N^1 -(Fmoc) aminoethyl-pyrrolidine-2-carboxylic acid (8)



In round bottom flask equipped with magnetic stirrer bar, Fmoc-amino propanaldehyde **23** (1.3 g, 4.3 mmol) was taken, to which dry MeOH:DCM:THF (70:30:70 mL) and stirred for 10 min. to the solution of aldehyde, proline **7** (1g, 4.3 mmol) with free amine was added. To this reaction mixture $NaCNBH_3$ (0.32 mg, 5.2 mmol) was added followed by $ZnCl_2$ (1.3 g, 30 mmol). This reaction mixture was stirred for 6 h, solvent was concentrated to 50 mL. To this ethyl acetate was added and washed with saturated solution of $NaHCO_3$. The aqueous layer was removed and organic layer was washed with $NaHCO_3$ followed by brine and dried over an anhydrous Na_2SO_4 . It was filtered and the organic layer was evaporated and solid was purified by column chromatography using DCM and MeOH to yield **8** (2.8 g, 65% yield); MS (MALDI-TOF) m/z calcd for $C_{22}H_{24}N_2O_4$ $[M+Na]^+$ 403.16 found 403.38.

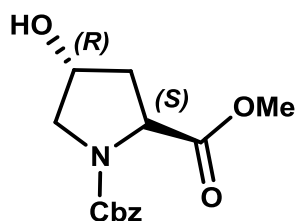
(2S, 4R)- N^1 -(benzyloxycarbonyl)-4-hydroxyproline (10)



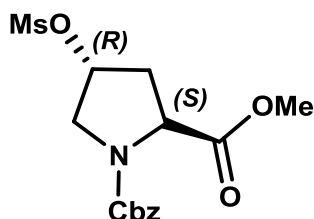
A solution of *trans*-4-hydroxy-L-proline **9** (20.0 g, 152 mmol) in THF:H₂O (1:3) $NaHCO_3$ (28 g, 183 mmol) was added and cooled in an ice bath to which a solution of Cbz-Cl (62.5 mL, 183 mmol) in toluene (50%) was added. The reaction mixture was stirred for 12 h at room temperature and the solvent toluene was removed under vacuum.

The aqueous layer was washed with diethyl ether for 3-4 times to remove the unreacted Cbz-Cl. It was acidified to pH 2 with aqueous HCl (2N) and then extracted with ethyl acetate (3 x 200 mL). The combined organic solution was washed with water followed by saturated brine solution. The organic layer was dried over anhydrous Na₂SO₄ and concentrated under reduced pressure to yield white sticky solid of compound **10**. (39.7 g, 98%); [α]_D²⁵ -86.70 (c 1.0, CH₂Cl₂); ¹H NMR (CDCl₃, 400 MHz) δ : 7.36-7.28 (m, 5H), 5.17-5.09 (m, 3H), 4.54-4.45 (m, 2H), 3.62-3.62 (m, 2H), 2.38-2.10 (m, 2H); ¹³C NMR (100 MHz, CDCl₃) δ : 176.6, 175.0, 156.2, 154.98, 136.1, 135.9, 128.6, 128.5, 128.3, 128.0, 127.6, 69.9, 69.31, 67.6, 58.1, 57.6, 55.0, 54.6, 38.9, 37.9, 29.7; MS (MALDI-TOF) m/z calcd for C₁₃H₁₅NO₅ [M+1]⁺ 265.09 found 266.05.

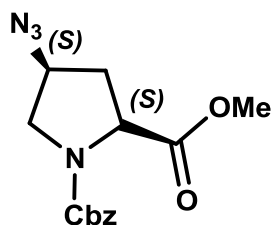
(2S, 4R)-N¹-(benzyloxycarbonyl)-4-hydroxyproline methyl ester (11)



A solution of compound **10** (25.0 g, 94 mmol) in anhydrous acetone (250 mL), anhydrous K₂CO₃ (32.5 g, 235 mmol) and dimethylsulphate (11 mL, 113 mmol) was stirred in a flask. The mixture was then refluxed under nitrogen for 4 h. The acetone was removed under vacuum and the resulting residue was dissolved in water followed by extraction with ethyl acetate (3 x 250 mL). The combined organic layers was washed with water (3 x 100 mL) followed by saturated brine solution (3 x 50 mL), dried over Na₂SO₄ and concentrated under vacuum. The crude material was purified by silica gel chromatography eluting ethyl acetate:hexane (1:1) afford compound **11** as colourless thick oil. (20.4 g, 97% yield); [α]_D²⁵ -61.15 (c 1.0, CH₂Cl₂); ¹H NMR (CDCl₃, 400 MHz) δ : 7.35-7.29 (m, 5H), 5.19-4.46 (m, 2H), 4.50-4.42 (m, 2H), 3.76-3.53 (m, 5H), 2.33-2.24 (m, 1H), 2.08-2.0 (m, 1H); ¹³C NMR (100 MHz, CDCl₃) δ : 173.4, 173.9, 155.2, 154.8, 136.4, 136.2, 128.5, 128.1, 127.9, 69.9, 69.2, 67.4, 58.0, 57.8, 55.3, 54.7, 52.5, 52.3, 39.2, 38.4; MS (MALDI-TOF) m/z calcd for C₁₄H₁₇NO₅ [M+1]⁺ 279.29 found 280.04.

(2S,4R)-N¹-(benzyloxycarbonyl)-4-(methanesulfonyloxy) proline methyl ester (12)

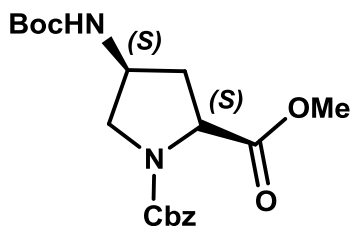
A solution of methyl ester **11** (10.0 g, 35.8 mmol) and triethylamine (7.8 mL, 53.7 mmol) in dry DCM (150 mL) was cooled to 0 °C in ice bath under nitrogen. While stirring, methanesulfonyl chloride (3.3 mL, 43 mmol) was added drop-wise over a period of 3 h at 0 °C. After completion of the reaction, the mixture was washed with water followed by saturated aqueous brine solution. The organic layer was dried over anhydrous Na₂SO₄ and concentrated under vacuum. The crude material was purified by silica gel chromatography (elution with 30% ethyl acetate/hexane) to afford mesylated compound **12** as colorless thick oil. (12.4 g, 97% yield); ¹H NMR (CDCl₃ 200 MHz) δ: 2.19-2.33 (1 H, m), 2.63-2.67 (1 H, m), 3.01 (3H, d), 3.76 (3H, s), 3.83 (1H, d), 3.98-4.15 (1H, m), 4.44-4.56 (1H, dd, *J* = 7.96), 4.98-5.26 (2H, m), 7.30-7.34 (5H, s). ¹³C NMR (100 MHz, CDCl₃) δ: 36.1, 37.2, 38.5, 52.2, 57.1, 57.3, 67.3, 77.4, 127.7, 128.3, 136.0, 153.8, 154.3, 172.1; MS (MALDI-TOF) *m/z* calcd for C₁₅H₁₉NSO₇ [M]⁺ 357.08 found 357.05.

(2S, 4S)-N¹-(benzyloxycarbonyl)-4-azidoproline methyl ester (13)

The compound **12** (10.0 g, 23 mmol) and NaN₃ (15.0 g, 230 mmol) was dissolved in dry DMF (100 mL). The solution was stirred for 8 h at 55-60 °C under nitrogen atmosphere. To remove DMF excess water (620 mL) was added to reaction mixture and the aqueous layer was extracted with ethyl acetate (3x150 mL). The combined organic layer was washed with water (3x200 mL) followed by brine. The organic layer was dried

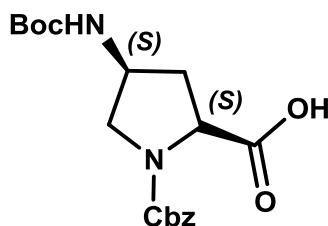
over anhydrous Na_2SO_4 and concentrated under vacuum. The crude product obtained was purified by silica gel chromatography (elution with 40% ethyl acetate/hexane) to afford **13** as colourless thick oil. (8 g, 94% yield); $[\alpha]_D^{25}$ -23.32 (c 1.0, CH_2Cl_2); ^1H NMR (CDCl_3 , 400 MHz) δ : 7.38-7.28 (m, 5H), 5.28-4.99 (m, 2H), 4.52-4.43 (m, 1H), 4.24-4.12 (m, 1H), 3.81-3.53 (m, 5H), 3.36-3.26 (m, 1H), 2.50-2.40 (m, 1H), 2.25-2.15 (m, 1H); ^{13}C NMR (100 MHz, CDCl_3) δ : 171.8, 171.6, 154.5, 154.1, 136.3, 128.5, 128.4, 128.4, 128.2, 128.1, 128, 127.9, 67.4, 67.2, 59.2, 58.3, 57.8, 57.7, 57.5, 52.6, 52.4, 51.5, 51.4, 51.2, 36.4, 36.1, 35.1; MS (MALDI-TOF) m/z calcd for $\text{C}_{14}\text{H}_{16}\text{N}_4\text{O}_4$ $[\text{M}+1]^+$ 305.30 found 305.05

(2S, 4S)-N¹-(benzyloxycarbonyl)-4-(*t*-butoxycarbonylamino) proline methyl ester (14)



The azide **13** (7.0 g, 23 mmol) was dissolved in of dry ethyl acetate (75 mL) to which Raney-Nickel (14 mL of suspension in ethyl acetate) and di-*t*-butyl-dicarbonate (6.1 g, 27 mmol) were added. The reaction mixture was subjected to hydrogenation (H_2 gas, 55-psi) for 4 h. After completion of the reaction, the catalyst from reaction mixture was filtered off and the filtrate was concentrated under reduced pressure followed purification by silica gel chromatography to obtain compound **14** as a colorless liquid. (8.4 g, 96% yield); $[\alpha]_D^{25}$ -32.44 (c 1.0, CH_2Cl_2); ^1H NMR (CDCl_3 , 400 MHz) δ : 7.31-7.24 (m, 5H), 5.41 (br, 1H), 5.16-4.97 (m, 2H), 4.37-4.29 (m, 2H), 3.74-3.55 (m, 5H), 2.49-2.38 (d, 1H), 2.0-1.91 (m, 1H), 1.39 (s, 9H); ^{13}C NMR (100 MHz, CDCl_3) δ : 174, 155.2, 154.8, 154.1, 136.3, 128.6, 128.2, 128.1, 128, 79.2, 67.4, 67.2, 58, 57.7, 53.5, 53.3, 52.7, 52.5, 50, 49.2, 36.9, 35.9, 28.4; MS (MALDI-TOF) m/z calcd for $\text{C}_{19}\text{H}_{26}\text{N}_2\text{O}_6$ $[\text{M}+1]^+$ 379.42 found 379.05.

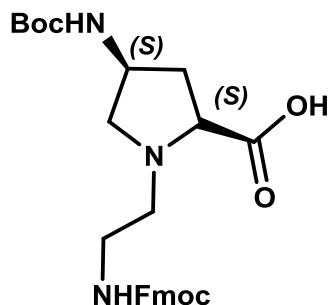
(2*R*,4*S*)-N¹-((benzyloxy)carbonyl)-4-((*tert*-Boc)amino)pyrrolidine-2-carboxylic acid (15)



The methyl ester **14**, 5 g (16.4 mmol) was subjected to hydrolysis using NaOH in MeOH (2N) for 1 h. MeOH was removed under vacuum and the aqueous layer was washed with ethyl acetate (3 x 50 mL) to remove unreacted organic compound. The crude product obtained was purified by silica gel chromatography (70% ethyl acetate/hexane) to afford a white solid powder **15**. (4.57 g, 95% yield); $[\alpha]_D^{25}$ -39.15 (c 1.0, CH₂Cl₂); ¹H NMR (CDCl₃, 400 MHz) δ : 7.99 (br, 1H), 7.37-7.31 (m, 5H), 5.37-5.12 (m, 3H), 4.47-4.21 (m, 2H), 3.80-3.49 (m, 2H), 2.46-2.39 (m, 1H), 2.20-2.17 (m, 1H), 1.42 (s, 9H); ¹³C NMR (100 MHz, CDCl₃) δ : 175, 174.8, 154.4, 135.7, 128.6, 128.5, 128.4, 128.2, 127.8, 80.0, 67.4, 68.3, 67.4, 58.5, 53.7, 53.4, 50.0, 37.1, 34.6, 28.4; MS (MALDI-TOF) *m/z* calcd for C₁₈H₂₄N₂O₆. [M+1]⁺ 365.39 found 365.15.

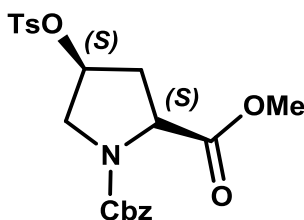
(2*S*, 4*S*)-N¹-(*Fmoc*) aminoethyl-4-((*t*-Boc)amino)pyrrolidine-2-carboxylic acid (17)

In round bottom flask equipped with magnetic stirrer bar, Fmoc-amino propanaldehyde **23** (1.3 g, 4.3 mmol) was taken, to which dry MeOH:DCM:THF (70:30:70 mL) and stirred for 10 min. to the solution of aldehyde, proline derivative **16** (1g, 4.3 mmol) with free amine was added. To this reaction mixture NaCNBH₃(0.32 mg, 5.2 mmol) was added followed by



ZnCl₂ (1.3 g, 30 mmol). This reaction mixture was stirred for 6 h, solvent was concentrated to 50 mL. To this ethyl acetate was added and washed with saturated solution of NaHCO₃. The aqueous layer was removed and organic layer was washed with NaHCO₃ followed by brine and dried over an anhydrous Na₂SO₄. It was filtered and the organic layer was evaporated and solid was purified by column chromatography using DCM and MeOH to yield **17**. (1.73 g, 62 % yield); ¹H NMR (CDCl₃, 400 MHz) δ: 7.73-7.74 (2H, t, J = 4), 7.55-7.57 (2H, dd, J = 8), 7.29-7.30 (4H, m), 5.88 (1H, s), 5.52 (1H, s), 4.37-4.65 (2H, m), 3.95-4.17 (2H, m), 3.65-3.73 (2H, m), 3.50-3.57 (2H, m), 2.99-3.08 (2H, m), 2.07-2.23 (2H, m), 1.41 (9H, s); ¹³C NMR (100 MHz, CDCl₃) δ: 174.0, 143.7, 143.6, 141.4, 127.8, 127.2, 125.4, 125.2, 120.5, 80.1, 69.2, 68.8, 67.8, 54.1, 47.2, 47.05, 38.2, 36.7, 28.4; MS (MALDI-TOF) m/z calcd for C₂₇H₃₃N₃O₆ [M+Na]⁺ 518.22 found 518.58.

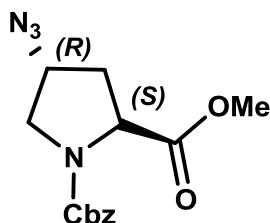
(2S, 4S)-N¹ (t-butoxy-carbonyl)-4-(p-toluenesulfonyloxy) proline methyl ester (18)



The compound **11** (10.0 g, 36 mmol), PPh₃ (11.9 g, 43 mmol) and methyl-*p*-toluenesulfonate (8.5 mL, 43 mmol) was dissolved in dry THF (120 mL) and cooled to -11 °C on ice bath under nitrogen. The mixture was stirred for 30 min. Diethyl azodicarboxylate (9.2 mL, 43 mmol) was added slowly with syringe. The reaction mixture was stirred at 0 °C for first 4 h then stirred at room temperature for 8 h after which THF was removed under vacuum. The resulting orange colored thick oil was dissolved in ethyl acetate (20 mL) to which petroleum ether (500 mL) was added. After triturating with spatula, the solution was kept at room temperature for 2 h. The white powder settled was filtered and the residue was washed with diethyl ether (6 x 60 mL) to obtain compound **18**. (14.8 g, 80% yield); [α]²⁵_D -24.44 (c 1.0, CH₂Cl₂); ¹H NMR (CDCl₃ 200 MHz) δ: 1.80 (1H, s), 2.34-2.40 (1H, m), 2.45 (3H, s), 2.48 (1H, s), 3.58 (2H, s), 3.65-3.73 (3H, m), 4.42-4.55 (1H, m), 5.02-5.23 (3H, m), 7.28-7.36 (7H, m), 7.73-7.77 (2H, d, J = 8.46). ¹³C NMR δ: 21.6, 36.8, 37.2, 52.1, 52.4, 52.5, 57.3, 57.6, 67.3, 67.4, 78.8, 127.7, 127.9, 127.9,

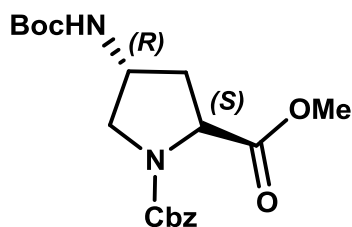
128.1, 128.5, 130.0, 133.5, 136.3, 145.3, 153.9, 154.4, 171.3, 171.5; MS (MALDI-TOF) m/z calcd for $C_{21}H_{23}NO_7S$ $[M+1]^+$ 434.47 found 434.12.

(2*S*, 4*R*)-*N*¹-(benzyloxycarbonyl)-4-azido proline methyl ester (19)



The compound **18** (10.0 g, 23 mmol) and NaN_3 (15.0 g, 230 mmol) were dissolved in dry DMF (100 mL). The solution was stirred for 8 h at 55-60 °C under nitrogen atmosphere. To remove DMF excess water (620 mL) was added to reaction mixture and the aqueous layer was extracted with ethyl acetate (3x150 mL). The combined organic layer was washed with water (3 x 200 mL) followed by brine. The organic layer dried over anhydrous Na_2SO_4 and concentrated under vacuum. The crude product obtained was purified by silica gel chromatography (4:6; ethyl acetate/hexane) to afford **19** as colourless thick oil. (6.9 g, 99% yield); $[\alpha]_D^{25}$ -45.75 (c 1.0, CH_2Cl_2). 1H NMR ($CDCl_3$, 400 MHz) δ : 7.38-7.27 (m, 5H), 5.22-5.07 (m, 2H), 4.53-4.42 (m, 1H), 4.25-4.18 (m, 1H), 3.84-3.54 (m, 5H), 2.52-2.42 (m, 1H), 2.27-2.18 (m, 1H). ^{13}C NMR (100 MHz, $CDCl_3$) δ : 171.9, 171.7, 154.6, 154.2, 136.3, 128.6, 128.5, 128.3, 128.1, 128, 67.5, 67.4, 59.3, 58.4, 57.9, 57.6, 52.7, 52.5, 51.5, 51.2, 36.4, 36.2, 35.4, 35.2; MS (MALDI-TOF) m/z calcd for $C_{14}H_{16}N_4O_4$ $[M]^+$ 304.30 found 304.21.

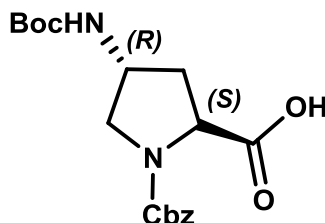
(2*S*, 4*R*)-*N*¹-(benzyloxycarbonyl)-4-(*t*-butoxycarbonylamino) proline methyl ester (20)



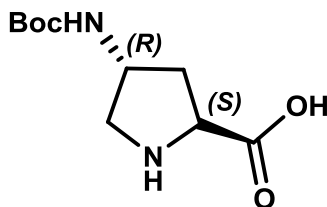
Compound **19** (7.0 g, 23 mmol) was dissolved in dry ethyl acetate (75 mL) to which Raney-Nickel (14 mL suspension in ethyl acetate) and di-*tert*-butyl-dicarbonate (6.1

g, 27 mmol) were added. The mixture was subjected to hydrogenation (H_2 gas, 60-psi). After completion of the reaction, the catalyst from reaction mixture was filtered off and the filtrate was concentrated under reduced pressure followed purification by silica gel chromatography to obtain compound **20**. (6.26 g, 72 % yield); $[\alpha]_D^{25}$ -29.41 (c 1.0, CH_2Cl_2). ^1H NMR (CDCl_3 , 400 MHz) δ : 7.37-7.28 (m, 5H), 5.42 (br, 1H), 5.30-5.0 (m, 2H), 4.44-4.34 (m, 2H), 3.79-3.48 (m, 5H), 2.53-2.43 (m, 1H), 2.11-1.96 (m, 1H), 1.44(s, 9H). ^{13}C NMR (100 MHz, CDCl_3) δ : 173.9, 155.2, 154.7, 154, 136.3, 128.5, 128.4, 128.1, 128, 127.9, 79.7, 67.4, 67.2, 58, 57.9, 57.6, 56.7, 53.5, 52.6, 52.4, 50, 49.1, 36.9, 36.4, 35.9, 35.2, 28.4; MS (MALDI-TOF) m/z calcd for $\text{C}_{19}\text{H}_{26}\text{N}_2\text{O}_6$ $[\text{M}]^+$ 378.42 found 378.02.

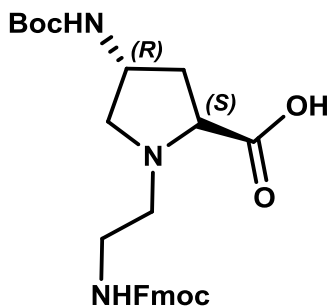
(2S, 4R)-N¹-(fluorenylmethoxycarbonyl)-4-(*t*-butoxycarbonylamino) proline (21)



The ester compound **20** (5.0 g, 14 mmol) was subjected to hydrolysis using NaOH (2N, 10 mL) for 1 h. MeOH was removed under vacuum and the aqueous layer was washed with ethyl acetate (3 x 50 mL) to remove unreacted organic compound. The residual aqueous layer was acidified by 2N HCl to pH 2 and extracted with ethyl acetate (3 x 75 mL) followed by concentration. The crude product obtained was purified by silica gel chromatography (3% MeOH/DCM) to afford a white solid powder **21**. (4.6 g, 96% yield); $[\alpha]_D^{25}$ -40.41 (c 1.0, CH_2Cl_2); ^1H NMR (CDCl_3 , 400 MHz) δ : 7.37-7.32 (m, 5H), 5.35-5.15 (m, 3H), 4.48-4.17 (m, 2H), 3.81-3.50 (m, 2H), 2.45-2.37 (m, 1H), 2.26-2.19 (m, 1H), 1.42(s, 9H); ^{13}C NMR (100 MHz, CDCl_3) δ : 174.5, 155.4, 135.7, 128.7, 128.5, 127.2, 127.8, 80.0, 68.4, 67.4, 58.7, 53.8, 53.4, 50.1, 37.1, 34.3, 28.4; MS (MALDI-TOF) m/z calcd for $\text{C}_{18}\text{H}_{24}\text{N}_2\text{O}_6$ $[\text{M}]^+$ 364.39 found 364.25.

(2*S*, 4*R*)-4-((*t*-Boc)amino)pyrrolidine-2-carboxylic acid (22**)**

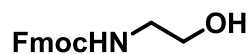
Compound **22** (5.0 g, 13.7 mmol) was dissolved in dry methanol (15 mL) to which 10% Pd/C (0.5 g) was added. The mixture was subjected to hydrogenation under H₂ gas (60-psi pressure) for 6 h. Water (200 mL) was added to the reaction mixture which was filtered through Whatman filter paper and the filtrate was concentrated under reduced pressure to yield **22**.

(2*S*, 4*R*)-N¹-(*Fmoc*) aminoethyl-4-((*t*-Boc)amino)pyrrolidine-2-carboxylic acid (24**)**

In a round bottom flask equipped with magnetic stirrer bar, aldehyde **23** (1.3 g, 4.3 mmol) was taken, to which dry MeOH:DCM:THF (70:30:70 mL) was added and stirred for 10 min. To the solution of aldehyde, proline derivative **22** (1 g, 4.3 mmol) with free amine was added. To this reaction mixture NaCNBH₃ (0.32 mg, 5.2 mmol) was added followed by ZnCl₂ (1.3 g, 30 mmol). This reaction mixture was stirred for 6 h, solvent was concentrated to 50 mL to this ethyl acetate was added and washed with saturated solution of NaHCO₃. The aqueous layer was removed and organic layer was washed with NaHCO₃ followed by brine, and dried over an anhydrous Na₂SO₄. It was filtered and the organic layer was evaporated and solid was purified by column chromatography using DCM and MeOH to yield **24**. (1.67 g, 60% yield); ¹H NMR (CDCl₃, 400 MHz) δ: 7.73-7.74 (2H, t, J = 4), 7.55-7.57 (2H, dd, J = 8), 7.29-7.30 (4H, m), 5.88 (1H, s), 5.52 (1H, s), 4.37-4.65 (2H, m),

3.95-4.17 (2H, m), 3.65-3.73 (2H, m), 3.50-3.57 (2H, m), 2.99-3.08 (2H, m), 2.07-2.23 (2H, m), 1.41 (9H, s); ^{13}C NMR (100 MHz, CDCl_3) δ : 174.0, 143.7, 143.6, 141.4, 127.8, 127.2, 125.4, 125.2, 120.5, 80.1, 69.2, 68.8, 67.8, 54.1, 47.2, 47.05, 38.2, 36.7, 28.4; MS (MALDI-TOF) m/z calcd for $\text{C}_{27}\text{H}_{33}\text{N}_3\text{O}_6$ $[\text{M}+\text{Na}]^+$ 518.22 found 518.18.

(N^1 -Fmoc) (2-hydroxyethyl)carbamate (25)



Ethanolamine (1 g, 16 mmol) was dissolved in 15 mL water and the pH was adjusted to ~ 10 by the slow addition of solid Na_2CO_3 . Solution of Fmoc-OSu (5.6 g, 16 mmol) in THF (10 mL) was added slowly to the reaction mixture. The reaction mixture was stirred overnight at room temperature. After completion of the reaction, the reaction mixture was acidified with aq. HCl (1N, 20 mL) in cold. The product was extracted with ethyl acetate (3x50 mL). Combined organic layers were washed with brine (30 mL) and dried over anhydrous Na_2SO_4 . The solvent was concentrated under reduced pressure to give **25**. (4.5 g, 98% yield); ^1H NMR (CDCl_3 , 400 MHz) δ : 7.78-7.30 (m, 8H), 5.22 (br, 1H), 4.44 (d, $J=8$ Hz, 2H), 4.24 (t, $J=16$ Hz, 2H), 3.70 (br, 2H), 3.34 (br, 2H), 2.11 (br, 1H); ^{13}C NMR (100 MHz, CDCl_3) δ : 143.94, 141.41, 127.80, 127.14, 125.08, 120.08, 66.86, 62.31, 47.31, 43.56; MS (MALDI-TOF) m/z calcd for $\text{C}_{17}\text{H}_{17}\text{NO}_3$ $[\text{M}+\text{Na}]^+$ 306.32 found 306.05.

(N^1 -Fmoc) (2-oxoethyl)carbamate (23)



Compound **25** (500 mg, 1.8 mol) was dissolved in ethyl acetate (10 mL) and IBX (1.8 g, 5.4 mol) was added to it. The resulting suspension was immersed in an oil bath set to 80°C and stirred vigorously open to atmosphere. After 3.25 h (TLC monitoring), the reaction was cooled to room temperature and filtered through medium glass frit. The filtered cake was washed with ethyl acetate and the combined filtrates were concentrated to yield Fmoc-amino propanaldehyde **23** which was used without purification for next reaction.

2.10.3 Peptide synthesis

All peptides were synthesized manually in a sintered vessel equipped with a stopcock. The readily available Rink amide resin with loading value 0.5-0.6 mmol/g was used and standard Fmoc chemistry was employed. The resin bound Fmoc group was first deprotected with 20% piperidine in DMF and the coupling reactions were carried out using *in situ* active ester method, using HBTU as a coupling reagent and HOBt as a recemization suppresser and DIPEA as a catalyst. All the materials used were of peptide synthesis grade (Sigma-Aldrich) and was used without further purification. Analytical grade DMF was purchased from Merck (India) and was distilled over P₂O₅ under vacuum at 45°C, stored over 4Å molecular sieves for 2 days before using for peptide synthesis.

2.10.3a Resin functionalization

The resin (2',4'-Dimethoxyphenyl-Fmoc-aminomethyl)-phenoxy, (100 mg) was taken in sintered vessel (25 mL) and rinsed with 5 mL of dry DCM and filtered. The process was repeated 3-4 times and the resulting resin was kept for 2 h in DCM (10 mL) for swelling. The solvent was removed and the resin was rinsed 3 times with dry DMF and kept 2 h in dry DMF (10 mL) for swelling before the first coupling. The deprotection of Fmoc group attached to the resin was done with 20% piperidine in DMF (3x5 mL) before proceeding for first amino acid coupling.

- The resin was washed and swollen in dry DCM for at least 2 h.
- Further washing and swelling with dry DMF for 2 h.
- Immediate coupling of 1st amino acid desired in C-terminus of peptide.

2.10.3b General method for solid phase peptide synthesis

All peptides were assembled on solid phase method by sequential amino acid coupling. Protected amino acids were well dried over P₂O₅ in vacuum desiccator before coupling. Fmoc protecting group was used for main chain amino group. The *t*-Boc protection was used for side chain amine protection and cleaved with 20% TFA in DCM for final cleavage of peptide from the resin. The peptide obtained after cleavage was stirred in 95% TFA in DCM for 2 h for complete deprotection *t* Boc.

2.10.3c *Synthesis protocol for solid phase synthesis*

The resin was pre-swollen overnight and the following steps were performed for each cycle.

- Wash with DMF 4 x 5 mL.
- 20% piperidine in DMF 2 x 5 mL (15 min for each) for deprotection of Fmoc group.
- Wash with DMF 3 x 5 mL, MeOH 3 x 5 mL and DCM with 3 x 5 mL.
- Test for complete deprotection (chloranil test).
- Coupling reaction with amino acid, DIPEA, HOBt and HBTU (3 eq.) in DMF (1 mL).
- Repeat of the coupling reaction in NMP for better yield.
- Test for completion of coupling reaction (chloranil test).

This cycle was repeated for every amino acid.

2.10.3d *General procedure for peptide couplings on Rink Amide Resin*

Fmoc-AA-OH (3 eq), HBTU (3 eq) and HOBt (3 eq) dissolved in DMF/NMP followed by *i*Pr₂NEt (7-8 eq) were added to the amino-functionalized resin in DMF. The mixture was kept for 2 h and bubbled with N₂ during last 5 min and washed with DMF (3x), MeOH (3x) and DCM (3x). The loading value for peptide synthesis is taken as 0.5~0.6.

2.10.3e *General procedure for Fmoc deprotection*

20% Piperidine in DMF was added to the resin and the reaction mixture was kept for 15 min, drained and the piperidine treatment was repeated 3 times. Finally the resin was washed with DMF (3x), MeOH (3x) and DCM (3x).

2.10.3 *Chloranil test*⁶

This sensitive test is used for reliable detection of secondary amino groups but it will also detect primary amines. A few beads of resin were taken in a small test tube and were washed with methanol. To this of 2% acetaldehyde in DMF and 2% chloranil in

DMF (5 drops each) were added. After a short mixing, the mixture was left at room temperature for 5 min and the beads inspected. A dark blue to green colour on by beads indicates a positive test (presence of NH group). A colourless to yellowish beads indicates then the test to be negative.

2.10.3g General procedure for acetylation

Triethylamine (20 eq, 1mL) and acetic anhydride (20 eq, 1mL) were added to the resin in DMF (\approx 100 mM). The mixture was kept for 1 h followed by bubbling with N₂ for 5 min and washed with DMF (3x), MeOH (3x) and DCM (3x).

2.10.3h Preparation of resin with peptide for cleavage

After the final coupling/acetylation, the resin was washed sequentially with DMF (5 x 10 mL), DCM (5x10 mL), toluene (5x10 mL) and finally with methanol (5x10 mL) and dried with nitrogen gas for 3 min. The resin in sintered flask was dried in a vacuum desiccator over P₂O₅.

2.10.3i General procedure for cleavage of peptides from the solid support

The dry peptide-resin (20 mg) was taken in round-bottomed flask to which of 20% TFA in DCM (10 mL) and Triisopropylsilane (as scavengers) (2-3 drops) were added. The resulting mixture was kept for 2 h by gentle shaking. The mixture was filtered through a sintered funnel and the resin was washed with 3x5 mL of above solution. The filtrate was collected in pear shape round-bottom flak and evaporated under reduced pressure. The resin was washed with MeOH (3X5 mL) and the washings were evaporated to dryness. The crude peptide obtained containing a N⁴-*t*-Boc group, was deprotected by stirring the peptide solution with 95% TFA in DCM (10 mL) for 2 h. The TFA: DCM mixture was removed under reduced pressure. The residue obtained was dissolved in anhydrous methanol (0.4 mL) to which anhydrous diethyl ether (4 x 1.5 mL) was added. The off-white precipitate obtained was centrifuged. The precipitation procedure was repeated twice to obtained peptide as a colourless powder.

2.10.4 High performance liquid chromatography (HPLC)

Peptides (**1-3**) were purified by reverse phase-HPLC on Waters 600 equipped with 2998-Photodiode array detector (PDA). Semi-preparative RP-C18 columns (250x10 mm, 10 μ m) of was used for peptides. The solvent system comprised of MeCN:Water (5:95) with 0.1% TFA for solution A and for solution B MeCN: Water (50:50), 0.1% TFA. A gradient of 0-100% at a flow rate of 3 mL/min was used to elute the peptide and the eluant was monitored at 220 nm. The peak corresponding to the peptide was collected and the fractions were freezed. Subsequently these peptides were concentrated by using speed vacuum. The purity of the final peptides were further analyzed on the Merck LiChrospher 100 RP-18 (250 x 4 mm, 5 μ M) column by using a gradient flow of 0 to 100% B in 30 min at a flow rate of 1.5 mL/min. The absorbance of the eluant was monitored at its corresponding wavelength and the purity was obtained from the integrator output. The purities of the hence purified peptides were found to be more than 95%.

2.10.4 MALDI-TOF characterization

MALDI-TOF mass spectra were obtained on either Voyager-Elite instrument (PerSeptive Biosystems Inc., Farmingham, MA) equipped with delayed extraction or on Voyager-De-STR (Applied Biosystems) instrument. Sinapinic acid and α -cyano-4-hydroxycinnamic acid (CHCA) both were used as matrix for peptides of which CHCA was found to give satisfactory results. A saturated matrix solution was prepared with typical dilution solvent (50:50:0.1 Water: MeCN: TFA) and spotted on the metal plate along with the oligomers. The metal plate was loaded to the instrument and the analyte ions are then accelerated by an applied high voltage (15-25 kV) in reflector mode, separated in a field-free flight tube and detected as an electrical signal at the end of the flight tube. HPLC purified peptides were characterized through this method and were observed to give good signal to noise ratio, mostly producing higher molecular ion signals.

2.10.5 Circular dichroism (CD) spectroscopy

CD spectrometric study was carried out on JASCO J-815 spectropolarimeter using cylindrical, jacketed quartz cell (10 mm path length), which was connected to Julabo-UC-

25 water circulator. For reproducible data, each set of spectra were measured using at least three individually prepared solutions. CD spectra were recorded using a spectral bandwidth of 1.0 nm at 25 °C with a time constant of 1 s and a step resolution of 1 nm. All the spectra were corrected for respective buffer condition and are typically averaged over 5-10 scans. The spectra are the result of 5-10 accumulations. A quartz cell with a path length of 1 cm was used with solutions containing approximately 0.9 mL (100 μ M) peptide solutions. For the spectra in buffer the blank spectrum of the solution was subtracted. All samples were equilibrated for at least 10 h before measurement except some TFE experiment.

Resolution: 1 nm
Band width: 1.0 nm
Sensitivity: 100 mdeg
Response: 1 sec
Speed: 100 nm/min
Accumulation: 5-10

All peptides had same peptide concentration (200 μ M) for CD measurements done in Na-phosphate buffer (pH 7.2). The data processing and curve fitting were performed using Origin 8.0 software. All spectra were collected at 25 °C with a 1 nm resolution and a scan rate of 100 nm min⁻¹. Spectra are the averages of 5 scans. The spectra could not be collected below a wavelength of 210 nm because of the absorbance properties of the salt solution.

2.11. References:

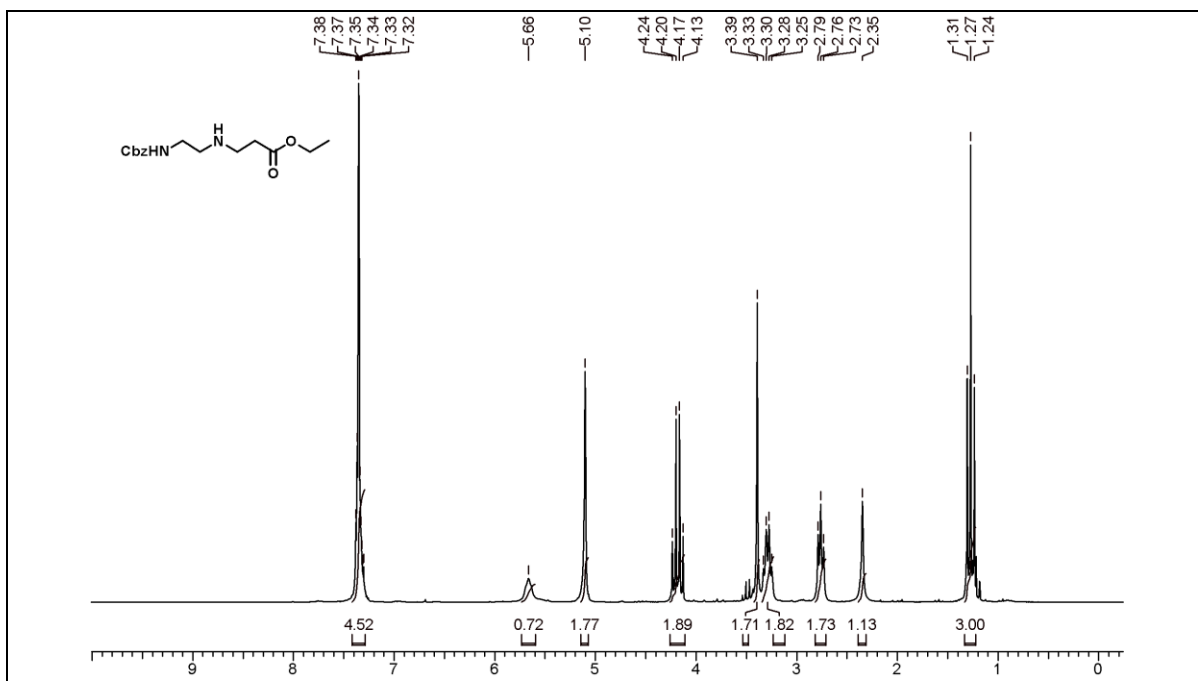
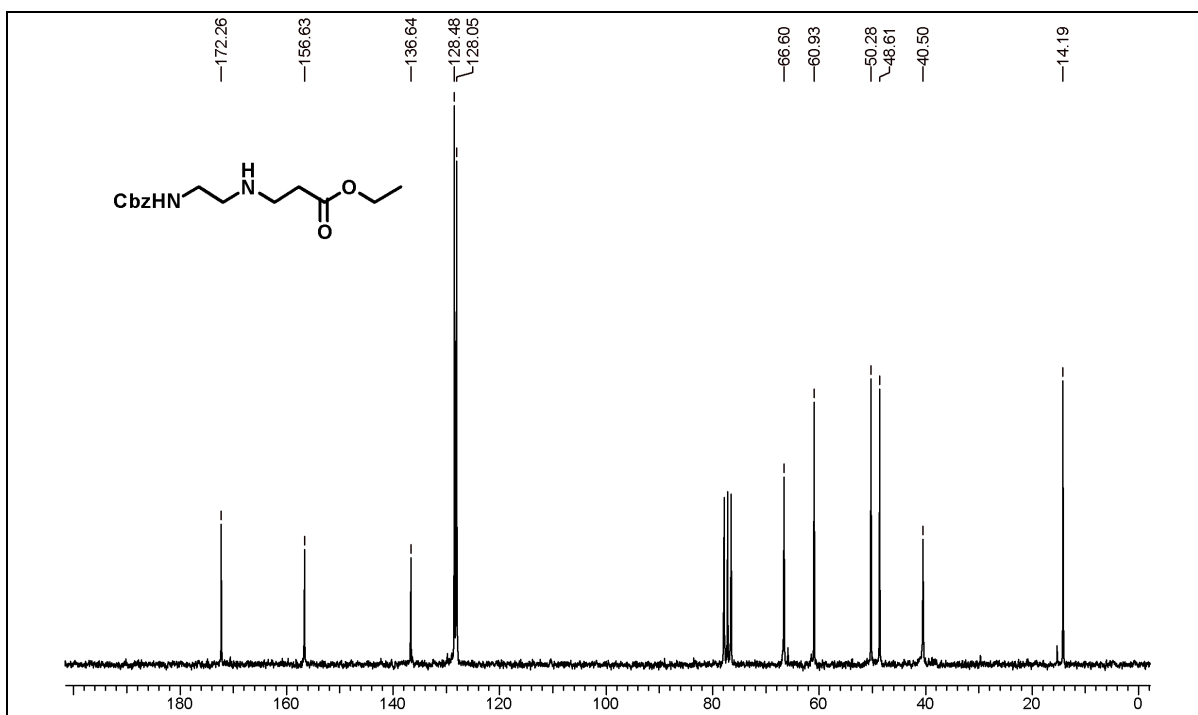
1. Karshikoff, A., Non-Covalent Interactions in Proteins. *Imperial College Press, United Kingdom, London* **2006**.
2. Roy, A.; Prabhakaran, P.; Baruah, P. K.; Sanjayan, G. J., Diversifying the structural architecture of synthetic oligomers: the hetero foldamer approach. *Chem. Commun.* **2011**, *47*, 11593-11611.
3. Cooley, R. B.; Arp, D. J.; Karplus, P. A., Evolutionary origin of a secondary structure: π -helices as cryptic but widespread insertional variations of α -helices enhancing protein functionality. *J. Mol. Biol.* **2010**, *404*, 232-246.
4. Varala, R.; Nuvula, S.; Adapa, S. R., Molecular Iodine-Catalyzed Facile Procedure for N-Boc Protection of Amines. *J. Org. Chem.* **2006**, *71*, 8283-8286.
5. Assem, N.; Yudin, A. K., Convergent synthesis of aminomethylene peptidomimetics. *Nat. Protocols* **2012**, *7*, 1327-1334.
6. Vojtkovsky, T., Detection of secondary amines on solid phase. *Pept.res.* **1995**, *8*, 236-7.
7. Bodansky, M. B., A., The Practice of Peptide Synthesis *Springer-Verlog, Berlin*.
8. Wu, Y.; Huang, H. W.; Olah, G. A., Method of oriented circular dichroism. *Biophys. J.* **1990**, *57*, 797-806.
9. Woody, R. W., Circular dichroism. *Methods enzymol.* **1995**, *246*, 34-71.
10. Appella, D. H.; Christianson, L. A.; Klein, D. A.; Powell, D. R.; Huang, X.; Barchi, J. J.; Gellman, S. H., Residue-based control of helix shape in [beta]-peptide oligomers. *Nature* **1997**, *387*, 381-384.
11. Appella, D. H.; Christianson, L. A.; Karle, I. L.; Powell, D. R.; Gellman, S. H., Synthesis and Characterization of trans-2-Aminocyclohexanecarboxylic Acid Oligomers: An Unnatural Helical Secondary Structure and Implications for β -Peptide Tertiary Structure. *J. Am. Chem. Soc.* **1999**, *121*, 6206-6212.
12. (a) Hamuro, Y.; Schneider, J. P.; DeGrado, W. F., De Novo Design of Antibacterial β -Peptides. *J. Am. Chem. Soc.* **1999**, *121*, 12200-12201; (b) Molski, M. A.; Goodman, J. L.; Craig, C. J.; Meng, H.; Kumar, K.; Schepartz, A., Beta-peptide bundles with fluororous cores. *J. Am. Chem. Soc.* **2010**, *132* (11), 3658-9; (c) Korendovych, I. V.; Shandler, S. J.; Montalvo, G.; DeGrado, W. F., Environment and sequence-dependence

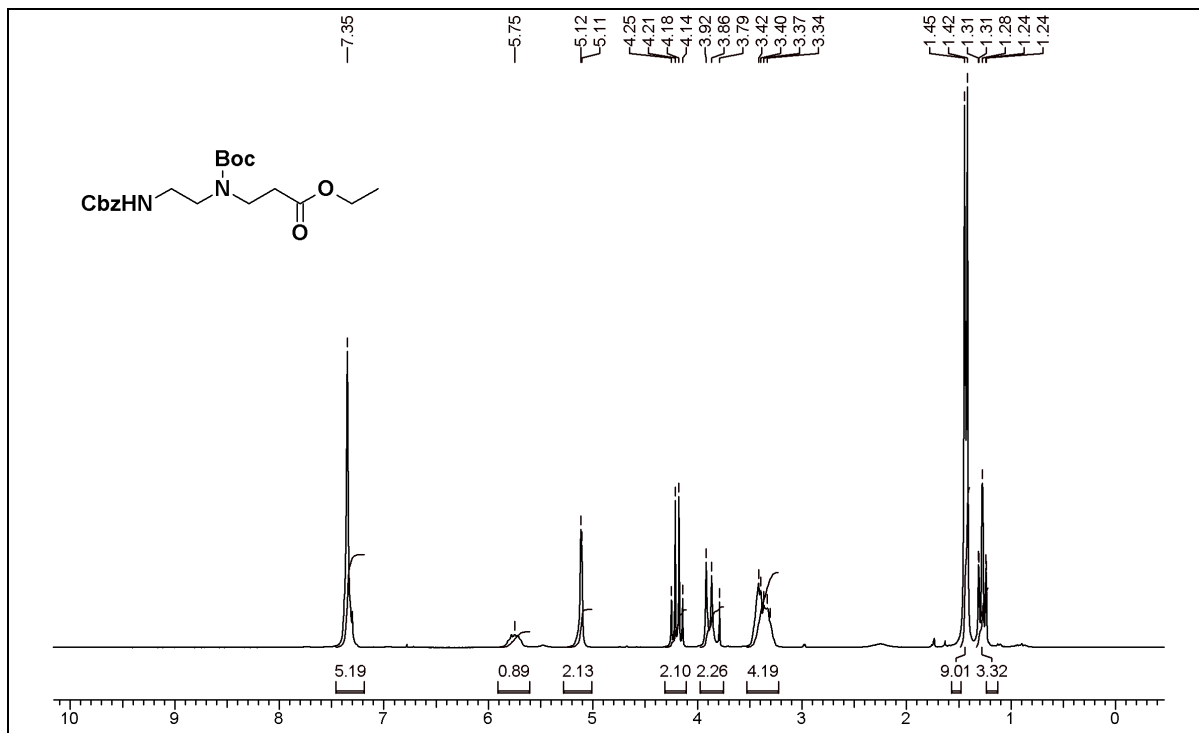
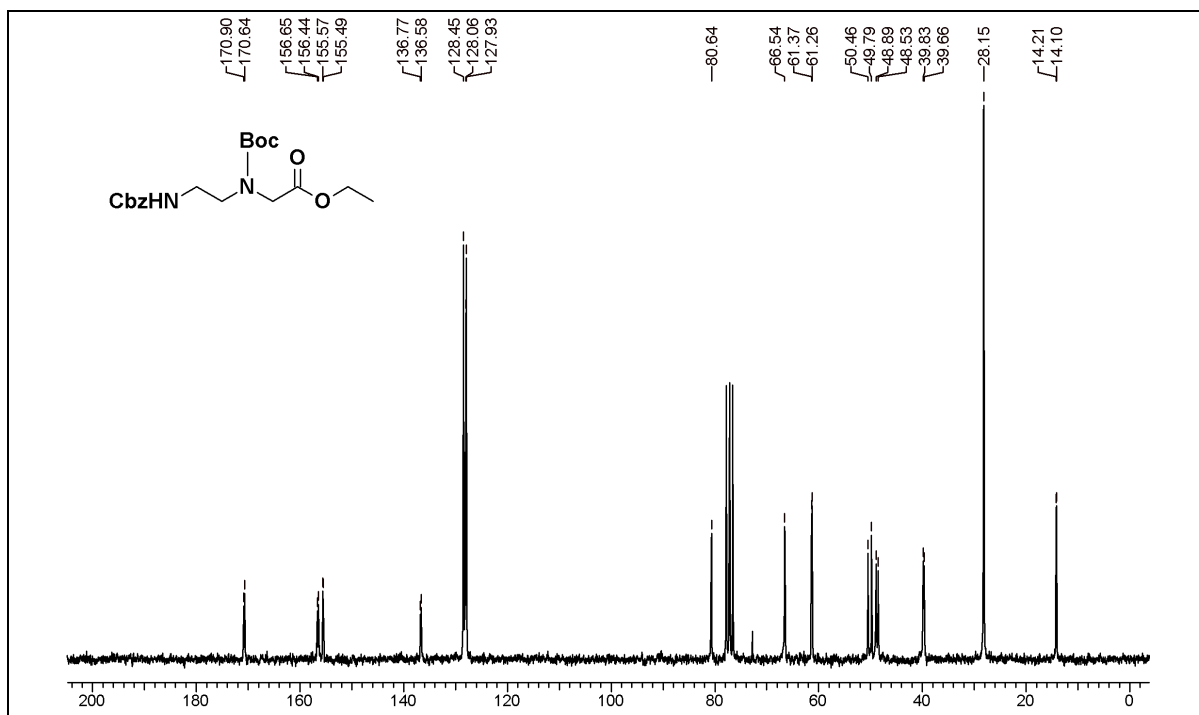
- of helical type in membrane-spanning peptides composed of $\beta(3)$ -amino acids. *Org. Lett.* **2011**, *13*, 3474-3477.
13. Rueping, M.; Schreiber, J. V.; Lelais, G.; Jaun, B.; Seebach, D., Mixed $\beta(2)/\beta(3)$ -Hexapeptides and $\beta(2)/\beta(3)$ -Nonapeptides Folding to (P)-Helices with Alternating Twelve- and Ten-Membered Hydrogen-Bonded Rings. *Helv. Chim. Acta* **2002**, *85*, 2577-2593.
14. Kumaran, S.; Roy, R. P., Helix-enhancing propensity of fluoro and alkyl alcohols: influence of pH, temperature and cosolvent concentration on the helical conformation of peptides. *J. Pept. Res.* **1999**, *53*, 284-293.
15. Sonar, M. V.; Ganesh, K. N., Water-Induced Switching of β -Structure to Polyproline II Conformation in the 4S-Aminoproline Polypeptide via H-Bond Rearrangement. *Org. Lett.* **2010**, *12*, 5390-5393.
16. Seebach, D.; Overhand, M.; Kühnle, F. N. M.; Martinoni, B.; Oberer, L.; Hommel, U.; Widmer, H., β -Peptides: Synthesis by Arndt-Eistert homologation with concomitant peptide coupling. Structure determination by NMR and CD spectroscopy and by X-ray crystallography. Helical secondary structure of a β -hexapeptide in solution and its stability towards pepsin. *Helv. Chim. Acta* **1996**, *79*, 913-941.
17. Feng, Y.; Melacini, G.; Taulane, J. P.; Goodman, M., Acetyl-Terminated and Template-Assembled Collagen-Based Polypeptides Composed of Gly-Pro-Hyp Sequences. 2. Synthesis and Conformational Analysis by Circular Dichroism, Ultraviolet Absorbance, and Optical Rotation. *J. Am. Chem. Soc.* **1996**, *118*, 10351-10358.
18. Cai, S.; Singh, B. R., A Distinct Utility of the Amide III Infrared Band for Secondary Structure Estimation of Aqueous Protein Solutions Using Partial Least Squares Methods†. *Biochemistry* **2004**, *43*, 2541-2549.
19. Chirgadze, Y. N.; Fedorov, O. V.; Trushina, N. P., Estimation of amino acid residue side-chain absorption in the infrared spectra of protein solutions in heavy water. *Biopolymers* **1975**, *14*, 679-94.
20. Barth, A.; Zscherp, C., What vibrations tell about proteins. *Q. rev. biophys.* **2002**, *35*, 369-430.

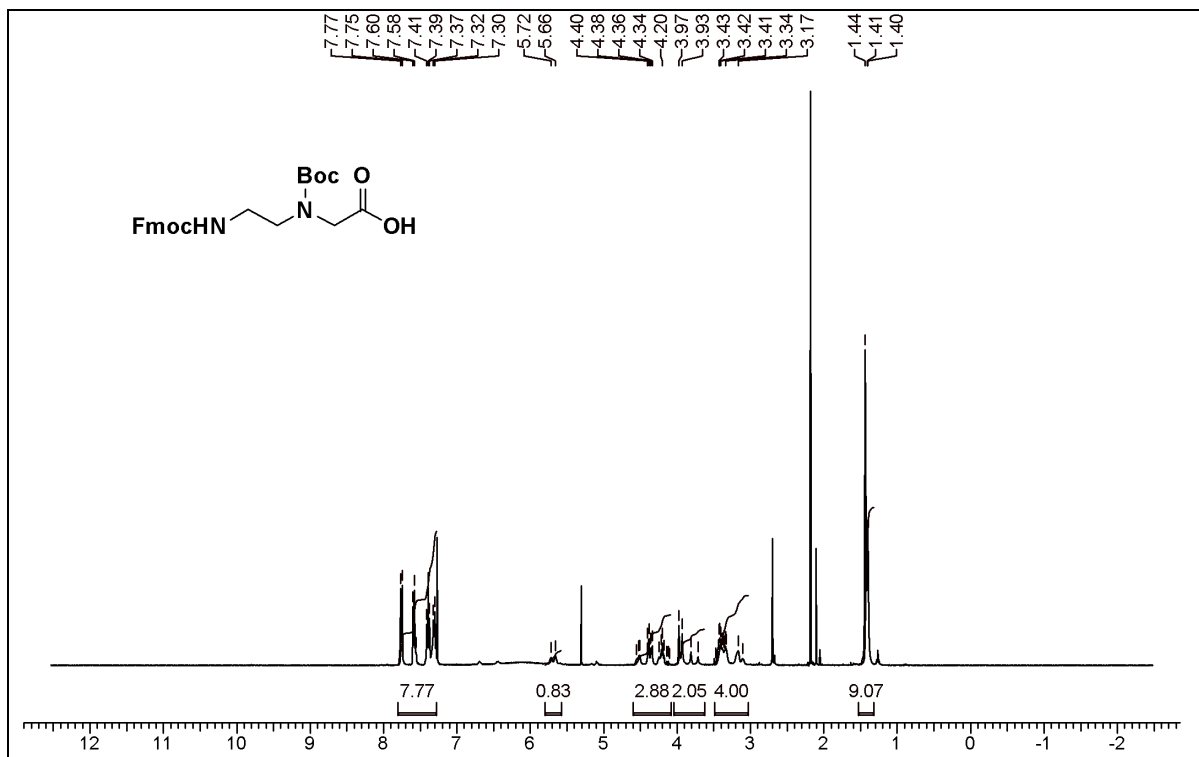
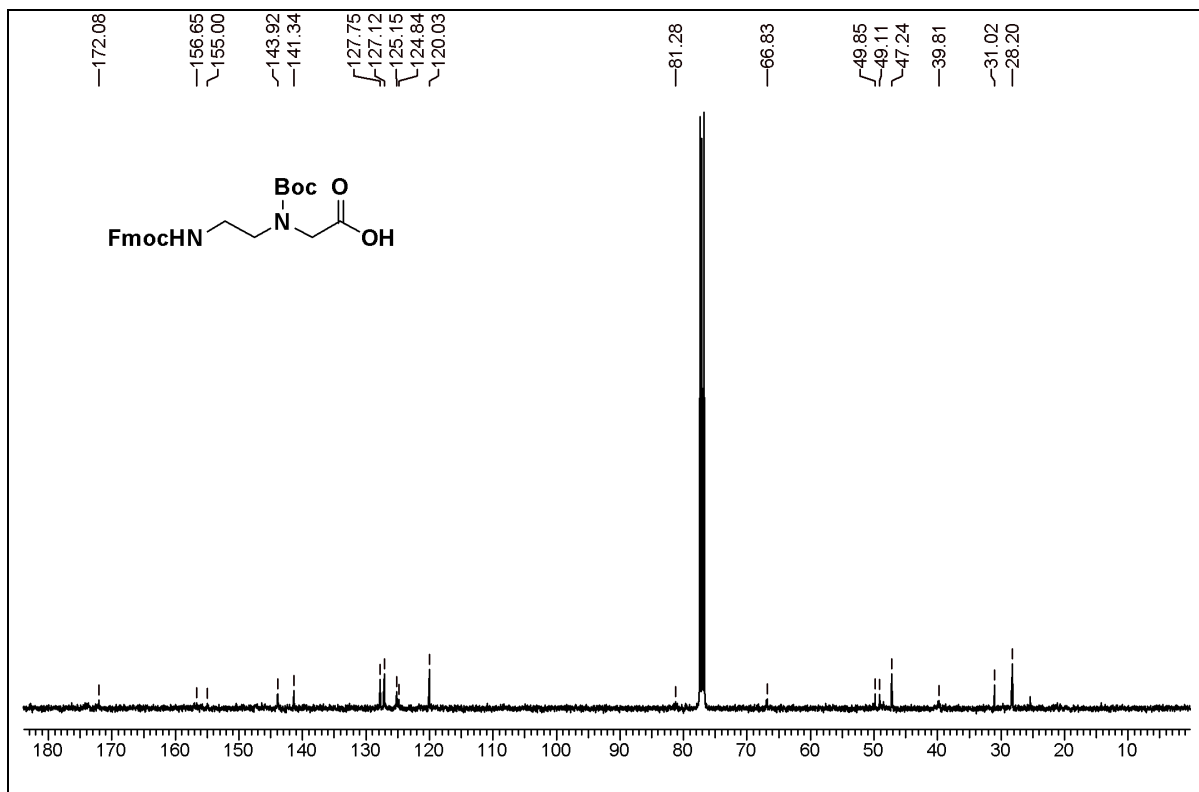
21. Englander, S. W.; Downer, N. W.; Teitelbaum, H., Hydrogen exchange. *Annu. rev. of biochem.* **1972**, *41*, 903-24.
22. Venyaminov, S.; Kalnin, N. N., Quantitative IR spectrophotometry of peptide compounds in water (H₂O) solutions. I. Spectral parameters of amino acid residue absorption bands. *Biopolymers* **1990**, *30*, 1243-57.
23. Zanetti-Polzi, L.; Aschi, M.; Amadei, A.; Daidone, I., Simulation of the Amide I Infrared Spectrum in Photoinduced Peptide Folding/Unfolding Transitions. *J. Phys. Chem. B* **2013**, *117*, 12383-12390.
24. Baginska, K.; Makowska, J.; Wiczak, W.; Kasprzykowski, F.; Chmurzynski, L., Conformational studies of alanine-rich peptide using CD and FTIR spectroscopy. *J. pept. sci. : an official publication of the European Peptide Society* **2008**, *14*, 283-9.
25. (a) Pomerantz, W. C.; Grygiel, T. L.; Lai, J. R.; Gellman, S. H., Distinctive circular dichroism signature for 14-helix-bundle formation by beta-peptides. *Org. Lett.* **2008**, *10*, 1799-802; (b) Byler, D. M.; Susi, H., Examination of the secondary structure of proteins by deconvolved FTIR spectra. *Biopolymers* **1986**, *25*, 469-487; (c) Jackson, M.; Mantsch, H. H., The use and misuse of FTIR spectroscopy in the determination of protein structure. *Crit. rev. biochem. mol. biol.* **1995**, *30*, 95-120; (d) DeFlores, L. P.; Ganim, Z.; Nicodemus, R. A.; Tokmakoff, A., Amide I'-II' 2D IR Spectroscopy Provides Enhanced Protein Secondary Structural Sensitivity. *J. Am. Chem. Soc.* **2009**, *131*, 3385-3391.

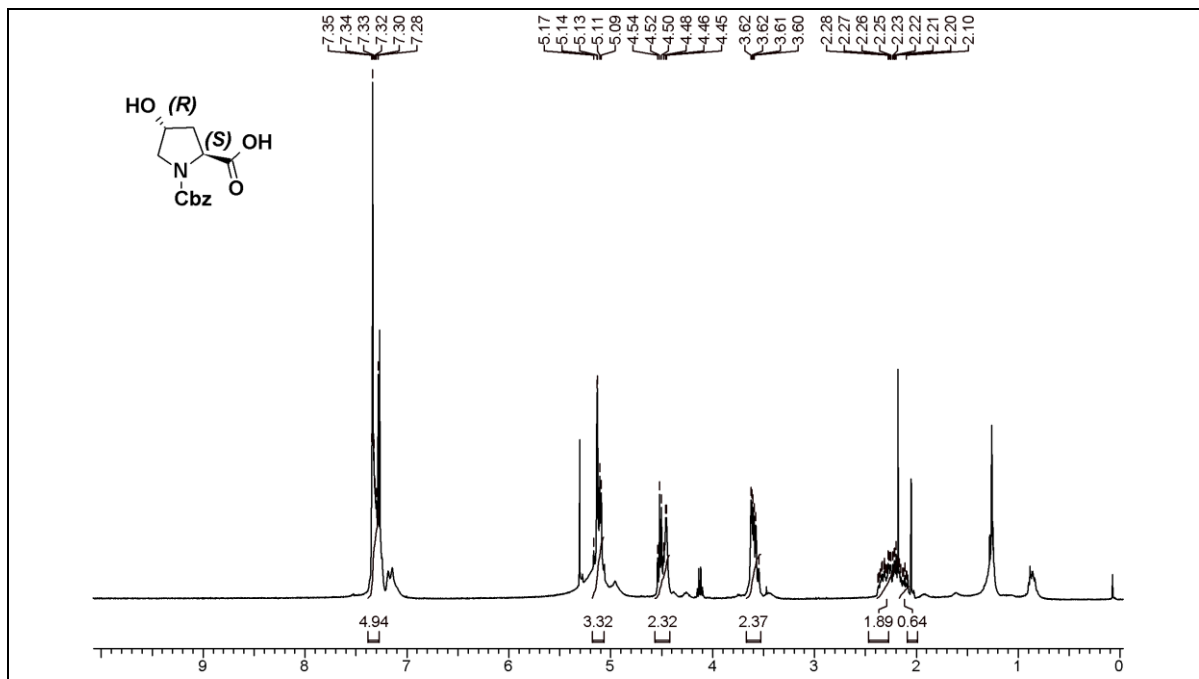
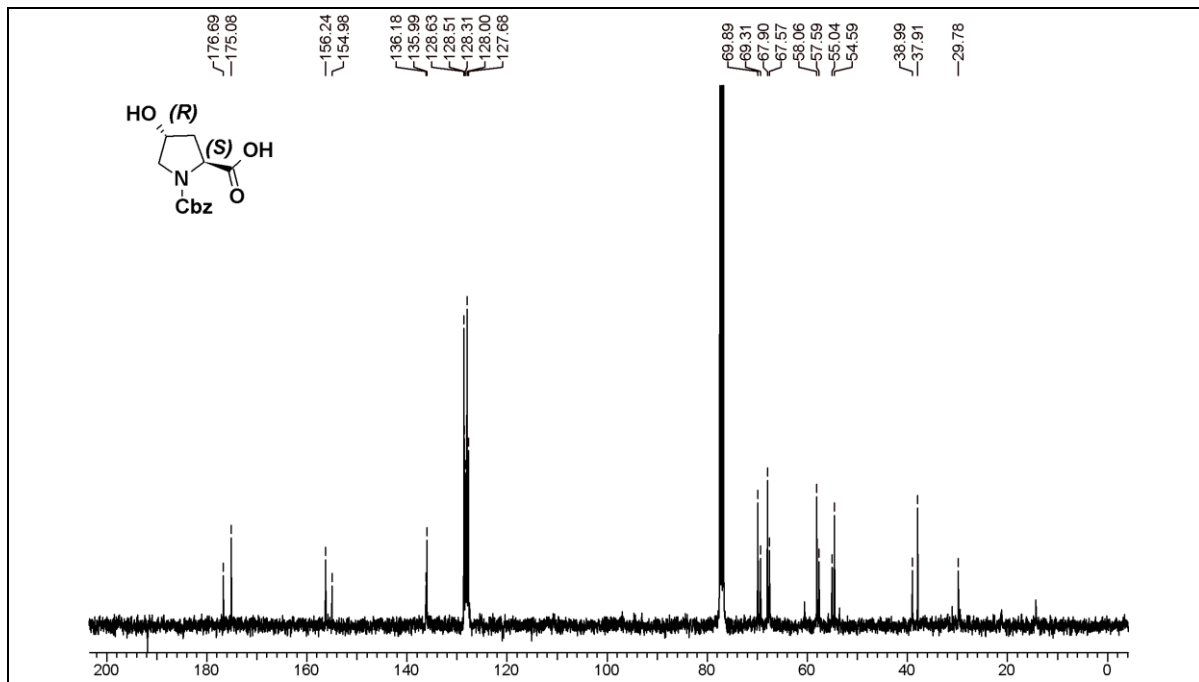
2.12 Appendix 2: Characterization data of synthesized compounds and peptides

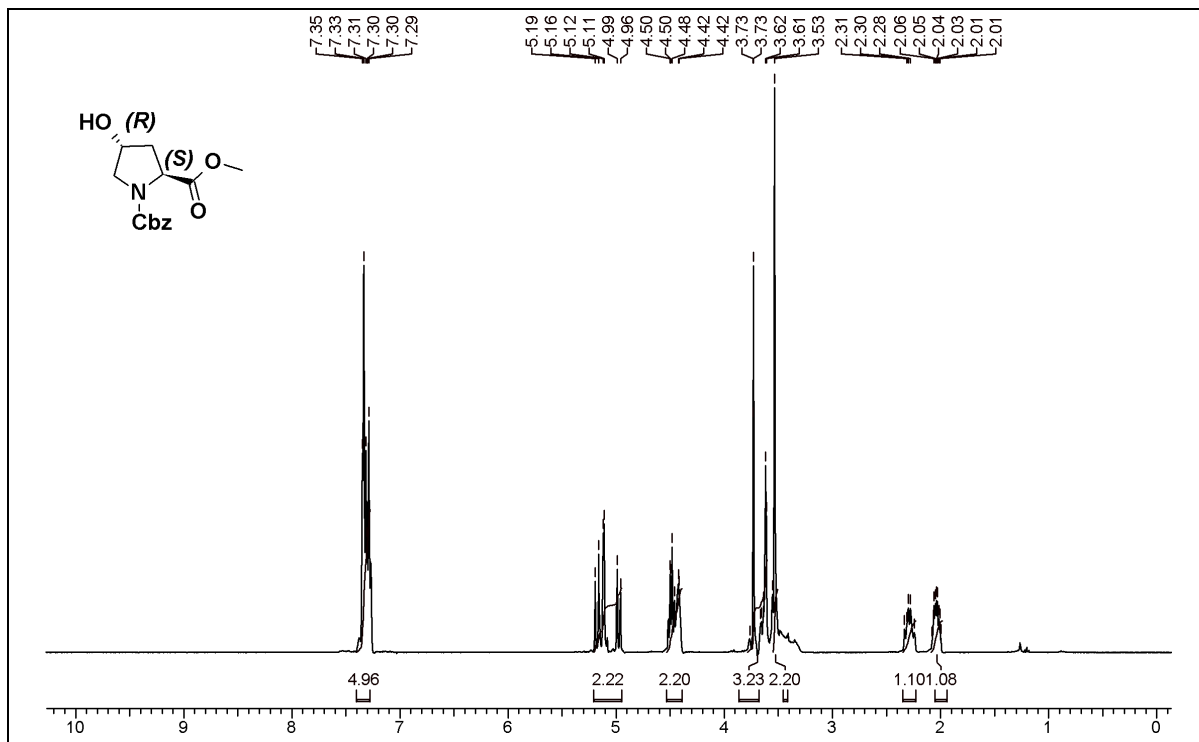
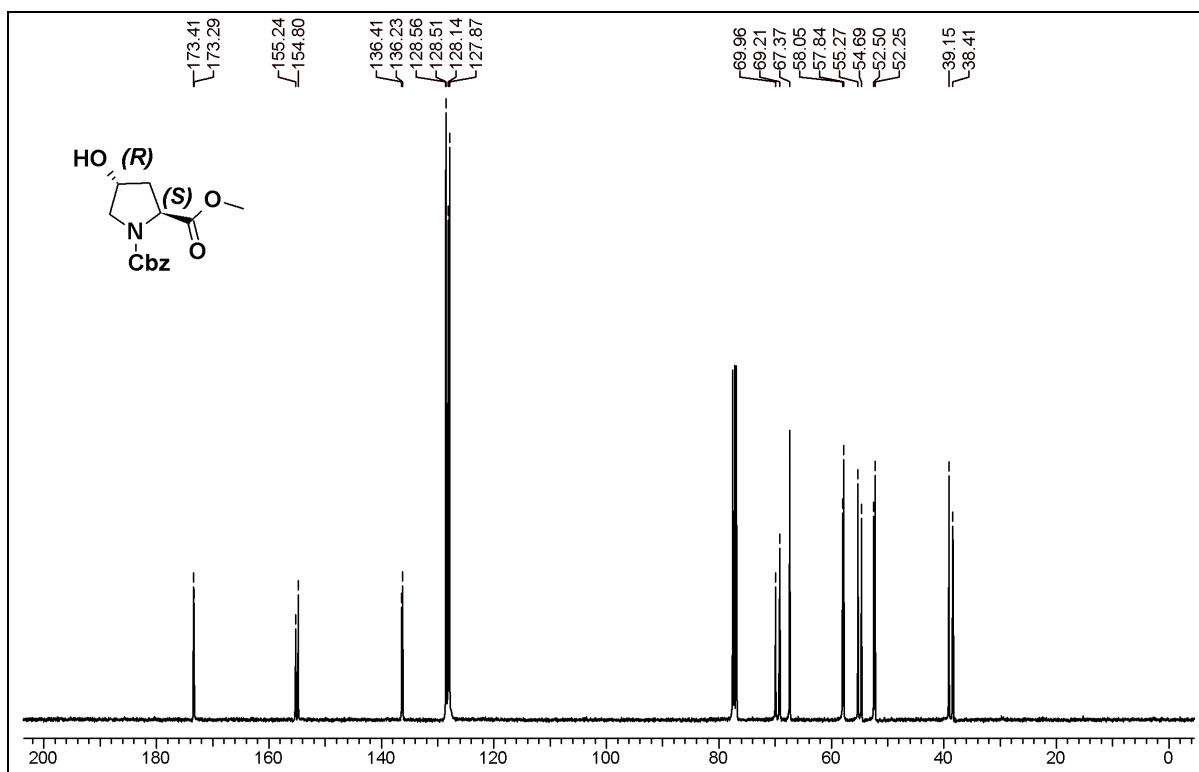
Entry	Page No.
A) ^1H , and ^{13}C NMR spectra of compounds (2-25)	113-125
B) HPLC of Peptides (1-4)	126-131
C) MALDI-TOF of peptides (1-4)	132-137

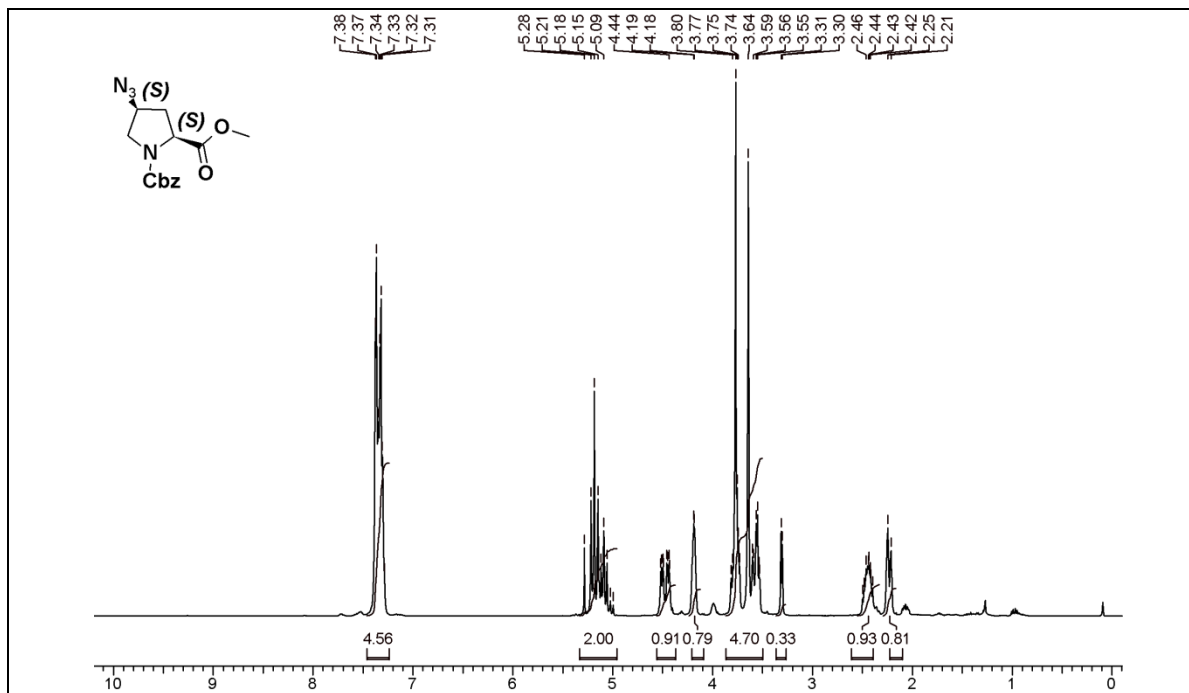
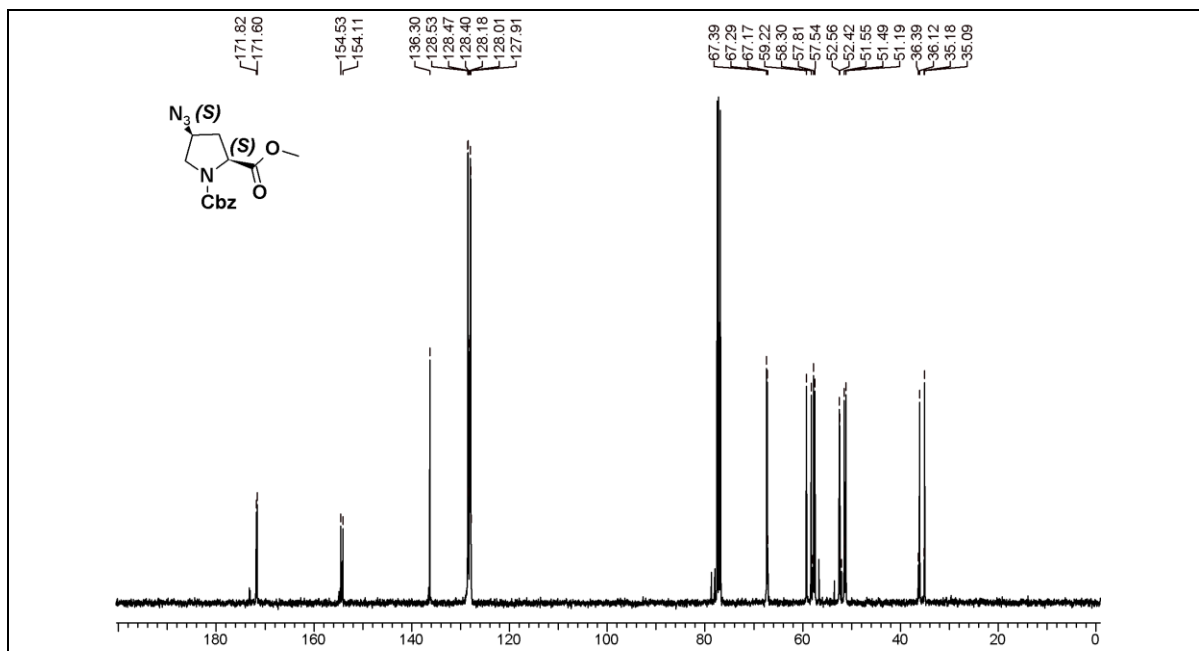
(A) ^1H , ^{13}C and DEPT NMR spectra of compounds (2-26) ^1H NMR of compound 3 ^{13}C NMR of compound 3

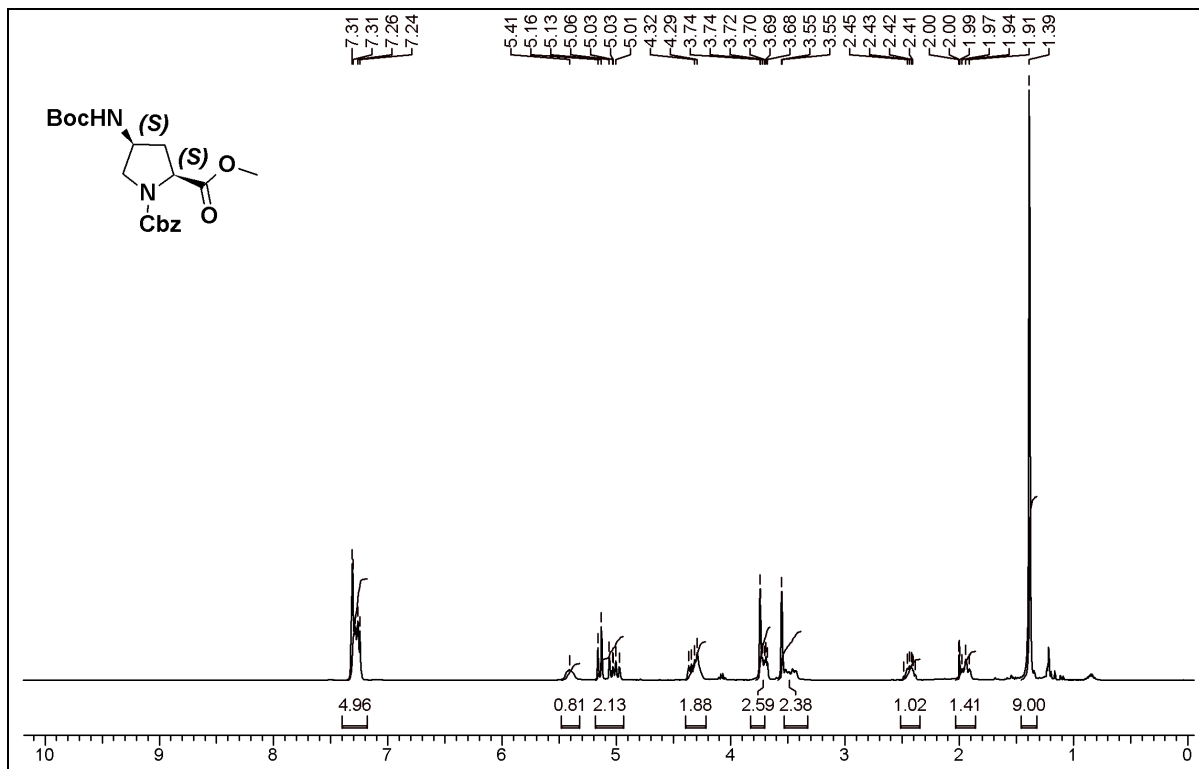
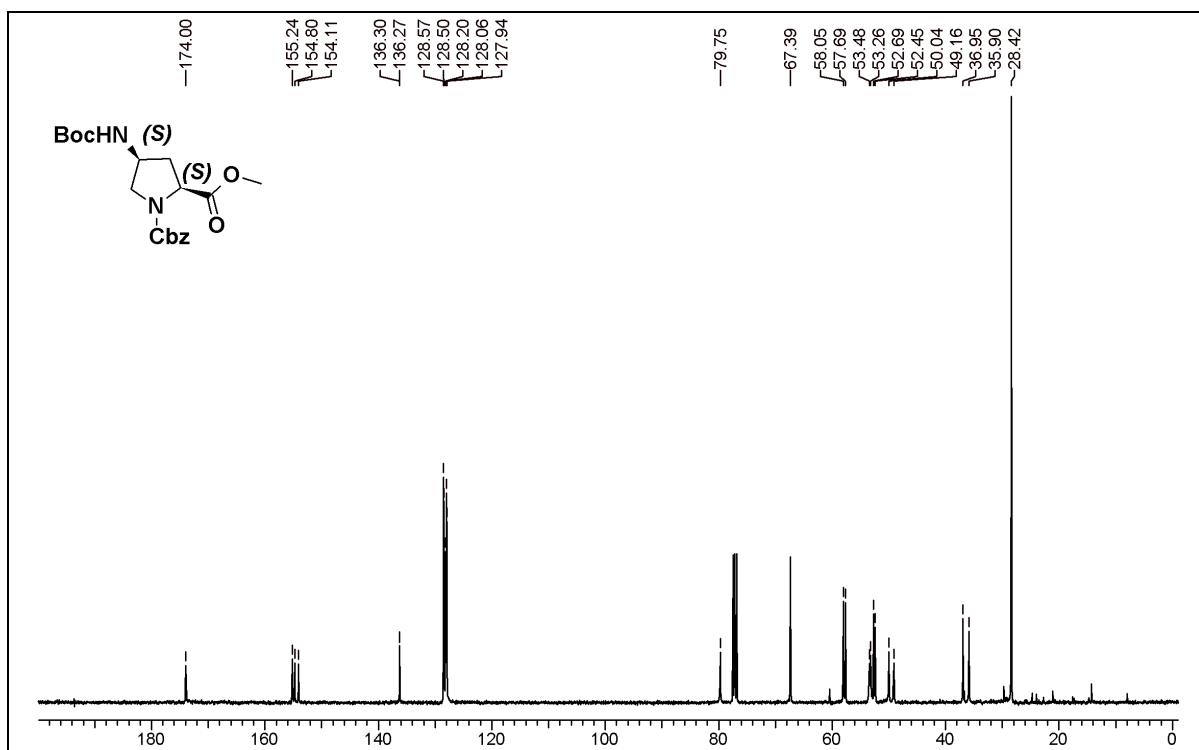
^1H NMR of compound 4 ^{13}C NMR of compound 4

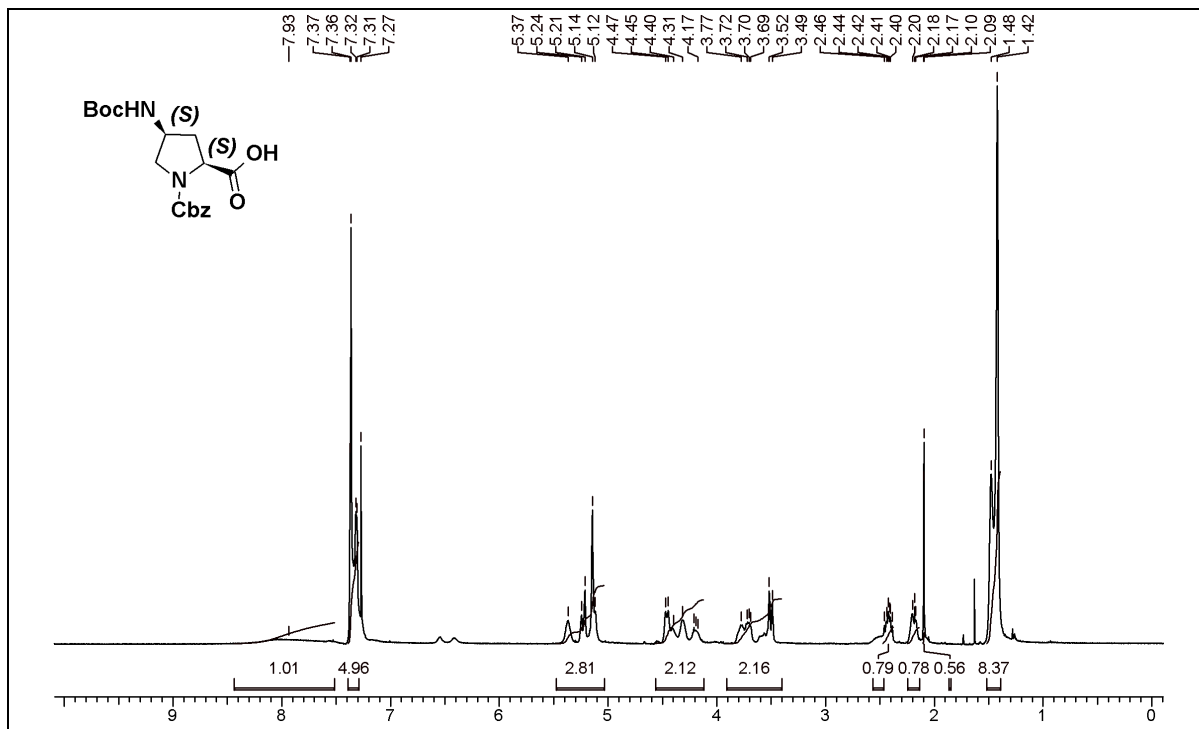
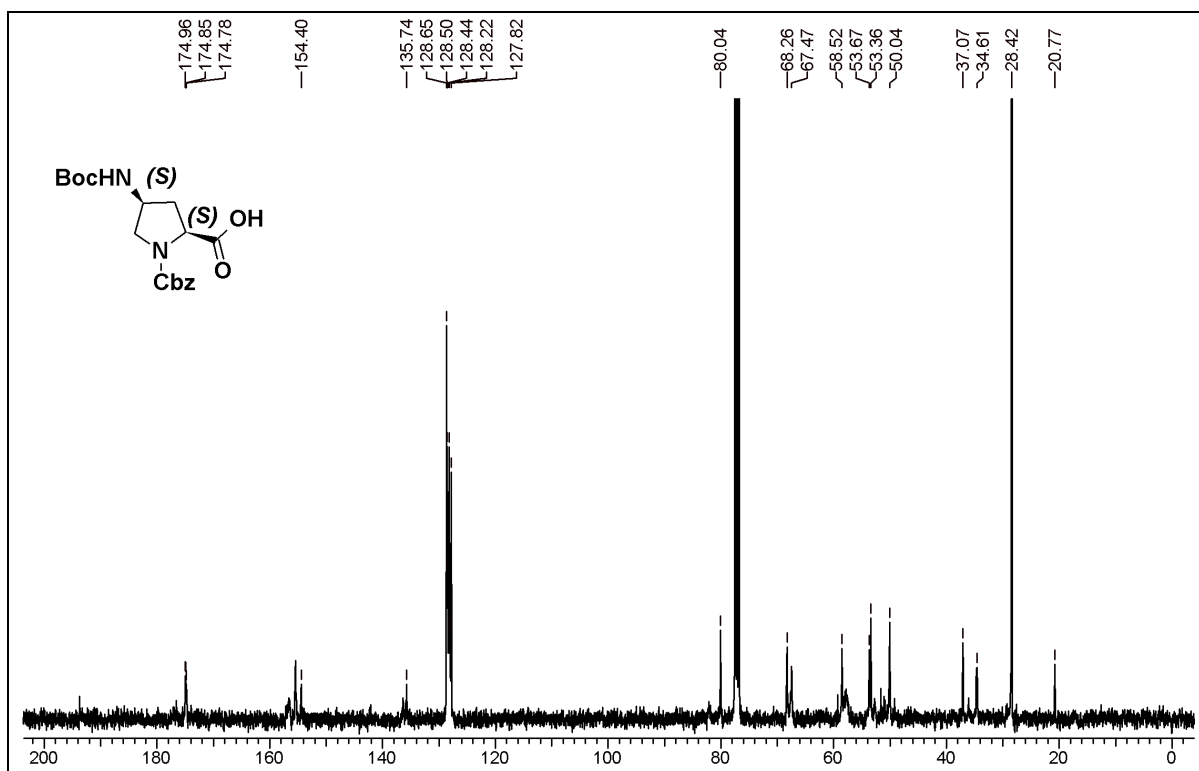
^1H NMR of compound 6 ^{13}C NMR of compound 6

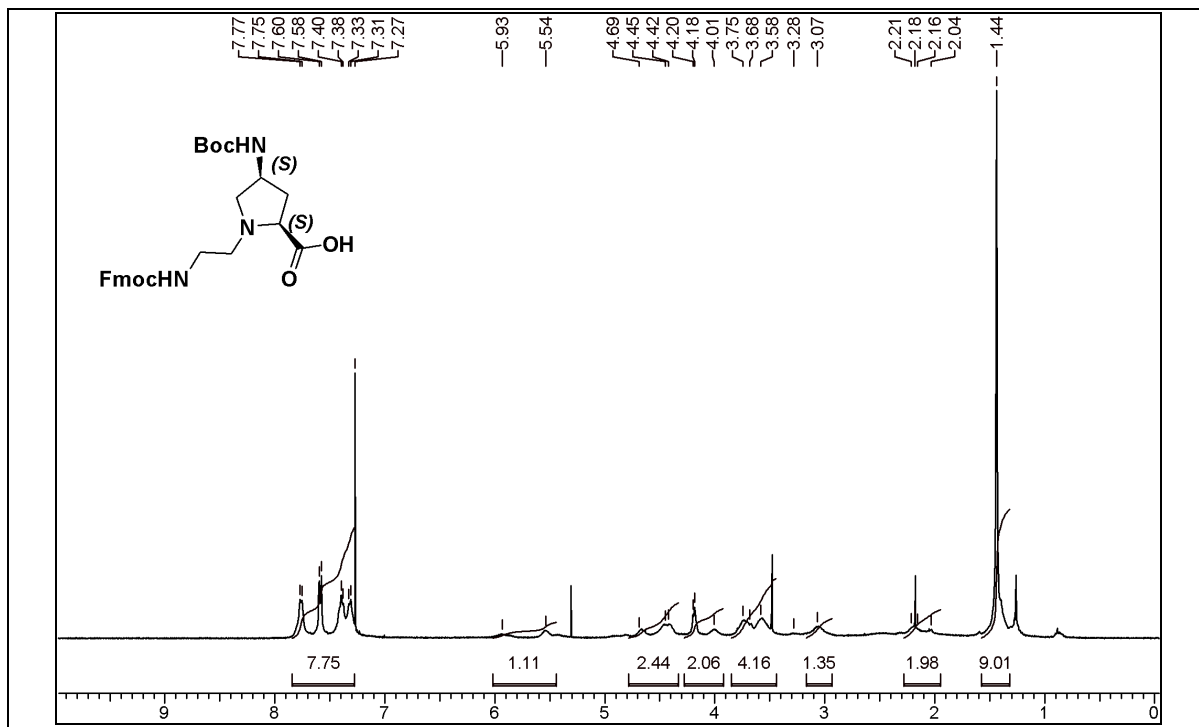
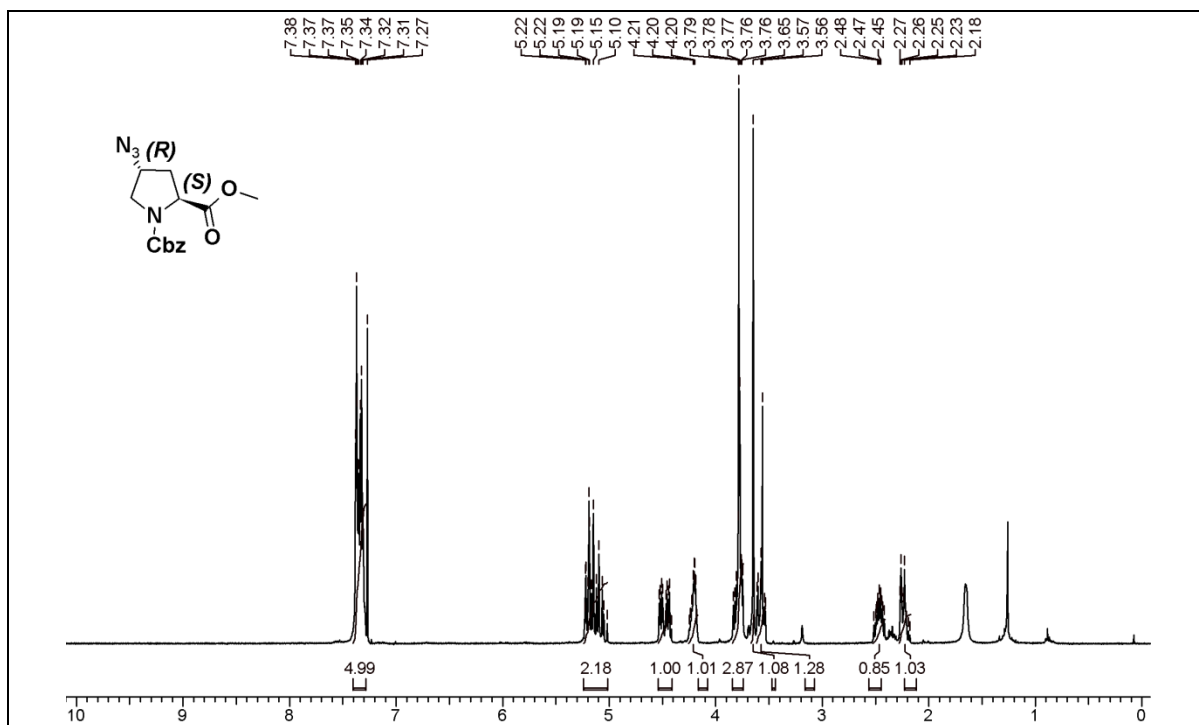
^1H NMR of compound 10 ^{13}C NMR spectrum of compound 10

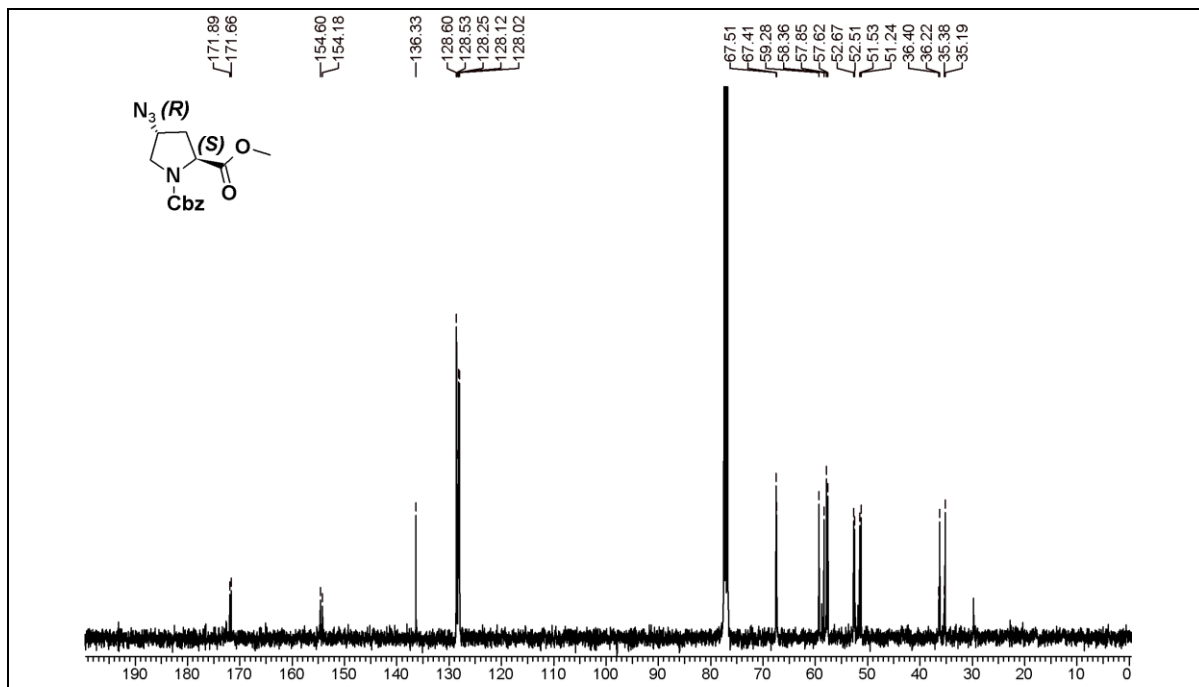
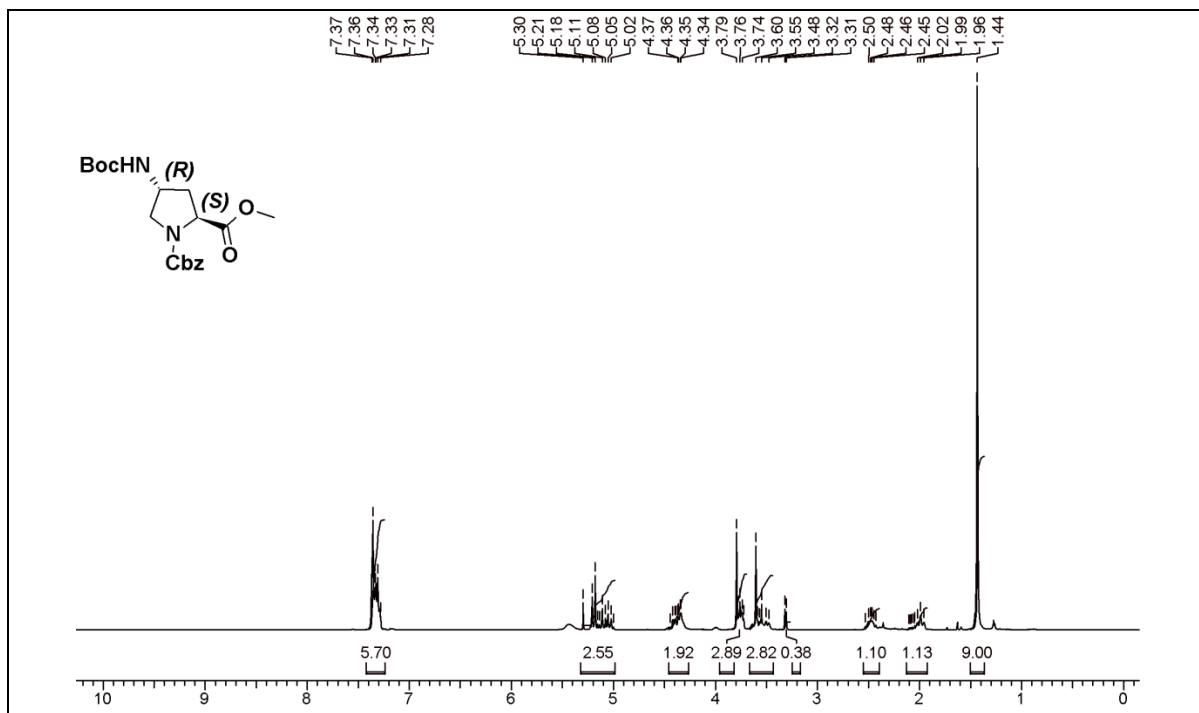
^1H NMR of compound 11 ^{13}C NMR spectrum of compound 11

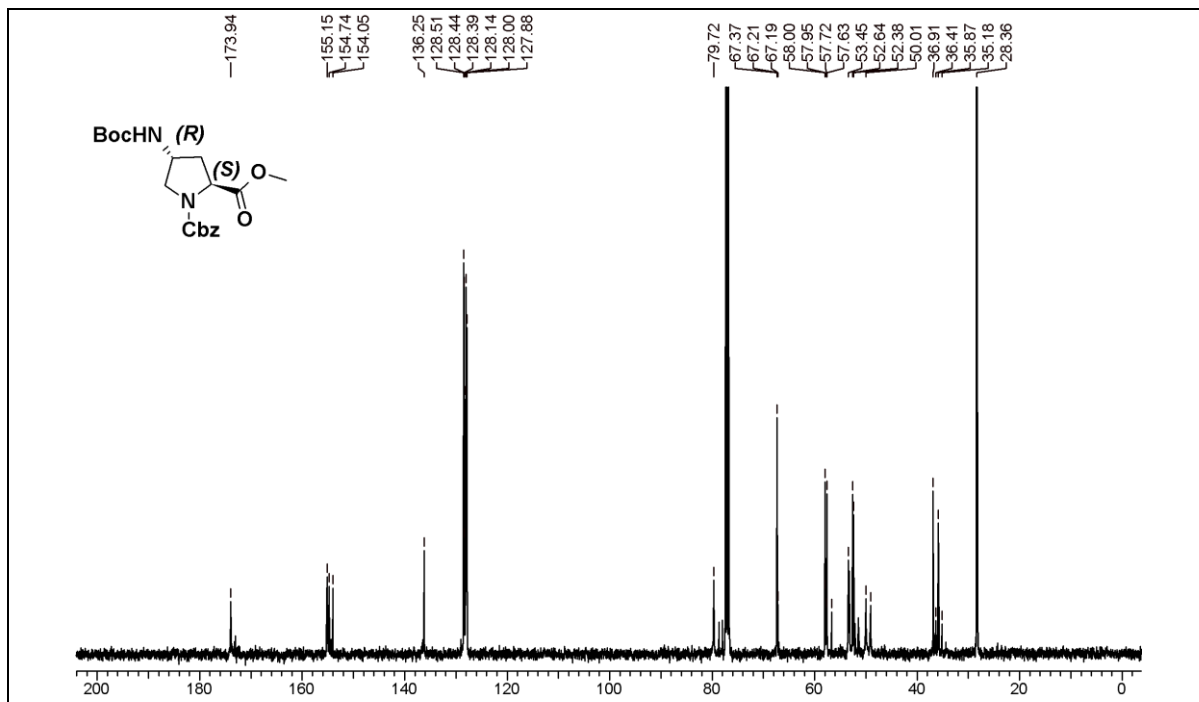
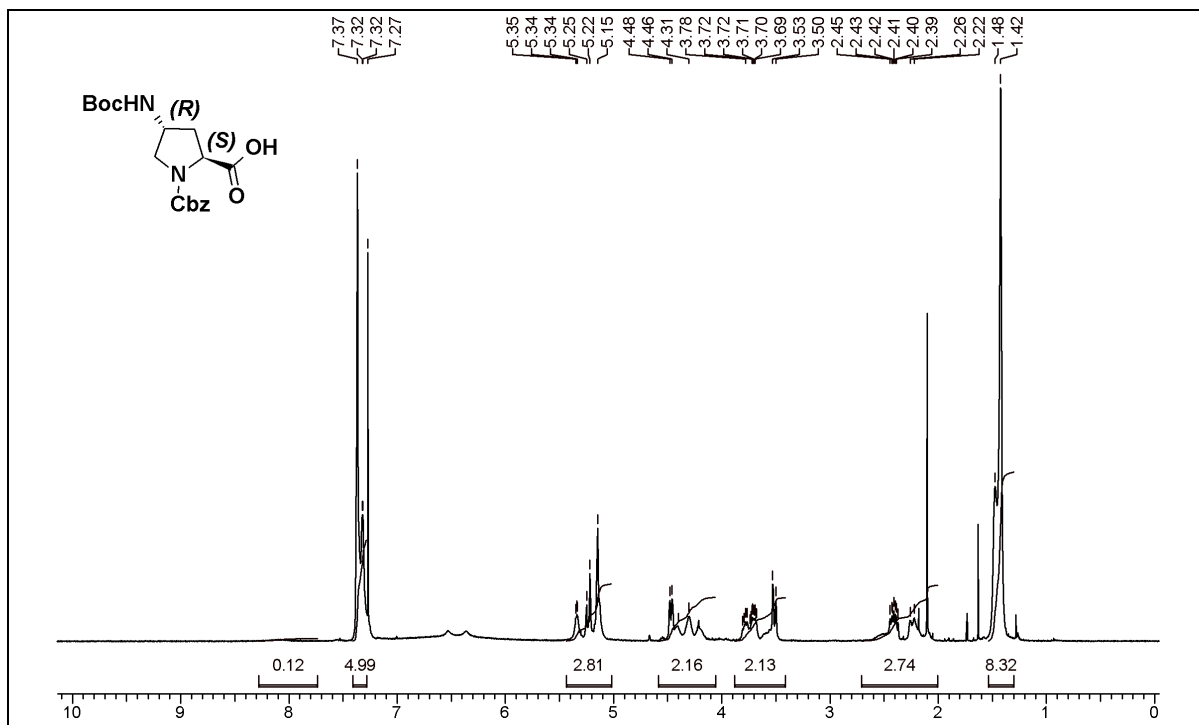
^1H NMR of compound 13 ^{13}C NMR of compound 13

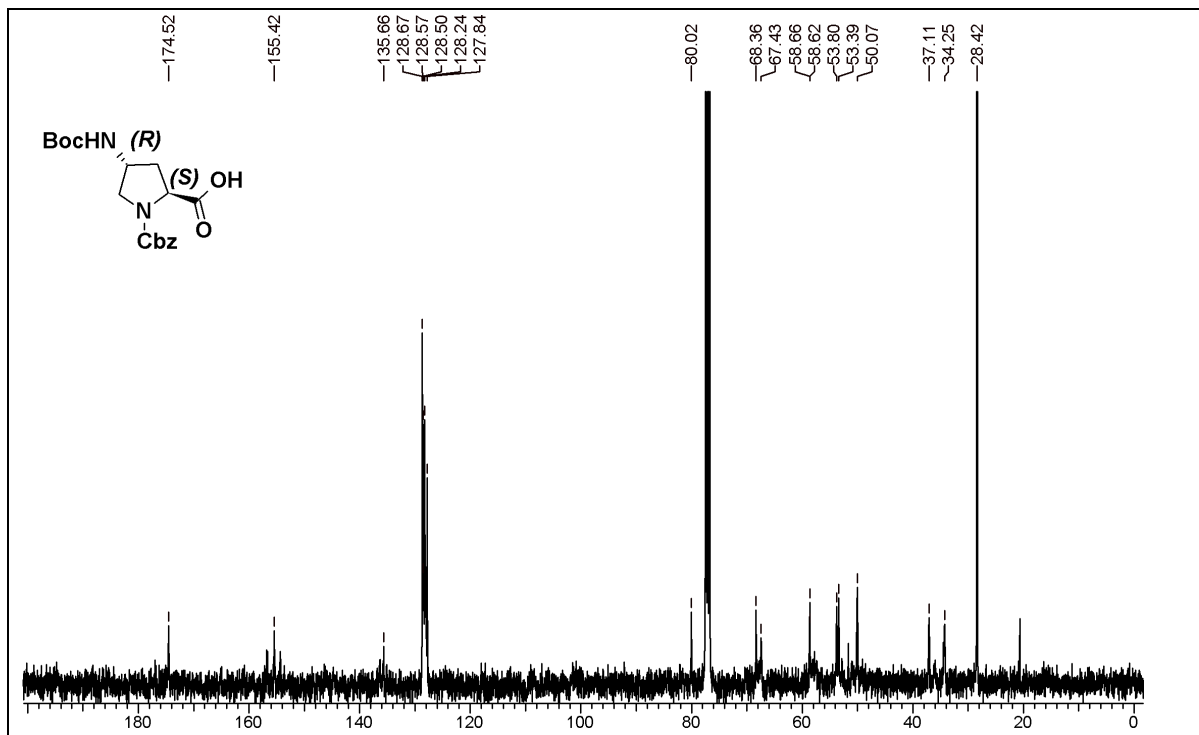
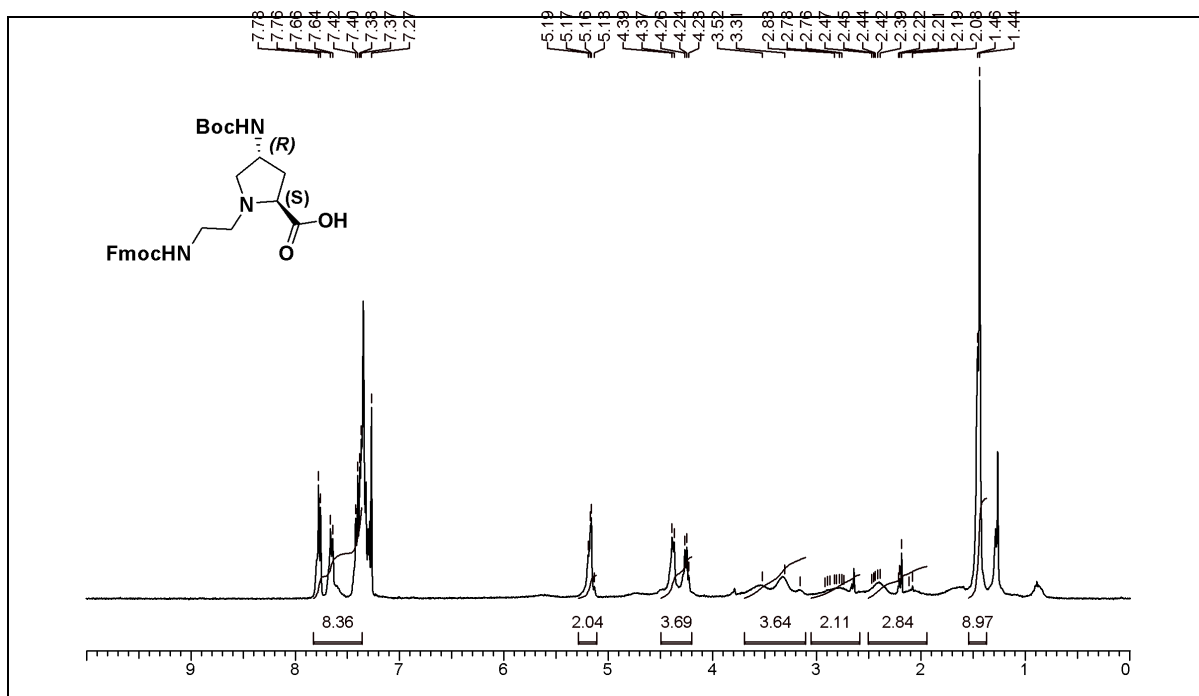
^1H NMR of compound 14 ^{13}C NMR spectrum of compound 14

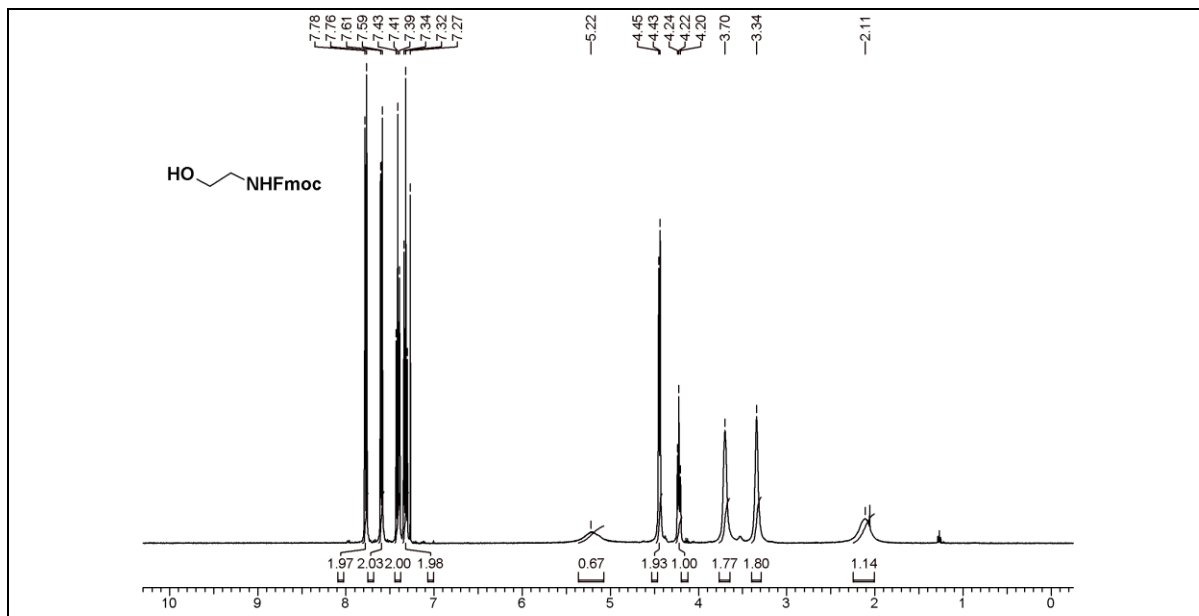
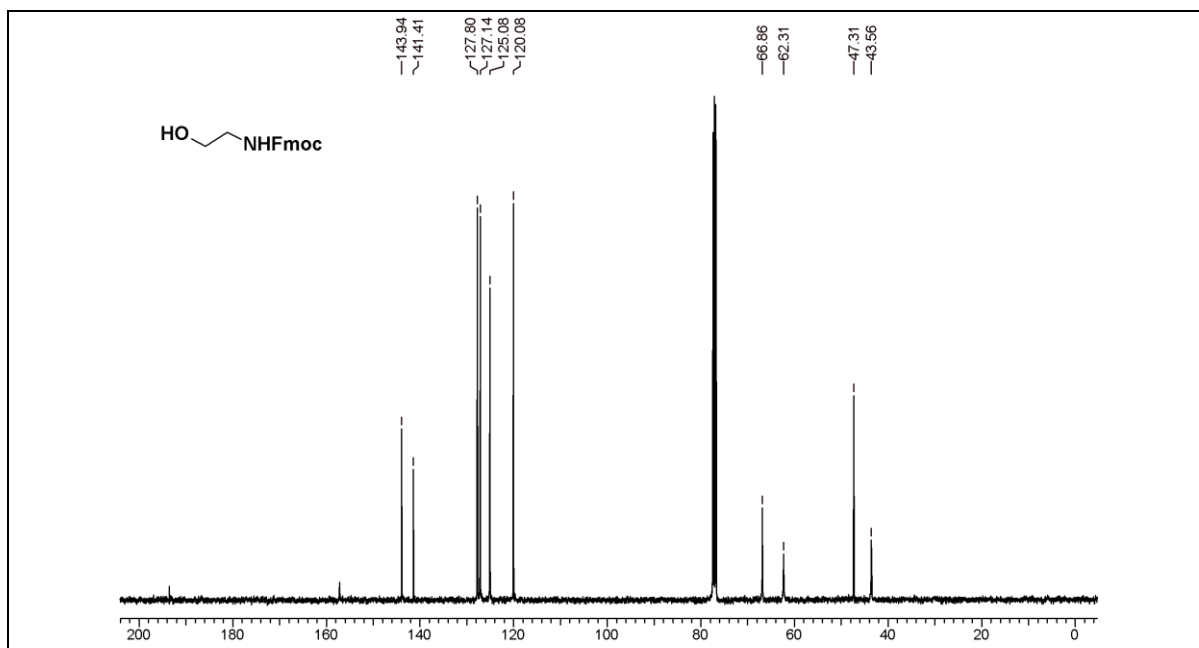
^1H NMR of compound 15 ^{13}C NMR of compound 15

^1H NMR of compound 17 ^1H NMR of compound 19

^{13}C NMR of compound 19 ^1H NMR of compound 20

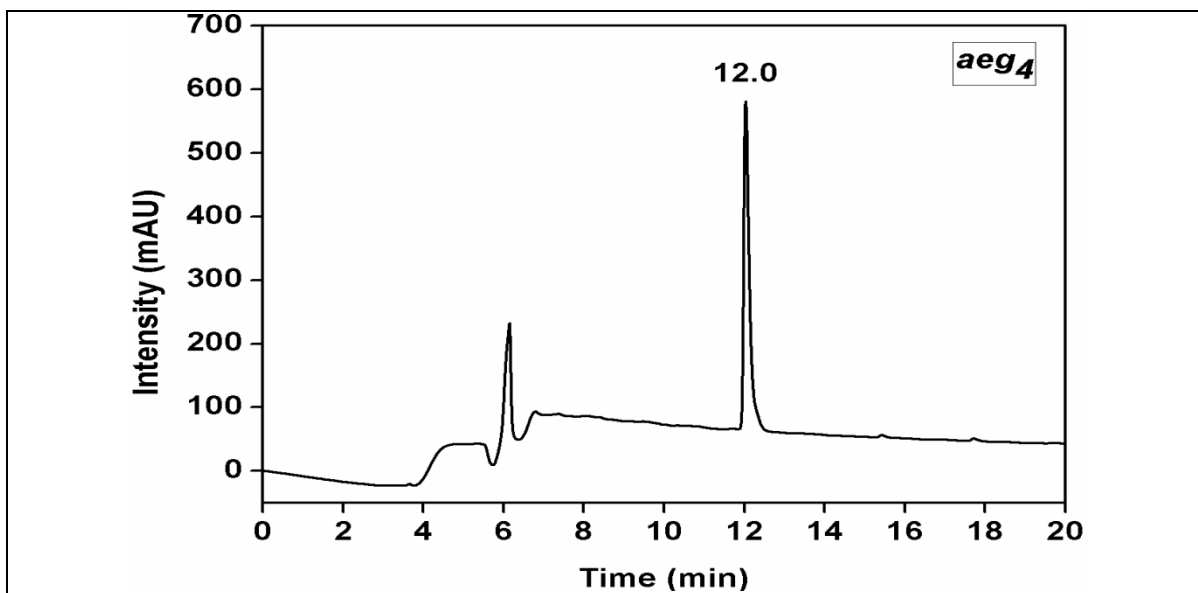
^{13}C NMR of compound 20 ^1H NMR of compound 21

^{13}C NMR of compound 21 ^1H NMR of compound 24

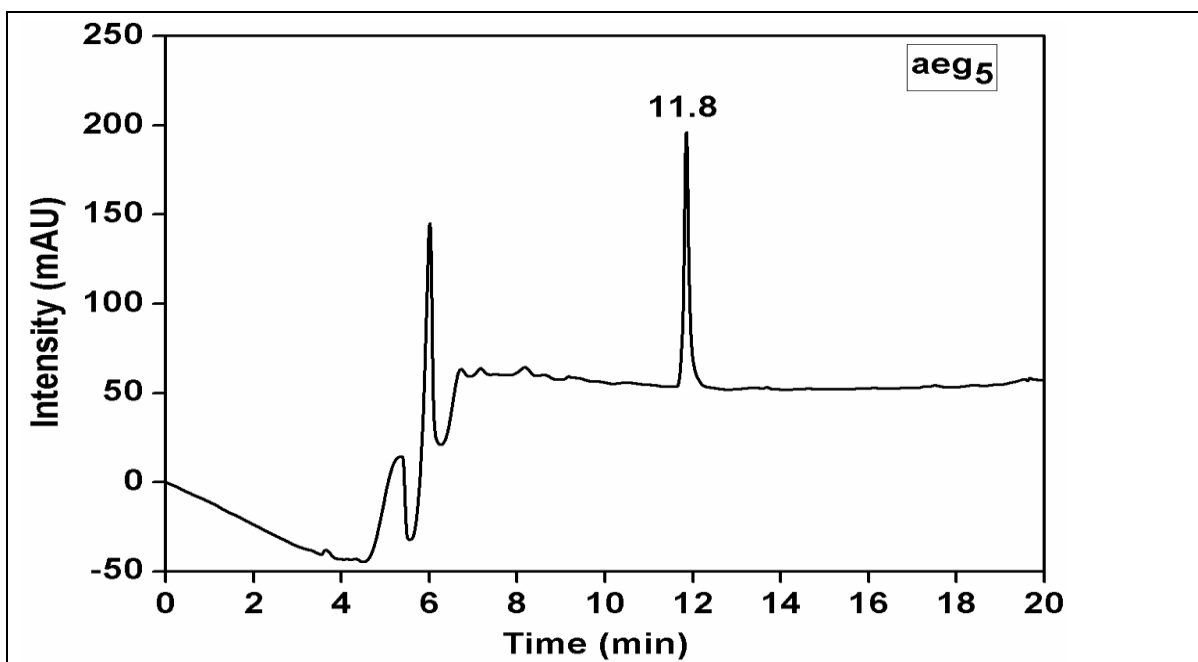
^1H NMR of compound 25 ^{13}C NMR spectrum of compound 25

B) HPLC Trace of 1-4

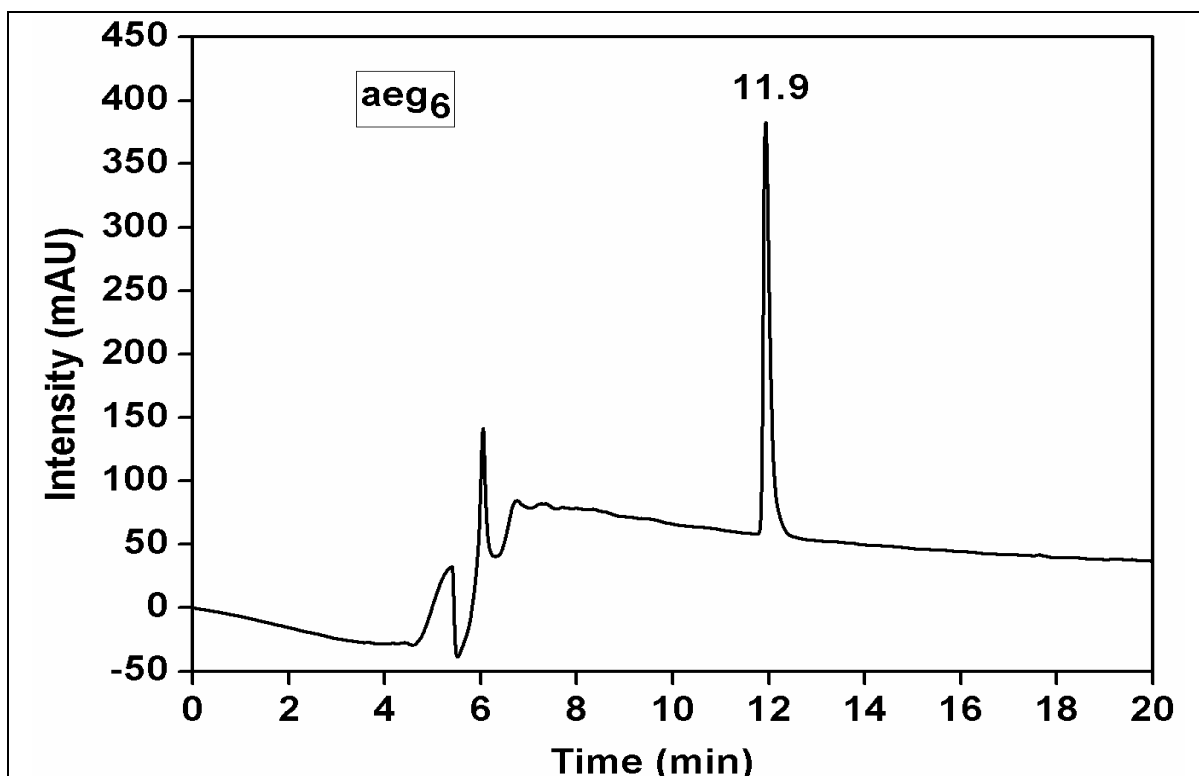
HPLC Trace of *aeg*₄



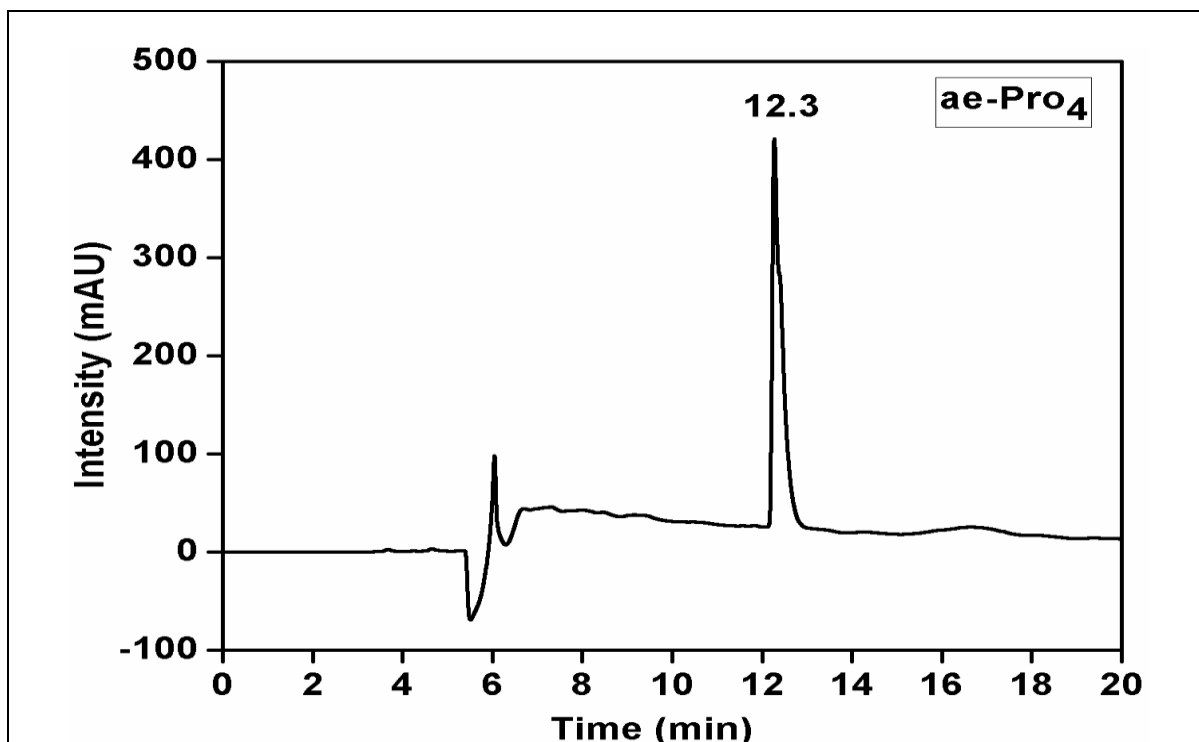
HPLC Trace of *aeg*₅



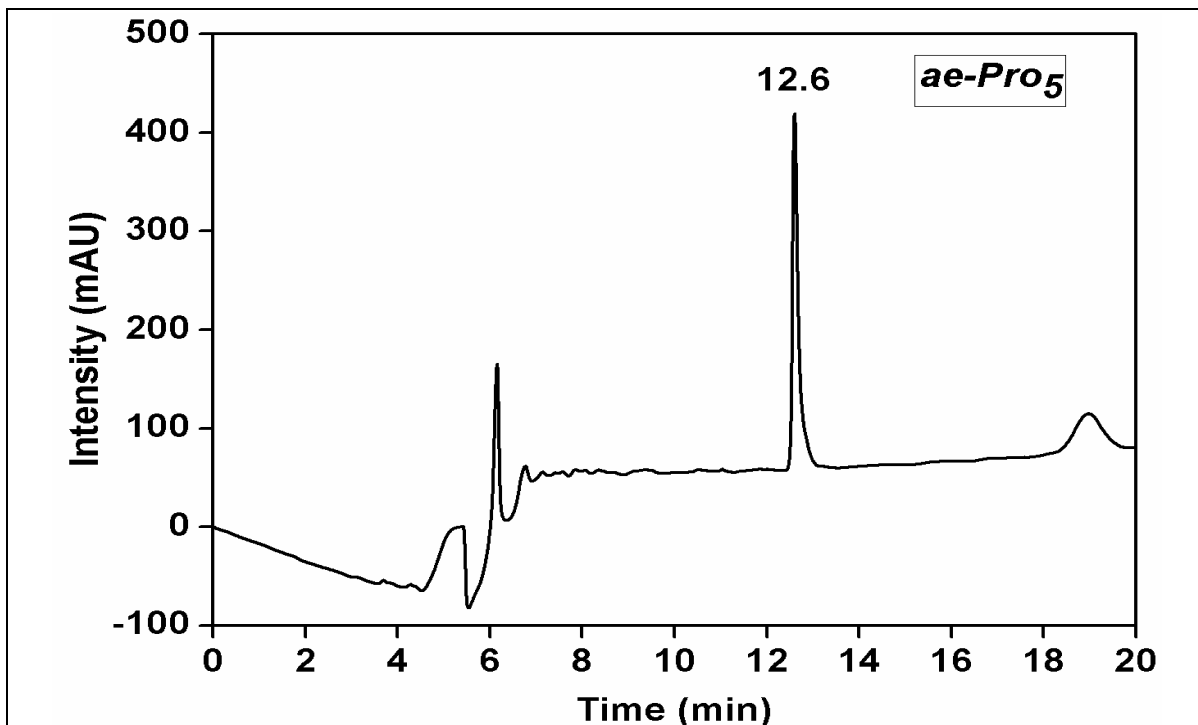
HPLC Trace of *aeg*₆



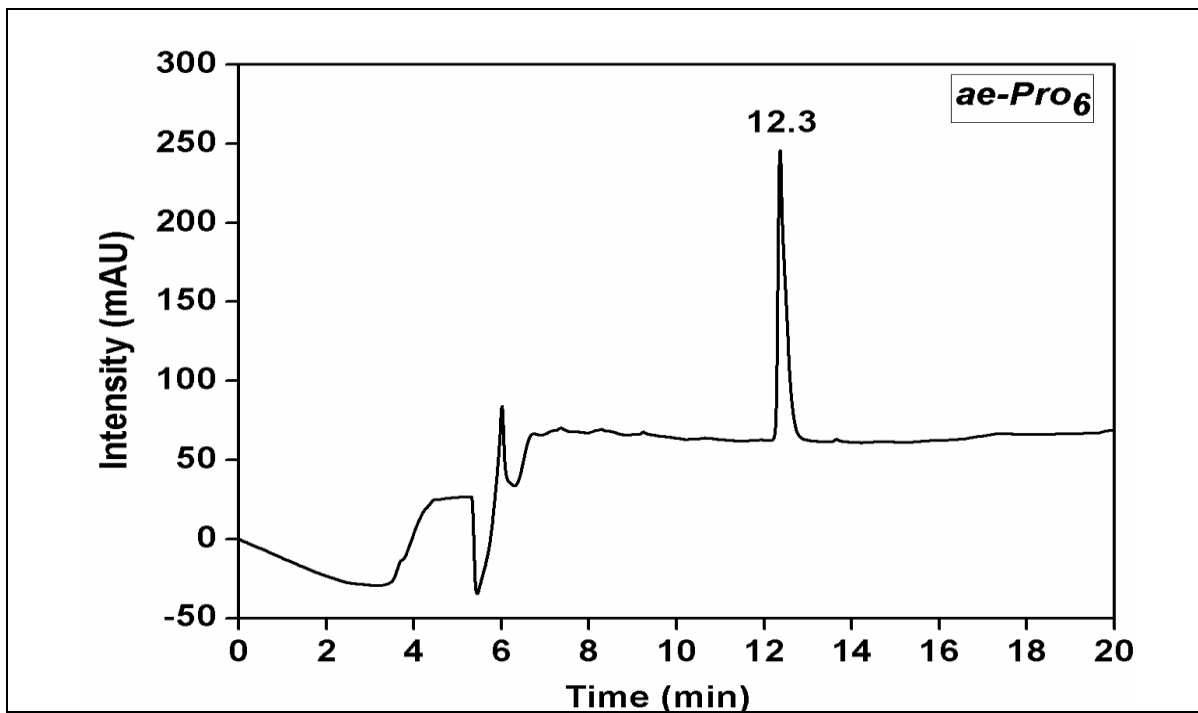
HPLC Trace of *ae-Pro*₄



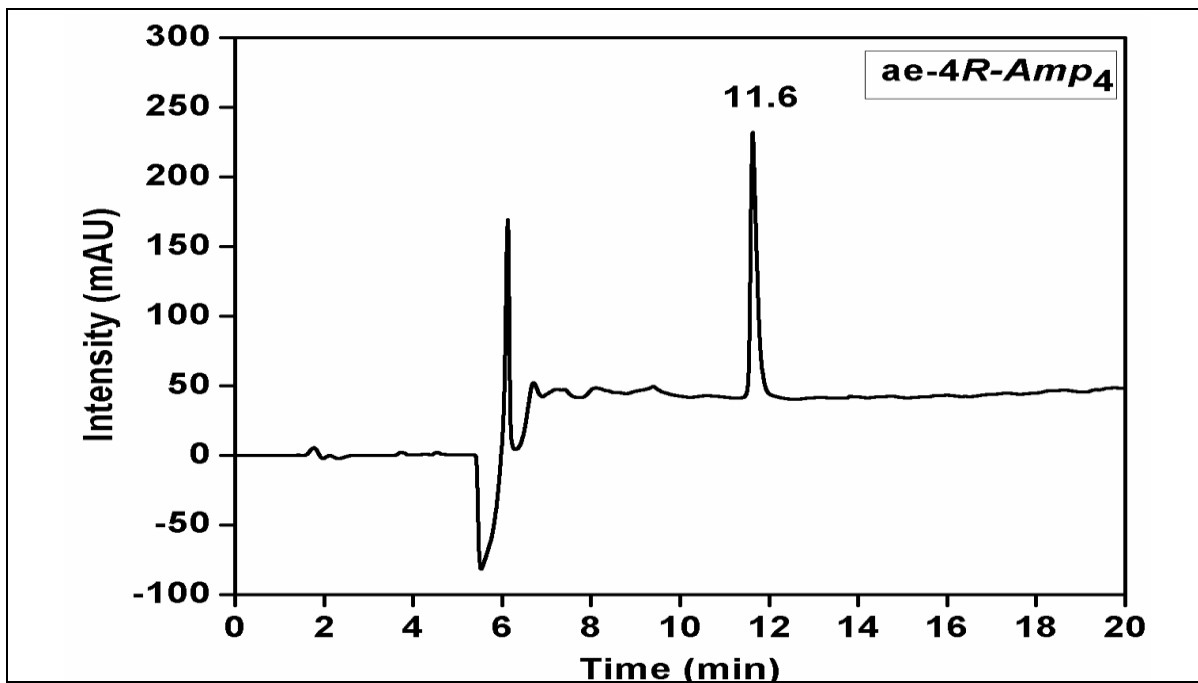
HPLC Trace of *ae-Pro*₅



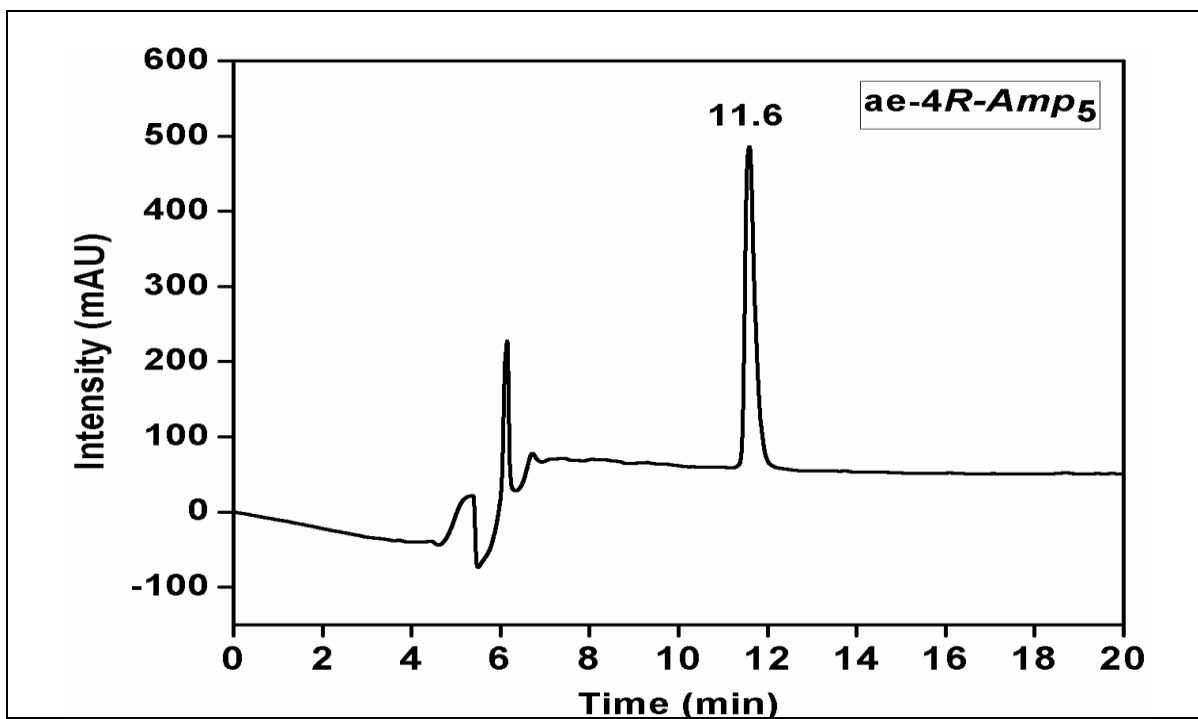
HPLC Trace of *ae-Pro*₆



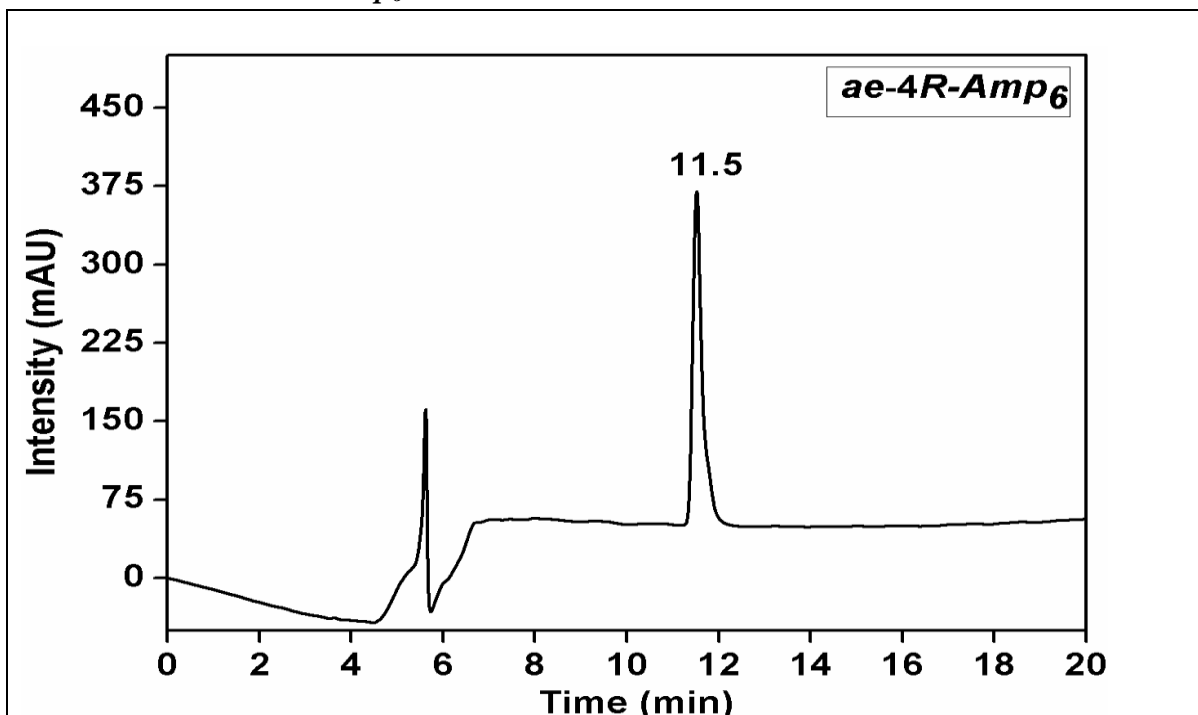
HPLC Trace of *ae-4R-Amp₄*



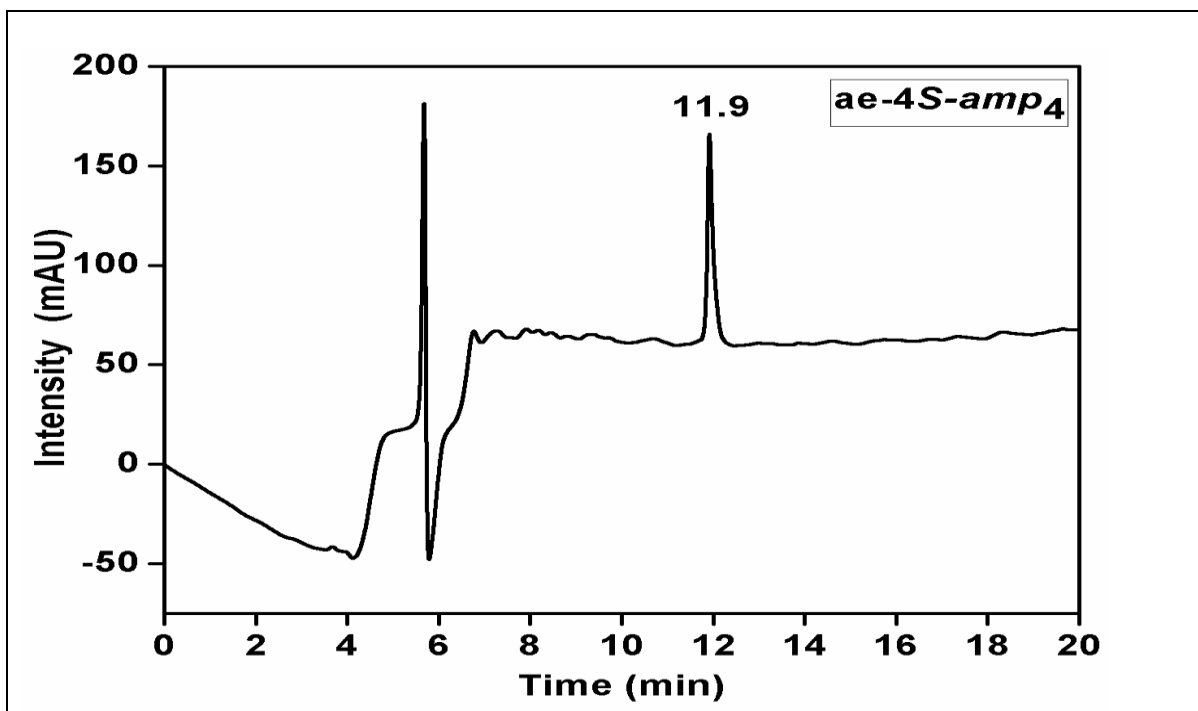
HPLC Trace of *ae-4R-Amp₅*



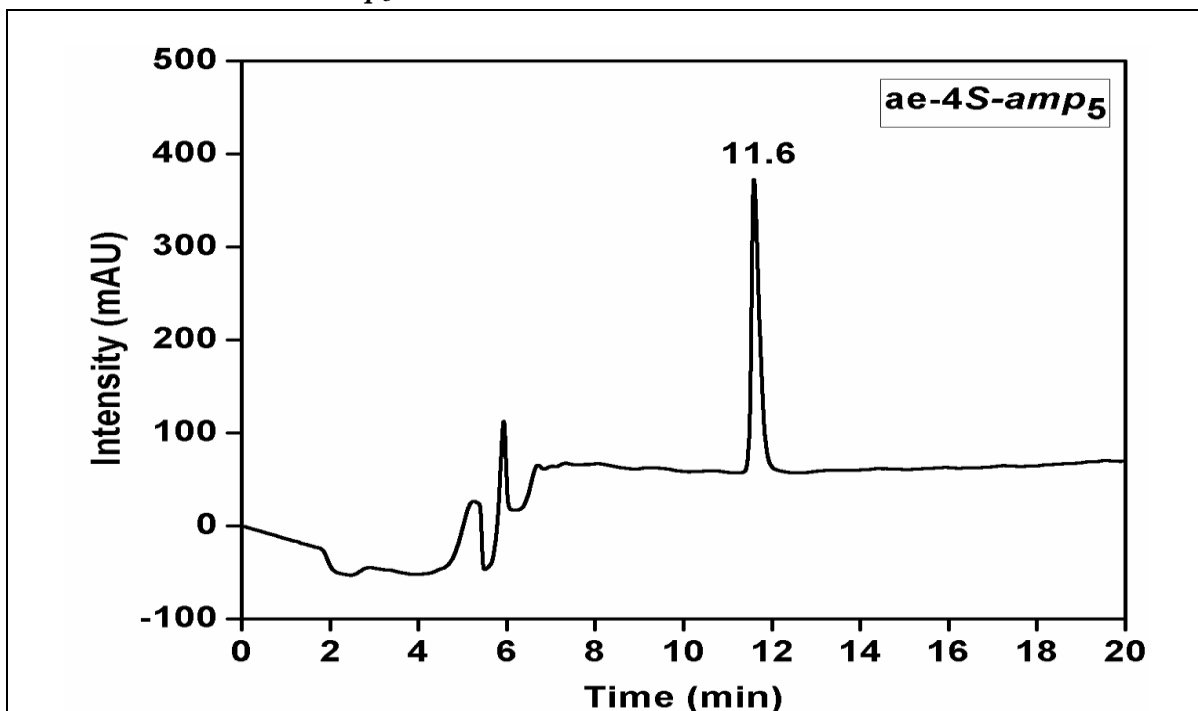
HPLC Trace of *ae-4R-Amp₆*



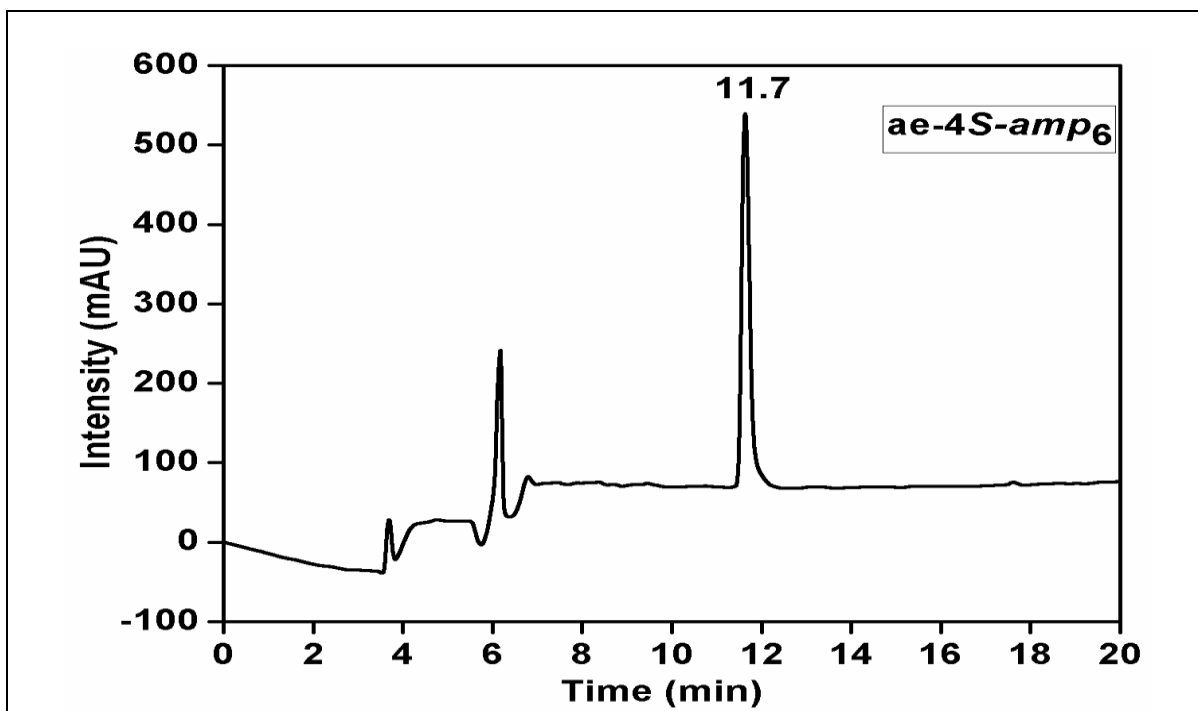
HPLC Trace of *ae-4S-amp₄*



HPLC Trace of *ae-4S-amp₅*

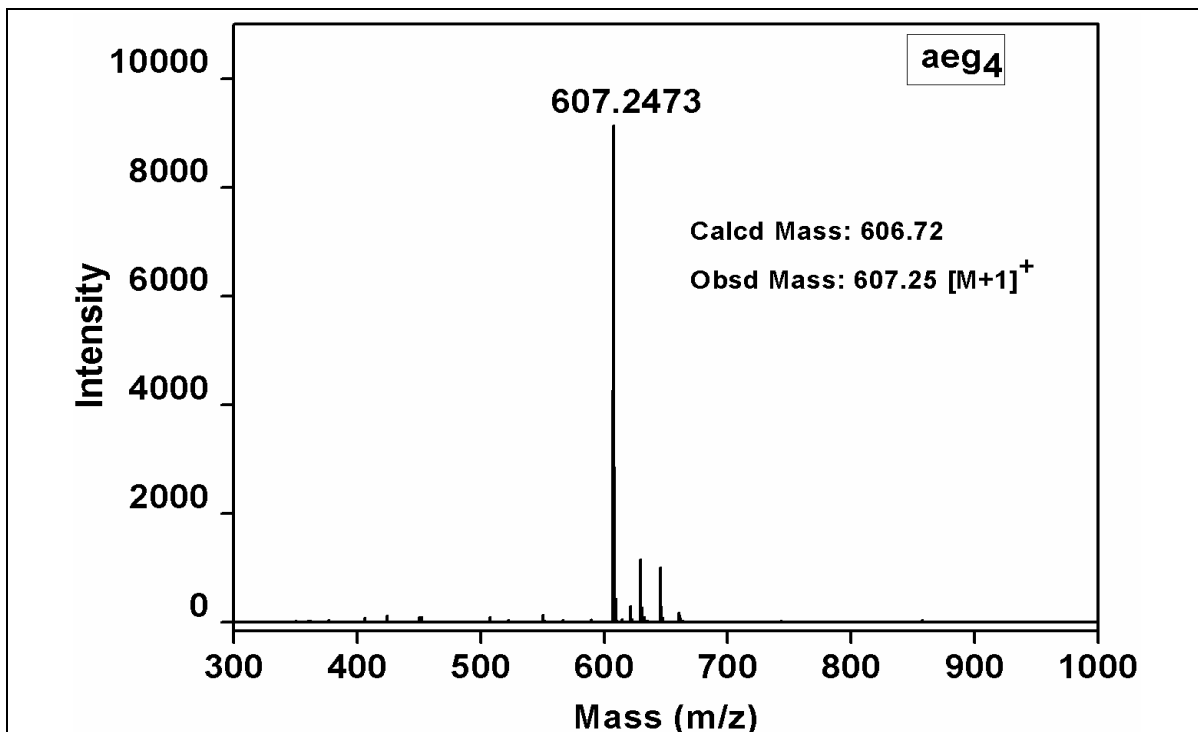


HPLC Trace of *ae-4S-amp₆*

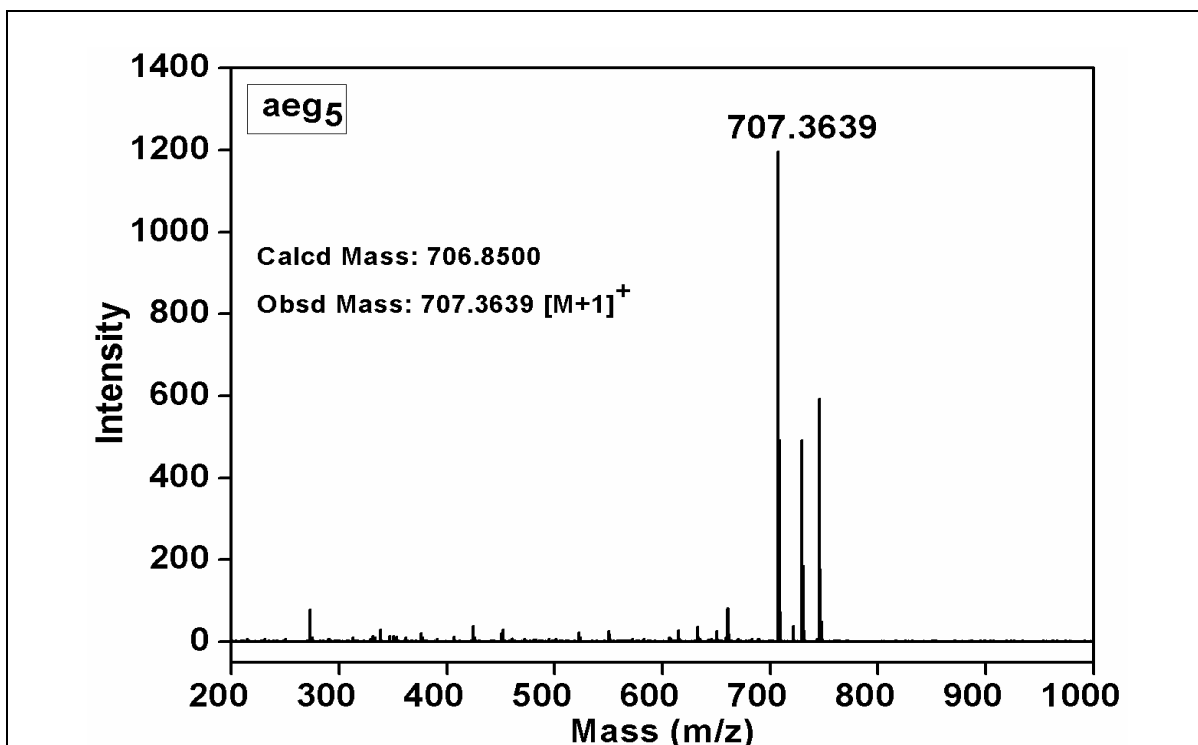


C) MALDI-TOF Mass of (1-4)

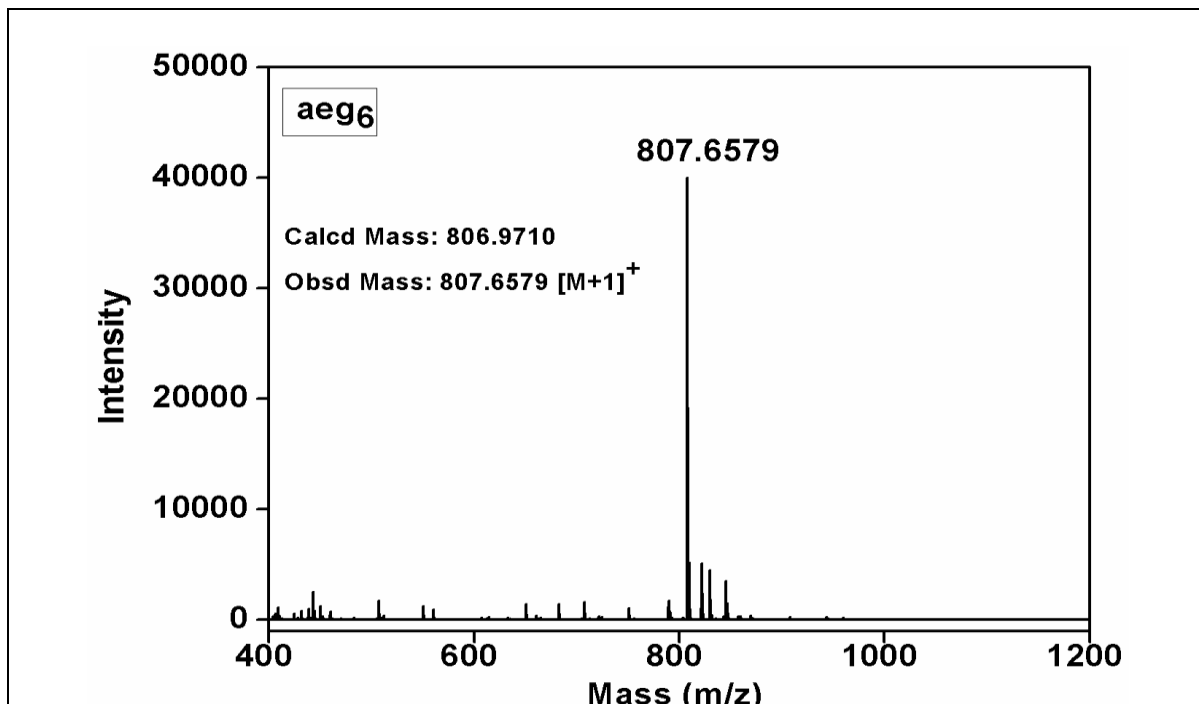
MALDI-TOF Mass of *aeg*₄



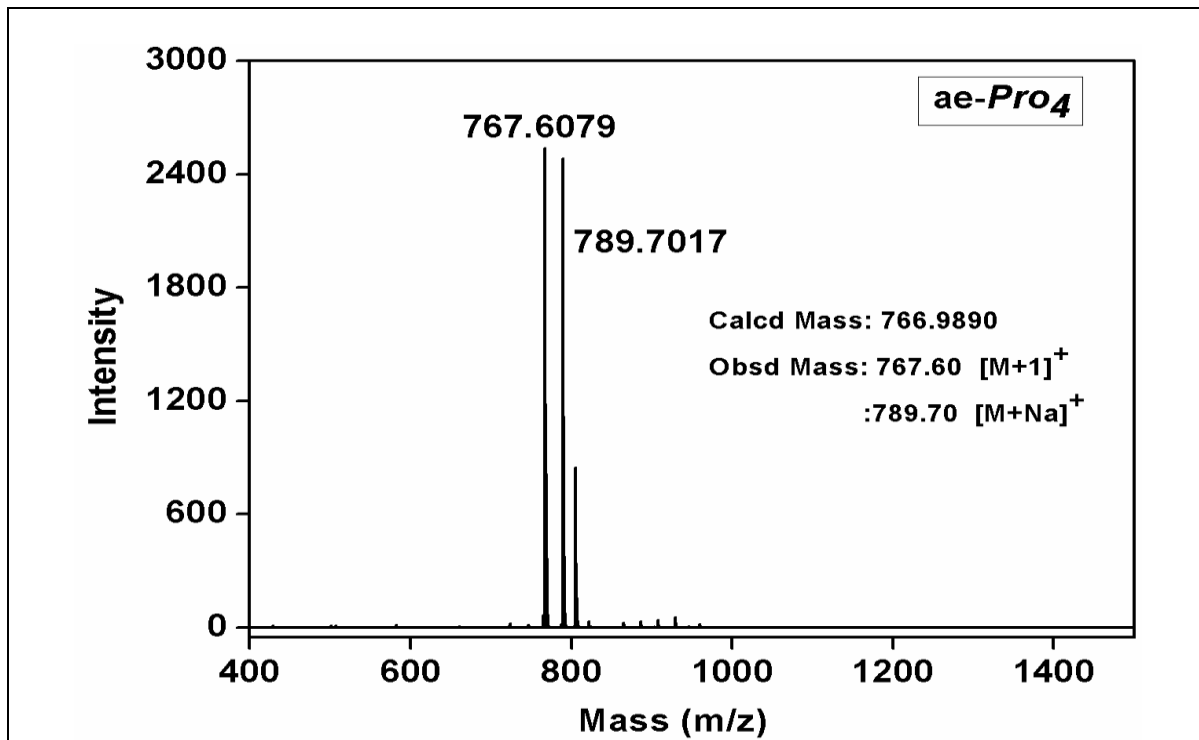
MALDI-TOF Mass of *aeg*₅

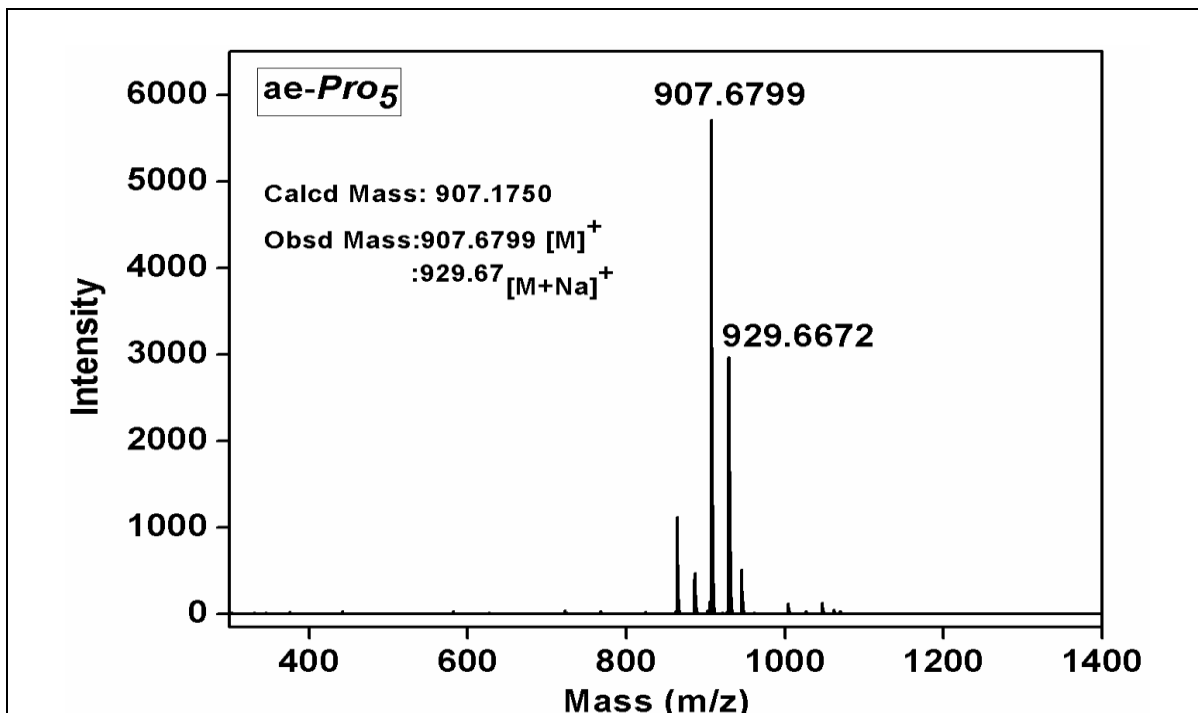
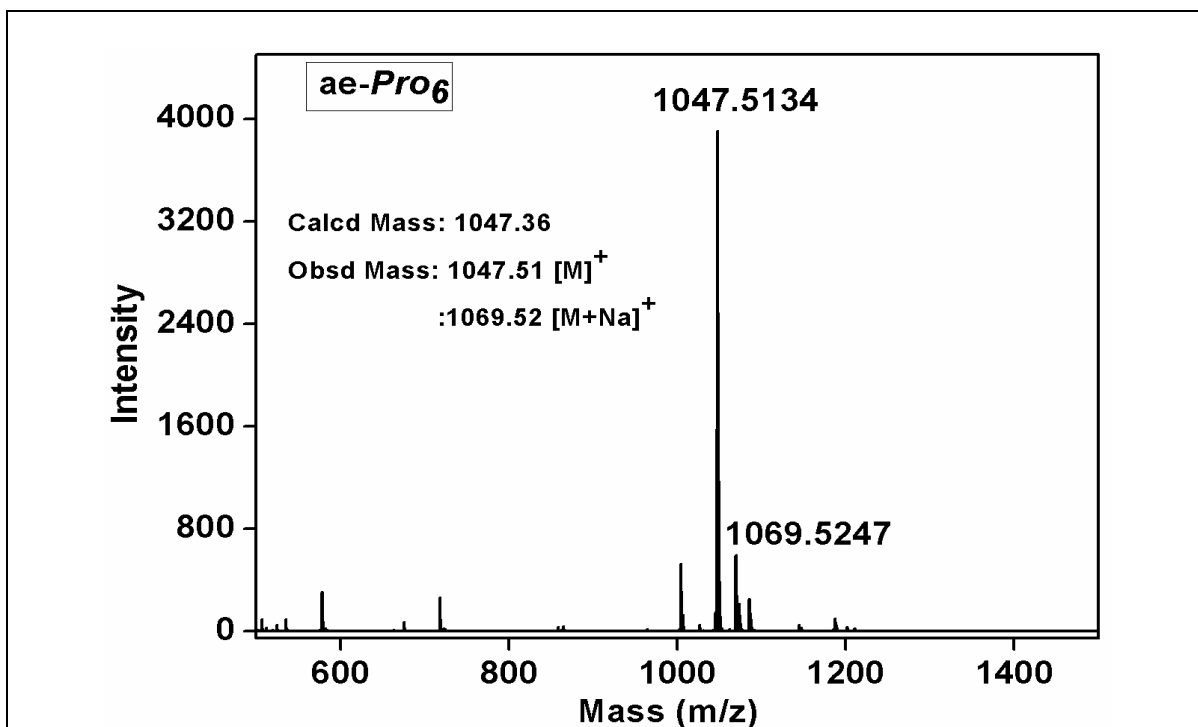


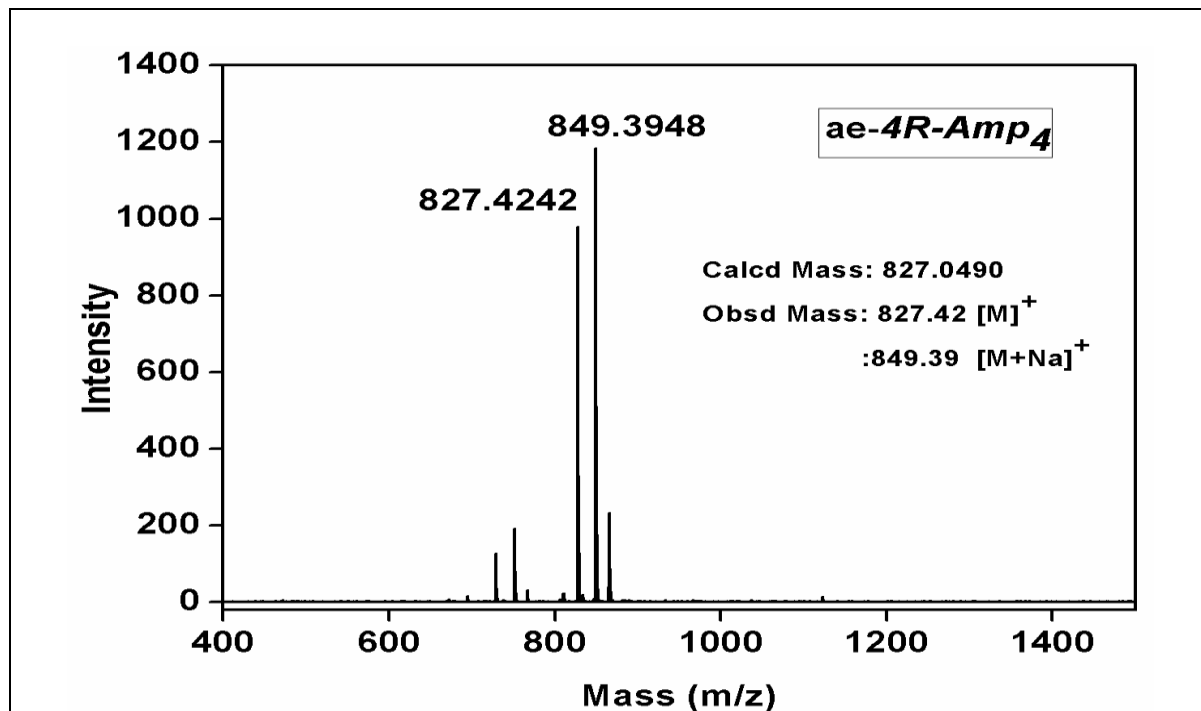
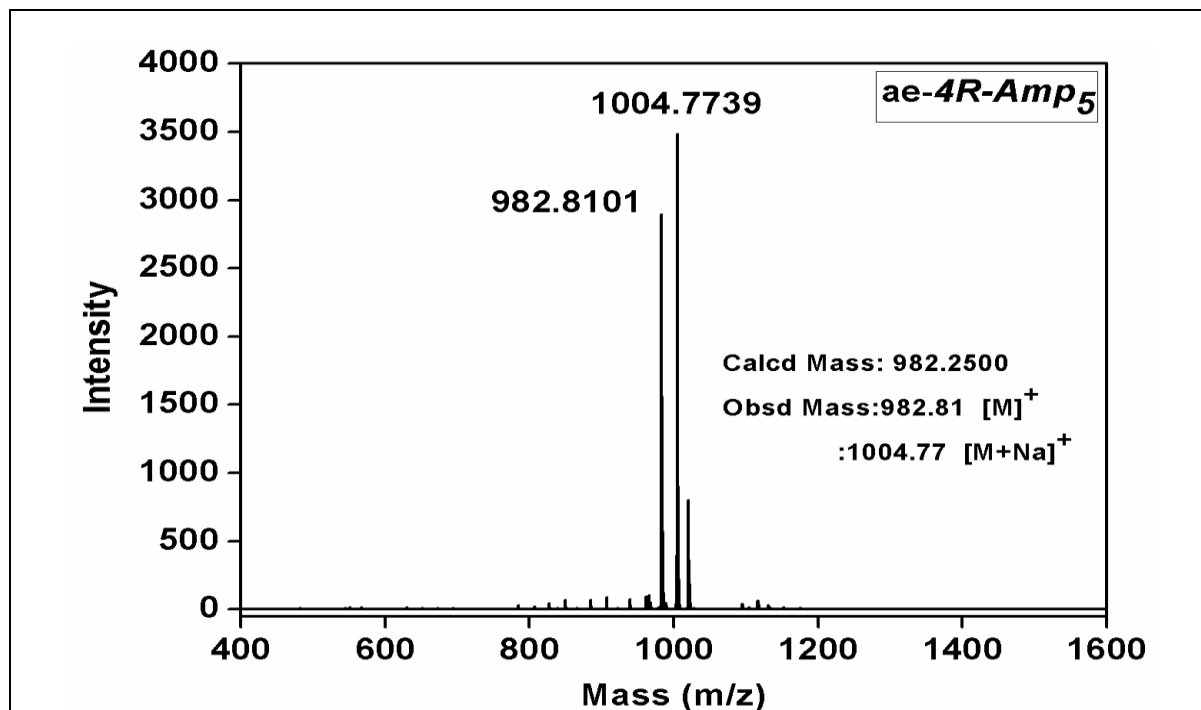
MALDI-TOF Mass of *aeg*₆

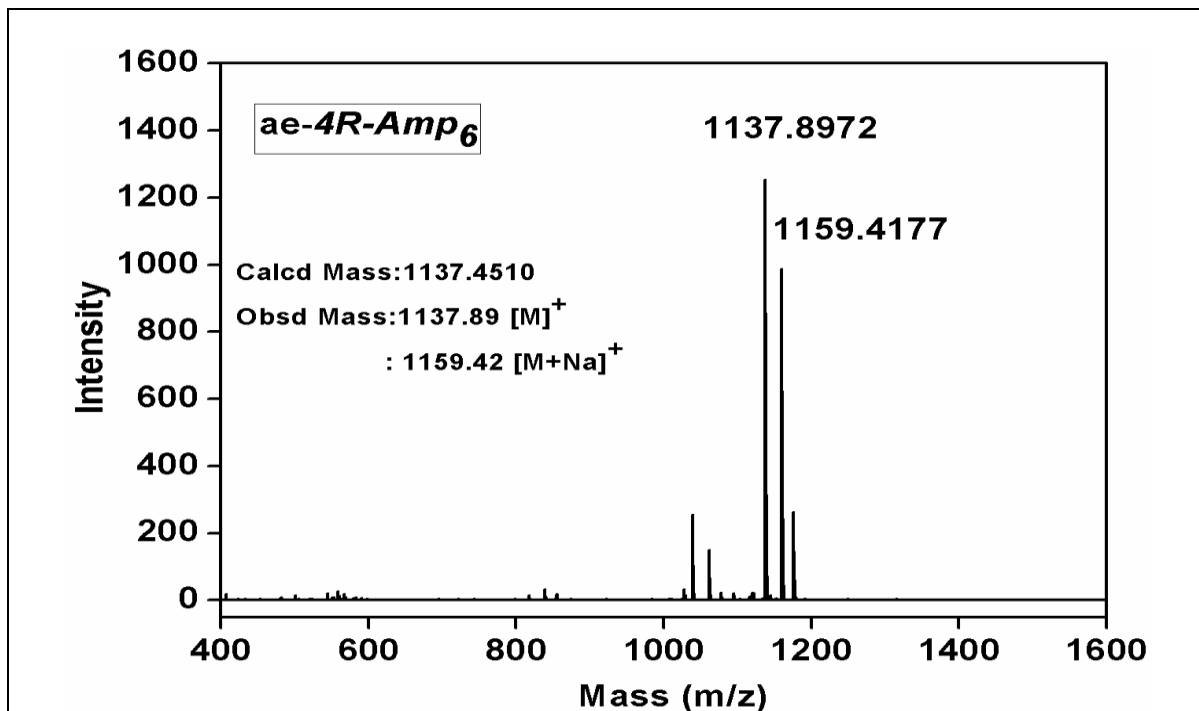
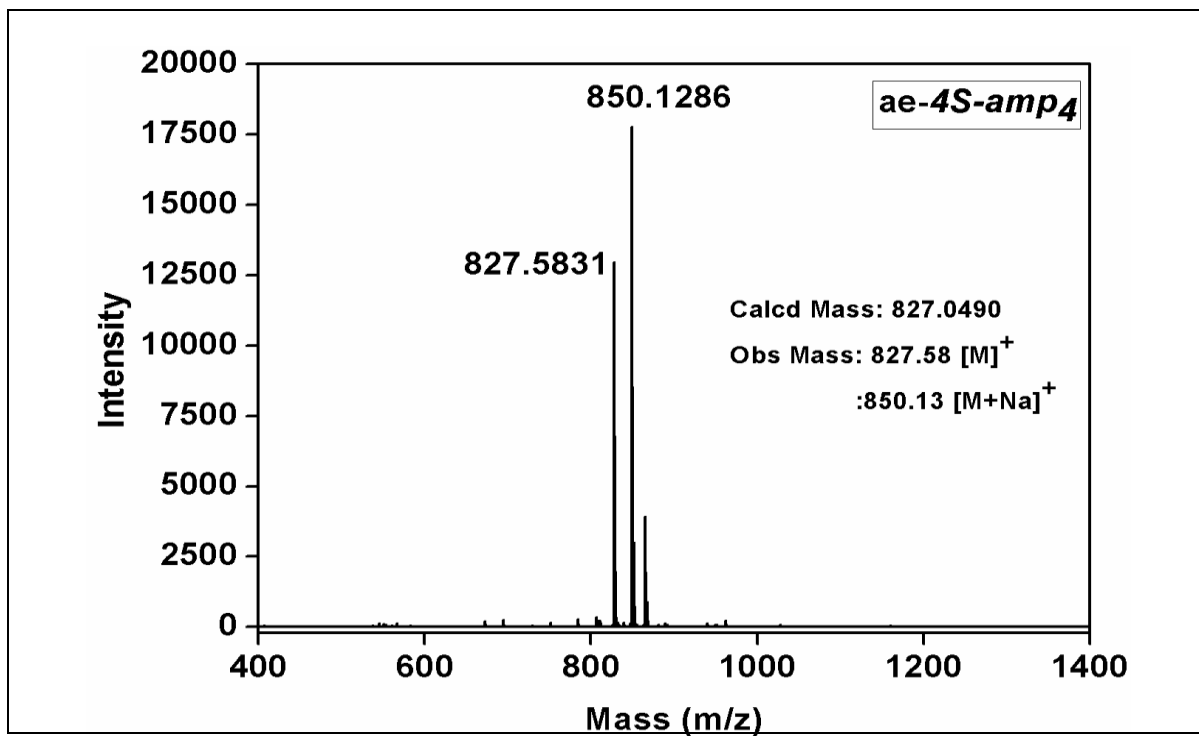


MALDI-TOF Mass of *ae-Pro*₄

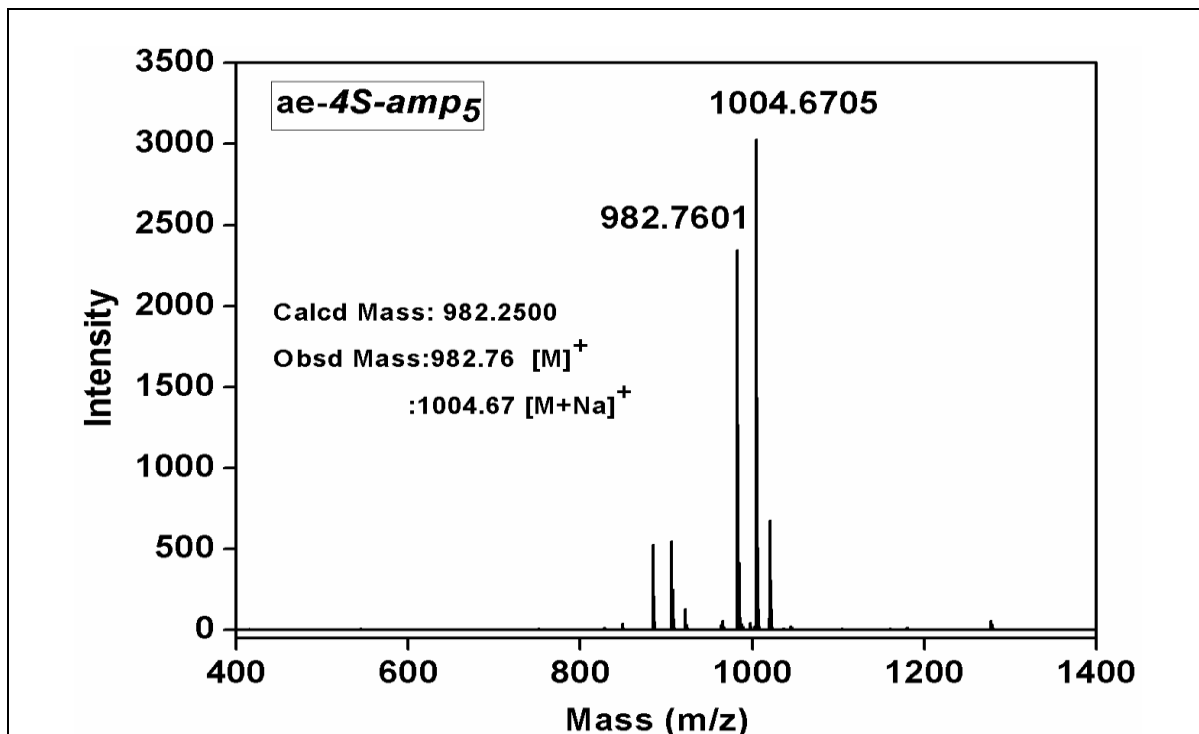


MALDI-TOF Mass of ae-Pro₅MALDI-TOF Mass of ae-Pro₆

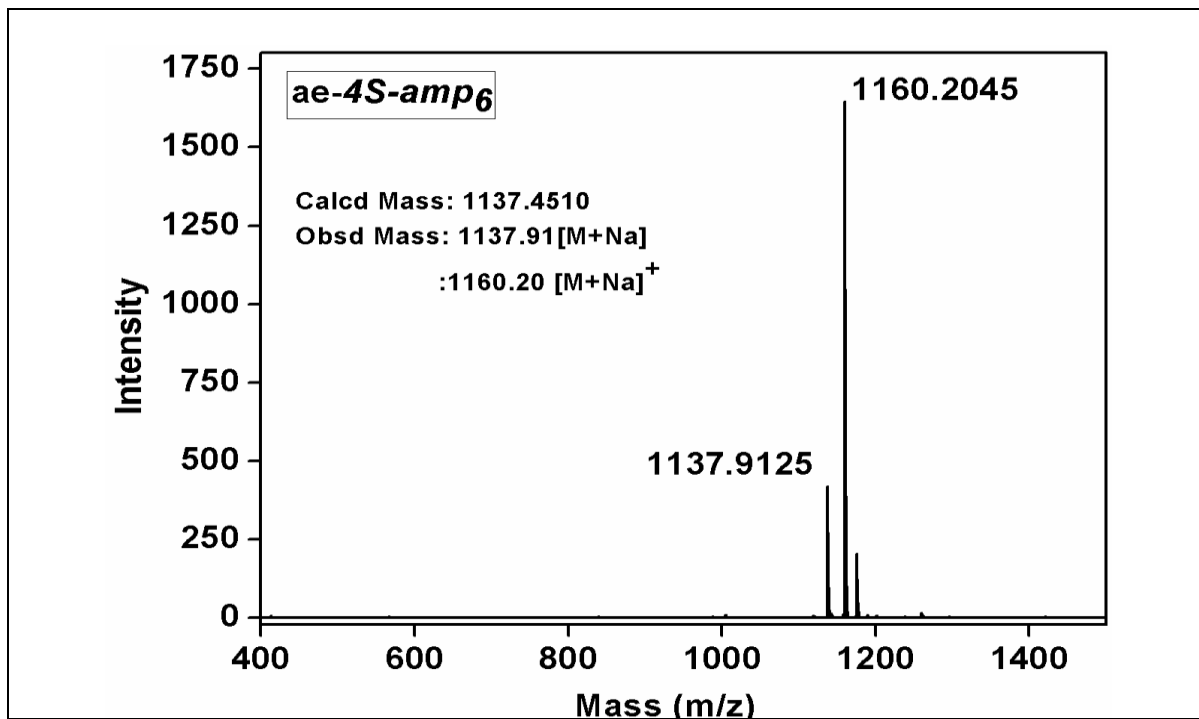
MALDI-TOF Mass of *ae-4R-Amp₄*MALDI-TOF Mass of *ae-4R-Amp₅*

MALDI-TOF Mass of *ae-4R-Amp*₆MALDI-TOF Mass of *ae-4S-amp*₄

MALDI-TOF Mass of *ae-4S-amp₅*

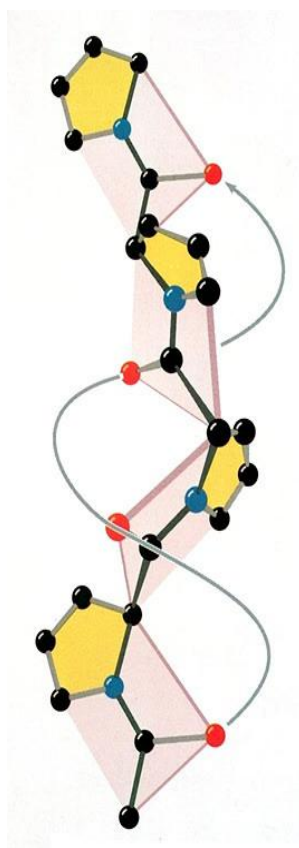


MALDI-TOF Mass of *ae-4S-amp₆*



Chapter-3

Poly-4*S*(*hyp*)/4*R*(*Hyp*)Proline Peptides, Characterization of β -Structure



3. Introduction

Post-translational modifications play an important role in defining the biological functions of proteins. In vertebrates, the most common post-translational modification observed is hydroxylation of proline to (4*R*)-hydroxy-L-proline (*Hyp*). The hydroxylation of proline residues in pro-collagen enhances the thermal stability of the collagen triple helix and provides mechanical strength to collagen fibers, which are the main component of the extracellular matrix.¹ It has been perceived that increase in stability of collagen triplex is primarily due to stereoelectronic effects with little or no additional stability arising from the hydration of the hydroxyproline residues.^{2,3,4} The presence of significant amounts of *Hyp* has also been observed in elastin, another structural protein of the extracellular matrix responsible for the elasticity and resilience of vertebrate tissues and organs.⁵

Polyproline adopts two stable secondary structures: left handed polyproline II helix (PPII) and the right handed polyproline I helix (PPI).⁶ The PPI helix is predominant in organic solvents, such as *n*-propanol, whereas the PPII helix is preferred in aqueous solution.⁷ PPI helices are rare in biological context but over the past decade, the poly-L-proline (PPII) secondary structure has received much attention due to finding that it is the prevalent conformation in both folded and unfolded proteins.⁸ It is also found to play an important role in a wide variety of biological processes, such as signal transduction, transcription, immune response, and cell motility.⁹

In collagen, the tripeptide repeat unit [*Pro-Hyp-Gly*]_n has glycine whose amide linkage is involved in an interchain H-bond and allow the twisting of three polypeptide chains in the polyproline II conformation (PPII) to form the triple helix structure.^{10,11} It was initially proposed that the stabilization induced by *Hyp* was due to water molecules forming a hydrogen bonding network linking the prolyl hydroxyl groups and the main-chain carbonyl groups.^{12,13} It is now recognised that it is primarily due to the stereoelectronic effects^{3,14} which arise essentially from the presence of electron-withdrawing substituent at C4 in *R/S* stereo-disposition which favourably pre-organizes the polypeptide chain, promoting assembly into a triple helix. The other consequences of the introduction of the electronegative group in the 4*R/S* configuration are a higher *trans/cis*

ratio of the tertiary prolyl amide bond as well as a favoured C^{γ} -*exo*/ C^{γ} -*endo* ring puckering, necessary for the compatible packing of the three polypeptide chains into a triple helix.^{15,16}

In contrast to collagen, polyproline peptides without any intervening glycine and lacking amide NH are unable to form a triplex *via* interchain H-bonds and remain as single helix of PPI or PPII type. Unlike other 4-substituents on proline studied so far (OH, F, N₃),^{17,18} the ionisable 4-NH₂ group is a good functional probe to examine the pH effects on polyproline conformation. The 4-aminoproline at acidic pH in protonated form (NH₃⁺) may influence the proline puckering *via* its electron withdrawing effects,^{2,19,20} while at basic pH, the NH₂ group has the ability to form hydrogen bonding.

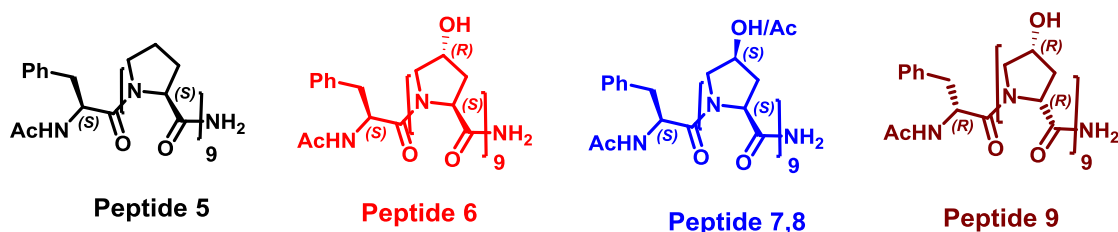
3.1 Present work: Rationale

Previous studies from our laboratory demonstrated that 4*S*-aminoprolyl polypeptide forms a novel β -structure in trifluoroethanol (TFE) unlike most polyproline peptides that prefer the PPI form in hydrophobic/fluorinated media, switching to PPII form in aqueous medium.²¹ This property is observed exclusively for peptide derived from 4*S*-aminoproline and not seen for peptide from 4*R*-aminoproline.

In view of the importance of polyproline peptides in biology and the influence of 4-substitution, this chapter is intended to study molecular conformations adopted by 4(*R/S*)-hydroxy-(*D/L*)-proline polypeptides. Such study would lead to an understanding of the importance of 4(*R/S*)-OH group in dictating the PPII conformation and influence the ring puckering. 4-Hydroxy group should act like the 4-amino group in terms of its ability to form hydrogen bonding and influence the PPI and PPII conformation of proline polypeptides. A recent computational study^{22,23} has suggested that in 4*S*-aminoproline, intramolecular hydrogen bond that is feasible between 4*S*-NH₂ and the carbonyl carbon of same proline moiety, leads to increase in the *trans/cis* ratio of peptide bond.

Incorporating D-amino acid in molecular design has the potential to improve protein stability and create new topologies. Molecular mechanism involved in proteins to stabilize left handed elements by L-amino acids are structurally enantiomeric to potential strategy for stabilizing right-handed amino acid elements with D-amino acids. To explore the proposed structural handedness and stability of polyproline or β -structure, peptide **9**

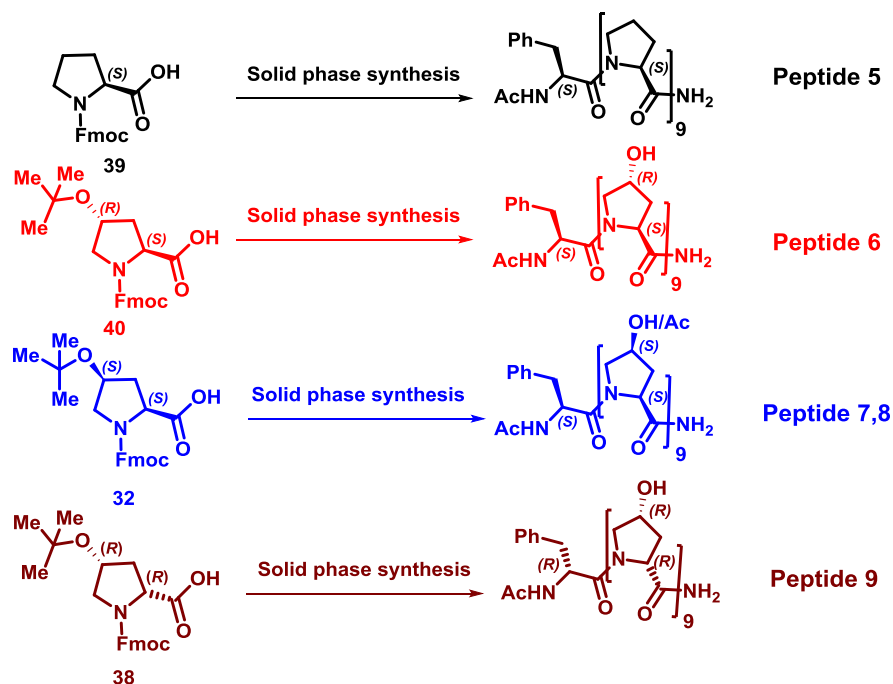
was designed. The target polypeptides synthesised for these works are peptides **5** (*Pro*)₉, **6** (*4R-Hyp*)₉, **7** (*4S-hyp*)₉, **8** (*4S-Achyp*)₉ and **9** (*4R-hyp-D-pro*)₉.



3.2 Results

3.2.1 Synthesis of protected (2*S*,4*R*)- and (2*S*,4*S*)-hydroxyproline monomers for polypeptide synthesis

Scheme 1. Synthesis of homooligopeptides **5-9** from proline and 4*R/S*-hydroxyproline monomers



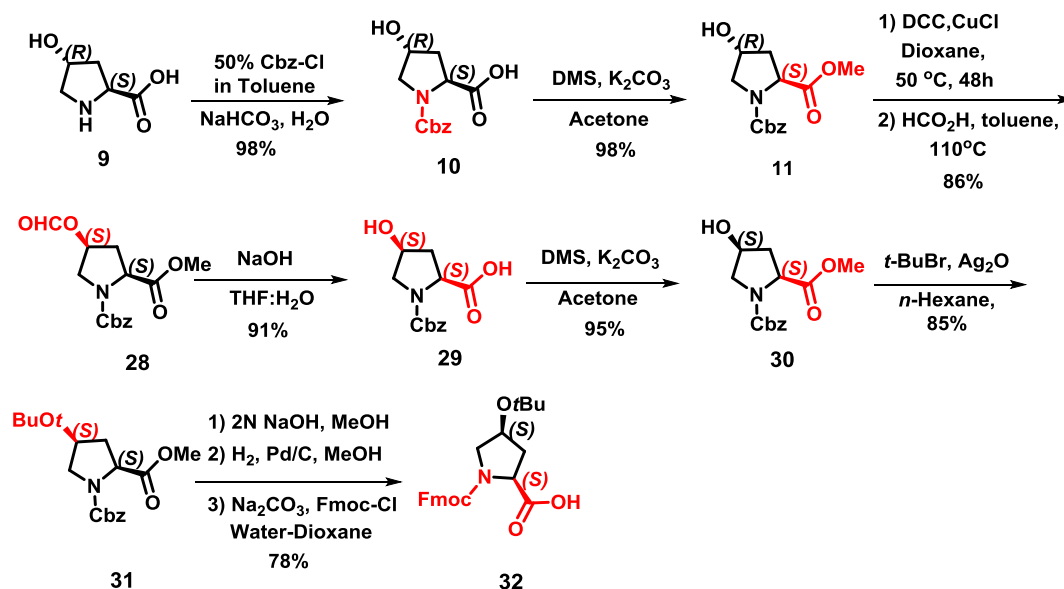
The peptides **5** and **6** were synthesized from the commercially available Fmoc proline **39** and (2*S*,4*R*)-*N*¹-(Fmoc)-4-OH-(*t*-Butyl)-hydroxyproline **40**. To achieve the synthesis of peptides **7** and **8** the monomers (2*S*,4*S*)-*N*¹-(Fmoc)-4-OH-(*t*-Butyl)-hydroxyproline **32** with a combination of *N*¹(Fmoc) and *O*⁴-*t*-butyl protection were chosen.

Orthogonally protected monomer (2*R*,4*R*)-*N*¹-(Fmoc)-4OH-(*t*-butyl)-hydroxyproline **38** was used to synthesize peptide **9**.

3.2.1a Synthesis of (2*S*,4*S*)-*N*¹-(Fmoc)-4-O-(*t*-Bu)-hydroxyproline (**32**)

The synthesis of orthogonally protected (2*S*,4*S*)-*N*¹-(Fmoc)-4O-(*t*-Butyl)-hydroxyproline (**32**) monomer was achieved in ten steps from the naturally occurring *trans*-4*R*-hydroxyproline **9** (Scheme 2). The reaction of **9** with benzyloxycarbonylchloroformate in water/dioxane in the presence of Na₂CO₃, yielded *N*1-benzyloxycarbonyl-4*R*-hydroxyproline **10**. The appearance of aromatic ($\delta = 7.2$ -7.3 and benzylic $\delta = 5.1$) signals in ¹H NMR spectrum of compound **10** confirmed its structure.

Scheme 2. Synthesis of fully protected (2*S*,4*S*)-*L*-hydroxyproline monomers



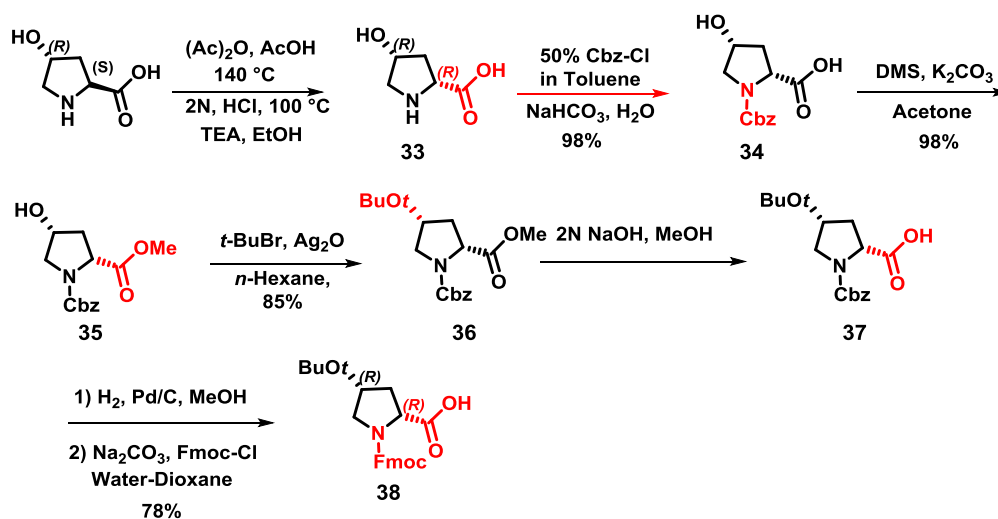
The compound **10** upon treatment with DMS in acetone/K₂CO₃ gave the corresponding methyl ester **11**, which showed two signals at $\delta = 3.75$ and 3.54 in the ¹H NMR spectrum corresponding to the methyl (-CH₃) group of the ester (minor and major rotamers respectively). Treatment of **11** with DCC in the presence of a catalytic amount of copper (I) chloride in toluene at 45-50°C and subsequent refluxing with formic acid for 24 h afforded the (4*S*)-O-formyl prolyl derivative **28** in an 86% yield. The reaction was accompanied by an inversion of configuration at C-4. Hydrolysis of **28** under basic

conditions afforded (2*S*,4*S*)-N1-benzyloxycarbonyl-4-hydroxyproline **29**. To avoid esterification in next reaction, compound **29** was treated with DMS in acetone/ K_2CO_3 to get the corresponding methyl ester **30**. The hydroxyl group at C4 was protected with *tert*-butyl group to give **31** which showed signal at $\delta = 1.17$ -1.18 in the 1H NMR spectrum corresponding to the *tert*-butyl group. The hydrolysis of ester function in **31**, subsequent deprotection of N1-Cbz and reprotection with Fmoc gave (2*S*,4*S*)-N¹-(Fmoc)-4-*O*-(*t*-Butyl)-hydroxyproline **32**.

3.2.1b Synthesis of (2*R*,4*R*)-N¹-(Fmoc)-4-*O*-(*t*-Butyl)-hydroxyproline (**38**)

The *cis*-4(*S*)-hydroxy-D-proline **33** was obtained by epimerization of *trans*-4-hydroxy-L-proline²⁴ by heating it with acetic anhydride followed by acid hydrolysis and fractional crystallization of the epimeric hydroxyprolines (Scheme 3). The reaction of *cis*-4*R*-hydroxy-D-proline with benzyloxycarbonyl chloride in water/dioxane in the presence of Na_2CO_3 , yielded N¹-benzyloxycarbonyl-4*R*-hydroxyproline **34**. This upon treatment with DMS in acetone/ K_2CO_3 gave the corresponding methyl ester **35**, which showed two signals at $\delta = 3.75$ and 3.54 in the 1H NMR spectrum corresponding to the methyl ($-CH_3$) group of the ester (minor and major rotamers respectively).

Scheme 3. Synthesis of fully protected (2*R*,4*R*)-D-hydroxyproline monomers



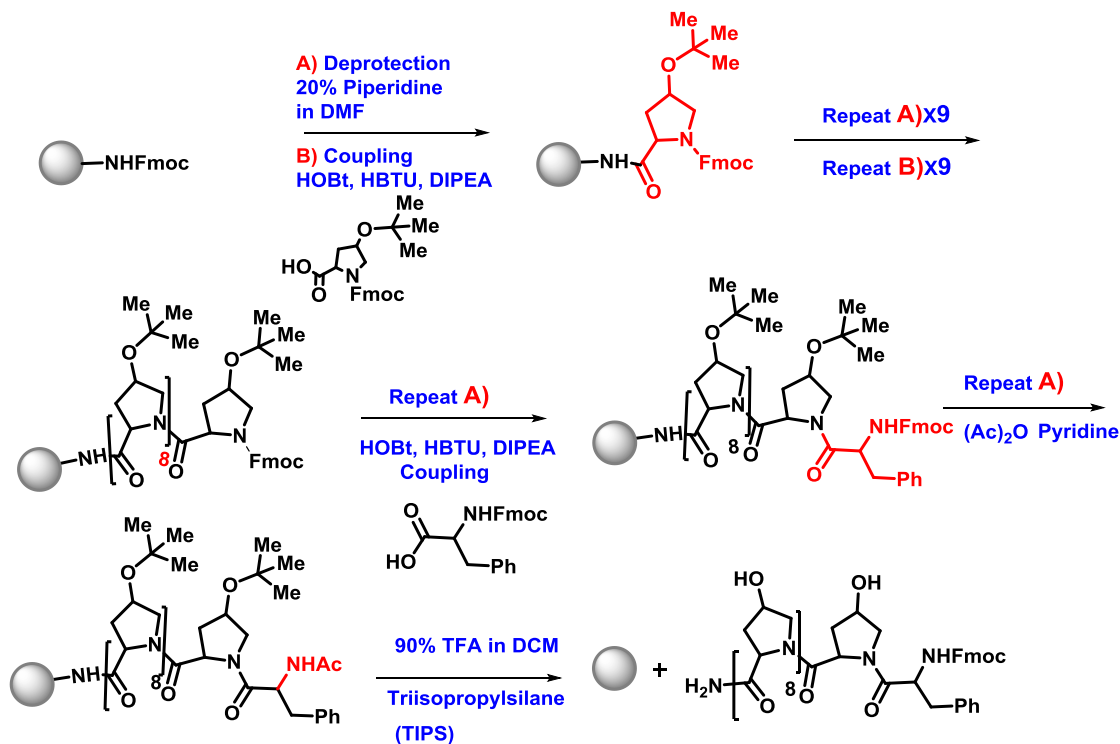
The hydroxyl group at C4 was protected with *tert*-butyl group by treatment with *t*-butylbromide to give **36** which showed signal at $\delta = 1.17$ - 1.18 in the ^1H NMR spectrum corresponding to the *tert*-butyl group. The hydrolysis of ester group in **36** to the corresponding acid, subsequent deprotection of N^1 -Cbz and reprotection with Fmoc gave (2*R*,4*R*)- N^1 -(Fmoc)-4-*O*-(*t*-Bu)-hydroxyproline **38**.

3.2.2 Synthesis of homo oligopeptides 5-8 by using solid phase protocol

The target peptides (**5-7**, **9**) were synthesized by manual solid phase synthesis on readily available rink amide resin using standard Fmoc chemistry (Scheme 4), followed by cleavage to yield the peptides as C-terminal amides. The commercially available Kieselghur supported N,N-dimethylacrylamide resin (with Rink-amide linker) with Fmoc substitution was deprotected by 20% piperidine in DMF. The monomers as free acids were coupled using *in situ* activation procedure using amino acid (3 eq.), HBTU as a coupling reagent and HOBt as catalyst and racemisation-suppressant in DIPEA. The coupling reaction was repeated by using *N*-methyl-2-pyrrolidone (NMP) as solvent. The deprotection reactions were done with 20% piperidine in DCM and monitored by qualitative Chloranil test²⁵ for iminoacids. The terminal amino group of the final peptide was capped with Ac_2O and the peptide was cleaved from the resin using 20% TFA in DCM. The deprotection of sidechain *t*-butyl on hyp residues of the peptide was carried out with 90% TFA in DCM. Since *t*-butyl cation formed during the deprotection the final peptide can lead to N-alkylation of the amines, 0.1% TIPS (triisopropylsilane) was used as a scavenger to prevent side reactions during peptide-cleavage and *t*-butyl deprotection. The N-terminal acetylated and C-terminal amidated peptides were purified on semi-preparative RP-18 HPLC column using water-acetonitrile gradient containing 0.1% TFA. The treatment of peptide **7** (4*S*-hyp₉) with acetic anhydride/DIPEA in DMF afforded peptide **8** (4*S*-Achyp₉).

All oligomers were purified by HPLC and characterized by MALDI-TOF. The purity of the peptides as determined using analytical RP-18 HPLC was found to be greater than 98%. The structural integrity of the peptides was further confirmed by MALDI-TOF mass spectral data which agreed closely with the calculated values (Table 1).

Scheme 4. Solid phase synthesis of peptides 5-7, 9



The oligopeptides **5-7, 9** were synthesized from appropriate N-Fmoc-protected monomers (2*S*,4*S*)-*N*¹-(Fmoc)-4*S*-OH-(*t*-butyl)-hydroxyproline (**32**), (2*R*,4*R*)-*N*¹-(Fmoc)-4*R*-OH-(*t*-butyl)-hydroxyproline (**38**), and the readily available *N*¹-(Fmoc)-4*R*-hydroxyproline (**39**), (2*S*,4*R*)-*N*¹-(Fmoc)-4*R*-OH-(*t*-butyl)-hydroxyproline (**40**) monomers assembled on the solid phase is shown in Scheme 4. The peptides were purified by reverse phase HPLC and characterised by MALDI-TOF.

Table 1. Characterization of peptides **5-8**

Sr.No.	Peptides	Mol. Formula	Mass (cal) [M+Na] ⁺	Mass (obs)
5		C ₅₆ H ₇₇ N ₁₁ O ₁₁	1103.28	1102.89 [M+Na] ⁺

6		$C_{56}H_{77}N_{11}O_{20}$	1247.27	1246.89 $[M+Na]^+$
7		$C_{56}H_{77}N_{11}O_{20}$	1247.27	1246.81 $[M+Na]^+$
8		$C_{74}H_{95}N_{11}O_{29}$	1625.61	1624.48 $[M+Na]^+$
9		$C_{56}H_{77}N_{11}O_{20}$	1247.27	1246.67 $[M+Na]^+$

3.2.3 CD Spectroscopic Studies

Several methods are known in literature for determination of polyproline conformation, which includes NMR, UV, resonance Raman spectroscopy and chiroptical spectroscopies. In the present study, circular dichroism spectroscopy was used to investigate the conformational behavior of peptides **5-9**.

3.2.4 Identification of PPII by UV-CD spectroscopy

In order to investigate the conformational nature of peptides **5** (*Pro*₉), **6** (*4R-Hyp*₉) and **7** (*4S-hyp*₉), CD spectral analyses were carried out as a function of urea, salt and solvents (buffer and trifluoroethanol). The CD spectra of the three peptides **5-7** were

recorded with 100 μM peptide concentration at pH 7.2 in sodium-phosphate buffer and shown in Figure 1.

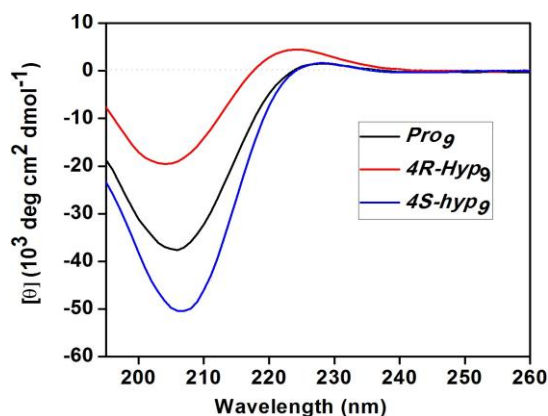


Figure 1. CD profiles of peptides **5** (*Pro*₉), **6** (*4R-Hyp*₉) and **7** (*4S-hyp*₉) at 100 μM (pH 7.2).

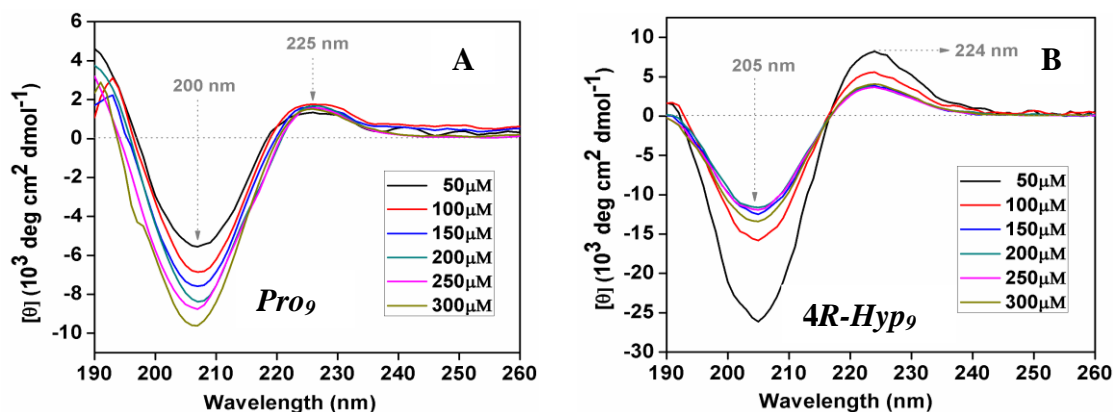
The CD spectra of peptides **5-7** (Figure 1) show a positive band between 220 to 230 nm and a negative band between 200 to 210 nm, which are the hallmarks of the PPII conformation with the intensity of the positive band being proportional to the PPII helical content.^{26,27} Conformational averaging resulting from the presence of other local structures can lead to negative ellipticity in 200-210 region. It is seen from Figure 1 that both peptide **6** (*4R-Hyp*₉) and peptide **7** (*4S-hyp*₉) have more positive intensity in the region (225-227 nm) than the unsubstituted proline oligomer *Pro*₉ (**5**), with *4R-hyp*₉ having maximum PPII helix content. The intensity of the positive band at 225-227 nm is seen to decrease in the order *4R-Hyp*₉ **6** > *4S-hyp*₉ **7** > *Pro*₉ **5**. The *4S-hyp*₉ peptide **7** shows a more negative ellipticity (205 nm) than *4R-Hyp*₉ peptide **6** and *Pro*₉ peptide **5**.

3.2.5 Concentration dependent CD spectroscopy of peptides 5-7

The conformational behavior of peptides is mediated by the complex interactions between the amino acids in the peptide and the surrounding environment. The helix stability can be measured from the concentration dependence of CD spectra. In collagen peptides, glycine NH involved in interchain hydrogen bonding leads to formation of the triple helix structure whose propensity will increase with concentration. In contrast, polyproline peptides lack amide NH and hence are unable to form a triplex *via* interchain

H-bonds even at higher concentrations, ending up as a single helix of PPI or PPII type. Formation of triple-helical structure is thus a concentration dependent phenomenon with single stranded chains shifting to the triple-helix upon increase in concentration.²⁸ The percent of triple-helicity is maximum when the concentration is greater than its critical triple-helical concentration. Unlike in unsubstituted proline the peptides **6** and **7**, the presence of hydroxyl group may form structure other than PPII.

Figure 2 (A-C) shows the CD spectra of peptides **5-7** recorded at 25 °C in the concentration range of 100–300 μM . The peptides **5** (*Pro*₉), **6** (*4R-Hyp*₉) and **7** (*4S-hyp*₉) show CD spectra in water typical of PPII conformation with a positive band around 223–226 and a negative band at 204–205 nm. It emerges from Figure 2 that both peptides **5** (*4R-Hyp*₉) and **6** (*4S-hyp*₉) have more positive intensity in the region (225–227 nm) than the unsubstituted proline peptide **5** (*Pro*₉).



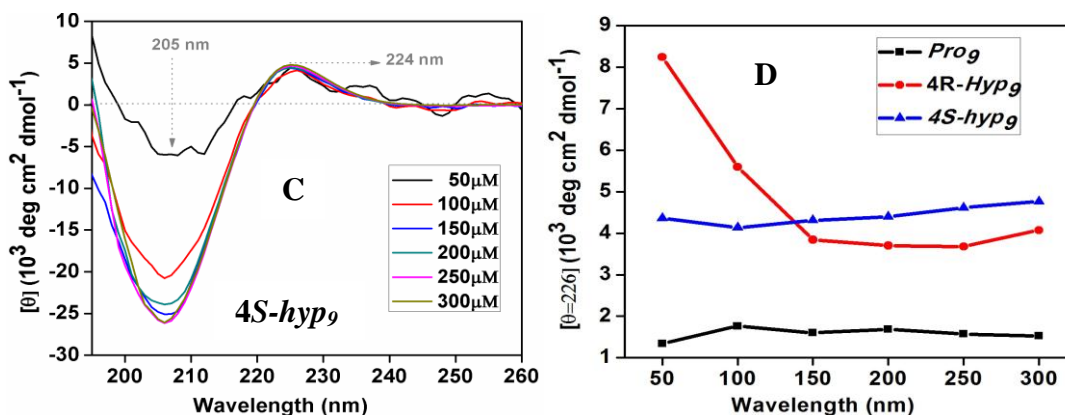


Figure 2. CD profiles of peptides **5-7** (A) **5** (*Pro*₉), (B) **6** (*4R-Hyp*₉), (C) **7** (*4S-hyp*₉), at concentration 50 to 300 μM , (D) Intensity of positive band of CD spectra as a function of concentration of peptide in sodium-phosphate buffer (pH 7.2).

Figure 2D depicts a plot of the intensity of positive band as a function of concentration of the peptides and it is seen that the plot is more or less linear. Any change in conformation should result in a biphasic pattern. Peptide **6** (*4R-Hyp*₉) has maximum PPII helix content and the intensity of the positive band at 225-227 nm decreases in the order peptide **6** (*4R-Hyp*₉) > peptide **7** (*4S-hyp*₉) > peptide **5** (*Pro*₉).

3.2.6 Effect of urea on peptides 5-7

It is commonly known that urea denatures proteins by promoting disorder in peptide backbone. The first step of unfolding is opening up of the hydrophobic core, which then gets solvated by water and later by urea.²⁶ Urea promotes the formation of left-handed polyproline II helical structures in both polypeptides and denatured proteins.²⁶ PPII helix content is known to increase in the presence of urea, which interacts favourably with the polypeptide backbone. Hence the effect of varying concentrations of urea on polyproline peptides **5-7** was investigated through CD spectral analysis at pH 7.2. CD spectra were recorded for peptides at same concentration (100 μM) in sodium-phosphate buffer (pH 7.2) in presence of increasing concentrations of urea. The inherent UV absorbance of urea at high concentrations prevented recording spectra below 215 nm wavelength. The intensity of the positive band is taken to be proportional to the PPII helical content.

3.2.6a Peptide 5 (*pro*₉): The CD spectra (220-230 nm) for peptide **5** (*Pro*₉) as a function of urea concentration are shown in Figure 3A and the positive band intensity at 226 nm is

plotted as a function of urea concentration in Figure 2B. The plot indicates a linear increase suggesting mere enhancement of the PPII helical content of peptide **5** (*Pro*₉) with increase in urea concentration. At 5M urea concentration, the PPII helical content of peptide **5** (*Pro*₉) is almost doubled, demonstrating that urea stabilized the PPII helix in case of peptide **5**.

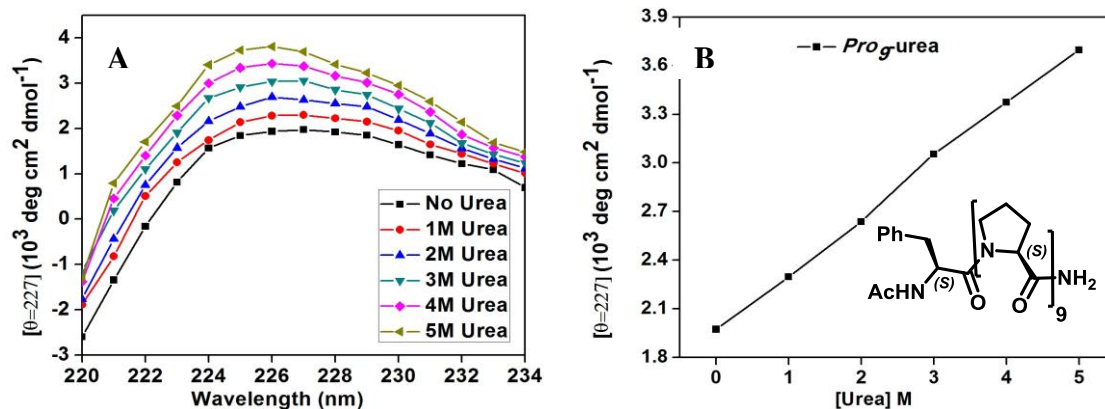


Figure 3. (A) CD profile of peptide **5** (*Pro*₉) as a function of concentration of urea at pH 7.2 (B) Intensity of positive band of CD spectra as a function of concentration of urea.

3.2.6b Peptide 6(4*R*-Hyp₉): The positive band at 224 nm in CD spectra for peptide **6** (4*R*-Hyp₉) as a function of urea concentration are shown in Figure 4A. The positive band intensity at 224 nm plotted as a function of urea concentration shown in Figure 4B.

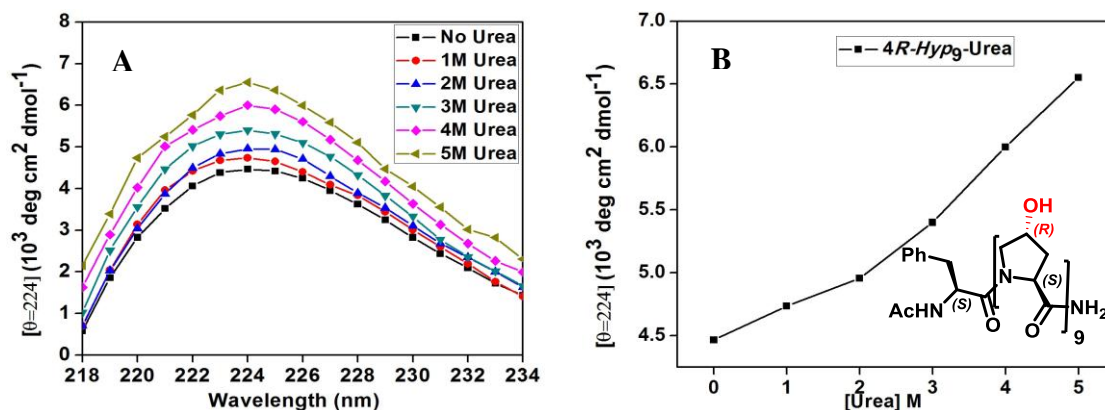


Figure 4. (A) CD profile of peptide **6** (4*R*-Hyp₉) as a function of concentration of urea at pH 7.2 (B) Intensity of positive band of CD spectra as a function of concentration of urea.

It is seen from the data that as the concentration of urea increases, the PPII helix content of peptide **6** (*4R-Hyp*₉) also increased linearly. The PPII helicity of peptide **6** (*4R-Hyp*₉) was enhanced by 5-10% by addition of 1M urea and increased linearly by 50-60% upto 5 M urea concentration, demonstrating that urea stabilized the PPII helix in case of peptide **6** (*4R-Hyp*₉) without changing its conformation.

3.2.6c Peptide 7 (*4S-hyp*₉): The CD spectra (220 nm - 230 nm) for peptide **7** (*4S-hyp*₉) as a function of urea concentration are shown in Figure 5A. The positive band intensity in CD spectra at 224 nm plotted as a function of urea concentration is shown in Figure 5B. The peptide **7** (*4S-hyp*₉) has less PPII helical content in the absence of urea and at 0.25M concentration of urea, the PPII helical content for peptide **7** (*4S-hyp*₉) rapidly increased, upto 1 M urea. At this concentration, the PPII helical content is comparable with that of peptide **6** (*4R-Hyp*₉) and from 1M to 5 M urea, the increase was much lower. The low PPII helical content of peptide **7** (*4S-hyp*₉) was enhanced enormously (>250%) by addition of 1M urea. The intensities of the positive band increases linearly by 300% upto 5M urea concentration, indicating that urea significantly stabilized the PPII helix in case of peptide **7** (*4S-hyp*₉). It is possible that low PPII helical content (more disordered) assumes regular PPII conformation at 1M NaCl concentration. Thus the neat PPII conformation in buffer needed at least 1M NaCl is needed to reasonably stabilize PPII conformation.

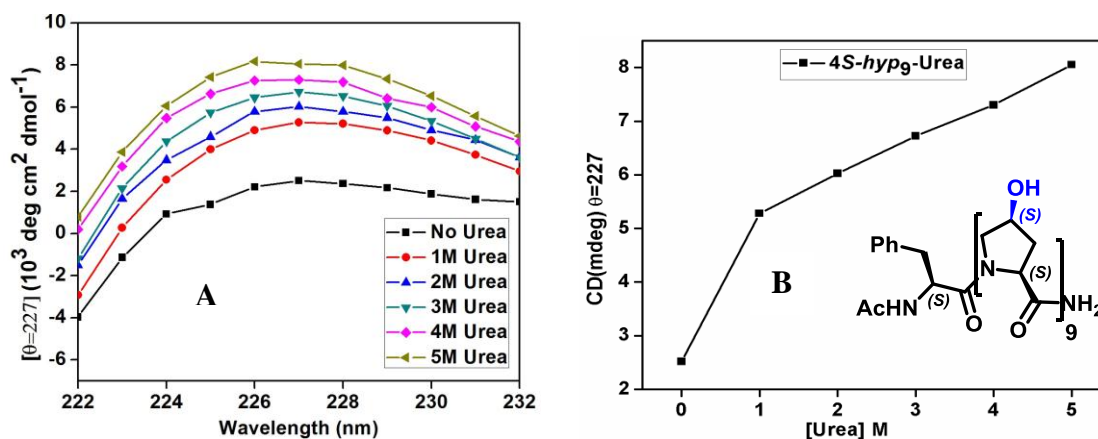


Figure 5. (A) CD profile of peptide **7** (*4S-hyp*₉) as a function of concentration of urea at pH 7.2 (B) Intensity of positive band of CD spectra as a function of concentration of urea.

3.2.6d Comparative behavior of peptides 5-7 as a function of urea concentration

The positive band intensity in CD spectra of peptides **5-7** between 224-226 nm plotted as a function of urea concentration is shown in Figure 6. In peptides **5** and **6**, urea increased the PPII helix content linearly in the range 1M to 5M concentrations.

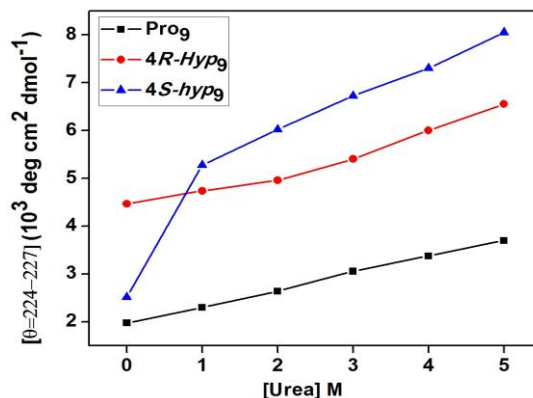


Figure 6. Intensity of CD spectra positive band of peptides **5-7** as a function of urea concentration.

In case of peptide **7** (*4S-hyp₉*) which initially had low PPII helix content in the absence of urea, the PPII helical content increased very rapidly upto 1M urea after which the PPII content increased linearly but gradually. The low PPII helicity of peptide **7** (*4S-hyp₉*) was enhanced enormously by three folds upon addition of 5M urea (pH 7.2), while that for peptide **6** (*4R-Hyp₉*) and peptide **5** (*Pro₉*) the increased was only one fold. These results demonstrate that 1M urea was critical to stabilize the PPII helix in case of *4S*-hydroxyprolyl peptide while *4R*-hydroxyprolyl peptide was inherently stable in PPII form even in absence of urea.

3.2.7 Effect of salt (NaCl) on peptides 5-7

It is known that, salt bridges stabilize α -helices²⁹ and β -sheets.³⁰ Stabilization of an α -helix occurs when the oppositely charged side chains are located on the same side spaced at $i \rightarrow i+3$ or $i \rightarrow i+4$ and on the same face of a β -sheet with the side chains on adjacent strands.³¹ On the other hand, salt bridges do not stabilize PPII helix, in both proline-rich peptides and in denatured proteins.^{32,33} Charge neutralization of cationic side chain of polylysine by counter ions at higher pH induces α -helix formation, suggesting the

important role of electrostatic interaction in stabilizing the helices. Hence the effect of varying concentrations of salt on peptides **5-7** was investigated through CD spectral changes. All CD experiments were done at the same peptide concentration (100 μM) in sodium-phosphate buffer (5 mM) at pH 7.2 with increasing concentrations of salt (NaCl). The spectra could not be recorded below wavelength of 210 nm due to high absorbance of the salt solution.

3.2.7a Peptide 5 (*Pro*₉): The CD spectra (positive band) for peptide **5** (*Pro*₉) as a function of salt concentration is shown in Figure 7A. The positive band intensity at 227 nm in CD spectra plotted as a function of salt (NaCl) concentration is shown in Figure 7B.

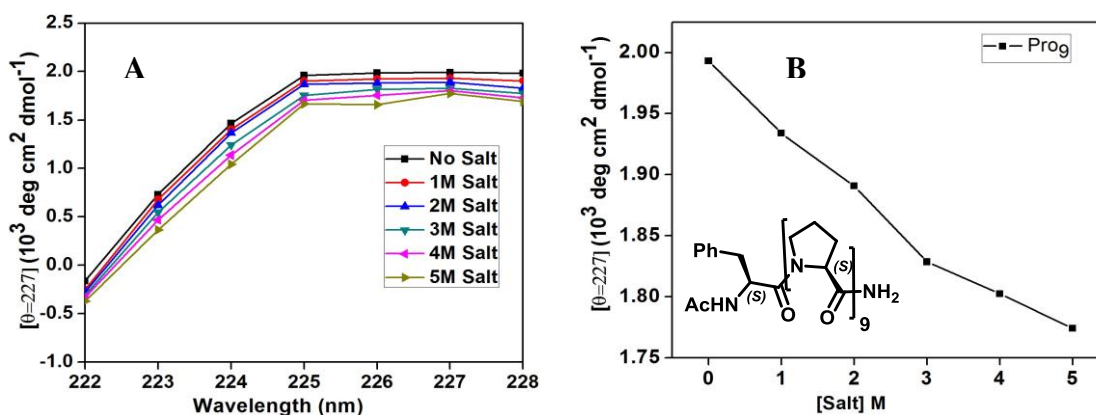


Figure 7. (A) CD profile of peptide **5** (*Pro*₉) as a function of concentration of salt at pH 7.2, (B) Intensity of positive band of CD spectra as a function of concentration of salt.

It is seen that as the concentration of salt is increased from 1M to 5M, the PPII helical content of peptide **5** (*Pro*₉) decreased linearly by 8-10%, suggesting slight disruption of the PPII helix presence of salt.

3.2.7b Peptide 6 (4*R-Hyp*₉): The CD spectra (positive band) for peptide **6** (4*R-Hyp*₉) as a function of salt (NaCl) concentration are shown in Figure 8A. The plot of intensity of positive band at 225 nm as a function of salt concentration (Figure 8B) shows a decrease of the PPII helical content of peptide **6** (4*R-Hyp*₉) by <8% in presence of increasing concentration of salt from 1M to 5M. The relative intensity of positive band at 225 nm was higher in case of peptide **6** (4*R-Hyp*₉) compared to peptide **5** (*Pro*₉).

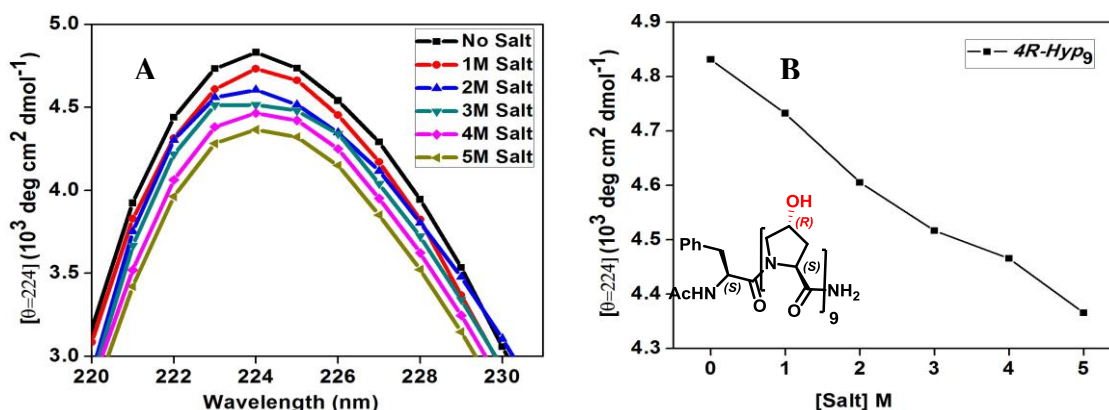


Figure 8. (A) CD profile of peptide 1 (*4R-Hyp*₉) as a function of concentration of salt at pH 7.2, (B) Intensity of positive band of CD spectra as a function of concentration of salt.

3.2.7c Peptide 7 (*4S-hyp*₉): The change in intensity of positive band at 225nm for peptide 7 (*4S-hyp*₉) as a function of salt concentration (Figure 9A), indicated an initial large decrease upto 1M (50%) followed by a gradual decrease upto 5M.

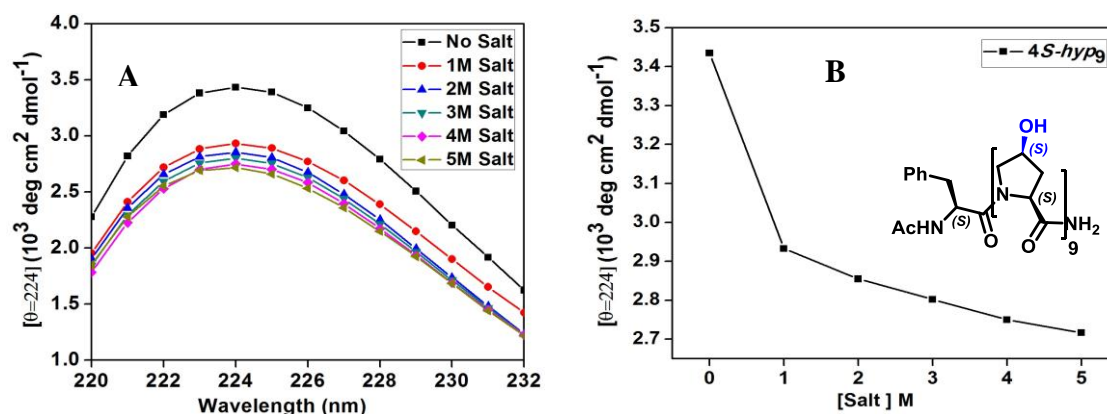


Figure 9. (A) CD profile of peptide 7 (*4S-hyp*₉) as a function of concentration of salt at pH 7.2, (B) Intensity of positive band of CD spectra as a function of concentration of salt.

3.2.7d Comparative effect of salt on PPII stability of peptides 5-7

PPII helix content is known to decrease in presence of salt. A comparison of the intensity of positive band as a function of salt concentration for peptides 5-7 is shown in Figure 10. The initial PPII helical content of peptides was in the order *4R-Hyp*₉ > *4S-hyp*₉ > *Pro*₉ and decreased by 8-10% in all cases as the salt concentration increased in the range of 1M to 5M concentration.

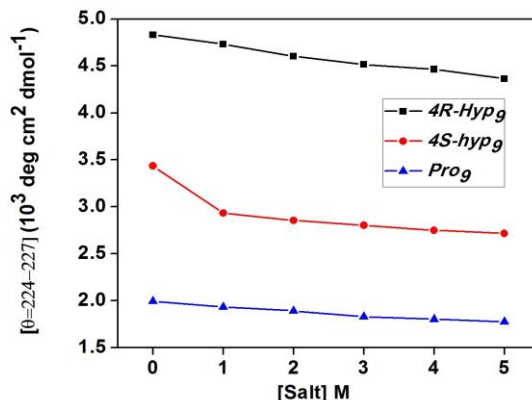


Figure 10. Intensity of CD spectra positive band as a function of salt concentration.

However, in peptide **7** (*4S-hyp*₉) PPII helical content decreased very rapidly (6%) upto 1M, while the decrease of PPII helical content of peptide **6** (*4R-Hyp*₉) and peptide **5** (*Pro*₉) was gradual. These results suggest that salt specifically destabilized the PPII helical content in peptide **7** (*4S-hyp*₉), with greater susceptibility of intramolecular H-bond between 4S-OH and C2 carbonyl.

3.2.8 Effect of NaClO₄ on peptides **7**

The arrangement of water molecules around a protein is governed by hydrogen bonding that gets altered in the presence of salt counter ions, thus influencing the conformation and the activity of proteins. Water molecules solvate the cations by orienting their oxygen atoms toward the ion, whereas the anions are solvated by adopting the opposite configuration. Such solvent orientations perturb the hydrogen-bonded network. In proteins, the preferential binding affinity to different types of ions thus influences the conformation of the polypeptide.

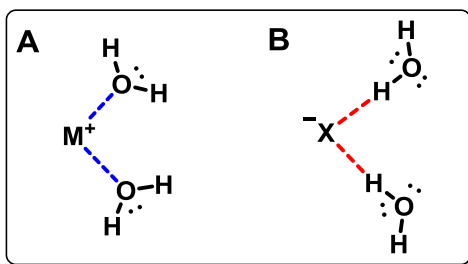


Figure 11. (A) Solvation of cations and (B) Solvation of anions by water molecules

To investigate the effect of nature of counter ions and solvation on H-bonding in peptide **7** (*4S-hyp₉*), comparative CD spectral analyses were carried out as a function of concentration of the salts NaCl and NaClO₄. These have the same cations (Na⁺) but different anions (Cl⁻ and ClO₄⁻) which have different solvating ability. The CD spectra for peptide **7** (*4S-hyp₉*) as a function of NaClO₄ concentration (Figure 12 A) show that the intensity of positive band at 225 nm slightly increases with the concentration of NaClO₄ i.e. opposite to the behaviour observed with NaCl. The PPII helical content for peptide **7** (*4S-hyp₉*) increased by 2.5 folds at 5M salt in presence of ClO₄⁻.

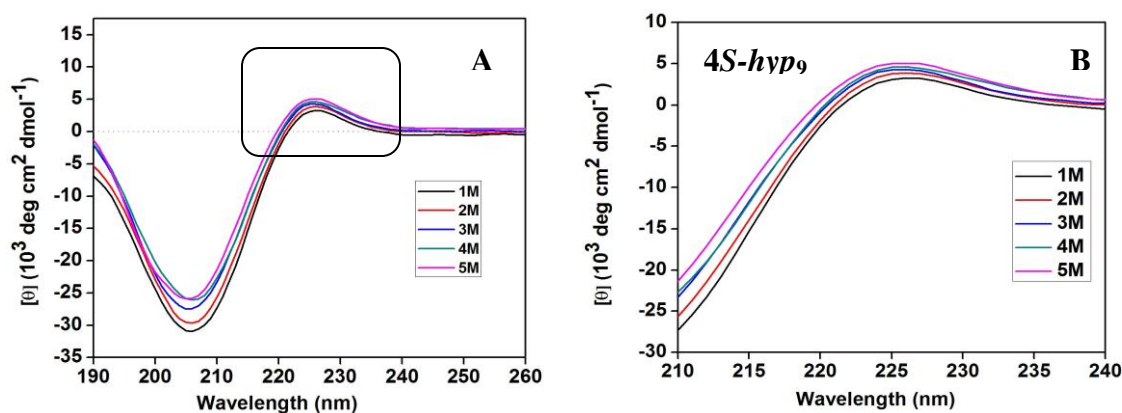


Figure 12. (A) CD profiles of peptide **7** (*4S-hyp₉*) as a function of NaClO₄ concentrations, (B) Intensity of the positive band of CD spectra of peptide **7** (*4S-hyp₉*) as a function of NaClO₄.

The stabilization found for NaClO₄ (ClO₄⁻) compared to NaCl (Cl⁻) can be explained according to Hofmeister effect³⁴ which proposes differential “salt-in” or “salt-out” of peptides by salts that interact with H-bonded water molecules, and alter water of hydration. The Hofmeister series orders ions in their decreasing ability to perturb water structure.



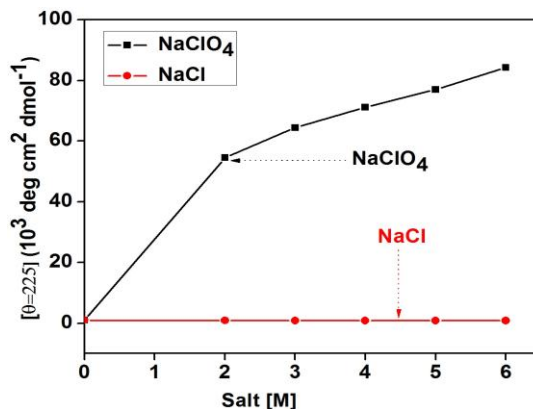


Figure 13. Intensity of the positive band of CD spectra of peptides **7** (*4S-hyp*₉) as a function of NaClO₄ and NaCl concentration.

Cl⁻ (hydrophilic) perturbs the water structure more than ClO₄⁻ causing more dehydration of peptide by stronger interaction with water, while ClO₄⁻ (more hydrophobic) leaves more water available for peptide hydration. Thus, ClO₄⁻ stabilizes water mediated hydrogen-bonded PPII conformations better than Cl⁻, which dehydrates the peptide with less water available for peptide hydration. This explains the stabilization of PPII conformations by ClO₄⁻ (NaClO₄) as compared to destabilization by Cl⁻ (NaCl) (Figure 13).

3.2.9 Effect of trifluoroethanol on peptides 5-7

In case of polyproline peptides, TFE and other hydrophobic solvents (isopropyl alcohol) are known to shift the conformation from PPII to PPI. To investigate the effects of solvent environment on peptide conformation and stability, 2,2,2-trifluoroethanol (TFE) is often used as a solvent in CD studies due to its ability to promote and reinforce the secondary structure.³⁵ The effect of alcohols on protein conformations is considered to arise from their lower polarity compared to water.³⁶ The low polarity weakens the hydrophobic interactions that stabilize the compact native structure of proteins, but simultaneously strengthens electrostatic interactions and hydrogen bonds, which stabilize the secondary structures.

The CD spectra of three polyproline peptides **5-7** were recorded at 100 μM concentration in pure TFE and the spectra are shown in Figure 14. The CD spectral profile of peptides **5** (*Pro*₉) and **6** (*4R-Hyp*₉) in TFE are typical of PPII conformation with a

positive band around 223-226 and a negative band at 204-205 nm as seen in water. Interestingly, the CD profile of peptide **7** (*4S-hyp*₉) in TFE is unlike the PPII pattern that changed to bisignate shape with a negative maximum around 214 nm, a broad shoulder at 228 nm and a positive band emerging around 197 nm. Such a spectral profile is characteristics of β -structure^{21,37} and similar to that observed previously with the 4(*S*)-amino-prolyl peptides.²¹

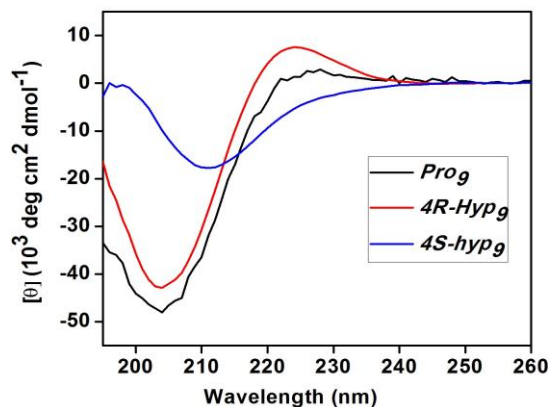


Figure 14. CD spectral profile of peptides **5-7** in trifluoroethanol (TFE).

3.2.10 Effect of peptide concentration 5-7

The β -structure arises from the inter-strand interactions and hence should be favored at a higher peptide concentration.³⁸ Hence the effect of increasing the peptide concentration for peptides **5-7** from 50 μ M to 300 μ M in TFE as solvent was recorded. In case of peptide **5** (*Pro*₉), and peptide **6** (*4R-Hyp*₉) increasing the peptide concentration lead to a mere enhancement of negative band at 208 nm without any change in CD profile itself (Figure 15). These results imply that peptide **5** (*Pro*₉) and peptide **6** (*4R-Hyp*₉) retain PPII form in trifluoroethanol, in general undergoing only minor changes to alter the PPII helical content.

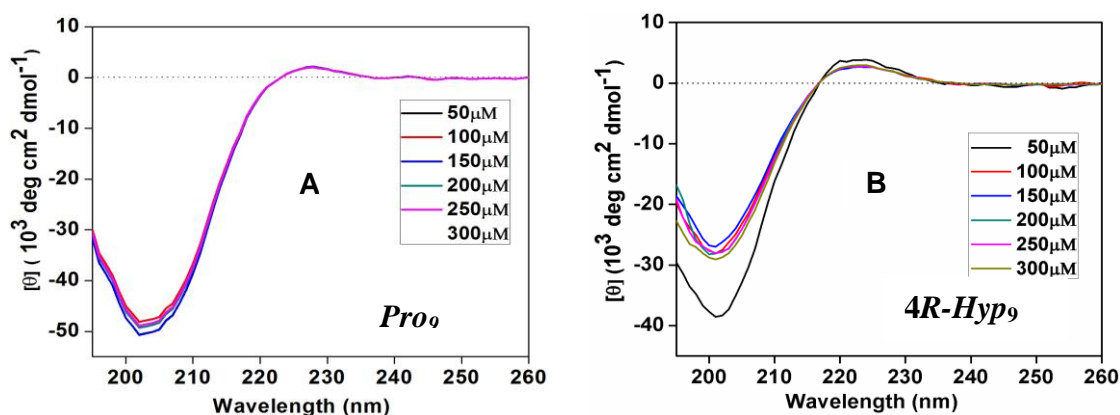


Figure 15. Increasing peptide concentration for (A) Peptide **5** (*Pro*₉), (B) **6** (*4R-Hyp*₉) from 50 to 300 μM in TFE.

Figure 16 shows the CD profiles for peptide **7** (*4S-hyp*₉) recorded from 50 to 300 μM concentration in TFE. The spectra exhibited the negative band intensity at 210 nm accompanied by the positive band at 200 nm. The bisignate profile typical of a β -structure (minima at 216 nm, maxima at 198 nm) was showed a marked decrease in intensity at 100 μM followed by a somewhat saturation at higher concentrations.

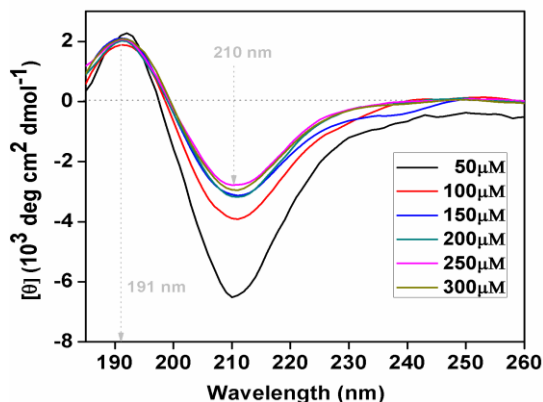


Figure 16. (A) Increasing peptide concentration of peptide **7** (*4S-hyp*₉) from 50 to 300 μM .

Hydrophobic (alcohol) solvents generally change PPII conformation to PPI. However the present results assert that peptide **7** (*4S-hyp*₉) specifically assumes a β -structure,²¹ while peptides **5** (*Pro*₉) and **6** (*4R-Hyp*₉) retain PPII conformation in TFE (Figure 15). No evidence of any PPI structure was seen in any case.

3.3 Identification of β -structure by Raman Spectroscopy

In order to support the formation of interesting β -structure by another technique, Raman spectroscopy, studies were carried out for peptide **6** (*4R-Hyp₉*) and peptide **7** (*4S-hyp₉*) in TFE. Raman spectroscopy has been abundantly used in analysis of protein conformations wherein one-to-one correspondence between the amide bands and the type of secondary structure has been established.³⁸⁻⁴¹ The peptides **5-7** were dissolved in TFE and Raman spectra were recorded using 532 nm frequency-doubled Nd:YAG laser. As the sensitive spectral band changes are of low intensity. The blank TFE Raman spectra were subtracted from the original spectra to of peptides highlight the induced changes (Figure 17). It is well established that the position of amide I band around 1630 -1640 cm^{-1} corresponds to α -helix, 1640–1660 cm^{-1} represents to random coil and 1660-1675 cm^{-1} indicates β -structure

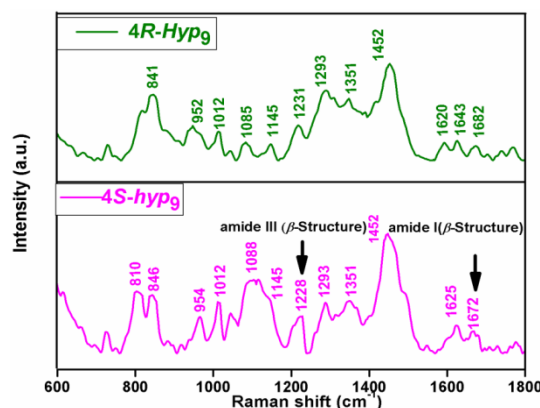


Figure 17. Raman spectra of peptide **6** (*4R-Hyp₉*) and peptide **7** (*4S-hyp₉*) from 600 cm^{-1} to 1800 cm^{-1} .

It is seen from Figure 17 that for the peptide **7** (*4S-hyp₉*), the amide I and amide III bands were observed at 1628 cm^{-1} and 1670 cm^{-1} respectively which clearly suggests the formation of β -structure (Figure 17). Significantly the characteristic band seen for peptide **7** (*4S-hyp₉*) at 1670 cm^{-1} is absent in the Raman spectra of peptide **6** (*4R-Hyp₉*). A comprehensive Raman bands assignment for peptide **6** and peptide **7** are given in Table 12.

Table 2: Raman band assignments for peptides **6** and **7**

Peptide 6 (4 <i>R</i> -Hyp ₉)		Peptide 7 (4 <i>S</i> -hyp ₉)	
Raman shift (cm ⁻¹)	Band assignment	Raman shift (cm ⁻¹)	Band assignment
841	δ (proline ring)	848	δ (proline ring)
952	δ(N-H)	954	δ(N-H)
1012	ν (N-C) + δ(N-C-C)	1012	ν (N-C)+δ(N-C-C)
1085	ν (C-C)	1088	ν (C-C)
1145	τ(CH ₂)	1145	τ(CH ₂)
1231	amide III	1228	amide III - β structure
1351	ν (COO ⁻)	1351	ν (COO ⁻)
1452	δ(CH ₂)	1452	δ(CH ₂)
1620	ring (C-C)	1625	-
1643	amide I – random coil	1672	amide I – β structure
1682 (very weak mode)	amide I – random coil/β structure		

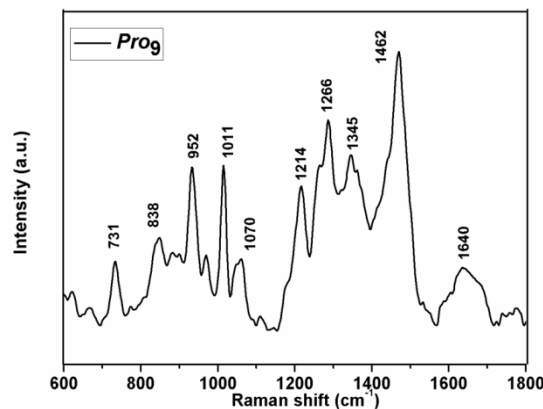
**Figure 18.** Raman spectra peptide **5** *Pro*₉ from 600 cm⁻¹ to 1800 cm⁻¹.

Figure 18 is the Raman spectra obtained from the control proline oligomer recorded with the same experimental parameters as above. The amide I band for the control peptide **5** (*Pro*₉) is around 1640 cm⁻¹ corresponding to a random coil/polyproline conformation. No bands at 1228 cm⁻¹ and 1672 cm⁻¹ characteristics of β-structure were seen.

3.4 Water-induced switching of β -structure to PPII conformation in the 4*S*-hyp₉

In order to investigate the β -structure seen for (4*S*-hyp₉) peptide **7** in trifluoroethanol, aliquots of aqueous phosphate buffer solution (pH 7.2) was titrated into TFE solution and the changes monitored by CD spectra is shown in Figure 19.

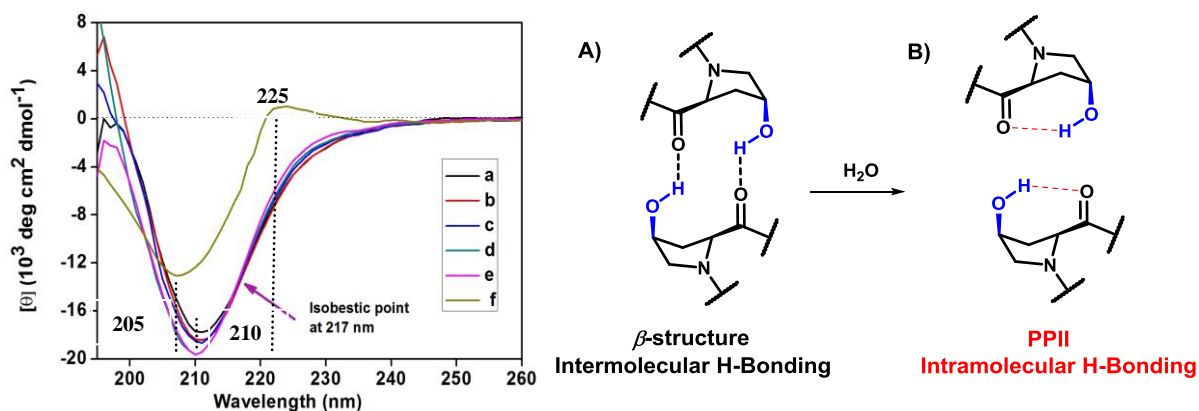


Figure 19. CD spectra of peptide **7** (4*S*-hyp₉) in TFE with incremental addition of phosphate buffer (pH 7.2) from 0.2%-1.0% (a-e) and (f) 2.0%.

Upon addition of buffer, the bisignate CD spectrum characteristic of a β -structure gradually shifted to spectral profile corresponding to that of polyproline II structure. The negative band at 214 nm slowly shifted to 205 nm, accompanied by growing broad negative shoulder at 228 nm into a positive band at about 224 nm, typical of PPII helical form. The isobestic point seen at 216 nm is indicative of the conversion of (4*S*-hyp₉) peptide **7** from β -structure in 100% TFE to full PPII form with 0.8% buffer in TFE. The conformation adopted by the 4*S*-peptide **7** in TFE is thus the result of intermolecular H-bonding that switches to intramolecular H-bonding in water.

3.5 Effect of O-acylation on β -structure

If β -structure arises due to intermolecular hydrogen bonding between two strands caused by 4*S*-OH groups, its protection by *acyl* (-OAc) group should prevent the formation of intermolecular hydrogen bonding. The CD spectra of O-acylated peptide **8** (4*S*-Achyp₉) were recorded with 100 μ M peptide concentration in sodium-phosphate buffer and in TFE (Figure 20). It is seen that the peptide **8** 4*S*-(OAc)-Pro₉ failed to form β -structure in TFE

unlike the hydroxyl peptide **7** 4*S*-(OH)-*Pro*₉, and remains in PPII conformation even in TFE like peptide **6** 4*R*-(OH)-*Pro*₉.

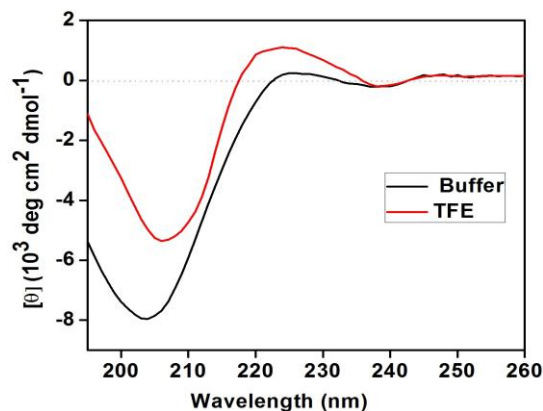


Figure 20. CD spectra of peptide **8** (4*S*-*Achyp*₉) in water and TFE.

It can be reasoned that due to non-availability of hydrogen bond donor in (4*S*-OAc) proline, which behaves like unsubstituted proline, the hydrogen bonding between two strands is not possible in TFE and PPII conformation is retained in both water as well as in TFE (Figure 20).

3.6 β -Structure requires *cis*-disposition of 4-OH and C2-CO groups

Most essential biological molecules exist only in one of the two possible enantiomers (mirror-image structures) and are either left- or right-handed. Most proteins contain only L-amino acids, while DNA is made up of D-deoxyribose. Chirality of amino acids and helical polypeptide structure are well correlated because naturally occurring L-amino acids predominantly form right-handed helices, whereas the stereoisomeric D-amino acids favor left-handed helices.

Polyproline peptide composed of L-*cis*-hydroxyproline forms PPII in water (Figure 1) but β -structure in TFE (Figure 14). The *cis* disposition of C4-OH and C2-carboxyl of L-proline encourages intramolecular H-bonding in H₂O and interstrand H-bonding in TFE. This *cis* disposition seems to be key for the differential conformations in TFE and H₂O, since the 4*R*-(*trans*)-OH-L-proline does not exhibit this behavior. Such a *cis* disposition is possible in the mirror image stereomer 4*R*-(*trans*)-(OH)-D-Proline. The polypeptide derived

from this stereomer should exhibit a opposite handed PPII in H₂O (Figure 21 A-B) and β -structure in TFE (Figure 21 C-D) respectively. To examine such a possibility of mirror image secondary structures, the CD spectra of peptide **9** (*4R-D-hyp*₉) was measured in trifluoroethanol (TFE) and water.

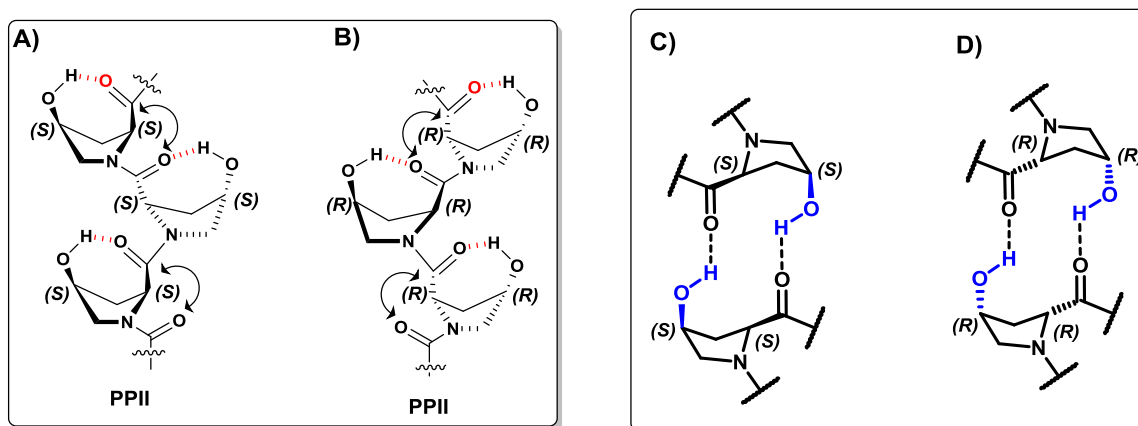


Figure 21. Proposed structure for polyproline in (A) 4*S*-hydroxy-L-proline, (B) 4*R*-hydroxy-D-proline; proposed β -structure in (C) 4*S*-hydroxy-L-proline, (B) 4*R*-hydroxy-D-proline.

3.6.1 Conformational study of 4*R*-D-peptide **9** (*4R-D-hyp*₉) in water

The CD spectra of peptide **9** (*4R-D-hyp*₉) at 100 μ M in water was recorded from 190 to 260 nm wavelength and compared with that of peptide **7** (*4S-L-hyp*₉). The CD profile of peptide **9** (*4R-D-hyp*₉) derived from D-hydroxyproline (Figure 22A, black) shows a weakly negative peak at 225-228 nm, while that at lower wavelength of 205 nm a strong positive peak is seen. The CD peaks of the (*4R-D-hyp*₉) peptide **9** appear as close mirror image of that of (*4S-L-hyp*₉) peptide **7**, which is known to be right-handed PPII form. This indicates that the D-peptide **9** forms the mirror image PPII form. Although the PPI form is opposite handed of PPII form, the CD profile of D-peptide **9** is different from that expected for the PPI form (Figure 22).

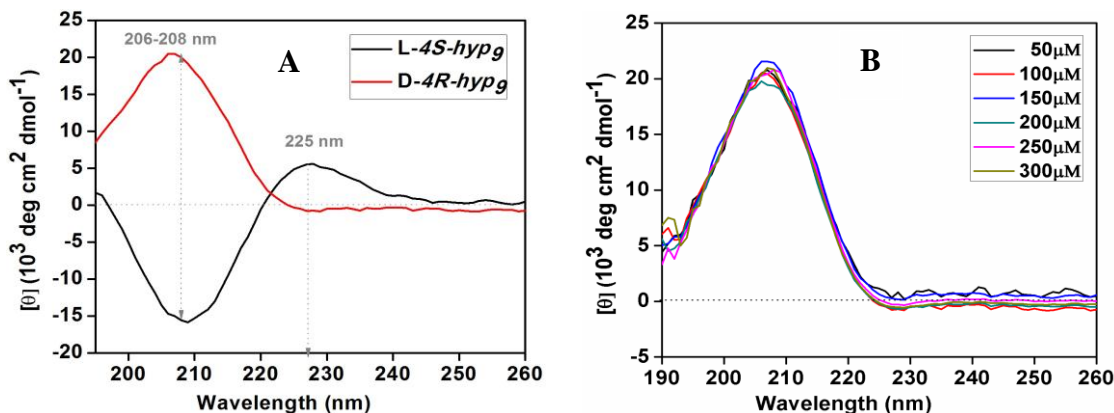


Figure 22. CD profiles of (A) peptide **7** (*4S-L-hyp*₉, red) and **9** (*4R-D-hyp*₉, black) at concentration 100 μM , (B) CD profiles of peptide **9** (*4R-D-hyp*₉) at concentration 50-300 μM in buffer at 25 $^{\circ}\text{C}$.

Increasing the concentrations of D-peptide **9** in buffer gave rise to CD amplitude with opposite signs (Figure 23B) to the PPII showed by L-peptide **7** (*4S-L-hyp*₉). Thus the peptide derived from *4R*-(OH)-D-proline induces reversal of PPII helix from left-handed to right-handed sense. Although the CD profiles are mirror images, the amplitudes are not exactly mirror image in magnitude. The CD bands thus reflect the prevalence of one screw sense over the other one (Figure 23B).⁴⁰

3.6.2. Conformational study of (*4R-D-hyp*₉) peptide **9** in TFE

In order to study the structural switch of the peptide **9** induced by TFE, CD spectra of (*4R-D-hyp*₉) peptide **9** was recorded in TFE from 190 to 260 nm wavelength. It showed a negative peak around 195 nm and a positive peak at around 210 nm. In comparison, the CD spectra of peptide **7** (*4S-L-hyp*₉), showed negative peak at around 210 nm and positive peak around 195 nm (Figure 24). The relative signs of CD bands of peptide **7** and **9** are completely opposite to each other suggesting mirroring chirality of induced structure (Figure 24). Once again although the CD profiles are of opposite signs, the magnitude of the peak intensities (amplitude) were not exactly opposite in magnitude. Thus, it is seen that the *cis* disposed *4R*-(OH)-D-Pro peptide **9** forms a β -structure in TFE but opposite in handedness to β -structure of *cis* *4S*-(OH)-L-Pro peptide **7**.

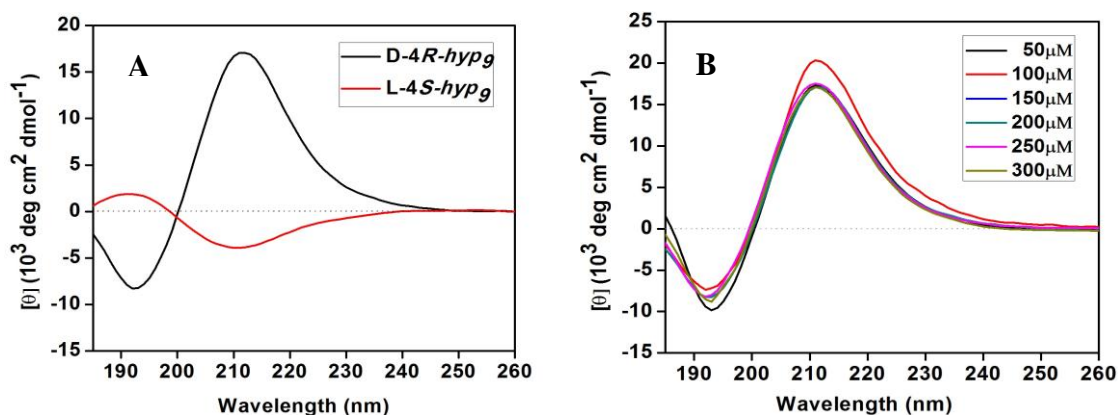


Figure 24. (A) CD profiles of peptide **7** (4S-L-hyp₉, red) and **9** (4R-D-hyp₉, black) at concentration 100 μM , (B) CD profiles of peptide **9** (4R-D-hyp₉) at concentration 50-300 μM in TFE

Further proof of formation of β -structure by **9** is provided by CD at increasing concentration in the range (50 μM -300 μM) that shows decreased amplitude of positive peak 210 nm and negative peak at 192-195 nm as a function of concentration (Figure 24B), indicates that there is no switch between conformations.

The results prove that β -structure arises in polyproline peptides derived from hydroxyproline in which stereochemistry of C4-substituent is *cis* to that of carboxylic group. The intensity of the CD bands reflect the prevalence of β -structure formed by **9** (4R-D-hyp₉) over the β -structure formed by peptide **7** (4S-L-hyp₉) (Figure 21). This observation strongly supports the interchain association of peptide in TFE possible only with *cis* disposed 4-OH group intermolecular hydrogen bonding, giving rise to β -structures (Figure 21).

3.6.3. Effect of N-terminal Phenylalanine :

To examine the effect of N-terminal Phe, 4S-Peptides without phenylalanine at N-terminus was synthesised and checked for its CD properties. It exhibited a positive band at 197-199 nm, a negative maximum around 213 nm and a broad shoulder around 227 nm, which are characteristic features of β -structure (Figure 25).

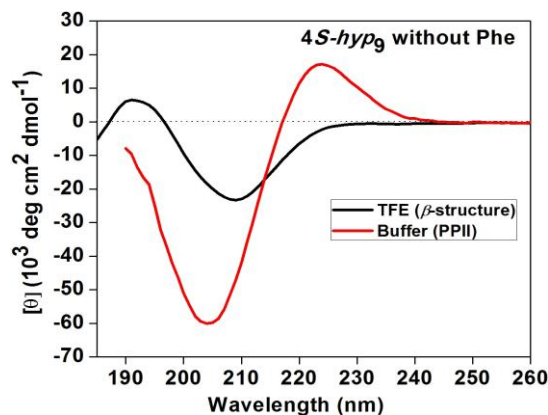


Figure 25. (A) CD profiles of peptide **7** (*4S-L-hyp*₉) at concentration 100 μM in TFE (black) and Buffer (red).

The CD spectrum of *4S-L-hydroxy* peptides without phenylalanine retained PPII conformation in aqueous medium. This data provided additional evidence that the β -structure originates from an interchain association favoured by the *cis* disposed *4S*-substituent and the amide carbonyl on same proline residue.

3.7 Discussion

The properties of α -amino acids influence the folding and functions of peptides and proteins. Proline residues are often found in natural peptides and facilitate different conformations and increase structural diversity as a result of *cis/trans* isomerization across the prolyl peptide bond. Hydroxylation of proline at the C4-position has been found to substantially enhance the stability of collagen, via the induction of stereoelectronic effect.^{17,41} This is facilitated by the preferred *gauche* relationship of the 4-hydroxyl substituent and the carbon–amide bond. In *4R-Hyp* and *4S-hyp*, two major hyperconjugative interactions stabilize the conformation. The sterically disfavored *gauche* conformation is preferred due to favorable hyperconjugative interactions from overlap of electron-rich σ_{C-H} orbitals and the electron-deficient σ^*_{C-X} orbitals (X = amide or hydroxyl in Hyp (Figure 26).

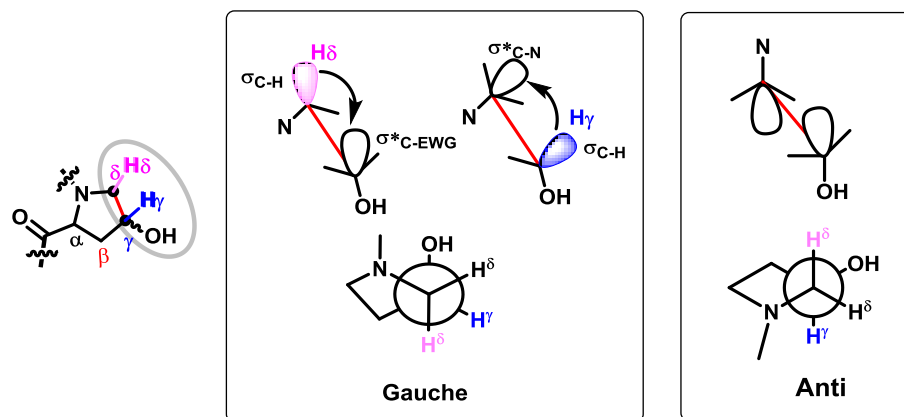


Figure 26. Stereoelectronic effects in 4-substituted prolines.

In addition to the stereoelectronic (*gauche*) effect on controlling ring pucker of peptides containing proline residues, conformations are also influenced by a favorable $n \rightarrow \pi^*$ interaction between adjacent carbonyls of peptide backbone.⁴² This interaction, originates due to overlap between a lone pair (n) on the carbonyl oxygen of the i residue with the π^* orbital of the carbonyl at the carbon of the $i+1^{\text{th}}$ residue. The geometry for $n \rightarrow \pi^*$ interaction is ideal when the carbonyl at the carbon of the $i+1$ residue is pointing inwards of the pyrrolidine ring (Figure 27). This orientation is observed in *exo*-puckered proline derivatives, in particular those with electron-withdrawing groups at C4 and a 4*R*-configuration.^{10, 43} On the other hand, in *endo*-puckered derivatives, the carbonyl group at $i+1$ residue is turned away from the ring centre. On the basis of this conformational analysis, an inward orientation of the carbonyl is disfavored in *endo*-puckered proline derivatives because of repulsion between the substituent at C4 and the oxygen of the carbonyl at the carbon of the $i+1$ site. Introduction of a C4 substituent that can attractively interact with CO of $i+1$ residue would therefore stabilize a C4 *endo* pucker and this is realised with 4*S*-hydroxy/amino proline derivatives.

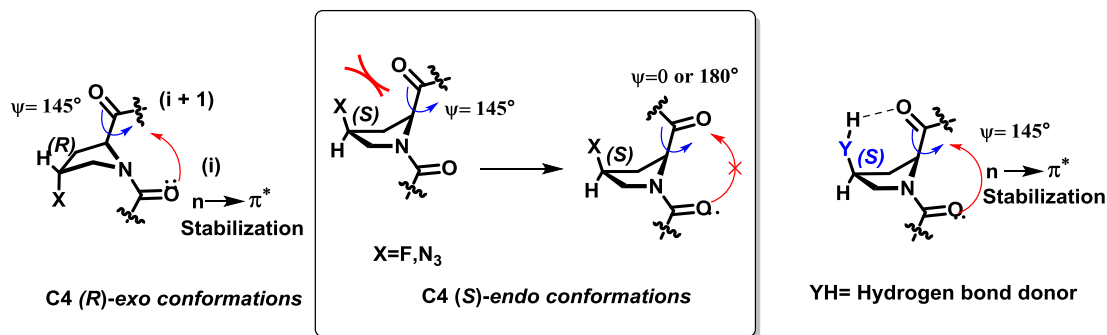


Figure 27. C4-*exo* conformations of 4*R*-derivatives and C4-*endo* conformations of 4*S*-derivatives without (middle) and with (right) H-bond donors at C4.

In peptides derived from 4-(*R/S*)-substituted proline derivatives that bear H-bond-donating groups at C4 (OH, NH₂), additional interactions possible from the inter-residue H-bonding influences of such interactions on the secondary structure of the derived polypeptides. L-Peptides **5-7** form PPII helix at physiological pH as indicated by established CD pattern of the PPII conformation. The intensity of positive band in CD spectrum is proportional to the PPII helical content is higher in and 4-substituted peptides **6** (4*R*-Hyp₉) and peptide **7** (4*S*-hyp₉) have more positive intensity in the region (225-227 nm) than the unsubstituted proline peptide **5** (Pro₉). The 4*R*-peptide **6** (4*R*-Hyp₉) has maximum PPII helical content and the intensity of the positive band at 225-227 nm decreases in the order peptide **6** (4*R*-Hyp₉) > peptide **7** (4*S*-hyp₉) > peptide **5** (Pro₉). The ratio of intensity of positive to negative bands in CD spectra (Figure 2) for the peptides (**5-7**) show a linear increase with concentration, indicating that the peptide strands do not associate into higher order structures and maintain single chain PPII helix form, even at higher concentrations.

Urea: PPII helical content is known to increase in presence of urea that interacts favorably with the polypeptide backbone. The effect of increasing concentrations of urea on CD of 4-(*R/S*)-hydroxy-L-proline polypeptides showed enhanced stability. The PPII helix in case of both 4*R*- and 4*S*-hydroxyprolyl peptides is more than that with unsubstituted prolyl polypeptide. The initial large increase with peptide **7** (4*S*-hyp₉) arises from a slight reorientation of the 4*S*-hydroxy group to accommodate urea-mediated hydrogen bonding with the amide carbonyl carbon (Figure 28) and thereby favoring the PPII helix. Such type

of complementary H-bonding of urea with the amide groups in protein is known in literature.^{26,44} The steady increase of PPII helical content with urea for peptide **6** (*4R-Hyp*₉) and peptide **5** (*Pro*₉) suggests a rigidification of peptide backbone by bidentate H-bonding with urea.

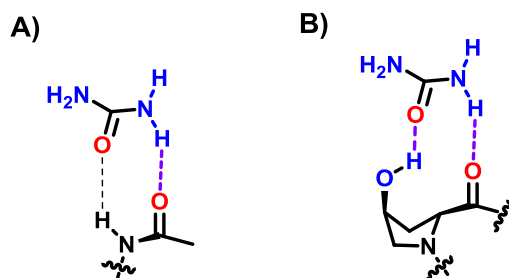


Figure 28. Urea mediated hydrogen bonding in (A) Peptide backbone (B) Polyproline peptide **7** (*4S-hyp*₉) dictating the PPII conformation.

Salt: PPII helical content is known to decrease in presence of salt.⁴⁵ The effect of varying concentrations of salt on 4-hydroxyproline polypeptides analysed through CD spectral analysis (Figure 10) suggest that salt (NaCl) destabilized the PPII helix in all cases. These observations are consistent with the findings that the PPII helical content of proline homopolymers or peptides decreased with increasing salt concentration.⁴⁵⁻⁴⁶ The initial larger decrease with peptide **7** (*4S-hyp*₉) may be due to salt immediately disrupting the intraresidue hydrogen bonding resulting in a rapid decrease of PPII helical content, clearly pointing to the role of H-bond promoting PPII form. This is supported by experiments to examine the relative effects with salts having same cations but different anions. While the PPII helical content decreased linearly with NaCl for peptide **5** (*Pro*₉) and **6** (*4R-Hyp*₉), the helical content increased for peptide **7** is in presence of NaClO₄. This suggests that conformation of peptide **7** is influenced by chaotropic effect caused by solvation effects of the counter anion. The hydrophobic NaClO₄ encourages the H-bonds in 4*S*-peptides to favour PPII form. The hydrophilic Cl⁻ ion disengages H₂O molecules from solvation network, while hydrophobic ClO₄⁻ strengthens the H₂O network. Both the effects influence the PPII form.

Larger changes seen specifically for peptide **7** (*4S-hyp*₉) in the presence of urea and salts (NaCl/NaClO₄) points to the combined role of H-bonding and stereoelectronic effects

in dictating the PPII conformation. Recently, 4*S*-(OH/NH₃⁺) groups on proline monomers were shown to form intramolecular H-bonds with the amide carbonyl (Figure 28), increasing the *trans/cis* amide ratio, promoting PPII conformation in the derived polypeptides.⁴⁷

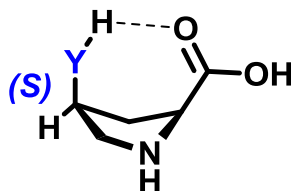


Figure 29. C4-*endo* conformations of 4*S*-derivatives with H-bond donors at C4.

Solvent: H-bonding interactions are sensitive to solvent. In order to evaluate the effect of non-aqueous solvent on conformations of poly-4(*R/S*)-hydroxyproline, the CD spectra of peptides **5-7** were recorded in trifluoroethanol (TFE) (Figure 14). The CD profiles showed that peptide **5** (*Pro*₉) and peptide **6** (4*R-Hyp*₉) retain their PPII conformation. Interestingly, the CD profile of 4*S*-peptide **7** (4*S-hyp*₉) in TFE exhibited a pattern characteristic of a β -structure. Intermolecular associations should get enhanced at higher peptide concentrations and hence the CD spectra of 4*S*-OH-substituted peptides were recorded in TFE at increasing concentrations from 50 μ M to 300 μ M. It was found that the strong negative band at 210 nm present in all peptides at 50 μ M, showed a marked decrease in intensity at 100 μ M followed by a somewhat saturation at higher concentrations. Titration of water reverses β -structure to PPII form, indicating that water disturbs the interchain H-bonding, destabilising the β -structure. Further confirmation for presence of β -structure was seen from Raman spectroscopy data, in which the bands at 1228 and 1670 cm⁻¹ characteristics of β -structure were seen specifically for peptide **7** (4*S-hyp*₉) and not for peptides **5** and **6**.

These observed results could be overall rationalized by following description. In the peptide **7** (4*S-hyp*₉), the -OH group can form an *intramolecular* H-bond with the amide carbonyl of the same proline moiety, which promotes PPII conformation.⁴⁷ The possibility of the 4*S*-OH group engaging the amide carbonyl of another chain of 4*S-hyp*₉ through an *intermolecular* H-bond would lead to formation of β -structure, which is facilitated at higher peptide concentration in TFE. In aqueous solution even at high peptide concentrations, no β -structure is seen due to competition of H₂O molecules, which disrupt

intermolecular H-bonds seen for β -structure. As β -structure is not observed with *trans* 4*R*-OH prolyl peptides, it is certain that *cis* disposition of the H-bonding groups is necessary even to form β -structure. The proposed synthon for β -structure is shown in Figure 30A.

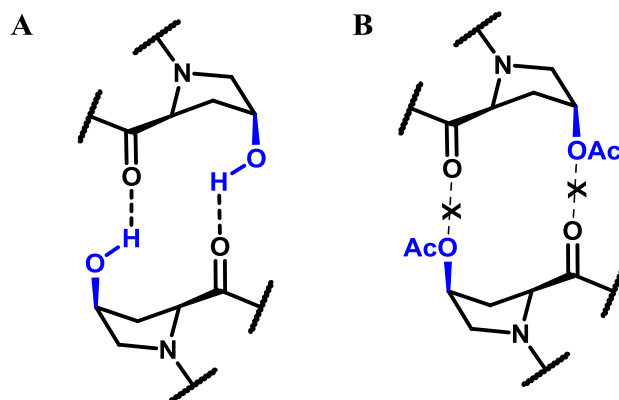


Figure 30. (A) Proposed structure for β -structure in presence of H-bond donor, (B) β -structure in absence of H-bond donor

When the hydrogen bond donor groups (-OH) are protected by *acyl* (-OAc) group, hydrogen bonding is not possible (Figure 30) and the CD spectroscopic analyses performed both in H₂O and the aprotic solvent TFE, suggesting the existence of only PPII form. It was found that the, peptide **8** (4*S*-*Achyp*₉) shows PPII conformation both in water as well as in trifluoroethanol due to absence of H-bond donor. This confirms that the association of two polyproline strands in TFE is possible only when substituent at C4 position has at least one H-bond donor and *S*-stereochemistry with carbonyl group.

D-peptide: The *cis* position of 4*S*-OH and 2-carboxyl essential for β -structure in L-proline can be realised with 4*R*-OH- D-proline that has inverted stereochemistry of both C4 and C2 and hence 4*R*-OH-D-prolylpeptide **9** was investigated. The 4*R*-OH-D-prolyl peptide exhibited PPII form of opposite handedness compared to the natural right-handed PPII form of 4*S*-OH-L-proline in water (mirror image CD), although the CD amplitudes are not exactly inverted in magnitude. Significantly, in TFE, 4*R*-D-peptide **9** showed the CD with exactly mirror relationship of the β -structure profile seen with 4*S*-OH-L-proline peptide **7**. This strongly supported the formation of intermolecular hydrogen bonding between 4*R*-hydroxy (-OH) of one strand and C2 carbonyl of another strand even in D-

peptide, which are *cis* to each other necessary to form mirror image β -structure. There are perhaps the first examples of mirror image β -structures realised in polypeptides.

3.8. Water-induced switching of β -structure to PPII conformation in the 4*S*-hyp₉

When aqueous phosphate buffer (pH 7.2) was titrated into TFE solution of peptide **7** (4*S*-hyp₉) in tiny incremental steps of 0.1%, the 214 nm negative band slowly shifted to 205 nm, accompanied by a growing of the broad negative shoulder at 228 nm into a positive band at about 224 nm (Figure 18) typical of PPII form. The isobestic point seen at 218 nm is indicative of the conversion of peptide **7** (4*S*-hyp₉) from β -structure in 100% TFE to full PPII form with 0.8% buffer in TFE. The overall results imply that peptide **7** (4*S*-hyp₉) assumes a β -structure in TFE that is transformed to the PPII form in aqueous medium.

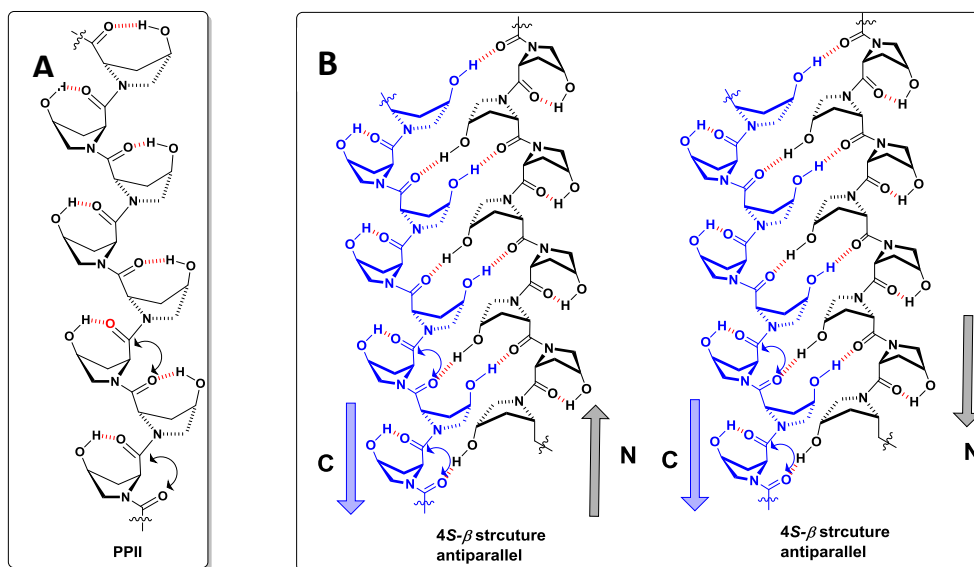


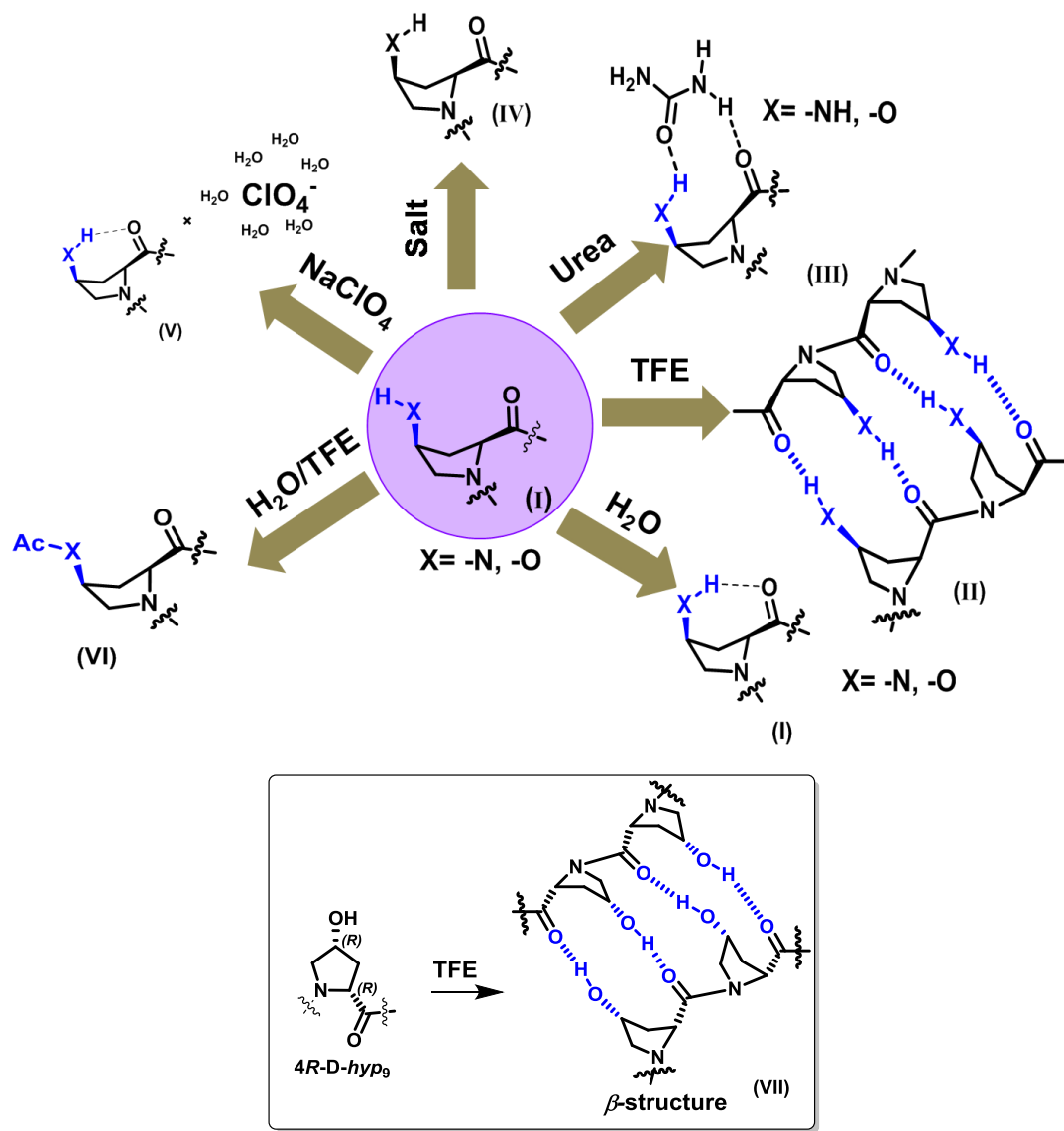
Figure 31. (A) Intramolecular H-bonding favors the PPII form *via* enriching the *trans* amide geometry (B) Interchain hydrogen bonds involving 4*S*-OH in β -structure.

The β -structure arising from *interchain* hydrogen bonds involving 4*S*-OH and amide carbonyl can be pictorially depicted as in Figure 31B in which H-bond from 4*S*-OH and the backbone carbonyl in 4*S*-substituted polypeptides. The β -structure can be either parallel or antiparallel. Although theoretical studies are needed, it appears that

antiparallel structure is favored with 4*S*-OH in equatorial form. The present results have importantly unearthed novel mirror image PPII helix (non-PPI form) and β -structure.

3.9 Conclusion

A plausible molecular picture for various structural transitions under different conditions for peptide **6-7** is depicted in Scheme 5. The *intramolecular* H-bonding of 4*S*-OH with amide carbonyl possible only in (4*S*-hyp₉) peptide **7** (I) promotes PPII form in buffer, while in a fluorinated solvent TFE, the intramolecular H-bonding between 4*S*-OH and the amide carbonyl switches to interchain H-bonding (II).



Urea rigidifies the backbone by complementary H-bonding (III) to *cis*-disposed 4*S*-OH group and amide carbonyl to enhance the PPII form; salt weakens the PPII by breaking the H-bond (IV). NaClO₄ promotes intramolecular H-bonding which enhances PPII conformation (V). *Intramolecular* H-bonding is absent in O-*Acyl* peptide due to lack of H-bond donor (VI) The *cis* disposition of 4*R*-OH in D-proline also leads to interchain H-bonding in the derived peptide to form β -structure with opposite handedness to that of *cis* disposition of 4*R*-OH in L-proline (VII).

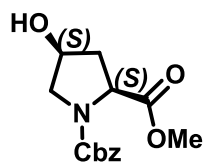
In summary, it is demonstrated here that peptide **7** (4*S*-hyp₉) adapts an unusual β -structure like (4*S*-NH₂) in TFE unlike most polyproline peptides, which prefer the PPI form in hydrophobic/fluorinated media. The β -structure arises from *interchain* hydrogen bonds involving 4*S*-OH and amide carbonyl, which are broken in water and rearranged to *intramolecular* H-bonding that favors the PPII form *via* enriching the *trans* amide geometry. This structural conversion illustrates a fine balance between stereoelectronic and H-bonding effects in novel tuning of the secondary structure of 4*R/S*-hydroxyproline polypeptides. β -structure in polyproline will add a new design principle to a growing repertoire of strategies for engineering peptide secondary structural motifs for new biomaterials and nanoassemblies.

3.10. Experimental section

Materials and reagents were of the highest commercially available grade and used without further purification. Reactions monitored by thin layer chromatography (TLC) were carried out on precoated silica gel 60 F254 plates (E. Merck). TLCs were visualized under UV light, iodine and/or ninhydrin spray followed by heating upto 110 °C with heat gun. Silica gel 60-120 and 100-200 mesh (Merck) was used for routine column chromatography. Elution was done with ethyl acetate/petroleum ether or dichloromethane/methanol mixture depending upon the compound polarity and chemical nature. ^1H and ^{13}C NMR spectra were recorded on Bruker AV 500 and AV 400 spectrometers. Chemical shifts are reported in ppm using TMS and CDCl_3 as a reference. Spectra were analyzed using ACD spectviewer software from ACD labs. Analytical HPLC was performed using a LiChrospher 100 RP-18e 5 μm (250 mm x 25 mm) column from Merck. Preparative HPLC was carried out on a LiChrospher RP-18e 5 μm (250 mm x 10 mm) column from Merck. Mass spectra were obtained by ESI-MS technique on AP-QSTAR spectrometer. Jasco J-815 (Japan) instrument was used for CD measurements. All graphs presented for CD spectra's are drawn by Origin 8 software.

3.10.1 Synthesis of 4S-hydroxyproline monomer

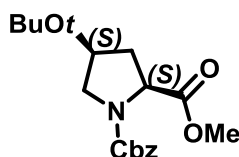
(2S, 4S)-N¹-Benzyloxycarbonyl-4-hydroxyproline methyl ester (**30**)



A solution of compound **29** (4.0 g, 150 mmol) in anhydrous acetone (25 mL), K_2CO_3 (5.2g, 275 mmol) and dimethylsulphate 1.7 mL (180 mmol) was refluxed under nitrogen atmosphere for 4 h. The acetone was removed under vacuum and the resulting residue was dissolved in water followed by extraction with ethyl acetate (3x50 mL). The combined organic layers were washed with water (3x50 mL) followed by saturated brine solution (3 x 30 mL) then dried over Na_2SO_4 and concentrated under vacuum. The crude material was purified by silica gel chromatography afford compound **30** as a colourless

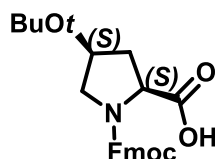
thick oil (4 g, 95% yield); ^1H NMR (400 MHz, CDCl_3) δ 7.32-7.38 (m, 5H), 5.05-5.22 (m, 2H), 4.39 (t, 1H), 3.81 & 3.62 (s, 3H, rotamer), 3.65-3.74 (dd, 2H), 2.82 (bs, 1H), 2.15-2.36 (m, 2H); ^{13}C NMR (100 MHz, CDCl_3) δ 175.3, 175.0, 155.1, 136.4, 128.6, 128.1, 128, 71.3, 70.3, 67.5, 58.2, 57.8, 55.8, 53.0, 52.7, 38.8, 37.8; ESI-MS m/z calcd for $\text{C}_{14}\text{H}_{17}\text{NO}_5$ $[\text{M}+\text{Na}]^+$ 302.0800, found 302.1012.

(2S, 4S)-N¹-Benzyloxycarbonyl-4-O-tert-butyl proline methyl ester (31)



The mixture of compound **30** (5.0 g, 179 mmol), Ag_2O (8.5g 358mmol) and *tert*-butyl bromide (6.0 mL, 537mmol) in cyclohexane (50 ml) was stirred for 24 h at room temperature. The resulting suspension was filtered out and the filtrate was concentrated under reduced pressure and crude product was purified by silica gel chromatography eluting with petroleum ether:ethyl acetate (80:20) to give a desired product **31**. (5.11 g, 85% yield); ^1H NMR (400 MHz, CDCl_3) δ 7.29-7.37 (m, 5H), 5.0-5.21 (m, 2H), 4.27-4.49 (m, 2H), 3.78-3.81 (t, 1H), 3.76 & 3.56 (s, 3H, rotamer), 3.26-3.39 (m, 1H), 2.09-2.21 (m, 2H), 1.17-1.18 (d, 9H); ^{13}C NMR (100 MHz, CDCl_3) δ : 173.4, 154.8, 154.3, 136.6, 136.5, 128.5, 128.3, 74.2, 69.2, 68.5, 67.2, 57.7, 53.9, 53.3, 52.4, 52.2, 38.7, 37.7, 28.3; MS (MALDI-TOF) m/z calcd for $\text{C}_{18}\text{H}_{25}\text{NO}_5$ $[\text{M}+\text{Na}]^+$ 358.1630, found 358.1271.

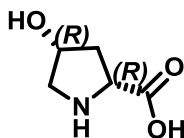
(2S,4S)-N¹-fluorenylmethyloxycarbonyl-4-O-tert-butyl proline (32)



The ester compound **7** (5.0 g, 15 mmol) was subjected to hydrolysis using NaOH (1.7g 45mmol) in THF:H₂O (1:1) for 1 h. THF was removed under vacuum and the aqueous layer was washed with ethyl acetate (3x50 mL) to remove unreacted organic compound. The aqueous layer was acidified by KHSO_4 to pH 2 and extracted with ethyl

acetate (3x60 mL) followed by concentration. The crude product obtained was purified by silica gel chromatography and eluted with ethyl acetate/hexane (65:35) to afford a white solid powder **32** (4.6 g, 97% yield). Compound **32** was dissolved in dry methanol (15 mL) to which of 10% Pd/C (0.5 g) was added. The mixture was subjected to hydrogenation under H₂ gas (60-psi pressure) for 6 h. Water (200 mL) was added to the reaction mixture which was filtered through Whatman filter paper and the filtrate was concentrated under reduced pressure. The product obtained as a white solid powder was dissolved in water:dioxane, 1:1 (50 mL). The pH was maintained at 10 by addition of 10% Na₂CO₃. The reaction mixture was stirred at 0 °C for 15 minutes. Fmoc-Cl (5.17 g, 20 mmol) was added in portion wise during 45 minutes maintained the temperature at 0 °C for first 4 h and then allowed to come at room temperature and was stirred for 18 h. The dioxane was removed under vacuum and the aqueous layer was washed with ethyl acetate (3x80 mL). The aqueous layer was acidified with KHSO₄ to pH 2 followed by extraction with ethyl acetate (3x70 mL). Concentration of solvent gave crude product which was purified by silica gel chromatography (70% ethyl acetate/hexane) to afford compound **32** as white solid (4.75 g, 78% yield); ¹H NMR (400 MHz, CDCl₃) δ 7.32-7.78 (m, 8H), 4.51-4.53 (d, 1H), 4.40-4.43 (m, 2H), 4.28-4.30 (t, 2H), 3.43-3.61 (t, 2H), 2.18-2.42 (m, 2H), 1.24 (s, 9H); ¹³C NMR (100 MHz, CDCl₃) δ 174.2, 144.2, 142.4, 127.8, 127.2, 125.1, 120.0, 69.6, 67.9, 58.5, 54.7, 53.9, 47.2, 38.2, 37.0, 28.1; ESI-MS m/z calcd for C₂₄H₂₇NO₅ [M+Na]⁺432.1787 found 4432.1788.

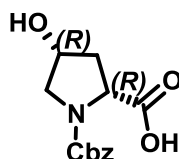
(2R, 4R)-Cis-4-hydroxy-D-proline (33)



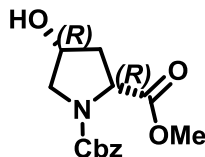
A suspension of trans-4-hydroxy-L-proline (13.1 g, 10.0 mmol) in a mixture of acetic anhydride (10 ml) and glacial acetic acid (20 ml) was heated under reflux at 140 °C for 5.5 h. The dark solution was cooled, and evaporated under reduced pressure to give thick oil. The oil was dissolved in 2N HCl (250 ml) and the solution was refluxed at 100 °C for 3 h, then was decolourised with charcoal and filtered. The filtrate was concentrated under reduced pressure to give light yellow oil. Trituration with diethyl ether gave a

precipitate which was a mixture of epimeric hydrochloride salts. Recrystallisation from ethanol gave a crystalline solid (13.7 g, 82%); mp 145–149 °C; A portion of the hydrochloride salt (0.50g, 3.0 mmol) was dissolved in water (2 ml), and triethylamine (1ml) and absolute ethanol (40 ml) were added. The solution was stored at room temperature until crystallisation was complete. The crystals were collected by suction filtration and were recrystallised twice from water-ethanol to give pure *cis*-4-hydroxy-D-proline as needles (7 g, 53.4% yield); $[\alpha]_D^{25} +56.30$ (c 2.0 H₂O); ¹H NMR (CDCl₃, 400 MHz) δ 4.57-4.54 (m, 1H), 4.21-4.17 (m, 1H), 3.46-3.42 (m, 1H), 3.37-3.32 (m, 1H), 2.52-2.44 (m, 1H), 2.25-2.20 (m, 1H); ¹³C NMR (100 MHz, CDCl₃) δ 174.5, 69.2, 59.7, 53.0, 37.2; ESI-MS m/z calcd for C₂₄H₂₇NO₅ [M+Na]⁺ 131.0582 found 131.0580.

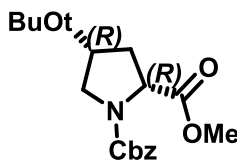
(2*R*, 4*R*)-¹N-((benzyloxy) carbonyl)-4-hydroxyproline (33)



A solution of *trans*-4-hydroxy-D-proline (2.0 g, 15.3 mmol) and NaHCO₃ (1.54g 18.4 mmol) in THF: H₂O (1:1) was cooled in an ice bath to which solution of Cbz-Cl (6.3g, 18.4 mmol) in toluene (50%) was added. The reaction mixture was stirred for 12 h at room temperature, and solvent toluene was removed under vacuum. The aqueous was washed with diethyl ether for 3-4 times to remove unreacted Cbz-Cl. The aqueous layer was acidified to pH 2 with aqueous HCl (2N) and then extracted with ethyl acetate (3 x 50 mL). The combined organic layers were washed with water followed by saturated brine solution. The organic layer was dried over anhydrous Na₂SO₄ and concentrated under reduced pressure to yield white sticky solid of compound **33**. This compound was used for the next reaction without purification (1.96 g, 98% yield); $[\alpha]_D^{25} +21.0$ (c 2.0 CHCl₃); ¹H NMR (CDCl₃, 400 MHz) δ 7.35-7.24 (m, 5H), 5.19-5.06 (m, 2H), 4.47-4.37 (m, 2H), 3.63-3.51 (m, 2H), 2.29-2.17 (m, 2H); ¹³C NMR (100 MHz, CDCl₃) δ 175.9, 155.7, 155.2, 136.2, 128.6, 128.3, 128.1, 128.0, 127.9, 127.9, 127.7, 70.6, 69.6, 67.7, 58.2, 57.9, 55.3, 55.1, 38.6, 37.7; HRMS (ESI-MS) m/z calcd for C₁₃H₁₅NO₅ [M+Na]⁺ 288.0848, found 288.0846.

(2*R*, 4*R*)-¹N-((benzyloxy) carbonyl)-4-hydroxyproline ester (34)

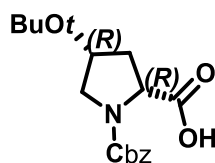
A solution of compound **33** (5 g, 18.9 mmol) in anhydrous acetone (60 mL), anhydrous K_2CO_3 (6.5 g, 47.3 mmol) and dimethylsulphate 2.2 mL (23.1 mmol) was stirred in a flask. The mixture was then refluxed under nitrogen for 4 h. The acetone was removed under vacuum and the resulting residue was dissolved in water followed by extraction with ethyl acetate (3 x 50 mL). The combined organic layer was washed with water (3 x 50 mL) followed by saturated brine solution (3 x 30 mL) then dried over Na_2SO_4 and concentrated under vacuum. The crude material was purified by silica gel chromatography (50% ethyl acetate/hexane) afford compound **34** as colourless thick oil. (19.5 g 98% yield); $[\alpha]_D^{25} +22.8$ (c 1.0 $CHCl_3$); 1H NMR ($CDCl_3$, 400 MHz) δ 7.35-7.24 (m, 5H), 5.20-5.02 (m, 2H), 4.45-4.37 (m, 2H), 3.79-3.56 (m, 5H), 2.37-2.27 (m, 1H), 2.14-2.09 (m, 1H); ^{13}C NMR (100 MHz, $CDCl_3$) δ 175.3, 175.0, 155.1, 154.9, 154.3, 136.4, 136.3, 128.6, 128.5, 128.2, 128.1, 127.9, 71.3, 70.3, 67.4, 58.2, 57.8, 56.2, 55.8, 53.0, 52.7, 38.8, 37.8; HRMS (ESI-MS) m/z calcd for $C_{14}H_{17}NO_5$ $[M+Na]^+$ 302.1004, found 302.1006.

(2*R*, 4*R*)-¹N-((benzyloxy) carbonyl)-4(*t*-butoxy)-hydroxyproline ester (35)

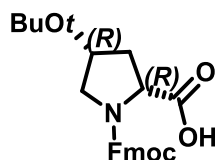
The mixture of compound **34** (5.0 g, 179 mmol), Ag_2O (8.5g 358 mmol) and *tert*-butyl bromide (6 mL, 537mmol) in cyclohexane (50 ml) was stirred for 24 h at room temperature. The resulting suspension was filtered out and the filtrate was concentrated under reduced pressure and crude product was purified by silica gel chromatography eluting with petroleum ether:ethyl acetate (80:20) to give a desired product **35** (5.11 g,

85% yield); $[\alpha]_D^{25} +39.6$ (c 1.0 CHCl₃); ¹H NMR (CDCl₃, 400 MHz) δ 7.37-7.29 (m, 5H), 5.21-5.04 (m, 2H), 4.42-4.33 (m, 1H), 4.20-4.13 (m, 1H), 3.80-3.68 (m, 3H), 3.59 (s, 2H), 3.37-3.31 (m, 1H), 2.40-2.30 (m, 1H), 2.09-2.03 (m, 1H), 1.16 (s, 9H); ¹³C NMR (100 MHz, CDCl₃) δ 172.8, 172.6, 154.9, 154.4, 136.7, 136.6, 128.5, 128.1, 127.9, 74.0, 69.4, 68.6, 67.1, 57.8, 57.5, 53.6, 53.4, 52.3, 52.1, 38.7, 37.9, 28.3; HRMS (ESI-MS) m/z calcd for C₁₈H₂₅NO₅ [M+Na]⁺ 358.1630, found 358.1629.

(2*R*, 4*R*)-¹N-((benzyloxy) carbonyl)-4(*t*-butoxy)-hydroxyproline (36)



The ester compound **35** (5.0 g, 15 mmol) was subjected to hydrolysis using 2N NaOH in MeOH for 1 h. MeOH was removed under vacuum and the aqueous layer was washed with ethyl acetate (3 x 50 mL) to remove unreacted organic compound. The aqueous layer was acidified by 2N HCl to pH 2 and extracted with ethyl acetate (3 x 60 mL) followed by concentration. The crude product obtained was purified by silica gel chromatography (65% ethyl acetate/hexane) to afford a white solid powder **36** (4.6 g, 97% yield); $[\alpha]_D^{25} +18.6$ (c 1.0 CHCl₃); ¹H NMR (CDCl₃, 400 MHz) δ 8.77 (br, 1H), 7.37-7.28 (m, 5H), 5.22-5.11 (m, 2H), 4.45-4.38 (m, 1H), 4.28-4.22 (m, 1H), 3.69-3.66 (m, 1H), 3.51-3.37 (m, 1H), 2.43-2.12 (m, 2H), 1.21 (s, 9H); ¹³C NMR (100 MHz, CDCl₃) δ 177.0, 175.6, 155.5, 154.6, 136.4, 128.5, 128.2, 127.9, 75.4, 74.7, 69.6, 69.1, 67.6, 67.4, 58.2, 54.3, 53.8, 38.2, 37.4, 28.1, 20.6; HRMS (ESI-MS) m/z calcd for C₁₇H₂₃NO₅ [M+Na]⁺ 344.1474, found 344.1473.

(2*R*, 4*R*)-¹N-((Fmoc) carbonyl)-4(*t*-butoxy)-hydroxyproline (37)

Compound **36** (1.5 g, 4.7 mmol) was dissolved in dry methanol (15 mL) to which of 10% Pd/C (0.2 g) was added. The mixture was subjected to hydrogenation under H₂ gas. Water (200 mL) was added to the reaction mixture which was filtered through Whatman filter paper and the filtrate was concentrated under reduced pressure. The product obtained as a white solid powder was dissolved in water: dioxane, 1:1 (50 mL). The pH was maintained at 10 by addition of 10% Na₂CO₃. The reaction mixture was stirred at 0 °C for 15 minutes. Fmoc-Cl (1.5 g, 5.6 mmol) was added in portion wise during 45 minutes maintained the temperature at 0 °C for first 4 h and then allowed to come at room temperature and was stirred for 18 h. The dioxane was removed under vacuum and the aqueous layer was washed with ethyl acetate (3 x 80 mL). The aqueous layer was acidified with 2N HCl to pH 2 followed by extraction with ethyl acetate (3 x 70 mL). Concentration of solvent gave crude product which was purified by silica gel chromatography (70% ethyl acetate/hexane) to afford compound **37** as white solid (1.49 g, 78% yield); $[\alpha]_D^{25} +73.6$ (c 1.0 CHCl₃); ¹H NMR (CDCl₃, 400 MHz) δ 7.77-7.24 (m, 8H), 4.48-4.22 (m, 5H), 3.62-3.37 (m, 2H), 2.43-2.33 (m, 1H), 2.21-2.13 (m, 1H), 1.21 (s, 9H); ¹³C NMR (100 MHz, CDCl₃) δ 173.7, 143.8, 143.7, 141.4, 127.8, 127.2, 125.4, 125.1, 120.0, 69.6, 69.2, 68.2, 67.9, 58.6, 54.8, 53.9, 47.2, 47.1, 38.2, 37.0, 28.2, 28.1; HRMS (ESI-MS) m/z calcd for C₂₄H₂₇NO₅ [M+Na]⁺ 432.1787, found 432.1786.

3.11. Peptide synthesis

All peptides were synthesized manually in a sintered vessel equipped with a stopcock. The readily available Rink amide resin with loading value 0.5-0.6 mmol/g was used and standard Fmoc chemistry was employed. The resin bound Fmoc group was first deprotected with 20% piperidine in DMF and the coupling reactions were carried out using *in situ* active ester method, using HBTU as a coupling reagent and HOBt as a recemization

suppressor and DIPEA as a catalyst. All the materials used were of peptide synthesis grade (Sigma-Aldrich) and was used without further purification. Analytical grade DMF was purchased from Merck (India) and was distilled over P₂O₅ under vacuum at 45°C, stored over 4Å molecular sieves for 2 days before using for peptide synthesis.

3.11a. General procedure for peptide couplings on Rink Amide Resin: Fmoc-AA-OH (3 eq), HBTU (3 eq) and HOBT (3 eq) dissolved in DMF/NMP followed by *i*Pr₂NEt (7-8 eq) were added to the amino-functionalized resin in DMF (≈100 mM concentration). The mixture was stand for 2 h and last 5 min bubbled with N₂ and washed with DMF (3x), methanol (3x) and CH₂Cl₂ (3x) was omitted. The loading value for peptide synthesis is taken as 0.5~0.6.

3.11b. General procedure for Fmoc-deprotection: 20 % piperidine in DMF was added to the resin and the reaction mixture was kept for 15 min, drained and the piperidine treatment repeated for 3 times. Finally the resin was washed with DMF (3x), Methanol (3x) and CH₂Cl₂ (3x).

General schematic representation of solid phase peptide synthesis is shown in supporting information. Couplings and deprotection reaction were monitored by the qualitative Chloranil test.

3.11c. General procedure for acetylation: NEt₃ (20 eq) and 20 eq Ac₂O (20 eq) were added to the resin in DMF (≈ 100 mM). The mixture was stand for 1 h and washed with DMF (3x), Methanol (3x) and CH₂Cl₂ (3x).

3.11d. General procedure for cleavage of peptides from the solid support: The solid supported peptides were cleaved off the resin by kept in a mixture of acid in CH₂Cl₂ Rink Amide Resin (20 % TFA in DCM) for 1 h and a second time for 20 min. Pulling of filtrates and removal of all volatiles under reduced pressure followed by stirring the peptide in 90 % TFA in 10 % DCM for Boc deprotection. Precipitation with Et₂O afforded the peptides.

3.12 References:

1. Berg, R. A.; Prockop, D. J., The thermal transition of a non-hydroxylated form of collagen. Evidence for a role for hydroxyproline in stabilizing the triple-helix of collagen. *Biochem. Biophys. Res. Commun.* **1973**, *52*, 115-20.
2. Holmgren, S. K.; Taylor, K. M.; Bretscher, L. E.; Raines, R. T., Code for collagen's stability deciphered. *Nature* **1998**, *392* (6677), 666-667.
3. Kotch, F. W.; Guzei, I. A.; Raines, R. T., Stabilization of the collagen triple helix by O-methylation of hydroxyproline residues. *J. Am. Chem. Soc.* **2008**, *130*, 2952-3.
4. Pepe, A.; Crudele, M. A.; Bochicchio, B., Effect of proline analogues on the conformation of elastin peptides. *New J. Chem.* **2013**, *37*, 1326-1335.
5. Wagenseil, J. E.; Mecham, R. P., New insights into elastic fiber assembly. *Birth defects research. Part C, Embryo today : reviews* **2007**, *81*, 229-40.
6. (a) Steinberg, I. Z.; Harrington, W. F.; Berger, A.; Sela, M.; Katchalski, E., The Configurational Changes of Poly-L-proline in Solution. *J. Am. Chem. Soc.* **1960**, *82*, 5263-5279; (b) Assem, N.; Yudin, A. K., Convergent synthesis of aminomethylene peptidomimetics. *Nat. Protocol.* **2012**, *7*, 1327-1334.
7. (a) Knof, S.; Engel, J., Conformational Stability, Partial Specific Volumes and Spectroscopic Properties of Poly-L-Proline, Poly-L-Hydroxyproline and Some of Its O-Acyl-Derivatives in Various Solvent Systems. *Isr.J. of Chem.* **1974**, *12*, 165-177; (b) Krimm, S.; Tiffany, M. L., The Circular Dichroism Spectrum and Structure of Unordered Polypeptides and Proteins. *Isr. J. Chem.* **1974**, *12*, 189-200; (c) Kakinoki, S.; Hirano, Y.; Oka, M., On the Stability of Polyproline-I and II Structures of Proline Oligopeptides. *Polym. Bull.* **2005**, *53*, 109-115.
8. (a) Cowan, P. M.; McGavin, S., Structure of Poly-L-Proline. *Nature* **1955**, *176*, 501-503; (b) Traub, W.; Shmueli, U., Structure of Poly-L-Proline I. *Nature* **1963**, *198*, 1165-1166.
9. (a) Rath, A.; Davidson, A. R.; Deber, C. M., The structure of "unstructured" regions in peptides and proteins: Role of the polyproline II helix in protein folding and recognition*. *Pept. Sci.* **2005**, *80*, 179-185; (b) Holt, M. R.; Koffer, A., Cell motility: proline-rich proteins promote protrusions. *Trends Cell Biol.* **2001**, *11*, 38-46; (c)

- KAY, B. K.; WILLIAMSON, M. P.; SUDOL, M., The importance of being proline: the interaction of proline-rich motifs in signaling proteins with their cognate domains. *FASEB J.* **2000**, *14*, 231-241.
10. Shoulders, M. D.; Raines, R. T., Collagen structure and stability. *Annu. rev. biochem.* **2009**, *78*, 929-58.
11. Ramshaw, J. A.; Shah, N. K.; Brodsky, B., Gly-X-Y tripeptide frequencies in collagen: a context for host-guest triple-helical peptides. *J. struct. biol.* **1998**, *122*, 86-91.
12. Ramachandran, G. N.; Bansal, M.; Bhatnagar, R. S., A hypothesis on the role of hydroxyproline in stabilizing collagen structure. *Biochim. biophys. Acta* **1973**, *322*, 166-71.
13. Bella, J.; Eaton, M.; Brodsky, B.; Berman, H. M., Crystal and molecular structure of a collagen-like peptide at 1.9 Å resolution. *Science* **1994**, *266*, 75-81.
14. Holmgren, S. K.; Taylor, K. M.; Bretscher, L. E.; Raines, R. T., Code for collagen's stability deciphered. *Nature* **1998**, *392*, 666-7.
15. Eberhardt, E. S.; Panisik, N., Jr.; Raines, R. T., Inductive Effects on the Energetics of Prolyl Peptide Bond Isomerization: Implications for Collagen Folding and Stability. *J. Am. Chem. Soc.* **1996**, *118*, 12261-12266.
16. DeRider, M. L.; Wilkens, S. J.; Waddell, M. J.; Bretscher, L. E.; Weinhold, F.; Raines, R. T.; Markley, J. L., Collagen stability: insights from NMR spectroscopic and hybrid density functional computational investigations of the effect of electronegative substituents on prolyl ring conformations. *J. Am. Chem. Soc.* **2002**, *124*, 2497-505.
17. Bretscher, L. E.; Jenkins, C. L.; Taylor, K. M.; DeRider, M. L.; Raines, R. T., Conformational Stability of Collagen Relies on a Stereoelectronic Effect. *J. Am. Chem. Soc.* **2001**, *123*, 777-778.
18. Kuemin, M.; Sonntag, L.-S.; Wennemers, H., Azidoproline containing helices: Stabilization of the polyproline II structure by a functionalizable group. *J. Am. Chem. Soc.* **2007**, *129*, 466-467.
19. Hodges, J. A.; Raines, R. T., Stereoelectronic and Steric Effects in the Collagen Triple Helix: Toward a Code for Strand Association. *J. Am. Chem. Soc.* **2005**, *127*, 15923-15932.

20. Siebler, C.; Erdmann, R. S.; Wennemers, H., Switchable Proline Derivatives: Tuning the Conformational Stability of the Collagen Triple Helix by pH Changes. *Angew. Chem. Int. Ed.* **2014**, *53*, 10340-10344.
21. Sonar, M. V.; Ganesh, K. N., Water-Induced Switching of β -Structure to Polyproline II Conformation in the 4S-Aminoproline Polypeptide via H-Bond Rearrangement. *Org. Lett.* **2010**, *12*, 5390-5393.
22. Flores-Ortega, A.; Casanovas, J.; Nussinov, R.; Alemán, C., Conformational Preferences of β - and γ -Aminated Proline Analogues. *J. Phys. Chem. B* **2008**, *112*, 14045-14055.
23. Flores-Ortega, A.; Casanovas, J.; Assfeld, X.; Alemán, C., Protonation of the Side Group in β - and γ -Aminated Proline Analogues: Effects on the Conformational Preferences. *J. Org. Chem.* **2009**, *74*, 3101-3108.
24. Lowe, G.; Vilaivan, T., Amino acids bearing nucleobases for the synthesis of novel peptide nucleic acids. *J. Chem. Soc. Perkin Trans. 1* **1997**, *4*, 539-546.
25. Vojtkovsky, T., Detection of secondary amines on solid phase. *Pept. res.* **1995**, *8*, 236-7.
26. Whittington, S. J.; Chellgren, B. W.; Hermann, V. M.; Creamer, T. P., Urea Promotes Polyproline II Helix Formation: Implications for Protein Denatured States†. *Biochemistry* **2005**, *44*, 6269-6275.
27. Woody, R. W., Circular dichroism and conformation of unordered polypeptides. *Adv. Biophys. Chem.* **1992**, *2*, 37-79.
28. Feng, Y.; Melacini, G.; Taulane, J. P.; Goodman, M., Acetyl-Terminated and Template-Assembled Collagen-Based Polypeptides Composed of Gly-Pro-Hyp Sequences. 2. Synthesis and Conformational Analysis by Circular Dichroism, Ultraviolet Absorbance, and Optical Rotation. *J. Am. Chem. Soc.* **1996**, *118*, 10351-10358.
- 29.(a) Lyu, P. C.; Gans, P. J.; Kallenbach, N. R., Energetic contribution of solvent-exposed ion pairs to alpha-helix structure. *J. Mol. Biol.* **1992**, *223*, 343-50; (b) Marqusee, S.; Baldwin, R. L., Helix stabilization by Glu-...Lys+ salt bridges in short peptides of de novo design. *Proc. Natl. Acad. Sci. U S A* **1987**, *84*, 8898-902; (c) Merutka, G.;

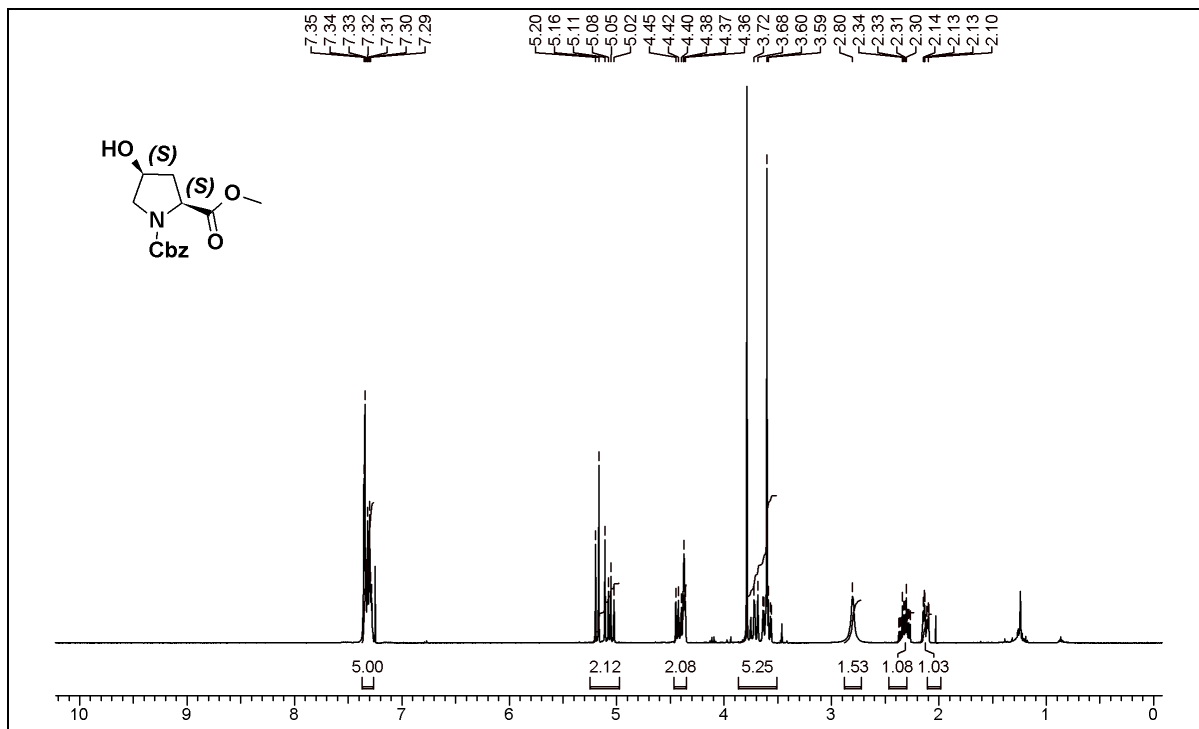
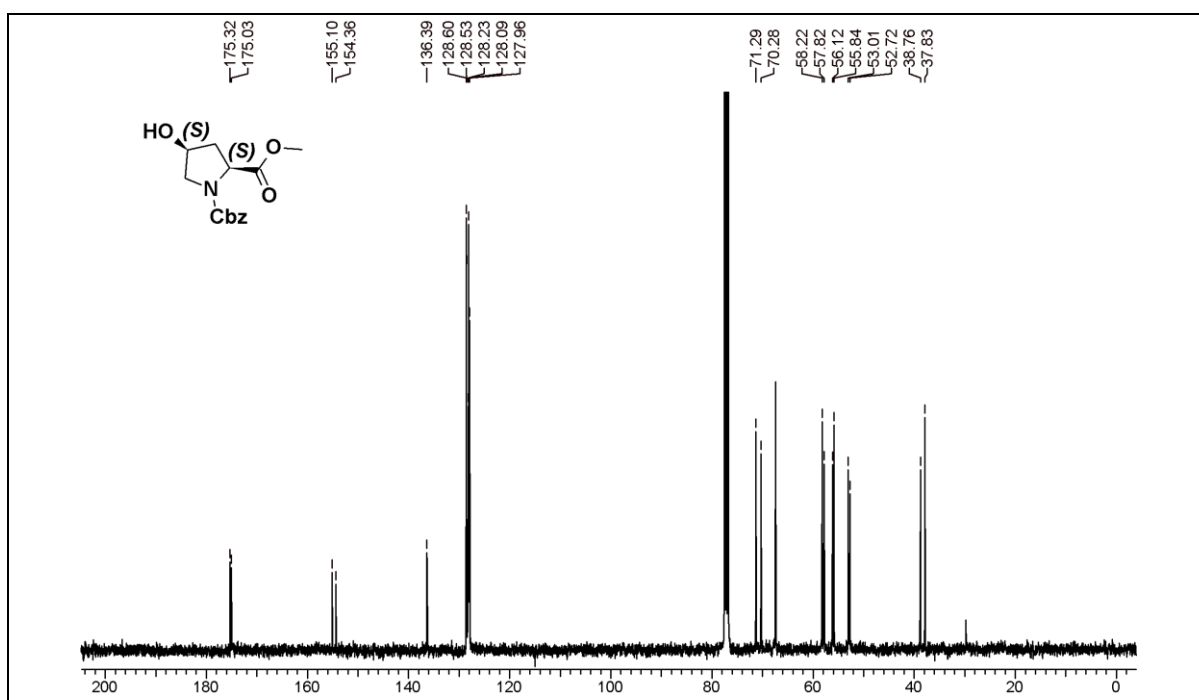
- Stellwagen, E., Effect of amino acid ion pairs on peptide helicity. *Biochemistry* **1991**, *30*, 1591-4.
30. Blasie, C. A.; Berg, J. M., Electrostatic interactions across a beta-sheet. *Biochemistry* **1997**, *36*, 6218-22.
31. Makabe, K.; Tereshko, V.; Gawlak, G.; Yan, S.; Koide, S., Atomic-resolution crystal structure of *Borrelia burgdorferi* outer surface protein A via surface engineering. *Protein Sci. : A Publication of the Protein Society* **2006**, *15*, 1907-1914.
32. Whittington, S. J.; Creamer, T. P., Salt Bridges Do Not Stabilize Polyproline II Helices†. *Biochemistry* **2003**, *42*, 14690-14695.
33. Arunkumar, A. I.; Kumar, T. K.; Yu, C., Non-specific helix-induction in charged homopolypeptides by alcohols. *Biochim. biophys. Acta* **1997**, *1338*, 69-76.
34. Collins, K. D.; Washabaugh, M. W., The Hofmeister effect and the behaviour of water at interfaces. *Q. rev. biophys.* **1985**, *18*, 323-422.
- 35.(a) Kumaran, S.; Roy, R. P., Helix-enhancing propensity of fluoro and alkyl alcohols: influence of pH, temperature and cosolvent concentration on the helical conformation of peptides. *J. Pept. Res.* **1999**, *53*, 284-293; (b) Buck, M., Trifluoroethanol and colleagues: cosolvents come of age. Recent studies with peptides and proteins. *Q. rev. biophys.* **1998**, *31*, 297-355; (c) Povey, J. F.; Smales, C. M.; Hassard, S. J.; Howard, M. J., Comparison of the effects of 2,2,2-trifluoroethanol on peptide and protein structure and function. *J. struct. biol.* **2007**, *157*, 329-38; (d) Hong, D.-P.; Hoshino, M.; Kuboi, R.; Goto, Y., Clustering of Fluorine-Substituted Alcohols as a Factor Responsible for Their Marked Effects on Proteins and Peptides. *J. Am. Chem. Soc.* **1999**, *121*, 8427-8433.
36. (a) Gerlsma, S. Y.; Stuur, E. R., THE EFFECT OF POLYHYDRIC AND MONOHYDRIC ALCOHOLS ON THE HEAT-INDUCED REVERSIBLE DENATURATION OF LYSOZYME AND RIBONUCLEASE. *Intl. J. Pept. Protein Res.* **1972**, *4*, 377-383; (b) Thomas, P. D.; Dill, K. A., Local and nonlocal interactions in globular proteins and mechanisms of alcohol denaturation. *Protein Sci.* **1993**, *2*, 2050-2065; (c) Liu, Y.; Bolen, D. W., The Peptide Backbone Plays a Dominant Role in Protein Stabilization by Naturally Occurring Osmolytes. *Biochemistry* **1995**, *34*, 12884-12891.

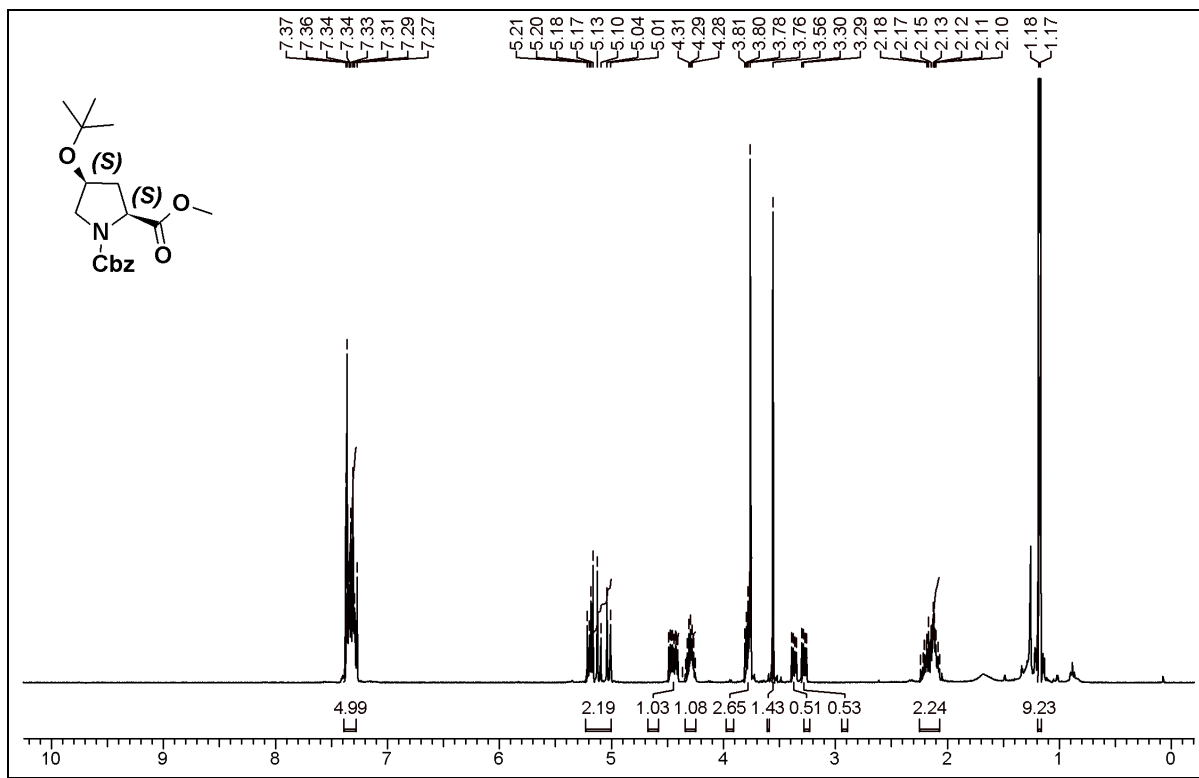
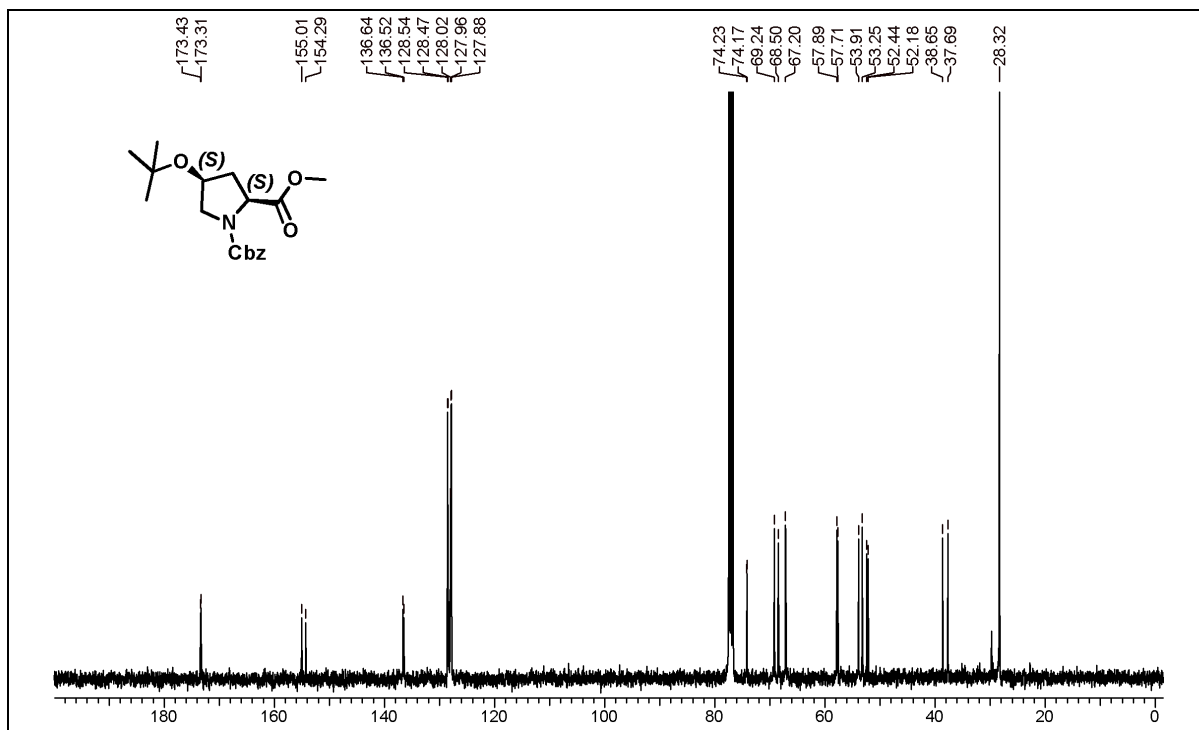
37. Korevaar, P. A.; Newcomb, C. J.; Meijer, E. W.; Stupp, S. I., Pathway Selection in Peptide Amphiphile Assembly. *J. Am. Chem. Soc.* **2014**, *136*, 8540-8543.
38. Luo, Z.; Akerman, B.; Zhang, S.; Norden, B., Structures of self-assembled amphiphilic peptide-heterodimers: effects of concentration, pH, temperature and ionic strength. *Soft Matt.* **2010**, *6*, 2260-2270.
39. (a) Podstawka, E.; Ozaki, Y.; Proniewicz, L. M., Part I: Surface-enhanced Raman spectroscopy investigation of amino acids and their homodipeptides adsorbed on colloidal silver. *Appl. Spectrosc.* **2004**, *58*, 570-580; (b) Podstawka, E.; Ozaki, Y.; Proniewicz, L. M., Part II: Surface-enhanced Raman spectroscopy investigation of methionine containing heterodipeptides adsorbed on colloidal silver. *Appl. Spectrosc.* **2004**, *58*, 581-590; (c) Podstawka, E.; Ozaki, Y.; Proniewicz, L. M., Adsorption of S-S containing proteins on a colloidal silver surface studied by surface-enhanced Raman spectroscopy. *Appl. Spectrosc.* **2004**, *58*, 1147-1156; (d) Podstawka, E.; Ozaki, Y.; Proniewicz, L. M., Part III: Surface-enhanced Raman scattering of amino acids and their homodipeptide monolayers deposited onto colloidal gold surface. *Appl. Spectrosc.* **2005**, *59*, 1516-1526.
40. (a) Xu, F.; Khan, I. J.; McGuinness, K.; Parmar, A. S.; Silva, T.; Murthy, N. S.; Nanda, V., Self-Assembly of Left- and Right-Handed Molecular Screws. *J. Am. Chem. Soc.* **2013**, *135* (50), 18762-18765; (b) Zotti, M. D.; Formaggio, F.; Crisma, M.; Peggion, C.; Moretto, A.; Toniolo, C., Handedness preference and switching of peptide helices. Part I: Helices based on protein amino acids. *J. Pept. Sci.* **2014**, *20*, 307-322.
41. (a) Hodges, J. A.; Raines, R. T., Stereoelectronic Effects on Collagen Stability: The Dichotomy of 4-Fluoroproline Diastereomers. *J. Am. Chem. Soc.* **2003**, *125*, 9262-9263; (b) DeRider, M. L.; Wilkens, S. J.; Waddell, M. J.; Bretscher, L. E.; Weinhold, F.; Raines, R. T.; Markley, J. L., Collagen Stability: Insights from NMR Spectroscopic and Hybrid Density Functional Computational Investigations of the Effect of Electronegative Substituents on Prolyl Ring Conformations. *J. Am. Chem. Soc.* **2002**, *124*, 2497-2505; (c) Eberhardt, E. S.; Panasik, N.; Raines, R. T., Inductive Effects on the Energetics of Prolyl Peptide Bond Isomerization: Implications for Collagen Folding and Stability. *J. Am. Chem. Soc.* **1996**, *118*, 12261-12266.

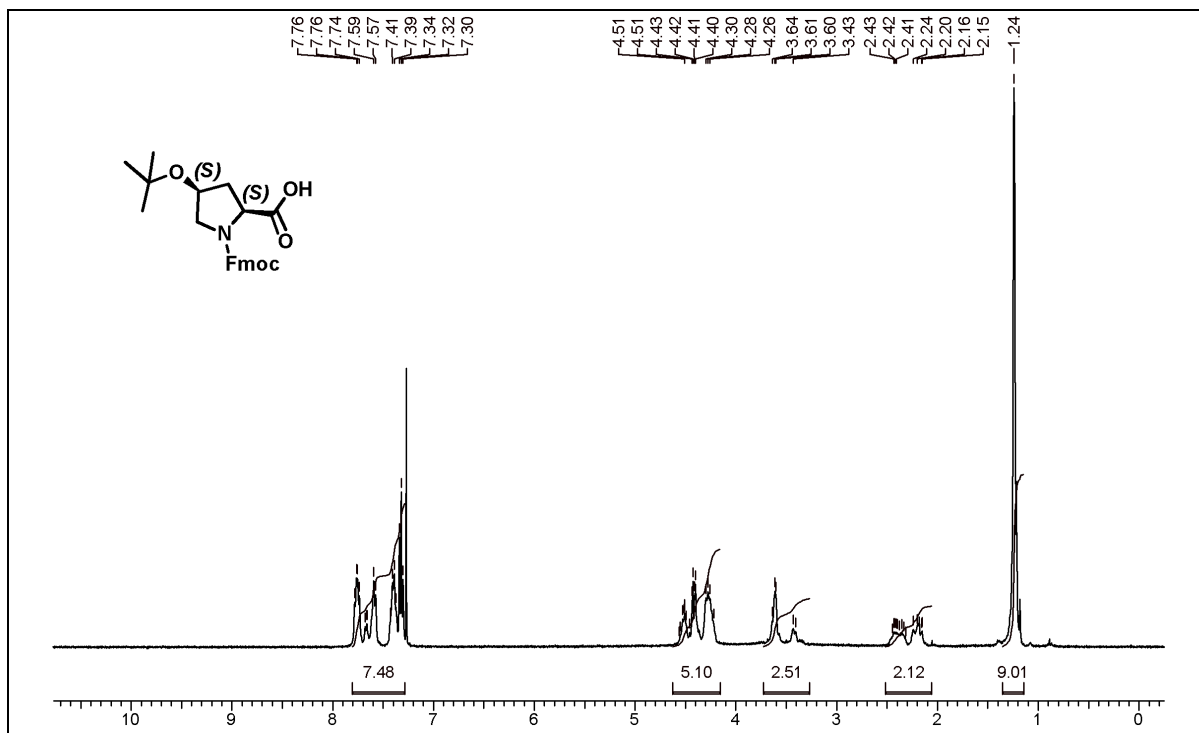
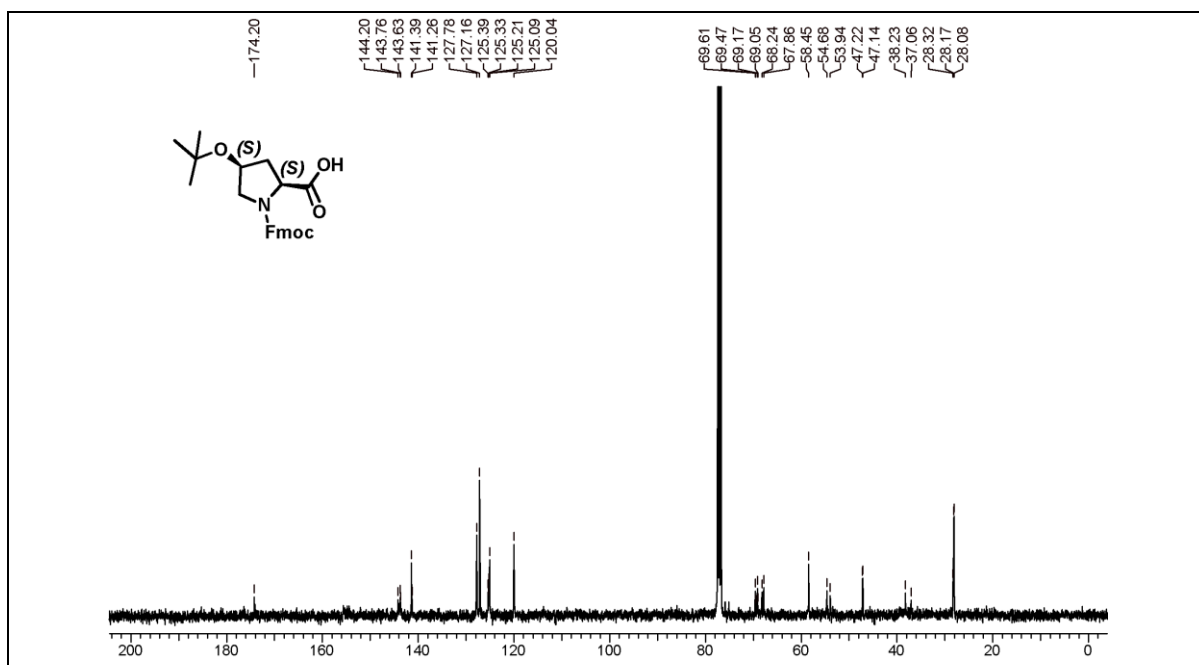
42. (a) Dai, N.; Wang, X. J.; Etzkorn, F. A., The Effect of a Trans-Locked Gly-Pro Alkene Isostere on Collagen Triple Helix Stability. *J. Am. Chem. Soc.* **2008**, *130*, 5396-5397; (b) Horng, J.-C.; Raines, R. T., Stereoelectronic effects on polyproline conformation. *Protein Sci. : A Publication of the Protein Society* **2006**, *15*, 74-83; (c) Bartlett, G. J.; Choudhary, A.; Raines, R. T.; Woolfson, D. N., $n \rightarrow \pi^*$ interactions in proteins. *Nat. chem. biol.* **2010**, *6* (8), 615-620.
43. (a) Sonntag, L. S.; Schweizer, S.; Ochsenfeld, C.; Wennemers, H., The "azido gauche effect"-implications for the conformation of azidoprolines. *J. Am. Chem. Soc.* **2006**, *128*, 14697-703; (b) Shoulders, M. D.; Guzei, I. A.; Raines, R. T., 4-chloroprolines: synthesis, conformational analysis, and effect on the collagen triple helix. *Biopolymers* **2008**, *89*, 443-54; (c) Jenkins, C. L.; McCloskey, A. I.; Guzei, I. A.; Eberhardt, E. S.; Raines, R. T., O-acylation of hydroxyproline residues: effect on peptide-bond isomerization and collagen stability. *Biopolymers* **2005**, *80*, 1-8; (d) Koskinen, A. M.; Helaja, J.; Kumpulainen, E. T.; Koivisto, J.; Mansikkamaki, H.; Rissanen, K., Locked conformations for proline pyrrolidine ring: synthesis and conformational analysis of cis- and trans-4-tert-butylprolines. *J. Org. Chem.* **2005**, *70*, 6447-53.
44. Robinson, D. R.; Jencks, W. P., The Effect of Compounds of the Urea-Guanidinium Class on the Activity Coefficient of Acetyltetraglycine Ethyl Ester and Related Compounds¹. *J. Am. Chem. Soc.* **1965**, *87*, 2462-2470.
45. Mattice, W. L.; Mandelkern, L., Conformational properties of poly-L-proline in concentrated salt solutions. *Biochemistry* **1970**, *9*, 1049-58.
46. Rucker, A. L.; Creamer, T. P., Polyproline II helical structure in protein unfolded states: Lysine peptides revisited. *Protein Sci. : A Publication of the Protein Society* **2002**, *11*, 980-985.
47. (a) Kuemin, M.; Nagel, Y. A.; Schweizer, S.; Monnard, F. W.; Ochsenfeld, C.; Wennemers, H., Tuning the cis/trans Conformer Ratio of Xaa-Pro Amide Bonds by Intramolecular Hydrogen Bonds: The Effect on PPII Helix Stability. *Angew. Chem. Int. Ed.* **2010**, *49*, 6324-6327; (b) Shoulders, M. D.; Kotch, F. W.; Choudhary, A.; Guzei, I. A.; Raines, R. T., The Aberrance of the 4S Diastereomer of 4-Hydroxyproline. *J. Am. Chem. Soc.* **2010**, *13*, 10857-10865.

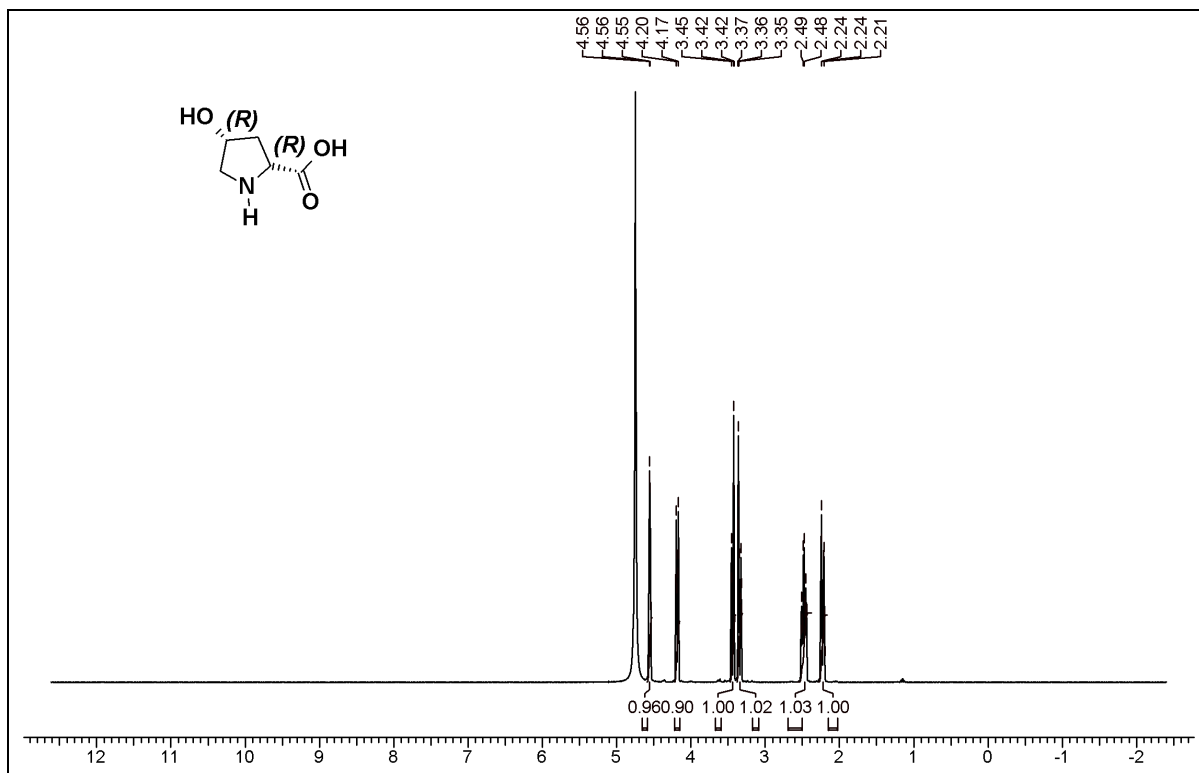
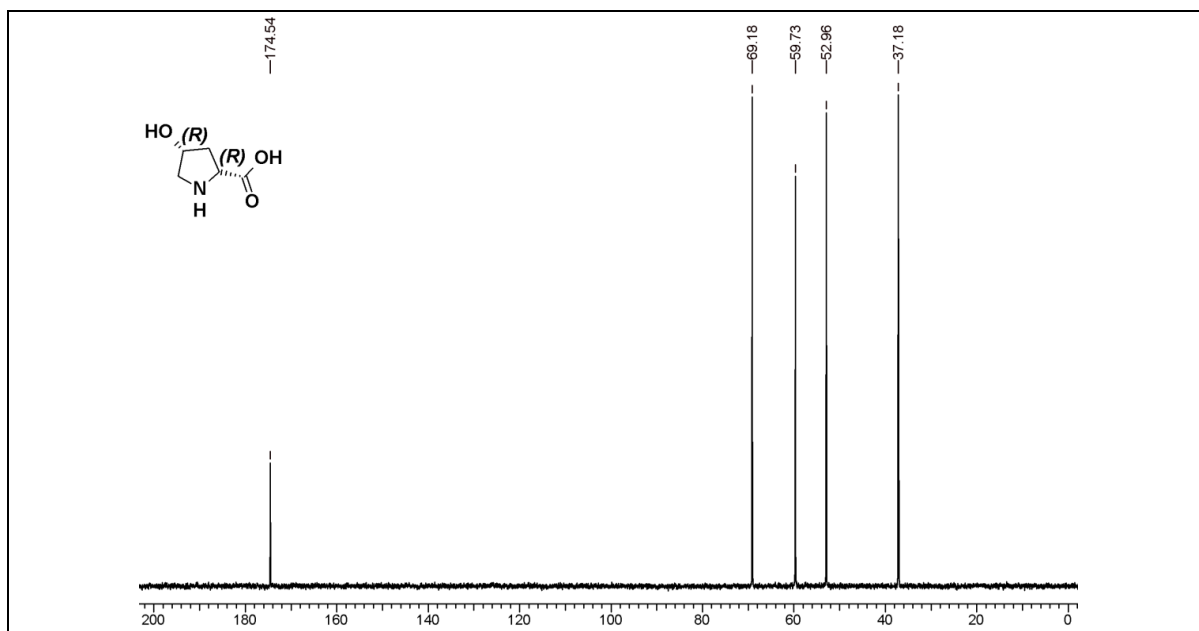
3.13 Appendix 3: Characterization data of synthesized compounds and peptides

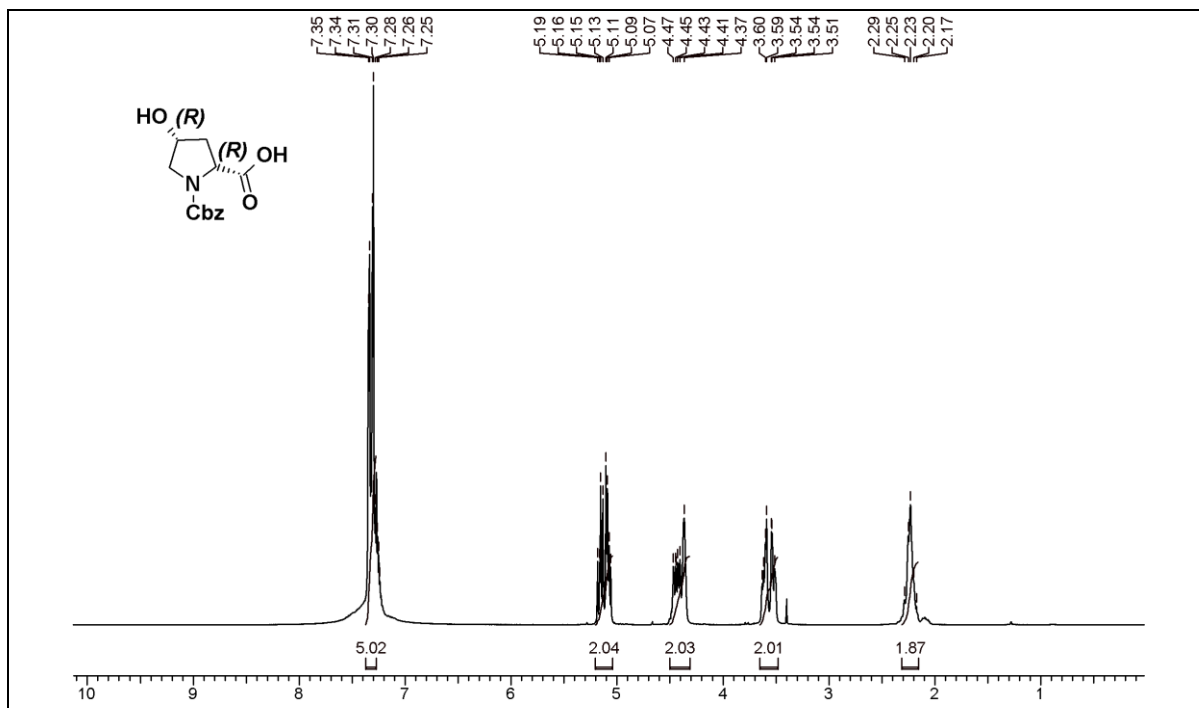
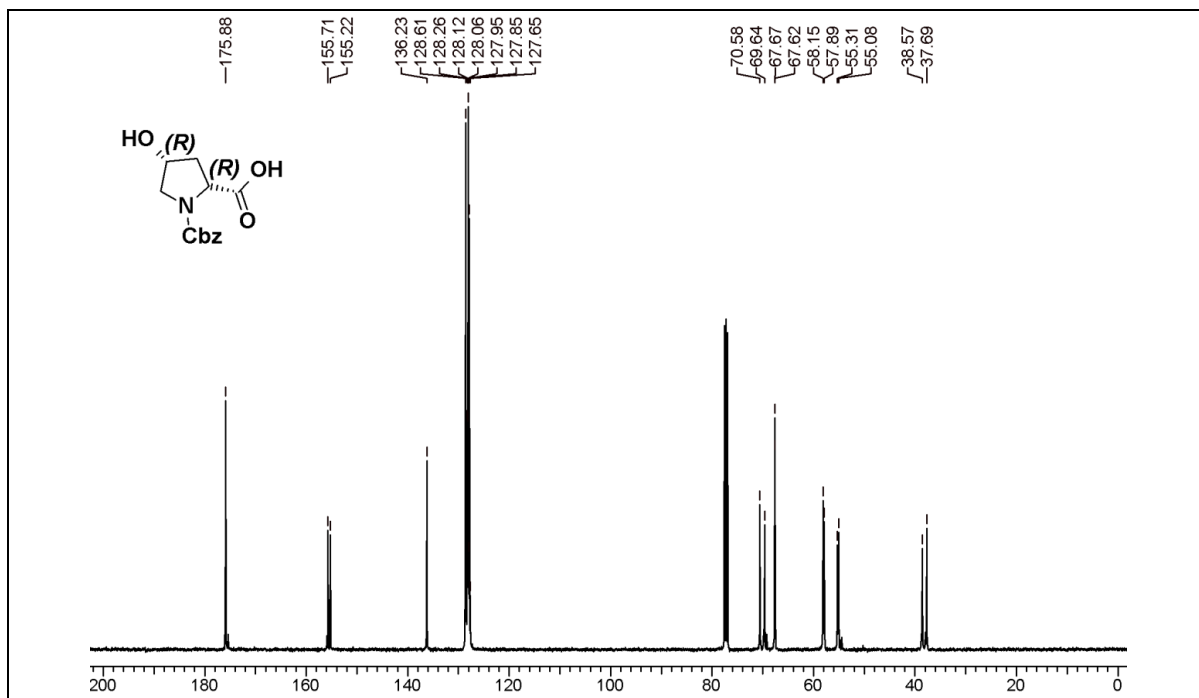
Entry	Page No.
^1H , and ^{13}C NMR spectra of compounds (29-38)	191-199
HPLC of Peptides (5-9)	200-202
MALDI-TOF of peptides (5-9)	202-204

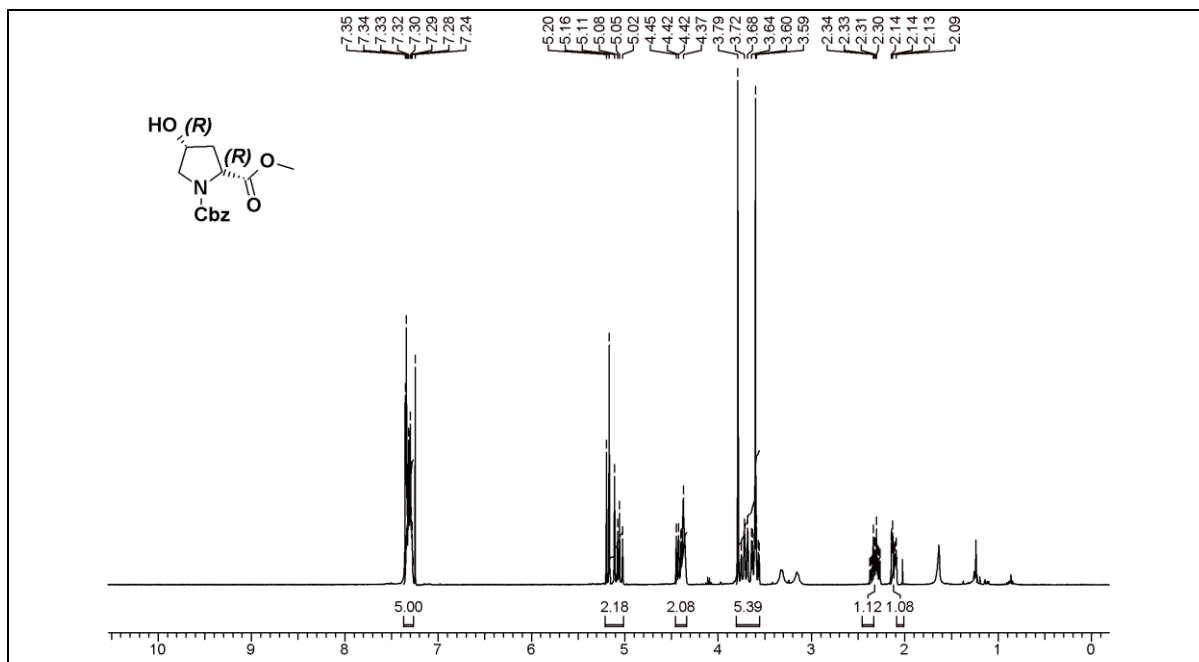
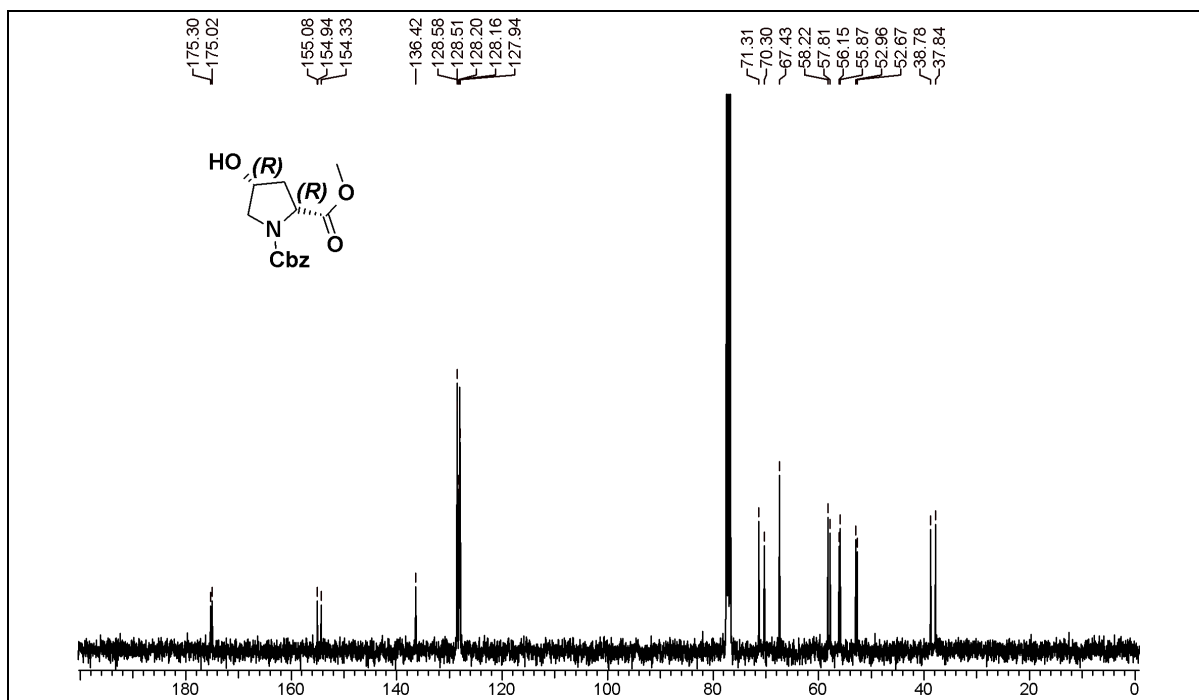
^1H , ^{13}C and NMR spectra of compounds (29-38) ^1H NMR of compound 29 ^{13}C NMR of compound 29

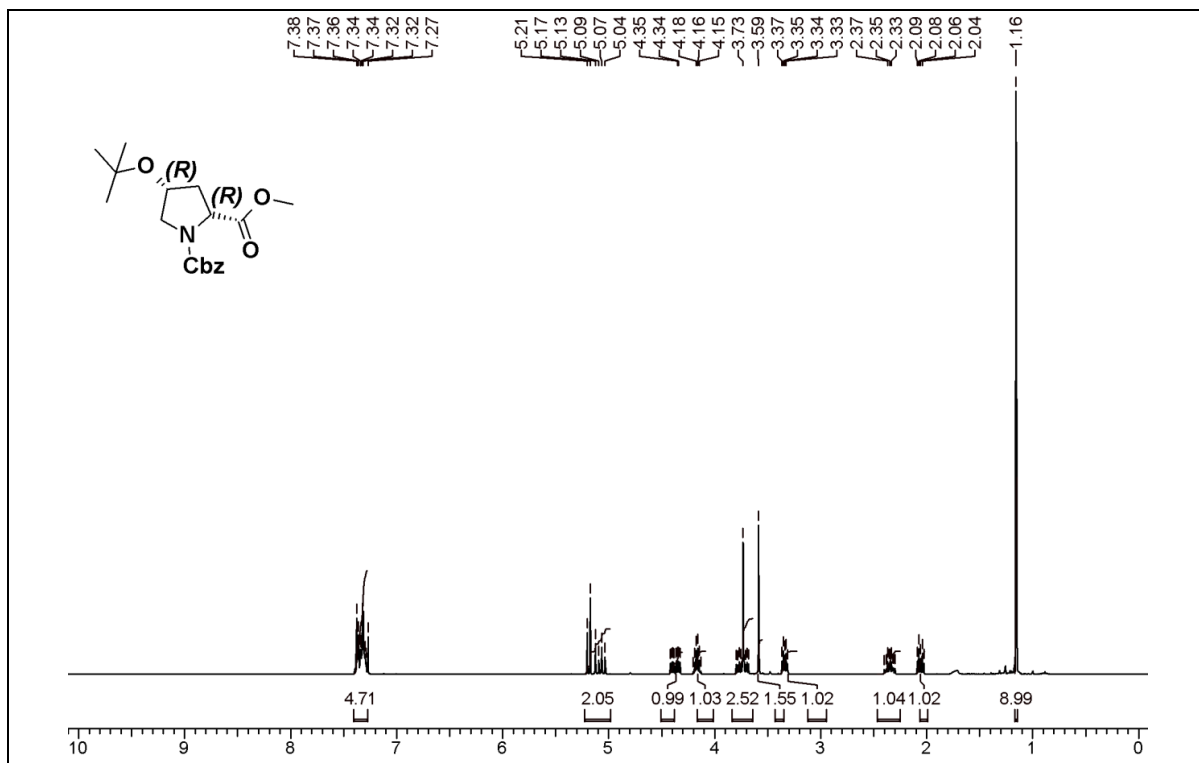
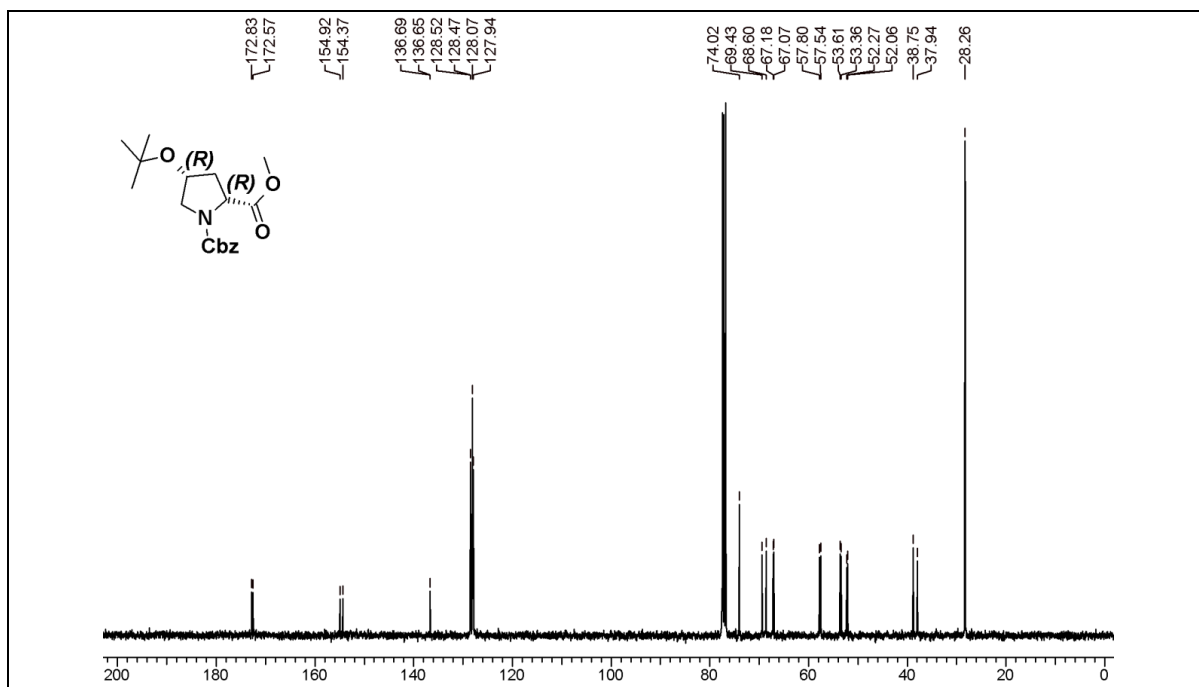
^1H NMR of compound 30 ^{13}C NMR of compound 30

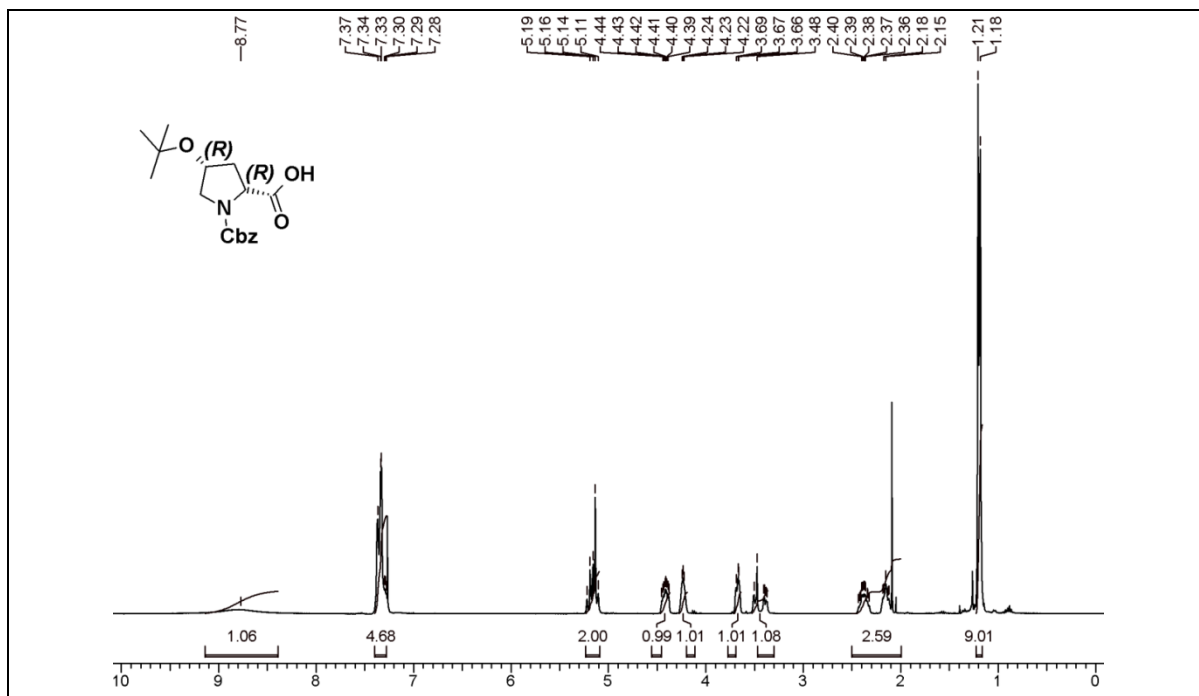
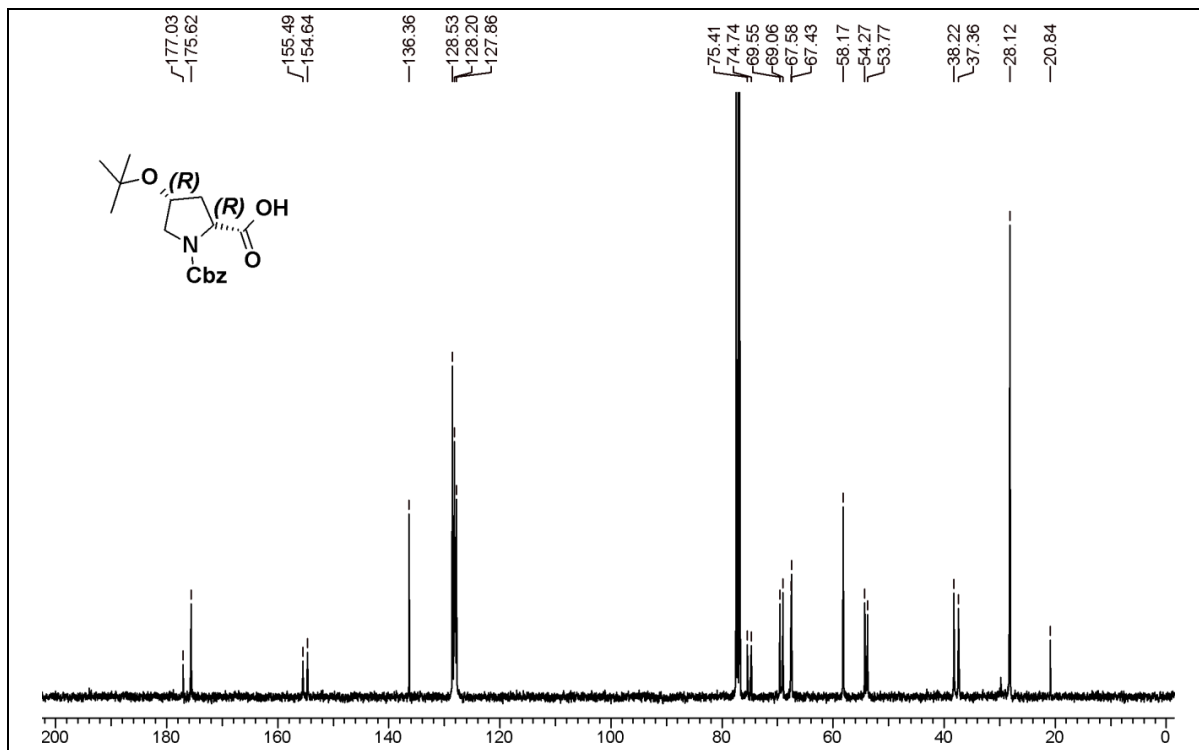
^1H NMR of compound 32 ^{13}C NMR of compound 32

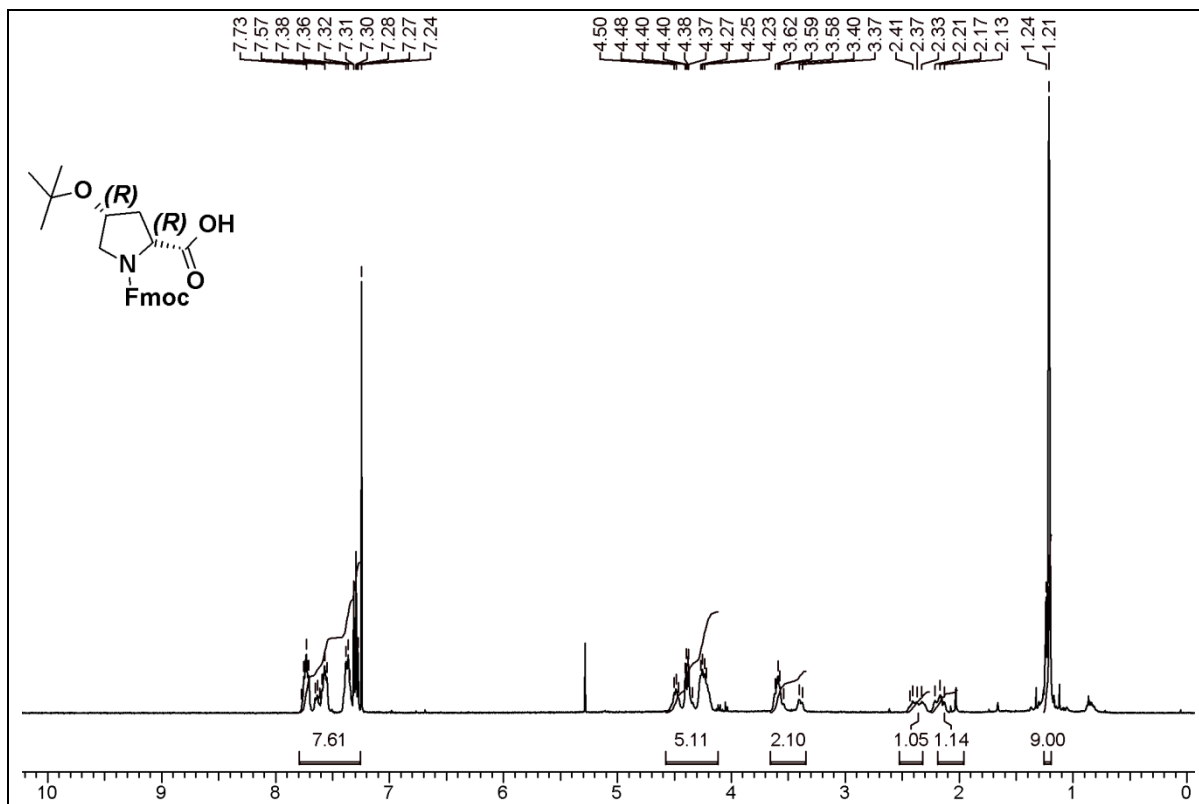
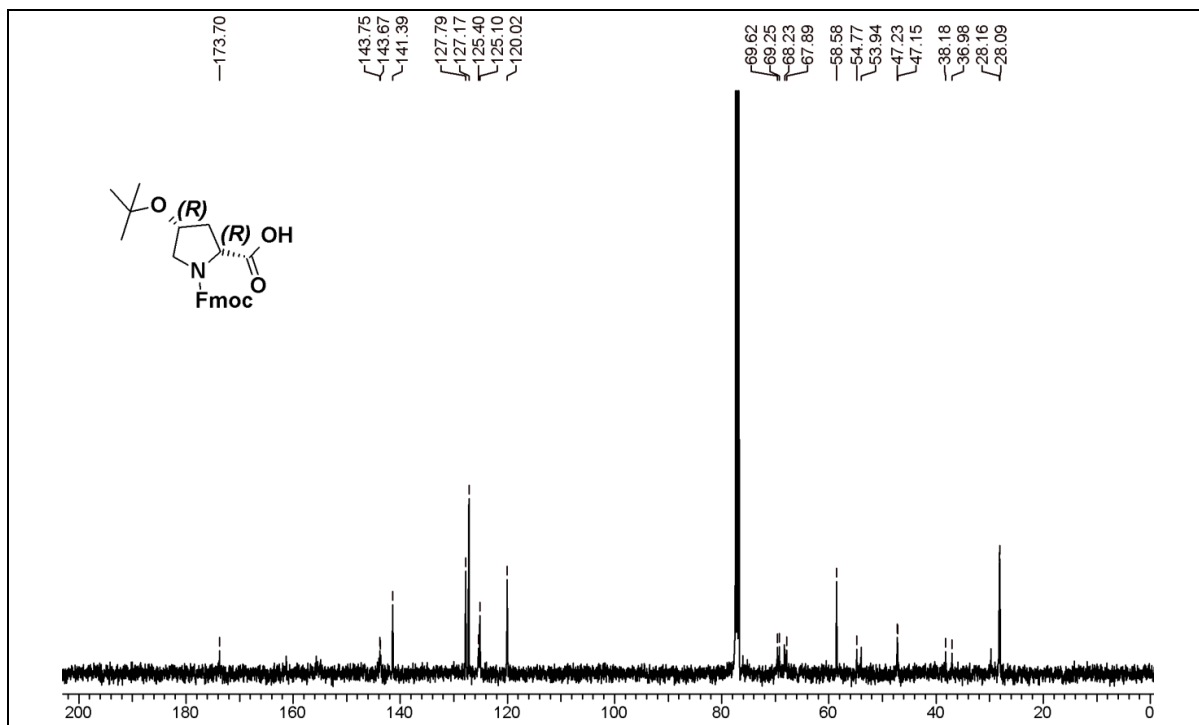
^1H NMR of compound 33 ^{13}C NMR of compound 32

^1H NMR of compound 34 ^{13}C NMR spectrum of compound 34

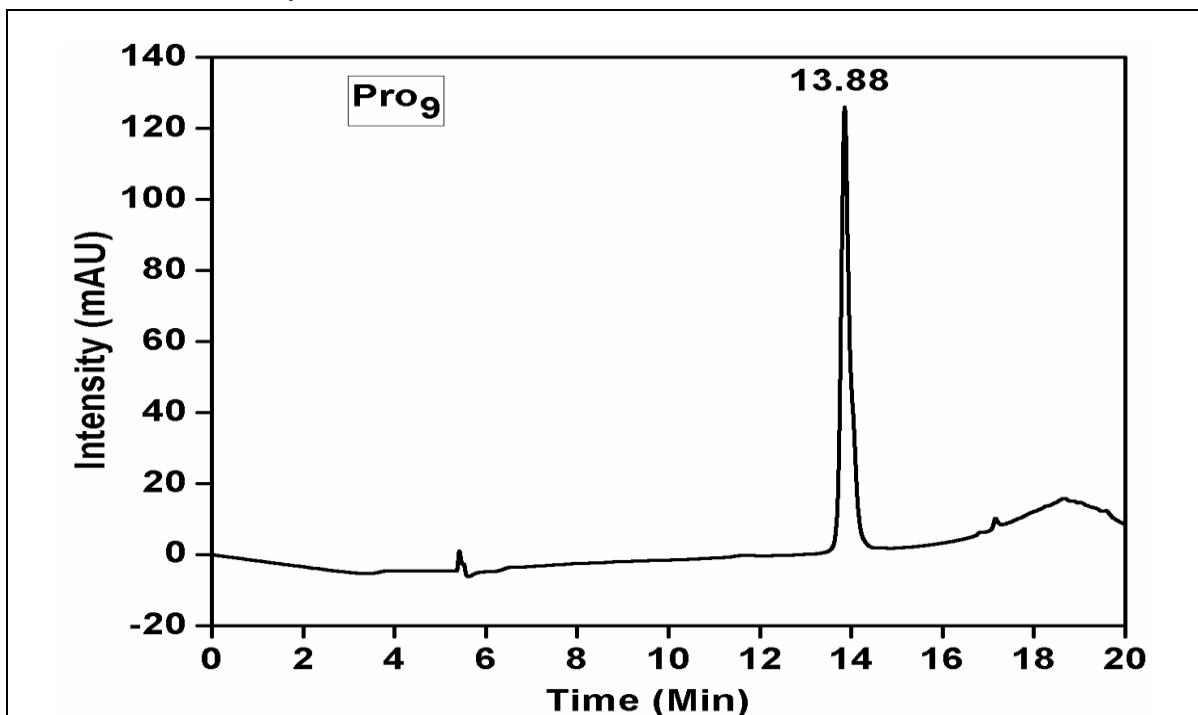
^1H NMR of compound 35 ^{13}C NMR of compound 35

^1H NMR of compound 36 ^{13}C NMR spectrum of compound 36

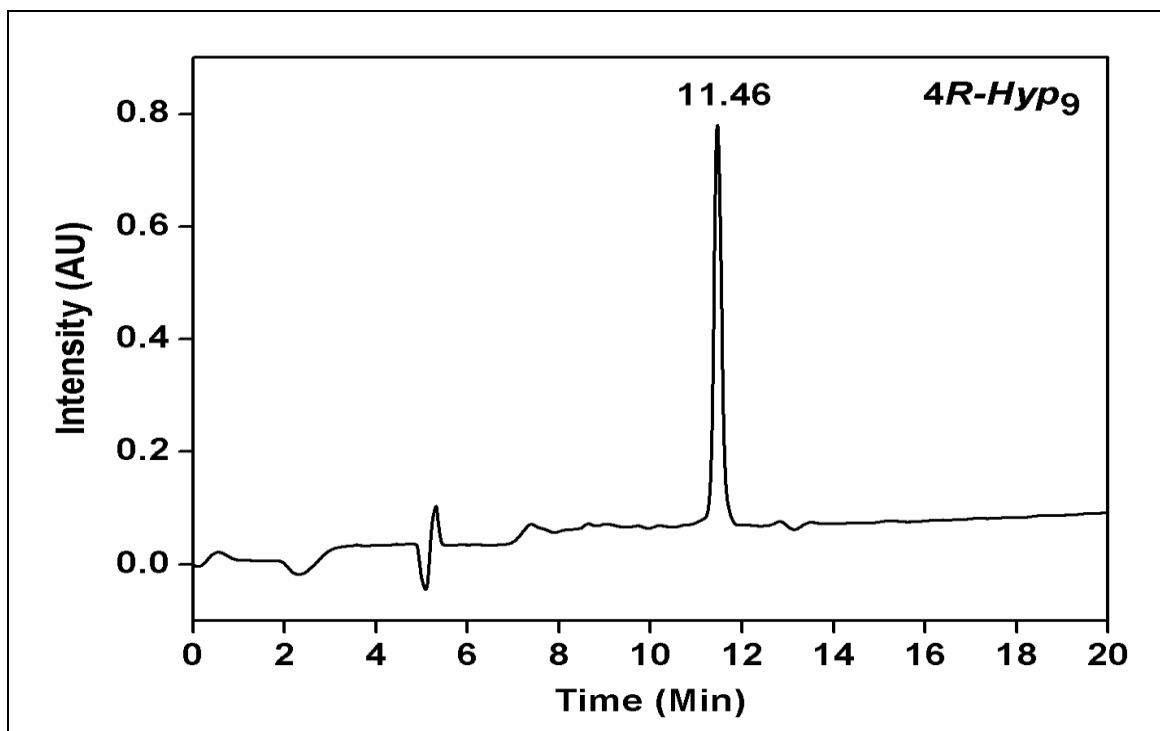
^1H NMR of compound 37 ^{13}C NMR of compound 37

^1H NMR of compound 38 ^{13}C NMR of compound 38

HPLC Trace of *Pro*₉

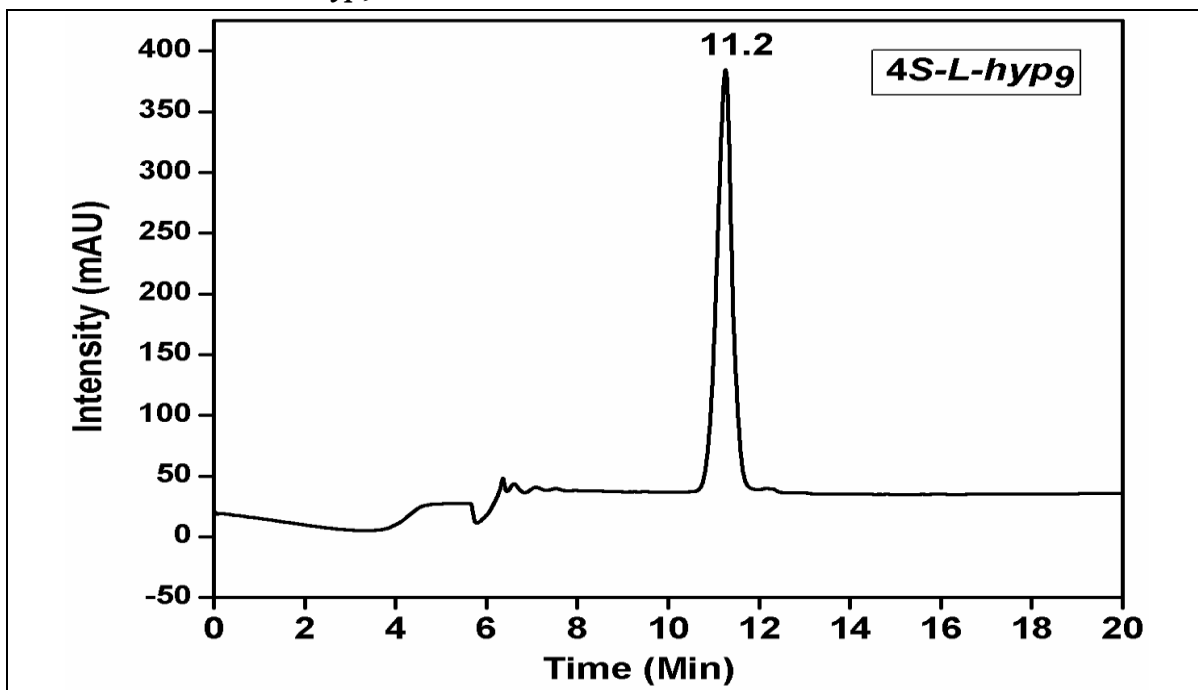


HPLC Trace of *4R-Hyp*₉

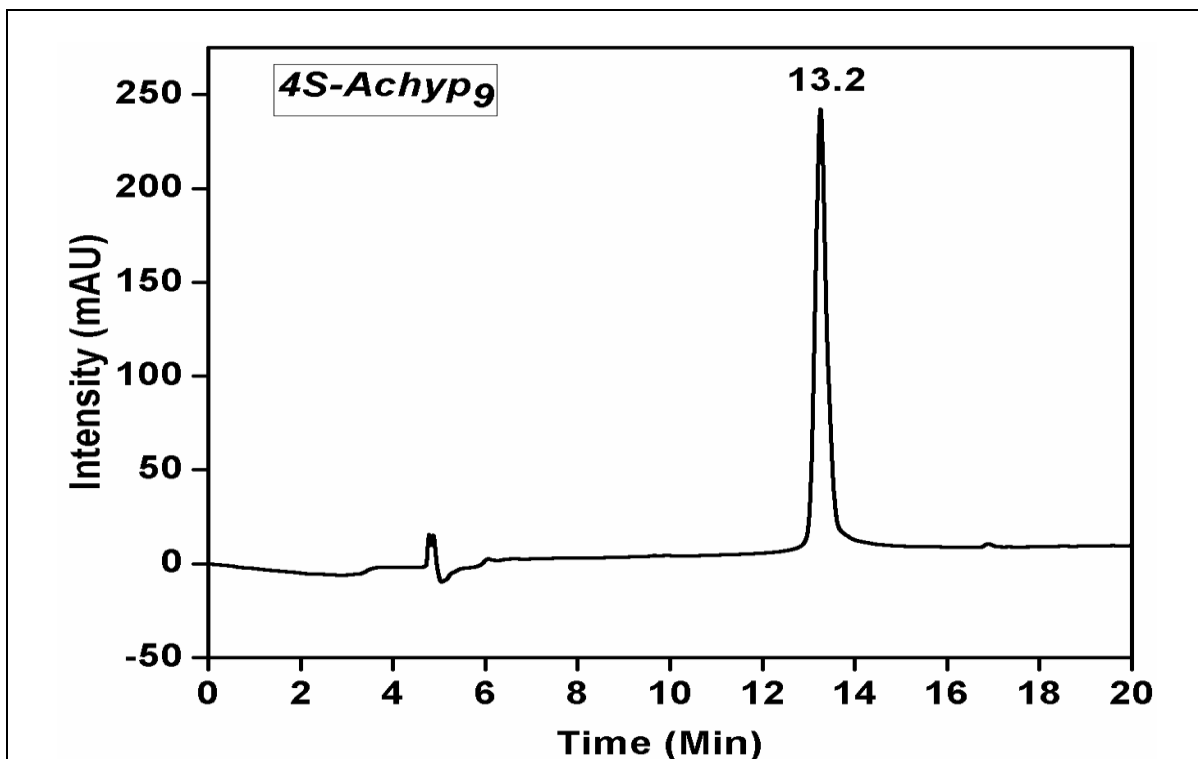


B) HPLC of Peptides (5-9)

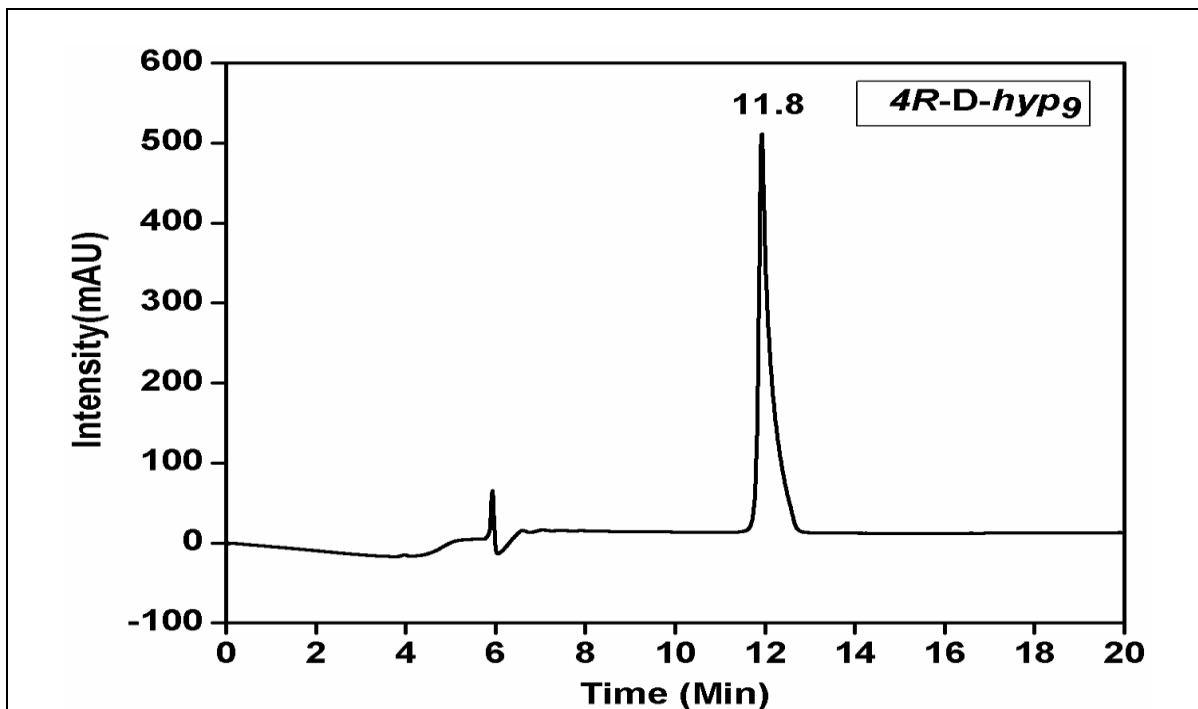
HPLC Trace of 4S-L-hyp₉



HPLC Trace of 4S-Achyp₉

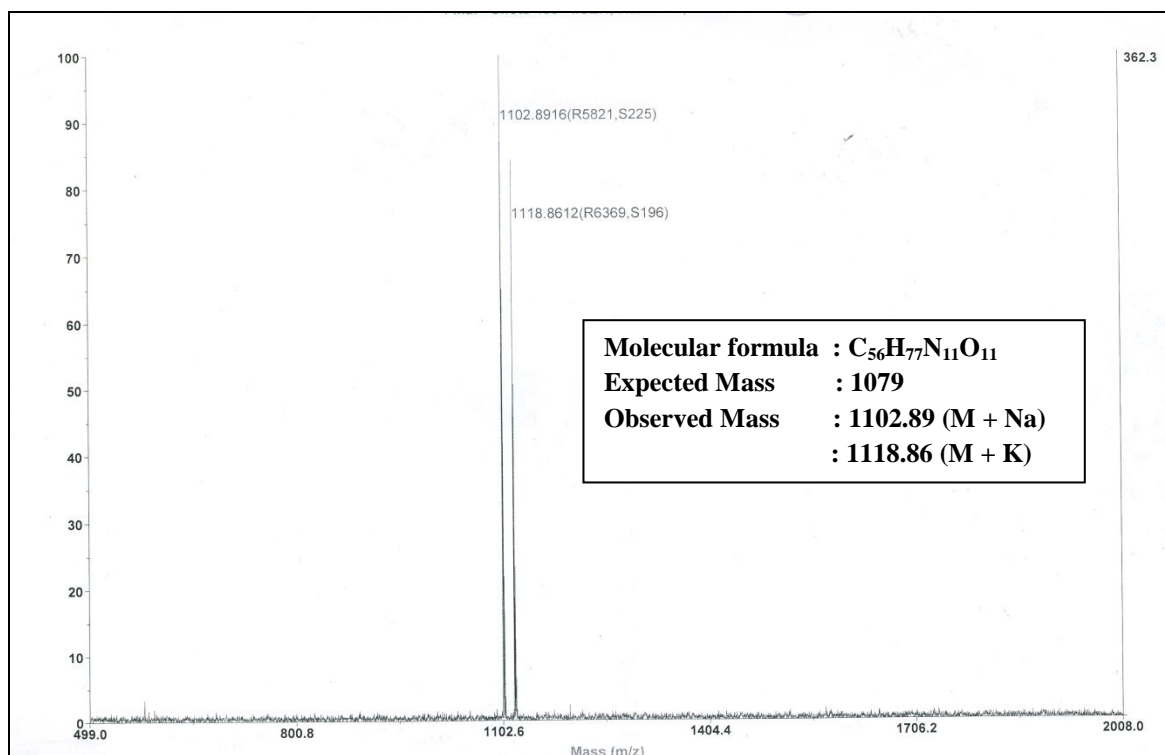


HPLC Trace of 4R-D-hyp₉

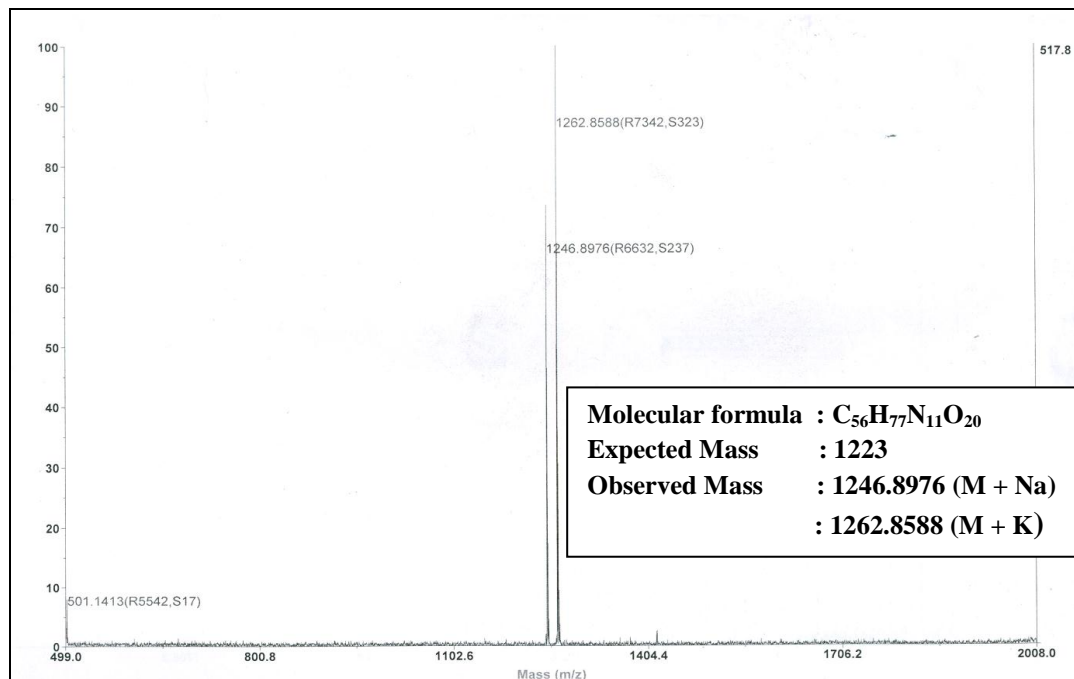


C) MALDI-TOF Mass of 5-9

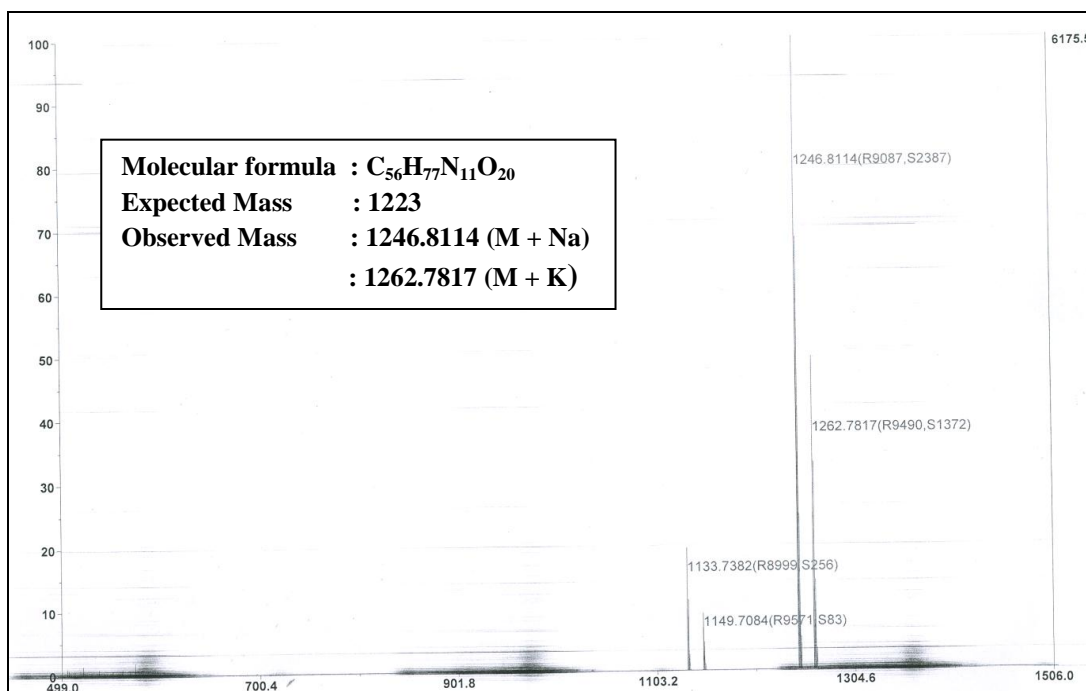
MALDI-TOF Mass of Pro₉



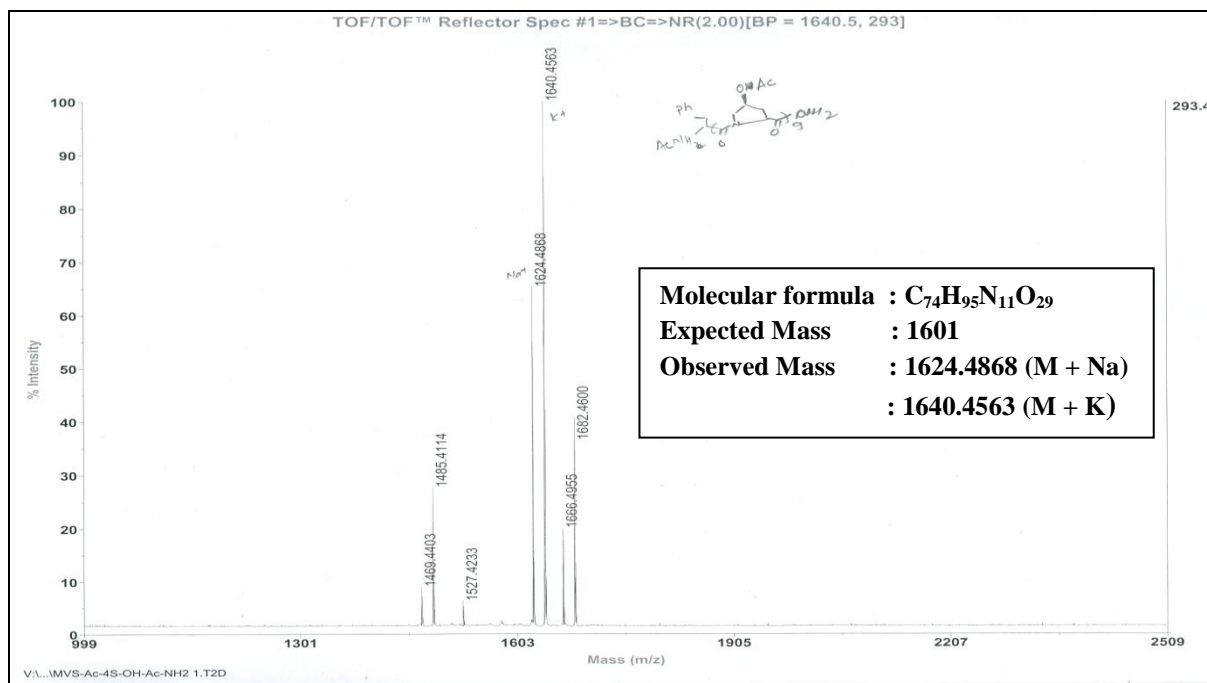
MALDI-TOF Mass 4R-Hyp₉



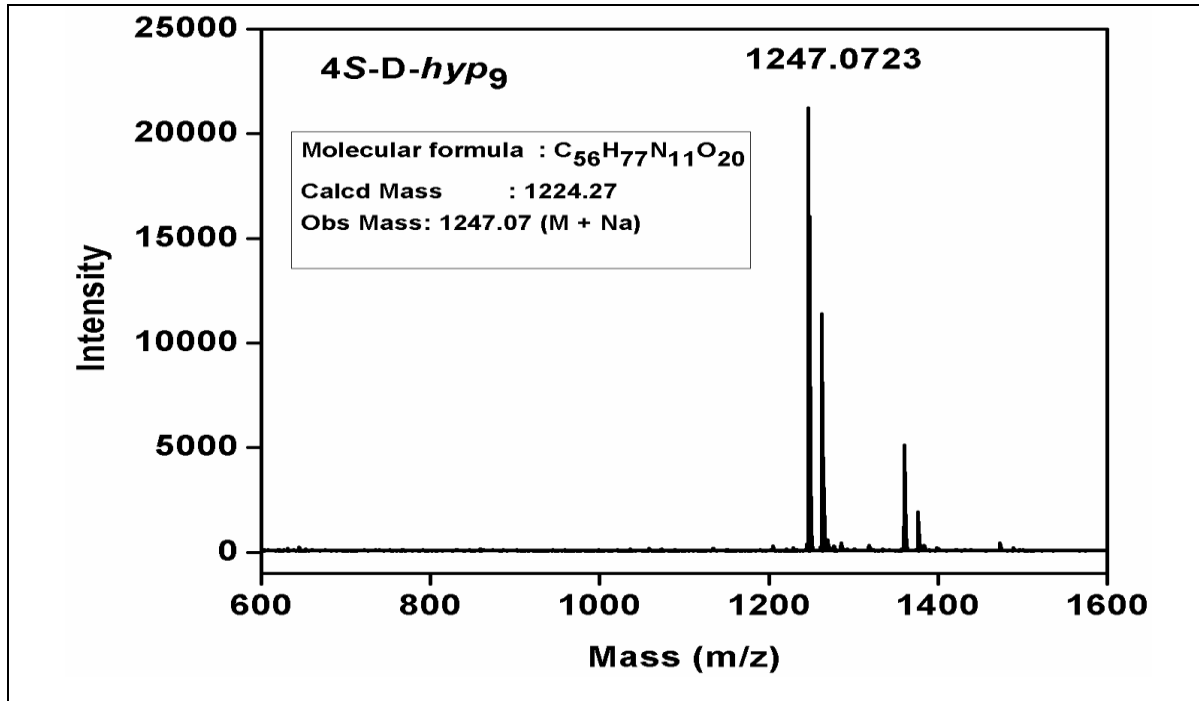
MALDI-TOF Mass 4S-L-hyp₉



MALDI-TOF Mass 4S-Achyp₉

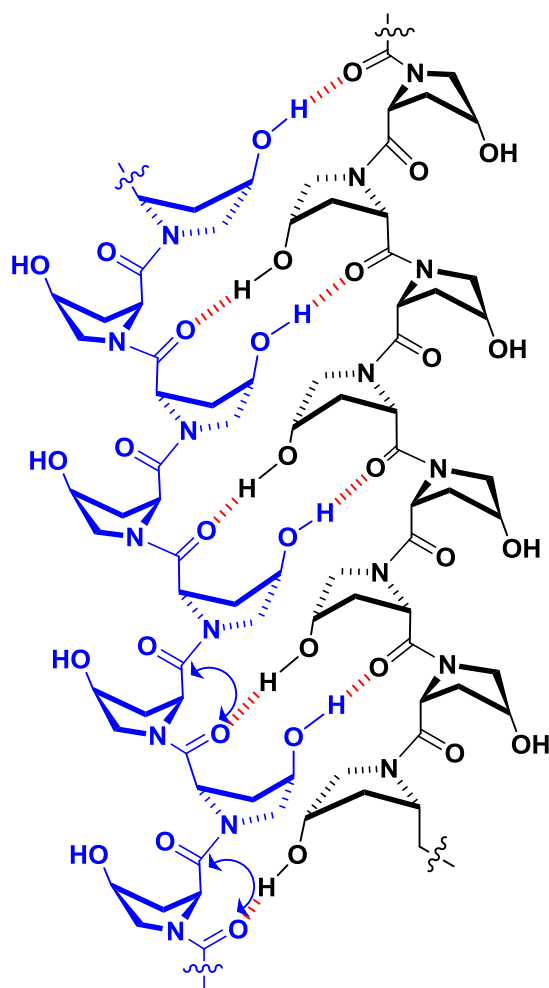


MALDI-TOF Mass 4R-D-hyp₉



Chapter 4

Orientation of β -Structure: Parallel or Antiparallel?



Section 1: Distinguishing the β -structure arrangements by FRET

4.0 Introduction

The ability of polypeptides and nucleic acids to adopt unique three-dimensional structures in aqueous solution is one of the most fundamental consequences of biological self-assembly.¹ Crucial to understanding of protein folding is also the characterization of the levels of denatured states and the conformational ensemble of unfolded protein chains. The initial event of folding is thought to be intramolecular contact of amino acid residues, a process that is mediated by chain diffusion.² Similar conformational events are thought to be crucial for functionality of intrinsically disordered protein domains. Proteins and peptides play a crucial role in many biological applications and processes in living organisms. They transform under certain cellular conditions from their soluble forms into highly ordered fibrillar aggregates.³ Such transitions can give rise to protein misfolding, which is basis of diseases ranging from neurodegenerative disorders to systemic amyloidoses. A broad range of human diseases arises because of failure of specific peptides to fold rightly to its native functional conformation. The largest group of misfolding diseases is associated with the conversion of specific peptides or proteins from their soluble functional states into highly organized fibrillar aggregates.⁴ Structure determination of these proteins and characterizing the misfolded shapes are important for understanding their function and to design the molecules that can more effectively mediate or interfere with cellular events.

In order to understand the conformation of complex proteins, it is necessary to examine orientations of component secondary structures of peptide fragments in the protein. Two most frequent secondary structures in proteins are α -helices and β -sheets. α -Helices arise from a repetitive helical arrangement of amino acids through intrachain H-bonding of amide groups from i^{th} residue to $i-3^{\text{rd}}$ residue. β -Sheets originate from interchain H-bonding of amide groups leading to a pleated collection of β -strands with either a parallel or an antiparallel arrangement of chains⁵ (Figure 1). Many membrane-associated proteins and peptides have a β -barrel of β -sheets. Conformational transitions of protein components to β -sheets have also been observed, which lead to mad cow and Creutzfeldt-Jakob disease etc.⁶ The formation of β -sheets at the membrane interface can result in the accumulation of fibrous structures that can disrupt cellular processes. The

amyloid β -peptide ($A\beta$ -) fibrous plaques can accumulate on the brain, leading to Alzheimer's disease.⁷ The occurrence of β -sheet structures in membrane-associated proteins as well as in $A\beta$ -plaques has raised much interest about β -sheet formation. The ability to determine the structures of the β -sheets, including their orientation at interfaces and on surfaces, could aid in the understanding of the origin of such important protein behaviors.⁸

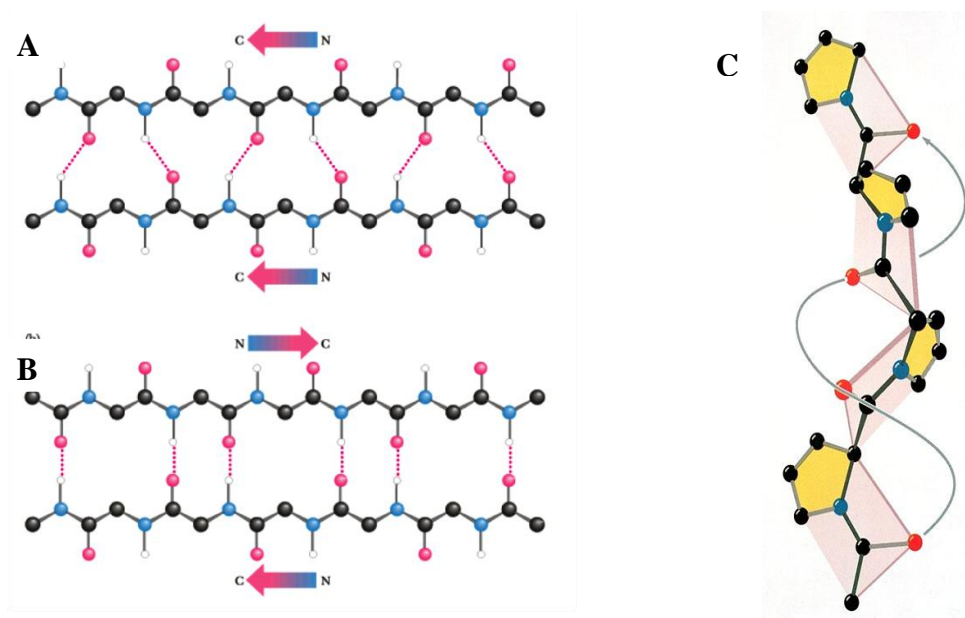


Figure 1. (A) Parallel orientation β -strand pair, (B) an antiparallel orientation of β -strand pair, (C) Polyproline II structure (without H-bond).

An important type of secondary structure arising without any H-bonding is the polyproline type structures (PPII/PPI) in which the structural constraints of amide bonds from proline (that lacks ability to form H-bond), forces to form helices. These forms are prevalent in denatured states and in special case aggregate to form triplex (collagen triplex).

A wide range of spectroscopic techniques has been applied to the study the relative orientation of peptide secondary structures in proteins. The most important ones include the use FT-IR⁹ and Raman spectroscopy,¹⁰ providing structural information of these molecules in solution or adsorbed on surfaces. Nuclear magnetic resonance (NMR) technique has been successfully applied to determine detailed structural information including that of membrane-associated proteins/peptides, which are difficult to crystallize.¹¹ Fluorescence resonance energy transfer (FRET) is another

powerful technique used to study orientation of peptides by measuring interactions between FRET pairs.¹² Recently, a nonlinear optical spectroscopic method of sum frequency generation (SFG) vibrational spectroscopy has been developed to determine the orientation of interfacial α -helices.¹³ Fluorescence spectroscopy is a versatile sensitive technique to measure the distances, monitor dynamics, or observe molecular interactions. In particular, Fluorescence resonance energy transfer (FRET) is very useful in measuring intramolecular interactions at Å distances.^{14,15}

4.1 Fluorescence resonance energy transfer (FRET)

In FRET, a donor chromophore absorbs energy, gets excited, followed by the transfer of the excitation energy to a nearby acceptor molecule under certain conditions. This energy transfer decreases the emission intensity from the donor and leads to emission of fluorescence from acceptor without its direct excitation. The rate of energy transfer is characteristically dependent on (i) the extent of overlap of the emission spectrum of the donor with the excitation spectrum of the acceptor (Figure 2A), (ii) the distance (r) between the donor and acceptor molecules, being most efficient when the acceptor and donor fluorophores are within 2-10 nm of one another (Figure 2B) and (iii) the relative orientation of the transition dipoles (Figure 2C). It is least favorable when the donor and acceptor dipoles are perpendicular to one another, with fluorescence seen only from donor and not acceptor and efficient when dipoles are parallel to each other, FRET will occur.

Fluorescence resonance energy transfer (FRET) has been a widely used to determine distances within and between biological molecules.^{17,18} Polyproline, a rigid rod like structure has been recently used as a spacer between donor and acceptor chromophores measure distances from single-molecule FRET measurements.¹⁹ Stryer and Haugland²⁰ used a series of L-proline oligomers as spacers of known lengths between naphthyl and dansyl chromophores to measure the efficiency of electronic excitation energy from donor to acceptor as a function of distance.

Amyloid fibrils are characterized by a common structural component, the cross- β spine whose detailed arrangement was difficult to determine because of the fibrillar nature of the material. Lai et al.²¹ determined arrangement of such cross- β spine based on the magnitude of the FRET signal.

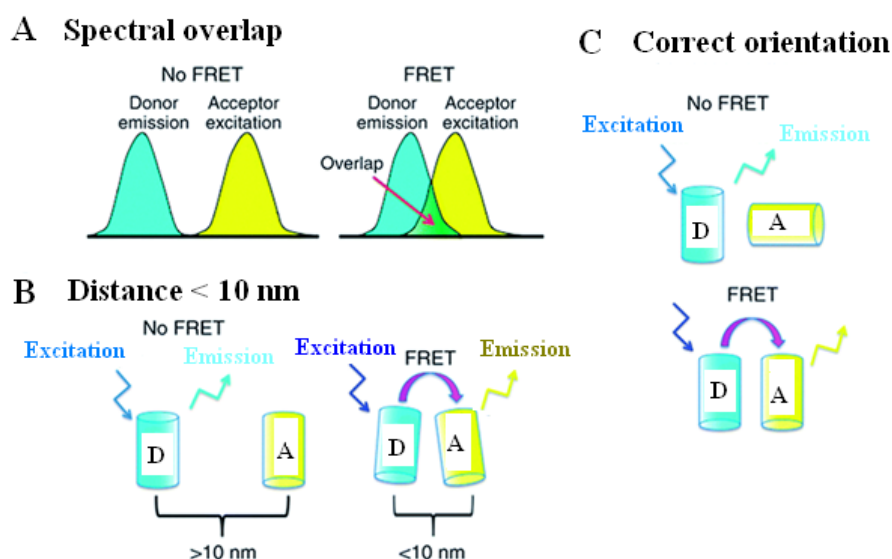


Figure 2. Schematic diagrams depicting the three conditions required for efficient FRET. (A) The emission spectrum from the donor must overlap with the excitation spectrum of the acceptor, (B) Donor and acceptor to be within ~ 10 nm for energy transfer to occur from the donor to the acceptor and (C) FRET is efficient when donor and acceptor dipoles are parallel to each other.¹⁶

4.2 Rationale of the work

The work presented in this is directed towards distinguishing the parallel/antiparallel orientation of β -structure formed in polypeptides derived from 4*S*-hydroxy-L-proline and 4*R*-hydroxy-D-proline in TFE. For this, two set of experiments have been designed: (i) fluorescence resonance energy transfer (FRET) and (ii) hydrophobic interactions of conjugated fatty acyl chains to induce nanostructures. In first strategy (i) the hypothesis is that when donor/ acceptor are linked to N-terminus, FRET signals can be seen only when the chains in the β -structure are in parallel orientation but not in the antiparallel orientation (Figure 3). In second strategy, if the N-terminus is labeled with a long chain fatty acid, parallel orientation should result in a simple aggregation, while antiparallel orientation should lead to a concatameric arrangement, giving rise to long wires (Figure 4), which can be characterized by microscopy.

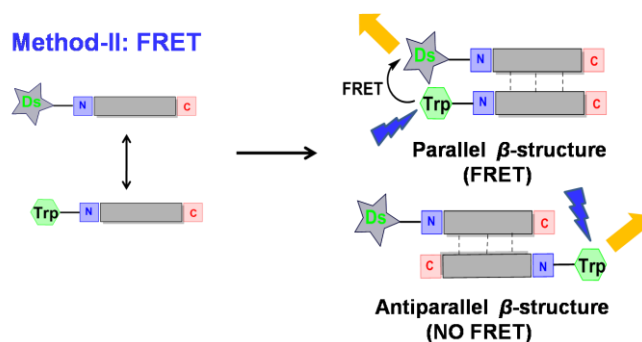


Figure 3. Possible arrangement of two peptide strands in β -structure (Parallel and Antiparallel).

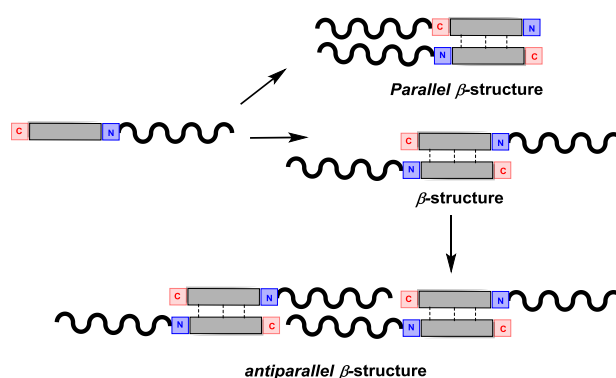
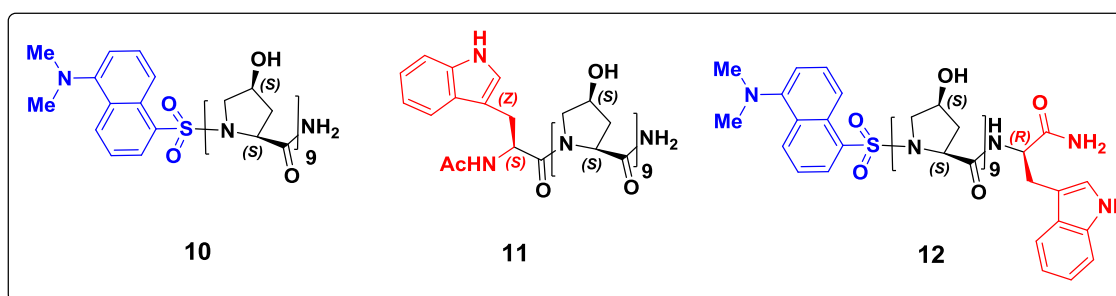
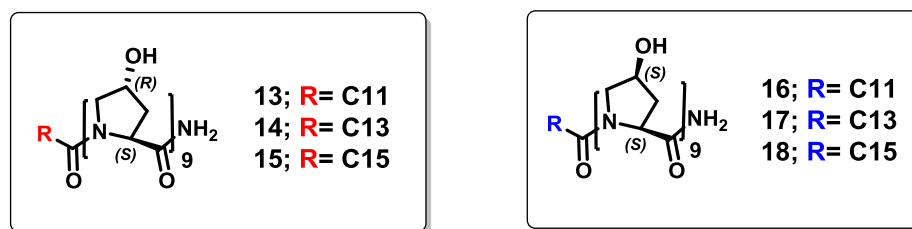


Figure 4. Possible arrangement of fatty acid conjugated peptide strands in β -structure (Parallel and Antiparallel).

Based on these rationales, for FRET experiments the peptides **10-12** were designed to contain a tryptophan or dansyl at N-terminus in two different peptides and both in same peptides with tryptophan at C-terminus and dansyl at N-terminus. Tryptophan as donor and dansyl as acceptor are well known to serve as a FRET pairs to monitor biomolecular geometries.



The peptides **13-18** were designed to monitor orientation dependent morphology through morphology (Figure 4).



4.3 Results and discussion

4.3.1 Peptide synthesis and labeling

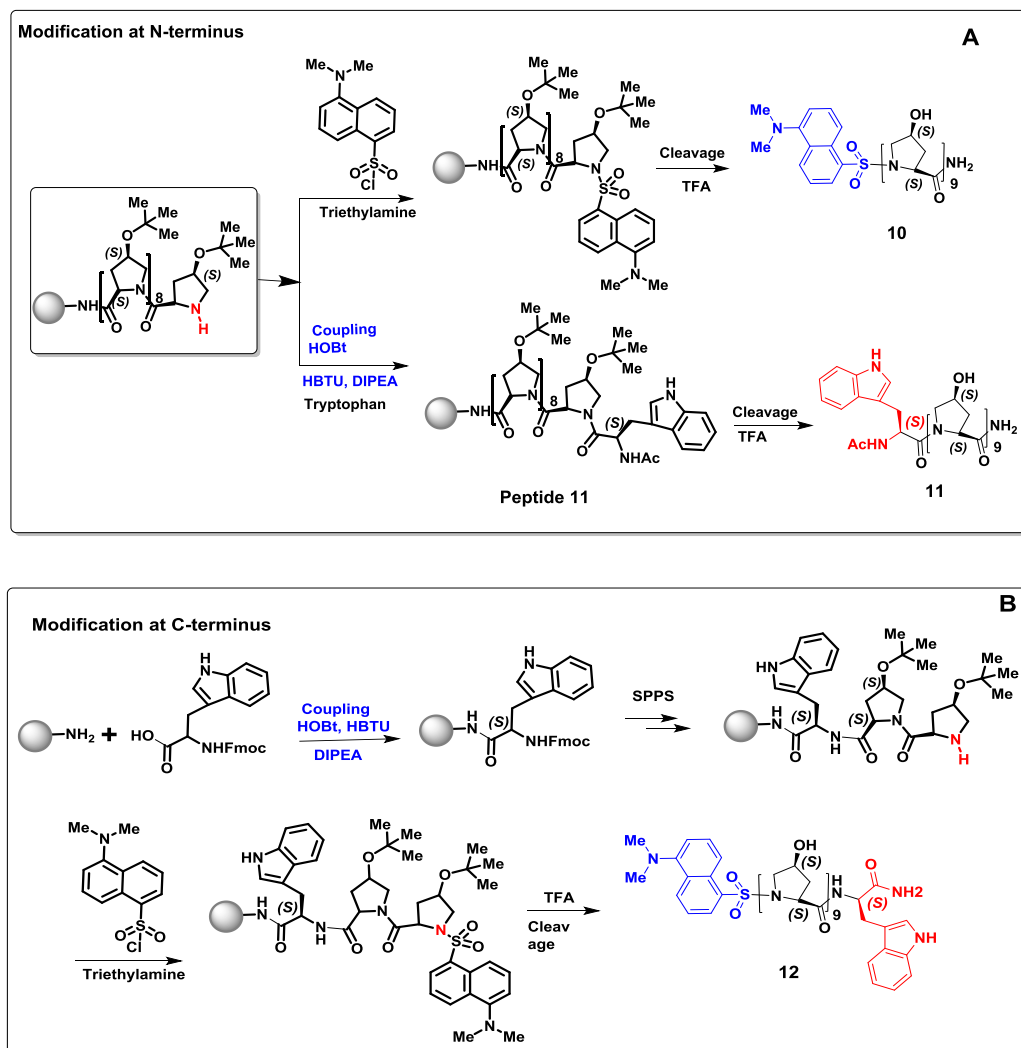
The fluorescent labeled peptides were synthesized by solid phase synthesis from C-terminus to N-terminus, with either first labeled with a fluorophore at C-terminus or labeling at the end at N-terminus. The hybrid peptide was synthesized by a combination of both approaches.

4.3.1a Fluorescent peptides

The synthesis of homo oligopeptides **10** (4*S*-hyp₉-Ds), **11** (4*S*-hyp₉-Trp) and **12** (Trp-4*S*-hyp₉-Ds) were done using solid phase peptide synthesis protocol on the commercially available rink amide resin using standard Fmoc chemistry as described in last chapter (Scheme 1A). The syntheses were done from the C-terminus to the N-terminus using protected monomer **32** (Chapter 3). The Kieselghur supported N,N-dimethylacrylamide resin (with Rink-amide linker) carrying terminal Fmoc group was deprotected with 20% piperidine in DMF to free amine. The monomers as N-protected free acids (3 eq) were coupled sequentially using the *in situ* activation with HBTU (coupling reagent) and HOBt (catalyst) and racemisation-suppressant. The coupling reaction was repeated by using *N*-Methyl-2-pyrrolidone (NMP) as solvent.

The peptide **12** labeled with a tryptophan residue at the C terminus and dansyl at N-terminus was synthesized as follows (Scheme 1B). Tryptophan was attached to peptide at C-terminus by standard Fmoc synthesis before the addition of first propyl residue and synthesis was continued. After the deprotection of the last amino acid, dansyl chloride and triethylamine in DMF was added to the resin to couple dansyl at N-terminus.

Scheme 1. Solid phase synthesis for 10-12



4.3.1b Peptides conjugated with fatty acids

The resin (Rink amide)-bound peptide of desired length with Fmoc group at N-terminus was used to attach fatty acid chains at N-terminus of peptide. *Fmoc*-group was deprotected with 20 % piperidine in DMF for 2 h. All peptides were coupled with phenylalanine at N-terminus before coupling of fatty acid to determine concentration of peptide stock-solutions by using phenylalanine absorption. It was coupled with fatty acid (lauric acid myristic acid, palmitic acid) using a 4-fold molar excess of HTBU, HOBt, *N,N'*-diisopropylethylamine (DIPEA) (Scheme 2), the N-terminal acetylated and C-terminal amidated peptides were purified on semi-preparative RP-18 HPLC column using water-acetonitrile gradient containing 0.1% TFA.

Scheme 2. Solid phase synthesis for 13-18

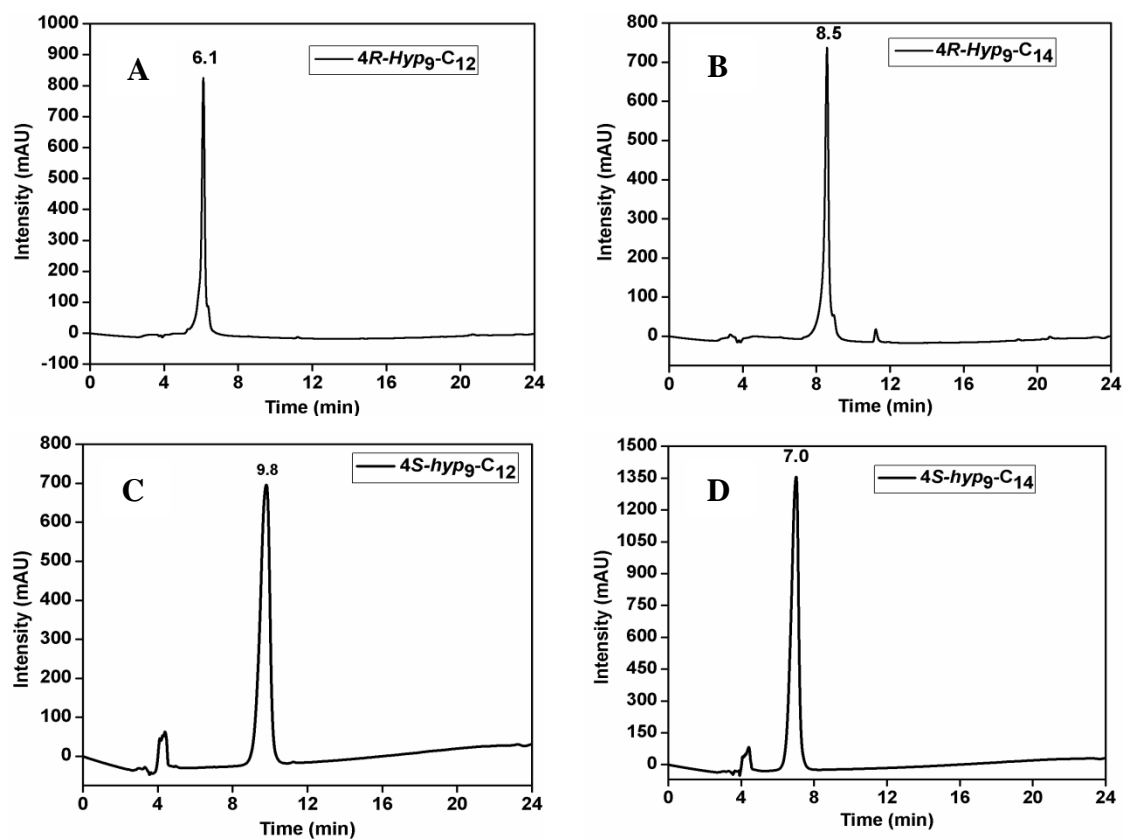
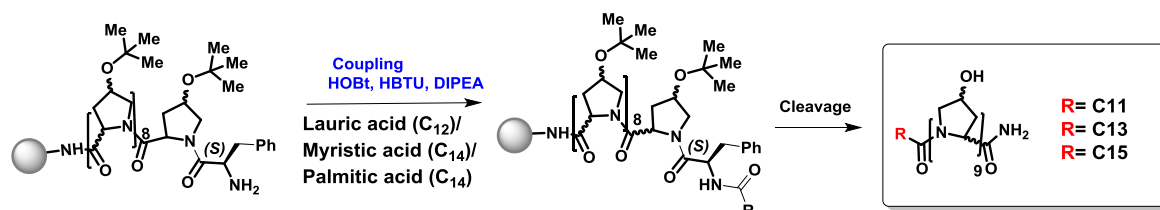


Figure 5. HPLC profiles of peptides (A) **13** (4R-Hyp₉-C₁₂), (B) **14** (4R-Hyp₉-C₁₄), (C) **16** (4S-hyp₉-C₁₂) and (D) **17** (4S-hyp₉-C₁₄); the conditions used in HPLC are 30 min, Gradient: A gradient of 0-100% MeCN/H₂O with 0.1% TFA, flow rate = 3 ml/min; λ = 220 nm.

The MALDI-TOF spectra recorded for the peptides reported in this section, DHB (2,5-Dihydroxybenzoic acid) was used as matrix and the molecular mass obtained for them were within the calculated range are shown in Figure 6.

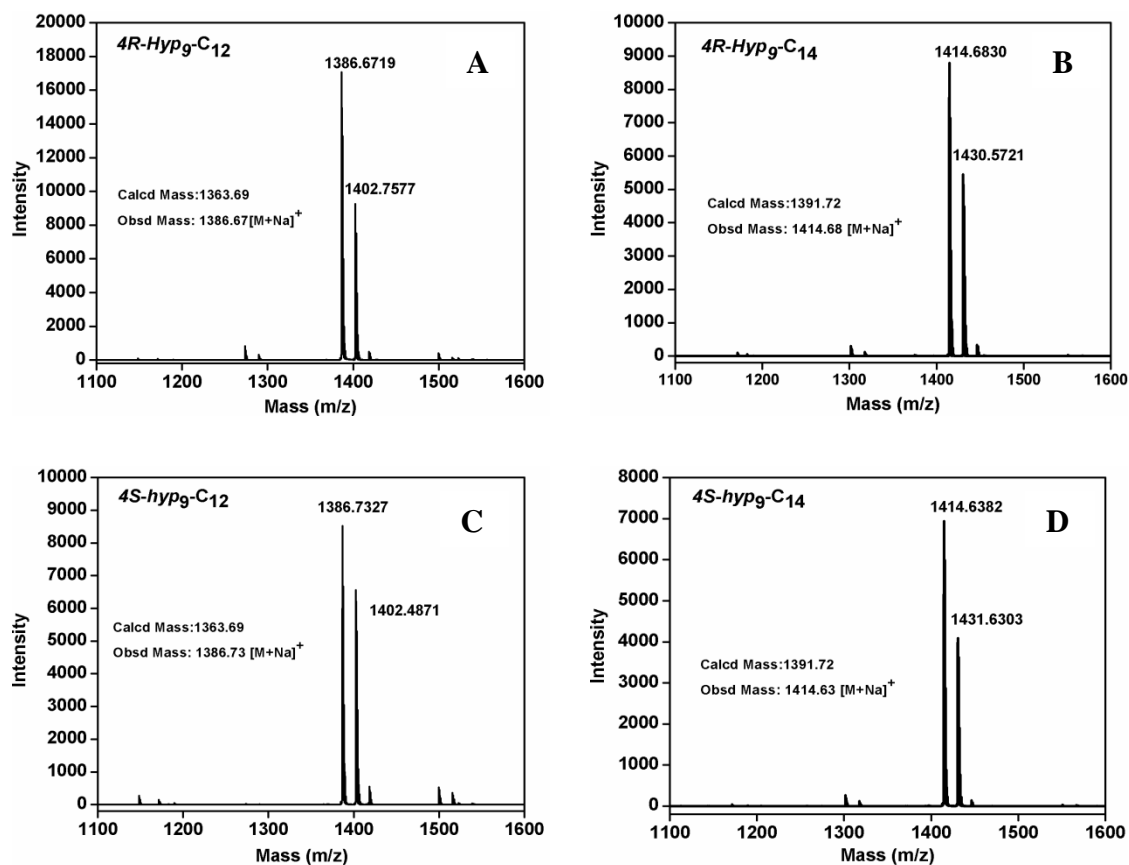
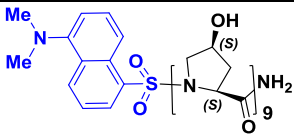
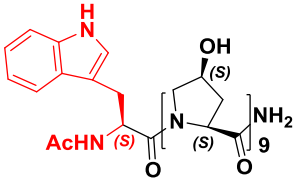


Figure 6. MALDI-TOF spectra of peptides (A) **13** (*4R-Hyp*₉-C₁₂), (B) **14** (*4R-Hyp*₉-C₁₄), (C) **16** (*4S-hyp*₉-C₁₂) and (D) **17** (*4S-hyp*₉-C₁₄).

Table 1. Characterization of peptides **10-18**.

Sr.No	Peptides	Mol. Formula	Mass (cal)	Mass (obs)
10		$C_{57}H_{77}N_{11}O_{20}SNa$	1290.49	1290.58 [M+Na] ⁺
11		$C_{58}H_{78}N_{12}O_{20}Na$	1285.53	1285.50 [M+Na] ⁺

12		$C_{68}H_{87}N_{13}O_{21}SNa$	1476.56	1476.58 [M+Na] ⁺
13		$C_{66}H_{97}N_{11}O_{20}Na$	1386.67	1386.67 [M+Na] ⁺
14		$C_{68}H_{101}N_{11}O_{20}Na$	1414.70	1414.68 [M+Na] ⁺
15		$C_{70}H_{106}N_{11}O_{20}Na$	1443.58	1443.19 [M+Na] ⁺
16		$C_{66}H_{97}N_{11}O_{20}Na$	1386.67	1386.73 [M+Na] ⁺
17		$C_{68}H_{101}N_{11}O_{20}Na$	1414.70	1414.63 [M+Na] ⁺
18		$C_{70}H_{106}N_{11}O_{20}Na$	1443.58	1443.18 [M+Na] ⁺

4.3.2 Determination of the peptide concentration in stock solution

The concentrations of the peptides conjugated with dansyl (Ds) and tryptophanyl fluorophores (Trp) were determined based on the dansyl absorption maximum (Ds = 330 nm, Trp = 280 nm) and extinction coefficient (Ds = $4800 \text{ M}^{-1}\text{cm}^{-1}$, Trp = $5500 \text{ M}^{-1}\text{cm}^{-1}$). To determine the concentrations of the peptides conjugated with fatty acid chains, the amino acid phenylalanine (Phe) was included at the N-terminal side for all peptides. Since it has aromatic side chain, the concentration of peptide stock-solutions can be determined by using phenylalanine absorption maximum at 254 nm and extinction coefficient of $195 \text{ M}^{-1}\text{cm}^{-1}$. All peptides contained phenylalanine at N-terminus and hence any effect from this residue on polyproline helix stability is same for all peptides.

4.3.3 CD Spectroscopic Studies

The effect of dansyl and tryptophanyl conjugation on the conformation of polyproline peptides was studied by CD spectroscopy.

4.3.4 Circular Dicroism (CD) studies of fluorescent peptides in sodium phosphate buffer (pH 7.2)

The CD spectra of all three peptides **10** (*4S-hyp₉-Ds*) and **11** (*4S-hyp₉-Trp*) were recorded in the range of 50-250 μM peptide concentrations in sodium-phosphate buffer (pH 7.2) and shown in Figure 7.

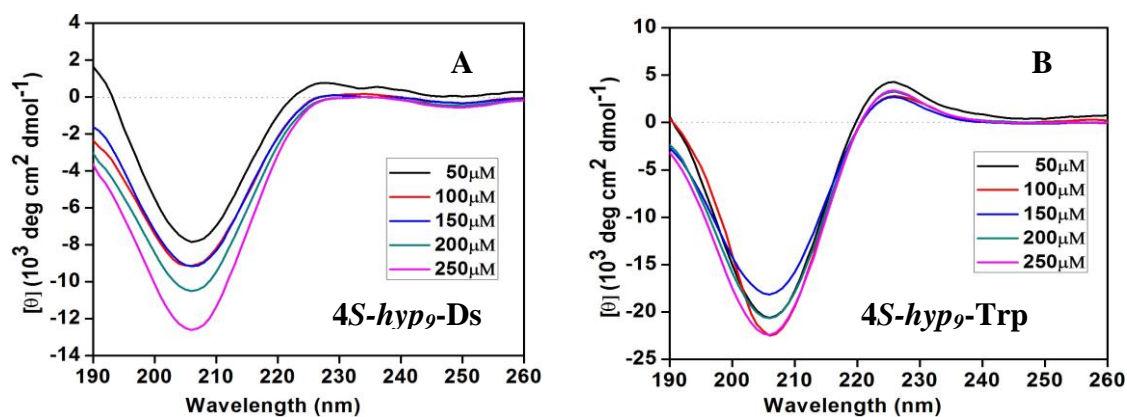


Figure 7. CD spectra of (A) **10** (*4S-hyp₉-Ds*), (B) **11** (*4S-hyp₉-Trp*); All CD spectra are recorded in 5 mM sodium phosphate (pH 7.2) buffer at 50-250 μM .

The spectra of the peptide **11** (*4S-hyp₉-Trp*) show characteristic CD signature of polyproline II (PPII), with strong maxima around 222-225 nm, and minima around 205 nm. Although spectral changes are apparent for the dansylated peptide **10** (*4S-hyp₉-Ds*), the spectra resemble PPII form with small minima around 250 nm (Figure 5A). This arises from the absorption of naphthalene ring of the dansyl group.²² CD studies of individual peptides showed that conjugation with dansyl or tryptophan units in polyproline peptides does not alter the PPII conformation in water (Figure 7A, 7B) and resembled that of the peptides described in Chapter 3.

4.3.5 Circular Dichroism (CD) studies in trifluoroethanol

The CD spectra of peptide **10** (*4S-hyp₉-Ds*, **11** (*4S-hyp₉-Trp*) and **12** (*Trp-4S-hyp₉-Ds*) in TFE has positive maxima at 195 nm and intense negative minima at around 210 nm.

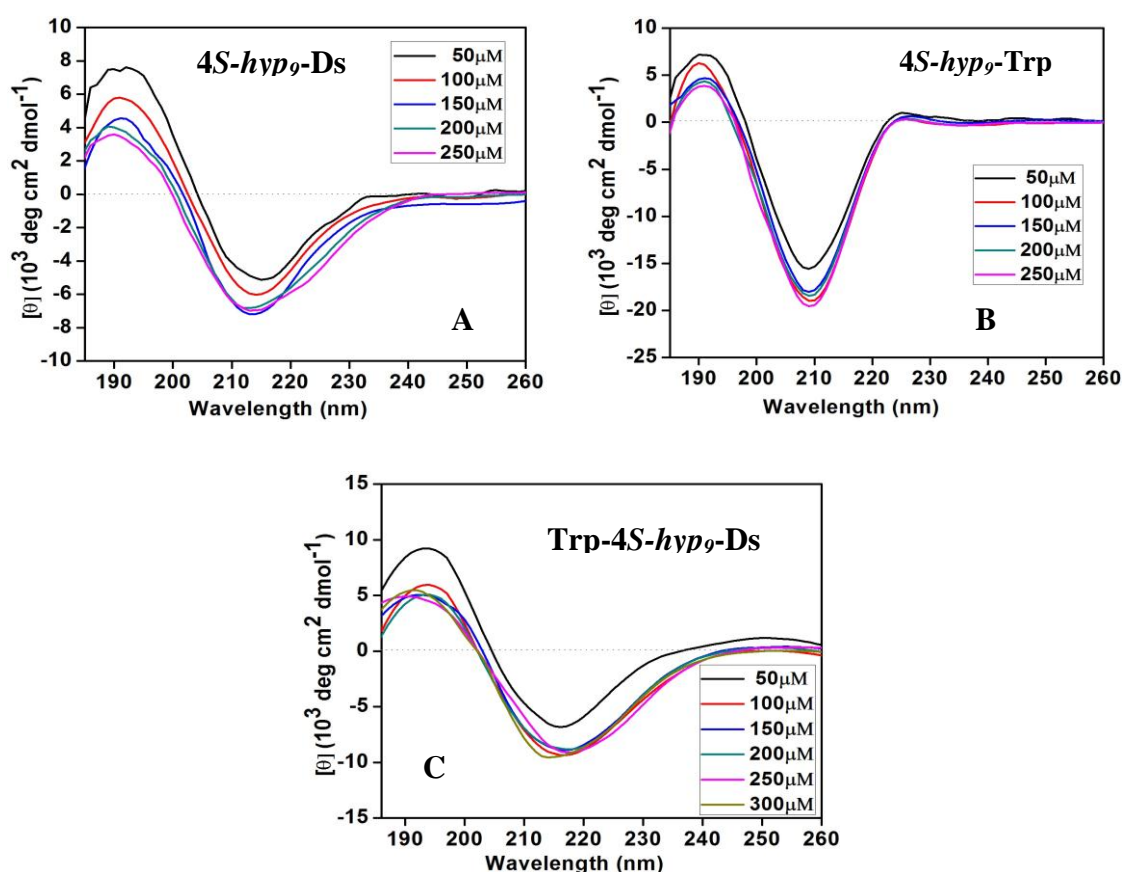


Figure 8. CD spectra of (A) **10** (*4S-hyp₉-Ds*), (B) **11** (*4S-hyp₉-Trp*), (C) **12** (*Trp-4S-hyp₉-Ds*); All CD spectra are recorded in TFE at 50-250 μM .

In the entire concentration range both peptides show similar positive and negative maxima. (Figure 8A, 8B) These are similar to that seen for free peptides (Chapter 3) and confirm that the fluorescent peptides form β -structure in TFE.

4.4 Fluorescence spectroscopic studies

4.4.1. Fluorescence emission of peptide 10 and 11 in sodium phosphate buffer (pH 7.2)

The excitation and fluorescence emission spectra for peptide **10** (*4S-hyp₉-Ds*) and **11** (*4S-hyp₉-Trp*) in sodium phosphate buffer (pH 7.2) are shown in Figure 9. The tryptophanyl and dansyl polyproline *4S-hyp* peptides upon excitation at 290 nm (Tryptophan ext) and 330 nm (dansyl ext) showed the emission spectra with maximum at 357 nm and 570 nm respectively.

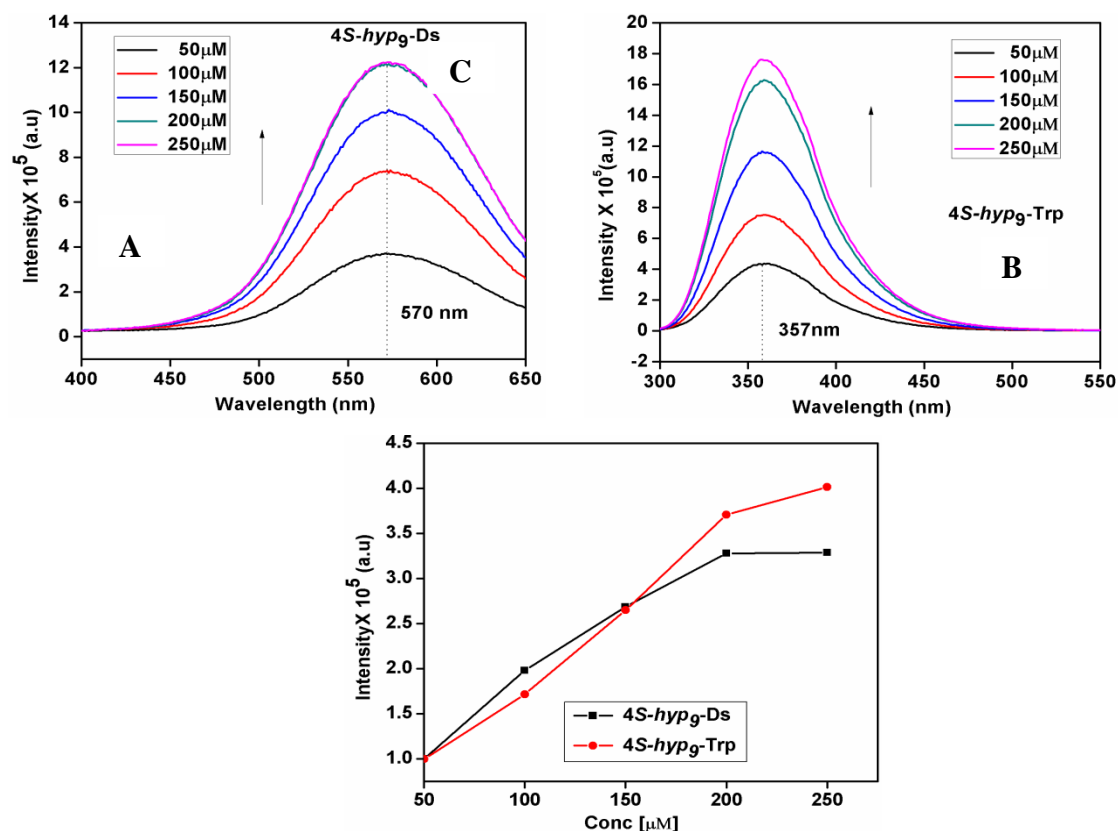


Figure 9. Fluorescence spectra of peptides (A) **10** (*4S-hyp₉-Ds*) and (B) **11** (*4S-hyp₉-Trp*), (C) Intensity of fluorescence spectra of as a function of concentration of peptide; All fluorescence spectra are recorded in sodium phosphate buffer (pH 7.2) at 50-250 μ M.

The fluorescent intensities were enhanced linearly in both peptides with increase in concentration from 50 μM to 200 μM and beyond this concentration, fluorescent intensities enhancements slightly decreased perhaps due to concentration quenching (Figure 9C). Hence all of the FRET experiments were conducted at concentrations lower than 200 μM .

4.4.2 Fluorescence emission of peptides 10 and 11 in TFE

The fluorescence spectra were recorded for peptide **10** (*4S-hyp₉-Ds*) and **11** (*4S-hyp₉-Trp*) in TFE and typical fluorescence emission spectra for the peptides are shown in Figure 10. These fluorescent polyproline peptides upon excitation at 330 nm and 290 nm showed the emission spectra with maximum at 546 nm and 350 nm respectively. Unlike in H_2O , concentration quenching in TFE was seen beyond 150 μM perhaps due to association /aggregation in TFE.

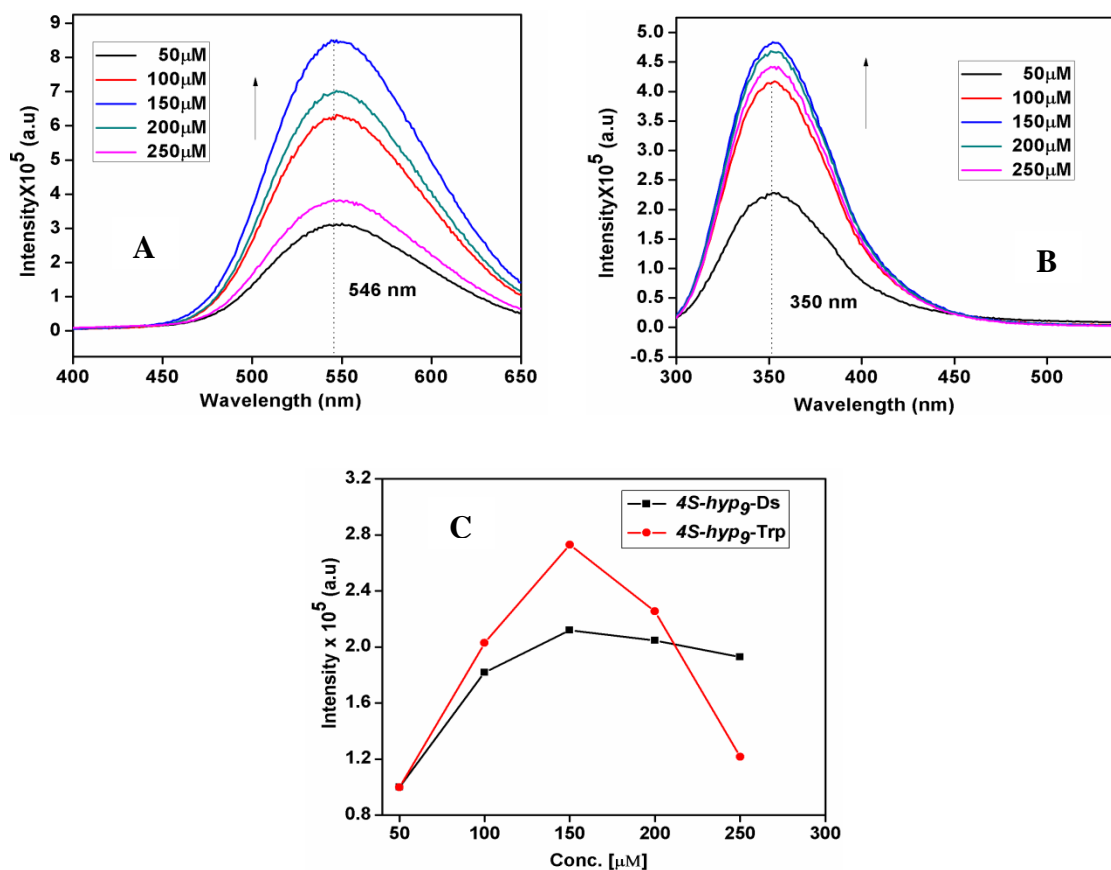


Figure 10. Fluorescence spectra of peptides (A) **10** (*4S-hyp₉-Ds*), (B) **11** (*4S-hyp₉-Trp*), (C) Intensity of fluorescence spectra of as a function of concentration of peptide; All fluorescence spectra are recorded in TFE at 50-250 μM .

4.5 The FRET experiments

4.5.1. Excitation and emission spectra of peptides

The fluorescence excitation and emission spectra recorded for peptides **10** (4*S*-hyp₉-Ds) and **11** (4*S*-hyp₉-Trp) in TFE are shown in Figure 10. The emission spectrum of **11** (4*S*-hyp₉-Trp) overlaps considerably with the absorption spectrum of **10** (4*S*-hyp₉-Ds). Effective emission-excitation spectral overlap seen for peptides **10** (4*S*-hyp₉-Trp) and **11** (4*S*-hyp₉-Trp) (Shaded Figure 11) suggests that the dansyl and tryptophan fluorophore pair conjugated to polyproline peptide are good FRET pair (Figure 11).

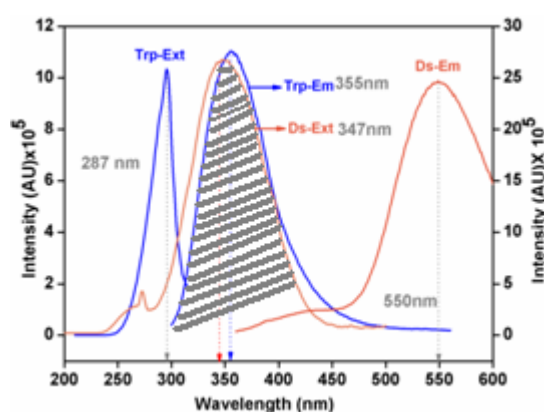


Figure 11. Spectral overlap of donor **11** (4*S*-hyp₉-Trp, Blue), emission and acceptor **10** (4*S*-hyp₉-Ds) organic dye absorption; All fluorescence spectra are recorded in TFE at 100 μM.

In order to determine the relative orientation of two strands in β -structure, from FRET data, three types of experiments were performed.

(i) The acceptor-tagged peptide **10** (4*S*-hyp₉-Ds) is added to the donor-tagged partner **11** (4*S*-hyp₉-Trp) and the emission spectra of both fluorophores were monitored in TFE (Figure 12). The concentration of donor Trp-tagged peptide **11** (4*S*-hyp₉-Trp) was kept constant (100 μM) and the acceptor Ds-tagged peptide was added with increased concentration and the emission spectra at λ_{540} are monitored as shown in (Figure 12A) upon excitation at Trp (λ). Only the emission from tryptophan at 350 nm was observed and the emission from the dansyl was negligible indicating that there was no FRET occurring from Trp to Ds. The non-absorbance of FRET signal suggests that the two fluorophores are away from each other that is possible only in an antiparallel orientation in β -structure (Figure 12B).

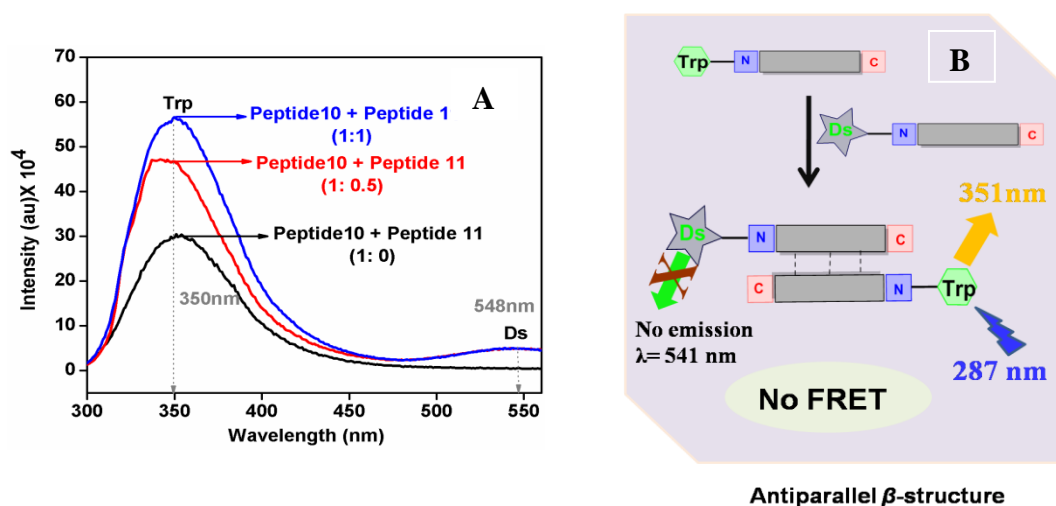


Figure 12. (A) Emission spectra (at λ_{351} nm) of **11** (4*S*-hyp₉-Trp) (100 μM) after addition of peptide **10** (4*S*-hyp₉-Ds) with excitation at λ_{287} nm (Trp) at 1:0.5 and 1:1 ratios, (B) Plausible antiparallel orientation of peptides in β -structure.

(ii) In a reverse experiment, the Trp-tagged peptide **11** was added to dansyl-tagged peptide **10** (acceptor) and the emission spectra of acceptor at λ_{540} nm monitored upon excitation of donor (Figure 13A). Only Trp emission increased, with negligible effect on dansyl emission. This situation arises only in anti-parallel orientation of strands in which both N-terminus containing FRET probes are away from each other.

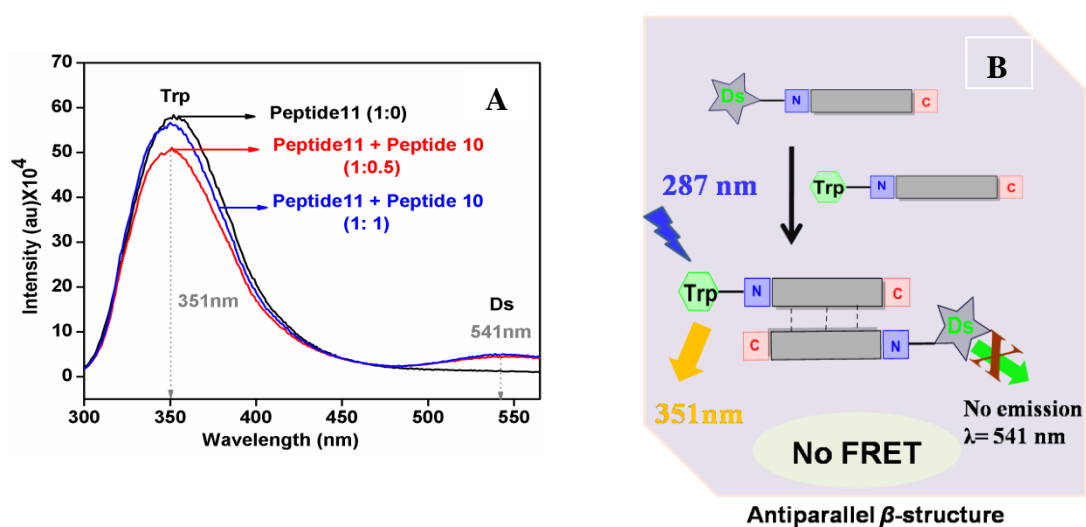


Figure 13. FRET spectra (A) Peptide **10** (4*S*-hyp₉-Ds) after addition of **11** (4*S*-hyp₉-Trp); For FRET excited at λ_{287} nm. Monitored donor emission at λ_{351} nm emission and acceptor emission λ_{541} nm, (B) Plausible orientation of peptides in β -structure.

Although both experiments indicated the formation of anti-parallel β -structure, the evidence is based on the non-observance of a signal. In order to provide a positive evidence, third experiment was performed using the doubly labeled peptide **12**. The doubly labeled peptide **12** (Trp-4*S*-hyp₉-Ds) with donor tryptophan at the C-terminus and a dansyl group at the N-terminus was mixed with peptide **10** (4*S*-hyp₉-Ds) having dansyl at N-terminus of two different ratios 1:0.5 and 1:1 Formation of complex was monitored by emission intensities of donor-acceptor.

The lack of dansyl emission in these experiments upon Trp excitation can be explained if strands are in antiparallel orientation. However this is a negative evidence. Positive evidence sought by a different experiment.

The peptide **12** (Trp-4*S*-hyp₉-Ds) alone, upon excitation at 287 nm gave only the emission of tryptophan at 350 nm with no emission at 541 nm. This suggests that no FRET occurs within the peptide **12** (Trp-4*S*-hyp₉-Ds) that has both tryptophan and dansyl (Figure 14).

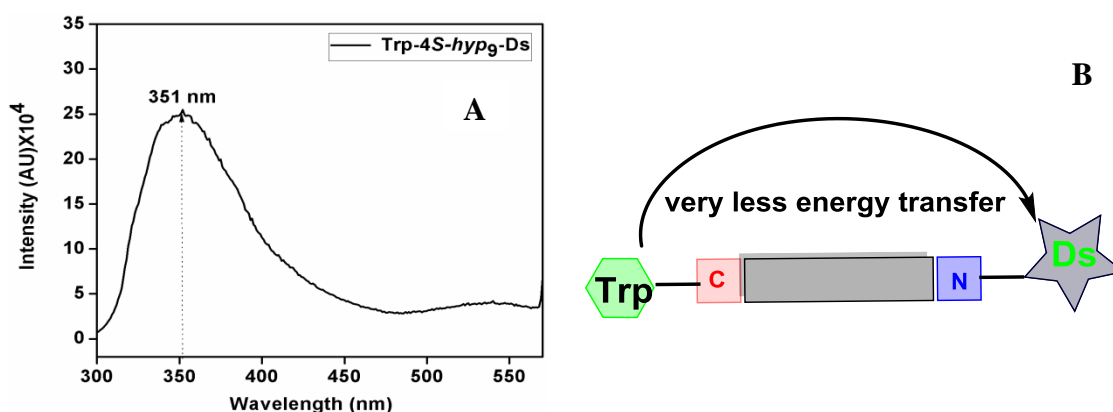


Figure 14. (A) Emission spectra of peptide **12** (Trp-4*S*-hyp₉-Ds) alone, excited at λ_{287} nm; Monitored donor emission at $\lambda_{351\text{nm}}$ and acceptor emission $\lambda_{351\text{nm}}$ (B) Possibility of intramolecular energy transfer.

After the addition of acceptor peptide **10** (4*S*-hyp₉-Ds), it is found that emission signal intensity at 549 nm corresponding to dansyl fluorescence increased upon excitation at Trp 287 nm (Figure 15). Importantly, the emission corresponding to donor tryptophan decreases which is due to transfer of fluorescence energy from tryptophan to excite dansyl followed by emission from dansyl at 541 nm (Figure 15). This is a positive evidence fluorescence arising from dansyl due to FRET rather than by direct excitation/emission. The incremental increase of FRET (dansyl emission) upon

increasing concentrations can only arise from an intermolecular anti-parallel packing of two strands in β -structure as shown in Figure 15B. These results along with the control experiment in which the doubly labeled peptide **12** (Trp-4*S*-hyp₉-Ds) alone failed to show any FRET signal provides a direct positive evidence for antiparallel β -structure in 4*S*-peptides.

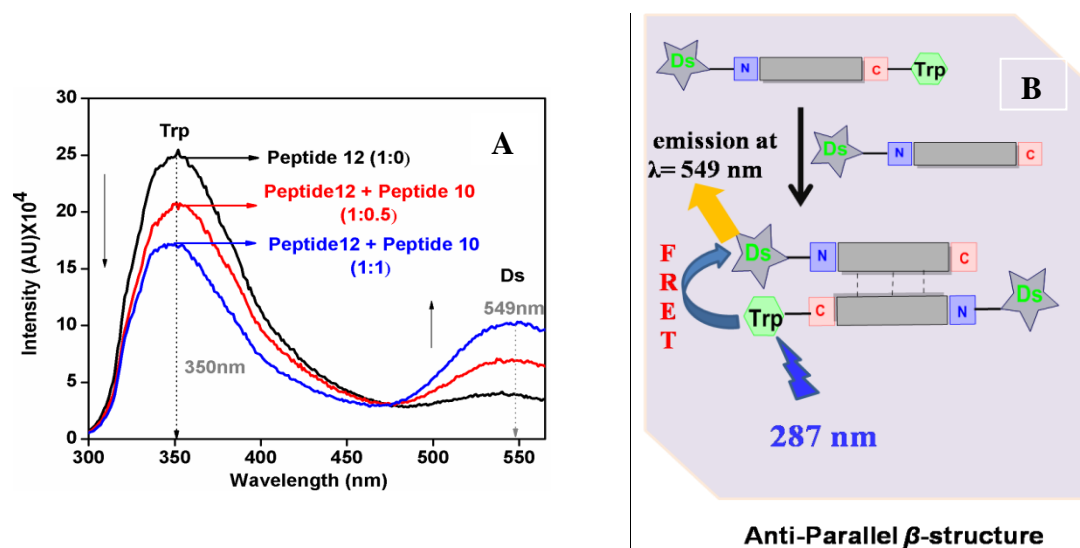


Figure 15. (A) Emission spectra of the modified peptide **12** (Trp-4*S*-hyp₉-Ds) before and after addition of **10** (4*S*-hyp₉-Ds), For FRET excited at λ_{287} nm (donor emission monitored at $\lambda_{351\text{nm}}$ emission and acceptor emission $\lambda_{549\text{nm}}$) (B) Plausible orientation of peptides in β -structure.

These experiments clearly proved the hypothesis that β -structure is formed with an antiparallel structural arrangement and gives the FRET signal, with the parallel arrangement not showing any FRET signal.

4.5.3 CD evidence for β -structure of fluorescent peptides mixture in water and in TFE

In order to ensure that the fluorophore labeled 4*S*-peptides retain their conformation as in unlabeled peptides, CD spectra of the fluorescent peptides **10** (4*S*-hyp₉-Ds) and **11** (4*S*-hyp₉-Trp) were recorded in water and TFE (Figure 16).

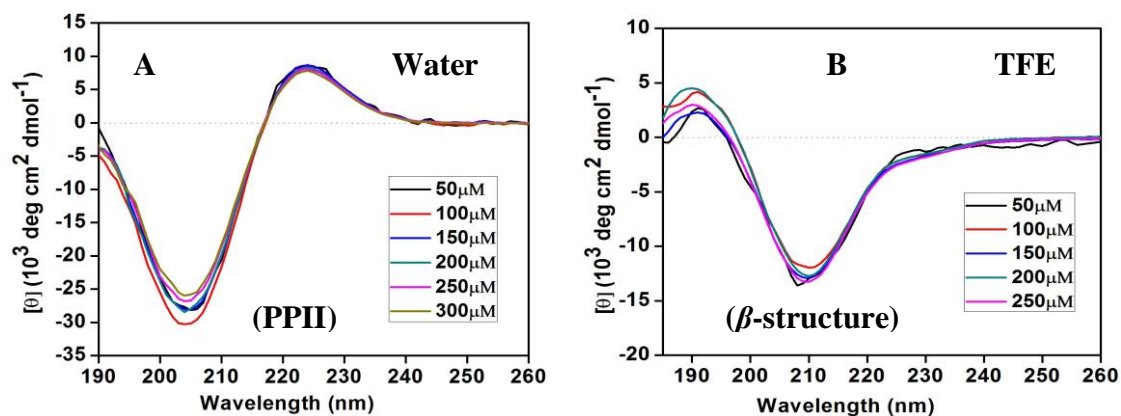


Figure 16. CD of mixture of (1:1) of peptide **10** (4*S*-hyp₉Ds) and **11** (4*S*-hyp₉-Trp); (A) in water and (B) in TFE.

These are similar to the results obtained (Figure 7, 8) with single peptides. The results in Figure 16 suggest that the ability of the fluorescent peptides to form PPII in water and β -structure in TFE is not altered by mixing of two peptides at various concentrations. Thus, the interpretation of results of FRET experiments to identify the antiparallel arrangement of two chains of β -structure is validated.

Section 2. Morphology and polymorphism of self-assembling polyproline peptides conjugated with fatty acid chains

Peptides are very useful building blocks for self-assembling nanostructures useful for various medical and materials applications.²³ Their secondary structures provide a unique platform for the design of materials with controllable structural features at the nanoscale.²⁴ β -Structure forming peptides demonstrate an extraordinary ability to develop their assemblies into their various nanostructures like nanotubes, ribbons, and helices through intermolecular hydrogen bonding.²⁵ The different nanostructures arise from an interplay of several factors, such as hydrophobic interactions, hydrogen bonding, crystal packing, electrostatic interactions, steric effects, and π - π stacking of aromatic amino acids within and amongst the different peptide chains.²⁶ Conjugation of peptides with other functional groups such as perylene monoimides (PMIs) is lead to the formation of hierarchical supramolecular assemblies with tunable properties.²⁷ Conjugation of hydrophilic cell-penetrating peptides with polyproline rods self-assemble them into nanocapsules, useful as potential intracellular delivery carriers.²⁸

Wennemers et al.²⁷ demonstrated the value of functionalizable peptidic scaffolds that have no tendency to self-aggregate but govern the spatial orientation between π -systems for directed self-assembly (Figure 17). The length of the conjugate and the absolute configuration of stereocenters at the outside of the helix, allowed for tuning the supramolecular aggregation. With increasing lengths of the oligoproline– π -system conjugates, higher ordered nanostructures resulted from flexible worm-like threads via fibrils to nanosheets and nanoribbons.

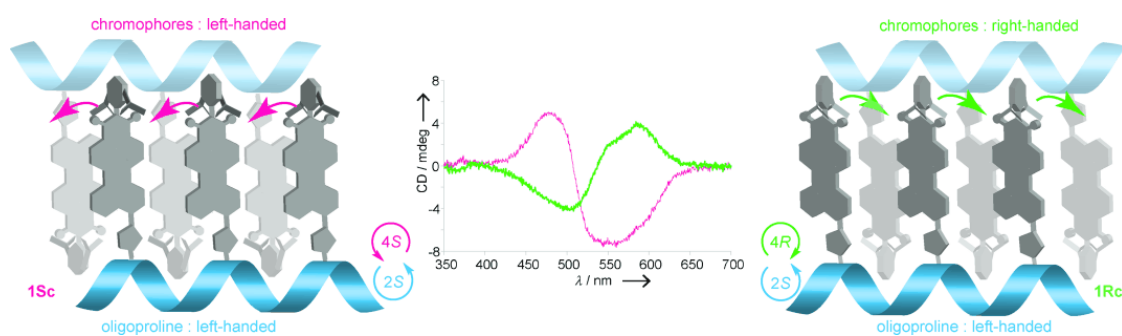


Figure 17. CD spectra of diastereoisomers in THF/H₂O; Representation of the counter-clockwise and clockwise orientation of chromophores.²⁷

Lee et al.²⁹ reported the self-assembly of bioactive peptide rod-coils where polyproline used to create rod while a hydrophilic cell-penetrating peptide Tat induced coil. Conjugations of hydrophilic cell-penetrating peptide with polyproline rods self-assemble into nanocapsules (Figure 18) useful as potential intracellular delivery carriers.

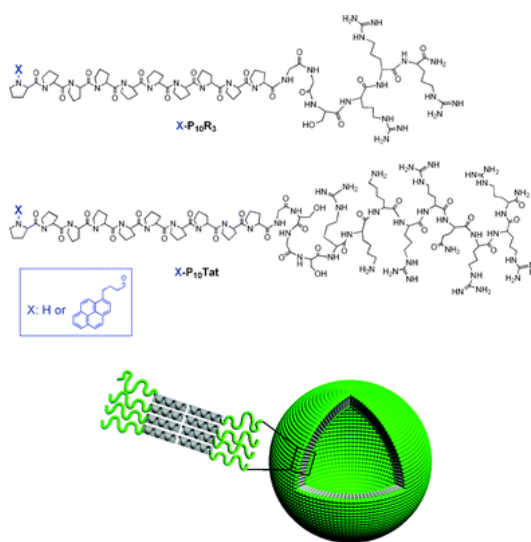


Figure 18. Structures of peptide rod-coil building blocks and their self-assembly into nanocapsule structures.²⁸

4.7 Rationale of work

Our previous findings that 4*S*-amp₉/*hyp* adapt an unusual β -structure (Figure 19) in TFE arising from *interchain* association of two polyproline peptide strands in antiparallel fashion, has been explored in this section to form of nanowires by conjugation with hydrophobic chains.³⁰

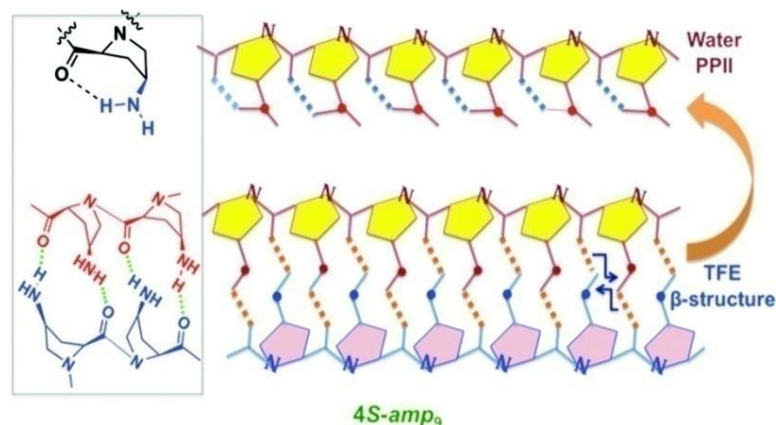


Figure 19. Water induced switching β -structure to PPII conformation in peptide 2 (4*S*-amp₉).³⁰

To investigate antiparallel orientation of peptide strands in β -structure, fatty acyl chains of different lengths were conjugated at N-terminus of these peptides.

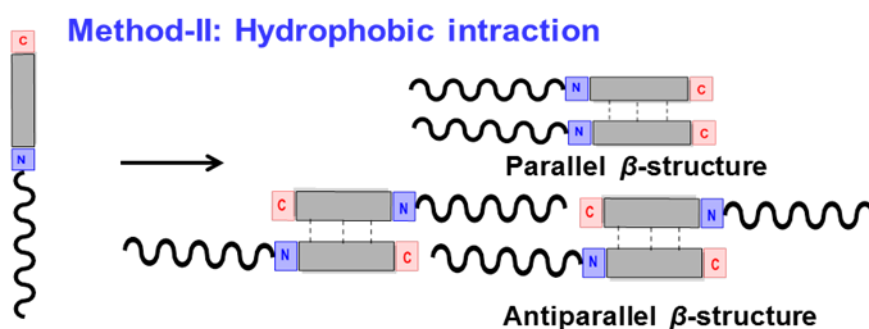


Figure 20. Possible arrangement of two peptide strands in β -structure (Parallel and Antiparallel).

The possible assemblies may induce β -structure formation via hydrogen bonding in the oligopeptide blocks while aggregative interactions among the fatty acid tails may superorganize the peptides (Figure 20) in an antiparallel β -structure. Peptide segments conjugated to aliphatic lipid tail may form continuous fibers whereas such an assembly is not possible in parallel orientation.

4.8 Results and discussion

4.8.1 Circular dichroism studies of 4R-peptides 13-15 in buffer

To examine the potential stabilization of secondary structure by covalently attached acyl chains, the CD spectra of peptide **6** (*4R-Hyp*₉) and fatty acid conjugated peptides **13** (*4R-Hyp*₉-C₁₂), **14** (*4R-Hyp*₉-C₁₄) and **15** (*4R-Hyp*₉-C₁₆) were recorded at 25 °C in the concentration range 50 μM–300 μM in sodium phosphate buffer (pH 7.2) (Figure 21).

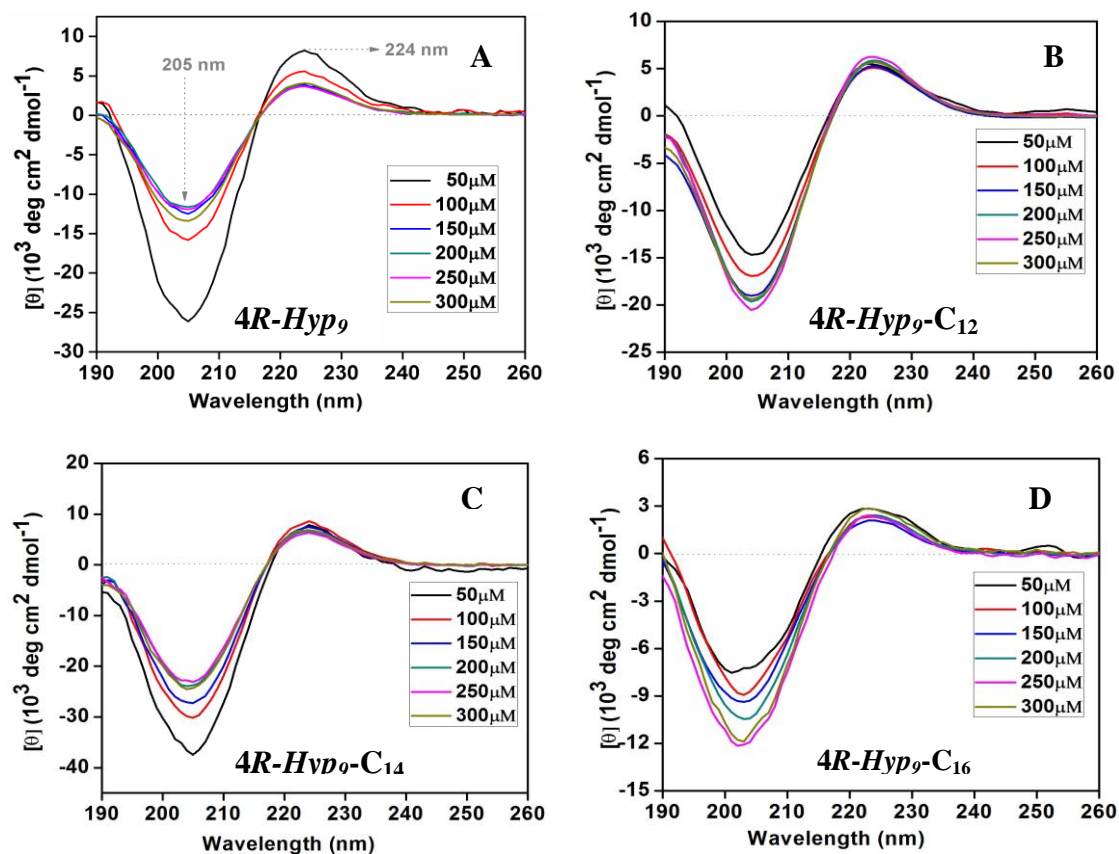


Figure 21. CD spectra recorded at 25°C for increasing peptide concentrations of peptides (A) peptide **6** (*4R-Hyp*₉), (B) **13** (*4R-Hyp*₉-C₁₂), (C) **14** (*4R-Hyp*₉-C₁₄), and (D) **15** (*4R-Hyp*₉-C₁₆) from 50 to 300 μM in sodium-phosphate buffer.

As shown in Figure 21, the CD spectra of peptides **6**, **13-15** showed a positive peak at around 225 nm and a large negative peak at around 205-207 nm. This is characteristics of PPII form. suggesting, that the peptide does not form any structures other than PPII in water.

The intensity of the positive band at 225 nm taken as proportional to the PPII helical content, was plotted as a function of peptide concentration (Figure 22). It is seen from the data that as the length of fatty acid chain in peptides increase, the PPII helix content of peptide **6** (*4R-Hyp*₉), **13** (*4R-Hyp*₉-C₁₂), and **14** (*4R-Hyp*₉-C₁₄) increased but for peptide **15** (*4R-Hyp*₉-C₁₆) decreased. The intensity of the positive band at 225-227 nm is seen in the order *4R-Hyp*₉ **6** < *4R-Hyp*-C₁₂ **13** < *4R-Hyp*-C₁₄ **14** > *4R-Hyp*-C₁₆ **15**. Thus, increase in concentration enhanced the aggregation of peptides in water promoted by hydrophobic chains, but retained overall PPII conformation for all peptides.

4.8.2 Circular dichroism studies of 4*R*-peptides 13-15 in TFE

In hydrophobic solvents, aggregation is not encouraged but H-bonding is favored. Hence the CD spectra of 4*R*-peptides **6**, **13-15** were recorded in TFE as a function of concentration in the range of 50 μ M-300 μ M (Figure 23).

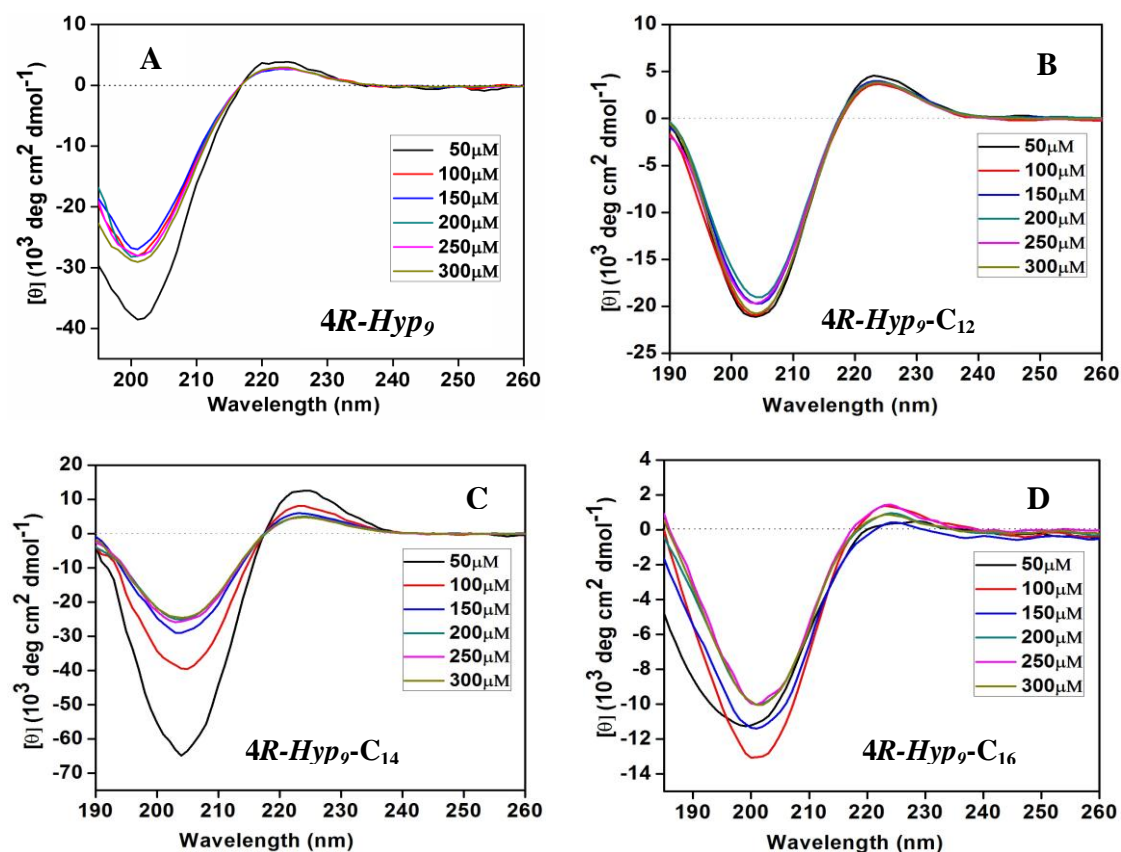


Figure 23. CD spectra recorded at 25°C for increasing peptide concentrations for (A) Peptide **6** (*4R-Hyp*₉), (B) **13** (*4R-Hyp*₉-C₁₂), (C) **14** (*4R-Hyp*₉-C₁₄), (D) **15** (*4R-Hyp*₉-C₁₆) from 50 to 300 μ M in TFE.

The peptides derived from 4*R*-hydroxyproline showed increased PPII CD signature and the conformation of the peptides did not change with conjugation of fatty acids at N-terminus. However, for peptide **15** (4*R*-Hyp₉-C₁₆) minor changes were observed perhaps due to formation of some irregular structure with less PPII (Figure 23), due to higher hydrophobicity.

4.8.3 Circular dichroism studies of 4*S*-peptides **7**, **16-18** in water

Figure 24 (A-B) shows the CD spectra of 4*S*-peptides **7**, **16-18** in sodium-phosphate at pH 7.2 at various molar concentrations. In case of 4*S*-peptides, the CD spectra has positive maxima at 225 nm and intense negative maxima at around 200-205 nm. In the entire concentration range, peptides show similar positive and negative maxima with the magnitude of positive and negative bands varying as a function of concentration.

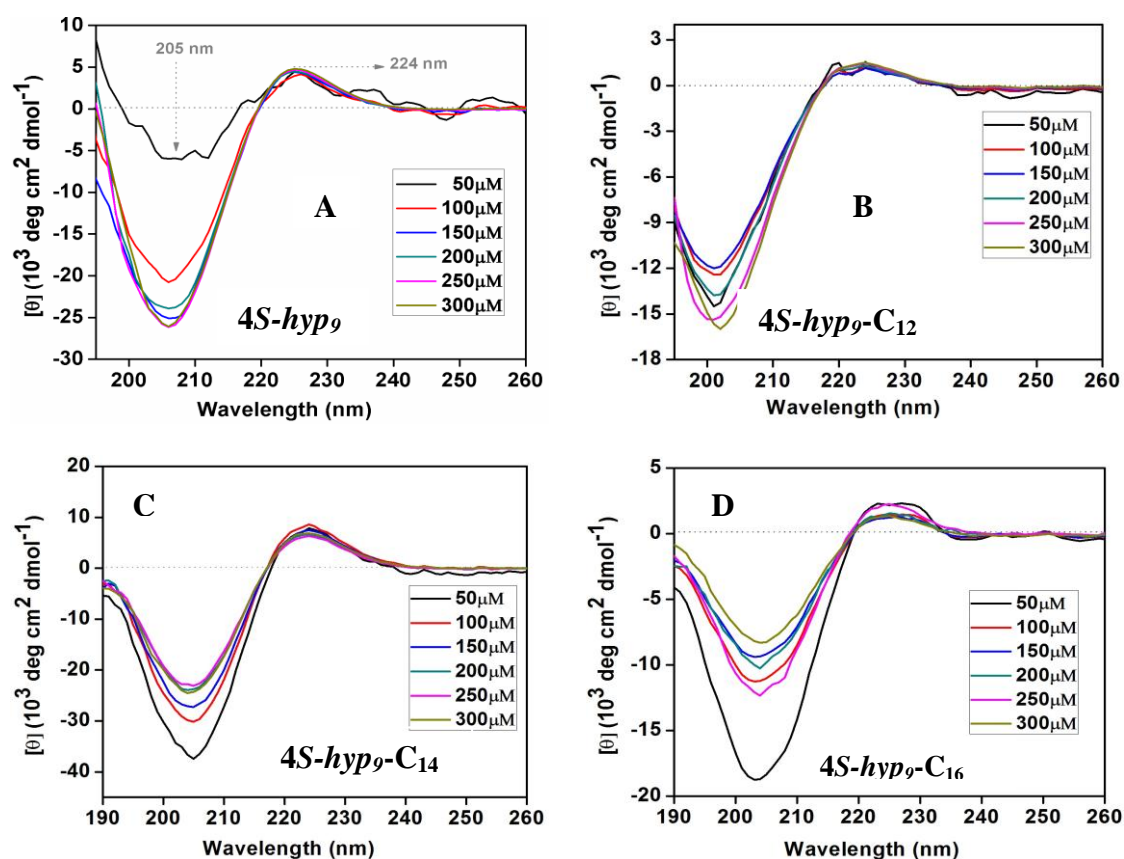


Figure 24. CD spectra recorded at 25°C for increasing peptide concentration for (A) Peptide **7** (4*S*-hyp₉), (B) **16** (4*S*-hyp₉-C₁₂), (C) **17** (4*S*-hyp₉-C₁₄), (D) **18** (4*S*-hyp₉-C₁₆) from 50 to 300 μM in sodium-phosphate buffer.

The 4*S*-peptides (Figure 24) show characteristic presence of PPII conformation in water and not altered by conjugation of fatty acid chains at N-terminus. These results comply with the trend observed in 4*R*-peptide (Figure 21). Overall the CD results for 4*R*-peptides in water (Figure 21), TFE (Figure 23) and for 4*S*-peptides in water (Figure 24) clearly confirm formation of PPII and the fatty acid conjugation does not perturb PPII conformation.

4.8.4 Circular dichroism studies of 4*S*-peptide 7, 16-18 in TFE

To test the effect of introduced hydrophobic modification at the N-terminus of 4*S*-peptides **16-18** which have ability to form β -structure in TFE, the CD spectra of fatty acid chain conjugated peptides **7, 16-18** were recorded in TFE in the concentration range of 50 μ M-300 μ M (Figure 25).

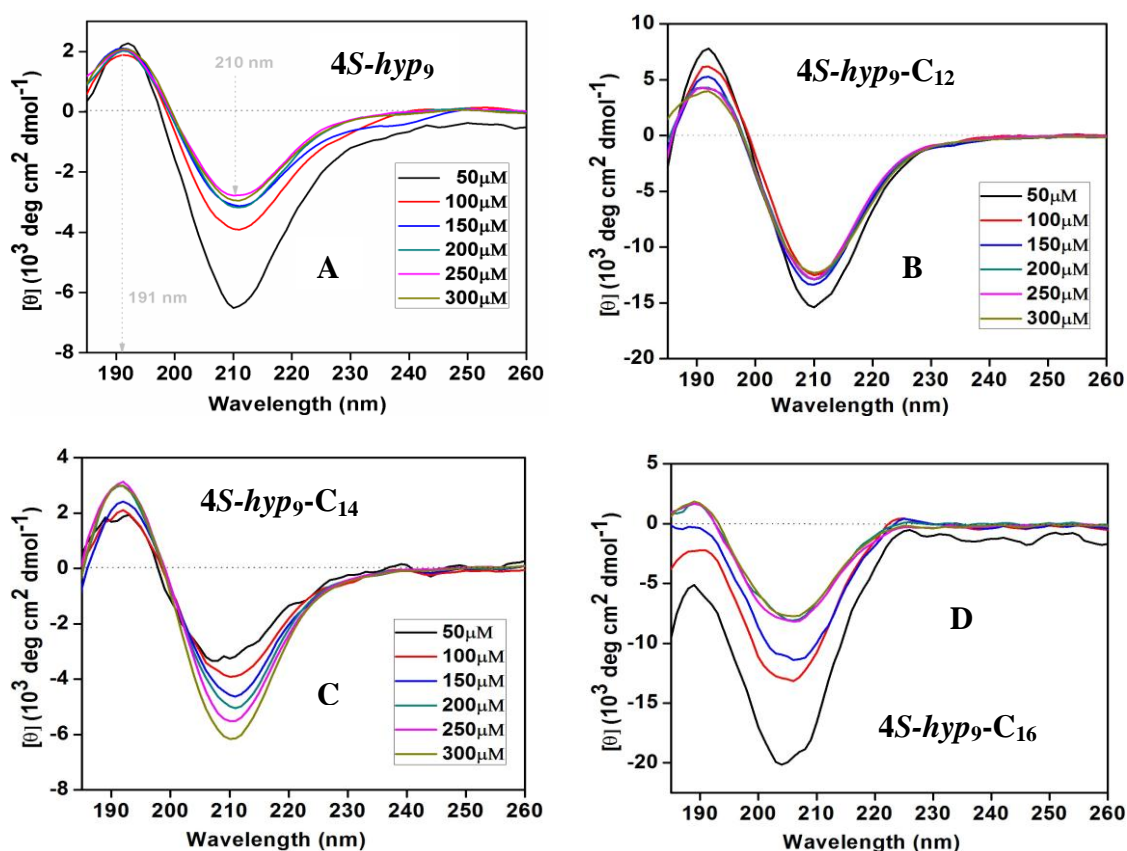


Figure 25. CD spectra recorded at 25°C for increasing peptide concentration for (A) Peptide **7** (4*S*-hyp₉), (B) **16** (4*S*-hyp₉-C₁₂), (C) **17** (4*S*-hyp₉-C₁₄) and (D) **18** (4*S*-hyp₉-C₁₆) from 50 to 300 μ M in TFE.

4.9 Field Emission Scanning Electron Microscopy (FESEM)

To examine the morphologies of self assembled structures with and without fatty acid conjugation, FE-SEM imaging was carried out for each of the acylated peptides at a lower concentration of 50 μM and a higher concentration of 300 μM in water as well as in TFE.

4.9.1 4*R*-peptides 6, 13-15 in water

The 4*R*-peptides **6** (4*R*-Hyp₉), **13** (4*R*-Hyp₉-C₁₂), **14** (4*R*-Hyp₉-C₁₄) and **15** (4*R*-Hyp₉-C₁₆) show only PPII form in water as seen by CD. The FESEM images (Figure 28, 29) of these peptides indicate short rods of 40-60 nm diameter and 100-200 nm lengths. The effect of different length of conjugated carbon chains was not apparent, with size of rods remaining similar. The C₁₆ chain peptide exhibited somewhat longer rods compared to C₁₂ and C₁₄ peptides.

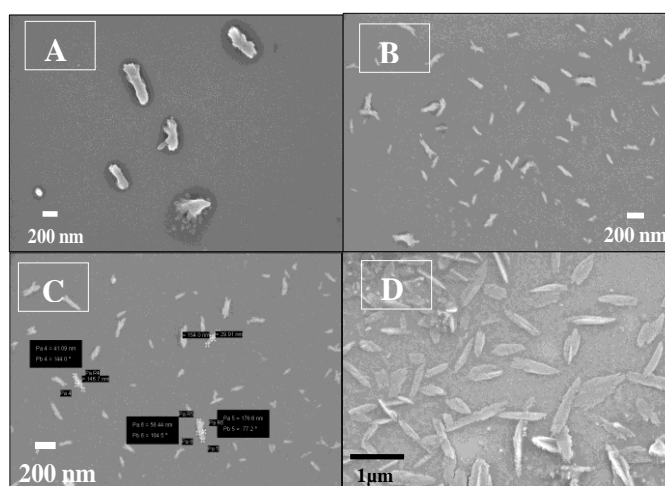


Figure 28. FESEM images for 4*R*-peptides (A) **6** 4*R*-Hyp₉, (B) **13** (4*R*-Hyp₉-C₁₂), (C) **14** 4*R*-Hyp₉-C₁₄, (D) 4*R*-Hyp₉-C₁₆ in water at 50 μM .

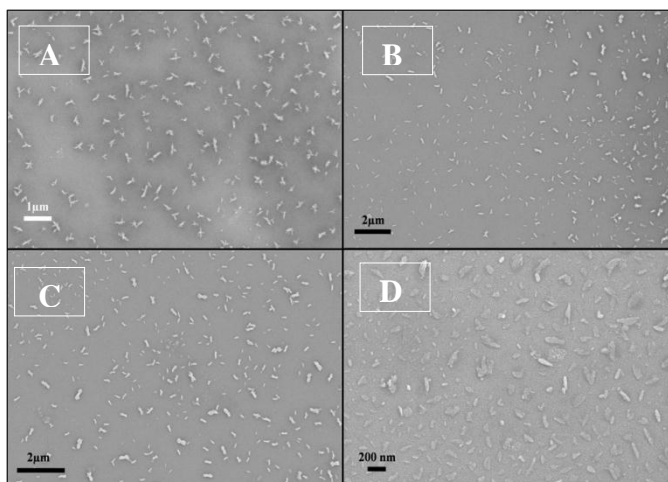


Figure 29. FESEM images for 4*R*-peptides (A) **6** 4*R*-Hyp₉, (B) **13** (4*R*-Hyp₉-C₁₂), (C) **14** 4*R*-Hyp₉-C₁₄, (D) 4*R*-Hyp₉-C₁₆ in water at 300 μM.

Thus, the PPII conformation of 4*R*-polyproline peptides seen in water, results in rod type nanostructures in the size range 40-60 nm X 100-200 nm.

4.9.2 4*S*-peptides **7**, **16-18** in water

To examine the supramolecular organization of the 4*S*-oligoproline FESEM images of peptides **7**, **16-18** were recorded at 50 μM and 300 μM concentration in TFE.

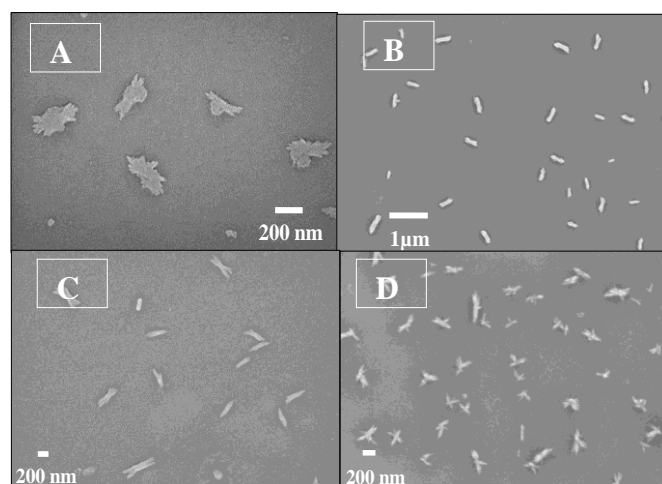


Figure 30. FESEM images for peptides (A) **7** (4*S*-hyp₉), (B) **16** (4*S*-hyp₉-C₁₂), (C) **17** (4*S*-hyp₉-C₁₄), (D) **18** (4*S*-hyp₉-C₁₆) in water at 50 μM.

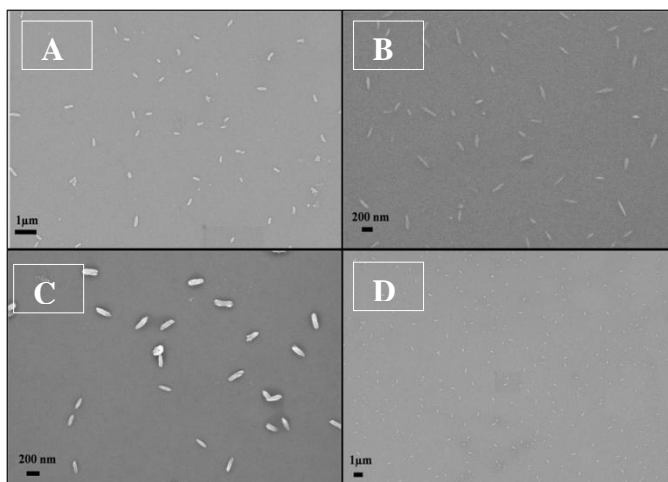


Figure 31. FESEM images for peptides (A) **7** (*4S-hyp₉*), (B) **16** (*4S-hyp₉-C₁₂*), (C) **17** (*4S-hyp₉-C₁₄*), (D) **18** (*4S-hyp₉-C₁₆*) in water at 300 μM.

FESEM images for peptides **7**, **16-18** were similar to that seen *4R*-peptides wherein they associated to form rod like microstructures at low as well as high concentrations (Figure 30, 31). This is in complete agreement with comparative CD results.

4.9.3 FESEM of *4R*-peptides 6, 13-15 in TFE

The *4R*-peptides **13-15** conjugated with different fatty acid chains show PPII conformation in TFE as seen by CD spectroscopy. The FESEM images were recorded for *4S*-peptides **6**, **13-15** in TFE (Figure 32, 33) indicated highly aggregated structures without any distinct morphologies.

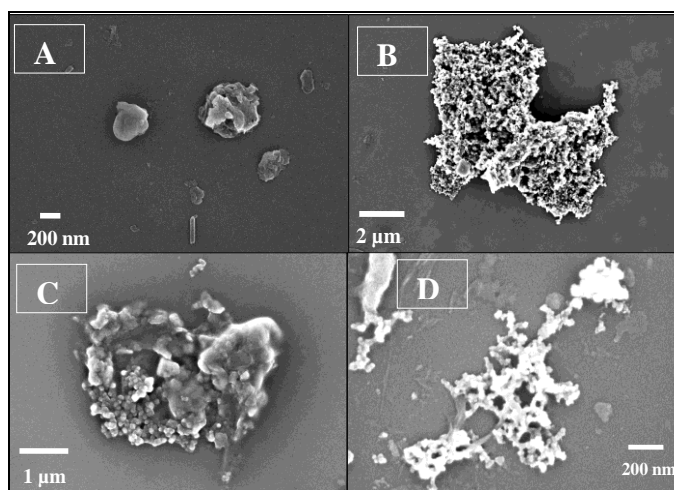


Figure 32. FESEM images for peptides (A) **6** (*4R-Hyp₉*), (B) **13** (*4R-Hyp₉-C₁₂*), (C) **14** (*4R-Hyp₉-C₁₄*), (D) **15** (*4R-Hyp₉-C₁₆*) in TFE at 50 μM.

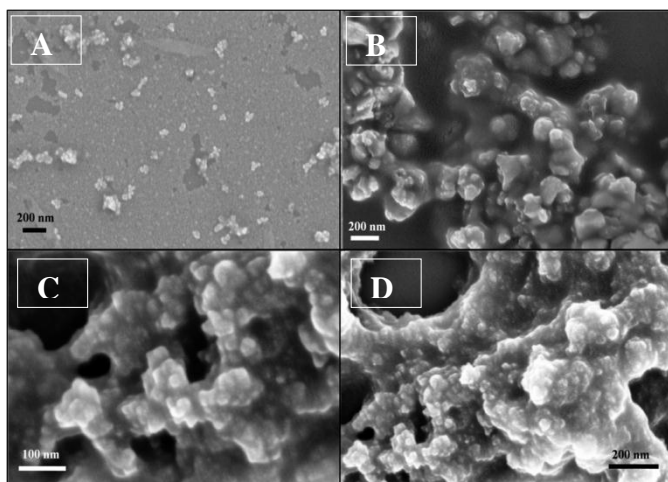


Figure 33. FESEM images for peptides (A) **6** (*4R-Hyp*₉), (B) **13** (*4R-Hyp*₉-C₁₂), (C) **14** (*4R-Hyp*₉-C₁₄), (D) **15** (*4R-Hyp*₉-C₁₆) in TFE at 300 μ M.

The hydrocarbon chains do not self assemble in TFE and the peptides do not grow into any ordered structures, but simply formed irregular clumps. The PPII conformation seen in CD spectra does not seem to translate into ordered self assembled structures in TFE.

4.9.4 FESEM of 4S-peptides 7, 16-18 in TFE

These peptides have been shown by CD spectroscopy to form β -structure in TFE through interchain H-bonding. The morphology of unconjugated 4S-peptide **7** (*4S-hyp*₉), and conjugated peptides **16** (*4S-hyp*₉-C₁₂), **17** (*4S-hyp*₉-C₁₄) and **18** (*4S-hyp*₉-C₁₆) was investigated by FESEM in TFE. The peptide **7** (*4S-hyp*₉), without fatty acid chain at N-terminus did not exhibit noticeable morphological features (Figure 34A, 35A). In contrast, the 4S-peptides **16-18** conjugated with fatty acid tail showed formation of long nanofibers (Figure 34, 35) indicating the role of fatty acid in seeding supramolecular morphologies through additional hydrophobic interactions. This demonstrates synergistic effect of hydrogen bonding in the peptide core of the 4S-polyproline peptides and hydrophobic interactions in the terminus in promoting nanofiber formation (aggregation of nanowires).

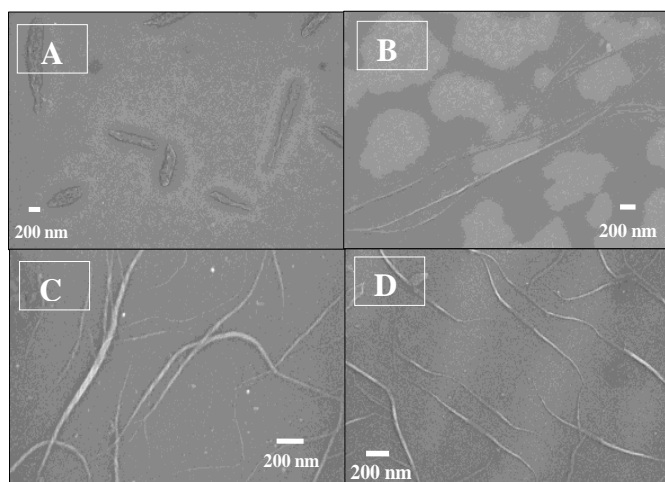


Figure 34. FESEM images for peptides (A) **7** (*4S-hyp*₉), (B) **16** (*4S-hyp*₉-C₁₂), (C) **17** (*4S-hyp*₉-C₁₄) (D), **18** (*4S-hyp*₉-C₁₆) in TFE at 50 μ M.

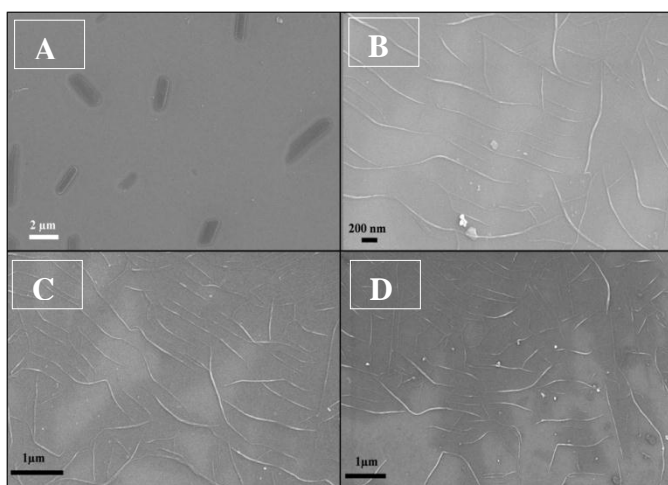


Figure 35. FESEM images for peptides (A) **7** (*4S-hyp*₉), (B) **16** (*4S-hyp*₉-C₁₂), (C) **17** (*4S-hyp*₉-C₁₄), (D), **18** (*4S-hyp*₉-C₁₆) in TFE at 300 μ M.

This unique observation indicates that the rigid, well-extended nanofiber morphology seen for 4*S*-peptides by FESEM is a result of combination of interactions involved to stabilize β -structure. These results demonstrate that the presence of fatty acid chains affects the morphology of peptides in TFE. The formation of nanofibers cannot simply be attributed to hydrogen bonds, since 4*S*-peptide **7** without fatty chain does not show nanofibers. The hydrophobic aliphatic tail at N-terminus of one peptide chain makes the nanofiber assembly stable by hydrophobic interactions of alkyl tail attached to another peptide chain (Figure 36).

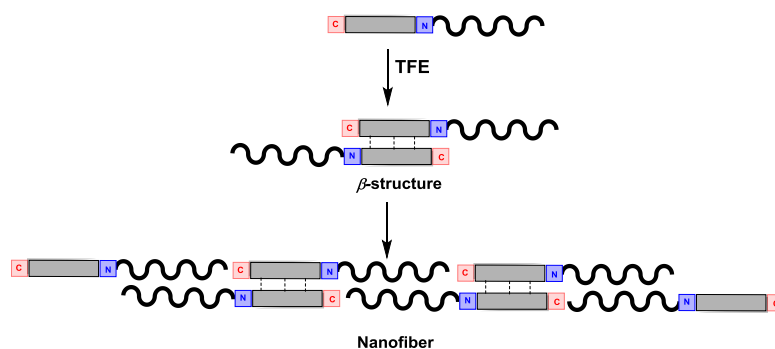


Figure 36. Proposed self assembly of β -structure to nanofibers.

This continuous assembly into a long fiber is possible only in antiparallel orientation of two peptide strands. The formation of elongated self-assembled aggregates can be explained by the propagation of hydrophobic interactions along the axis of the fiber (Figure 34, 35) which synergistically stabilizes the H-bonded β -structure arrangement in TFE (Figure 36).

4.10 FT-IR Studies

The antiparallel and parallel β -sheets are two of the most abundant secondary structures found in proteins and variety of vibrational and electronic spectroscopic methods have been employed to distinguish the antiparallel and parallel β -sheets.³¹ The amide I IR-absorption has been widely used to distinguish different secondary structures. The position of amide I band around $\sim 1650\text{ cm}^{-1}$ corresponds to α -helix, $1640\text{--}1650\text{ cm}^{-1}$ corresponds to random coil and band $\leq 1640\text{ cm}^{-1}$ and $\geq 1680\text{ cm}^{-1}$ corresponds to β -structure.³²

4.10.1 FT-IR studies of peptides 7, 10-13

Both β -structures are distinguishable because only the antiparallel β -sheets are characterized by a large splitting of the amide I mode caused by interstrand interactions.³³ FT-IR absorption spectra distinguish the anti-parallel orientation from other secondary structures of which the amide I band consists of overlapped components forming a single band at a frequency higher than the characteristic low-frequency β -sheet peak at $1620\text{--}1630\text{ cm}^{-1}$. A characteristic intense low-frequency peak around $1620\text{--}1630\text{ cm}^{-1}$ and a weaker high-frequency peak at $1680\text{--}1690\text{ cm}^{-1}$ are signatures that the protein contains antiparallel β -sheet polypeptide segments³³⁻³⁴ while

characteristic absorption bands for the parallel β -sheet are observed at 1626–1639 cm^{-1} (strong) and close to 1675 cm^{-1} (weak).³⁵

In order to support the formation of β -structure by an independent technique, FT-IR spectroscopic studies were carried out for 4*S*-peptide **7** (4*S*-hyp₉), **10** (4*S*-hyp₉-Ds), **11** (4*S*-hyp₉-Trp) and **10** (Trp-4*S*-hyp₉-Ds) in TFE.

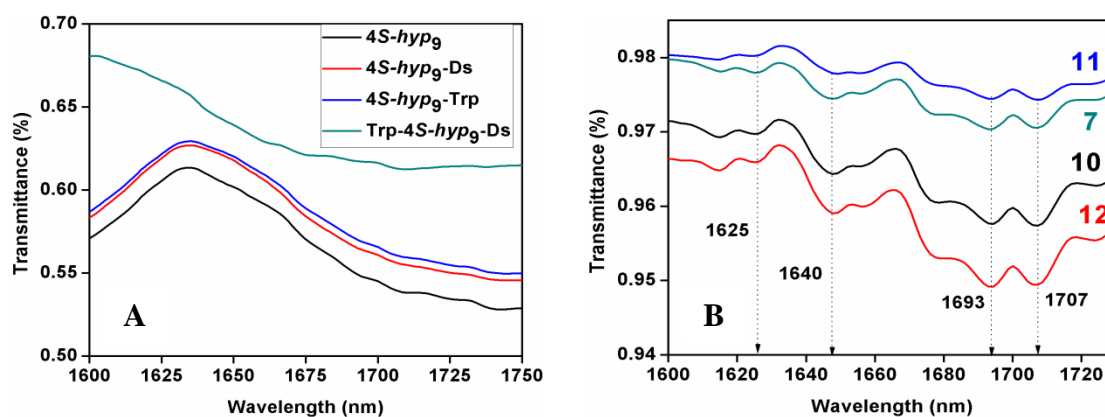


Figure 37. FT-IR spectra of peptide **7**, **10-12** from 1600 cm^{-1} to 11730 cm^{-1} , (A) Water and (B) TFE.

It is seen from Figure 36 that for the all peptides **7**, **10-12**, the amide I bands were not observed in 1600 cm^{-1} and 1700 cm^{-1} region but in TFE, band at 1625 cm^{-1} (weak), 1640 cm^{-1} (strong), and 1693 cm^{-1} were observed (Figure 37), which clearly suggests the formation of *anti*-parallel β -structure. This provides additional support to conclusion from fluorescence and FESEM image data for antiparallel antiparallel β -structure formation in 4*S*-peptides.

4.12 Discussion

It is demonstrated in Chapter 3 that 4*S*-peptide **7** (4*S*-hyp₉) adapts a non-classical β -structure in TFE unlike 4*R*-substituted polyproline peptides that do not show β -structure. It is recalled from literature that unsubstituted polyproline peptides form PPI structure in alcohol/hydrophobic medium. The β -structure arises from *interchain* hydrogen bonds involving 4*S*-OH and carbonyl (amide), which are broken in water and rearranged to *intramolecular* H-bonding that favors the PPII form *via* enriching the *trans* amide geometry. Such *interchain* H-bonds are possible only when 4-OH/NH₂ and 2*S*-CO substituents are in *cis* disposition; since *trans* 4*R*-OH/NH₂ prolyl peptide do not form β -structure.

To delineate the parallel or antiparallel orientation of two strands in β -structure, a pair of FRET probes (dansyl and tryptophan) was introduced into the peptides with dansyl at N-terminus in peptide **11** (4*S*-hyp₉-Ds) and tryptophan at the N-terminus in another peptide (**10**, 4*S*-hyp₉-Trp). Further, both components of FRET pair were introduced into same peptide chain (dual labeled) with dansyl at N-terminus and a tryptophan at C-terminus in peptide **12** (Trp-4*S*-hyp₉-Ds). These terminal modifications either alone (**10**, **11**) or together (**12**) do not perturb the PPII conformation in water and β -structure in TFE, as confirmed by CD spectra of each of these peptides individually as well as mixing the FRET pair peptides in water and TFE respectively.

In FRET experiments, the concentration of either donor or acceptor peptide was kept constant, the second component peptide was added in 0.5 or 1.0 equivalent and the signal from the emission of acceptor (dansyl) was recorded at the excitation frequency (287 nm) of donor (tryptophan).

Increasing amount of acceptor peptide **10** (4*S*-hyp₉-Ds) (Figure 38 A), was added to the constant amount of donor peptide **11**(4*S*-hyp₉-Trp) and vice versa. Samples were excited at 287 nm (tryptophan absorption) recorded and did not show any emission from acceptor dansyl fluorophore at 540-560 nm. The non-observance of FRET signal can be attributed to an antiparallel orientation of two strands with the FRET components at opposite termini. Upon excitation of tryptophan at 287 nm, fluorescence was observed only at tryptophan emission 351 nm (Figure 38). Same result was observed in reverse experiment when donor was added to acceptor.

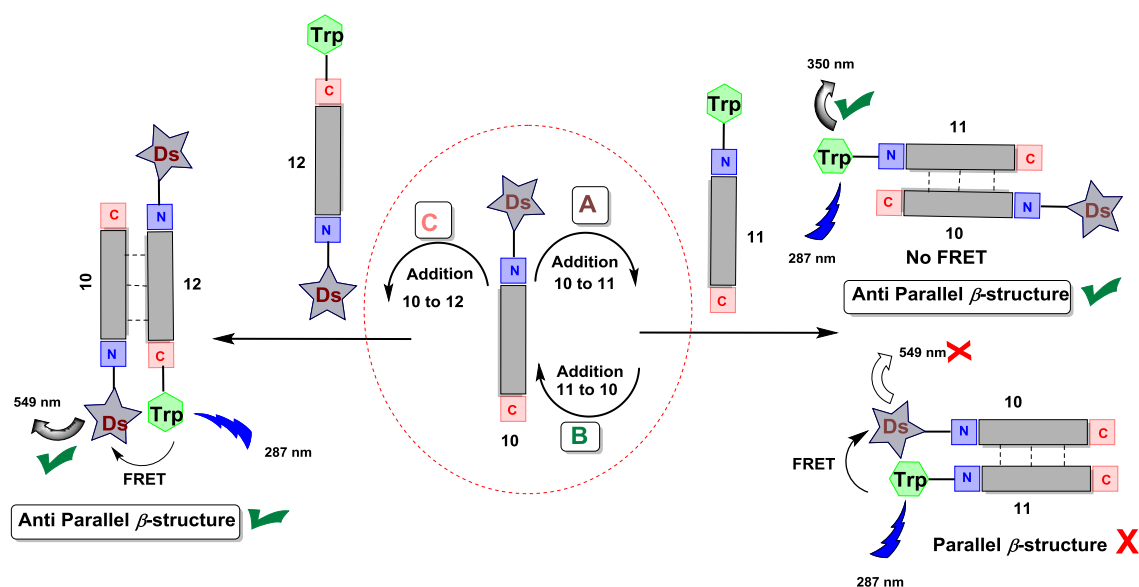


Figure 38. Predicting β -Structure based on FRET signal (A) addition of acceptor **10** (4*S*-hyp₉-Ds) to donor **11** (4*S*-hyp₉-Trp), (B) addition of donor **10** (4*S*-hyp₉-Trp) to acceptor **11** (4*S*-hyp₉-Trp), (C) addition of acceptor **10** (4*S*-hyp₉-Ds) to dual labeled peptide **12** (Trp-4*S*-hyp₉-Ds).

In order to provide a positive proof, the acceptor **11** (4*S*-hyp₉-Ds) added to the donor-acceptor hybrid peptide **12** (Trp-4*S*-hyp₉-Ds), FRET signal from dansyl emission at 550 nm (Figure 38C), was seen upon excitation of donor tryptophan at 287 nm. This can be explained only when peptide **11:12** associates in an antiparallel orientation. Since the hybrid peptide **12** alone does not emit at dansyl upon tryptophan excitation, the observed dansyl emission seen is not from intrachain FRET, but from *interchain* transfer (Figure 38C), in antiparallel fashion. All results are summarized in Table 2.

Table 2. Summary of FRET Experiments.

Expt No	Addition of peptide X (diff. conc.)→Y (const)	Excitation (nm)	Observed emission (nm)	Orientation of two strands
A	10 (4 <i>S</i> -hyp ₉ -Ds) to 11 (4 <i>S</i> -hyp ₉ -Trp)	287 (Trp)	350 (Tryptophan)	(No FRET) Antiparallel
B	11 (4 <i>S</i> -hyp ₉ -Trp) to 10 (4 <i>S</i> -hyp ₉ -Ds)	287 (Trp)	350 (Tryptophan)	(No FRET) Antiparallel
C	10 (4 <i>S</i> -hyp ₉ -Ds) to 12 (4 <i>S</i> -hyp ₉ -Ds)	287 (Trp)	549 (Dansyl)	(FRET) Antiparallel

The antiparallel disposition of β -structure of 4*S*-polyprolyl peptides seen in TFE is further substantiated from morphological features of nano-structure formed visualized through FESEM images of their fatty acid conjugates. The hydrophobic interactions among the chains are superimposed on the interchain hydrogen bonding in β -structure. Only the 4*S*-peptides-lipid conjugates that show β -structure and exhibit nanofiber structures while those from 4*R*-peptides remains as rods. These nanostructures arise from an antiparallel arrangement in which fatty acid chains from opposite strands can hydrophobically interact leading to continuous extension of structures to form nanofibers. A parallel arrangement of strands will remain as non-extendible rods. Peptides or proteins with one or more β -structure strands are known to exhibit the extraordinary assemblies into long, fibrillar nanostructures via intermolecular hydrogen bonding.³⁶

Polyproline peptides adopt conformationally well-defined left-handed polyproline II (PPII) helix in water and their conjugates with desired functionality are known for their good solubility in both aqueous and organic solvents and further modulating their assembly.³⁷ Single tail peptide-amphiphiles (PAs) along with other peptide-based self-assembling nanomaterials are a new class of biomaterials. β -sheet formation between the peptide region of a molecule should play a crucial role in directing the self-assembly into nanofibers as opposed to spherical micelles or vesicles.³⁸

Polyproline peptides are easily modifiable within the molecular structure, such as the different lengths of the conjugate at N-terminus and the absolute configuration of stereocenters at C4 position of proline. Such modifications allow for tuning the supramolecular aggregation which dictates the antiparallel orientation of two strands in β -structure (Figure 39). The short length rods are a consequence of the aggregation from of mere PPII form in water and in TFE. This hierarchical self-assembly demonstrates that increasingly ordered supramolecular structures are formed with increasing lengths of the fatty acid in conjugates.

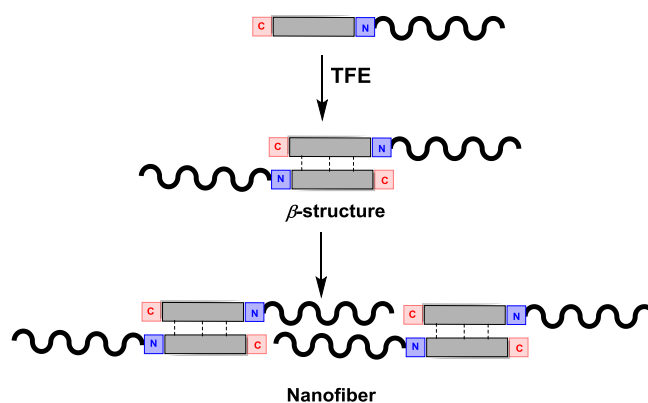


Figure 39. Predicting β -Structure based on hydrophobic interactions: Antiparallel β -structure leads to nanofibers.

4.13 Conclusion

In conclusion, it is shown that peptides composed of 4*S*-hydroxyproline (*hyp*) adapt an unusual β -structure in TFE unlike unsubstituted polyproline peptides which prefer the PPI form in hydrophobic/fluorinated media. The 4*R*-substitution retains PPII form in TFE unlike the reported unsubstituted proline peptides that show PPI form. The self-assembled β -structure arises from *interchain* association of two polyproline peptide strands.

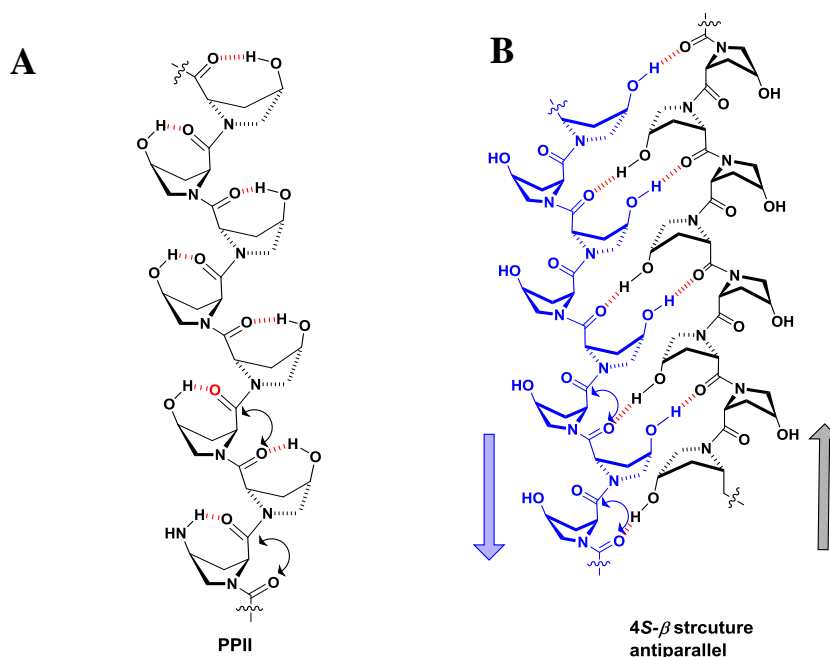


Figure 39. (A) polyproline II structure in water (Intramolecular H-bonding), (B) Predicted antiparallel β -structure (Intermolecular H-bonding).

FRET between fluorescent tags provided proof of antiparallel orientation of the two strands in TFE. β -structure observed in 4S-peptides because of association of two polyproline strands through *interchain* H-bond and addition of fatty acid tail at the end of these peptides formed elongated fibers. The formation of fiber is possible only in the antiparallel orientation of two strands in β -structure (Figure 39B).

The current results add a new design principle to a growing repertoire of strategies for engineering peptide secondary structural motifs to create new biomaterials and nanoassemblies.³⁰ It increases the scope of potential applications to which polyproline peptides can be applied including models for β -sheets or collagen. The present findings will provide additional basis for the manipulations of the polyproline peptides nanostructure and will lead to the development of new tunable nanostructured materials with additional control structural elements.

4.14 Experimental

4.14.1 Peptide synthesis

All peptides were synthesized manually in a sintered vessel equipped with a stopcock. The readily available Rink amide resin with loading value 0.5-0.6 mmol/g was used and standard Fmoc chemistry was employed. The resin bound Fmoc group was first deprotected with 20% piperidine in DMF and the coupling reactions were carried out using *in situ* active ester method, using HBTU as a coupling reagent and HOBt as a recemization suppresser and DIPEA as a catalyst. All the materials used were of peptide synthesis grade (Sigma-Aldrich) and was used without further purification. Analytical grade DMF was purchased from Merck (India) and was distilled over P₂O₅ under vacuum at 45°C, stored over 4Å molecular sieves for 2 days before using for peptide synthesis.

4.14.1a Resin functionalization

The resin (2',4'-dimethoxyphenyl-Fmoc-aminomethyl)-phenoxy resin, (100 mg) was taken in sintered vessel (25 mL) and rinsed with of dry DCM (5 mL) and filtered. The process was repeated 3-4 times and the resulting resin was kept in DCM (10 mL, for 2 h) for swelling. The solvent was removed and the resin was rinsed 3 times with dry DMF and kept in dry DMF (10 mL, for 2 h) for swelling before the first coupling. The deprotection of Fmoc group attached to the resin was done with 20% piperidine in DMF (3x5 mL) before proceeding for first amino acid coupling. The resin was

- Washed and swollen in dry DCM for at 2 h.
- Washed and swollen with dry DMF for 2 h.
- Coupled of 1st amino acid with C-terminus of peptide.

4.14.1b General method for solid phase peptide synthesis

All peptides were assembled on solid phase method by sequential amino acid coupling. Protected amino acids were well dried over P₂O₅ in vacuum desiccator before coupling. Fmoc protecting group was used for main chain amino group. The *t*-Boc protection was used for side chain amine protection and cleaved with 20% TFA in DCM for final cleavage of peptide from the resin. The peptide obtained after cleavage was stirred in 95% TFA in DCM for 2 h for complete deprotection *t* Boc.

4.14.1c *Synthesis protocol for solid phase synthesis*

The resin was pre-swollen overnight and the following steps were performed for each cycle.

- Wash with DMF 4 x 5 mL
- Deprotect Fmoc with 20% piperidine in DMF 2 x 5 mL (15 min for each)
- Wash with DMF 3 x 5 mL, MeOH 3 x 5 mL and DCM with 3 x 5 mL
- Test for complete deprotection (chloranil test)
- Coupled reaction with amino acid, DIPEA, HOBT and HBTU (3 eq.) in DMF (1 mL)
- Repeat the coupling reaction in NMP for better yield
- Test for completion of coupling reaction (chloranil test)

This cycle was repeated for every amino acid.

4.14.1d *General procedure for peptide couplings on Rink Amide Resin*

Fmoc-AA-OH (3 eq), HBTU (3 eq) and HOBT (3 eq) dissolved in DMF/NMP followed by *i*Pr₂NEt (7-8 eq) were added to the amino-functionalized resin in DMF. The mixture was kept for 2 h and bubbled with N₂ during last 5 min and washed with DMF (3x), MeOH (3x) and DCM (3x). The loading value for peptide synthesis is taken as 0.5~0.6.

4.14.1e *General procedure for Fmoc deprotection*

20% Piperidine in DMF was added to the resin and the reaction mixture was kept for 15 min, drained and the piperidine treatment was repeated 3 times. Finally the resin was washed with DMF (3x), MeOH (3x) and DCM (3x).

4.12.1f *Chloranil test*³⁹

This sensitive test is used for reliable detection of secondary amino groups but it will also detect primary amines. A few beads of resin were taken in a small test tube and were washed with methanol. To this of 2% acetaldehyde in DMF and 2% chloranil in DMF (5 drops each) were added. After a short mixing, the mixture was left at room temperature for 5 min and the beads inspected. A dark blue to green colour on by beads

indicates a positive test (presence of NH group). A colourless to yellowish beads indicates then the test to be negative.

4.14.1g General procedure for acetylation

Triethylamine (20 eq, 1 mL) and acetic anhydride (20 eq, 1 mL) were added to the resin in DMF (\approx 100 mM). The mixture was kept for 1 h followed by bubbling with N₂ for 5 min and washed with DMF (3x), MeOH (3x) and DCM (3x).

4.14.1h Preparation of resin with peptide for cleavage

After the final coupling/acetylation, the resin was washed sequentially with DMF (5 x 10 mL), DCM (5x10 mL), toluene (5x10 mL) and finally with methanol (5x10 mL) and dried with nitrogen gas for 3 min. The resin in sintered flask was dried in a vacuum desiccator over P₂O₅.

4.14.1i General procedure for cleavage of peptides from the solid support

The dry peptide-resin (20 mg) was taken in round-bottomed flask to which of 20% TFA in DCM (10 mL) and Triisopropylsilane (as scavengers) (2-3 drops) were added. The resulting mixture was kept for 2 h by gentle shaking. The mixture was filtered through a sintered funnel and the resin was washed with 3x5 mL of above solution. The filtrate was collected in pear shape round-bottom flask and evaporated under reduced pressure. The resin was washed with MeOH (3X5 mL) and the washings were evaporated to dryness. The crude peptide obtained containing a N⁴-*t*-Boc group, was deprotected by stirring the peptide solution with 95% TFA in DCM (10 mL) for 2 h. The TFA: DCM mixture was removed under reduced pressure. The residue obtained was dissolved in anhydrous methanol (0.4 mL) to which anhydrous diethyl ether (4 x 1.5 mL) was added. The off-white precipitate obtained was centrifuged. The precipitation procedure was repeated twice to obtain peptide as a colourless powder.

4.15 High performance liquid chromatography (HPLC)

Peptides (**10-12**) were purified by reverse phase-HPLC on Waters 600 equipped with 2998-Photodiode array detector (PDA). Semi-preparative RP-C18 columns (250x10 mm, 10 μ m) of was used for peptides. The solvent system comprised of MeCN:Water (5:95) with 0.1% TFA for solution A and for solution B MeCN: Water (50:50), 0.1%

TFA. A gradient of 0-100% at a flow rate of 3 mL/min was used to elute the peptide and the eluant was monitored at 220 nm.

Peptides (**13-18**) were purified by reverse phase-HPLC on Waters 600 equipped with 2998-Photodiode array detector (PDA). Semi-preparative RP-C18 columns (250x10 mm, 10 μ m) of was used for peptides. The solvent system comprised of MeCN:Water (50:50), 0.1% TFA for solution A and for solution B MeCN:water (5:95) with 0.1% TFA. A gradient of 0-100% at a flow rate of 3 mL/min was used to elute the peptide and the eluant was monitored at 220 nm.

The peak corresponding to the peptide was collected and the fractions were freezed. Subsequently these peptides were concentrated by using speed vacuum. The purity of the final peptides were further analyzed on the Merck LiChrospher 100 RP-18 (250 x 4 mm, 5 μ M) column by using a gradient flow of 0 to 100% B in 30 min at a flow rate of 1.5 mL/min. The absorbance of the eluant was monitored at its corresponding wavelength and the purity was obtained from the integrator output. The purities of the hence purified peptides were found to be more than 95%.

4.16 MALDI-TOF characterization

MALDI-TOF mass spectra were obtained on either Voyager-Elite instrument (PerSeptive Biosystems Inc., Farmingham, MA) equipped with delayed extraction or on Voyager-De-STR (Applied Biosystems) instrument. Sinapinic acid and α -cyano-4-hydroxycinnamic acid (CHCA) both were used as matrix for peptides of which CHCA was found to give satisfactory results. A saturated matrix solution was prepared with typical dilution solvent (50:50:0.1 Water:MeCN:TFA) and spotted on the metal plate along with the oligomers. The metal plate was loaded to the instrument and the analyte ions are then accelerated by an applied high voltage (15-25 kV) in reflector mode, separated in a field-free flight tube and detected as an electrical signal at the end of the flight tube. HPLC purified peptides were characterized through this method and were observed to give good signal to noise ratio, mostly producing higher molecular ion signals.

4.17 Circular dichroism (CD) spectroscopy

CD spectrometric study was carried out on JASCO J-715 spectropolarimeter using cylindrical, jacketed quartz cell (10 mm path length), which was connected to Julabo-

UC-25 water circulator. For reproducible data, each set of spectra were measured using at least three individually prepared solutions. CD spectra were recorded using a spectral bandwidth of 1.0 nm at 25 °C with a time constant of 1 s and a step resolution of 1 nm. All the spectra were corrected for respective buffer condition and are typically averaged over 5-10 scans. The spectra are the result of 5-10 accumulations. A quartz cell with a path length of 1 cm was used with solutions containing approximately 0.9 mL (100 μ M) peptide solutions. For the spectra in buffer the blank spectrum of the solution was subtracted. All samples were equilibrated for at least 10 h before measurement except some TFE experiment.

Resolution: 1 nm
Band width: 1.0 nm
Sensitivity: 100 mdeg
Response: 1 sec
Speed: 100 nm/min
Accumulation: 5-10

All peptides had same concentration (200 μ M) for CD measurements done in Na-phosphate buffer (pH 7.2). The data processing and curve fitting were performed using Origin 8.0 software.

All spectra were collected at 25 °C with a 1 nm resolution and a scan rate of 100 nm min⁻¹. Spectra are the averages of 5 scans. The spectra could not be collected below a wavelength of 210 nm because of the absorbance properties of the salt solution.

4.18 Fluorescence measurement of peptide in various solvents

Fluorescence measurements of peptide conjugated with fluorescent dye were performed on Horiba Jobin Yvon Fluorolog 3 spectrophotometer. The samples for fluorescence spectra were prepared by mixing calculated amounts of polyproline peptides in sodium phosphate buffer (pH 7.2, 5 mM) and TFE. The prepared samples were used to record fluorescence spectra in a quartz cell (Hellma, path length 1.0 cm) at ambient temperature. The λ_{exc} 287 for tryptophan and 330 nm for dansyl with scan range from 300 nm to 580 nm; The excitation slit width of 3 nm and emission slit width of 7 nm were used.

4.18. Fluorescence resonance energy transfer (FRET) studies in TFE

Horiba Jobin Yvon Fluorolog 3 spectrophotometer was used to measure the fluorescence intensity of FRET. The samples for FRET studies were prepared by mixing calculated amounts of polyproline peptides in Trifluoroethanol (TFE). To avoid the dilution effect, calculated amount of peptides were taken into eppendorf from stock solution and water was evaporated by using speed vacuum and desired solvent was added. Intensity of FRET was measured with the exciting wavelength of 295 nm and scan range from 310 nm to 580 nm. The excitation slit width of 3 nm and emission slit width of 7 nm were used. Each sample was measured three times in parallel to be averaged.

4.19 Field Emission Scanning Electron Microscopy (FESEM)

Calculated amounts of polyproline peptides were taken into eppendorf from stock solution and water was evaporated by using speed vac. Desired solvent was added to it and solution was vortexed for 1 min and centrifuged. 5 μ L of supernatant solution was then drop casted on silicon vapor. Samples were allowed to dry at room temperature in vacuum desiccators and then coated with gold. Scanning electron microscopic imaging was performed using ZEISS ULTRA PLUS electron microscope operating at 30 kV.

4.15 References

1. Doose, S.; Neuweiler, H.; Sauer, M., Fluorescence Quenching by Photoinduced Electron Transfer: A Reporter for Conformational Dynamics of Macromolecules. *Chem.Phys.Chem.* **2009**, *10*, 1389-1398.
2. Bieri, O.; Wirz, J.; Hellrung, B.; Schutkowski, M.; Drewello, M.; Kiefhaber, T., The speed limit for protein folding measured by triplet-triplet energy transfer. *Proc. Natl. Acad. Sci. U S A* **1999**, *96*, 9597-601.
3. Chiti, F.; Dobson, C. M., Protein misfolding, functional amyloid, and human disease. *Annu. rev. biochem.* **2006**, *75*, 333-66.
4. Bemporad, F., *Folding and aggregation studies in the acylphosphatase-like family*. Firenze University Press: 2009.
5. Lifson, S.; Sander, C., Antiparallel and parallel [beta]-strands differ in amino acid residue preferences. *Nature* **1979**, *282*, 109-111.
6. Pan, K. M.; Baldwin, M.; Nguyen, J.; Gasset, M.; Serban, A.; Groth, D.; Mehlhorn, I.; Huang, Z.; Fletterick, R. J.; Cohen, F. E.; et al., Conversion of alpha-helices into beta-sheets features in the formation of the scrapie prion proteins. *Proc. Natl. Acad. Sci. U S A* **1993**, *90*, 10962-6.
7. Hardy, J.; Selkoe, D. J., The amyloid hypothesis of Alzheimer's disease: progress and problems on the road to therapeutics. *Science* **2002**, *297*, 353-6.
8. Nguyen, K. T.; King, J. T.; Chen, Z., Orientation Determination of Interfacial β -Sheet Structures in Situ. *J. Phys. Chem. B* **2010**, *114*, 8291-8300.
9. (a) Marsh, D.; Muller, M.; Schmitt, F. J., Orientation of the infrared transition moments for an alpha-helix. *Biophys. J.* **2000**, *78* (5), 2499-510; (b) Tamm, L. K.; Tatulian, S. A., Infrared spectroscopy of proteins and peptides in lipid bilayers. *Q. rev. biophys.* **1997**, *30*, 365-429.
10. (a) Overman, S. A.; Tsuboi, M.; Thomas, G. J., Jr., Subunit orientation in the filamentous virus Ff(fd, f1, M13). *J. Mol. Biol.* **1996**, *259*, 331-6; (b) Lee, S.-H.; Krimm, S., Polarized Raman spectra of oriented films of α -helical poly(L-alanine) and its N-deuterated analogue. *J. Raman Spectrosc.* **1998**, *29*, 73-80; (c) Overman, S. A.; Bondre, P.; Maiti, N. C.; Thomas, G. J., Structural Characterization of the Filamentous Bacteriophage PH75 from *Thermus*

- thermophilus by Raman and UV-Resonance Raman Spectroscopy†. *Biochemistry* **2005**, *44*, 3091-3100.
11. (a) Bechinger, B., The structure, dynamics and orientation of antimicrobial peptides in membranes by multidimensional solid-state NMR spectroscopy. *Biochim. biophys. Acta* **1999**, *1462*, 157-83; (b) Bechinger, B.; Aisenbrey, C.; Bertani, P., The alignment, structure and dynamics of membrane-associated polypeptides by solid-state NMR spectroscopy. *Biochim. biophys. Acta* **2004**, *1666*, 190-204; (c) Durr, U. H.; Yamamoto, K.; Im, S. C.; Waskell, L.; Ramamoorthy, A., Solid-state NMR reveals structural and dynamical properties of a membrane-anchored electron-carrier protein, cytochrome b5. *J. Am. Chem. Soc.* **2007**, *129*, 6670-1.
- 12.(a) Deng, W.; Cao, A.; Lai, L., Detecting the inter-peptide arrangement and maturation process of transthyretin (105–115) amyloid fibril using a FRET pair with short Förster distance. *Biochem. Biophys. Res. Commun.* **2007**, *362*, 689-694; (b) Deng, W.; Cao, A.; Lai, L., Distinguishing the cross- β spine arrangements in amyloid fibrils using FRET analysis. *Prot. Sci.* **2008**, *17*, 1102-1105.
- 13.(a) Nguyen, K. T.; Le Clair, S. V.; Ye, S.; Chen, Z., Orientation determination of protein helical secondary structures using linear and nonlinear vibrational spectroscopy. *J. phys. chem. B* **2009**, *113*, 12169-80; (b) Chen, X.; Wang, J.; Boughton, A. P.; Kristalyn, C. B.; Chen, Z., Multiple orientation of melittin inside a single lipid bilayer determined by combined vibrational spectroscopic studies. *J. Am. Chem. Soc.* **2007**, *129*, 1420-7; (c) Wang, J.; Lee, S. H.; Chen, Z., Quantifying the ordering of adsorbed proteins in situ. *J. phys. chem.. B* **2008**, *112*, 2281-90; (d) Chen, X.; Boughton, A. P.; Tesmer, J. J.; Chen, Z., In situ investigation of heterotrimeric G protein betagamma subunit binding and orientation on membrane bilayers. *J. Am. Chem. Soc.* **2007**, *129* (42), 12658-9.
14. (a) Sapsford, K. E.; Berti, L.; Medintz, I. L., Materials for Fluorescence Resonance Energy Transfer Analysis: Beyond Traditional Donor–Acceptor Combinations. *Angew. Chem Int. Ed.* **2006**, *45*, 4562-4589; (b) Jares-Erijman, E. A.; Jovin, T. M., FRET imaging. *Nat. Biotech.* **2003**, *21*, 1387-1395.
15. Lakowicz, J. R., *Principles of Fluorescence Spectroscopy*. Springer: 2007.
16. (a) Broussard, J. A.; Rappaz, B.; Webb, D. J.; Brown, C. M., Fluorescence resonance energy transfer microscopy as demonstrated by measuring the

- activation of the serine/threonine kinase Akt. *Nat. Protocol.* **2013**, *8*, 265-281; (b) Kochuveedu, S. T.; Kim, D. H., Surface plasmon resonance mediated photoluminescence properties of nanostructured multicomponent fluorophore systems. *Nanoscale* **2014**, *6*, 4966-4984.
17. Schuler, B.; Lipman, E. A.; Steinbach, P. J.; Kumke, M.; Eaton, W. A., Polyproline and the "spectroscopic ruler" revisited with single-molecule fluorescence. *Proc. Natl. Acad. Sci. U. S. A.* **2005**, *102*, 2754-2759.
18. Michalet, X.; Kapanidis, A. N.; Laurence, T.; Pinaud, F.; Dose, S.; Pflughoeft, M.; Weiss, S., The power and prospects of fluorescence microscopies and spectroscopies. *Annu. rev. biophys. biomol. struct.* **2003**, *32*, 161-82.
19. (a) Schuler, B.; Lipman, E. A.; Steinbach, P. J.; Kumke, M.; Eaton, W. A., Polyproline and the "spectroscopic ruler" revisited with single-molecule fluorescence. *Proc. Natl. Acad. Sci. U S A* **2005**, *102*, 2754-9; (b) Sahoo, H.; Roccatano, D.; Hennig, A.; Nau, W. M., A 10-A spectroscopic ruler applied to short polyprolines. *J. Am. Chem. Soc.* **2007**, *129*, 9762-72.
20. Stryer, L.; Haugland, R. P., Energy transfer: a spectroscopic ruler. *Proc. Natl. Acad. Sci. U S A* **1967**, *58*, 719-26.
21. Deng, W.; Cao, A.; Lai, L., Distinguishing the cross-beta spine arrangements in amyloid fibrils using FRET analysis. *Protein Sci* **2008**, *17*, 1102-5.
22. Stella, L.; Venanzi, M.; Carafa, M.; Maccaroni, E.; Straccamore, M. E.; Zanotti, G.; Palleschi, A.; Pispisa, B., Structural features of model glycopeptides in solution and in membrane phase: a spectroscopic and molecular mechanics investigation. *Biopolymers* **2002**, *64*, 44-56.
23. (a) Cui, H.; Webber, M. J.; Stupp, S. I., Self-assembly of peptide amphiphiles: From molecules to nanostructures to biomaterials. *Pept. Sci.* **2010**, *94*, 1-18; (b) McCloskey, A.; Gilmore, B.; Lavery, G., Evolution of Antimicrobial Peptides to Self-Assembled Peptides for Biomaterial Applications. *Pathogens* **2014**, *3*, 791-821.
24. Mandal, D.; Nasrolahi Shirazi, A.; Parang, K., Self-assembly of peptides to nanostructures. *Org. Biomol. Chem.* **2014**, *12*, 3544-3561.
25. (a) Zelzer, M.; Ulijn, R. V., Next-generation peptide nanomaterials: molecular networks, interfaces and supramolecular functionality. *Chem. Soc. rev.* **2010**, *39*, 3351-7; (b) Aida, T.; Meijer, E. W.; Stupp, S. I., Functional supramolecular

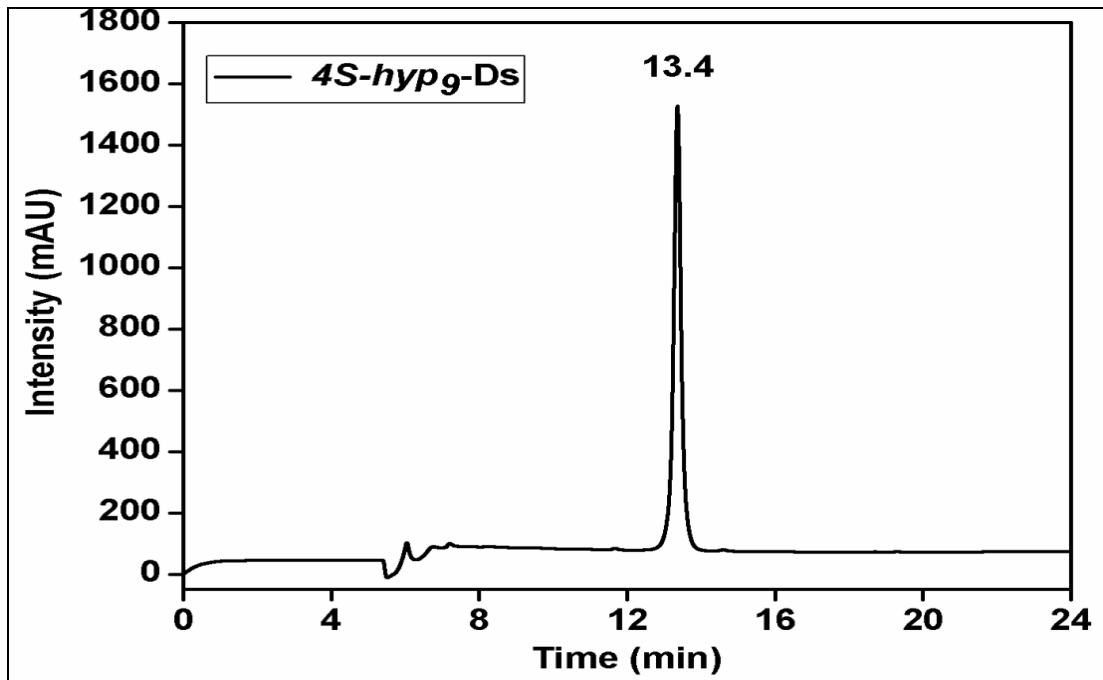
- polymers. *Science* **2012**, *335*, 813-7; (c) Hauser, C. A.; Zhang, S., Nanotechnology: Peptides as biological semiconductors. *Nature* **2010**, *468*, 516-7.
26. Subramani, K.; Ahmed, W., *Emerging Nanotechnologies in Dentistry: Processes, Materials and Applications*. Elsevier Science: 2011.
27. Lewandowska, U.; Zajaczkowski, W.; Chen, L.; Bouillièrè, F.; Wang, D.; Koynov, K.; Pisula, W.; Müllen, K.; Wennemers, H., Hierarchical Supramolecular Assembly of Sterically Demanding π -Systems by Conjugation with Oligoproline. *Angew. Chem. Int. Ed.* **2014**, *53*, 12537-12541.
28. Yoon, Y. R.; Lim, Y. B.; Lee, E.; Lee, M., Self-assembly of a peptide rod-coil: a polyproline rod and a cell-penetrating peptide Tat coil. *Chem. commun.* **2008**, *16*, 1892-4.
29. (a) Yoon, Y.-R.; Lim, Y.-b.; Lee, E.; Lee, M., Self-assembly of a peptide rod-coil: a polyproline rod and a cell-penetrating peptide Tat coil. *Chem. Commun.* **2008**, 1892-1894; (b) Lim, Y.-b.; Moon, K.-S.; Lee, M., Recent advances in functional supramolecular nanostructures assembled from bioactive building blocks. *Chem. Soc. rev.* **2009**, *38*, 925-934.
30. Sonar, M. V.; Ganesh, K. N., Water-Induced Switching of β -Structure to Polyproline II Conformation in the 4S-Aminoproline Polypeptide via H-Bond Rearrangement. *Org. Lett.* **2010**, *12*, 5390-5393.
31. (a) Richardson, J. S., The anatomy and taxonomy of protein structure. *Advances in protein chem.* **1981**, *34*, 167-339; (b) Efimov, A. V., Structural Similarity between Two-layer α/β and β -Proteins. *J. Mol. Biol.* **1995**, *245*, 402-415; (c) Hahn, S.; Kim, S.-S.; Lee, C.; Cho, M., Characteristic two-dimensional IR spectroscopic features of antiparallel and parallel β -sheet polypeptides: Simulation studies. *J. Chem. Phys.* **2005**, *123*, 084905; (d) Demirdöven, N.; Cheatum, C. M.; Chung, H. S.; Khalil, M.; Knoester, J.; Tokmakoff, A., Two-Dimensional Infrared Spectroscopy of Antiparallel β -Sheet Secondary Structure. *J. Am. Chem. Soc.* **2004**, *126*, 7981-7990.
32. (a) Surewicz, W. K.; Mantsch, H. H.; Chapman, D., Determination of protein secondary structure by Fourier transform infrared spectroscopy: a critical assessment. *Biochemistry* **1993**, *32*, 389-94; (b) Haris, P. I.; Chapman, D., Does

- Fourier-transform infrared spectroscopy provide useful information on protein structures? *Trends biochem. sci.* **1992**, *17*, 328-33.
33. Krimm, S.; Bandekar, J., Vibrational spectroscopy and conformation of peptides, polypeptides, and proteins. *Adv. protein chem.* **1986**, *38*, 181-364.
34. Susi, H.; Byler, D. M., Fourier transform infrared study of proteins with parallel beta-chains. *Arch. biochem. biophys.* **1987**, *258*, 465-9.
35. Surewicz, W. K.; Mantsch, H. H., New insight into protein secondary structure from resolution-enhanced infrared spectra. *Biochim. Biophys. Acta- Protein Struct. Mol. Enzymol.* **1988**, *952*, 115-130.
36. Cui, H.; Muraoka, T.; Cheetham, A. G.; Stupp, S. I., Self-Assembly of Giant Peptide Nanobelts. *Nano Lett.* **2009**, *9*, 945-951.
37. Lewandowska, U.; Zajaczkowski, W.; Chen, L.; Bouillière, F.; Wang, D.; Koynov, K.; Pisula, W.; Müllen, K.; Wennemers, H., Hierarchical Supramolecular Assembly of Sterically Demanding π -Systems by Conjugation with Oligoprolines. *Angew. Chem.* **2014**, n/a-n/a.
38. Paramonov, S. E.; Jun, H.-W.; Hartgerink, J. D., Self-Assembly of Peptide–Amphiphile Nanofibers: The Roles of Hydrogen Bonding and Amphiphilic Packing. *J. Am. Chem. Soc.* **2006**, *128*, 7291-7298.
39. Vojtkovsky, T., Detection of secondary amines on solid phase. *Pept. res.* **1995**, *8*, 236-7.

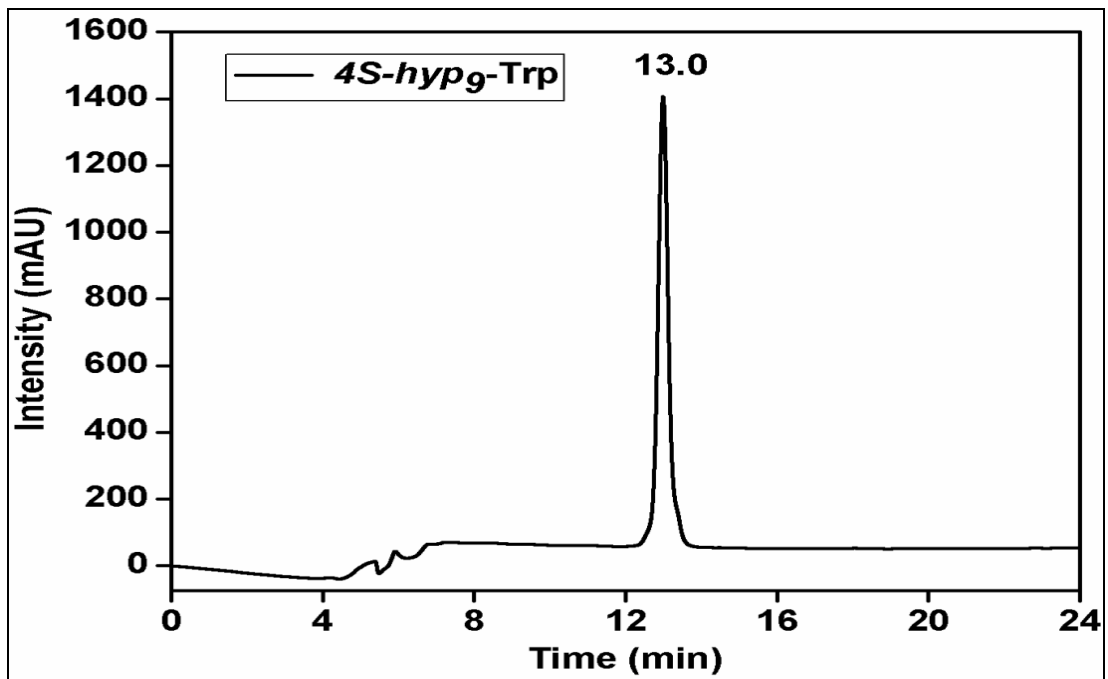
4.16 Appendix 4: Characterization data of synthesized peptides 10-18

Entry	Page No.
HPLC of Peptides (10-18)	255-259
MALDI-TOF of peptides (10-18)	259-263

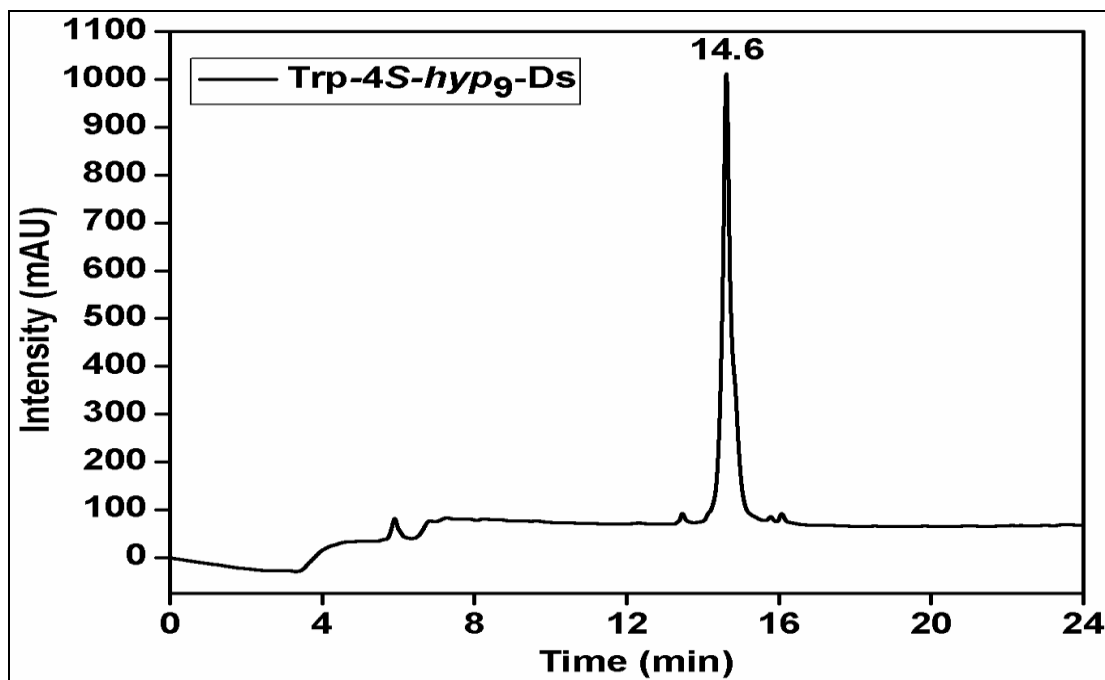
HPLC Trace of 4*S*-hyp₉-Ds



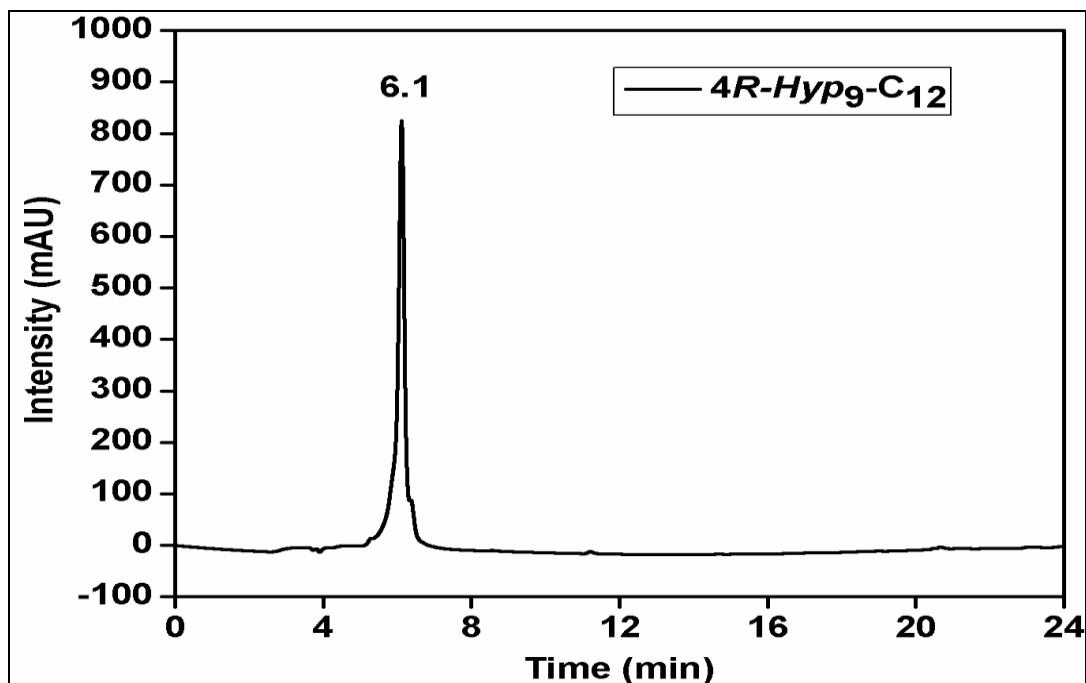
HPLC Trace of 4*S*-hyp₉-Trp



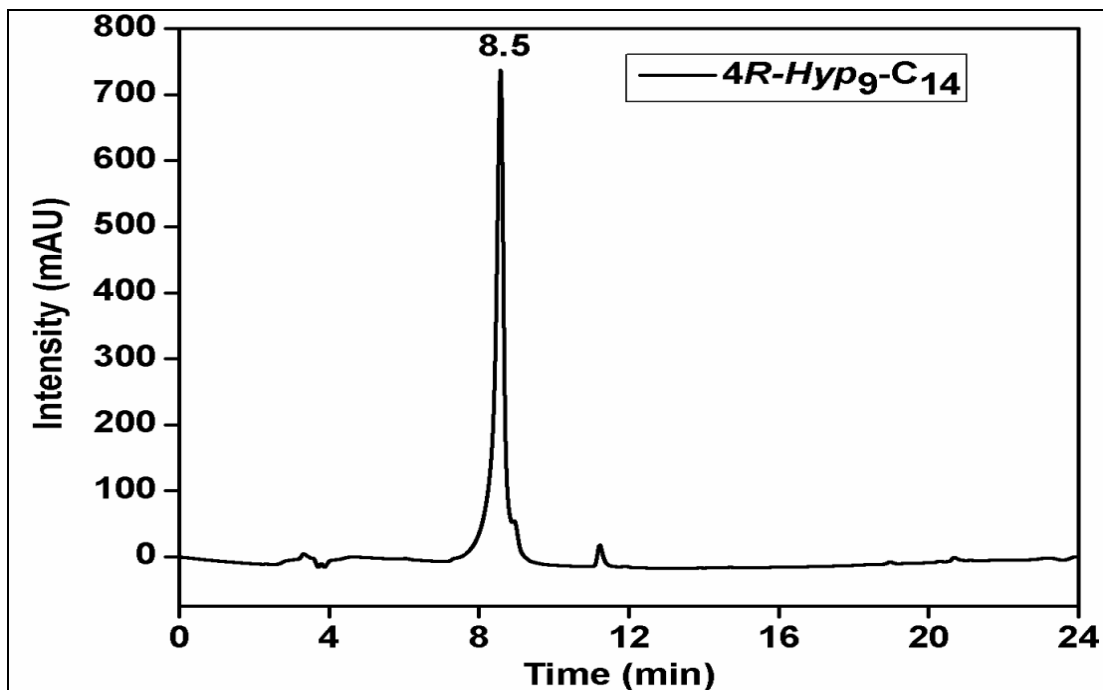
HPLC Trace of Trp-4S-hyp₉-Ds



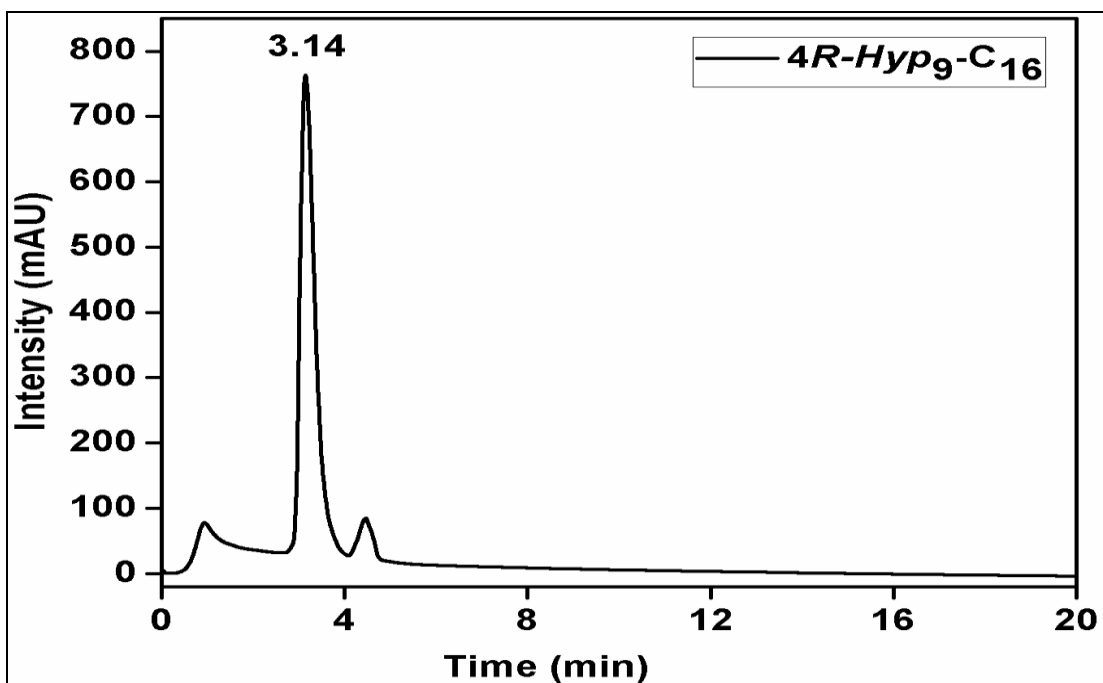
HPLC Trace of 4R-Hyp₉-C₁₂



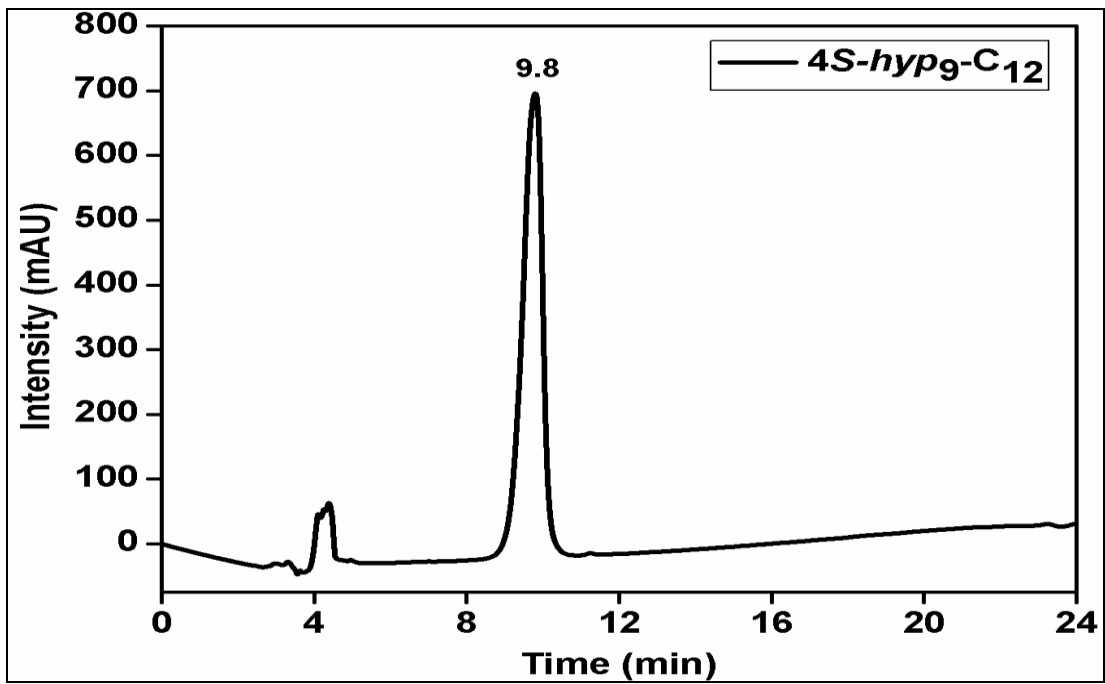
HPLC Trace of 4*R*-Hyp₉-C₁₄



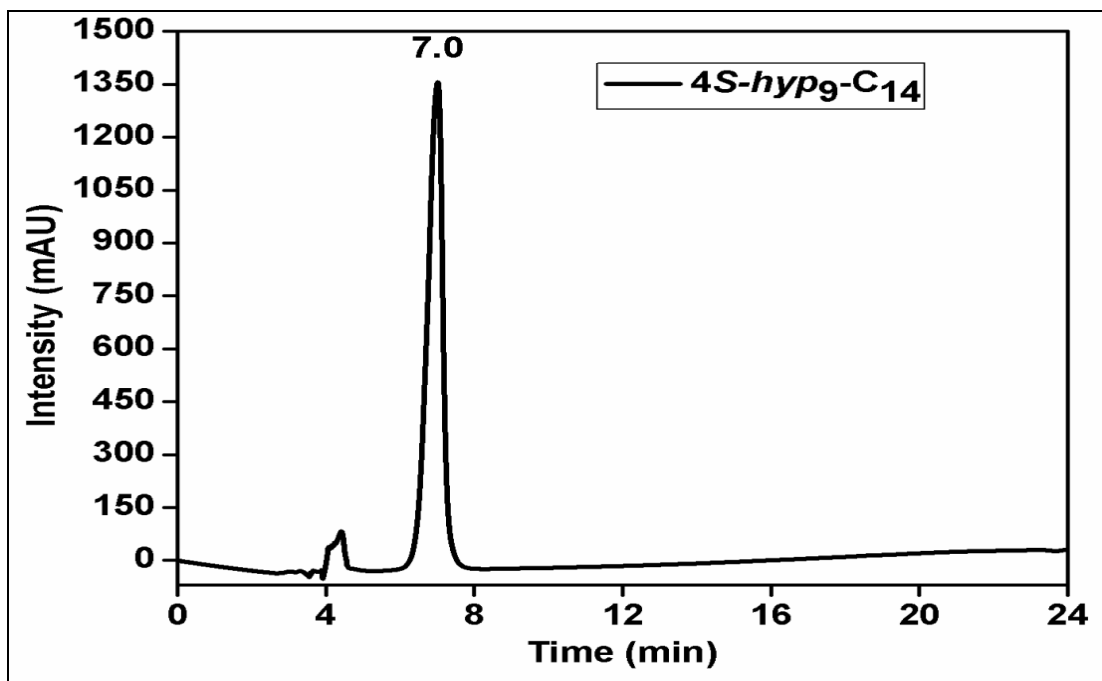
HPLC Trace of 4*R*-Hyp₉-C₁₆



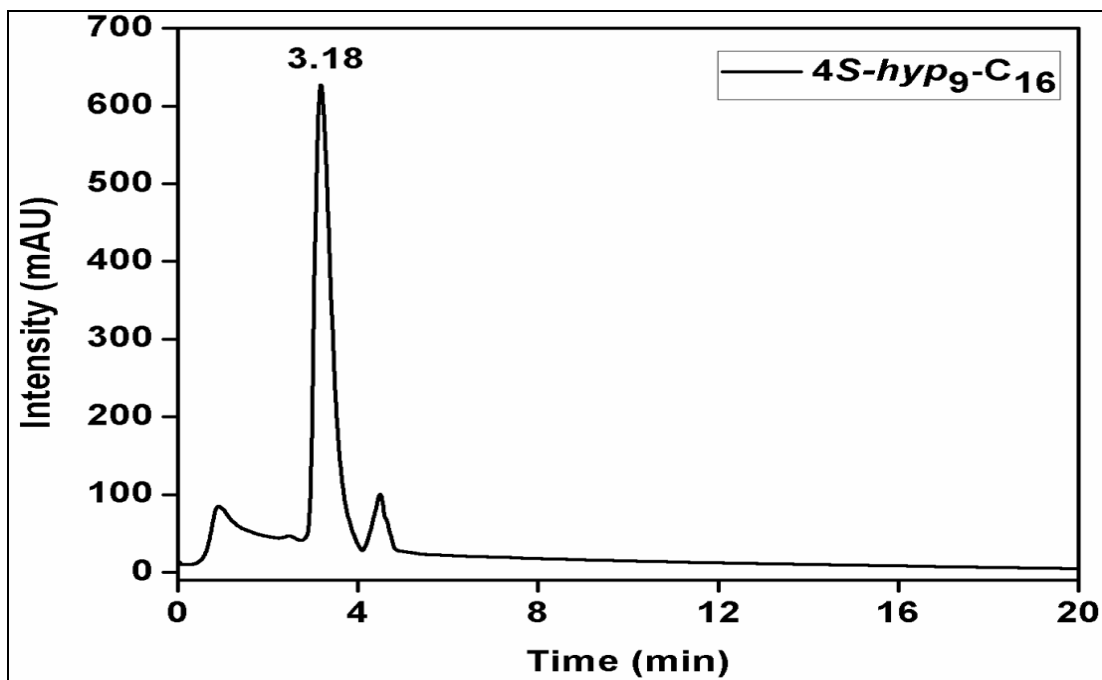
HPLC Trace of 4*S*-hyp₉-C₁₂



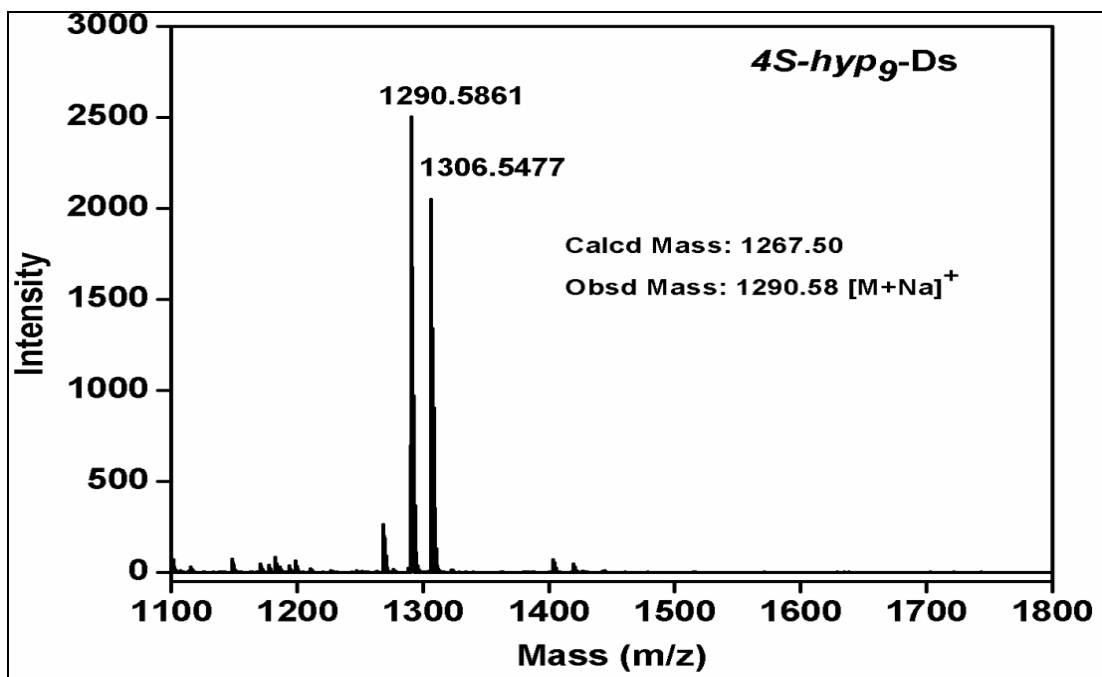
HPLC Trace of 4*S*-hyp₉-C₁₄



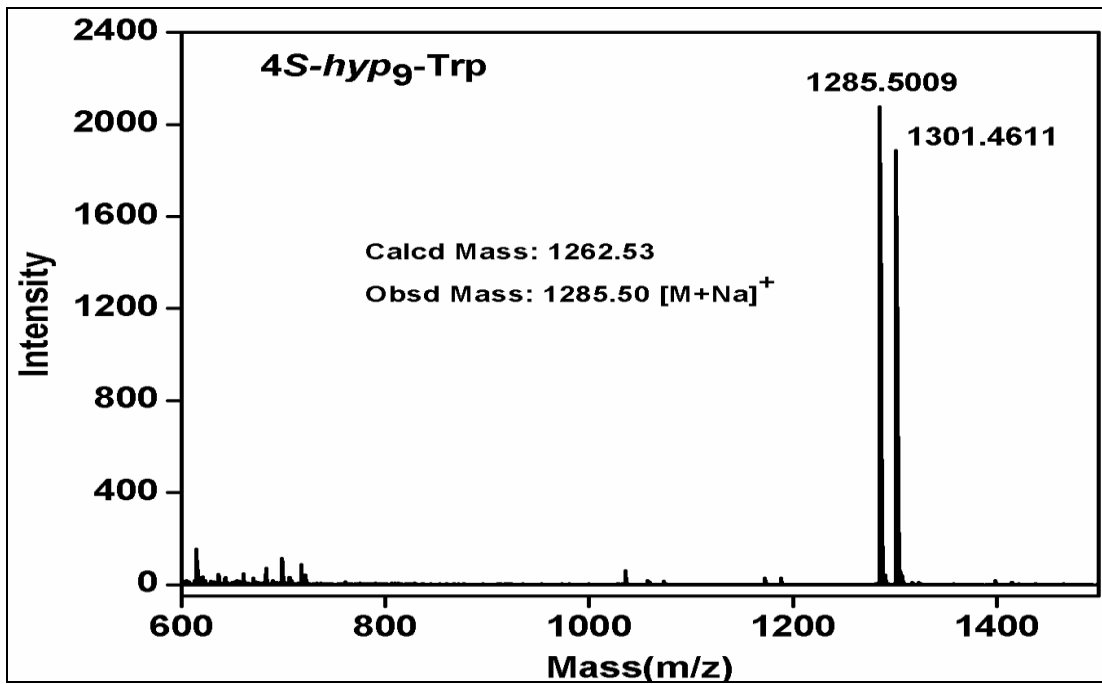
HPLC Trace of 4*S*-hyp₉-C₁₆



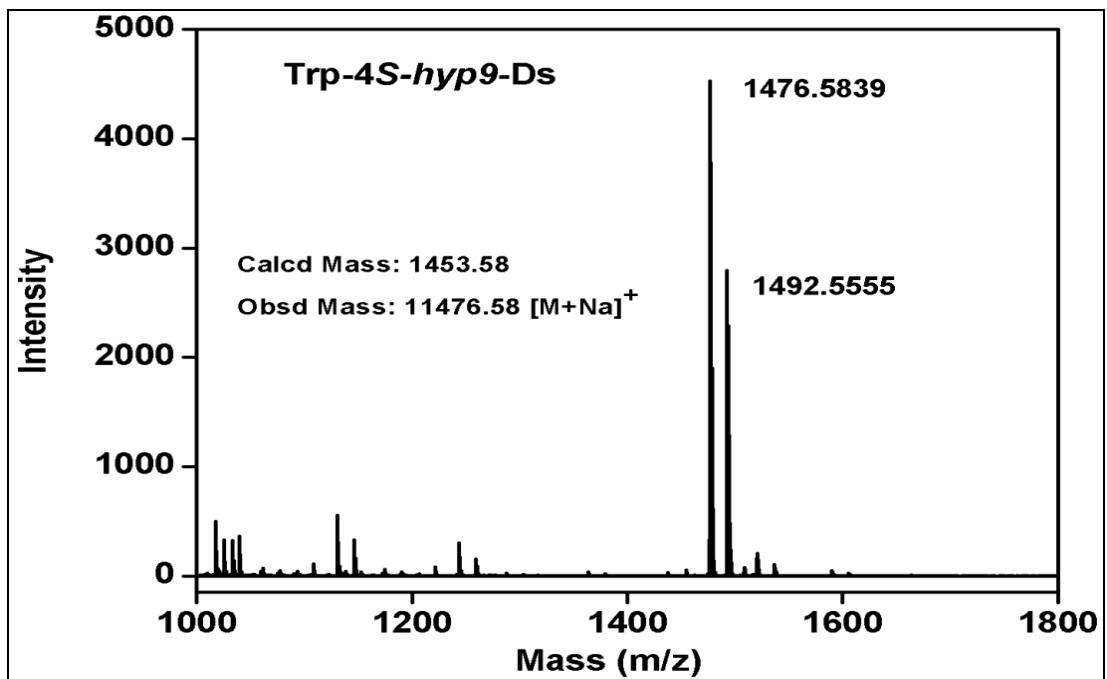
MALDI of 4*S*-hyp₉-Ds



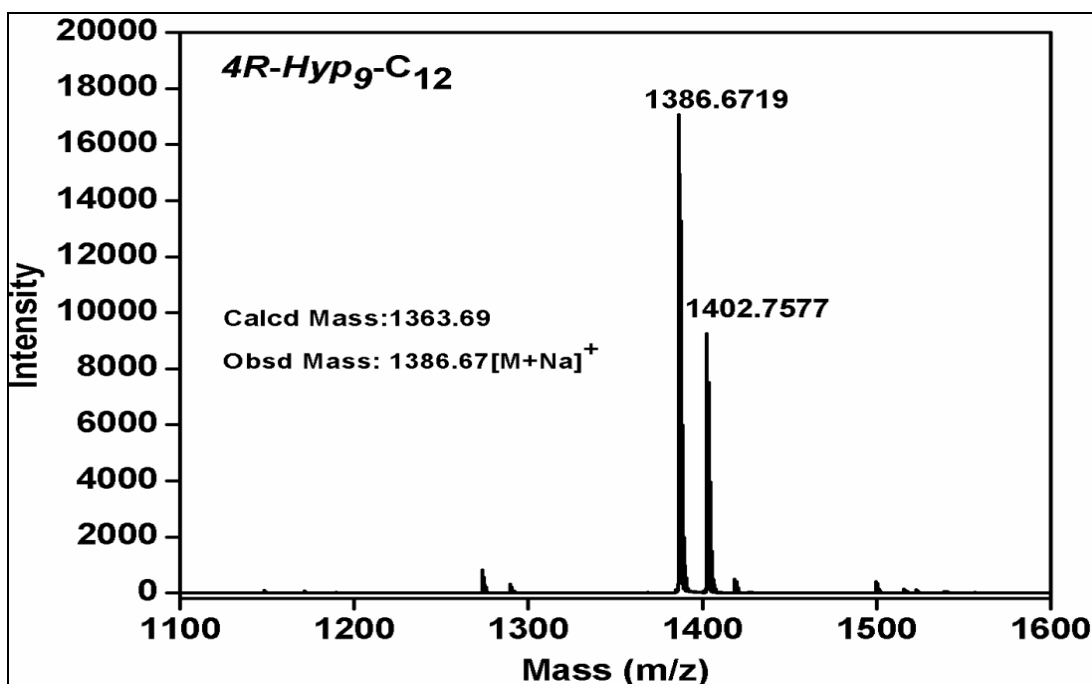
MALDI-TOF of 4S-hyp₉-Trp



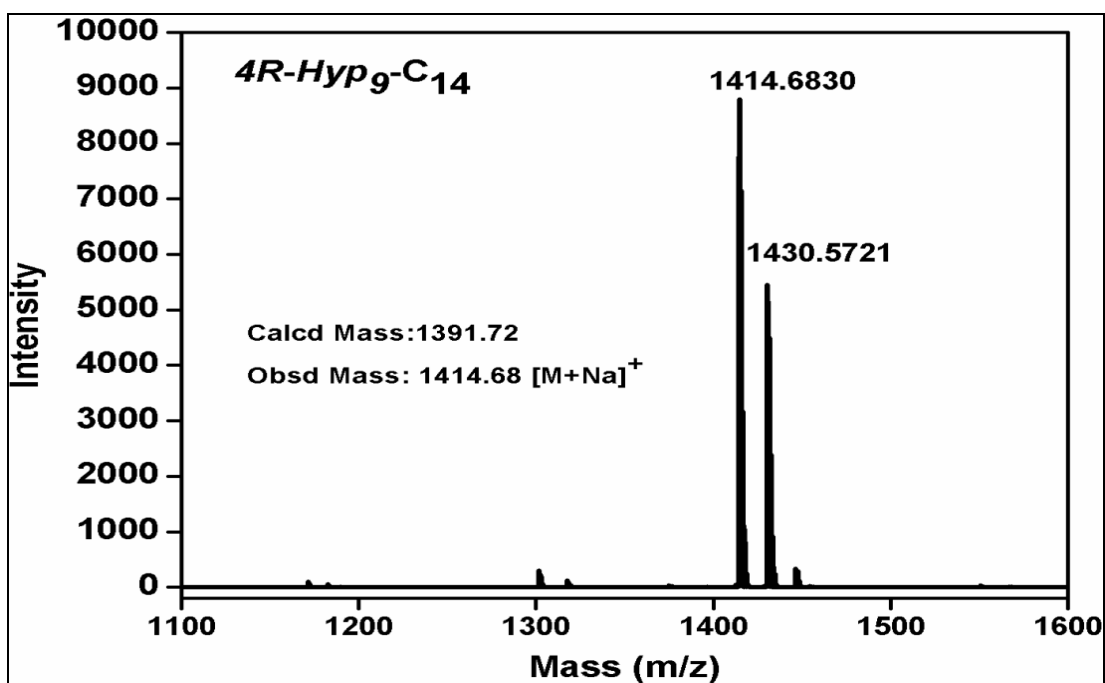
MALDI-TOF of Trp-4S-hyp₉-Ds



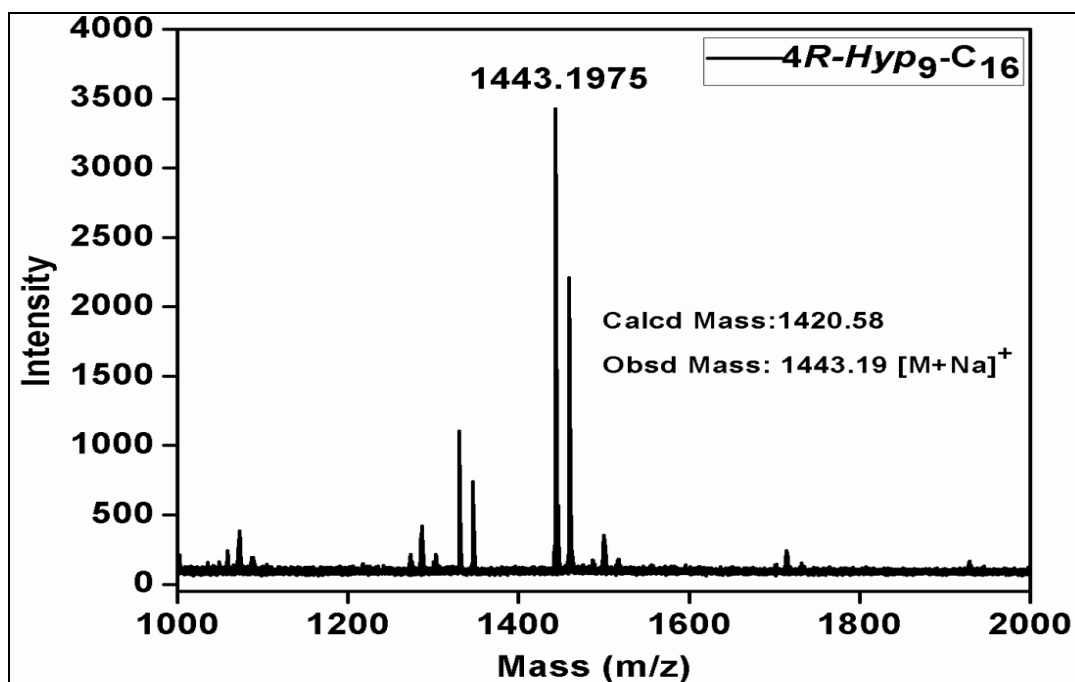
MALDI-TOF of 4*R*-Hyp₉-C₁₂



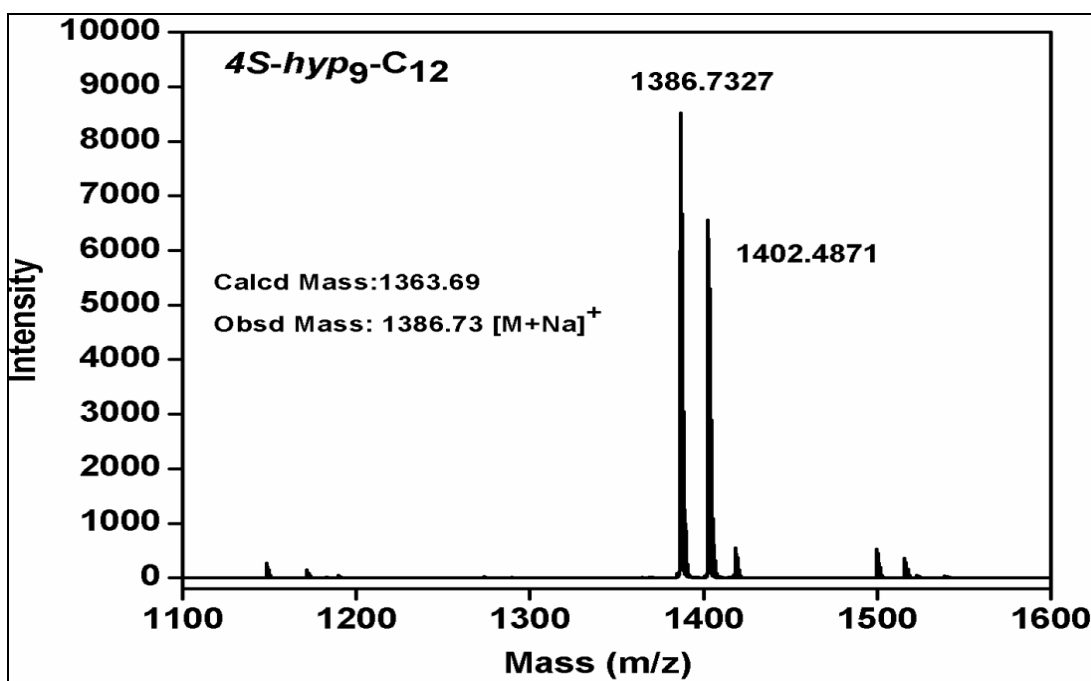
MALDI-TOF of 4*R*-Hyp₉-C₁₄



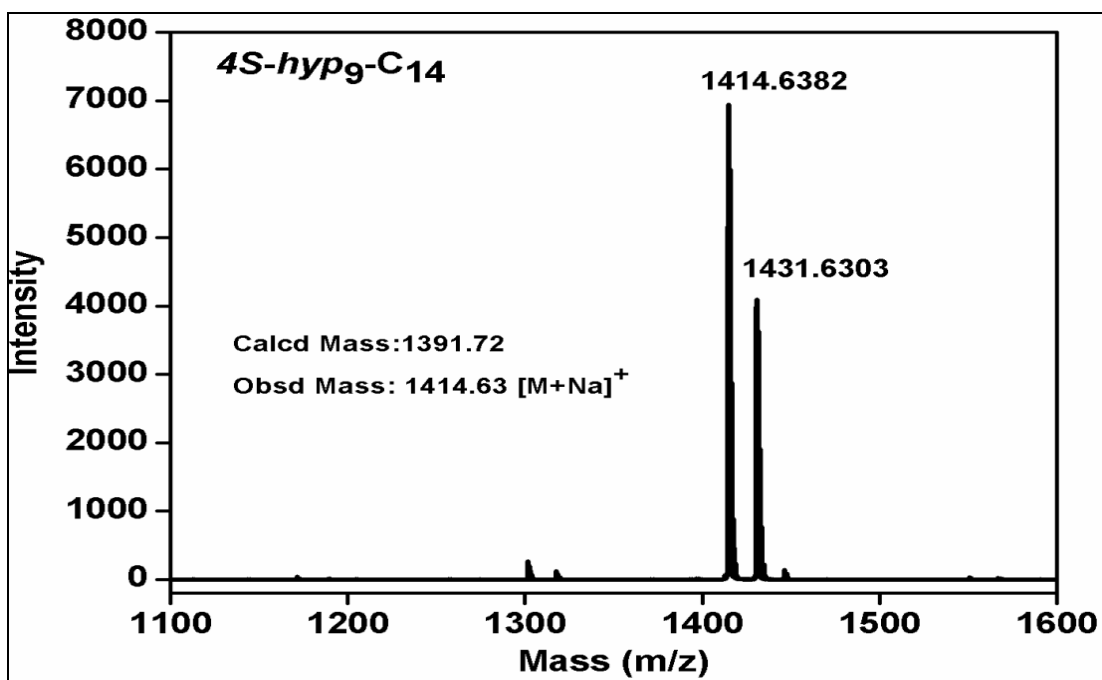
MALDI-TOF of 4*R*-Hyp₉-C₁₆



MALDI-TOF of 4*S*-hyp₉-C₁₂



MALDI-TOF of 4*S*-hyp₉-C₁₄



MALDI-TOF of 4*S*-hyp₉-C₁₆

